Volume 3, Issue 10(4), October 2014
INTERNATIONAL JOURNAL OF MULTIDISCIPLINARY EDUCATIONAL RESEARCH

Published by
Sucharitha Publications
Visakhapatnam – 530 017
Andhra Pradesh – India
Email: victorphilosophy@gmail.com
Website: www.ijmer.in

Editorial Board

Editor-in-Chief
Dr. Victor Babu Koppula
Faculty
Department of Philosophy
Andhra University – Visakhapatnam -530 003
Andhra Pradesh – India

EDITORIAL BOARD MEMBERS

Prof. S.Mahendra Dev
Vice Chancellor
Indira Gandhi Institute of Development Research
Mumbai

Prof.Y.C. Simhadri
Vice Chancellor, Patna University
Former Director
Institute of Constitutional and Parliamentary Studies, New Delhi &
Formerly Vice Chancellor of
Benaras Hindu University, Andhra University
Nagarjuna University, Patna University

Prof. (Dr.) Sohan Raj Tater
Former Vice Chancellor
Singhania University, Rajasthan

Prof.K.Sreerama Murty
Department of Economics
Andhra University - Visakhapatnam

Prof. K.R.Rajani
Department of Philosophy
Andhra University – Visakhapatnam

Prof. A.B.S.V.Rangarao
Department of Social Work
Andhra University – Visakhapatnam

Prof.S.Prasanna Sree
Department of English
Andhra University – Visakhapatnam

Prof. P.Sivunnaidu
Department of History
Andhra University – Visakhapatnam

Prof. P.D.Satya Paul
Department of Anthropology
Andhra University – Visakhapatnam

Prof. Josef HÖCHTL
Department of Political Economy
University of Vienna, Vienna &
Ex. Member of the Austrian Parliament
Austria

Prof. Alexander Chumakov
Chair of Philosophy Department
Russian Philosophical Society
Moscow, Russia

Prof. Fidel Gutierrez Vivanco
Founder and President
Escuela Virtual de Asesoría Filosófica
Lima Peru

Prof. Igor Kondrashin
The Member of The Russian Philosophical Society
The Russian Humanist Society and Expert of the UNESCO, Moscow, Russia

Dr. Zoran Vujisiæ
Rector
St. Gregory Nazianzen Orthodox Institute
Universidad Rural de Guatemala, GT, U.S.A

Swami Maheshwarananda
Founder and President
Shree Vishwa Deep Gurukul
Swami Maheshwarananda Ashram Education & Research Center
Rajasthan, India

Prof.U.Shameem
Department of Zoology
Andhra University Visakhapatnam

Dr. N.V.S.Suryanarayana
Head
Dept. of Education, A.U. Campus
Vizianagaram

Dr. Momin Mohamed Naser
Department of Geography
Institute of Arab Research and Studies
Cairo University, Egypt

I Ketut Donder
Depasar State Institute of Hindu Dharma
Indonesia

Prof. Roger Wiemers
Professor of Education
Lipscomb University, Nashville, USA

Prof. G.Veerraju
Department of Philosophy
Andhra University
Visakhapatnam

Prof.G.Subhakar
Department of Education
Andhra University, Visakhapatnam

Dr.B.S.N.Murthy
Department of Mechanical Engineering
GITAM University –Visakhapatnam

N.Suryanarayana (Dhanam)
Department of Philosophy
Andhra University
Visakhapatnam

Dr.Ch.Prema Kumar
Department of Philosophy
Andhra University
Visakhapatnam

Dr.S.V Lakshmana Rao
Coordinator
AP State Resource Center
Visakhapatnam

Dr.E. Ashok Kumar
Department of Education
North- Eastern Hill University, Shillong

Dr.K.Chaitanya
Postdoctoral Research Fellow
Department of Chemistry
Nanjing University of Science and Technology
People's Republic of China

Dr.Merina Islam
Department of Philosophy
Cachar College, Assam

Dr R Dhanuja
PSG College of Arts & Science
Coimbatore

Dr. Bipasha Sinha
S. S. Jalan Girls' College
University of Calcutta
Calcutta

Dr. K. John Babu
Department of Journalism & Mass Comm
Central University of Kashmir, Kashmir

Dr. H.N. Vidya
Government Arts College
Hassan, Karnataka

Dr.Ton Quang Cuong
Dean of Faculty of Teacher Education
University of Education, VNU, Hanoi

Prof. Chanakya Kumar
University of Pune
Pune

© Editor-in-Chief, IJMER
Typeset and Printed in India
www.ijmer.in

IJMER, Journal of Multidisciplinary Educational Research, concentrates on critical and creative research in multidisciplinary traditions. This journal seeks to promote original research and cultivate a fruitful dialogue between old and new thought.

CONTENTS

Volume 3 Issue 10(4) October 2014

S. No		Page No
1.	The Non-Inclusion of Turkey in The European Union (EU) **Pradyut V. Hande**	1
2.	Rape - Social Disaster and its Impact in India **Nasidul Islam and Maniruzzamann Sk**	7
3.	A Study of Relationship Between Teacher Professional Pleasure and Teacher Stress Among the Engineering College Lecturers in North Coastal Districts of Andhra Pradesh **N.V.S.Suryanarayana,Goteti Himabindu and K.Victor Babu**	24
4.	Ambedkar's Perspective on Democracy and Challenges to its Today **Rohit Gangoli**	40
5.	Gatti Community of Tulunadu: A Study **Naveen**	53
6.	Normalization of Indo-Pak Relations and its Impact on Regional Security **Varam.Venkata Narasaiah**	62
7.	International Convention on Child Rights and India's Legal System-A Review of Juvenile Justice **Nutakki Sateesh**	69
8.	Employee Attitude Towards Corporate Social Responsibility – Evidence from Indian Corporate Sector **Ch. Sri Rama Murthy**	79
9.	Self – Help Groups – A Tool to Weaker Sections' Women Empowerment	87

10.	Exploring Service Design for Aquarium Business Using Service Mix **Sankaran A and Selvarasu A**	95
11.	A Study on Causes of Low Achievement in English Among Telugu Medium Pupils at Secondary Level **M. Solomon Raju**	126
12.	High Step up Solar Power Optimizer for DC Micro Grid Systems **V R S Kumar and P. Vijaya Ramarao**	137
13.	Dual Buck Conveter Fed Full Bridge Inverter for Renewable Energy Power Generation **S Rambabu and M.Pavani**	155
14.	Dual Active Bridge (DAB) Converter Stage with High Frequency SST'S Between AC & DC Distribution Systems **B. Satya Varaprasad and B. Lalitha Kumari**	175
15.	A CYCLO-Converter Based LFAC System Interfaced with the Main Power Grid for Wind Power **S. Rajasekhar and P. Vijaya Ramarao**	193
16.	Two String Buck Boost Converters in PV Panels with Two MPPT'S for Distribution System **T Siva Kumar and M.Pavani**	210
17.	Sinusoidal Pulse Width Modulation Based Multiple-Loop Digital Control Method Inverter System **V.N.D Sailaja and B. Lalitha Kumari**	226
18.	Voltage Balancing Technique for Reactive Power Compensation in 3-Level NPC Inverters Using TPWM Technique **Ch. Ramya and P. Vijaya Ramarao**	246
19.	Single Stage DC/DC Converter & DC/AC Converter for PV-Battery Applications **V. Rama Lakshmi and M.Pavani**	264
20.	PV Based Single & Three Phase Integrated Energy	278

Systems for Micro Grids
K Anitha and B. Lalitha Kumari

21. Transient Stability & Voltage Unbalances Improvement Using TCSC & SFCL — 302
B. Sai Krishna and P. Vijaya Ramarao

22. Bidirectional Power Flow Controller for The Electric Vehicle and DC or AC Grid — 313
J. Ramesh and M. Pavani

23. Enhancement of Three-Phase Shunt Active Power Filters with Current Control Strategy with FSTPI — 330
K. Srinivasulu and B. Lalitha Kumari

24. A Multi Objective Current & Power Controller for Distributed Generation (DG) Resources — 352
K. Sravani Sandhya and P. Vijaya Ramarao

25. A Pulse Width Modulation DC–DC Non-Isolated Buck Converter Using the Three-State Switching Cell — 373
K. Bhanu Deepika and M.Pavani

26. Electrolytic Capacitor-Less DC Anti-Islanding Technique in DC Distribution Systems — 392
K Surya Tejaswi and B. Lalitha Kumari

27. Space Vector Pulse Width Amplitude Modulation for Voltage Source Inverter — 411
T. M. Rayudu and P. Vijaya Ramarao

28. Performance of A DG System Connected to Three-Phase Power Converter & Boost Converter — 424
K. Madhavarao and B. Lalitha Kumari

29. IFBTL DC/DC Converter FOR Wind Turbines IN A DC GRID — 444
M. Kavya and M.Pavani

30. Disaster Management in Andhra Pradesh – A Study of Hudhud Cyclone — 460
B. Sunitha Padmavathi

Dr. K.VICTOR BABU
Editor-in-Chief

ISSN: 2277-7881; Impact Factor -2.735

INTERNATIONAL JOURNAL OF MULTIDISCIPLINARY EDUCATIONAL RESEARCH

Visakhapatnam -530 003, Andhra Pradesh – India, www.ijmer.in

Editorial ……..

Provoking fresh thinking is certainly becoming the prime purpose of International Journal of Multidisciplinary Educational Research (IJMER). The new world era we have entered with enormous contradictions is demanding a unique understanding to face challenges. IJMER's contents are overwhelmingly contributor, distinctive and are creating the right balance for its readers with its varied knowledge.

We are happy to inform you that IJMER got the high Impact Factor 2.972, Index Copernicus Value 5.16 and IJMER is listed and indexed in 34 popular indexed organizations in the world. This academic achievement of IJMER is only author's contribution in the past issues. I hope this journey of IJMER more benefit to future academic world.

In the present issue, we have taken up details of multidisciplinary issues discussed in academic circles. There are well written articles covering a wide range of issues that are thought provoking as well as significant in the contemporary research world.

My thanks to the Members of the Editorial Board, to the readers, and in particular I sincerely recognize the efforts of the subscribers of articles. The journal thus receives its recognition from the rich contribution of assorted research papers presented by the experienced scholars and the implied commitment is generating the vision envisaged and that is spreading knowledge. I am happy to note that the readers are benefited.

My personal thanks to one and all.

(Dr.Victor Babu Koppula)

INTERNATIONAL JOURNAL OF MULTIDISCIPLINARY EDUCATIONAL RESEARCH
ISSN : 2277-7881; IMPACT FACTOR - 2.972; IC VALUE:5.16
VOLUME 3, ISSUE 10(4), OCTOBER 2014

THE NON-INCLUSION OF TURKEY IN THE EUROPEAN UNION (EU)

Pradyut V. Hande
Student Manager
Symbiosis Institute of Management Studies (SIMS)
Pune,Maharashtra

Introduction

Since its official foundation in 1993 as a product of the Maastricht Treaty of 1992; the European Union (EU) has espoused the values of "respect for human dignity, liberty, democracy, equality, the rule of law and respect for human rights"; as outlined in Article 1-2 of its Constitution. Furthermore, member states ought to embrace an attitude of "pluralism, tolerance, justice, solidarity and non-discrimination". Prima facie evidence would suggest that these are universal tenets that any civilized society ought to live by in an endeavour to forge a more cohesive, productive and meaningful existence. However, closer inspection into the history leading up to the creation of the EU reveals a starker reality; from a values standpoint.

The pitched ideological battle that many fellow EU member nation states and Turkey have often waged in an attempt to resist/pursue integration into the EU has been tinged with various hues of mistrust, skepticism and broken promises. While Turkey has the right to feel slighted on many occasions, there is no denying the fact that it has not consistently fulfilled the systemic and charter requirements requisite for being considered for inclusion in the EU. To Turkey's credit, they have refused to cow down to the sometimes restrictive diktats of the influential EU clique and have instead chosen to pursue their independent trajectory of growth and development. Matters have gradually undergone a paradigm shift, especially after the 2008 global economic crisis and its spillover effects that have left the Eurozone in tatters. The same period has witnessed Turkey's strong economic performance, prompting many to question what they would have to actually gain from integration with the EU at large. However, the incumbent government has not just abandoned plans to pursue integration in totality.

In this regard, it is critical to examine the factors that have collectively connived to prevent the entry of an Islamic state like Turkey into the ambit of the EU through multiple lenses.

Study Objectives

The objectives of undertaking this inspectional study are threefold:

1. To examine the potential factors responsible for keeping Turkey out of the European Union (EU) thus far
2. To highlight the current state of the accession requirements mandated by the EU
3. To inspect the mutual benefit that both the EU and Turkey would gain in the event of plausible integration

A Geographic Reluctance

While most of Turkey lies in the Asian peninsula, it is only Western Turkey that lies in the European Continent. Its largest city of Istanbul with a population of over 9 million straddles both sides of the Bosporus Strait; laying half in Asia and the other half in Europe. Additionally, the capital city of Ankara lies entirely outside Europe. Thus, from a geographical standpoint, many are of the staunch opinion that Turkey does not qualify to be a member state of the EU. With a majority of the nation in terms of land and population external to Europe, this happens to be superficial reason at best. The fact that the EU has clarified that it is fuelled by "values and political will rather than the location of rivers and mountains" has done precious little to quell the aforementioned concern. Is this a legitimate factor? Or is there a more deeper and basic reason at play?

Christian Values: The Beneficial Bedrock of European Civilisation?

Christianity has certainly been the crucible within which the intellectual and political cultures of Western Europe have developed over the past two millennia. But the claim that Christianity embodies the "bedrock values of European civilisation", and that the weakening of Christianity inevitably means the weakening of liberal democratic values, is ethically debatable. It greatly simplifies both the history of Christianity and the roots of modern democratic values. What we now think of as the Judeo-Christian tradition has been created as much despite the efforts of the Christian Church, as because of them. Western Europe endured the Dark Ages between the extinguishing of the final sparks of Hellenism in the fifth century and the re-ignition of cultural life in the Renaissance almost a millennium later. This is often seen as a period ushered in by the barbaric invasions of the fourth and

fifth centuries that brought down the Roman Empire. In fact, the intellectual darkness was ushered in by the policies of the Church itself. The collapse of the Roman imperial institutions under the weight of the myriad invasions left the Church as almost the only body capable of maintaining some semblance of social order in Western Europe. It also left the clergy as the sole literate class in the Western world and the Church as the lone patron of knowledge and the arts. This formed the springboard for its growing influence across the land and its continual attempts at quelling the spread of "non-Christian" elements; namely Islam.

A Clash of Religious Values: An Uncomfortable Question

Is it this "tainted" religious history that has laid the foundations for the EU's contemporary attitude towards Europe's only Islamic state; Turkey? Pitched against largely Christian values across a disparate Continent, Turkey has always faced an ideological and identity crisis of sorts in its attempt to align itself with its neighbours for long term socio-economic gains. However, the EU's reluctance in welcoming Turkey under its umbrella with open arms over the years has raised multiple uncomfortable questions and theories that go beyond complying with laid down stipulations.

A Game of Musical Chairs: Turkey's Historical Attempts at Aligning with the EU

Turkey has striven for membership to the EU and its predecessor organisations for many decades. It was in 1959 that Turkey first applied for full time membership to the European Economic Commission (EEC), founded in 1958. 1963 turned out to be a watershed year when an agreement was signed between the EEC and Turkey. The EU Association Council established a Customs Union with the Islamic Republic in 1995; that has played a crucial role in much of the country's recent socio-economic success. After years of being a peripheral player, Turkey was granted Accession Country status in 1999. The official enlargement negotiations that inspect the alignment of Turkish and EU law began in 2005.

Accession Tales: The EU's Reservations

On paper, Turkey is subject to the same stipulations that every other potential member state inductee is supposed to fulfill. Turkey has made significant progress in ensuring the establishment of "functional market economy and stability of institutions guaranteeing democracy". However,

there are severe shortcomings with regards to the country's human rights situation, limited freedom of expression and press and gender inequality.

Most glaring in this respect is the civil suppression, suspension of rights and "cultural genocide" of the local Kurdish population; the largest ethnic minority that composes almost 15% of the total populace. Viewed as a threat to the Turkish primacy, the Kurds have faced decades of repression at the hands of successive governments. The well documented intolerance displayed by the central leadership despite international calls to remedy the domestic situation has not won Turkey any new fans in the EU. This mood was captured by the European Commission in 2006 when it said that, "overall Turkey made little progress in ensuring cultural diversity and promoting respect for and protection of minorities in accordance with international standards". There has been marginal improvement in this direction over the last four years; ever since Recep Tayyip Erdogan assumed the Prime Minister's office. There is still a long way to go before holistic national integration is achieved and the Kurds as a whole are bestowed with greater rights and political representation.

With regards to the existing gender inequality argument, there are certain notable statistics that offer a dichotomous view. According to the 2010 Millennium Development Goals (MDG) Report, while Turkey has almost eliminated gender inequality in primary education; the proportion of girls who do not enter the realms of secondary education is a cause for worry. There are primary gaps observed in the participation of women in decision making and the labour force. The representation of women in the parliament is a lowly 9.1% and that at the local governmental level is just over 2%. The proportion of women as part of the labour force is 25%, a figure that puts Turkey well below all other OECD members. With a position of 77th out of 138 counties on the Gender Inequality Index (GII), fellow EU members are liable to view Turkey through a jaundiced eye on this front.

Turkey has historically been known for curtailing freedom of personal expression and stringent censorship of the press machinery. Major media establishments are owned either by the government or leading business houses that collude with the incumbent party to foster an environment of self-censorship in order to avoid the wrath of Erdogan's Justice and Development Party (AKP). In fact, Turkey ranked 148th out of 169 countries in the Reporters Without Borders Annual Worldwide Press Freedom Index of 2012-

13. Censorship has taken a turn for the worse what with a contentious new law passed in February, 2014 that further regulates the Internet. The European Court of Human Rights has repeatedly found Turkey in violation of Article 10 of the European Convention on Human Rights for blocking access to the likes of Google and social media outlets such as Twitter; multiple times. This has further given the decision makers at the EU more fodder to stall Turkey's inclusion into the Union.

Another factor that has thrown the proverbial spanner in the wheels is Turkey's staunch reluctance to recognise Cyprus as an independent state. Cyprus is full-fledged permanent member of the EU. Turkey would have to bestow Cyprus with a degree of recognition if it hopes to make it to the EU eventually.

Integration: A Question of Mutual Benefit?

Despite its inherent reservations, the EU would have a lot to gain from Turkey's inclusion. For starters, Turkish membership would definitely strengthen the EU's foreign policy weight on the global arena. Turkey's geographic location positions it as an ideal country for the transit of oil and natural gas; playing a potentially strategic role in fulfilling the EU's energy requirements. The nation can also serve as a counterweight to the volatile and fractious influence of Russia in the region. In light of the Arab Spring and volatility in the Middle East, integrating an Islamic state into the fabric of the EU can have multifarious benefits.

For Turkey, per se, decades of trying to gain Continental acceptance and Union membership have left the general populace with a feeling of *Schadenfreude.* The attractiveness of joining the EU has further diminished in the wake of the prolonged sovereign debt crisis of 2008 and its still prevalent spillover effects. The fact that Turkey has created more private sector jobs that all EU member states combined in the last five years, coupled with strong economic growth has further shrouded a potential integration in doubt.

Thus, it is a collection of factors steeped in on-ground domestic realities, rigid ideologies stemming from age-old Christian values and the perceived threat of the rise of "Eurabia" that has kept Turkey outside the EU until now. It has now come to a point where after being snubbed for years, Turkey has managed to carve a niche all of its own in Europe and literally speaking does not require the EU to further its socio-economic and political

interests. It remains to be seen whether integration ensues in the future. For now though, both the EU and Turkey have their own set of functional demons, value constraints, systemic inadequacies and socio-economic problems to grapple with.

References

1. Enlargement

   http://ec.europa.eu/enlargement/countries/detailed-country-information/turkey/

   [Accessed: September, 2014]

2. EU-Turkey Relations

   http://www.euractiv.com/enlargement/eu-turkey-relations/article-129678

   [Accessed: September, 2014]

3. Turkey Profile

   http://www.bbc.com/news/world-europe-17988453

   [Accessed: September, 2014]

RAPE - SOCIAL DISASTER AND ITS IMPACT IN INDIA

Nasidul Islam
Department of Disaster Management
Pondicherry University,
Brookshabad,
Port Blair, Andaman and Nicobar Island

Maniruzzamann Sk
Department of Disaster Management
Pondicherry University, Brookshabad,
Port Blair, Andaman and Nicobar Island

1. INTRODUCTION

Rape in India is one of India's most common crimes against women [1]. January 4, 2014 India has become a top ten rape crime record all over the world. Marital rape that occurs when spouses are living together can only be dealt under the Protection of Women from Domestic Violence Act 2005 which only provides civil remedies to victims (it is a form of non-criminal domestic violence). Marital rape is not a criminal offense, except when spouses are separated. Rape cases in India have doubled between 1990 and 2008[2]. Penile and non-penile penetration in bodily orifices of a woman by a man, without the consent of the woman, constitutes the offense of rape under the Criminal Law (Amendment) Act, 2013. [3]Recent day the rape became a social disaster all over the world. Rape is a type of sexual assault usually involving sexual intercourse, which is initiated by one or more persons against another person without that person's consen. The act may be carried out by physical force, coercion, abuse of authority or against a person who is incapable of valid consent, such as one who is unconscious, incapacitated, or below the legal age of consent [4][5]. The term rape is sometimes used inter changeably with the term sexual assault [6]. There are several types of rape, generally categorized by reference to the situation in which it occurs, the sex or characteristics of the victim or the sex or characteristics of the perpetrator. Different types of rape include date rape, gang rape, marital rape, incestual rape, child sexual abuse, prison rape, acquaintance rape, war rape and statutory rape. When part of a widespread and systematic practice during international conflict, rape and sexual slavery are recognized as crimes against humanity and war crimes. Rape is also recognized as an element of the crime of genocide when committed with the intent to destroy, in whole or in part, a targeted ethnic group. People who have been raped can be severely traumatized and may suffer from posttraumatic stress disorder [7] in addition to psychological harm resulting from the act; rape may cause physical injury, or have additional effects on the

victim, such as acquiring of a sexually transmitted infection or becoming pregnant. Furthermore, following a rape, a victim may face violence or threats thereof from the rapist, and, in some cultures, from the victim's own family and relatives [8][9].

1.1. ISLAMIC CONCEPT

Rape is forbidden under Islamic law [10]. Some female rape victims are accused and punished for having sex outside of marriage. But there must be sufficient evidence before any sort of penalty is given. "Local Sharia courts in some third world countries regularly punish raped minor girls and women by flogging and beating them with shoes. But this is not according to the orthodox Sharia (Quran and Sunnah) [11]. "In 1979, the government of Pakistan adopted the Zina Ordinance to bring the Penal Code into accord with Islamic principles. Under this ordinance, women who report having been raped must prove that the intercourse was without consent. If unable to prove this lack of consent, they can be charged with fornication. As a result, women are less likely to report rape [12] some rights advocates say that this aspect of Sharia law "not only negates the rights of women but is also a misinterpretation of Islam. [13] (See also Hudood Ordinance.) Mainstream Sunni Islamic scholars, like Imam Malik, clearly state that no punishment is applied on the raped women. "The hadd (punishment) in such cases is applied to the rapist, and there is no punishment applied to the raped woman [14] [15].

In Islamic criminal jurisprudence (Islamic shariya), the overwhelming majority of Muslim scholars believe that there is no punishment for a woman forced to have sex. According tohadith, the punishment for committing rape is death, there is no sin on the victim, nor is there any worldly punishment ascribed to her. Most scholars treat rape as hirabah (disorder in the land). Rape is defined as 'zinabiljabr' fornication/adultery with the use of coercion or compulsion. Rape is defined as 'zinabiljabr' fornication/adultery with the use of coercion or compulsion. Note it has to be extra marital i.e. fornication/adultery; the rape charge can not be brought against the husband by the wife, i.e. it can not be within marriage, as indeed was the case in English Law until 1991 when the House of Lords ruling in R v R [16] stated it was anachronistic to maintain such position in modern western society. The interpretation and application of these laws is very controversial, not least due to modern ill-fated legislation, such as Pakistan's Hudood Ordinance, under General Zia ul-Haq, which arguably criminalise the victim who fails to produce

four witnesses. Thus perverting the aim behind the law, to protect the victim of rape and grant her justice. In Islamic military jurisprudence, classical jurists laid down severe penalties for rebels who use "stealth attacks" and "spread terror". In this category, Muslim jurists included abductions, poisoning of water wells, arson, attacks against wayfarers and travelers (highway robbery), assaults under the cover of night, and rape. The punishment for such crimes was severe, including death, regardless of the political convictions and religion of the perpetrator [17].

2. RESEARCH OBJECTIVE

The main research objective is to systematically study rape scenario and to identify and estimate its impact on women in Indian.

- To estimate and quantify the number of rape scenario and its impact of victim in India.

3. HISTORICAL ANALYSIS

The methodological study of rape scenario based upon the historical analysis of reported rape case by National Crime Records Bureau in India. The quantities Analysis Technique (QAT) was use for growth trend intensity analysis of state wise in India.

4. RESULT AND DISCUSSION

Rape in India has been defined by Radha Kumar as one of the most common crimes against women in India [18] and by the UN's human-rights chief as a "national problem" [19]. Marital rape is not a criminal offence [20].While this means they are more likely to be sexually abused, it also means they are more likely -compared with women of a previous generation — to report rapes and confront sexual predators. India's National Crime Records Bureau recorded 16,000 reported cases of rape in 2001.

In 2010, 14,263 cases of rape were decided, with the accused being convicted in 3,788 cases, or 26.6%. According to the National Crime Records Bureau, 24,206 rape cases were registered in India in 2011 and Northeastern state of Manipur recorded a 100% conviction rate in rape trials in 2011.

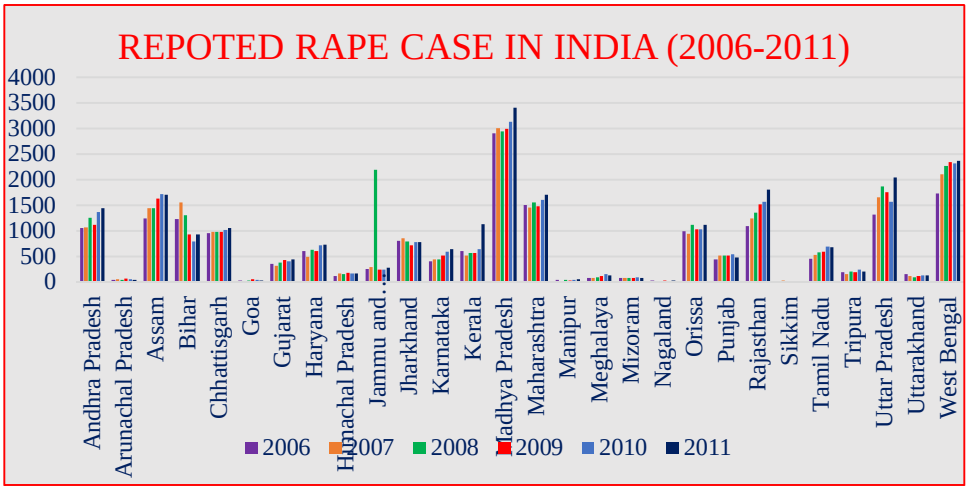

FIG: 1. STATE WISE REPORTED RAPE CASE IN INDIA

According to the National Crime Records Bureau, in 2012, 25,000 rape cases were reported across India. New Delhi has the highest number of rape-reports among Indian cities, while Jabalpur has the per capita incidence of reported rapes [21][22]. In the three months after the Delhi gang rape, the number of rapes reported in the city more than doubled to 359, from the 143 reported in January-March of 2012. Rape cases in India have doubled between 1990 and 2008[23].In fact, Mizoram has the absolute highest rape rate in India.

The NCRB was sharp that West Bengal recorded 2,046 cases of rape registered in 2012 alone. India is one of the most verdict countries right now in rape cases among the top ten in the word (2014). Every day a new case is reported every 20 minutes [24]. If we can see state-wise statistic of rape in India it is cleared that Madhya Pradesh is highest rang and west Bengal first growing state in India. (Figure: 1). during the partition of India, rape was an extensive issue. It is estimated that during the partition, up to 100,000 women were kidnapped and raped.

TABLE: 1. STATE-WISE RAPE CASES STATITICS IN INDIA

Name of State	Years						Total number of rape (2006-2011)
	2006	2007	2008	2009	2010	2011	
Andhra Pradesh	1049	1070	1257	1118	1362	1442	7298
Arunachal Pradesh	37	48	42	59	47	42	275
Assam	1244	1437	1438	1631	1721	1700	9171
Bihar	1232	1555	1302	929	795	934	6747
Chhattisgarh	955	982	978	976	1012	1053	5956
Goa	21	20	30	47	36	29	183
Gujarat	354	316	374	433	408	439	2324
Haryana	608	488	631	603	720	733	3783
Himachal Pradesh	113	159	157	183	160	168	940
Jammu and Kashmir	250	288	2190	237	245	277	3487
Jharkhand	799	855	791	719	773	784	4721
Karnataka	400	436	446	509	586	636	3013
Kerala	601	512	568	568	634	1132	4015
Madhya Pradesh	2900	3010	2937	2998	3135	3406	18386
Maharashtra	1500	1451	1558	1483	1599	1701	9292
Manipur	40	20	38	31	34	53	216

Meghalaya	74	82	88	112	149	130	635
Mizoram	72	83	77	83	92	77	484
Nagaland	23	13	19	22	16	23	116
Orissa	985	939	1113	1023	1025	1112	6197
Punjab	442	519	517	511	546	479	3014
Rajasthan	1085	1238	1355	1519	1571	1800	8568
Sikkim	20	24	20	18	18	16	116
Tamil Nadu	457	523	573	596	686	677	3512
Tripura	189	157	204	190	238	205	1183
Uttar Pradesh	1314	1648	1871	1759	1563	2042	10197
Uttarakhand	147	117	87	111	121	129	712
West Bengal	1731	2106	2263	2336	2311	2363	13110
Total	18682	20096	20953	20804	21603	23582	125720

Source: NCRB, PRS

4.1. MADHYA PRADESH

Madhya Pradesh has a highest rank of Rape among all the state in India. The total account of rape was estimated 18386 women from 2006 to 2011 and during 2006 it was reported 2900 that account reached up to 3010 during 2007. After 2007 it amount was slightly decreased to be 2937 during the year 2008 and during 2009 to 2011 it was slowly increasing 2998 women up to 3406 women rape in the state(table:1, fig:1). In March 2013 a Swiss couple who were cycling from Orchha to Agra, were physically assailed by 8 locals, the man was overpowered and tied up while the 39-year old woman was gang-raped in front of her husband at a village in Datia District where they decided to camp for a night. [25][26] The Supreme Court on 5 August 2013 directed the Madhya Pradesh Government to pay Rs 10 lakh as compensation each to the two school-going girls gang raped last year in Betma town of Indore district and issued show cause notice to a senior police officer as to why criminal case be

not lodged against him for disclosing the names of victims in his affidavit, which is an offence under section 228A of the Indian Penal Code [27].

4.2.WEST BGENGAL

West Bengal has a second rank of reported rape case in India. It was estimate as13110 women were rape during the year 2006 to 2011(table: 1). NCRB (National Crime Records Bureau) reported that in the future of West Bengal has highly trend to increasing the number of rape in India. If we can see the previous reported history of rape cases then we can appraisal and compute the growth intensity of rape in the state. During the year 2006 West Bengal embrace its account was 1731 women and after 2006 to 2011 rape intensity rapidly increased 2106 women during the 2007, 2263 women during 2008, 2336 women during 2009, 2311 women during 2010 and 2363 women during (fig: 1).According to The time of India and The Telegraph "if the Government do not taken any act again the criminal then West Bengal has exceedingly trend to growth intensity of rape in the future".

4.3.UTTAR PRADESH

Uttar Pradesh has third position after West Bengal for explosion rape recorded by NCRB in India. During the year 2006 it was estimate 1314 women and from the next year 2007 it was increase 1648 women and again rape 1871 women during 2008 and During the year 2009 and 2010 the growth intensity of rape marginally declined but the nest year suddenly increased up to 2042 women (table:1,fig:1) and during the year 2011 number of brutal assaults on women were reported in Uttar Pradesh and according to the People's Union for Civil Liberties (PUCL), the majority of those assaulted were poor women from remote areas and Dalits. SR. Darapuri vice president of the PUCL stated, "I analyzed the rape figures for 2007 and I found that 90% of victims were Dalits and 85% of Dalit rape victims were underage girls"[28].

4.4.MAHARASHTTRA

After Uttar Pradesh, Maharashtra has fourth rank of rape in India. Total amount was estimated 9292 women during 2006-2011. Where during the year 2006, it account was 1451 women rape and next year rapidly increased the trend of growth intensity of rape to be 1558 women during 2007. But this amount slowly increased 1701 during 2011(table: 1).NCRB assess the state Maharashtra has positive trend to increasing rape intensity in Indian.

4.5. ASSAM

Assam is another significant state for reported rape in India, it has fifth position all among the state. After the calculation Assam projected that the account of 9071 women were rape during 2006 to 2011 and during 2008 its amount was 2244 women and after 2008 progressively declined the growth rate during 2009, 2010 and 2011 and during1700 women were rape in the 2011(table: 1) which is suggest that there has been negative trend to growth intensity of rape.

4.6. JAMMU AND KASHMIR

Jammu and Kashmir during the year 2006 and 2007 rape was estimate 250 women. But during the nest year 2008 it was give highest allegations of rape and mass rape in Jammu and Kashmir which account as 2190 women(table:1,fig:1). The Indian government carried out three inquiries into the allegations and concluded that it had been a hoax for that number of increased rape. There was doubt that the sudden increased number of rape in Jammu and Kashmir. The International Commission of Jurists has stated that though the attacks had not been proven beyond a doubt, there was credible evidence that it had happened. In 2011, the State Human Rights Commission (SHRC) asked for the reopening of the case. After 2008 growth intensity of rape marginally decreased during the years of 2009 and 2010 but again it is increased in 2011whichaccount was 277 women.

4.7. OTHERS STATE OF INDIA

In the north east India was remark as a lowest account of growth intensity of rape in India. Nagaland and Sikkim give its total amount 116 women both and nest was Manipur during the year 2011(table: 1 fig: 1).Human rights groups allege that the Indian armed forces under the protection of the Armed Forces (Special Powers) Act, 1958 have carried out a large amount of rapes in the Nagaland, Assam and Manipur provinces [29]. In August 2013, a School Teacher in Arunachal Pradesh was arrested for raping fourteen underage girls in a hostel where he was warden. The sexual exploitation allegedly continued for over 3 years, until one of the girls filed a police complaint [30]. After historical analysis consequence show that the other state like Bihar, Chhattisgarh, Rajasthan, Gujarat, Haryana, Kerala, Karnataka, Jharkhand and Tamil Nadu has moderate trend to growth intensity of rape in India.

4.8. RECENT REPORT IN INDIA

According to BBC report in February 2013, more than 7,200 children are raped each year in India. Underage victims who do report the assaults are often subjected to mistreatment and humiliation from the police [31]. A landmark government survey in 2007 revealed that a lot of children in India are physically abused and that such occurrences are "disturbingly common".[32] In January 2013, a 7-years old girl was raped in the school toilet while studying at school in Goa[33][34].Young girls are trafficked into prostitution in India, often by women who have been trafficked themselves. As adults they use personal relationships and trust in their villages of origin to recruit additional girls. India is categorized as one of the 'extreme risk' countries for trafficking children by Maplecroft [35]. Communal riots in India have seen rapes and gang rapes become a common phenomenon in recent history. Perhaps the first riot where rape was used by rioters as a weapon (along with attacks on pregnant women) was the 2002 post-Godhra riots in the western state of Gujarat [36]. Sexual violence was a strong component of the rioting in the 2013 Muzaffarnagar riots in Uttar Pradesh; 13 rape and assault cases were reported.

5. IMPACT OF RAPE ON WOMEN

For rape victims the more common consequences of sexual violence are those related to reproductive health, mental health, and social wellbeing. Common consequences experienced by rape victims include are Vaginal or anal bleeding or infection, Hypoactive sexual desire disorder, Vagin it is or vaginal inflammation, Dyspareunia — painful sexual intercourse, Vaginismus - a condition affecting a woman's ability to engage in any form of vaginal penetration, Chronic pelvic pain, Urinary tract infections, Pregnancy, HIV/AIDS, Social exclusion, Mental and physical suffering, Coping with hate, grim and scorn, Family trouble, Feeling of lost world, A way to prostitution, Social anarchy Sexually transmitted diseases: Violent or forced sex can increase the risk of transmitting HIV. In forced vaginal penetration, abrasions and cuts commonly occur, thus facilitating the entry of the virus through the vaginal mucosa. Adolescent girls are particularly susceptible to HIV infection through forced sex, and even through casual sex, because their vaginal mucous membranes have not yet acquired cellular density sufficient to provide an effective barrier that develops sin the later teenage years. Self-blame: is among the most common of both short- and long-term effects and functions as an

avoidance coping skill that inhibits the healing process and can often be remedied by a cognitive therapy technique known as cognitive restructuring. The victim will often already internally blame themselves, especially because the violation of boundaries, broken trust, and the feeling of personal danger occurs with rape. And lack of motivation to seek care, lack of empathy; cutting themselves off from other people; anger; aggression. Suicide: Childhood and adulthood victims of rape are more likely to attempt or commit suicide. The association remains, even after controlling for sex, age, education, symptoms of post-traumatic stress disorder and the presence of psychiatric disorders. Victim blaming: The term *victim blaming* refers to holding the victim of a crime to be responsible for that crime, either in whole or in part. In the context of rape, it refers to the attitude that certain victim behaviors (such as flirting or wearing sexually provocative clothing) may have encouraged the assault. Adult-on-child rape: Rape and other forms of sexual assault on a child can result in both short-term and long-term harm, including psychopathology in later life. Psychological, emotional, physical, and social effects include depression, post-traumatic stress disorder, anxiety, eating disorders, poor self-esteem, dissociative and anxiety disorders; general psychological distress and disorders such as somatization, neurosis, chronic pain, sexualized behavior, school/learning problems; and behavior problems including substance abuse, destructive behavior, criminality in adulthood and suicide.

6. MEASUREMENT TO BE TAKEN ABSTAINED

"Rape "has become a term that can be seen daily in news and just like a termite it is undermining the roots of India. Recently Dr. Indira Sharma, President of the Indian Psychiatric Society has said that early marriage can solve the problem of rape in India. To prove her viewpoint she said that as soon as a boy starts earning his parents lose 50% control over him and then he is free to drink, smoke etc. In Dr. Indira Sharma's wording "One of the advantages of early marriage is that it is a socially acceptable channel for sexual desire". Various factors may aid or inhibit the survivors' ability to resolve the issues associated by the rape. Positive feelings of self-esteem, good support systems, previous success in dealing with crisis and economic security all enhance the ability to heal. Survivors who can minimise, (deal with one small segment of the problem at a time) often find success. The woman's personality and her previous coping mechanisms influence her ability to cope with the rape. Women with a past or current history of physical, psychiatric or social problems appear to be more likely to develop severe depression,

psychotic behaviour, psychosomatic disorders, suicidal behaviour and acting out behavior associated with alcoholism, drug abuse and/or sexual activity. Social network support is a factor affecting the woman's coping capacity. Secondly, these people need to be supportive. They need to allow the woman the opportunity to discuss the assault if she wants to and to listen to her. Some families and partners tell the woman "to forget it" refusing to accept the extent of the trauma. Life cycle stage may also affect the victim's coping capacity. The rape means different things to women at different stages of their life. The younger adolescent for whom the rape is her first sexual experience may become concerned about her sexual behaviour in the future. She may become afraid of entering into relationship with her adolescent peers. The way the woman is treated as a victim may also influence her ability to cope. Good treatment, co-operation of police and jurisdiction response can minimize the intensity of rape.

6.1. LEGAL ACT TAKEN BY GOVERNMENT IN INDIA

In April 2013 the Indian Parliament introduced amendments to the Indian Penal Code making various changes to the anti-rape laws in India [37]. The offence of rape under Section 375, have made both penile and non-penile insertion into bodily orifices of a woman by a man an offence. The definition is broadly defined in some aspect, with acts like penetration by penis, or any object or any part of body to any extent, into the vagina, mouth, urethra or anus of a woman or making her to do so with another person or applying of mouth to sexual organs without the consent or will of the woman constitutes the offence of rape [38]. The section has also clarified that penetration means "penetration to any extent", and lack of physical resistance is immaterial for constituting an offence. Except in certain aggravated situation the punishment will be Imprisonment not less than seven years but which may extend to imprisonment for life, and shall also be liable to fine. In aggravated situations, punishment will be rigorous imprisonment for a term which shall not be less than ten years but which may extend to imprisonment for life, and shall also be liable to fine [38]. A new section, 376A has been added which states that if a person committing the offence of sexual assault, "inflicts an injury which causes the death of the person or causes the person to be in a persistent vegetative state, shall be punished with rigorous imprisonment for a term which shall not be less than twenty years, but which may extend to imprisonment for life, which shall mean the remainder of that person's natural life, or with death [38]. In the case of "gang rape", persons involved regardless

of their gender shall be punished with rigorous imprisonment for a term which shall not be less than twenty years, but which may extend to life and shall pay compensation to the victim which shall be reasonable to meet the medical expenses and rehabilitation of the victim. Certain changes has been introduced in the Criminal Procedure Code, 1973 and Indian Evidence Act, like the recording of statement of the victim has been made more friendly and easy, character of the victim is irrelevant for consideration, presumption of no consent where sexual intercourse is proved and the victim states in the court that there has been no consent, etc. The age of consent in India has been increased to 18 years, which means any sexual activity irrespective of presence of consent with a woman below the age of 18 will constitute statutory rape. Although, the decision of death penalty for the most extreme rape cases was approved by the Indian parliament, marital rape is still not accepted as a criminal offense within Indian legal framework, [39] except during the period of judicial separation of the partners. In the 1980s, women's rights groups lobbied for marital rape to be declared unlawful, as until 1983, the criminal law (amendment) act stated that "sexual intercourse by a man with his own wife, the wife not being under fifteen years of age is not rape. The government officials argued that the contract of marriage presumes consent to sex and that criminalising marital rape in turn would weaken family values in India.[39] The Protection of Women from Domestic Violence Act 2005 (PWDVA) which came into force in 2006, provides protection against marital rape or other forms of sexual perversions and domestic violence.[40] However, it offers only a civil remedy for the offence. In April 2013, Additional Sessions Judge Virender Bhat noted that the legal principle of reliance on the sole testimony of the victim had become "an easy weapon" to implicate anyone in a case of rape [41]. Justice Kailash Ghambhir of the Delhi High Court stated that penal provisions for rape are often being misused by women as a "weapon for vengeance and vendetta" to harass and blackmail their male friends by filing false cases to extort money and to force them get married .

7. CONCLUSION

The present research was carried out by the historical analysis of register rape case in Indian by NCRB. This research given a clear optical view of trend to increasing of the growth intensity of rape some of the state in India. Madhya Pradesh remark as a maximum number of rape in India but West Bengal has a highest trend to growth of rape intensity in the future in the contemporary India. Rape in India is one of the most common crimes against women. Now

modern India rape becomes a social disaster which refers to as social crime. Marital rape that occurs when spouses are living together can only be dealt under the Protection of Women from Domestic Violence Act 2005 which only provides civil remedies to victims (it is a form of non-criminal domestic violence. Marital rape is not a criminal offense, except when spouses are separated. Rape cases in India have doubled between 1990 and 2008 Penile and non-penile penetration in bodily orifices of a woman by a man, without the consent of the woman, constitutes the offense of rape under the Criminal Law (Amendment) Act, 2013.

References

1. Kumar, Radha (1993). The History of Doing: An Account of Women's Rights and Feminism in India. Zubaan. p. 128. ISBN 978-8185107769.
2. "Indian student gang-raped, thrown off bus in New Delhi" (http://www.arabnews.com/indian-student-gang-raped-thrown-bus-new-delhi). Arabnews.com. 2012-12-17. Retrieved 2013-12-04.
3. "Criminal Law (Amendment) Act, 2013" (http://mha.nic.in/pdfs/TheCrimnalLaw030413.pdf). Ministry of Home Affairs, Government of India. Retrieved 7 April 2013.
4. ab "Rape" (http://www.merriam- webster.com/dictionary/rape%5B3%5D). Merriam-Webster. April 15, 2011.
5. a b "Sexual violence chapter 6" (http://whqlibdoc.who.int/publications/2002/9241545615_chap6_eng.pdf). World Health Organization. April 15, 2011.
6. Hedge, edited by Jenny Petrak, Barbara (2003). The Trauma of Sexual Assault Treatment, Prevention and Practice. (http://books.google.ca/books?id=6KZfQ6cSVHoC&pg=PA2). Chichester: John Wiley & Sons. p. 2. ISBN 9780470851388.
7. "Post Traumatic Stress Disorder in Rape Survivors" (http://www.aaets.org/article178.htm). The American Academy of Experts in Traumatic Stress. 1995. Retrieved 2013-04-30.

8. a b "Rape victim threatened to withdraw case in UP"(http://zeenews.india.com/news/uttar-pradesh/rapevictim-threatened-to-withdraw-case-in-up_694364.html).Zeenews.india.com.2011-03-19. Retrieved 2013-02-03.
9. a b Harter, Pascale (2011-06-14). "BBC News - Libya rape victims 'face honour killings' " (http://www.bbc.co.uk/news/world-africa-13760895). BBC News. Retrieved 2013-02-03.
10. Uzma Mazhar (2002) Rape & Incest: Islamic Perspective (http://www.muslimaccess.com/articles/Women/rape_in_islam.asp)
11. How Sharia Law Punishes Raped Women (http://www.aina.org/news /20081117111817.htm). Aina.org. Retrieved on 2011-10-01.
12. Polk, Michael F. (1998). "Women Persecuted under Islamic Law: The Zina Ordinance in Pakistan as a Basis for Asylum Claims in the United States" (http://heinonline.org/HOL/LandingPage?collection=journals&handle=hein.journals/geoimlj12&div=26&id=&page=). Georgetown Immigration Law Journal 12: 379.
13. Will Pakistan ease harsh Sharia rape laws? (http://www.jihadwatch.org/2006 /07/will-pakistan-ease-harshsharia-rape-laws.html). Jihad Watch. July 2006
14. Imam Malik. "Book 36 (Judgements): Section 16, Judgment about raped women" (http://www.sultan.org/books/Muatta.pdf) (pdf). Malik's Muwatta.
15. Malik, Imam. "Al-Muwatta' of Imam Malik – Judgements – SunniPath Library – Hadith" (http://www.sunnipath.com/Library/Hadith/H0001P0036.aspx). Sunnipath.com. Retrieved 2012-08-24.R v R [1992] 1 A.C. 599, House of Lords
16. Abou El Fadl, Khaled. [Commentary: Terrorism Is at Odds With Islamic Tradition]. Muslim Lawyers
17. [18] Kumar, Radha (1993). The History of Doing: An Account of Women's Rights and Feminism in India. Zubaan. p. 128. ISBN 978-8185107769.

18. "India's women: Rape and murder in Delhi" (http://www.economist.com/news/leaders/21569031-horribleattack-could-prove-turning-point-indias-women-rape-and-murder-delhi).Economist.com. Retrieved 2013-01- 07.

19. a b Kinnear, Karen L. (2011). Women in Developing Countries: A Reference Handbook. ABC-CLIO. pp. 26– 27. ISBN 1598844261.

20. Data busts some myths on sexual violence (http://www.thehindu.com /news/national/data-busts-some-mythson- sexual-violence/article5089690.ece)

21. "Rape statistics around the world" (http://www.indiatribune.com/index.php?option=com_content&view=article&id=10195: rape-statistics-around-the-world&catid=107:coverpage&Itemid=471). Indiatribune.com. 2012-09-11. Retrieved 2013-03-17.

22. "Indian student gang-raped, thrown off bus in New Delhi" (http://www.arabnews.com/indian student-gangraped- thrown-bus-new-delhi) Arab News. Retrieved 29 May 2013.

23. "Court sentences 4 men to death in New Delhi gang rape case" (http://edition.cnn.com/2013/09/13/world/asia/india-gang-rape-sentence/). CNN. 2013-09-14. Retrieved 2013- 09-15.

24. "BBC News - Swiss woman 'gang-raped' in central India" (http://www.bbc.co.uk/news/world-asia-india- 21812849). Bbc.co.uk. 1970-01-01. Retrieved 2013-03-16.

25. "India: Tourist Gang-Raped And Husband Beaten" (http://news.sky.com/story/1065513/india-tourist-gangraped- and-husband-beaten). News.sky.com. Retrieved 2013-03-16.

26. "Police: Swiss tourist gang-raped in India - CNN.com" (http://edition.cnn.com/2013/03/16/world/asia/indiatourist- gangrape/). Edition.cnn.com. Retrieved 2013-03-17.

27. "Rape and murder in Uttar Pradesh" (http://www.bbc.co.uk/ news/world-south-asia-14058814). BBC. 18 July 2011.

28. Karlsson, B. G. (2011). Unruly Hills: A Political Ecology of India's Northeast. Berghahn. p. 51. ISBN 978- 0857451040.

29. "Hostel Warden arrested for raping 14 Girls in Arunachal Pradesh" (http://news.biharprabha.com/2013/08/hostel-warden-arrested-for-raping-14-girls-in-arunachal-pradesh/). Retrieved, 4 September 2013.

30. a b Geeta Pandey (2013-02-07). "BBC News - India child sex victims 'humiliated' - Human Rights Watch" (http://www.bbc.co.uk/news/world-asia-india-21352102). Bbc.co.uk. Retrieved 2013-03-15.

31. Pandey, Geeta (2007-04-09). "South Asia | Abuse of Indian children 'common' " (http://news.bbc.co.uk/2/hi/south_asia/6539027.stm). BBC News. Retrieved 2013-03-15.

32. "BBC News - India protests in Goa after rape of schoolgirl" (http://www.bbc.co.uk/news/world-asia-india- 21022478). Bbc.co.uk. 2013-01-15. Retrieved 2013-03-15.

33. "Goa rape case: Headmistress knows who the school girl's rapist is? - India - DNA" (http://www.dnaindia.com/india/report_goa-rape-case-headmistress-knows-who-raped-the-school-girl-saysbjp-legislator_1791439). Dnaindia.com. 2013-01-22. Retrieved 2013-03-15.

34. a b Alyson Warhurst; Cressie Strachan, Zahed Yousuf, Siobhan Tuohy-Smith (August 2011). "Trafficking A global phenomenon with an exploration of India through maps" (http://maplecroft.com/about/news/trafficking_report.html) (PDF). Maplecroft. p. 51. Retrieved December 25, 2012.

35. http://world.time.com/2012/08/31/gujarat-riots-new-court-verdict-raises-the-heat-on-narendra-modi/

36. "Criminal Law (Amendment) Act, 2013" (http://mha.nic.in/pdfs/ TheCrimnalLaw030413.pdf). Government of India. Retrieved 16 April 2013.

37. a b c Section 376A, Criminal Law (Amendment) Act, 2013

38. a b "Marital rape not criminal offence: MPs committee backs govt" (http://www.ndtv.com/article/india/marital-rape-not-criminal-offence-mps-committee-backs-govt-337053). NDTV.com. 2013-03-01. Retrieved 2013-04-16.

39. Peter Foster (2006-10-27). "India outlaws wife-beating and marital rape" (http://www.telegraph.co.uk/news/worldnews/1532567/India-

outlaws-wife-beating-and-marital-rape.html). The Telegraph. Retrieved 2012-12-28.

40. "Men falsely accused of rape should be rehabilitated" (http://www.indianexpress.com/news/-men-falselyaccused- of-rape-should-be-rehabilitated-/1100590/#sthash.XS37YArh.dpufIn) The Indian Express. Retrieved 29 May 2013.
41. "Women sometime file rape cases as weapon for vengeance: HC" (http://newindianexpress.com/nation/Women-sometime-file-rape-cases-as-weapon-for-vengeance- HC/2013/05/25/article1605616.ece) The New Indian Express. Retrieved 29 May 2013.

INTERNATIONAL JOURNAL OF MULTIDISCIPLINARY EDUCATIONAL RESEARCH
ISSN : 2277-7881; IMPACT FACTOR - 2.972; IC VALUE:5.16
VOLUME 3, ISSUE 10(4), OCTOBER 2014

A STUDY OF RELATIONSHIP BETWEEN TEACHER PROFESSIONAL PLEASURE AND TEACHER STRESS AMONG THE ENGINEERING COLLEGE LECTURERS IN NORTH COASTAL DISTRICTS OF ANDHRA PRADESH

Dr.N.V.S.Suryanarayana
Head
Department of Education
Andhra Universality Campus
Vizianagaram

Goteti Himabindu
Consultant Psychologist
Abhaya Mind and Personality
Counselling Center
Vizianagaram

Dr.K.Victor Babu
Guest Faculty
Department of Philosophy
Andhra University , Visakhapatnam

Teachers in the idea of Kellen - Teachers are custodians of the nation's human capital the guardians of nation's youth helpers of nation's most precious treasure and the shapers of nation's future. How a teacher teaches in the classroom matters as much as or even more than 'what' a Teachers. The Teacher will be effective if he lives teaching, shows affection towards children and respects his profession. Thus the key stone in the education edifice is doubtless, the teacher. The teacher qualities like sincerity and sobriety have great impact on behavior of students. The Education in India in the 21st Century is moving with advanced steps towards maintaining high standards right from Primary to Higher Education. Owing to day-to-day changing trend and competition in the world Technology Education, it is inevitable to provide more opportunities to the future generation with high standards at all levels of Education. This is the right time to focus the significance of Teacher Professional Competency in relation to Teacher Stress among the Faculty Members of Engineering and Technology Institutions.

It is evident that the effective and efficient functioning of any institute primarily depends on the quality and commitment of its human resources. The right attitude towards the profession, involvement in teaching, concern over the profession, aptitude towards teaching, zeal and enthusiasm in his profession, mental health of the teacher are essential requisite conditions to prevail in a teacher who could definitely bring success in his Institutional programme. Since the early eighties, due to rapid industrialization and economic growth, engineering and technical education in India have been

developing faster than anywhere else in the world, and India now has the second largest number of engineering students in the world. India also has the second largest population, with more than nine hundred and forty million people, fourteen officially recognized regional languages, twenty five states and seven union territories. English is taught at every school and is the only medium of instruction at all engineering institutions. In a recent assessment by the United Nations, the Indian economy was rated as the sixth largest in the world and is expected to move into the fourth place by the end of this century. India, the largest democracy in the world, is very much proud of her rich traditional cultural heritage and technically skilled manpower. Recent Indian scientific, industrial and technological development, particularly in space, nuclear and missile technology, computer engineering and information science has earned India world recognition as an emerging global power.

Growing concern about Teachers:

Recently, however, teachers and their problems have been attracting a great deal of attention throughout the world, especially in Western countries like U.S.A., Teacher Pleasure aspects and Stress have become topics of increasing public and professional concern. In addition to number of articles that have been appearing in professional journals, some have dedicated entire special issues on the topics – Teacher Professional Pleasure and Teacher Stress.

Need for the present Study:

Under these circumstances, the investigator felt that a systematic study of Teacher Professional Pleasure in relation to Teacher Stress among the Teachers of Colleges of Engineering and Technology in the Indian context is very much needed. Identification of major sources of Professional Pleasure, the extent of the Stress experienced by teachers, to what extent Professional Pleasure and Stress have 'a say' on the teacher performance should be made. It is also necessary to identify the rewarding factors in the professional life of teachers, which make teaching more effective.

An inquiry into the above problems will provide us with information which may be highly valuable for counselors, administrators and above all for teachers themselves to plan coping strategies for preventing Professional Pleasure, less Stress and make teachers more and more effective.

A deep understanding of the present situation has prompted the investigator to take up a humble piece of research to probe into the allied aspects of Teacher Professional Pleasure and Stress.

Statement of the Problem:

Taking the unexplored aspects of Teacher Professional Pleasure into consideration and with the presumption that there exists a relation to Teacher Stress, the investigator was encouraged to undertake the study of the following problem.

'**A Study of relationship between Teacher Professional Pleasure and among the Engineering College Lecturers'.**

Scope of the Study:

No doubt, much research has been done on the teacher Professional Pleasure and Stress, but very little is achieved. As pointed by Barr, evaluation of teachers was, is and always will be carried on. The research for identifying an effective teacher with his personal characteristics and the situations in which he is more effective is continuous.

The present study is designed to investigate into various components of Teachers' Professional Pleasure and Stress, which influencing the effect of probable intervening variables such as Sex, qualification, designation, Age, experience, Marital Status and Teaching discipline etc., on it.

Professional Pleasure among Teachers:

Professional pleasure gives happiness success and efficiency in one's Professional activity. It indicates individual's ability to strike a balance between the requirements of the job and his own potentialities. Deprofessionalization takes place when there is erosion of the characteristics of the profession.

Scheneider and Synder (1975) explained job satisfaction as 'it is most adequately conceptualized as a personalitistic evaluation of conditions existing on the job (work supervision) or outcomes that arise as a result of having a job security. Job Satisfaction consists of filtered and processed perceptions. Perceptions filtered through the individual's system forms, values expectations and so forth'.

There are many controversies about the very meaning of professional pleasure. As Evans (1969) and Schewab and Comings (1970) have correctly pointed out, there is a serious lack of good theory of job satisfaction and the tendency among the investigators has been to construct job satisfaction measures without careful attention to what theory of satisfaction might implied by their measures.

Through the thirties and forties many studies were carried out to determine the correlates of high and low job satisfaction. Such studies related job satisfaction to seniority. Age, sex education occupation and income are to mention a few from among the personal and demographic variable of the individual. Lawlar (1967) argued that it was important to consider which people and what kinds of needs were satisfied in the organizations, rather than how to maximize satisfaction. For this one should concentrate on the personal characteristics of employees. The situational factors like the type of school and the conditions of school are also important factors on which the level of job satisfaction and teaching success evidently depend. Relationship among personality measures and job satisfaction has shown no trends of sufficient generally to be summarized (Woman, 1977). But many of the studies conducted to find out the relationship between professional pleasure and personality measures indicate a possibility of predicting professional pleasure to some extent. Predictions of turnover, absenteeism are significantly related to measures of job satisfaction. The most dissatisfied workers are the most likely to have such resultant factors with them. Butter (1961) found that satisfaction was related to tenure. A satisfied teacher tended to stay in teaching and dissatisfied teaches tend to leave the job. Thus on one hand the professional pleasure influences the productivity a task performance measures and on the other hand it is influenced by job factors, personal demographic variables and personality characteristics of workers.

TEACHER STRESS:

Hans Selye feels that complete freedom from stress is 'death'. Stress appears to be as common as 'Sweat' to anybody now-a-days. It appears at every level, and in every profession. 'Teaching' is no exception. In fact, it is strongly felt that teachers are more prone to stress because dealing with children all day is in itself a stressful occupation.

School is considered to be a major source of stress in the lives of both students and teachers. The potential of stress is present in a bureaucratic

setup, intense interpersonal relationships, time-space restrictions and constant evaluation of effort.

Kyriacou and Sutcliffe (1977, 1978) have defined teachers stress as a response syndrome of negative effects (such as anger, anxiety or depression) arising from aspects of the teacher's job and mediated by the perception that the demands made upon the teacher constitute a threat to his self-esteem or well being and by coping mechanisms activated to reduce the perceived threat. Alecia Youngblood Jackson (2008) studied 'Power and Pleasure in ethnographic home-work: Producing a recognizable ethics'. Through two data stories, the author recounts her own pleasurable acts while carrying out an ethnographic study in her hometown high school. The pleasures of conducting such home-work are analyzed to point out the ethics of constituting the experience of the self in qualitative research. Clare Woolhouse & Matt Cochrane (2009) studied 'Is Subject knowledge to be all and end all? Is the investigating Professional Development for Science Teachers? The authors disclosed that reports on the initial findings of research carried out with a cohort of science teachers engaged in a professional development course at a northwest England university. Balwinder Kaur in the doctoral study listed out the objectives to study relationship among professional, personal organizational characteristics and job satisfaction. The finds of the study were: (1) from among personal variables (age, intelligence, socio-economic status and need satisfaction) – need satisfaction including physical securities, social, ego and total need satisfaction was found to be a correlate of job satisfaction. (2) Professional characteristics (experience, salary and qualification) did not act as a correlate of job satisfaction. (3) Eight of the eleven organizational characteristics appeared as correlates of job satisfaction.

Kulsum, U., in his doctoral study took age, sex, marital status, teaching experience, medium of instructions, job performance, attitude towards teaching, teacher effectiveness, school organizational climate, leadership behaviour, school strength as independent variables and teachers' job satisfaction and their job involvement as dependent variables. Coats and Thoresen (1976) in their review of studies on Teacher anxiety quote the NEA report to show the growing incidence of teacher anxiety. In the 1987 survey of 2,290 teachers 16.2% reported they were working under considerable strain and another 67%, under moderate strain (total 78%). While the incidence of strain, tension and anxiety may be no greater for teachers than for other professional groups, because of its possible negative effects on students, it is

more serious. Kyriacou and Sutcliffe (1978) in a study of 257 in a study of 257 teachers of 16 schools in England noted that 15.6% found being a teacher 'very' stressful while 4.3% found it 'extremely' stressful (total 19.9%). In other study (1979) by the authors 23.5% teachers indicated that it was 'fairly' or 'very' unlikely that they would be school teachers in ten years' time. Gyanani (1998) studied the impact of organizational climate on stress and strain among the teachers working in higher education institutions. Saini and Das (1999) studied the relationship of secondary school female teachers' stress in personal and occupational life. Paratkar (1994) made a psychosocial study of role stress among primary, secondary and university teachers. Bankat and Parveen (1999) compared organizational role stress among bank managers and university teachers. Mishra (1991) studied relationship between organizational climate in school, teacher's stress and burn-out in relation to teacher's personality.

Definitions of the terms used:

In the present study the present investigator is concerned with Teacher Professional Pleasure and Teachers Stress and definitions of these constructs are dealt with.

Teacher:

The term 'Teacher' used in this present study is referring to the Teachers working in Colleges of Engineering and Technology in Vizianagaram District only.

Teacher Professional Pleasure:

Teacher Professional Pleasure in this study has been defined as a satisfactory relationship between the individual teacher and his environment. In this the Personal, Intellectual, Professional and Social aspects are the influencing factors lead to Professional Pleasure with reference to Classroom and School environmental activities and his feelings while in teaching profession.

Teacher Stress:

The definition of Teacher Stress in this study that, Stress can be viewed in a number of different ways and has been described as most imprecise work in the scientific dictionary. But analysis of various definitions reveal that 'Stress is a response syndrome of negative effects (as anger, anxiety or

depression), which threatens self-esteem or well being, operationalize as a response of negative effect resulting from imbalance or discrepancy between the demands made and the ability to cope with them.

Problem:

The problems posed in this study are to establish reliability and validity of Teacher Professional Pleasure and Stress in this study has been defined as a satisfactory relationship between the individual teacher and his environment. In this the Personal, Intellectual, Professional and Social aspects are the influencing factors lead to Professional Pleasure with reference to Classroom and School environmental activities and his feelings while in teaching profession.

(1) Development of suitable tool to measure Teacher Professional Pleasure
(2) Development of suitable tool to measure the Teacher Stress.
(3) Finding out the relationship between Teacher Professional Pleasure and Teacher Stress.

Objectives of the Study:

- To study the significance of relationship between Teacher Professional Pleasure and Teacher Stress.
- To study the significance of relationship between the dimensions of Teacher Professional Pleasure.
- To study the significance of relationship between the dimensions of Teacher Stress.
- To study the comprehensive inter-correlation between the dimensions of Teacher Professional Pleasure and Teacher Stress.
- To Study the significance of difference between different categories of demographic variables in respect of Teacher Professional Pleasure and Teacher Stress.
- To study the significance of difference between high and low Teacher Professional Pleasure in relation to Teacher Stress.
- To study the significance of difference between high and low Teacher Stress in relation to Teacher Professional Pleasure.

Hypotheses:

In the present study the investigator has proposed the following hypotheses for testing the tools with reference to the above objectives.

Major Hypotheses:

1. There is no significant relationship between Teacher Professional Pleasure and Teacher Stress.
2. There is no significant relationship between various dimensions of Teacher Professional Pleasure.
3. There is no significant relationship between various dimensions of Teacher Stress.
4. There is no significant relationship inter and intra relationship between Teacher Professional Pleasure in relation to Teacher Stress.
5. There is no significant difference between Low and High groups of Teacher Professional Pleasure in relation to Teacher Stress and vice-versa.

Subsidiary Hypotheses:

6. There is no significant difference between the Teachers in their Teacher Professional Pleasure taking the Sex into consideration.
7. There is no significant difference between the Teachers in their Teacher Professional Pleasure taking the Qualification into consideration.
8. There is no significant difference between the Teachers in their Teacher Professional Pleasure taking the Designation into consideration.

Procedure:

In order to test the hypotheses the investigator is planned and executed in four phases.

In the first phase developing and standardization of Teacher Professional Pleasure and Teacher Stress self-rating scales.

In the second phase measuring the Teachers' opinionnaire with the help of above two self-rating scales.

In the third phase using appropriate statistical procedure is adopted to find out the significant relationship between Teacher Professional Pleasure and Teacher Stress.

In the fourth phase using appropriate statistical procedures to find out the significant difference between the different demographic variables of teachers in their Teacher Professional Pleasure and Teacher Stress.

Tools Administration:

After developing and standardizing the tools viz., Teacher Professional Pleasure and Teacher Stress of the present study followed the Predictive Validity as suggested by John, W.Best and James V.Khan, the final and fresh

scales are prepared for the final study and to administer with a specific instruction. Each statement in both the tools –

The Teacher Professional Pleasure Measurement Tool (PPMT) is consisting of 35 items with five alternatives viz., Extremely Important (1), Moderately Important (2), Slightly Important, (3) and Not Important (1) provided against each statement.

Whereas, Stress Inventory is consists of 40 items. Four Point Scale viz., Little or no Stress, Mild Stress, Moderate Stress and Great Stress was provided against each statement.

The investigator gave necessary instructions and made an appeal to the respondents to answer for all the items of the above tools administered among the sample of selected Engineering College Teachers in North Coastal Districts of Andhra Pradesh. Each scale is started with personal data sheet. These two scales are administered among 200 Teachers working in different Engineering Colleges situated in North Coastal Districts of Andhra Pradesh.

Collection Data:

For collecting the data the investigator visited each Institution and administered the scales to the selected teachers personally. They are requested to record the details as per the demographic data sheet for both the scales. Teachers are further advised not to leave any item of the tools. Most of the teachers filled the tools on the spot and return to the investigator. Thus these two tools collected are scored according to the scoring procedure.

Scoring Procedure:

The responses scored according to the key of each Tool as detailed herewith –

The Teacher Professional Pleasure Measurement Tool (PPMT) total of 35 items is scored ranging from 4 to 1 for the statements viz., Extremely Important (4), Moderately Important (3), Slightly Important (2) and Not Important (1). There are no negative statements. Hence, the total score of the tool will be in between 35 – 140.

While in the case of Teacher Stress Measurement Tool is scored i.e., Little or no Stress, Mild Stress, Moderate Stress and Great Stress for all 40 items weightage given from 4 to 1 in respect of positive items and the scores

given 1 to 4 is awarded for negative items. Thus the total score of this tool will be in between 40 to 160.

Sample:

The present study is confined to 20 Engineering Colleges in North Coastal Districts of Adhra Pradesh. Random sampling technique is followed to draw the sample for the present study. In the study the variables like – Sex (Male and Female), Qualification (Post-graduates and Post-graduates with M.Phil/Ph.D.), Designation (Professors, Readers and Lecturers), Age (below 40 years and above 40 years), Experience (below 5 years and above 5 years), Marital Status (Married and Unmarried), and Teaching Discipline (Mechanical, Electronic Communication, Electrical, Civil, Computer Science, Information Technology, Metallurgy and Aeronautical Engineering courses) are taken into consideration.

Limitations of the Study:

This study is confined to the Teachers working in Colleges of Engineering in the North Coastal Districts only. The Research tool Professional Pleasure Measurement Tool (PPMT) of Dr.U.Nageswara Rao (1998) is consisting of 35 items with four areas viz., Personal, Professional, Academic and Co-curricular aspects. The Research tools – Teacher Stress (Dr.B.Indira, 1996) tool consists of 40 items covering with four areas viz., Intensity of work, Students Behaviour, Professional Growth and Extrinsic Annoyers are taken into consideration. The independent variables like Sex (Male and Female), Qualification (Post-graduate and Post-graduate with M.Phil), Designation (Professor, Readers and Lecturers), Age (below and above 40 years), Experience (below and above 05 years), Marital Status (Married and Unmarried) and Teaching Discipline (Mechanical, Electronic Communication, Electrical, Civil, Computer Sciences, Information Technology, Metallurgy and Aeronautical) are taken into consideration. After distribution and collection of tools from the respondents, the data analyzed with reference to the opinionnaire of the respondents and keeping the results of the study the following conclusions are arrived at.

Table showing the Comprehensive Inter-correlation Matrix for all Dimensions of Teacher Professional Pleasure and Teacher Stress

Professional Pleasure (1-5) Stress (6-10)

	1	2	3	4	5	6	7	8	9	10
1	1.00	0.48	0.54	0.59	0.53	0.27	0.19	0.25	0.11	0.23
2		1.00	0.61	0.63	0.56	0.24	0.26	0.21	0.22	0.18
3			1.00	0.51	0.62	0.25	0.28	0.20	0.19	0.27
4				1.00	0.64	0.19	0.17	0.21	0.16	0.14
5					1.00	0.22	0.18	0.23	0.28	0.17
6						1.00	0.54	0.47	0.52	0.61
7							1.00	0.53	0.64	0.49
8								1.00	0.51	0.62

Professional Pleasure

1.Personal
2.Professional
3.Academic – and
4.Co-curricular
5.Total of Professional Pleasure

Teacher Stress

6.Intensity of Work
7.Students' Behaviour
8.Professional growth
9.Extrinsic Annoyers - and
10.Total of Stress

Besides testing the other hypothesis, the investigator has also conducted the study of Comprehensive Inter-correlation Matrix for all the Dimensions of Teacher Professional Pleasure and Teacher Stress as mentioned in the above table. The above table is clearly disclosed that positive and significant relationship is found between all the dimensions of Teacher Professional Pleasure and Teacher Stress. The coefficients of correlation between all the values of 'r' are in accordance with the principles stipulated by Garrette, H.E. (1981). Hence, the null hypothesis is rejected.

CONCLUSIONS:

There is positive and significant relationship between Teacher Professional Pleasure and Teacher Stress.

There is positive and significant relationship between the dimensions of Teacher Professional Pleasure.

There is positive and significant relationship between the dimensions of Teacher Stress.

There is positive and significant inters and intra relationship between the dimensions of Teacher Professional Pleasure and Teacher Stress.

Teacher Professional Pleasure:

There is significant difference between the Teachers taking the sex into consideration. Female Teachers possessed higher mean than Male Teachers.

There is significant difference between the Teachers taking the qualification. Post-graduate with M.Phil/Ph.D., Teachers possessed higher mean than their counterparts i.e., Post-graduate Teachers.

There is no significant difference between Professors and Readers.

There is no significant difference between Professor and Lecturers.

There is no significant difference between Readers and Lecturers.

There is significant difference between the Teachers taking the age into consideration. The mean value obtained by above 40 years age is greater than the mean value obtained below 40 years age.

There is significant difference between the Teachers taking the experience into consideration. The mean value obtained below 5 years experience teachers possessed higher mean value than above 5 years experience teachers.

There is significant difference between the Teachers taking the marital status into consideration. The mean value obtained unmarried teachers is greater than the mean value obtained by their counterparts i.e., married Teachers.

Regarding the verification of the results taking teaching discipline into consideration are as follows.

Teaching Mechanical and Teaching Electronic Communication do not differ significantly.

Teaching Mechanical and Teaching Electrical do not differ significantly.

Teaching Mechanical and Teaching Civil do not differ significantly.

Teaching Mechanical and Teaching Computer Science do not differ significantly.

Teaching Mechanical and Teaching Information Technology do not differ significantly.

Teaching Mechanical and Teaching Metallurgy do not differ significantly.

Teaching Mechanical and Teaching Aeronautical science do not differ significantly.

Teaching Electronic Communication and Teaching Electrical do not differ significantly.

Teaching Electronic Communication and Teaching Civil do not differ significantly.

Teaching Electronic Communication and Teaching Computer Science do not differ significantly.

Teacher Stress:

Male and Female Teachers do differ significantly. Female Teachers possessed higher mean than Male Teachers.

Post-graduates possessed higher mean score than Post-graduates with M.Phil/Ph.D.

Professors and Readers do not differ significantly.

Professors and Lecturers do differ significantly. The mean value obtained by Lecturers is greater than the mean value obtained by Professors.

Readers and Lecturers do not differ significantly.

There is significant difference between the Teachers keeping the age into consideration. The mean value obtained by above 40 years age teachers is greater than the mean value obtained by the Teachers below 40 years age.

There is significant difference between the Teachers keeping the experience into consideration. The mean value obtained by below 5 years experience is greater than the mean value obtained above 5 years experience.

There is significant difference between the Teachers taking the Marital Status into consideration. The mean value obtained by Married Teachers is greater than Unmarried Teachers.

There is significant difference between low and high of Teacher Stress in relation to Teacher Professional Pleasure. The mean value obtained by High Teacher Stress is greater than the mean value obtained by low Teacher Stress.

Study Implications:

This study disclosed that the dimensions of Teacher Professional Pleasure are significantly related. While in the case of all the dimensions of Teacher Stress are related positively significant. The significance of difference is found between the Teachers in their Teacher Pleasure in respect of the variables – Sex (Female Teachers > Male Teachers), Age (above 40 years age > below 40 years age), Experience (below 5 years experience > above 5 years experience), Marital Status (Unmarried > Married) Teaching Discipline (Teaching Electronic Communication > Teaching Information Technology).

Whereas, significance of difference is found between the Teachers in their Teacher Stress in respect of the variables – Sex (Female > Male), Qualification (Post-graduates > Post-graduates with M.Phil/Ph.D.), Designation (Lecturers > Professors), Age (Above 40 years age > below 40 years age), Experience (Below 5 years experience > above 5 years experience), Marital Status (Married > Unmarried), Teaching Discipline (Teaching Information Technology > Teaching Civil and Teaching Aeronautical Science > Teaching Civil) . Though the Teacher Professional Pleasure and Teacher Stress aspects are independent but they are inter-dependent. These two aspects are played pivotal role in enhancing the quality in teaching. It is interesting to note that Teacher Professional Pleasure is better in respect of teachers considered under Sex category though the Teacher Stress aspect is influencing them. Teacher Professional Pleasure is better among the Teachers of different qualification even the Teacher Stress is influencing them. It is interesting to note that the Teacher Professional Pleasure among the Teachers of different age groups is better even though the Teacher Stress is influencing them. In similar way various experience category of teachers possessed Teacher Professional Pleasure is better though there is Teacher Stress is influencing among them. It is very interesting to note that the Teacher is more in Unmarried Teachers but they do not have Teacher Stress significantly and it is reverse situation in respect of Married Teachers. The differentiation between the Teachers with reference to demographic and professional variables of the teachers as mentioned there above is the preliminary facet of the teachers within a limited area. Since, it is a well known fact that the

teacher is the kingpin in any educational organization. Hence, the broad study on the above aspects might be discovering many problems. Taking the above results into consideration, the Educational Planners and Administrators are need to inquire into the problems taking the above aspects into consideration so as to overcome the difficulties or grievances of the Teachers to perform better and to enhance their quality in teaching learning process.

Suggestions for Further Research:

A Study of Teacher Professional Pleasure in relation to Teaching Competency may be attempted.

A study of Teacher Professional Pleasure in relation to Teacher Effectiveness may be conducted.

An investigation into Teacher Professional Pleasure in relation to Teacher Work Orientation may be conducted.

References :

1. Adaval, S.B.(Ed.), 'Teacher Education in the 3rd Year Book of Education', Educational Research, NCERT, 1968.
2. Balachandran, E.S., 'Teaching Effectiveness and Student Evolution of Teaching', Ph.D., Edu., Madras Univ., 1981.
3. Buch, M.B., (Ed.) Fourth Survey of Research in Education, NCERT, New Delhi, 1993
4. Charies L. Richman; Scott Bovelsky; Natalie Kroovand; Jamie Facca and Tara West of Wake Forest University, USA, 'Racism 102: The Classroom', Journal of Black Psychology, Vol.23, No. 4, Pp.378-387, 1997, DOI:10.1177/00957984970234005
5. Clare Wool-house and Matt Cochrane Edge Hill University, UK, 'Is Subject Knowledge the be all and end all? Investigating Professional Development for Science Teachers', Journal of Improving Schools, Vol.12, No.2, Pp.160-173, 2009, DOI:10.1177/1365480209106431
6. Farber, B.A., 'Stress and Burnout, implications for Teacher Motivation', Paper presented at the Annual Meeting of the AERA, New York, March, 1982.
7. Garrett, H.E., 'A Work Orientation Scale for the California Psychological Inventory', Journal of Applid Psychology, 1985, 70, 505 - 541.

8. Jenkins, C.D., 'Psychological modifiers of responses to Stress', Journal of Human Stress, Dec., 1979, 3.15.
9. Kyriacou, C. & Sutcliffe, J. 'Coping Action and Occupational Stress among School Teachers', Research in Education, 1981, 24, 57 – 61.
10. Levi, L (Ed), 'Stres and Distress in response to Psycho-social stimuli', Oxford, Pergmon Press, 1972.
11. Nageswararao, U. 'A Study of Meaning and Burnout and their impact on Stress among Lecturers of Vizianagaram District', Ph.D., Edu., Andhra Univ.
12. Neff, W.S., 'Work and Human Behaviour', New York, Atberton Press, 1968.
13. Sayles, L.K., 'Behaviour of Industrial Work Groups', New York, Wiley, 1958.
14. Vassilis Tsafos, University of Athens, Greece, 'Developing a practice-theory model in pre-service teacher education in Greece: The implications of action-research: a case study', Journal of Action Research, 2009, DOI:10.1177/1476750309335041

INTERNATIONAL JOURNAL OF MULTIDISCIPLINARY EDUCATIONAL RESEARCH
ISSN : 2277-7881; IMPACT FACTOR - 2.972; IC VALUE:5.16
VOLUME 3, ISSUE 10(4), OCTOBER 2014

AMBEDKAR'S PERSPECTIVE ON DEMOCRACY AND CHALLENGES TO ITS TODAY

Rohit Gangoli
P.hD Research Scholar
Panjab University,Chandigarh

Dr B R Ambedkar was a staunch protagonist of democracy and human rights. He was a far sighted person, so he could clearly envision the role of democracy for equality in society. The term democracy is derived from the Greek words 'Demos' and 'Kartos', the former meaning the people and the later power.[1] He was not content with the definition of democracy given by many thinkers. In particular he recalls Walter Bagehot when he defines democracy as a 'Government by discussion' as well as propounded by Abraham Lincoln as 'a Government of the people, by the people and for the people.' Deviating from these oft-repeated notions,[2] however, Ambedkar defines democracy as "a form and method of government, whereby, revolutionary changes in the economic and social life of the people are brought about without bloodshed"[3] In his view, democracy should be propagated by government to bring revolutionary changes in social, political and economical development of a state. He was against the bloodshed and violence for running government unlike Marx. Dr. Ambedkar further defined Democracy as, "democracy is a mode of associated living. The roots of Democracy are to be searched in social relationship, in terms of associated life between the people who form the society.[4] According to Ambedkar, Chaturvarnaya, Vedas and Upnishadas have misled people. These are the real causes of inequality in society. These have created a deep gulf among people in society. People from Ati shudra society were treated inhumanely. Shudras were not allowed to use the basic amenities in the village. They were kept aloof from the rest of society. It was believed that there was no healthy relationship among Indians in society in ancient times. Dr. Ambedkar states that, political democracy rests on four premises. They are:

1) The individual is an end in himself.
2) The individual has certain inalienable rights which must be guaranteed to him
3) by the Constitution.

4) The individual shall not be required to relinquish any of his constitutional rights as a price of any privilege.
5) The state shall not delegate power to private persons to govern others.[5]

Dr Ambedkar was a true democrat. He advocated the idea of liberty, equality and justice for all. Dr. Ambedkar's emphasis on morality was well integrated with his commitment to rationality and the scientific spirit. In particular, he considered that morality was always subject to rational scrutiny. Further, his notion of morality was quite close to what might be called "social rationality".[6] Dr Ambedkar believed that the changes in social and political life can be brought through democratic revolutions without bloodshed. The democracy has certain conditions:

1. **Public Conscience**-According to Dr. Ambedkar Public Conscience means, "Conscience which becomes agitated at every wrong, no matter who is the sufferer; and it means that everybody whether he suffers that particular wrong or not is prepared to join him in order to get him relieved." Dr Ambedkar considered public conscience essential for the successful functioning of democracy.

2. **No monopoly of Majority**-Dr. Ambedkar said, "The minority must always feel safe that although the majority is carrying on the Government, the minority is not being hurt."[7] The situation of violence among minority and majority creates the undemocratic environment in the society. If there will be supremacy of one group, it will definitely dominate other groups too. The government should always give equal space to every group in society.

3. **Moral Order**-He gave an idea of propagating morality in politics. According to him, politics is a kind of sewage system. So, we should try to clean this dirty system of our politics. India sincerely requires the leaders with moral ethics as were present during independence days.

4. **Constitutional Morality**-Dr. Babasaheb Ambedkar said that, "A Constitution which contains legal provisions, is only skeleton. The flesh of the skeleton is to be found in what we call constitutional morality."[8] According to Dr. Ambedkar Constitution is important for success of democracy but more important was constitutional morality in polity and society.

5. **Equality**-Indian society is divided into oppressed and suppressed class. Entire Indian society is affected from the evils of caste system. India is suffering from the problem of inequality. Our holy books like Vedas, Upnishads and Shastras are misleading the society according to Ambedkar. He said that our holy books have created the differences of thoughts among people. "Caste has killed public spirit. Caste has destroyed the sense of public charity. Caste has made public opinion impossible. A Hindu's public in his caste. His responsibility is only t o his caste. His loyalty is restricted only to his caste. Virtue has become caste-ridden and morality has become caste bound. There is no sympathy to the deserving. There is no charity to the needy.[9] Dr. Ambedkar said that caste was the root of undemocratic system and it was hurdle in success of Democracy. His idea of Democracy was based on principle of equality. According to him, "where equality is denied everything else may be taken to be denied".[10]

6. **Two Party System**-There should be a scope of strong opposition. In democracy, the Veto power lies in the hand of public but in dictatorship, it lies in the hands of one man only. There should always be a strong opposition in front of a ruling government. To avoid dictatorship and fascist tendency it is necessary in democracy to have two political party systems, one for ruling and other for opposition, to have counter check on ruling party.

7. **Equality in administration and law**- Equality before law is must but along with good administration. The administration must be well responsive, responsible and impartial; and it must be well determined. It should command obedience to authority, "We must have a Government," he said," in which the men in power will give their undivided allegiance to the best interest of the country. We must have a Government in which men in power, knowing where obedience will end and resistance will begin, will not be afraid to amend the social and economic code of life which the dictates of justice and expediency so urgently call for."[11]

Ambedkar says: "The conception of a secular state is derived from the liberal democratic tradition of the West. No institution which is maintained wholly out of state funds shall be used for the purpose of religious instruction irrespective of the question whether the religious instruction is given by the state or by any other body."[12] Ambedkar was the admirer of freedom and self-

government in India. Everyone should share the responsibility of governance which would nurture the behavior of public welfare and cooperation among all the citizens of society. While addressing the constituent assembly on November 25, 1949, he issued three warnings to democracy. The first warning is not to use any method of revolution including Satyagraha. He said these methods were used during British Raj. Now, our country has got its own Constitution. These methods have no relevance these days." India has witnessed sporadic armed rebellions throughout its history. It started with the peasant revolt in Telangana, and even today, 67 years after independence, we are still dealing with armed uprisings in some areas, mostly concentrated in the Naxal belt and parts of Kashmir and the Northeast. Though these activities haven't had a drastic effect on the overall democratic processes, they have certainly had a noteworthy localised impact."[13]The second warning was to get rid of Hero-worship. This can eventually lead to dictatorship and it is a blot on democratic institutions. The Emergency imposed in India in 1975 had already showed the consequences. It lasted for 21 months, Then Indira Gandhi realized her mistake after the results of election. "There is nothing wrong in being grateful to great men who have rendered life-long services to the country. But there are limits to gratefulness. As has been well said by the Irish Patriot Daniel O'Connel, no man can be grateful at the cost of his honour, no woman can be grateful at the cost of her chastity and no nation can be grateful at the cost of its liberty. This caution is far more necessary in the case of India than in the case of any other country. For in India, Bhakti or what may be called the path of devotion or hero-worship, plays a part in its politics unequalled in magnitude by the part it plays in the politics of any other country in the world. Bhakti in religion may be a road to the salvation of the soul. But in politics, Bhakti or hero-worship is a sure road to degradation and to eventual dictatorship."[14] The third warning is that the political democracy should not only be a prime motive of a country, it should also strive for social and economical democracy. The denial of a qualitative social and economical life will pose a serious threat to the political democracy one day. Dr Ambedkar suggest following reforms to make Hindu religion dynamic:

1) There should be one and only one standard book of Hindu religion, acceptable to all Hindus and recognized by all Hindus. All other religion books such as the Vedas, Shastras and Puranas should not be treated as sacred and authoritative and the preaching of any doctrine, religion or social, contained in these books should be penalized.

2) Preisthood must cease to be hereditary and there must be an examination to get entitled to be a preist and the person who wants to be a priest must hold a Sanad.
3) No ceremony performed by a priest who does not hold a Sanad shall be deemed to be valid in law and it should be made panel for a person who had no Sanad to officiate as a priest.
4) A priest should be a servant of the State and should be subject to disciplinary action by the State in matters of his morals, beliefs and worship.
5) The number of priests should be limited by law according to the requirements of the State-the priestly class must be brought under control by legislation. It will prevent it from doing mischief and from misguiding people. It will democratize it by throwing it open to everyone. It will certainly help to kill Brahmanism and will also help to kill caste, which is nothing but Brahmanism incarnate. Brahmanism is the poison which has spoiled Hinduism. You will succeed in saving Hinduism if you will kill Brahmanism." [15] By 'democracy' Ambedkar refers to fundamental changes in the social and economic life of the people and the acceptance of those changes by the people without resorting to disputes and bloodshed."[16] He wanted to cultivate one man, one vote, and one vote, one value in social, economical and political life. The social and economical inequalities are corroding the national integrity of India according to Dr Ambedkar. He said, "We must make our political democracy a social democracy as well. Political democracy cannot last unless there lies at the base of its social democracy."[17] There should not be any kind of tyranny over minority in the name of majority. Minority should always feel safe and secure whether majority is the part of Government.

Dr Ambedkar advocated the parliamentary form of government. He reiterated the need of parliamentary democracy. In this favour he said that political parties are necessary of this form of government. According to him, opposition is necessary for effective working of democracy. In this structure the ruling government is constantly under watch and observation by opposition. The official power to opposition confronts the absolute power of executives. He also emphasized the need of permanent civil services administrator which means there should not be under any political party. They should be free from any influence. A country may have Constitution with rules. When people in the country develop conventions and traditions

consistent with the constitution then only these rules become meaningful. Dr Ambedkar said majority may rule country but minority should feel safe and secure in their hand. This type of government can be considered as democratic. According to Ambedkar Neo-liberal market-economy is primarily based on capital markets, industrial liberalisation, removal of MRTP constraints, opening of yet newer areas hitherto reserved for the public sector, tax concessions, voluntary retirement scheme, hidden closing of non-viable units, delicensing, removal of import quotas, cutting down tariff levels, liberalisation of the inflow of foreign capital, capital goods, imported inputs, , widespread use of contracted/casual labour, sub-contacting work to the small scale sector, taming labour etc.

Social Democracy

This was always a point of discussion in Ambedkar's ideology, whether you take his ideas from Constitution or democracy. Dr Ambedkar in his paper wrote in three different parts. The first part includes his inclination towards social democracy which means liberalization of down-troddens. He always emphasized to alleviate the conditions of needy. He not only spoke for the dalits but also women, children and weaker sections of society. In his second part he openly confronted the casteism and in fact tried to relate neo-liberal market with economy to alleviate poverty. He was of the opinion that with the industrialization and globalization can bring bright future for our society. The third part draws heavily on the implications of the neo-liberal economic reforms for the emancipator project of social democracy in India and the birth of new contradictions that it gave rise to the disadvantage of Dalits. Before we could go ahead with this, we should develop in depth knowledge of economic liberalization." It is repulsion rather than fraternity that underlined the social structure of the Indian society. Repulsion promotes social exclusion. Repulsion is one of the three main agencies (the other two are hierarchy and hereditary occupation) of caste that determine the exclusionary boundaries of Indian social structures (Bougle 1971). In the views of Dr. Ambedkar:

In fact, it makes isolation of one caste from another a virtue. There is isolation in the class system. But it does not make isolation virtue nor does it prohibit social intercourse. The class system, it is true produces groups, but they are not akin to caste groups. The groups in the class system are only non-social while the castes in the caste systems are in their relations definitely and positively anti-social in the democracy."[18] The State shall strive to provide

economic, political, social and overall welfare to the citizens and the Constitution of India has also given the fundamental rights and Directive principles of state policy to feel freedom. The State shall inform all the institutions of the national life, and shall direct its policy towards securing, among other things –

(a) That the citizens, men and women have equal right to an adequate means of livelihood;

(b) That the ownership and control of the material resources of the community are distributed at the best to serve the common good; and

(c) That the operation of the economic system does not result in the concentration of wealth and means of production to the common detriment.

Thus the basic spirit of the constitution as well as the ambitious Five Year Planning projects of the Planning Commission of India underlines an all inclusive vision of development and an egalitarian social order. A number of special provisions are incorporated in the constitution and the Resolution for the creation of the Planning Commission to translate the ideals of the founding fathers. State affirmative action is the most prominent among them. It aimed at overcoming historic caste-based social exclusion and oppression. Along with reservations in education, employment and legislature, the Right to Education Act, mid-day meals programme, Mahatma Gandhi National Rural Employment Guarantee Act, the Food Security Act, the Sarva Shiksha Abhiyan, rural development programme, public distribution system, public health programmes, cooperatives, and the Sampoorna Grameen Rozgar Yojana are a few more significant state initiatives taken over the last many decades since independence to help emerge social democracy in India. Yet another important measure towards the formation of social democracy is the advent of decentralization of power from the grass-roots level (Panchayati raj institutions) which means providing autonomy of power at the basic level. Thus the constitution of India, as aptly argued by Dr. Manmohan Singh, Prime Minister of India, is “a unique social charter – the boldest statement ever of social democracy”. Whether these varied measures have been able to facilitate the growth of social democracy in India or not, is a matter of contention. The incorporation of such measures in the constitution is a vindication enough that the founding fathers of Independent India wanted to deepen the roots of liberal democracy while placing it on firm foundation of social democracy by incorporating such measures in the Constitution is a

vindictive. However, the adoption of the neo-liberal market-economy model by India in 1991 dilutes the social welfare concerns of the Indian state. It is in this context that the institution of social democracy has come under dark clouds of the free market economy model in the country. According to Dr Ambedkar poverty and caste had a symbiotic relation. They pose a serious challenge to social democracy in India and actually they club together. Even after the adoption of economic reform measures in India in 1991 this relationship was very tough to break and in fact had not been snapped yet completely. On the contrary, this relationship is further strengthening the anti-democracy nexus between caste and poverty in the country.

In actual we feel that this globalization may glue this gulf among the castes but this again is widening the gap between the castes. This globalization is only dancing in the hands of upper castes who is exploiting the opportunity in their own favour rather than giving benefits to the lower castes. Until the balance in the management of the economy among the different stratas of people is maintained, all the communities cannot get benefit out of it.. In other words, when the occupations of sewage disposal, scavenging and raw hides were performed in the *Jajmani* (hereditary system of asymmetrical reciprocity and patronage between landlords and occupational experts) set up, bereft of profit incentive, Dalits were forced to take them up. But when these same occupations became profit-generating businesses, Dalits find themselves at odd in their own tested fields. The process of globalization perpetuates the system of caste and inequality in a new form. It further pins them down, instead of liberalizing them. Shudras were cursed and isolated from the society because they use to do work in sewage disposable, now it excludes them by way of defeating them in the profit oriented open market system of the neo-liberal economy. In fact, this market is open only for those who have the capital to play the profit game on the chessboard of its unrestrained competition. In this new profit driven game of the process of globalization, Dalits – normally starved of capital – stand disqualified.

The accentuation of the phenomenon of their exclusion from land is the other way through which the process of globalization severely affects the lives of the Dalits. Significant parts of the vast majority of them who live in villages are landless labourers. Small cultivators have marginal holdings. The large-scale landlessness on the part of the Dalits led to their dependence on the upper caste land owning communities, which in turn deepened the caste based inequalities with the additional burden of asymmetrical class structures. The

neo-liberal economic policies adopted under the regimes of globalization, liberalization and privatization widen already existing caste and class divisions between the Dalits and the dominant castes, and further shortens the chances of the emergence of a sense of solidarity in different communities.

Challenges to Democracy in India

India has the largest democratic electorate in world. The democracy gives the power of governance in the hands of common public. We have got certain rights to live and grow freely in our country. Government is trying hard to achieve the motives of Democracy in India but there are a number of challenges to be achieved yet which are explained below:

1) Poverty-poverty is the biggest challenge among Indians today. A large proportion of people are living below BPL. Below this line people are living without the basic amenities like food, clothes and shelter etc. Government has started number of plans like Nirmal bharat Abhiyan, Annapurana Yojana, MNREGA, Jeevan Raksha. These are the plans initiated by the government to improve the standard of living among poor. By an estimate, around 21.92 % of Indians are extremely poor. In 1978, poverty line was fixed in terms of food requirements. People under BPL are not getting even this much of calories the standard calorie rate for rural area was 2400 and for urban area was 2100 for a normal individual each day. The persisting phenomenon of poverty is attributed to many factors, one of which is mass unemployment and under-employment. A large number of people in rural areas do not have regular and adequate work. In urban areas also the number of educated unemployed is very high. The growing population is regarded as a reason for poverty, though population is considered as the greatest resource in the country. In fact, the process of economic development has not been able to ensure social justice and gap between rich and poor has not been bridged.

2) Gender Discrimination- Our Country is inching towards becoming developed country. Urban areas have still come out this differentiation but rural areas are still fighting with this trauma. The Constitution of India has provided equal rights to all. Fundamental rights, directive Principle and Fundamental duties are given to every citizen of India irrespective of sex, caste, religion, place of birth etc. The 2005 census shows infant mortality figures for females and males are 61 and 56, respectively, out of 1000 live births,[19] with females more likely to be aborted than males due to biased attitudes. Literacy for females stands at 65.46%, compared to 82.14% for

males.[20] Gender discrimination impedes growth; with lower female-to-male workers ratios significantly reducing total output in both agricultural and non-agricultural sector.[21]

3) Illiteracy-Illiteracy is major threat to the successful functioning of democracy. India is largest among all in illiterate ratio. India has the highest population of illiterate adults, 287 million, 37% of the total population of such people across the world, according to UNESCO's Education for All (EFA) Global Monitoring report.[22] Recent right to Education has come to force, which is showing a hope for future. If a child is educated, the future of a country seems secure.

4) Communalism-communalism, casteism, and fundamentalism are the major blow to Indian democracy. What is more alarming is the mixing of caste and politics resulting into 'politicization of caste' and 'casteization of politics' in contemporary Indian polity which has become a greatest challenge to our Democracy. Communal violence held in Meerut in May 2014 was a shame on our democracy that we are not able to eradicate it since 67 years of our independence. As of May 11, 3 people were killed and 50 injured, including a top police officer and two media persons.[23] Honour killing prevalent in Haryana, Punjab are the heart shaking incidents happening blatantly in front of public and police.

5) Corruption-India scored 36 out of 100 in Corruption Perception Index ranks. India has yet to fight strictly against this ailment. Corruption is rampant in all the walks of life. Recently, Whistleblowers Protection Bill 2011 has yet to come into force. This bill would help to navigate the rate of corruption in India. Some of the largest scandals since 2010 have revealed very high level government officials, including Cabinet Ministers and Chief Ministers, such as in the 2G spectrum scam (1760 billion), the 2010 Commonwealth Games scam (700 billion), the Adarsh Housing Society scam, the Coal Mining Scam (1860 billion), the Mining Scandal in Karnataka and the Cash for Vote scam. These shows the level of corruption in India is not under control. Indian media has widely published allegations of corrupt Indian citizens stashing trillions of dollars in Swiss banks. Swiss authorities, however, deny these allegations.[24]

6) Regionalism-Regionalism is the major issue in India. Indians do not take them as Indians instead they take themselves as Punjabi, Marathi, Haryanavi and telugu etc. People from different states do not like to stay together.

Marriages are not allowed in different states even after 67 years of independence. On 20 October 2008, Thackeray was arrested in Ratnagiri after Mumbai police had received a non-bailable warrant issued by a Jamshedpur court against the MNS chief.[25] The terrorism in different parts of India are the results of regional imbalances only. ULFA (United Liberation Front of Assam) in Assam or by different groups in the North-Eastern region or separatist demands in Jammu and Kashmir are matters of grave concern for Indian polity.

7) Political Criminalization-Recently Supreme court has directed the Prime Minister and all the Chief Ministers to check the criminal records before providing tickets to ministers. Criminalization negates the democratic values. According to a survey done more than 20 % of members of parliament (MP's) of current 15th Lok Sabha (2009) have several cases pending against them."In Indian Parliament, 163 members have cases of heinous offences against them " .There are several charges of crime such as murder , attempt to murder , robbery , kidnapping , extortion & land grabbing etc .. its not just violation of IPC section 144 (forming unlawful assembly.[26]

8) **Political violence**-Violence has been with us for long, but use of violence for political end is dangerous for the existence of any system. In India we have been witnessing various forms of violence. Communal violence, caste violence and political violence in general have attained serious proportion. Communal riots are engineered by vested interests for political, religious and economic reasons. Caste violence in various shapes has been increasing. Despite agricultural development, abolition of *zamindari system*, and developments like green revolution and white revolution, there are still powerful feudal elements in the society. A serious conflict of interests has emerged between higher and middle castes and this has led to aggressive competition for political power which many a time leads to violence. Another aspect of caste violence is the backlash of the higher castes against the growing awareness and assertion of their rights by the Dalits and lower castes, particularly the Scheduled Castes and the backward castes. During elections, violence is being adopted either to mobilize voters or to prevent them from exercising their right to vote. Moreover, violence has been associated with demands for separate States, reorganization of States or adjustment of State boundaries. Violence has also been used quite frequently during industrial strikes, farmers' movements, and students' agitations.

Our government is taking every possible step to eliminate these problems from our path of progress. If all these are problem are taken seriously and government takes the cooperation of public, we will be able to achieve the objectives of our democracy very soon. Government of India is on the spree of cleansing all the evils in our democracy. The new government today has come. India has hopes from the new government in the arrival of society which is equality, liberal and just. The democratic form of Government is a boon to Indian citizen. The exploitation and wrong-doing by any Government can lead to its eradication and safeguard to citizens.

Conclusion-India is the largest democracy in the world. Ambedkar gave the teeth to weaker sections of Indian society by the mode of Constitution of India. Indian Constitution is the greatest gift of Ambedkar to all the sections of our society. Our Constitution serves the best purpose of equality, fraternity, justice, liberty and freedom.

References

1. Kshirsagar Ramchandra Kamaji, Political thought of Dr. Babasaheb Ambedkar, Intellectual publishing house, New Delhi, 1992, P-53.
2. Dr. Ambedkar's Thoughts On Democracy And Its Relevance In Existing Indian Scenario,by Ashok Kumar, Indian Streams Research Journal, Volume 2, Issue. 9, Oct 2012, ISSN:-2230-7850
3. Kshirsagar Ramchandra Kamaji, Political thought of Dr. Babasaheb Ambedkar , op. cit, P-53.
4. Jatava D.R. Political philosophy of B.R. Ambedkar, National publishing House, New Delhi, 2001, P-77.
5. Kshirsagar Ramchandra Kamaji, Political thought of Dr. Babasaheb Ambedkar , op. cit, P-55
6. On the latter, see particularly Anatol Rapoport (1960, 1995) and Amartya Sen (1985)
7. Kshirsagar Ramchandra Kamaji, *Political thought of Dr. Babasaheb Ambedkar* , Op. Cit,P-60.
8. ibid, P-59
9. Shashi S.S. (Dr.) (Editor), *Ambedkar and social justice, volume I, Director, Publicationsdivision, Ministry of Information and Broadcasting*, Government of India, New India, 1992, P-162.
10. Moon Vasant (ED), *Dr. Babasaheb Ambedkar writings and speeches, Vol III* , Ambedkar B.R. Philosophy of Hinduism, P-66.

11. Bhagwan Das (ED), *Thus spoke Ambedkar, Bheem Patrika* , Vol I, Jullundhar, 1977, P-22.
12. http://www.mainstreamweekly.net/article467.html
13. http://www.highbeam.com/doc/1P3-3270767211.html
14. http://www.dnaindia.com/analysis/standpoint-br-ambedkar-s-three-warnings-on-democracy-and-where-india-stands-today-1976571
15. Ambedkar B R, Annihilation of caste, P-75
16. Speech delivered by Dr B R Ambedkar before the members of the Poona District Law Library on 22 December 1952; quoted in Dr Ambedkar College, Magazine, Mahad, 1962.
17. Constituent Assembly Debates, (25-11-1949) Vol. XI, P- 972.
18. http://www.ambedkar.org/Babasaheb/Commandments_of_Baba_Saheb.htm.
19. "The India Gender Gap Review" (PDF). Retrieved 2012-09-10.
20. "Literacy in India". Census2011.co.in. Retrieved 2012-09-10.
21. "Gender Discrimination and Growth: Theory and Evidence from India" (PDF). Retrieved 2012-09-10.
22. http://www.livemint.com/Politics/3yYYIDoiLTWDiJAOg5J9SL/India-has-the-highest-population-of-illiterate-adults-Unesc.html?utm_source=copy
23. "50 injured in Meerut riot". *DNA India*. 10 May 2014. Retrieved 11 May 2014.
24. "Banking secrecy spices up Indian elections". SWISSINFO – A member of Swiss Broadcasting Corporation. 14 May 2009.
25. "MNS chief Raj Thackeray arrested". *The Times of India*. 21 October 2008. Retrieved 21 October 2008.
26. http://aqibsamicrimepoliticsandcorruption1.blogspot.in/

INTERNATIONAL JOURNAL OF MULTIDISCIPLINARY EDUCATIONAL RESEARCH
ISSN : 2277-7881; IMPACT FACTOR - 2.972; IC VALUE:5.16
VOLUME 3, ISSUE 10(4), OCTOBER 2014

GATTI COMMUNITY OF TULUNADU: A STUDY

Mr. Naveen
Associate Professor
Department of History
Government First Grade College
Car Street-01, Mangalore, Karnataka, India

The traditional society has been under attack by the march of civilization. Although this is a common trend, its impact has been felt acutely by the Tulu speaking communities of coastal Karnataka. Of late, there has been an increasing awareness and eagerness among these communities to re-assert their identity and to pass on their culture-specific practices to the younger generation.

The traditional cultivation-based castes and community system is dwindling under the influence of modernity. As a sense of anxiety about this is gripping the smaller communities, efforts have been underway to protect and preserve some of the traditional cultural practices. It is in this context that the researchers will have to assume the responsibility of documenting principal features of these communities, some of which are still in vogue while others might have to be gathered from the memory of those who witnessed them in the past. It would also be useful here to resort to an indigenous approach to studying the social context instead of simply copying the western understanding of castes and communities[1]. There are a large number of communities which do not have any documented system of rules and standards but are dependent mainly on the collective understanding of the norms defining their identity. This paper throws light on one such community called Gatti.

Man is a social animal and is used to community life. Human beings right from their birth are influenced by their environment and they build their culture in response to their immediate environment. While studying Tulu Nadu, if we use the conceptual lens of caste, Gattis constitute a caste of cultivators. The studies so far have contextually indentified Gatti community

[1]. Moahankrishna Rai (Tulu Samskruti Chaturmkukhi Adhyayana, Kannada University, Hampi, 1999, pp 6) says oral traditions although appear to be make-believe stories actuall represent real life accounts of communities.

as a community of cultivators[2]. Although cultivation has been a common profession of many caste groups, Gatti community has developed its own identity and culture over a period of time. At the same time it also maintained close ties with other communities of the region, especially in adopting worship of naga (serpent gods), matrilineal system of inheritance, folk traditions and so on[3]. Gatti community is one of the 42 communities which subscribe to the norms laid down by ancient king Bhootala Pandya, who is believed to have been the founder of the matrilineal system of inheritance in the region[4]. Despite this rich history there has not been any academic study on the community. While other important castes in this category such as Koraga, Bakuda, Mukhari, Mogaveera, Billava, Jaina and so forth have been subjects of several historical studies, there has been no significant study on Gatti community[5]. This paper is an attempt to fill this gap and it is based on evidence gathered through an extensive field-work spread over many years.

If we go beyond this limited conception to use the lens of community to understand Gattis, then they can also be understood as migrants from the north, their principal occupation being supplying fragrant material such as sandalwood paste.[6] Some scholars have argued that in this part of the country there were no castes as it is commonly understood in academic literature. Instead, they argue, what is found here are groups of people segregated broadly on the basis of their hereditary professions[7].

Certain caveats are in order while presenting the findings of this study on the Gatti community. There are two kinds of collective memories which constitute the received historical knowledge. The first type of collective memory is essentially inherent and inward looking. The other is some kind of

[2] Edgar Thurston, Castes and Tribes of South India, Volume 5, Madras 1909; fieldwork done for this study shows that Gattis generally consider themselves as cultivators and the word poladava which they use to describe their community alternatively means both forest and cultivator. Gattis have named their caste organization as Gattiyavara yane Poladavara Sangha. This was established in 1942 and similar organizations can be found in Kumble and Madhur.

[3] Polali Sheenappa Hegde, Dakshina Kannadada Praacheena Charitre mattu Bhootalapandyana Aliyakattu,

[4] Ibid

[5] For example in Indira Hegde's Tulunadina Gramadalita mattu Ajalugalu (Ka.Sa.Pa.Bangalore 2004, pp 12) documents the role played various caste groups in the village administration during Tulu Kings does not make any mention of Gatti community.

[6] Kannada Dictionary, Vol 2, Kannada Sahitya Parishat Bangalore (pp 2390-2)

[7] Balagangadhara, Smruti-Vismruti Bharathiya Smskriti, Kannada translation Rajarama Hegde, Akshara Prakashana, Heggodu, 2010. He says ancient travelers to the sub-continent have documented only broad professional groups and not castes as we know it today.

acquired knowledge, gathered from the memories of others. The former comprises sensibilities manifest in the folklore, awareness of the people, their orientations and agonies. Thus, they are part of organic memories of the society. However, when history becomes an academic discipline, the collective memories are dominated by some standard images and concepts, expressed in a scholarly language. Although historians are mainly producers of this historical knowledge, it also becomes a tool in the hands of laymen who selectively use some solidified images found in the formal historical knowledge as they use them with no hesitation to argue their view points[8]. Because of this, those who seek to understand history keenly come across a large number of doubts which prevent them from giving any conclusive judgments. They instead only engage in a dialogue and arrive at conclusions which are only closer to truth. This limitation is very much true in the case of the current study on Gatti community[9]. According to Ajalu system of Tulunadu, all the communities inhabiting a village participate in the activities relating to the worship of their deities[10]. They are guided by the headmen or a group of elders in this and take their assigned role in the administration of the village. However, the available records have no reference to Gatti community having had the administrative role in the villages.

Existing evidence suggest that members of the Gatti community were originally either agriculturists or agricultural labourers inhabiting the south western tip of Dakshina Kannada District and north western tip of Kasaragod District. Some of them have migrated in the recent times to different parts of the country and the world, but their number is miniscule. According to the community tradition, those of them residing up to Manjeshwar (in Kasaragod) are called Magane Gattis and those living to the south of Manjeshwara are called Seeme Gattis. A search on the origin of the word Gatti can take one as back as famous ancient Kannada poet Pampa's work – Vikramarjuna Vijaya.

[8] Surendra Rao B, Itihasa Mattu Samaja, Kannada University, Hampi, 2005 pp 6-7 Mohanakrishna Rai, Tulu Samskruti Chaturmukhi Adhyayana, Kannada University, Prasaranga, Hampi, 1999.

[9] The members of the caste, for example, even now have a practice of collecting sandal paste from the Somanatha temple of Ullal (Lord Somanatha being considered as their patron diety) to solemnize the marriage in the community. This is possibly be to perpetuate their past association with preparing fragrant materials, especially sandal paste.

[10] Pre-colonial period had a system in which various groups in society performed tasks assigned to them with a view to maintain overall cleanliness of the environment but the colonial powers attributed a sense of superior and inferior status to these performances leading to gradation. A secular understanding of the social roles slowly turned non-secular and caste-based then on.

There is a reference to a community called Ghattivala and Ghattivalti. However, it is not clearly established whether the words - Ghattivala and Gattivalti - mentioned in the ancient poet's work really refer to the community now known as Gatti. A probe into the available historical sources reveals a number of references to Gatti community especially to those who are now called Magane Gattis[11].

Much of the history of the community can be built around its association with Somanatheshwara temple in Ullal near Mangalore. The people of the community consider God Somanatheshwara as their patron deity. Members of the community are chosen to perform certain traditional managerial role in this temple over the years and the practice continues even now even though the temple is now under the Karnataka Government's Department of Muzarai and Religious Endowments. The two traditional positions that the members of Gatti community occupy in this temple are called *Nayaga* and *Melanta*. Those chosen for these positions are anointed with elaborate rituals[12].

The origin of these traditional offices held by the members of the Gatti community in Somanatha temple is not known but the earliest reference to it is made to the 16th century. The legend has it that when the Portuguese attacked Ullal in 1556, the Nayaga of the temple who was also in charge of protecting the Ullal port fought with the alien enemy ferociously and laid down his life[13]. The same legend also has it that several able bodied men of the community were part of the army of the famed Ullala queen Abbakka -I. After emerging victorious, Abbakka-I renovated the temple ruined during the battle and placed a stone edict[14] to record the services of the Gatti Nayaga. In another battle held two years later, it is said, a large number of youth from the community fought for queen Abbakka-I and the members of the community were especially adept at attacking the fleets of enemy boats with burning torches[15]. The association of the community with the rule of queen Abbakka-I

[11] Information gathered during the fieldwork.
[12] Achyuta Gatti Kallapu, Handbook of Gatti Community Customs and Traditions, 1997, pp 47-48
[13] Detailed in Jappu Padmanabha Gatti's novel Mayakoda Mandi, Hemavati Prakashana, Neermarga,2009. The novel gives a graphical fictional account of the role played by Gatti soldiers in the war between the Queen of Ullal and the Portuguese invaders.
[14] Information gathered during the fieldwork; Edicts to commemorate heroic exploits during the war are found across Karnataka.
[15] Information collected from the elders of the Gatty community during the fieldwork

is also supported by the fact that a number of Gatti families have been residing in Ombattukere area where the ruins of the Queen Abbakka's palace can be seen[16]. Gatti families of Pilar, Nurgemajal, Gattikudru and Sevantiguttu are especially mentioned in the context of the community's services to the Army of Queen Abbakka and it is these families which hold the hereditary positions in Somanatha temple to this day[17].

The martial tradition of the community is also borne by the fact that a number of Gatti households are located around ruins of another ruling dynasty of the region called Banga Kings of Nandavara. Evidences collected during the fieldwork for this study reveals that each of these households have a history of more than 300 years. There has also been a reference in some historical works to a lady who was holding a supervisory position in the Nandavara Palace[18]. Kuntla near Mudushedde is another place associated with the history of the community. This is a centre of a peculiar practice of conducting the weddings of the dead (Jakini or Preta weddings)[19] A Gatti household here called Nalkumane is the head household for the sept called Kojjaranna. Vajangalaya Bhoota (Bhootas are holy spirits that the Tuluvas) worship which is one of the Bhootas that Gatti community worships is said to have settled here[20]. The community has a stake in the Paryattur temple near Kotekar in the outskirts of Mangalore[21]. The chief patri (impersonator) at the Chamundi Bhootasthana is a member of Gatti community. There is a reference in the ballads (padthana) describing the history of this temple about the association of a female member of the community with Chamundi Bhoota of Paryattur.

The service links of the community with the royalty also extends to the present Kasaragod District of Kerala State also. The key families of the community here are Padumane, Pallatharu, Kallangadi, Madhur, Parakkila, Jodala, Mannippadi and Chowki. Ancestors of these families are said to have worked in the armies of the local Mayippadi and Kumble kings. The members of these families have also been given special responsibilities in the upkeep of

[16] There is a small Island called Gatti kudru on the river Netravati
[17] Information provided by Sharath Gatti, Managing Committee head, Ombattukere Temple near Ullal
[18] Kamalaksha P, Dakshina Kannada Jilleya Harijana mattu Girijanara Samajika Itihasa, Kannada Book Authority, Bangalore 1994, pp 93-94
[19] Information collected during the fieldwork
[20] From the archives of the Department of Muzari and Religious Endowments, Dakshina Kannada
[21] Information collected during the fieldwork

the temples built by these kings. This practice continues to this day in the temples of Kumble and Madhur, two of the famous four temples built by the King of Mayippadi (Adur and Kavu are the two other temples built by the kings)[22] Legend has it that there was a scholar and mystique in the community who was given substantial land grants from the kings and a platform (katte) called Munishwara Katte has been established in Padumane Taravad of the Community near Kumble. His visit to Tumbe near Mangalore has also been documented. Here, he is said to have performed miracles and he was remembered in this region for a long time as *ajjer*, meaning grand old man[23].

British ethnographer Edgar Thurston in his celebrated work Castes and Tribes of South India gives the following brief description about the Gatti community: A small caste of cultivators, found chiefly near Kumbla and Someswara in the Kasaragod tāluk of South Canara. Other names for the caste are Poladava and Holadava, both signifying men of the field. Like the Bants, they follow the aliya santāna law of inheritance (in the female line), have exogamous septs or balis, and, on the day of the final death ceremonies, construct car-like structures, if the deceased was an important personage in the community. The Bants and Gattis interdine, but do not intermarry.

As regards similarities between the Bunts and Gattis there is a lot more contemporary evidence than what Thurston had noted. Just as Bunts, Gattis also worship three category of Bhootas called Arasudaivas, Rajan Daivas and Kutumbadaiva[24]. Both Gattis and Bants have similar practices with regard to the selection of headman and their anointment besides the same being transferred in a matrilineal tradition from generation to generation. The extended family household or taravad is headed by the senior most woman in that lineage among the Gattis. The woman head is called kudaltedarti[25]. On important days of Tulu calendar the members of the matrilineal extended

[22] Information collected during the fieldwork – Gatti community members (specific families) have been given the task of protecting the wealth of four famous temples built by the erstwhile kings of Mayippadi. These temples are Adur, Madur, Kavu and Kanyara or Kumble. They continue to perform related tasks to this day.

[23] Information provided by K K Gatti and Mohini Gatti who is headwoman of Tanjeri Guttu Taravad, Tumbe

[24] Kuntla Taravad has Arasudaiva and worshipped by Kojjaranna sept, Kudelu taravad has vajangalaya worshipped by Kojjarennaya sept, Tanjeruguttu has Arasudaiva-Kanapadittaya, Chowkri, Padumane Taravadu in Kasaragod has Arasudaivas –Aivaru Paramathma, Pilaru has Arasudaiva Mahisandaya and so on.

[25] From the Kerala High Court order on a dispute relating to the property of Varkadi Tamaru Kojjarannaya Taravadu

family (all from the same sept) meet at the head household (taravad) and make offerings to the family gods – Berma, Naga (the serpent god) besides the Bhootas worshipped by the sept members. The offerings are also made to the dead ancestors on such occasions. Although the non-vegetarian food is offered to these gods, separate vegetarian offerings are made to some of these family gods which is a practice similar to the tradition of Jain families of the region. Similarly, along with the bhootas, the Gattis also worship Lord Venkataramana of Tirupati and on the day of making annual offering to Bhootas, the first event as of the occasion is worship of Lord Venkataramana and it is called Hariseve (meaning offering to the Lord Vishnu). Brahmin priests are called to perform this part of the worship.

Till around 1980s, the priestly functions on occasions such as marriage, funeral, celebrations around birth etc in Gatty community were performed by similarly placed other castes such as Madivala, Bhandari, Moily, Achari and so on. The purification of the site for any such ceremony was performed by a madivala and not by a Brahmin. However, of late, there has been a sanskritisation of all these practices and shudra priests have been replaced by Brahmin priests and the community-specific rituals have been replaced by vedic practices.

Another important historical feature of this community is that mass marriages were in vogue till around 1960s[26]. This might have been discontinued subsequently paving the way of individual marriages as the community grew both in numbers and economic terms. Intra-bali marriages are prohibited and the community leader called gurikara plays an important role in the conduct of the marriage ceremony. Non-vegetarian food is not allowed on the day of the marriage but it is used commonly in both pre-marriage and post-marriage ceremonies. Except for marriage ceremonies, Gatti community's practices are comparable with those of the Bunts in all other social ceremonies.

As noted in the account of Edgar Thurston, there are seven septs (baris/balis) with some sub-septs among the Gatti community. These septs are: bangerannaaya (Vashishta gotra); kojjarannaya (Angeerasa Gotra, Swadannaya (Gundodi, Somanettannaya), Kayyarannaya (Aggittodi,

[26] Pata Taravadu in Kasaragod and Sullanjeru Taravadu near Mangalore were centres of mass marriages for a long time – information gathered during the fieldwork.

Karingannaya, Kabberannaya), Perbannaya, Upyanyaya and Karibannaya. The last two septs are on the verge of extinction.

Although, the traditions practices, customs and ritual practices of this community are either disappearing or being altered, the members of the community have been conscious of this loss and are making efforts to preserve them, with some success. Increasing resort to modern occupations, increasing number of inter-caste marriages weakened the traditional practices on the one hand and at the same time they are creating an acute sense of loss resulting in a collective response to re-assert the identity of the community either by reviving the traditions or by developing a sense of community among the members which is a soft deterrent against forgetting the communal ties and inter-caste marriages.

The last caste-based census held in 1881 had documented the name of the community and the number of its members.[27] Although later census stopped caste enumeration, an organization of the Gatty community conducted another census of the community members in 2010. This census has recorded 1200 households of the community members across two districts and in some other major cities of the country.[28] Besides this, the customs and traditional practices of the community are also being documented systematically as part of the efforts of the current generation of the community members to preserve their identity. The census also found that there are about 75 taravad houses (extended family houses). The Karnataka State Government has recognized the Gatty community as socially and educationally backward caste and it has been included in the Category II-A of the Karnataka Backward Classes List.

References:

1. Achyuta Gatti Kallapu, Handbook of Gatti Community Customs and Traditions, 1997.
2. Balagangadhara, Smruti-Vismruti Bharathiya Smskriti, Kannada translation Rajarama Hegde, Akshara Prakashana, Heggodu, 2010.

[27] Herald H Stuart, Madras District Manual vol II, Madras 1885. (Male- 417, Female-446.)
[28] Information collected during the fieldwork :In Seeme 350 Households, Approximate number 3000, Magane 700 Householdes, Approximete number 5500, and in other states total 150 Households, Approximate number 500.

3. Edgar Thurston, Castes and Tribes of South India, Volume 5, Madras 1909.
4. Herald H Stuart, Madras District Manual vol II, Madras 1885.
5. Indira Hegde's Tulunadina Gramadalita mattu Ajalugalu, Ka.Sa.Pa. Bangalore 2004.
6. Jappu Padmanabha Gatti, Mayakoda Mandi, a novel, Hemavati Prakashana, Neermarga,2009.
7. Kamalaksha P, Dakshina Kannada Jilleya Harijana mattu Girijanara Samajika Itihasa, Kannada Book Authority, Bangalore 1994.
8. Kannada Dictionary, Vol 2, Kannada Sahitya Parishat, Bangalore.
9. Moahankrishna Rai (Tulu Samskruti Chaturmkukhi Adhyayana, Kannada University, Hampi, 1999.
10. Polali Sheenappa Hegde, Dakshina Kannadada Praacheena Charitre mattu Bhootalapandyana Aliyakattu. 1937.
11. Surendra Rao B, Itihasa Mattu Samaja, Kannada University, Hampi, 2005.

INTERNATIONAL JOURNAL OF MULTIDISCIPLINARY EDUCATIONAL RESEARCH
ISSN : 2277-7881; IMPACT FACTOR - 2.972; IC VALUE:5.16
VOLUME 3, ISSUE 10(4), OCTOBER 2014

NORMALIZATION OF INDO-PAK RELATIONS AND ITS IMPACT ON REGIONAL SECURITY

Varam.Venkata Narasaiah
Lecturer in Political Science
Silver Jubilee Govt. College(A)
Kurnool, Andhra Pradesh

Introduction

Partition left a legacy of animosity between India and Pakistan that continues to the present day and the division of the sub-continent gave rise to bitter territorial disputes that have persisted for last 63 years. The conflict over control of the territory of Kashmir has been especially intractable, giving rise to Indo-Pak wars. They have waged full-fledged wars with each other thrice during this period (1948, 1965, 1971), thrice they were involved in military stand offs (Brasstacks operation 1987, 1990 & Dec 2001), and twice in limited wars (Saichen 1985 & Kargil 1999). Kashmir issue continues to be the primary source of regional tension and would be the likely cause of any future Indo-Pakistani conflict.

As the fighting continued in this back and forth manner, Indian leaders concluded that the conflict would continue indefinitely unless they could devise a strategy to end Pakistani support for the Kashmir rebels. India referred the Kashmir question to the United Nations Security Coucil on January 1, 1948. On January 1, 1949 the U.N. imposed a ceasefire. At the time of ceasefire, Pakistan was in possession of about one third of the Princely states and India the remaining two-thirds.

In 1957, North – Western Kashmir was fully integrated into Pakistan becoming Azad Kashmir (Pakistan administered Kashmir), while the other portion was acceded to Indian control, and the Jammu & Kashmir (Indian administered Kashmir) was created.

A second Indo-Pakistan war of Kashmir erupted sixteen years later. In Aug-Sep 1965, Pakistan made yet another attempt to grab Kashmir. In the war that ensured, Pakistan was unsuccessful in accomplishing its mission.

Tashkent Agreement – 1966

It was an attempt to solve the Indo-Pakistan problems. The conference Tashkent was called on the initiative of Soviet Premeir Kosygin. He invited Ayub Khan, President of Pakistan, Lal Bahadur Sastri, Prime Minister of

India to meet on the Soviet soil to defuse the tensions. On Sep 20, the UN Security Council passed a unanimous resolution calling for a cease-fire under the Soviet-brokened Tashkent agreement, which officially ended the 1965 war. Both sides agreed in January 1966 to return to the Status Quo and to renounce the use of force in setting future disputes.

The Tashkent agreement could not ease the tension between India and Pakistan and a war involved the two countries in December 1971.

Pakistan, Since independence, was geopolitically divided into two major regions, West Pakistan and East Pakistan. East Pakistan was occupied mostly by Bengali people. In December 1971, following a political crisis in East Pakistan, the situation soon spiralled out of control in East Pakistan and India internvened in favour of the rebelling Bengali populance. The conflict, a brief but bloddy war, resulted in a independance of East Pakistan. In the war, the Pakistani army swiftly fell to India, forcing the independance of East Pakistan, which got seperated and become Bangladesh. The Pakistani military being a thousand miles away from its base and surrounded by enemies was forced to give in.

Simla Agreement – 1972

Since the 1971 war, Pakistan and India have made only slow progress towards the normalisation of relations. In July 3, 1972. Indian Prime Minister Smt. Indira Gandhi and Pakistan President Zulfikar Ali Bhutto met in the Indian hill station of Simla. They signed on the Simla agreement, by which India would return all Pakistani personnel (Over 90,000) and captured territory in the west, and the two countries would " settle their differences by Peaceful means through bilateral negotiations". Diplomatic and trade relations were also re-established in 1976.

India and Pakistan, however, were among a small group of States that insisted on retaining their right to develop nuclear weapons and refused to sign the N.P.T.

Lahore Summit – 1999

It was an attempt in the path of ending an era of conflict and confirmation between India and Pakistan. That was the time when both countries have acquired the so-called "Nuclear deterrent". In response to an invitation by the Prime Minister of Pakistan, Nawaz Shariff, the Prime

Minister of India A.B.Vajpayee visited Pakistan on the inaugural run of the Delhi – Lahore bus service. The Lahore declaration was signed on Feb 22, 1999. Both the Governments recognised nuclear dimension of security environment and committed themselves to universal disarmament and non-proliferation and on the importance of Confidence Building Measures. India and Pakistan agreed to refrain from the risk of accidental and un-authorised use of nuclear weapons.

These efforts have since been stalled by the intrusion of Pakistani forces into Indian Territory near Kargil in Jammu & Kashmir in May 1999. This resulted in intense fighting between Indian and Pakistani forces, known as the Kargil conflict. Backed by the Indian Air Force, the Indian Army successfully regained Kargil. A subsequent military coup in Pakistan that overturned the democratically elected Nawaz Shariff Government in October of the same year also proved a setback to relations.

Agra Summit – 2001

It was an attempt to solve the problems that emerged out of the July 1999 Indo – Pakistan war known as Kargil War. The Prime Minister A.B.Vajpayee took the initiative and invited the Chief Executive of Pakistan, General Parvez Musaraf , to visit India for a dialogue. No declaration, agreement or joint statements was signed because, both the Governments agreed to disagree on Jammu & Kashmir on the core issue.

Water Dispute

The water disputes also became another bone of contention between the two nation right from 1947 onwards. The Partition had left with India only a small strip of land irrigated by the Indus. Since most of the western rivers could not be relied upon, Pakistan wanted to draw water for agricultural development from the eastern rivers like Ravi, Beas and Sutlej. Pakistan is also currently having dialogue with India regarding the Baglihar Dam being built over the River Chenab in Jammu & Kashmir. It would have also been possible for both the nations to develp on adequate and mutually benefiting river system, but for the political reasons that strained their relations. In such an atomosphere of trouble and turbulance nothing could prevent an impending Indo-Pakistan conflict.

Terrorism Activities In Jammu& Kashmir

There have been numerous attempts to improve the relationship – namely, the Simla summitt, the Agra Summitt and the Lahore Summitt. Since, the early 1980's relations between the two nations soured particularly after the Siachen conflict, the intensification of Kashmir insurgency in 1989, Indian and Pakistani nuclear tests in 1998 and the 1999 Kargil War. Certain Confidence Building Measures – such as the 2003 cease fire agreement and the Delhi – Lahore bus service were successful in deescalating tensions.

Nuclear Factors

Although India and Pakistan tested nuclear weapons and become open nuclear powers in 1998, the nuclear era in South Asia began well before that. India first detonated a nuclear device in 1974. This peaceful nuclear explosion had few military implications. Nonetheless, the PNE demonstrated India's potential to develop a nuclear weapons capability in the relatively near future. Together with Pakistani's catastrophic loss of the 1971 Bangladesh war, the Indian test spurred the Pakistanis to energetically peruse their own nuclear weapons program. Both sides continued to develop their capabilities in the years that followed, and by the late 1980's the two countries had managed to acquire a defacto nuclear weapons capacity. From roughly 1990 forward, India and Pakistan didnot actually possess nuclear weapons but could probably have produced them in short order if necessary. As the years progressed, both sides increasingly viewed each other, and were seen by outside powers, as possessing a viable nuclear weapons capability. Thus South Asia's nuclear era dates back not just to the 1998 tests, but to India's and Pakistan's acquisition of an untested and undeclared nuclear capacity at the end of the previous decade.

Developments under UPA Government Since 2004

Violent activities in the region declined in 2004. There are two main reasons for this: warming of relations between New Delhi and Islamabad which consequently lead to a ceasefire between the two contries in 2003 and the fencing of the LOC being carried out by the Indian Army.

In 2006, a "Friends Without Borders" scheme began with the help of two British tourists. The idea was that Indian and Pakistani children would make pen pals and write friendly letters to each other. The idea was so successful in both countries that the organization found it "impossible to keep

up". The world's Largest Love Letter was recently sent from India to Pakistani.

In April 2010 a high profile Pakistani cricketer, Shoaib Malik married the Indian tennis star Sania Mirza. The wedding received much media attention and was said to transfix both India and Pakistan.

China, Russia and American Factors In Indo-Pak Relations

International relations are full of linkages-Relations between two nations are not only influenced by the bilateral issues but also by the relations these two countries have with the countries in their neighbourhood or with the countries across the globe. This is also true of Indo-Pakistan relations. Indo-Pakistan relations are mainly influenced and conditioned by these factors namely American factor, Chinese factor and Russian factor.

American factor

America has all along been good friends of Pakistan. Their relations have blossomed during the cold war era and continued after the cold war. Initially America tried to buildup India as western strategic partner but Indian non alignment policy came in the way. Pakistan was courted by United States and was buildup as a strategic partner because of American strategic interest in the Middle East. Pakistan was buildup also to check Indian ambitions and power by promoting a situation of military and diplomatic parity so that Indian power could be neutralized. In 1971 war America sent its seventh fleet into the Bay of Bengal in support of Pakistan. During the 1980's America gave financial aid and armaments to Pakistan and Pakistan used these weapons to strengthen itself against the Indian military might. The importance of Pakistan as an ally to protect American interest declined ofbe cold war by the end of 1990. Subsequently American notice the importance of India as an ally in south Asian region and start it befriending it. However of late America started cultivating Pakistan as a strategic ally in its war against terrorism in Afghanistan.

Chinese Factor

Immediately after India became an independent country in 1947 and china became people's Republic in 1948, there was an Euphoria of friendship and cooperation between two nations. Subsequently however due to the border dispute these two nations fought a war in 1962 which resulted in the

humiliated defeat of India by China. Since then these two countries were never on friendly terms. Pakistan exploited the situation and started moving closer towards china believing in the maxim "Enemey's enemy is my friend". China has also its own interest in be friending Pakistan because it had to pass through Pak occupied Kashmir to reach its southern provinces. China gave its moral support to Pakistan both in 1965 and 1971 wars. It also has been instrumental to giving aid, military hardware nuclear weapons know how and missile technology to Pakistan. Even to this day china is a trusted friend of Pakistan.

Russian Factor

Russia became a communist country in 1917 and China became a communist country in 1948. Initially there was a good relationship between Soviet Union and China. But subsequently because of the border problems and ideological differences between Soviet Union leadership and China leadership, their relationship got strained. Russia believed that India was a reliable friend in South Asia and started be friending to contain China. As a result in 1971 India and USSR signed the treaty of friendship and cooperation which assured each other that there will be assistance and cooperation for each other if a third party attacked one of them. Subsequently, Russia became the chief arm supplier and financed donor to India. By the end of cold war in 1990's America, Pakistan and China formed an axis against India and Soviet Union.

It is therefore imperative to study how these three factors namely America, china and Russia factors have influenced in the shaping and promoting India-Pakistan relations in the present study.

Conclusion

The issue of Jammu and Kashmir is one of the most important causes of the conflict between India and Pakistan since 1947. It has shaped the domestic politics of both countries and has been an important element in the calculus of foreign policy formulation on both sides. There is wisdom in saying that the resolution of the Jammu and Kashmir issue is a prerequisite to shape a better future for both India and Pakistan. The bottom-up approach is crucial to take the process of resolution forward and this includes the participation of people of the state on either side of the line of control in that process. For this purpose, the two countries have to take steps to usher in a process of genuine democratisation, which includes decentralisation of political and economic

powers on either side of the line of control to empower the people of the state to give them a direct say to shape their own destiny. Along with the improvement in bilateral relations the international environment along with US, Russia and Chinese foreign policies must be conducive to facilitate friendly relations and to provide an amicable and acceptable solution to them persistent problems.

References:

1. M.P.Ajith Kumar; India – Pakistan Relations, Kalpaz Publishers, New Delhi.2006.
2. T.V.Pal ; The Indian Pakistan Conflict, Cambridge University Press, 2006.
3. Bajaj, Premjath; Kashmir in the Crucible, Bombay, 1969.
4. Brinda,S.S; Indo-Pak Relations, New Delhi, 1981.
5. S.Ganguly & S.Paul Kapur; India, Pakistan and The Bomb, Columbia University, 2010.

INTERNATIONAL JOURNAL OF MULTIDISCIPLINARY EDUCATIONAL RESEARCH
ISSN : 2277-7881; IMPACT FACTOR - 2.972; IC VALUE:5.16
VOLUME 3, ISSUE 10(4), OCTOBER 2014

INTERNATIONAL CONVENTION ON CHILD RIGHTS AND INDIA'S LEGAL SYSTEM-- A REVIEW OF JUVENILE JUSTICE

Dr. Nutakki Sateesh

Background:

Human Rights have been of latest origin in the progress of civilizations. The scourge of war and massacre of people during wars, particularly, during Second World War has made the world community to resolve against all forms of violations of human dignity. The emergence of United Nations and the new consciousness of human rights jurisprudence has given fillip to draft various human rights conventions during the last fifty years.

In the growth of human rights, the first stage was the recognition by the international community that all individuals, including children, were the objectives of international law requiring legal protection. The second stage, which is still evolving, is the granting of specific substantive rights to individuals including children. The third stage, which is also still developing, is the acknowledgement that in order to ensure that individuals are able to enjoy the exercise of their fundamental rights they must be acknowledged to possess the necessary procedural capacity to exercise and claim these rights and freedom.[1] In the first phase of human rights era, attention was paid mostly on individual rights. But progressively the world human rights movement demanded for recognition of human rights of various neglected sections of humanity. In the course of time the rights of women and children came to be recognized as human rights, as a sequel to various demands and conferences on rights of children.

[1] Geraldine Van Bueren, the International Law on the Rights of the Child, Netherland: Kluwer Academic Publishers, 1995.

International Recognition of Child Rights

Recognition of Child rights in the international arena was a progressive one. Since the beginning of the twentieth century, the development of international law on the rights of the child has paralleled, in part, the development of the general body of the international human rights law. There are various Human Rights Instruments Specific to the rights of the child.

(a) The Declaration of the Rights of the Child 1924:

Adopted by the fifth Assembly of the League of Nations, this Declaration can be seen as the first international instrument dealing with children's rights. This Declaration is important as it highlights the social and economic entitlements of children and establishes internationally the concept of the rights of the child, thereby laying the foundation for setting future international standards in the field of children's rights.[2]

The Declaration of the Rights of the Child enshrines the principles that children are entitled to 'special protection' and that special protection should be implemented by reference to 'the best interest of the child', which 'shall be the paramount consideration' (principle 2 DRC).

(b) Charter of the United Nations:

The Constitutional document establishing the United Nations is the Charter of the United Nations which came in to force in 1945. It is clearly not a human rights instrument but it does contain provisions relevant to international human rights law. However, there is no express provision relating to children.

(c) Universal Declaration of Human Rights

The Universal Declaration of Human Rights 1948 proclaims a catalogue of human rights which apply to all human beings and therefore implicitly to children [CRC Art.1].It contains only two articles, which expressly

2. This declaration was the first to state the concept of 'best interests of the child' and laid down that in all matters relating to the placement of a child outside the care of the child's own parents, the best interest of the child, particularly his or her need for affection and right to security and continuing care, should be the paramount consideration.

refer to children. Article 25(2) on special care and assistance and Article 26 on education.

(d) International Covenant on Economic, Social, and Cultural Rights

It applies to all 'men and women' and therefore by implication to children[3]. The Covenant specially refers to children in Article 10 and 12. In Article 10, it is laid down that states recognize family as the 'natural and fundamental group unit of society' and therefore accord the widest possible protection and assistance to the family. This Covenant implicitly helped to raise the status of children in the resource allocation of the various countries[4].

(e) International Covenant on Civil and Political Rights (ICCPR)

The International Covenant on Civil and Political Rights complements the Economic, Social, and Cultural Rights Covenant[5]. Article 14(1) provides an express exception to the right to hearing in public, when it is in the interests of the juvenile or where it concerns the guardianship of children. Article 14(3) (f) provides that criminal proceedings should take account of juveniles' age and their 'desirability of promoting their rehabilitation'. The Covenant prohibits the imposition of death penalty for crimes committed by persons under eighteen years of age[6].

(f) Regional Instruments for the protection of Children

3. This is another way of classifying the rights under the Convention on the Rights of Child.
4. See Kabuta, 'Protection of Children's Rights', International Review of Criminal Policy, United Nations, Vol. 39-40, 1989,
No.108.
5. Geraldine van Buueren, the International Law on the Rights of the Child, Martinus Nijhoff Publishers, Netherland, 1995
[5]. Geraldine van Buueren, the International Law on the Rights of the Child, Martinus Nijhoff Publishers, Netherlands, 1995
6. See Henkin (ed.), The International Bill of Human Rights: The Covenant on Civil and Political Rights, 1981.
7. UN Doc A/C 3/L 650. This was done at the initiative of Japan.
8. This Convention came into force on 2nd September 1990. India ratified the Convention on 12 November 1992.

There are regional human rights instruments for the protection of children, adopted by the Council of Europe, the Organization of American States (OAS), and the Organization of African Unity (OAU).

(g) Convention on the Elimination on All Forms of Discrimination against Women (CEDAW):

Article 16(1) (d) of the Convention provides that in all matters relating to marriage and family relations, the interests of the children shall be paramount.[7]

(h) Convention on the Rights of the Child (CRC):

The United Nations Convention on the Rights of the Child (CRC) represents a turning point in the international movement on behalf of child rights. The CRC gives children their basic human rights- civil, economic, social, cultural, and political- which enable children to achieve their full potential[8]. Broadly, the Convention ensures the four categories of child rights, namely, The Right to Survival, The Right to Protection, The Right to Development, and The Right to Participation.

Enforcement of International Child Rights Instruments in India

The Government of India not only ratified the Convention on the rights of the Child but has endorsed the twenty-seven survival and developmental goals for the year 2000 laid down by the World Summit for children. Article 73 of the Constitution of India states: 'Subject to the provisions of this Constitution, the executive power of the Union shall extend to the matters with respect to which Parliament has power to make laws; and to the exercise of such rights, authority and jurisdiction as are exercisable by the Government of India by virtue of any treaty or agreement'. Article 253 of the Constitution states that 'Parliament has power to make any law for the whole or any part of the territory of the India for implementing any treaty.

International Treaties/ Conventions are not considered as binding or as part of Domestic Law in India until they are specifically transformed in to Parliamentary enactments[9]. In our Country, keeping in view the international

[9] In this regard India' practice differs from that of USA and other countries where International Treaties are considered automatically as part of domestic

obligations Child Rights have been duly recognized in various enactments. Important among them is Juvenile Justice (Care and Protection of Children) Act, 2000. This Act was specifically enacted to implement the CRC, Beijing Rules and other International Child Rights obligations.

Before the recognition of Child Rights as Human Rights, deviant children were considered and treated from the age old perspective of treating them as criminals. Earlier to the emergence of Human Rights perspective children were treated on par with ordinary offenders. Now, as terminology itself indicates, it is care and protection and not punishment that should be applied up to eighteen years of age in view of the international treaty obligations. Earlier as per IPC offences committed by children above the age of seven are offences. This is an important departure in the Indian Law in tune with international obligations.

The Child Rights Convention emphasized that all decisions concerning children should be guided by the single most consideration namely, 'promoting the best interest of the children.' n this brief article it is proposed to review how far Human Rights of the Child are implemented in India.

Law. See *Jolly George Verghese & Anr vs. The Bank Of Cochin* AIR 1980 S.C. 470.From the perspective of international law the question posed is whether it is right to enforce a contractual liability by imprisoning a debtor in the teeth of Art. 11 of the International Covenant on Civil and Political Rights.
The remedy for breaches of International Law in general is not to be found in the law courts of the State because International Law per se or *proprio vigore* has not the force or authority of civil law, till under its inspirational impact actual legislation is undertaken. I agree that the Declaration of Human Rights merely sets a common standard of achievement for all peoples and all nations but cannot create a binding set of rules. Member States may seek, through appropriate agencies, to initiate action when these basic rights are violated; but individual citizens cannot complain about their breach in the municipal courts even if the country concerned has adopted the covenants and ratified the operational protocol. The individual cannot come to Court but may complain to the Human Rights Committee, which, in turn, will set in motion other procedures. In short, the basic human rights enshrined in the International Covenants above referred to, may at best inform judicial institutions and inspire legislative action within member-States; but apart from such deep reverence, remedial action at the instance of an aggrieved individual is beyond the area of judicial authority.

Age of the Child

However for the beneficial protection of the JJ Act the foremost condition is establishing the age of the person as below eighteen at the time when the incident occurred. Since, it is laid down that all persons below eighteen years are to be considered as children, there is no scope for any one to look in to the maturity or mental capacity of the person. In other words it is a matter of technicality since it is a statutory rule. This has given rise to various problems in determination of age.

In most cases children accused of crimes come from poor and illiterate sections of the society for whom there exists no official records of the age. If the child has attended school, the school certificate can be considered as proof of the age. But if the child has not attended any school it is only through medical examination that age can be established. But the problem with medical examination is that its determination is approximate and cannot be accurate up to days. While this is one issue, another important question is; do the children who are charged with offences under other penal statutes get the benefit of child protective provisions of Juvenile Justice Act. In this regard, the question of the jurisdiction of a juvenile court to deal with offences punishable with death or life imprisonment arose for the first time in 1932 before the Calcutta High Court in *Lakhi Sahu v Emperor*[10] and became the focal point in numerous other cases right up to 1990s. The controversy was due to a provision in the Code of the Criminal Procedure 1898 as well as that of the Cr.P.C.1973.[11] laying down that any offence committed by a child, not punishable with death or life imprisonment, may be tried by the court of a chief judicial magistrate or a juvenile court or any other court specially empowered under the Children Act, or any other law in force providing for the treatment, training, and rehabilitation of youthful offenders. While the High courts of Punjab, Madhya Pradesh and Calcutta, in *Brij Kishore v State of Haryana*,[12] *Devi Singh v State of MP*[13] and *Lakhi Sahu v Emporer* [14] held that the juvenile court had no jurisdiction to deal with such cases, the High Courts

[10] AIR 1932(Cal) 437
[11] Section 29B of the CrPC 1898 and Section 27 of CrPC 1973.
[12] (1979) 91 Punj LR 214
[13] (1978) CriLJ 585 (MP); State v Ramesh Nai,1975 CriLJ 713 (FB) (MP) overruled in re Rupsingh Devjia,
1975/CriLJ500(MP)(DB)

of Rajasthan,[15] U.P[16], Mysore,[17] Madras,[18] and Sind,[19] held the opposite view. The matter reached the Supreme Court in *Rohtas v State of Haryana*,[20] in which case the Supreme Court held that the juvenile Court was competent to deal with all offences committed by children. It relied on section 5 of the Cr.P.C. 1973 protecting provisions for the trial of an offence under any special pr local law in force. The question, however, was raised again in *Raghbir v State of Haryana*[21] on the plea that the judgment in Rohtas was delivered without considering the impact of the language of Section 27 of the Cr.P.C., the Supreme Court reiterated its decision in *Rohtas*. It was observed that as Section 27 did not contain any expression like 'notwithstanding anything contained in any Children Act passed by any State Legislature', it is not a specific provision to the contrary within in the meaning of Section 5 which alone could have excluded the operation of the special law relating to children. the Supreme Court held that in all offences committed by children under various penal enactments it is the juvenile court that shall deal with children. In *Raj Singh v State of Haryana*[22] The Supreme Court had held that the Juvenile Justice Act applied to a child charged under the Narcotic Drugs and Psychotropic Substances Act[23]. Thus this judgment ensures that all children

[14] AIR 1932 (Cal) 487.
[15] 1980 WLN 472 as digested in 50years Digest 1900-1950.
[16] State of UP V Smt.Phoolmati (1979) CriLJ NOC 111 (All).
[17] State v Madubharti Chelabharthi (1961) Cri LJ 227 (Guj).
[18] Sessions Judge, Tirunelvli v Perumal, 1974 CrLJ 261 (Mad) (FB); In re Anthony, AIR 1960 (Mad) 308.
[19] Hiralal s/o Chuharamal v Emperor AIR1948 (Sind) 63 (DB).
20. AIR 1979(SC) 1839.
[21] (1981) CriLJ 1497
[22]. (2000) 6 SCC 759
[23] The provisions of Juvenile Justice (Care and Protection of Children) Act 2000 have an over riding effect on all other legislations irrespective of the nature of offence committed by a child who is less than 18 years of age as on the date of commission of offence. Section 1(4) provides: "Section 1(4) : Notwithstanding anything contained in any other law for the time being in force the provisions of this Act shall apply to all cases involving detention, prosecution, penalty or sentence of imprisonment of juveniles in conflict with law under such other law.". In Raj Singh case, it was held that juvenile legislation shall reign supreme in juvenile cases no matter the nature of offence committed. Thus irrespective of the provision/ Act under which a case is registered against a juvenile, the juvenile is to be dealt with only under the

irrespective of the penal Statute charged with get the protective umbrella of the JJ Act.[24]

Determination of Age:

Age determination has been a tricky and controversial issue in juvenile justice. A number of cases have been decided by the courts in this regard. In the context of juvenile legislation in India, a juvenile is a person who has not completed eighteen years of age can be traced under juvenile justice Act as children below seven years of age have been given blanket immunity, as mentioned above, by the Indian Penal Code. The object is not to treat such children as adults for their criminal behavior but to reform and rehabilitate them. The issue of age determination controversial because there is not clarity on the point. Even in the case of Indian Penal Code, Section 82and 83 talk about children below and above seven years of age but it is silent about seven year old children. Who is to determine the age bracket they fall in? Section 49 (1) of the Juvenile Justice Act, 2000 confers the power on competent authority to determine whether the person brought before it is a juvenile, if he/she appears to be so. But the procedure to determine juvenility of a person cannot be relied on[25]. The two ways to determine age of the accused are documentary evidence and medical evidenced. In Jaya Mala v. Home Secretary[26], Government of Jharkhand the apex court held that the age as certained by the medical examination is not conclusive proof of age. It is mere opinion of the doctor and a margin of two years could be on either side. In another high profile case, Bhoop Ram v. State of UP[27], the court held that in case of conflict between documentary evidence and medical report, the documentary evidence will be considered to correct. This leads one to the conclusion that it needs to establish and convince court that a criminal is a juvenile is documentary proof is one of the easiest things to obtain in our country whether it is to get a

J.J Act and not any other special Act for the purposes of inquiry and any final order pursuant thereto.

[24] JJ Act enshrines that child is taken care of by JJB and CWC which hve social workers in their composion. JJAct even prescribes that specially trained child friendly police to deal with children in conflict with the law.

[25]. Government of India, 'The Juvenile Justice (Care and Protection of Children) Act, (2000), publication Division, New Delhi. Section 49 (1), (2000)

[26]. AIR 1982 SC 1297

[27]. AIR 19891989

license one is legally not entitled to or for furnishing age proof in the court. In such case, even if we were to turn to medical examination, which is held not to be hundred percent conclusive proof by even medicos. By the Allahabad High Court's own admission, a doctor is not always truthful. In Smt. Kamlesh v. State of UP[28], the court maintained that a professional witness is prone to side with a party that engages his/her service. Thus, a doctor is not always truthful. Now, if age cannot be determined conclusively by using either documentary evidence or medical evidence, what is to be done? The apex court in Babloo Passi and v. State of Jharkhand[29] held that no fixed norm had been laid down by the Act for the age determination of a person and the plea of the juvenile must be judged strictly on its own merit. The medical evidence as to the age of a person, through a very useful guiding factor, is not conclusive and has to be considered along with other cogent evidence.

A part from the conclusive determination of age, the question of the date when age has to be taken into account has also been a matter of controversy. Arnit Das v. State of Bihar[30] overruled the judgment saying that the date of commission of offence is the court that has to be taken into account. This was again corrected in Pratap Singh v.State of Jharkhand where the court held that 'the reckoning date for the determination of the age of the juvenile is the date of an offence and not the date when he is produced before the authority or in the court.

Conclusion

At the international level age of child was fixed to be eighteen. This was accepted and implemented in the Indian Law. But whenever a serious crime is committed there is general prejudicial tilting of mind of the court and public to punish the juvenile. Recently also there was demand from the public in the aftermath of Delhi gang rape to reduce the age of the child in view of the ghastly crime committed by the juvenile in that incident. The Parliament also heeded to the public demand and amended the JJ Act reducing the age of child to sixteen. Thus this amendment goes against the international human rights standards.

[28]. 1997 CrLJ 3191
[29]. 2009 (1) JCR 73(SC)
[30]. (2001) 2 SCC (Jour) 9

However it is not India alone that has reduced the age. Similar amendments were brought in U.K, USA, and other western countries. Since this is a serious question involving with lot of controversy, emotional considerations should be kept aside and an expert committee like Law Commission shall be entrusted with the task of fixing the age of the child. Further it should also be noted that the changing trends in the period of globalization, marketisation or adversely affecting the children to resort to crimes, particularly rape. In the whole debate demanding for the reduction of age, the socio-economic process that is creating the type of juveniles was missing. Only an expert committee can thoroughly probe in to all aspects, including, socioeconomic, cultural and other causes for the growing criminality among the children below 18 years and made suitable recommendations not only on the question of age but also on other measures to be taken to protect the children from degenerating into criminals.

INTERNATIONAL JOURNAL OF MULTIDISCIPLINARY EDUCATIONAL RESEARCH
ISSN : 2277-7881; IMPACT FACTOR - 2.972; IC VALUE:5.16
VOLUME 3, ISSUE 10(4), OCTOBER 2014

EMPLOYEE ATTITUDE TOWARDS CORPORATE SOCIAL RESPONSIBILITY – EVIDENCE FROM INDIAN CORPORATE SECTOR

Dr. Ch. Sri Rama Murthy
Assistant Commercial Tax Officer
Commercial Taxes Department, Markapur
Prakasam District, Andhra Pradesh

1. INTRODUCTION

From time immemorial, welfare of the common man has been the cardinal concern of the governmental machinery. The corporations have started during the last 40 years across the world with a view to compensate for the damages meted out to the society in one form or the other as a result of their manufacturing process. Thus, corporate social responsibility has come of age.

Corporate social responsibility (CSR) is a concept whereby companies integrate social and environmental concerns in their business operations and in their interaction with their stakeholders on a voluntary basis.[1]

In India, the term corporate social responsibility might be relatively new but the concept is not. It has been there since the earliest times, going back to an age when society itself was in its formative stages.

The issue of corporate social responsibility became commonplace in the business press and among business and political leaders (Buhr and Grafstrom 2004), and a body of academic literature has also emerged around it (Walsh et al. 2003). There is a surprising dearth of research on perceptions or attitudes of executives in the academic literature (Narwal and Sharma, 2008). In India, only a few empirical studies, Singh et al. (1980); Krishna (1992) and Reddy (2006) etc., have been made analyzing the perceptions of Indian managers towards CSR.

While studying the attitudes of managers towards corporate social responsibilities, Krishna (1992) concluded that managers in Indian industry are very much favorable to corporate social responsibility. A further study of

[1] European Commission (EU:2001), Green Paper-Promoting a European Framework for Corporate Social Responsibility, COM (2001) 366 final, Brussels, *Official Publications of the European Commission*, July 18.

the perception of corporate managers on CSR revealed that the major drive of CSR in Indian industry is the drive to become good corporate citizen, maintaining social commitment, and improvement in employee relations, etc.[2]

Taking all the previous related research into consideration, this paper studies the attitude of the executives towards corporate social responsibility keeping in mind that a positive attitude of the executive may definitely tend to a good socially responsible behavior and the both result in achievement of the firm's success effectively.

2. REVIEW OF LITERATURE

Understanding the perceptions and attitudes regarding CSR is an important research dimension. Greening & Turban (2000) found that job applicant and employee perceptions of a firm's CSR determines their attractiveness towards the organisations. Moving on the same track, Cropanzano et al. (2001) demonstrated that employee attitudes and behaviours are heavily influenced by fairness of organisational actions towards them.

Abdul and Ibrahim (2002) examined the attitudes of Malaysian managers and executives towards social responsibility and the results showed that the most influential factor determining the attitude towards social responsibility was family upbringing. The other important factors were traditional beliefs and customs, and common practices in the industry. Quazi (2003) demonstrated that there is a significant relationship between the level of education, training, status and religiosity of managers and their perception on CSR. Hemingway (2004) suggested that there may be an association between different industries, the personal values of the managers who work in them and their commitment to CSR.

Jonung and Malhotra (2007) investigated the attitudes towards Corporate Social Responsibility among India's future business leaders. The results showed that the sample group has a positive attitude towards CSR. Brammer et al. (2007) emphasized the importance of gender variation and suggested that the contribution of CSR to organisational commitment is at

[2] Reddy, A.J.M. (2006), 'Corporate Social Responsibility for Sustainable Development', In Sahay, B.S.; Stough, Roger R.; Sohal, Amrik; and Goyal, Sonu, *Green Business*, Allied Publishers Pvt. Ltd., New Delhi.

least as great as job satisfaction. Zu and Song (2009) revealed that managers' CSR orientation is positively correlated with their firms' performance. According to Stawiski et al. (2010), the relationship between CSR and commitment is stronger for women than it is for men.

3. HYPOTHESES

To study the attitude of executives towards CSR, the following hypotheses are formulated in null form.

$H1_0$: Type of business sector does not have significant effect on executives' attitude towards CSR.

$H2_0$: Executive demographic profile will not have significant effect on attitude towards CSR in relation to: $H2_{0a}$: Gender; $H2_{0b}$: Education level; $H2_{0c}$: Level of management; $H2_{0d}$: Designation; $H2_{0e}$: Work experience.

4. RESEARCH METHODOLOGY

Simple random sampling technique was used in the selection a sample of executives from different industries across India. The final sample consisted of consisted of 317 executives. Both primary and secondary data were used. The primary data was collected through a well-structured survey. The self-administered questionnaire used 5-point Likert type statements (where 1 = strongly disagree, 2 = agree, 3 = undecided, 4 = agree, 5 = strongly agree) (Annexure). Inferential statistics were used selectively for the testing of hypotheses. Univariate ANOVA and test of homogeneity were computed. Reliability analysis, using Cronbach's alpha, was employed to check the reliability of the scale.

Table 1: Reliability analysis of the scale

S.No.	Item-Total Correlation	Cronbach's Alpha if Item Deleted
Q1	.692	.757
Q2	.697	.754
Q3	.367	.787
Q4	.548	.773
Q5	.553	.769
Q6	.469	.779
Q7	.506	.778
Q8	.412	.783

Q9	.615	.760
Q10	.080	.798
Q11	.729	.769
Q12	.158	.810
Q13	.158	.810
Q14	.682	.758
Q15	-.040	.821

Principal component analysis was used followed by Varimax rotation. The extraction of factors was stopped when Eigen values (latent roots) came to be less than 1.00. Five factors with Eigen value greater than 1 emerged explaining 85.234 per cent of variance with a Kaiser-Meyer-Olkin (KMO) measure of sampling adequacy of 0.655 which was in the acceptable range, being more than 0.5.

Table 2: Identified Variables and Factors

Factor No.	Factor Description	No. of variables	Variable Codes*	% of variance explained
F1	Economic Orientation	5	Q1 (.948), Q14 (.944), Q2(.892), Q11(.640), Q9 (.629)	26.667%
F2	Product/Service Quality	2	Q6 (.870), Q5(.736)	16.637%
F3	Corporate bonding	3	Q3(.900), Q4(.684), Q8(.677)	14.693%
F4	Calculative Consideration	2	Q12(.999), Q13(.999)	14.276%
F5	Corporate citizenship	2	Q10(.926), Q7(.744)	12.961%

Extraction Method: Principal Component Analysis.

Rotation Method: Varimax with Kaiser Normalization

*Values in brackets are factor loading in decreasing order.

5. DATA ANALYSIS AND RESULTS

5.1 Gender and Attitude towards CSR

From univariate ANOVA, it was implicit that gender had no significant effect on the dimensions of attitude towards CSR, namely 'Economic Orientation' $F(1,136)=0.428$, $p=.513$; 'Product/Service Quality' $F(1,136)=0.191$, $p=.663$; 'Corporate Branding' $F(1,136)=0.576$, $p=0.448$; 'Calculative Consideration' $F(1,136)=0.206$, $p=0.650$; and 'Corporate Citizenship' $F(1,136)=0.124$, $p=0.725$.

5.2 Educational Background and Attitude towards CSR

The univariate ANOVA results revealed that there was significant effect of educational background on the attitudes towards CSR, namely 'Economic Orientation' $F(1,136)=5.787$, $p=0.017$; 'Calculative Consideration' $F(1,136)=35.686$, $p=.000$; and 'Corporate Citizenship' $F(1,136)=11.829$, $p=.001$. Whereas, 'Product/Service Quality' $F(1,136)=3.657$, $p=0.057$ and 'Corporate Branding' $F(1,136)=3.718$, $p=0.055$ were insignificant.

The tests for homogeneity of variance were significant at 0.05 level for 'Product/Service Quality' (Levene=19.596, $p=0.000$), 'Corporate Branding' (Levene=6.053, $p=0.014$), 'Corporate Citizenship' (Levene=11.891, $p=0.001$) with the exception of 'Economic Orientation' (Levene=2.536, $p=0.112$) and 'Calculative Consideration' (Levene=2.369, $p=0.125$).

5.3 Level of Management and Attitude towards CSR

The results from univariate ANOVA revealed that level of management had significant effect on the attitudes towards CSR, namely 'Economic Orientation' $F(2,316)=282.821$, $p=0.000$; 'Product/Service Quality' $F(2,316)=37.898$, $p=0.000$; 'Corporate Branding' $F(2,316)=24.651$, $p=0.000$; and 'Corporate Citizenship' $F(2,316)=6.923$, $p=0.001$; with the exception of 'Calculative Consideration' $F(2,316)=2.833$, $p=0.060$.

The Levene's test for homogeneity of variances was applied between level of management and the attitudes. The tests for homogeneity of variance were significant at 0.05 level for 'Economic Orientation' (Levene=18.374, $p=0.000$), 'Product/Service Quality' (Levene=6.017, $p=0.003$), 'Corporate Branding' (Levene=49.212, $p=0.000$), 'Calculative Consideration' (Levene=6.672, $p=0.001$), and 'Corporate Citizenship' (Levene=20.271, $p=0.000$).

5.4 Designation of Respondents and Attitude towards CSR

The results of univariate ANOVA revealed that there was a significant effect of designation of the respondents on the attitudes towards CSR, namely 'Economic Orientation' $F(2,316)=98.309$, $p=0.000$; 'Product/Service Quality' $F(2,316)=19.446$, $p=0.000$; 'Corporate Branding' $F(2,316)=15.711$, $p=0.000$; and 'Corporate Citizenship' $F(2,316)=5.250$, $p=.006$ with the exception of 'Calculative Consideration' $F(2,316)=.920$, $p=.400$.

The Levene's test for homogeneity of variances was applied between the designations and the attitudes. The tests for homogeneity of variance were significant at 0.05 level for 'Economic Orientation' (Levene=38.582, $p=0.000$), 'Corporate Branding' (Levene=6.571, $p=0.002$), 'Calculative Consideration' (Levene=5.895, $p=0.003$), and 'Corporate Citizenship' (Levene=11.040, $p=0.000$). Whereas, 'Product/Service Quality' (Levene=0.367, $p=0.693$) was insignificant.

5.5 Work Experience and Attitude towards CSR

The univariate ANOVA test results revealed that there was no significant effect of work experience of the respondents on the attitudes towards CSR, namely 'Economic Orientation' $F(2,136)=0.568$, $p=0.567$; 'Product/Service Quality' $F(2,136)=0.436$, $p=0.647$; 'Corporate Branding' $F(2,136)=0.020$, $p=0.980$; and 'Corporate Citizenship' $F(2,136)=0.055$, $p=0.946$ with the exception of 'Calculative Consideration' $F(2,136)=202.091$, $p=0.000$.

The null hypothesis of work experience ($H2_{0e}$) was rejected for all the attitudes except for the attitude 'Calculative Consideration' where the null hypothesis was accepted. It was found that three out of five variables were found affecting significantly the attitude towards CSR. Therefore, it could be safely stated that the null hypothesis ($H2_0$) stood rejected and alternate hypothesis was accepted.

6. DISCUSSION OF RESULTS

It was found that type of sector has the significant effect on the attitude of executives towards CSR. Further, it was found from the results that executives from the manufacturing sector had much better attitude towards CSR than the executives from service sector companies on all the five attitude dimensions suggesting a significant difference between manufacturing

and service sectors in deciding the executives' CSR orientation. Gender variations on attitude towards CSR were found insignificant in this study. In other words, irrespective of the gender, executives have similar attitude towards CSR.

Postgraduate executives held much better attitude towards CSR than the undergraduate executives demonstrating a significant relationship between level of education and their perception on CSR. The findings revealed that top level management held much better attitude towards CSR than the middle level management whereas lower level management held poor attitude towards CSR. Such variation was also found statistically significant.

Designation of respondents influences their attitude towards CSR. CEOs/Presidents held much better attitude towards CSR than functional heads and other officers. Such variations were also found statistically significant. Regarding work experience, it was a surprising finding of invariance in all the attitudes of the executives except on one attitude namely 'calculative consideration'. This means years of experience need not have any influence on attitudes toward CSR.

7. CONCLUSIONS AND SUGGESTIONS

The results of this paper show that different business sectors have direct effects on the attitudes of executives towards corporate social responsibility. Significant interaction effects of attitudes of executives with personal and organisational attributes are present. With respect to the personal attributes, education has a significant effect on the attitudes of the executives. However, the direction of the interaction effects does not conform to gender of the executives. When it comes to organisational attributes, a strong correlation between position in the company and attitude towards CSR is identified. It appears that executives have a more straight forward perception about the term. Companies should establish an agenda on CSR and employees should be made responsible for implementation of CSR.

References

1. Abdul, M.Z. & Ibrahim, S. (2002). Executive and Management Attitudes towards Corporate Social Responsibility in Malaysia. Corporate Governance, 2(4), 10-16.
2. Brammer, S., Millington, A. & Rayton, B. (2007). The Contribution of Corporate Social Responsibility to Organisational Commitment. The International Journal of Human Resource Management, 18(10), 1701 – 1719.

3. Buhr, H., & Grafstrom, M. (2004), 'Corporate social responsibility', edited in the Business Press, Paper presented at the conference on Corporate Social Responsibility in the Era of the Transforming Welfare State, Florence, Italy.
4. Cropanzano, R, Byrne Z.S., Bobocel D.R., & Rupp, D.E. (2001). Moral Virtues, Fairness Heuristics, Social Entities, and Other Denizens of Organisational Justice. Journal of Vocational Behaviour, l(58), 164–209.
5. Greening, D.W. & Turban, D.B. (2000). Corporate Social Performance As A Competitive Advantage In Attracting A Quality Workforce, Business and Society, 39, 254–280.
6. Hemingway, C. A. & Maclagan, P. W. (2004). Managers' Personal Values as Drivers of Corporate Social Responsibility. Journal of Business Ethics, 50(1), 33-44.
7. Jonung, M. & Malhotra, M. (2007). Attitudes towards Sustainable Development and Corporate Social Responsibility among Future Business Leaders in Bangalore, India. Master's Thesis in International Business, Swedish International Development Cooperation Agency.
8. Krishna, C.G. (1992). Corporate Social Responsibility in India- A Study of Management Attitude, New Delhi: Mittal Publications.
9. Malhotra, N. (2008). Marketing Research: An Applied Orientation. New Delhi: Pearson Prentice Hall.
10. Narwal, M. & Sharma, T. (2008). Societal Perception of Corporate Social Responsibility: An Empirical Study In Jatana, Renu and Crowther, David (Ed.), Corporate Social Responsibility: Theory and Practice with Case Studies. New Delhi: DEEP & DEEP Publications Private Limited.
11. Nunnally, J. C. (1978). Psychometric Theory, 2nd edition, New York: McGraw-Hill.
12. Quazi, A.M. (2003). Identifying the Determinants of Corporate Managers' Perceived Social Obligations. Management Decision, 41(9), 822-831.
13. Reddy, A.J.M. (2006). Corporate Social Responsibility for Sustainable Development, In Sahay, B.S.; Stough, Roger R.; Sohal, Amrik; and Goyal, Sonu, Green Business, New Delhi: Allied Publishers Pvt.Ltd.
14. Singh, P., Maggu, A., & Warrier, S.K. (1980). Corporate Social Responsibility: Realities and Expectations. Vikalpa,5(2), 117-130.
15. Stawiski, S., Deal, J.J. & Gentry, W. (2010). Employee Perceptions of Corporate Social Responsibility – The Implications for Your Organization. Quick View Leadership Series, Center for Creative Leadership, USA.
16. Walsh, J. P., Weber, K., & Margolis, J. D. (2003). Social Issues and Management: Our Lost Cause Found. Journal of Management, 29, 859–881.
17. Zu, L., & Song, L. (2009). Determinants of Managerial Values on Corporate Social Responsibility: Evidence from China. Journal of Business Ethics, 88(1), 105-117.

INTERNATIONAL JOURNAL OF MULTIDISCIPLINARY EDUCATIONAL RESEARCH
ISSN : 2277-7881; IMPACT FACTOR - 2.972; IC VALUE:5.16
VOLUME 3, ISSUE 10(4), OCTOBER 2014

SELF – HELP GROUPS – A TOOL TO WEAKER SECTIONS' WOMEN EMPOWERMENT

Jyothi Guntaka
Research Scholar
Department of Commerce & Business Administration
Acharya Nagarjuna University, Nagarjuna Nagar
Guntur District, A.P

The important aspect of social lives now-a-days is mostly confined to the gender issues in various socio-economic-health-demographic and cultural classifications of people in India.. Especially the situation of Dalit women is very pathetic. They experience endemic gender - and - caste discrimination due to vulnerably position at the bottom of caste, class and gender hierarchies. These women also experience violence as the outcome of severely imbalanced social, economic and political power equations. Dalit women are one of the largest socially segregated groups anywhere in the world, and make up 2 per cent of the world's total population. Dalit women constitute about 16 per cent of the total Indian female population. The traditional taboos are the same for Dalit men and Dalit women. However, Dalit women have to deal with them more often. Dalit women are discriminated against not only by people of higher castes, but also within their own communities. Their socio - economic vulnerability and lack of political voice, when combined with the dominant risk factors of being Dalit and female, increase their exposure to potentially violent situations while simultaneously reducing their ability to escape. Therefore, the situation of Dalit women needs special attention.

Micro-finance with Self Help Groups plays an effective role for promoting women empowerment. It is not only an efficient tool to fight against poverty, but also as a means of promoting the empowerment of the most marginalized sections of the population, especially women. The role of self help groups is very significant in the present day context both in motivating women to save at least some money regularly and to use that amount as investment in income generating activities. At present, Self Help Groups (SHGs) are widely used as an instrument to change the conditions of women socially and economically, once socio-economic experiment is achieved it would have implication on the overall development of women.

Against this background, the present study is taken up to examine the socio-economic conditions of the Dalit women and their empowerment through

Self-Help Groups. The study is based on primary data collected using questionnaire. 120 sample respondents are selected randomly from Mangalagiri mandal of Guntur district.

Results and discussion

Age of the respondents

Age is a social variable. Table – 1 presents distribution of the respondents by age. It is noticed from the table that the study consists of about 58 per cent of the respondents who are below 35 years of age. It is further evident that age of the nearly one third of the respondents' ranges from 36 to 50 years. There are a few respondents above 51 years old (8.3 per cent).

Literacy level of the respondents

Distribution of the respondents by literacy level is furnished in Table – 2. It is revealed from the table that majority of the respondents are literates. However, majority had studied upto primary education only among literates (45.80 per cent). At the next level, majority had studied upto secondary education (23.30 per cent). It is also evident that one tenth of the respondents had studied upto intermediate, followed by negligible percentage of the respondents, degree and above. It is also evident that about 19 per cent of the respondents are illiterates.

Type of the family

Distribution of the respondents by type of family is given in Table – 3. It is portrayed from the table that type of family of the majority of the respondents is nuclear family (80 per cent). It is also evident that 20 per cent of the sample respondents are living in joint families.

Motivated persons to join SHGs

Table – 4 presents distribution of the respondents by motivation factors to join SHGs. It is found from the table that majority of the respondents reported that they are motivated by co-villagers to join SHGs (59.10 per cent), followed by 20 per cent, by other SHGs in their locality about 12 per cent, by friends and relatives, and about 9 per cent, by family members.

Number of years as members of the group

Distribution of the respondents by age of the group is furnished in

Table – 5. It is revealed from the table that around 87 per cent of the respondents are members of the group for the last five years. Further, it is noticed that 10 per cent of the respondents are members of the group from 5 to 10 years and merely 3 per cent of the respondents are members for more than 10 years.

Reasons for joining SHGs

Distribution of the respondents by reasons for joining SHGs in their opinion is given in Table – 6. It is found from the study that about 81 per cent of the sample respondents reported that they had joined SHGs to support family income. Further, it is found that 10per cent of the respondents said that they had joined SHGs to take up income generating activities, followed by 5 per cent, to develop social status and about 4 per cent, to improve savings level.

Independence to spend money earned through SHGs

An attempt is made in the present study to know whether sample respondents achieved independence to spend money earned through SHGs. Table – 7 shows the distribution of the sample respondents by their response. It is evident from the study that only little percentage of the sample respondents reported having independence to spend money earned through SHGs (11.70 per cent). On the contrary, about 88 per cent of the sample respondents reported that there is no independence to them to spend money earned through SHGs. This shows the existence of male domination over sample dalit women.

Changes in monthly income after joining SHGs

Distribution of the respondents by changes in monthly income after joining SHGs is shown in Table – 8. It is found from the table that monthly income of the respondents is increased to some extent in the case of 70 per cent of the sample respondents, while 10 per cent of the sample respondents reported considerable increase in their family income after joining SHGs. On the other hand, one fifth of the sample respondents reported no change in monthly income after joining SHGs.

Awareness about various things after joining SHGs

An attempt is made in the present study to know whether awareness of the sample respondents is increased after joining SHGs. Distribution of the

respondents by their response is given in Table – 9. It is obvious from the table that 80 per cent of the respondents felt that their awareness level is increased after joining SHGs and the rest 20 per cent felt that there are no changes in their awareness level is increased after joining SHGs.

Decision making power in the family after joining SHGs

Respondents are asked whether their decision making power is increased in their family after joining SHG. Distribution of the respondents by whether their decision making power is increased after joining SHGs is provided in Table –10. It is clear from the table that about 88 per cent of the respondents informed that their decision making power is not increased even after joining SHGs, while meager percentage of the sample respondents reported increase in decision making power in their family after joining SHGs (11 per cent).

Conclusion

It is found from the study that majority of the sample respondents are illiterates. Though vast proportion of the sample respondents are living in nuclear families, they are subject to male domination. They joined SHGs with motivation from their co-villagers. After joining SHGs, they are empowered economically to some extent only. They have no independence to spend the money earned through SHGs. Even after joining SHGs, decision making power in their families to these women is very poor. However, their awareness about various things is increased after joining SHGs. It is suggested that government should initiative steps to make it compulsory for each and every dalit women to enroll in SHGs. Dalit males also be encouraged to form SHGs so as to have awareness on the importance of women to the household economy.

Table – 1
DISTRIBUTION OF THE RESPONDENTS BY AGE

Age	Number of respondents	Per cent
Young (upto 35 years)	70	58.30
Middle (36 to 50 years)	40	33.30
Old (51 years and above)	10	8.30
Total	120	100.00

Source: Field survey

Table –2

DISTRIBUTION OF THE RESPONDENTS BY LITERACY LEVEL OF THE RESPONDENT

Literacy Level of the respondent	No. of respondents	Per cent
Illiterate	23	19.20
Primary	55	45.80
Secondary	28	23.30
Intermediate	12	10.00
Degree and above	2	1.70
Total	120	100.00

Source: Field survey

Table – 3

DISTRIBUTION OF THE RESPONDENTS BY TYPE OF THE FAMILY

Type of family	No. of respondents	Per cent
Joint family	96	80.00
Nuclear family	24	20.00
Total	120	100.00

Source: Field survey

Table –4

DISTRIBUTION OF THE RESPONDENTS BY MOTIVATED PERSONS TO JOIN SHGs

Reason	No. of respondents	Per cent
Family members	11	9.20
Friends & Relatives	14	11.70
Co-villagers	71	59.10
Other SHG in the Locality	24	20.00
Total	120	100.00

Source: Field survey

Table – 5

DISTRIBUTION OF THE RESPONDENTS BY AGE OF THE GROUP

Age of the group	No. of respondents	Per cent
Below 5 years	104	86.70

5-10 years	12	10.00
More than 10 years	4	3.30
Total	120	100.00

Source: Field survey

Table – 6

DISTRIBUTION OF THE RESPONDENTS BY REASONS FOR JOINING GROUP

Reason	No. of respondents	Per cent
To support family's income	97	80.80
To develop social status	6	5.00
To improve savings level	5	4.20
To take up income generating activities	12	10.00
Total	120	100.00

Source: Field survey

Table – 7

TABLE SHOWING DISTRIBUTION OF THE RESPONDENTS BY WHETHER THERE IS INDEPENDENCE TO THE SAMPLE RESPONDENTS TO SPEND THE MONEY EARNED THROUGH SHGs

Independence	No. of respondents	Per cent
Achieved	14	11.70
Not achieved	106	88.30
Total	120	100.00

Source: Field survey

Table – 8

TABLE SHOWING DISTRIBUTION OF THE RESPONDENTS BY CHANGES IN MONTHLY INCOME

Change	No. of respondents	Per cent
Increased considerably	12	10.00
Increased to some extent	84	70.00
No change	24	20.00
Total	120	100.00

Source: Field survey

Table – 9

TABLE SHOWING DISTRIBUTION OF THE RESPONDENTS BY AWARENESS ABOUT VARIOUS THINGS AFTER JOINING SHGs

Awareness	No. of respondents	Per cent
Increased	96	80.00
No change	24	20.00
Total	120	100.00

Source: Field survey

Table – 10

TABLE SHOWING DISTRIBUTION OF THE RESPONDENTS BY ACHIEVING DECISION MAKING POWER IN THE FAMILY AFTER JOINING SHGs

Decision making power	No. of respondents	Per cent
Achieved	14	11.70
Not achieved	106	88.30
Total	120	100.00

Source: Field survey

References

1. Gurumoorthy, T.R., (2000), "Self Help Groups Empower Rural Women", Kurukshetra, February, Vol.48, p.5.
2. Subhinra, H.R., (2002), "Devadasis reform into SHG Members", Social Welfare, November, Vol.49, No.8.
3. Nirmala, V., Shambhat K. and Buvaneswari P., (2004), "SHGs for Poverty Alleviation in Pandicherry", Journal of Rural Development, Vol.23, No.2.
4. Sunder Raj, D., (2004), "SHGs and Women's empowerment", Social Welfare, Vol. 50, No. 10, January, pp. 39-41.
5. Gangaiah C., Nagaraja B. and Vasudevulu Naidu C. (2006), "Impact of self Help Groups on income and Employment: A Case Study", Kurukshetra, March, Vol.54, No.5, pp.18.

6. Vinayagamoorthy A. (2007), "Women Empowerment through Self Help Groups - A Case Study in the North Tamil Nadu", Social Welfare, April, pp.32-35.

7. Murlidhar A. Lokhande1 (2013), " Micro Finance for Women Empowerment - A Study of Self-help Groups-Bank Linkage Programme", International Center for Business Research, Vol.2, April, pp.159-166.

8. Sooryamoorthy R (2013), "Microcredit, Self-Help Groups and NGOs in the Alleviation of Poverty: An Overview", Social Action, Vol.63, No.2, April-June, pp.165-179.

9. Sanjay V. Yadav (2013), "Women Empowerment through Self-Help-Group: A case study of Nagthane Village, Tal: Palus, Dist-Sangli", International Interdisciplinary Research Journal, Volume-III, Issue-III, May-June, pp.199-207

INTERNATIONAL JOURNAL OF MULTIDISCIPLINARY EDUCATIONAL RESEARCH
ISSN : 2277-7881; IMPACT FACTOR - 2.972; IC VALUE:5.16
VOLUME 3, ISSUE 10(4), OCTOBER 2014

EXPLORING SERVICE DESIGN FOR AQUARIUM BUSINESS USING SERVICE MIX

Sankaran A.
Ph.D., Research Scholar
Department of Business Administration, Annamalai University
Annamalai Nagar , Tamil Nadu, India

Selvarasu A.
Professor
Department of Business Administration, Annamalai University
Annamalai Nagar , Tamil Nadu, India

1. Introduction

The aquarium keeping is a age old hobby, popular even today, aquarium business service market is in the booming stage. Aquarium keeping has its origin in Japan and China. It is reported that it was a past time for the Japanese even before 1000 years. Now many countries such as Japan, Malaysia, Singapore, USA and European countries have made the aquarium keeping and ornamental fish culture and trade as a flourishing business. The top aquarium exporting country is Singapore, followed by Hong Kong, Malaysia, Thailand, Philippines Sri Lanka, Taiwan, Indonesia and India. The largest importer of ornamental fish is USA. Europe and Japan, China and South Africa are the emerging markets of ornamental fish trade (FAO, 2006).

1.1 Aquarium Fish Market in India

In India, out of total export of ornamental fish, 85% is based on wild collection Gurumayum et al., (2002). Majority of the indigenous ornamental fish trade is from the North Eastern states and Southern states in India. The capture of ornamental fish is based on development of the fish culture. Fish species grown for their importance, can be successfully bred in India. The ornamental fish trade depends upon supply and demand, which is possible only by mass breeding.

The increasing demand for aquarium fishes gradually paved the avenue towards global trade of ornamental fishes. World trade of ornamental fish is estimated to be about Rs. 2000 crores, but, India's share is only Rs. 15 crores, which is very insignificant (Sagar C. Mandal et al., 2013). Most of the fish species of North-Eastern region of India possess high values for their attractive coloration pattern, graceful behavior, peculiar body morphology and endemicity. Aquarium fish has become a popular hobby and aquarium fish selling is a popular trade in Tripura. The trade is mostly confined to

import of exotic ornamental fishes from other states of the country particularly from Kolkata which are then sold out on the basis of temporary management. The indigenous ornamental fishes which are available in the rivers of the state are being neglected due to lack of awareness. Most of these fishes are caught before their first maturity and sold in the market as food fishes. These indigenous ornamental fishes are collected from the wild resources and are cultured and reared for keeping in the aquarium.

1.2. Reasons for Service Design

1. Increased emphasis on customer satisfaction and increased pressure to be competitor.
2. Increased emphasis on time needed to introduce new products and service design in the market
3. Increased emphasis on reducing time to produce a product
4. Greater attention to environmental concerns (waste minimization, recycling, disposal of worn out products etc...)
5. Increased emphasis on user friendliness
6. Increased emphasis on the use of less material and or energy
7. Developing / strengthening the infrastructure facilities for hygienic handling and processing of business service
8. The customers to easy identify the service design industry

1.3. Aquarium Business Service Mix

The below Figure-3 to identify the aquarium business service mix implementation processes, that process is included on marketing mix 4P's and service mix 7 P's.

Figure 1

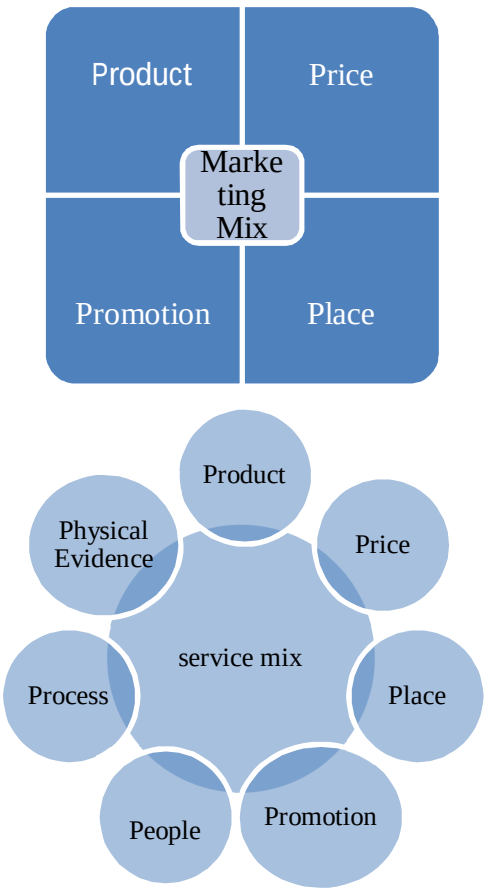

(Fig.1) Marketing Mix 4P's & Service Mix 7P's.

The services marketing mix is an extension of the 4-Ps framework. The essential elements of product, promotion, price and place remain but three additional variables – people, physical evidence and process – are included to 7–Ps mix. The need for the extension is due to the high degree of direct contact between the aquarium business providers and the aquarium keeping customers, the highly visible nature of the service process, and the simultaneity of the production and consumption. While it is possible to discuss people, physical evidence and process within the original-Ps framework (for example people can be considered part of the product offering) the extension allows a more thorough analysis of the marketing ingredients necessary for

successful services marketing. Booms and Bitner (1981) advise three new P's to service marketing: people, process, and physical evidence.

1.5. Service Design for Aquarium Business Using Service Mix

Service is most important one of the any business to develop our Product and service. Majority of Consumers is expected in new service design and service facilities offered by particular industry. Aquarium is a fast moving consumer service product and it is one of the developing stages in India. This industry in developed countries such as USA, Japan, Thailand etc., is offering the aquarium business service design for customers and hobbyist, a branded aquarium product, right place of parking, infrastructure, billing and ordering system, advertisement, and appointed aquarium technician with uniform, proper service facilities. But our countries particularly, Tamil nadu aquarium shop is not maintaining an equalent service design. So, in this research study, the need to is develop a new service design using service mix (7 P's) such as product, price, place, promotion, people, process and physical evidence suiting to aquarium business services.

Service mix for aquarium business service keeping in view of the service index, aquarium business service is faced with the following description for each component of 7p's.

Table 1: Aquarium Business Service Mix

Service mix	Description
Product	Aquarium Tank, Ornamental Fish, Food, Water Filter, Nature and Plants, Lighting and Aeration
Price	Service Delivery Charge, Tank Size, Fish Varieties, Use Of Equipment's and Cleaning Charge
Place	Aquarium Shop, Exhibition, Aquarium Fair, Fisheries Institution
Promotion	Advertising, Discount, Offer, Quick Service, Identities.
People	Aquarium Engineers, Maintenance Staff, Aquarium Researcher & Users.
Process	Order Processing, Bill Payment Process, Service Delivery Process and Tank Set Up Process.
Physical Evidence	Letter Head, Broachers, Service Vehicle, Logo, Display Board, Uniforms, Visiting Cards and Packaging Cover.

Product

A product is anything that is offered to a market to satisfy a need or want. The aquarium products mix includes such as Aquarium Tank, Ornamental Fish, Food, Water Filter, Nature and Plants, Lighting and Aeration.

Price

It is a flexible and dominant element, which determines the revenue/profitability/market share for the organization. From the customer's viewpoint aquarium business service price mix such as Service Delivery Charge, Tank Size, Fish Varieties, Use Of Equipment's and Cleaning Charge.

Place

It represents the distribution channels that an organization utilizes to convey its own physical products or services to the end users. The aquarium business service, place mix such as Aquarium Shop, Exhibition, Aquarium Fair, Fisheries Institution.

Promotion

This promotion activity involves the communication that marketer engages in with the customers in order to acknowledge the product. The aquarium business, promotion mix such as Advertising, price Discount, Offer, Quick Service, guarantee, and Identities.

People

People are the most important elements in aquarium service or experience. There are several ways in which people add value to an aquarium business service design such as Aquarium Engineers, Maintenance Staff, and Aquarium Researcher & Users.

Physical Evidence

The intangibility of service brings the difficulties of unclear, untouchable, and even doubtful. Strictly speaking there are no physical attributes in service, so a consumer often relies on those tangible evidences for confidence. Here, aquarium business service design considers such as Aquarium Shop Letter Head, Broachers, Service Vehicle, Logo, Display Board, Uniforms, Visiting Cards and Packaging Cover.

Process

In service business, process is an element that appreciates customer experiencing as an organizational offering. It's viewed as something that customer participates in at different point. Again we can see the importance of interaction with customers. It requires such as aquarium tank Order Processing, Bill Payment Process, Service Delivery Process and Tank Set up Process.

2. Review of Literature

There are different articles referred and the essence of ornamental fish aquarium business service design is presented. The concepts that are revisited in this section are as follows; market situation and export trade for aquarium business service; aquarium fish culture; availability of aquarium fish; aquarium fish industry; market risk analysis of ornamental fish aquarium business; business opportunities for ornamental fish production in India; aquarium management service; marketing strategies for ornamental fish aquarium business service; service design for other industry; service marketing mix.

Robert Fenner (2001) reported that the concept of running a service company in contrast with a retail business is not new to many industries. The service sectors provide employment for more economic growth. The critical elements of this retail business were stated as finance, personnel, location, set up and stock.

Sudhi K.S. (2002) stated that marine products export development authority supported financial aid for the analysis of ornamental fishes in Kerala as market development in India and abroad. Ornamental fish farming and aquarium keeping were reported as a major business in the state. The marketing of aquarium systems is also emerging in the state as a booming business, which mainly targets posh hotels, corporate offices and other business establishments.

Swain et al., (2001 & 2003) recognized common aquarium fishes and detailed the prospects of export oriented freshwater ornamental fish culture in India. Researcher suggested that commercial farms with necessary infrastructure facilities and due technical support are necessary to achieve mass production of ornamental fishes.

Tomey et al., (1986) conducted survey and reported about marine ornamental resources in Lakshadweep areas and freshwater fishes in Bombay and Madras. The export potential to The Netherlands was pointed out.

Sunderesan J (2011) stated that ornamental fish industry is the big industry with 4500 spices of freshwater fish, 1450 of marine fish, 650 marine corals. Ornamental fish keeping is measured as an easy and stress reliving hobby. Many states governments had initiate specific programme to support this industry. Kerala is planning for the first aqua park in the country at kochi for ornamental fish production and marketing. Kerala, west Bengal, utter Pradesh, Madhya Pradesh, and Tamil nadu has initiated attempt to train skilled manpower for the industry.

Robert Fenner (2001) stated that for the pet business primary objectives are desire in self employment as well as doing small business which is the backbone of the economy. The successful keeping and reproducing aquatic life well being, a good hobbyist should easily translate into being good retailers. Actually, the knowledge, skills, methods, and attitudes of being a good pet keeper are vital to successful retailing the business.

Duane Clark (2002) reported that two common ideas of pet business in ornamental fisher are-either breeding fish or starting an aquarium maintenance service. Breeding fish can certainly help pay for your hobby but running an aquarium maintenance service actually generate profit. However, before a person run off to start his own service, he must consider a few things such as motivation, research, necessities, finding clients, customer service, pricing, advice etc.

Adrian Lawler (2007) reported that aquarium management requires knowing enough about many subjects in order to do all aspects of an aquarium operation, plus practicing constant diligence, observation and work. As they are dealing with living organisms held under unnatural conditions some failures are expected.

Lucy Kimball (2009) reported that the contributions to the building of knowledge about service design by studying the practices of consultant who call themselves service designer. There were three service design consultancies worked on projects with three science and technology based venture are paying attention to the service experience design of touch point; making a service

tangible and visible; conceiving of a service as on arrangement of artifacts, people and practice.

Mc Carthy(1964) offered the marketing mix often referred to as the four Ps' as a means of translate marketing planning into practice. The product, for maximum customer's benefit, price book keeping to the buyer's ability to afford the product made available for the customers to buy place and promoted in order that prospective buyers know as much as required about the product on offer.

Bejarano et al (1997) exposed the important role played by small group interaction in helping students develop learning strategies. Very little research however has been looked at the effectiveness of learning strategies such as brainstorming in the teaching of productive skills such as writing.

Rao (2007) found that students who has been trained in brainstorming techniques and used them frequently over a twelve-month period produced measurably higher results in writing tasks. In addition to this, an attitudinal survey showed that students who participated in this research project felt positive about the effectiveness of the brainstorming techniques.

Thomas Wreiner, Ingrid Mårtensson et al.(2009) reported that service blueprints were usually included in schedule of standard methods within service design. The case study explored how a blueprint was applied in a situation with three key actors, all with different motives and wishes. The case study was within the domain of car parking, a service which at a first glance seemed simple, but was rather complex when scrutinized. Three ways of blueprinting the situation were presented and discussed in the study.

Betul C. Ozkan (2004) describes that how qualitative data analyses pack up, NVivo, was used in a study of genuine and constructivist learning and teaching in the classroom. The study started with a outline of the research study in which NVivo was used to analyze the data and overviews the methodology that was adopted in this study. It, described how NVivo was used in the analysis of observational (video) data, interviews and field notes.

3. Research Problem

India has a population estimate of above 1.22 billion (2012) and India is the second largest in the world population, based on the population the demand is proposed to increase, hence companies are introducing various

service design for their consumers like Banking service, Hotels service, Hospitals service etc, the services are standardized properly by corporate companies. The ornamental fish aquarium business service is developing and very little efforts are identified in developing service mix for the aquarium business. The aquarium business service is attempted to design a structured service design like restaurants, coffee shop, and ice crème parlor. The study is aimed to enhance business growth and to fulfill the customers' expectations as services. Hence, the study is attempted to provide design up to prototype and the experimentation of the study is directed for further study.

4. Need for the study

The research aims to create the aquarium business service design in the prototype form with its service mix. The study offers alternative forms of aquarium designs. The marketing strategies via-a-via consumer preference for ornamental fish aquarium business service (A.Sankaran, 2010) and Indigenous ornamental fish marketing Kerala (Mini Sekaran, 2006) have been reviewed. The extension of aquarium service design helps to focus on the potential for aquarium business service.

5. Research Objectives

The following are the objectives proposed for the study

i) To assess the aquarium service design attributes with demographic factors and service mix
ii) To specify the aquarium business service mix performance standards for product, price, place, promotion, people, process and physical evidence.
iii) To formulate the aquarium business service design concepts using service mix and service design tools such as servicescape, in aquarium business service design.
iv) To develop design details for alternative forms of aquarium business services

6. Research gap

Many researchers have studied in the area of service marketing (service quality) by Parasuraman et al. Especially in the Indigenous ornamental fish marketing only four dimensions are studied. The studies pre-deteminantly focused on the ornamental fish forming, another one of the study on consumer preference vis- a- vis marketing strategies for ornamental fish

aquarium business service, this study mainly focused identified target consumer and marketing strategies adopted by ornamental fish aquarium business service providers. In aquarium business service design and especially in aquarium service design sectors very limited studies have been found. So there is a research gap identified to study all 7 P's service mix such as Product, Price, Place, Promotion, People, Process and Physical Evidence. Also there is need to study in aquarium business service design. Hence, these study design the aquarium business service and exploring the aquarium business service design alternatives.

7. Methodology

a. Research design

The study on aquarium business service design is attempted using both qualitative and quantitative research. Qualitative research aims to generate further research and theories rather than to verify them. It relies on transforming information from observations, reports and recordings into data into the written word. There are several different methods used in qualitative research such as Phenomenological research, Grounded theory, Ethnographic research, Action research, Historical research and Narrative. The researcher has selected the grounded theory research method, based on the perspective of constructing word by word or line by line analysis about aquarium service designs. The primary source of data for grounded theory research is drawn using interview describing a particular experience which is supported by aquarium exhibition and aquarium service design videos. The identifications of target customers and proposition of design details have been proposed to be studied using quantitative method.

b. Pre test

i.) Brain storming;

A brain storming session survey was conducted on service design for aquarium business in the department of business administration, in the University. Above 100 students took part in this survey. The participants were divided into 10 teams and a leader was selected for each team **(Annexure 1).** Colour pen, colour chart board and yellow sticker slip were given to the participants. Each team was given the serial number and the colour charts were pasted on the wall. In the given sticker slips the participants were asked to write their expectation regarding the aquarium business service using

service mix. The views of the participants were pasted on their respective charts on the basis of 7P's of service mix. The instructions were given to the participants by the researcher for 5 minutes and the participants were guided by the team leaders for each service mix. The instructions were provided in three stages, in the first stage, their foremost views about the service design for aquarium business service. In the second stage, the remaining views about the service design and in the third stage the views are re checked and at last the sticker slips were pasted on the chart boards. In the way the qualitative data were collected and discussed about the basis of service mix for about 45 minutes. The outcome of the session is presented for understanding of aquarium business service.

Product:

The first service mix in designing the aquarium business service is the product. The product which includes the aquarium tank with characteristics of high quality which is made of imported 3D glass, varieties that are attractive and easy available. The aquarium tank should be branded, and the tank wall mounted model which attract most people. The aquarium tank be fitted with air motors, colour light fittings, aquatic tree and different colour stones be arranged and the verity of fishes suggested are arovana, gold fish, shark are given the first preference by the participants. The preferred colours for the fishes are yellow, red, green and orange, sky blue.

Aquarium tank kept in the entrance gate which attracts most people and the aquarium tanks also be placed in the business organization. The suggested area for keeping aquarium reception hall, meeting hall, and conference hall and in houses the preferred spots like bed room, showcase, TV hall, guest room and prayer hall are suggested spots for placing and maintaining the aquarium tank. Doctors, officers and the business people are suggested as the target customers for aquarium business.

Price:

The second service mix is the price and the opinion about the price of the tank is suggested, based on the size such as the small size aquarium tank worth Rs. 6500, middle size tank worth Rs.10000 and the large size tank worth Rs. 15000 have been suggested by the respondents. Some of the participants had suggested that the price of the aquarium tank may be up to Rs.50000. the ornamental fishes in the aquarium tank price range from Rs. 25 to Rs. 500 in

which the type of fish, size and the colour are taken into consideration for the selection of fish for the aquarium tank. In the same way for cleaning and maintaining the aquarium tanks the price would range from Rs.100 to Rs.500 for small size tank, Rs.500 to Rs.1000 for medium size tank and Rs.1000 to Rs. 2000 for the large sized tanks. Those are the range of amount suggested by the participants for maintaining the aquarium tank service cost.

Place:

The third service mix is the place which includes the local markets such as Chennai and Tuticoran and the abroad markets are Hong kong. These are the places are suggested by the participants to buy the aquarium tank.

Promotion:

The fourth service mix is the promotion. The customers buying 4 or 5 fishes to be offered 1 fish for free of cost which was suggested by most of the participants. While buying the aquarium fish tank 1 year guarantee offered is expected, fish food for discounted rates and the customer be offered fish toys, small gifts which would attract most of the customers. The service design of the aquarium business is to be advertised in media, news paper and through exhibitions. The awareness be created in the mind of people to increase the growth of aquarium business methods for maintaining aquarium tank. The shop name, logo of the aquarium shopper be designed in such a way to meet the customer's choice to remember of the service design.

People:

The fifth service mix is the people. The people visiting in the aquarium shop be highly skilled glass technician, chemical technicians and also the people should have the well experience in maintaining the aquarium and should have the minimum PG graduate level of educational qualifications and the person should have the skill to identify the needs of the customers and the in a position to fulfill and problems of the customers regarding the aquarium business.

Process:

The sixth service mix is the process. The process of buying the aquarium business through mobile orders and online orders in aquarium tank and accessories are expected. The service is processed by providing reach to the customers and easy payment options.

Physical evidence:

The last service mix in designing the aquarium business service is the physical evidence. The dress code for the people working in aquarium shop be easily identifiable by the customers and the expected colours for the dress Varity from white, brown, gray, red, sky blue and also tank symbols and fish logo be printed in the dress to enhance the aquarium business service.

ii) Expert opinion in-depth interview (Branding Aquarium Business Service).

The Model of Aquarium Business Service Mix describes four P's of marketing mix (Product, Price, Place and Promotion, Philip Kotlor et al., (2005). **(Annexure 2)**

Product consists of six qualities as size, model and shape of tank, equipments, and tank type and fish size. Each quality has three varieties as variation 1, variation 2 and variation 3. The Product variation 1 consists of small, round and bound tank shape with water filter and re-use glass type and containing small fishes. The Product variation 2 consists of medium, imported and squire tank with aquatic tree and glass tank containing medium size fishes. The Product variation 3 consists of large, furniture type and landscape tank with air motor and molding tank containing large size fishes.

Price consists of six dimensions as discount, geographic area, rural price, urban price, metro city and service cost. Each dimension of price consists of three varieties as variation 1, variation 2 and variation 3. Price variation 1 consists of discounted fishes in rural area having price range <500 in rural area, 1500-2500 in urban and 5000-10000 in metro city. The cost of service for price variation 1 is cleaning cost. Price variation 2 consists of discounted tanks in urban area having price range of 500-1000 in rural area, 2500-3500 in urban and 10000-15000 in metro city. The service cost for price variation 2 is maintenance cost. Price variation 3 consists of discount on maintenance costs in metro cities having price range of 1000-1500 in rural area, 3500-5000 in urban area and 15000-20000 in metro city. The service cost for variation 3 is step up cost.

Place consists of geographic area, rural area, urban area, metro city, export market and import country. Each variable of place have three varieties as variation 1, variation 2 and variation 3. Place variation 1 is in rural area, having a petty shop in super market and promotion through exhibition. The

export market for this product is Singapore and imported from China. Place variation 2 is in urban area, having aquarium shop in rural and urban markets while as malls in metro cities. The export market for this product is Japan and imported from India. The Place variation 3 is in metro city with school area, hotels and theater in rural, urban and metro cities respectively. The export market for this product is Thailand and imported from Sri Lanka.

Promotion consists of door delivery, installments, advertising, aquarium club, client campaign and brand name. Each variable of promotion consists of three varieties as variation 1, variation 2 and variation3. Promotion variation 1 does not provide home delivery and advertising is done through notices. Forum and students campaign are conducted in order to promote brand like BP. Promotion variation 2 delivers fishes at door step with an option of weekly twice payment. Advertising is done through newspapers. Aquarium promoters and hobbyists are used for promotion of brand like Vastu. Promotion variation 3 delivers aquarium tank at door step with an option of monthly payment. Advertising is done through TV ads. Hobbyist and households are used for promotion of brand like Visual Buffy.

iii) Service blueprinting for aquarium business service

Service Blueprinting is a service planning help tool. It has been used for developing aquarium business services as well as for improving existing services. The method is also appropriate for ensuring the service quality processes. It has been used for identifying users experience activities and service provider's action overview. The Service-Blueprinting output consists of a graphically-presented overview of the service process and its activities. Service-Blueprinting allows for visualization of the service development process in its early stages. In each process step, such as physical evidence, aquarium user's activities, contact service provider's actions, if tangible services become visible and invisibles and supportive process.

The service blueprint model for aquarium business service design using service mix, there are two main objectives of the Blueprint **(Annexure 3)**. The first is to analyze and see the aquarium customer's interactions, while the second is to have a map that enables better judgment of the business service design. For the purpose of service quality and service design generalization, the five genuine levels of the service Blueprint as.

The starting point of the service process is the aquarium business service design. The first stage of service blueprint is customer's activities in the aquarium business service. Typically, the aquarium keeping customers will plan to buy aquarium describe the reason from their perspective hobby, vastu and institutional use. Next, the customer arrives at aquarium service shop. After speaking and enquiry with the aquarium service providers about the aquarium models availability, fish varieties, accessories, price details and maintenance service details. During the customers visit to shop, they select suitable aquarium tank, color fish, and its accessories. After successful selection of aquarium, choose suitable place, the service shop provides an invoice for setup services rendered. The customer makes payment when the process is finished. In the shops, follow up customer service is considered as a separate service function. Finally, the aquarium keeping customers, benefits to playing, enjoying, get relaxing and establishing aquarium keepers as hobby.

The second step appears in the onstage visible contact level are all perceivable by the customers; he/she is integrated in the process such as customer's expectation, existing service, aquarium setup and maintenance. The third step of backstage processes includes fish breeding and ordering, maintaining customer's details, service instruction to service man, cost fixation, service man travels, service delivery and invoice preparation etc. are not perceivable by the customers.

The fourth step as supportive process are the backstage operations that needed in order for the service to function. These processes usually take the form of a database, purchase order system, knowledge based systems, service delivery systems, manufacturing systems and service quality system that the backstage service providers depend upon in order to complete the service request.

The fifth step showcases the evidence as one component of the service than the most readily available design input. For the service provider, it presents opportunities for introducing local TV advertisement, personal communication, sign board, family friends and compare another shop quality. Taking those design concepts to an aquarium business service environment is parking facility, waiting chair, employee uniform, discount, door delivery and good environment. At times, additional service evidence was needed to be created in order to complete the design for a positive service experience.

8. Main study

The aquarium keeping customers expectation regarding to the service design have been studied in this research. An advertisement has been announced at the fish - show exhibition in Chidambaram using print and multimedia tools. After collecting the details regarding the fish exhibition, I and my research supervisor got a possibility to meet one of the "Saravana Fish Show" exhibition partners. I explained about the plan of my research work and I got the details about the aquarium exhibition service as well as permission to collect the data regarding my research work.

The aquarium visitors 63 were interviewed regarding the aquarium service design and the consumers who are having an aquarium in their home, and the people who are willing to keep aquarium were interviewed using the well prepared interview schedule and the interview was video recorded.

The interview was conducted only to the users of fish show who have the interest in the interview. In this interview, the information regarding to the maintenance of aquarium, the expectation of the aquarium business service design have been exchanged.

a. Sampling

The sampling is based on purposive method conduct in depth interview with 63 aquarium customer and 25 aquarium service providers, 20 aquarium images, 5 video files and 12 aquarium WebPages.

b. Length of in-depth interview

Each interviews lasted from 10 minutes to half hour in exhibition area, and video recording for interview discussion.

c. Statistical analysis

The researcher has adopted relevant statistical tools for analysis data describing aquarium business service design the following are the relevant tools used for analysis of data viz., Grounded Theory Methodology (axial coding) Strauss and Corbin (1990) have been selected for the proper of analysis of servicescape measures (Gap Analysis, Blue Print Process).

9. Analysis and Findings

I) Mapping the Aquarium Business Service

In this section, we present the outcome of the interviews, according to the methodology explained. The aquarium business service customer's requirement was the main category of this research study. Then the research focuses each one as activity, interface, artifacts, and improvement of aquarium business service. After that the main challenge of this section was to express in a consistent way that contributed human activity modelling (HMA), service blueprint model. The service blueprint model was to introduce aquarium business service as customer requirement to the aquarium keeping service design. Also, we considered all the customers activities and customer expectations and focused on the overall customer's activity, interface, artifacts and service design.

i) Activities

Service analytical view of users' activities in rural area

Each activity in rural area encompasses several action or task specific to their lifestyles. Figure 1 shows that all representation of all the task, and activities of aquarium business service. Table 1 shows the partial coding tree for the aquarium business service activities in rural area and its source categories. There were 12 numbers of aquarium shops interviews, 5 numbers of image files,4 numbers of aquarium WebPages and 1 aquarium service related video having duration of 15 minutes and 33 numbers of aquarium users interview. The tables included that sources, code reference counts and respective percentages of aquarium service activities.

The user's requirements have been found as recreation of hobby (20%), children (8%), and museum (1%). Relaxation related responses have been found to relax (3%), to reduces stress (2%), and to other pet animals (2%) such as birds (1%), rabbit (1%). The responses have indicated to designing in residential (17%) house and interior office design (3%). Finally, up-gradation for aquarium related coding referred to marine tank (1%), aesthetic value for sentiments (6%) (vastu shastra), and customer need of seeing marine fish movements (3%).

The second category of customer activity link for searching information indicated that 11% of responses searched through referrals friends & relatives, 2% of responses have equally searched through both online & offline media. The customers were contacting through phone (18%) and personal (14%). There were 1% of responses depicted that the customers were

shopping with father and son, and 1% of customers have paid full. It was about 6% of responses have expected tank setting up for service man. In addition, the responses have shown the need for medication service (5%), self feeding service (4%), and aquarium keeping service in restaurant & Hotel (3%).

Service analytical views of aquarium users activities in urban area

The activities in urban area called for several action or task. Figure 1 shows all the tasks, and activities of aquarium business service. Table 1 shows the complete coding tree for all the aquarium business service activities and its source categories. There were 13 numbers of aquarium shop interviews, 15 numbers of image files,8 numbers of aquarium WebPages and 4 numbers of aquarium service related video with duration of 15 minutes and 30 numbers of aquarium users interview included. The tables included that sources, code reference counts and respective percentages of aquarium service activities.

The user's requirements have been identified as recreation of hobby (22%), for adults' fun for children (14%) and education through museum (4%). Relaxation related responses was found to relax (7%), to reduce stress (6%) and to keep other pet animals birds (3%), rabbit (3%) and dog (1%). The responses drawn for design activities have been categories as designing residential house (19%) and designing interior office (8%). Finally, up-gradation of aquarium activity have referred to breed aquarium fish (1%), to crate aesthetic value of sentiments (vastu shastra) (7%), to have special treat of seeing marine fish movements (5%).

The second category of customer activity link for searching information indicated that 13% of responses for referrals through friends and relatives, 5% online & offline media. The customers were contacting through phone (23%) and person (20%). Only 1% of users have got formal quotation for aquarium business service. There were 3% of responses depicted that customers experienced shopping with father and son. The purpose of hiring (1%) and cash purchase (4%) was reported for an aquarium purchasing activity. It was about 6% of responses have referred to tank setting up buy service man. In addition, the responses have referred medication service (8%), self feeding service (4%), and maintenance service, in restaurant & hotels (4%) and return service of aquarium tank either for up-gradation or after tired of cleaning & maintenance (1%).

Findings from activities based customer value constellation

As a result of understanding customer requirement, the constellation of customer value constellation reflected companion (Pet) and designing (aquascaping). In addition, aesthetic aquarium service, marine aquarium service and aquarium up- gradation service were the most closely related aquarium keeping value identified with aquarium business service. We expanded this analysis links by introducing other categories into picture like artifacts and interfaces. By doing this, we developed a better understanding of the contextual surrounding related with the aquarium service usage.

ii) Artifacts

Artifacts observed in rural area

It was inferred that the responses identified through the coding for aquarium tanks indicated glass tanks medium size (14%), moulding tanks of small size (5%) and small size tanks (3%). In the case of aquascaping artifacts, stone (6%), rocks (4%), artificial plants (7%) have been referred. The motorized artifacts included light (6%), air motor (5%) and non-motorized accessories. The design of wall papers (2%), fresh water (2%) have been referred. In addition, aquarium colour fishes as gold fish (13%), vastu fish's arowana (9%) and flower horn (8%) referred in the sources. Fish colour (1%) specified in the interview was clown marine fishes (1%) referred from sources. The fresh water fish food majorly referred by 4% of users. The users expected to have aquarium normal shop size (8%), with medium size design (2%). The service tools & equipments reference code was observed among 6% of responses from the rural area based sources of data.

Artifacts observed to urban area

It was found that most of respondents were of the view that the exhibit displayed medium size glass tank (21%), small size tanks (17%) and moulding tanks of small size (15%). In the case of aquascaping artifacts, stone (18%), rocks (15%), artificial plants (17%) have been widely pronounced. The motorized artifacts included light (15%), air motor (11%) and non-motorized accessories. The design of wall papers (7%) and fresh water (6%) have been referred. In addition, aquarium colour fishes as gold fish (24%), vastu fish's arowana (18%) have been mentioned and flower horn (18%) referred in the sources. Fish colour (4%) specified in the interview was clown marine fishes (5%) referred from sources. The fresh water fish food majorly referred by 8% of

users. The users preferred to buy from a normal shop size (11%), with moderate design (6%). The service tools & equipments reference code was shown 11% by artifacts categories.

Findings from artifacts of aquarium keeping

As a result of aquarium business service artifacts matrix, coding for the above item it was found that their aquarium fish tank and colour fish both for a new service and the existing service. Some of them even said that it was better to focus moderate fish variety and major eight varieties of glass tank models and additional service man and service design requirements to cope with changes. It gave rise to the concepts in aquarium service design as new business service.

iii) Interface

Interface observed from Rural area

It was found that most of respondents were of the view that majority of aquarium keeping for hobbyist (Living Street) 20% and aquarium shop/office (8%), and shopkeeper (6%), and internal aquarium service man (4%), aquarium technician (4%). Some other interface codes to the level of giving opinion below 6% have referred in sources

Interface observed from Urban area

It was found that most of respondents were of the view that majority of aquarium keeping for hobbyist (Living Street) 22% and aquarium shop/office (10%), and shopkeeper (8%), and internally aquarium service man (11%), technician (6%). Some other interface codes to the level of giving opinion below 5% have referred in sources.

Findings from interface

As a result of interface coding for the below item it was found that most of the respondent were of the view that their interaction point for aquarium was due to aquarium hobbyist in the living area, aquarium shop/office, technician and service man. It was a new service needed when the existing service was not addressing various issues. Some of them even said that it was better to launch aquarium hobbyist club and event for pet animals to identify new service design to make users more participative. It gave rise to consider design of a new aquarium business services.

iv) **Positive and Negative impact on aquarium service requirements**

Negative aspects of aquarium service in rural area

The product based customers requirement with negative coding categories referred in sources were aquarium manual tank cleaning (18%), daily attendance to aquarium(13%), no support medication (6%), high fish mortality (3%) . The negative coding referred in sources for price were such as high price of fish medicine (5%), food cost (3%), and high competitive price (1%), and expensive tanks (1%). Place based negative categories referred in sources were poor environment for aquarium shop (9%), and lack of delivery support (1%). Promotion based negative coding referred in sources were fish care (9%), no guarantee for fish/tank (1%), ordering and promoting (1%) and grown water plants (1%). People based negative categories coding referred in sources were unavailability service man (4%), as well as limited number of technician (4%). The process based negative categories referred in sources were water replacement process (18%), fish disease (15%), frequent feeding & maintenance (5%) and coordinating service setting up (1%). Finally, physical evidence based negative coding sources referred sign board (3%), no (uniform) dress code (2%), lack of bills and receipt (1%).

Negative aspects of aquarium service in urban area

The product based customers requirement with negative coding categories referred in sources were aquarium manual tank cleaning (25%), daily attendance to aquarium(14%), no support medication (6%), high fish mortality (5%) . The negative coding referred in sources for price were such as high price of fish medicine (8%), food cost (4%), and high competitive price (2%), and expensive new model tanks (1%). The negative categories referred in sources for place were poor environment for aquarium shop (8%), and lack of delivery support (1%). The negative coding referred in sources for promotion were fish care (9%), unavailable guarantee for fish/tank (1%), lack of support for ordering and promoting (1%) and unavailability of water plants (1%). People based negative categories coding referred in sources were unavailability service man (11%), as well as limited number of technician (6%). The negative categories referred in sources for process were water replacement process (25%), fish disease (22%), frequent feeding & maintenance (7%) and coordinating service setting up (4%). Finally, physical evidence based negative coding sources referred sign board (9%), no (uniform) dress code (3%), lack of bills and receipt (1%).

Findings of negative aspects in aquarium service requirement

As a result of aquarium business service customers' requirement negative matrix coding for the above item, it was found that most of the respondents were of the view that their aquarium fish tank manual cleaning, daily attendance, disease of fish, water replacement and shop sign board. Some of them even said that it was better to launch aquarium service- man support service and additional aquarium design service before the customers change their interest level. It gave rise to the aquarium concept considering additional business service. Finally, there was also a need for increased aquarium tank cleaning service, improvement in relation with aesthetic, marine & up-gradating the customer support service, aquascaping, setting up, competitive price of existing aquarium tank, and keeping quality of healthy colour fish.

Positive aspects of aquarium service in rural area

The positive categories coding tree for aquarium keeping customers' requirement levels was based upon service mix such as product, price, place, promotion, people, process and physical evidence. The positively categories for Product based coding in sources referred were 'good hobby' (20%), availability of fishes (9%), new arrival of fishes (13%), more types of fish tank (14%), availability of rare collections of colour fishes (1%), fun for children (13%) and low cost accessories (2%). The customers' positive responses for price were special price on size of tanks (8%), easy payment (4%), low price for ordering glass tank (2%), price benefits for customers (1%) and warranty for motorized accessories (1%). The positive aspects of aquarium service for place based sources design aquarium were shops (3%), suggesting for locating aquarium (1%) and modification of theme of aquarium using plants (1%). Aquarium keepers' opinions for promotion were local TV ads (4%), display of shop name (1%), festival exhibitions (campaign) (1%). The codes referred for people in aquarium service were shopkeepers' experience in offering instruction to customers (6%). The coding referred for process in aquarium business service were aquarium setting up process (2%), shoppers' contacting process (18%) and easy ordering process (4%). The coding for physical evidence in aquarium service were aquarium shop appearance (2%), vehicle parking (2%).

Positive aspects of aquarium service in urban area

The positive categories coding tree for aquarium keeping customers' requirement levels was based upon service mix such as product, price, place,

promotion, people, process and physical evidence. The positively categories for Product based coding in sources referred were 'good hobby' (22%), availability of fishes (18%), new arrival of fishes (23%), more types of fish tank (21%), availability of rare collections of colour fishes (4%), fun for children (13%) and low cost accessories (1%). The customers' positive responses for price were special price on size of tanks (6%), easy payment (4%), and low price for ordering glass tank (2%), price benefits for customers (1%). The positive aspects of aquarium service for place based sources design aquarium were shops (2%), suggesting for locating aquarium (1%) and modification of theme of aquarium using plants (1%). Aquarium keepers' opinion for promotion were local TV ads (6%), display of shop name (6%), festival exhibitions (campaign) (1%) and local newspaper advertising (1%). The codes referred for people in aquarium service were knowledgeable aquarium shopkeepers (1%) and shop keepers' experience in offering instruction to customers (8%). The coding referred for process in aquarium business service were aquarium setting up process (8%), shoppers' contacting process (23%) and easy ordering process (1%). The coding for physical evidence in aquarium service were aquarium shop appearance (8%), vehicle parking (6%), visiting card (6%) and shop logo (1%).

Findings of positive aspects in aquarium service requirement

As a result of assessing customer's requirement for positive matrix coding, it was found that most of the respondents were of the view that various sizes of aquarium fish tank, fish verities, accessibility, shop- keeper instructions, knowledgeable staff and aquarium keeping as a hobby. Some of them even said that it was better to launch aquarium service promotional activities and new service designs such as users changing life style. Finally, there was also desire for increased aquarium business service mix as combination of promotion, process, and physical evidence.

v) Suggested improvements category

Suggested improvements in aquarium service rural area

As a result of suggested improvements for aquarium service matrix coding, it was found that most of the respondents were of the view that additional cleaning was required by 11% with the help of service man, 12% of sources have referred to add more value of existing service, 9% of sources referred poor environment at the shop, 2% of sources indicated for colour of

fishes (aesthetic value fishes), 8% for more varieties of glass tank models (salt aquarium), 10% of sources for technical improvement, and even 1% of sources indicated that up-gradation of new model design tank. It gave rise to the concept of considering overall improvement for aquarium business service.

Suggested improvements in aquarium service urban area

As a result of suggested improvements for aquarium service matrix coding, it was found that most of the respondents were of the view that additional cleaning was required by 12% with the help of service man, 9% of sources have referred to add more value of existing service, 8% of sources referred poor environment at the shop, 6% of sources indicated for colour of fishes (aesthetic value fishes), 5% for more varieties of glass tank models (salt aquarium), 6% of sources for technical improvement, and even 4% of sources indicated that up-gradation of new model design tank. It gave rise to the concept of considering overall improvement for aquarium business service.

Findings of improvements for aquarium service

Finally, there was also a desire for increased aquarium tank models, new colour and pattern fishes for children and good-looking shop ambience in relation to the aquarium business service with customer support service. To fulfill designer skills in design of tanks with aquascaping model, fish for aesthetic value any family for future plant & themes, marine fish for exoistic fishes. Increased aquarium tank cleaning, technical service man and value addition of existing aquarium business service were the activities trusted upon service providers. In addition, up grading to setting up tanks and moderate to size of fishes.

10. Limitation of the study

The focus on the study is mainly based on aquarium keeping consumers. The study has been carried out to understand the consumer expectation and service design for aquarium business service. Since, aquarium consumers and aquarium fish exhibition visitors only interviewed for the study and this is the limitation of the study. Many aquarium visitors are partially willing to give the information and limited awareness of aquarium maintaining and also service design.

a. Scope of the study

Aquarium business service design provides enormous scope to carry out the continuous research. This study suggested a more areas for further research. More dimensions like service quality, customer satisfaction, service gap model.

The study on aquarium business service design facilitate study in other service sectors such as banking, couriers, postal, hospitals, pet care clinic and new innovative service business.

11. Conclusion

This study aimed to explore the current practice and the customer experience, expectation, perception and view of a aquarium keeping customers with regards to the service design. A qualitative research strategy has been selected as appropriate for this particular research area. A study collected data analysis has been utilized and purposive sampling has been used to identify potential research participants. A grounded theory approach and service design tools such as blue print and gap analysis approaches to data analysis was used for the study.

Reference

1. Robert Fenner (2001). "The pet business – is it for you?" www.wetwebmedia.com
2. Sudhi K.S. (2002) "All about ornamental fishes" The Hindu Online edition of India's National News papers, Thursday, Mar. 14.
3. LIffy Thomas (2010) "Demand on the rise for ornamental fish". The Hindu Newspaper, Jan. 21(P2).
4. Martin Theore (1999) "Ornamental Aquarium Fish in India". Wednesday 1, September
5. Paul Lajicek et al. (2009) "A Florida marine ornamental pathway risk analysis" Reviews in Fisheries Science, Vol. 17, Issue 2, page 156-169.
6. Robert Fenner (2001) "Aquarium Service Business" www.wetwebmedia.com
7. Jay Show (2002). "Setting up an aquarium maintance business part:11 marketing and services".
8. Mandal subhasis et al. (2006) "Agribusiness opportunities of ornamental fisheries in north-eastern region of India.

9. Duane Clark (2002). "Aquarium maintance service... who should start one" aquarium fish magazine.
10. Jason Shaw (2001). "Fish health" the fishy times, Campbell river aquarium society, B.C. Canada.
11. Kevin Thurston (2002). "The commercial aquarium fish supply chain", www.aquarticles.com
12. Dr. Adrian Lawler (2007). "Aquarium management" www.aquarticles.com
13. Andrew Palfreman (1999). "Strategy – marketing – development" fish business management.
14. Strauss and Corbin (1990)
15. Sankaran A. et al., .(2012) "Marketing For Ornamental Fish Aquarium Seller's Business Service", IJEMR – January 2012-Vol 2 Issue 1 - Online - ISSN 2249 – 2585 - Print - ISSN 2249 – 8672, Bangalore, India.
16. Christoph riedl etal (2009) "new service development for e-service-a literature review, proceeding of the 15th America conference on information systems, san Francisco, californiya, Aug.6th -9th .
17. Shu-ping lin (2012) "a study on the service design model in health care cloud industry". Business and information, Sapporo, July 3-5.
18. Larry J.mener etal. (2002)" new service development; areas for exploitation and exploration, journal of operation management, P.135-157.
19. Raberto M.saco (2008) "service design: an appraisal", design management review. P10-19.
20. Lucy Kimball (2009) "insights from service design practice", 8th European academy of design conference-1st -3rd April. The Robert Gordon University, Aberdeen, Scotland.
21. Frankel, R.M. & Devers, K.J. (2000b). Study design in qualitative research—1: Developing research questions and assessing research needs. *Education for Health*, *13*, 251–261
22. G Hollins and W Hollins, Total Design: Managing the design process in the service sector, Trans Atlantic Publications, 1991 (republished 2002 in its original form),ISBN 0273033387
23. Factfinder (2007) 'the value of design' design council, www.service-design-network.org

24. Sagar C. Mandal et al., (2013)"Culture of Ornamental Fishes and Entrepreneurship Development"
25. Fredrick Nyongesa Oduori (2010) "New Service Development:strategy and process in the hospitality sectors in Kenya".

Annexure 1

Attributes identified [Brain storming]

Product	Price	Place	Promotion	People	Process	Physical evidence
Tank : Quality tank 3,D glass Import glass tank Attractive design Branded Durability Availability **Tank size:** S- 2x2 M-4x2 L- 10x10 **Tank model:** Landscape Vertical Wall mound **Equipment's:** Air motor Colour light Aquatic tree E-bump	**Tank price:** S-O6500 M-O10000 L-O15000 Above O750-O50000 **Fish price:** O25-500 **Tank cleaner:** O240 **Service :** S-	**Market** Local Channai Tuticoran Ubroad (konghong) **Home :** Bet room Showcase TV hall Guest room Hall Entry gate **Industry / institutions** Reception Club Market place Meeting hall Conference hall	**Offer/Discount:** Festival offer Seasonal offer Offer 4F/1F Guarantee 1yr. Gift Toys Discount Free sample Free food Scheme coupons **Service :** Logo Shop look Shop name Demo Display Security User manual guide **Advertisement:**	**Technicians:** Glass tec. Chemical tec. A/c tec. Mechanical tec. Sales executives **Knowledge:** P.G qualification Experience **Behavior:** Good communication To attract person Nice person Rich family person	**Order :** Mobile Online Catalog Personnel meet **Service :** Delivery Repair Online Daily cleaning Cash payments	**Dress :** Formal dress with shoos & tie. School uniform **Colour:** White Brown Gray Red Sky blue **Evidence Symbols:** Fish glass Fish logo

E-board Food stand **Stone :** Colour stone **Medicine :** **Fish :** Arovana fish Gold fish Shark fish Horse fish Healthy fish Quality fish **Fish colour:** Yellow Steel Silver Green A ranch Red White	O2000-O5000 M-O500-O1000 L- O100-O500	Prayer hall Hotel Hospital Functions Mall's Super market Schools	T.V ads. Print media Internet Exhibitions Stress reduces related ads.	**Target people:** Doctors Officers Town people		

INTERNATIONAL JOURNAL OF MULTIDISCIPLINARY EDUCATIONAL RESEARCH
ISSN : 2277-7881; IMPACT FACTOR - 2.972; IC VALUE:5.16
VOLUME 3, ISSUE 10(4), OCTOBER 2014

Annexure 2

Product variants [Expert Opinion]

PRODUCT:	**Size**	**Model**	**Shape**	**Equipment**	**Tank Type**	**Fish**
Variant 1-	Small	Bound	Round	Water filter	Re-use glass	Small size
Variant 2-	Medium	Import tank	Square	Aquatic tree	Glass tank	Medium size
Variant 3-	Large	Furniture tank	Landscape	Air motor	Molding tank	Large size
PRICE:	**Discount**	**Geographic Area**	**Rural Price**	**Urban Price**	**Metro City**	**Service Cost**
Variant 1-	Fish	Rural	<₹500	₹ 1500-₹ 2500	₹ 5000-₹ 1000	Cleaning cost
Variant 2-	Tank	Urban	₹ 500-₹ 1000	₹ 2500-₹ 3500	₹ 10000-₹ 15000	Maintenance cost
Variant 3-	Maintenance	Metro city	₹ 1000-₹ 1500	₹ 3500-₹ 4500	₹ 15000-₹ 20000	Set up cost
PLACE:	**Geographic Area**	**Rural Area**	**Urban Area**	**Metro City**	**Export Market**	**Import Market**
Variant 1-	Rural	Petty shop	Super Market	Exhibition	China	India
Variant 2-	Urban	Aquarium shop	Aquarium shop	Malls	Japan	Srilanka
Variant 3-	Metro city	School area	Hotels	Theater	Thailand	Singapore
PROMOTION:	**Door Delivery**	**Installment**	**Advertisement**	**Aquarium Club**	**Client Campaign**	**Brand Name**
Variant 1-	Not applicable	Weekly	Notice	Forum	Students	BP
Variant 2-	Fish	Weekly twice	News paper	Aquarium Promoter	Hobbyist	Vastu
Variant 3-	Aquarium tank	Monthly	TV ads.	Hobbyist	House holder	Visual beauty

Annexure 3

Blueprinting Process Model (Proposed)

BLUE PRINT OF AQUARIUM BUSINESS SERVICE DESIGN USING SERVICE MIX- USER ACTION TO SERVICE PROVIDER'S REACTION

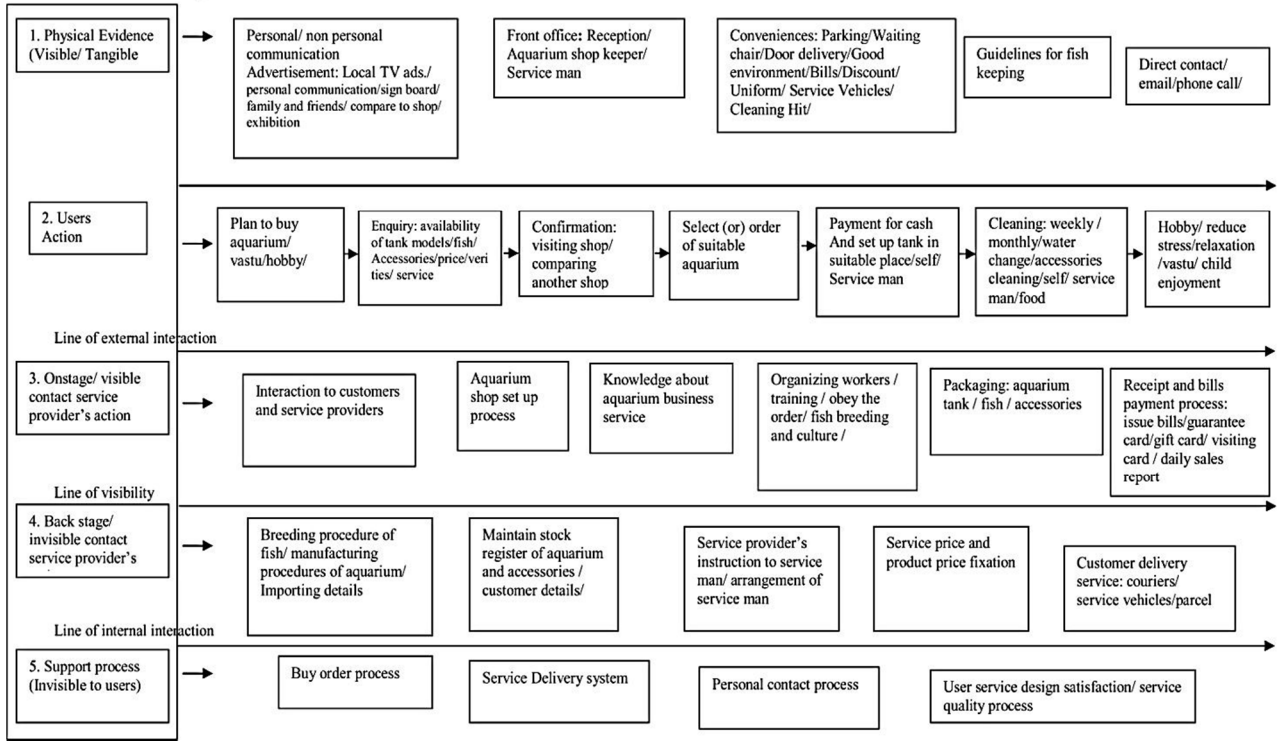

INTERNATIONAL JOURNAL OF MULTIDISCIPLINARY EDUCATIONAL RESEARCH
ISSN : 2277-7881; IMPACT FACTOR - 2.972; IC VALUE:5.16
VOLUME 3, ISSUE 10(4), OCTOBER 2014

A STUDY ON CAUSES OF LOW ACHIEVEMENT IN ENGLISH AMONG TELUGU MEDIUM PUPILS AT SECONDARY LEVEL

Dr. M. Solomon Raju
Assistant Professor
Department of Education
Andhra University Campus
Vizianagaram

INTRODUCTION:

Education plays a major role in the development of a nation. Where the people are more educated, there the development will also be more. Education is a process through which an individual develops his individuality and a person develops his personality. The main feature of an educational process is to bring about the best in the individuals. Different philosophers have given different interpretations in their own way about the purpose of education. So the education is a perfect tool that can shape a man into super human being. This transformation of man into superman who can adopt himself to the environment, through the language as the medium of exchange of ideas from one person to another, in this connection English place a vital role as a global language. According to F.G. French "No language, whether it is ancient or modern can be compared with English in the number of geographical distribution of homes, factories and offices in which that a language is spoken, written and read".

Man and the Language:

We learn how to think, how to feel, judge through the aid of and within the constraint imposed upon by the words, idioms and syntax of our language. Since the ages, even from the India Indus valley civilization, people tried to use verbal mode of communication carved in their seals in picot-graphic from. This is the same case with ancient civilizations of the world in preserving their experiences and expressions in the form of language. Language consists of words, idioms and syntax and it is through language that are learn to think, feel, Judge and express. The rich heritage of great ideas and actions possessed over to the young generation in terms of its own language. So every individual maintains his own languages.

Meaning and Definition of Language:

"Language is thought to be any means of expressing emotional or mental aspects by any living being what so ever through communication from one to the other living beings." In its specific sense, "Language is such expression and communication by human beings by means of speech and hearing". As we turn the pages of history, in the world as well as in our own country; we will be wondered to notice the role played by different languages. Especially in the case of English language, being a foreign language, it dramatically changed the human relations world over. It helped in strengthening the ties among the world nations. English language also helped unifying the different States of country.

Language is an essential part in human life. Everyone from birth to death makes use of it. Besides, it is a means of communication and social control, according to O. Jesperson language is set of human habits, the purpose of which is to give expression to thoughts and feelings of social group. But if is a foreign language for Indians. So it becomes necessary to think over about its place in school curriculum.

Place of English in India before and after Independence:

The history of English in India goes, back to pre-independence days when this country was ruled over by the British with the establishment of "East India Trading Company" in 1600 Ad; the language of the rulers was brought into India for running their business with the country on a more safer and profit lines. The Governor General of India, William Bentick appointed a commission headed by a famous law member of the directors of East India Trading Company, he is maculae and the suggestions to the government known after him as maculae's minutes passed in February, 1835. Then English was introduced in the Indian education system and since then English language had been dominating other Indian language and occupied an apex position in the field of education as well as administration in India.

Theses following reasons say English played a predominant role in the system in the post independence are:

1. It was the official languages of courts and administrative offices. 2. It was the medium of instruction in the educational institutions those were depended on government aid. 3. It was the medium of examinations. 4. It was a

compulsory subject 5. It was a language of the press and media and 6. It was a language of records.

After independence drastic changes come in the Indian panorama, about the place of English in India. The centuries, when the rule of birth was began, it was a language of rules. It is devious that English did not have the same place after independence which it had before. But in recent years the government of all states in Indian recognized the importance of English languages after 1992 owing to economical reformation (i.e.: liberalization, privatization and globalization). Every potential parent, in terms of finance which to join their children in English medium school in order to make their children compete in global markets of jobs.

The knowledge of English keeps a person at a highest pedestal than those around him when it comes to the question of employment opportunities. At present, the importance of English language in the educational system of India recognized widely from K.G. to P.G. Hence the place of English in the system of education elicited as follows.

Place of English in the System of Education:

V.K. Gokak, director of C.I.E.F.L, Hyderabad, rightly observes "whatever the controversy may exist regarding the validity of English of the official language or as medium of instruction in our educational institutes, almost everyone realizes the almost need to schools and colleges for many years to come. The four aims of English language are:

1. To listen English: The student can acquire the sound habits of English pronunciation
2. To speak English: They should able be conveys fluently in English with proper stress and intonation, accurate pronunciation.
3. To read English: He should more over be able to read and understand and English news papers, books, magazine and other English literature.
4. To write English: He should be able to write simple letters. Fill in application, write descriptions and report any event. This will enable the student to work effectively and to take notes lectures.

   b) To convenes freely on topics of every day interest within the prescribed language items.

c) To read with understanding books written in English within the prescribed range of vocabulary and sentence structures.

d) To write correctly in English on families topics cable to be expressed within the prescribed range of vocabulary and sentence structure.

Significance of the Study:

Man's greatest achievement and the sign that above all other distinguishes him from the great age is language. Language makes possible the communication of meanings and the sharing of experience among people enable them to from an enduring society and to create and transmit a distinctive culture. Thus language is one of the most important characteristics form of human beings. After independence, India could not accept English as her lingua-France, but English is an international language of science technology, politics, trade, civilization and culture. Indian English is till marked by its superior purity and free from modern along because it is a part of international heritage. The study of English is both necessity and an advantage. Even with English we may be bad keeping in view of national integration, but without it, we shall be worse. Secondary education commission (1953) recommended that the mother tongue or the regional language should generally be the medium of instruction throughout the secondary school stage. During the middle stage every child should be taught at least two languages.

English and Hindi should be introduced at the junior basic stage, subject to the principals that no two languages should be introduced in the same year. According to above requirement and importance of English language, it had been thought in Indian schools. Inspite of more efforts put for the development of the English languages skills among Telugu medium students at secondary stage, low achievement is seen in the results at various levels of examinations. The researcher has visited some schools and gathered the results of the students in English language.

- In government Boys High school, Vizianagaram, the researcher found the percentage of passed candidates in English in VIII, IX AND X classes below 65 where as it is more than 65 percent in remaining subjects in quarterly and Half yearly examinations.

- In Zilla parishad High school, Kadiyam, the percentage of passed candidates is less than 55, where as it is more than 60 percent in remaining subjects in quarterly and Half yearly examinations.
- In Sri Nannaya Municipal High school the percentage of passed candidates in low 50 and 55, in quarterly and Half yearly examination respectively, where as in other subjects it is above belongs to above 65 percent. By observing the scores of the students schools, it is clear that there is the low achievement in English than the remaining subjects. The researcher wants to study the factors responsible for low achievement in English. Hence the significance of the study is put for the with the title given below "Causes of Low Achievement in English among Telugu Medium students at Secondary Stage in Vizianagaram District".

Objectives of the Study:

The major objective of the present piece of research work is to study the causes of low achievement in English at secondary stage. The following are the specific objectives formulated for the present study.

1. To study the Academic factors responsible for low achievement in English.
2. To determine the personal factors responsible for low achievement in English.
3. To find out the environmental factors responsible for low achievement in English.
4. To study the difference re-going the factors formed for the study.

Hypothesis:

For the present piece of research work, the researcher has employed the Null Form of hypothesis for the purpose of the study. The hypothesis of present study are as follows.

1. There will be no significant difference in the opinions of the students with respect to academic factors responsible for low achievement in English.
2. There will be no significant difference in the opinions of the students with respect to personal factors responsible for low achievement in English.

3. There will be no significant difference in the opinions of the students with respect to environmental factors responsible for low achievement in English.
4. There will be no significant difference in the opinion of the students with respect to factors of the study.

Limitation of the Study:

- The present piece of research work is limited to Vizianagaram District only.
- This study confined to Telugu medium schools only.
- This study involves VIII, IX and X classes at secondary level only

REVIEW OF THE RELATED LITERATURE

The term 'review' means to organize the knowledge of the specific area of research to evolve an edifice of knowledge to show that his study would be an addition to this field.

- Satyavalli, A (1986), the study touched the causes of Backwardness in English among secondary school pupils. The researcher for formulated some of these objectives, to determine the causes of low achievement in English. To determine the relationship among academic and non-academic factors responsible for the low achievement in English. The study revealed significant difference has been observed between urban and rural sample covered under the investigator. Significant difference has been observed between different management schools. The schools covered under the study shown variation between boys and girls on low achievement in English at secondary stage. Though the above all studies revealed may findings regarding academic and environmental factors responsible for low achievement in English. This piece of research work is different from those study respect to population sample and the design.

DESIGN OF THE STUDY

Method of the Present Study:

For the present study the researcher has adopted the descriptive or the Normative survey method. This normative survey method of research concerns itself with the present phenomena in terms of conditions, practices, beliefs, process relationships or trends are variously termed as descriptive status, normative or trend study or survey.

This normative survey method is useful for collecting the responses from the sample chosen out of the population falls under the Jurisdiction of the areas covered for the researcher purpose. The population and sample for the present study was selected by the researcher as per his research work for causes of low achievement in English among Telugu medium schools as discussed below.

Population and Sample of the Study:

The entire mass of observations from which a sample is to be formed is its population. – J.W. Best. Accordingly to above quotation the population for the present study was laid in the district of Vizianagaram and that too Telugu medium schools under different managements. The size of the universe or the population covering Vizianagaram District. From the universe as taken above, the researcher has chosen the probable sample to carry out the research keeping the physical barriers and wide coverage of geographical area of the Vizianagaram District. The percentage of passed candidates in English when compared to other subjects is low and accordingly the sample was taken. Hence the population and the sample wherever is data possible for the research work is somewhat justifiable. This sample is covered in different management schools, the type of the school, locality and sex as variables. The variables taken into consideration for the research work is depicted as under:

1. Sex Boy / Girl
2. Locality of the School Urban / Rural
3. Type of Management Govt. / Local Body / Private
4. Type of the school Boys / Girls / co-education

Sampling Technique:

To conduct this piece of research work as discussed above, the researcher also employed simple Random sampling technique. In using this technique to this research work, he had chosen a series of even numbers from the attendance registers of secondary schools required for the study from VIII, IX and X classes. As per the selected population, the number of sample taken for this research is limited to 150 students.

ANALYSIS AND INTERPRETATION OF DATA

The research work done in any field is said to be more meaningful and purposeful when the data collected is carefully processed and systematically

analysed. On the basis of this analysis and interpretation, the researcher will be able to arrive at meaningful conclusions and draw proper inferences. Statistical Computations After the quantification of data, various statistical measures such as Means, Standard Deviations, 't' – Ratio and Analysis of Variance (ANOVA) with Scheffes Post Hoc Test have been calculated and presented in this chapter.

Table 1: showing the overall responses of students towards the causes of low achievement in English among Telugu medium pupils at secondary level in Vizianagaram District.

NO	Minimum	Maximum	Percent	Mean	Std. Deviation
150	78	103	77.36	92.83	4.71

It is revealed that the students showed more positive response the causes of low achievement English among Telugu medium pupils at Secondary level in Vizianagaram district. The mean value is 92.83 and the mean percent is 77.36.

Table 2 : showing the significant difference between boy and girl students towards the causes of low achievement in English among Telugu medium pupils at Secondary level in Vizianagaram District..

Gender	N	Mean	Std. Dev.	t-value	Df.
Boy	87	92.16	4.70	2.08*	148
Girl	63	93.76	4.61		

*Significant at 0.05 level As seen from the above table the mean response of girl students (93.76) is higher than the boy students (92.16). Thetvalue is found to be 2.08, which is significant at 0.05 level. This shows that there is a significant difference between both the samples. Hence, that "there is no significant difference between beyond girl students towards the cause so flow achievement in English among Telugu medium pupils at Secondary level in Vizianagaram district" is rejected. Graph showing the significant difference between boy and girl students towards the causes of low achievement in English among Telugu medium pupils at Secondary level in Vizianagaram district.

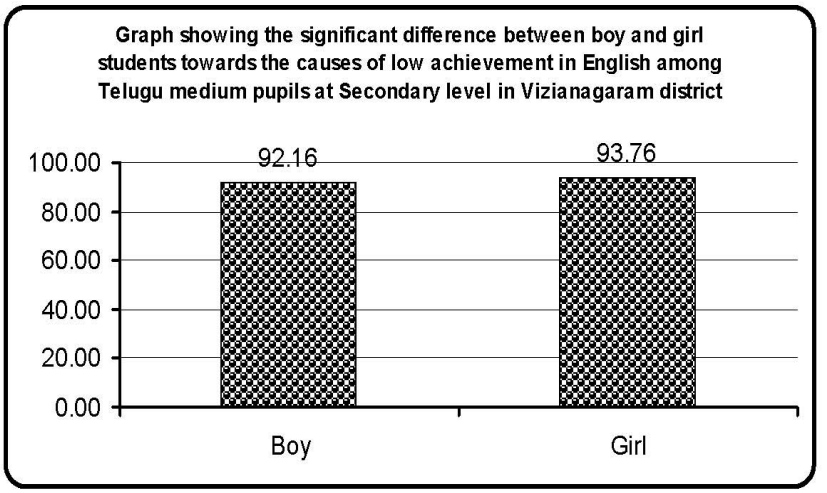

Table 3: showing the significant difference between rural and urban area students towards the causes of low achievement in English among Telugu medium pupils at Secondary level in Vizianagaram District.

Locality	N	Mean	Std. Dev.	t-value	Df
Rural	65	91.80	5.16	2.39*	148
Urban	85	93.62	4.20		

*Significantat0.05level Asseen from the above table the mean response of urban area students (93.62) is higher than the rural area students (91.80). That value is found to be 2.39, which is significant at 0.05 level. This shows that there is a significant difference between both the samples. Hence, that "there is no significant difference between rural and urban area students towards the causes of low achievement in English among Telugu medium pupils at Secondary level in Vizianagaram district" is rejected.

Findings of the study:

1. There is a significant difference between boy and girl students in their response towards the causes of low achievement in English among Telugu medium pupils at Secondary level in Vizianagaram district.
2. There is a significant difference between rural and urban area l students in their response towards the causes of low achievement in English among Telugu medium pupils at Secondary level in Vizianagaram district.

Conclusion of the Study:

The following are the items subjects expressed most favourable disposition. Hence, it can be concluded that the population have the following opinion

1. I want to learn English, 2. All the text books, Non-details and work books, stories should be attractive and motivating, 3. Work book, Assignment should be easy manner to understand clearly. 4. Our teachers are not encouraging to speak in the English class. 5. I want to read English news papers. 6. I don't have financial status to have English tuition.

The following are the items subjects expressed least favourable disposition. Hence, it can be concluded that the population is of the following opinion

1. There is no English teacher to teach English in our school. 2. Charts, Cassets Films etc., are not displaying in the English teaching class. 3. There is no special concentration on the English backward students. 4. The stories are not attractive in the English classroom. 5. They are not paying any concentration in teaching language techniques.

Suggestions of the study:

1. Special attention is to be paid to the slow and backward learners
2. The learners are to be encouraged to read English books / News papers in the school library.
3. The students are to be encouraged to speak in English in the class room.
4. Reading corner where the collection of poems / stories / anecdotes by the children is to be put in every class room for children to read.
5. Students are to be categorized in groups for effective teaching.

Therefore, according to my study if we laid down right foundation in secondary schools by using all sources, simply we can give the solutions for what are the causes for low achievement. Finally students will get more benefits and pay attention towards English language.

References

1. Abercxombie, D. (1956), "Problems & Principles in Language Study", Long Mans, London
2. Agnihotri, R. and Khanna, A.L. (1992). "Language in Education policy in India". The Administrator, 37.
3. Alatis, J.H. Altman and P. Alatis (Eds.) (1981), "The Second Language Classroom; Directions for the 1980's", Oxford University Press
4. Abha Rani Bishant (1984), "Teaching in India", Jalundhar: Krishna Bros, P.P. 76-98.
5. Aggarwal, V.N. (1984), "Teaching of English in India", Nebha: Pepsu Publications PP 26-42.
6. Baugh, A.C. (1975), "History of English Language", New Delhi: Prentice Hall PP 44-50
7. Best, J.W. (1948), "Research in Education", Madison: University of Wiconsis, USA.
8. Buch, M.B. (1981), "Syllabus of English", Fourth Survey of Educational Research, New Delhi: NCERT P 965.
9. Dutt, T.K. (1967), "India without English", Ambala: Nehru foundation P 21.
10. Humanyun Kabir, (1955), "English in India", London: Long man's Green and Co. P. 34.
11. Janson P (1981), "A study on English Language achievement in senior secondary schools of Belgam District in Karnataka", Sited in Fourth Survey of Educational Research, New Delhi NCERT P 864.
12. "Journal of English and Foreign Languages", Editor, B.T.Desai, 1996, No.18, by Central Institute of English and Foreign Languages, Hyderabad.
13. Kapada, M.K. (Feb. 2000) "Man and language skills" vol 3 No. 4 New Delhi NCERT, P .19
14. Mutaili, K & Borude R (1979), " Attitude of parents and students of Auranga Bad towards learning and performance in English", sited in Third survey of educational Research, New Delhi NCERT P 1051.
15. Nair, N.S. (2007), "Common language difficulties at primary level" sited in Journal of universal education, Volume 1 Issue No.1 Madras : Ponerageshan P 16
16. Singh, M.N. (1989), "A study of achievement in English in relation to intelligence, interest, socio economic status and facilities available for learning the language Ph.D. Edu. University of Gorakapur, sited in Fourth survey of educational Research, New Delhi NCERT, P 968.
17. Shivendra K. Verma, "Language in Education Problems and Principles", T.R. Publications.

INTERNATIONAL JOURNAL OF MULTIDISCIPLINARY EDUCATIONAL RESEARCH
ISSN : 2277-7881; IMPACT FACTOR - 2.972; IC VALUE:5.16
VOLUME 3, ISSUE 10(4), OCTOBER 2014

HIGH STEP UP SOLAR POWER OPTIMIZER FOR DC MICRO GRID SYSTEMS

Mr. V R S KUMAR
ravindra.satya224@gmail.com
Under the guidance of
Mr. P. VIJAYA RAMARAO
ASSISTANT PROFESSIOR
PYDAH COLLEGE OF ENGINEERING, KAKINADA

Abstract—This paper proposes a high step-up solar power optimizer (SPO) for DC Micro Grid System that efficiently harvests maximum energy from a photovoltaic (PV) panel then outputs energy to a dc-micro grid. A low voltage rating and low-conduction resistance switch improves system efficiency by employing the incremental conductance method for the maximum power point tracking (MPPT) algorithm. Its structure integrates coupled inductor and switched capacitor technologies to realize high step-up voltage gain. The leakage inductance energy of the coupled inductor can be recycled to reduce voltage stress and power losses. Because of its high tracking accuracy, the method is widely used in the energy harvesting of PV systems. Simulation results can be done by using MATLAB software.

Key words: SPO, MPPT, Micro grid

I. INTRODUCTION

A conventional PV generation system is either a single- or a Multi-string PV array that is connected to one or several central PV inverters. Numerous series-connected PV modules are connected in the PV array to achieve the DC link voltage that is high enough to be connected to electricity through the DCAC inverter. Fossil fuels continue to be depleted, and their use has been instrumental to climate change, a problem that grows more severe each year. A photovoltaic (PV) power generation system, which uses a renewable resource, has been extensively used in emergency facilities and in generating electricity for mass use. However, the power reduction that is caused by the shadow effect is an inevitable problem in a centralized PV system.

The use of a micro inverter or ac module has recently been proposed for individual PV panels [1], [2]. Although this discrete PV power generation solution may partially eliminate the shadow problem, a micro inverter

structure constrains the system energy's harvesting efficiency and entails high costs. A solar power optimizer (SPO) was developed as an alternative to maximize energy harvest from each individual PV module. An SPO is used as a dc–dc converter with maximum power point tracking (MPPT), which increases PV panel voltage to optimum voltage levels for a dc micro grid connection or through a dc–ac inverter for electricity [3]–[6]. Fig. 1 shows a single PV panel's energy, which passes through an SPO to a dc micro grid system. A 400 V dc-micro grid system was proposed as an energy-efficient distribution option for data center systems and telecommunication facilities [7]. The SPO attempts to improve the use of distributed renewable resources and lower system cost. It may also potentially improve the efficiency of PV systems, has an anti-shadow effect, and can monitor the status of PV modules [8]. Moreover, the dc-grid voltage is regulated by bidirectional inverter and battery tank. In case of low-loading condition, the redundant energy will store into battery or through bidirectional inverter to ac grid.

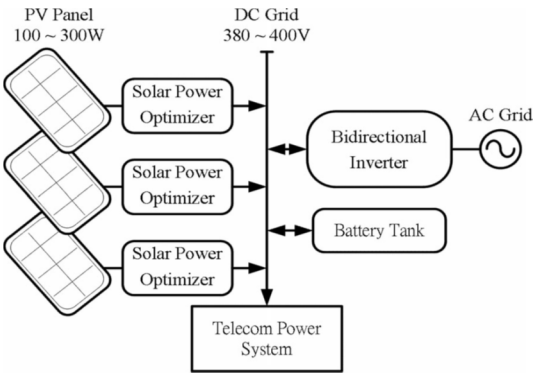

Fig. 1 Configuration of multiple parallel SPO for a dc-micro grid system

The maximum power point (MPP) voltage range of a single PV panel ranges from 15 to 40 V and has a power capacity of about 100 to 300 W [9]. An SPO has a high step-up converter that increases low-input voltage to a sufficient voltage level. Various step-up dc–dc converter topologies include a conventional boost and fly-back converters [10], [11], switched inductor converter, and switched capacitor converter [12]–[16], as well as a transformer-less switched capacitor types [17], [18], voltage-lift types [19]–[21], capacitor–diode voltage multipliers [22]–[25], and boost types that are integrated with coupled inductors [26]–[29].With increasing voltage gain, recycling the leakage inductance energy of a coupled inductor will reduce the

voltage stress on the active switch, which enables the coupled inductor and voltage multiplier or voltage-lift technique to realize high-voltage gain [9]–[29].

The proposed SPO is shown in Fig. 2; its configuration is based on a high step-up dc–dc converter with an MPPT control circuit. The converter includes a floating active switch S and a coupled inductor *T*1 with primary winding *N*1, which is similar to the input inductor of a conventional boost converter capacitor *C*1 , and diode *D*1 recycle leakage inductance energy from *N*1 . Secondary winding *N*2 is connected to another pair of capacitors, *C*2 and *C*3, and to diodes *D*2 and *D*3. Rectifier diode *D*4 connects to output capacitor *Co* and load *R*. The duty ratio is modulated by the MPPT algorithm, which uses the incremental conductance method [30]–[35] that is employed in the proposed SPO. It detects PV module voltage *V*pv and current *I*pv to determine the increase and decrease in the duty cycle of the dc converter. Therefore, the MPP can be obtained by comparing instantaneous conductance *I/V* and incremental conductance *dI/dV*. The algorithm is programmed into TMS320LF2407A, a digital signal microprocessor.

The proposed converter has the following features: 1) its voltage conversion ratio is efficiently increased by using the switched capacitor and coupled inductor techniques; 2) the leakage inductance energy of the coupled inductor can be recycled to increase efficiency, and the voltage spike on the active switch is restrained; 3) the floating active switch isolates the PV panel's energy during non-operating conditions, thereby preventing any potential electric hazard to humans or facilities. The MPPT control algorithm exhibits high-tracking efficiency; hence, it is widely used in the energy harvesting of PV systems.

The rest of the paper is organized as follows. Sections II and III discuss the operating principle and steady-state analysis of the proposed converter, respectively. Section IV addresses the practical implementation and component selection of the proposed converter. Section V presents the experimental results, and VI concludes the paper.

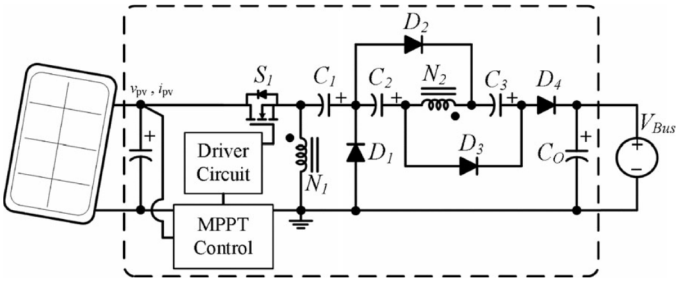

Fig. 2. Configuration of the proposed SPO

II. OPERATING PRINCIPLES

The operating principles for continuous conduction mode (CCM) and discontinuous conduction mode (DCM) are presented in detail.

To simplify the circuit analysis of the proposed converter, the following assumptions are made:

1) All components are ideal, except for the leakage inductance of coupled inductor *T*1, which is taken into account.

On-state resistance *R*DS (ON) and all the parasitic capacitances of main switch S are disregarded, as are the forward voltage drops of diodes *D*1 to *D*4;

2) Capacitors *C*1 to *C*3 and *Co* are sufficiently large that the voltages across them are considered constant;

3) The equivalent series resistance (ESR) of capacitors *C*1 to *C*3 and *Co,* as well as the parasitic resistance of coupled inductor *T*1, is neglected;

4) Turns ratio *n* of coupled inductor *T*1 windings is equal to *N*2 /*N*1.

The CCM operating modes are described as follows.

A. CCM Operation

*Mode I [t*0 *, t*1 *]:* During this interval, switch *S* and diodes *D*2 and *D*3 are conducted; diodes *D*1 and *D*4 are turned OFF. The current flow path is shown in Fig. 3(a). Magnetizing inductor

Lm continues to release energy to capacitors *C*2 and *C*3 through secondary winding*N*2 of coupled inductor *T*1. Leakage inductance *Lk* 1 denotes the stored energy from source energy *V*in. The energy that is stored in

capacitor *Co* is constantly discharged to load *R*. This mode ends when increasing *iLk*1 is equal to decreasing *iLm* at *t* = *t*1

$$vLm = Vin \quad (1)$$

$$\Delta iLm = Vin/Lm\ (t1 - t0) \quad (2)$$

*Mode II [t*1, *t*2*]:* During this interval, switch *S* and diode *D*4 are conducted. Source energy *V*in is serially connected to *C*1, *C*2, and *C*3, and secondary winding *N*2; *Lk*2 discharges the energy that is stored in charge output capacitor *Co* and loads *R*. Meanwhile, magnetizing inductor *Lm* also receives energy from *V*in. The current flow path is shown in Fig. 3(b). This mode ends when switch S is turned OFF at *t* = *t*2

$$v_{Lm} = \frac{V_o - V_{\text{in}} - V_{c1} - V_{c2} - V_{c3}}{n} \quad (3)$$

$$n = \frac{N_2}{N_1} \quad (4)$$

$$\Delta i_{Lm} = \frac{V_o - V_{\text{in}} - V_{c1} - V_{c2} - V_{c3}}{n \cdot L_m} \cdot (t_2 - t_1). \quad (5)$$

*Mode III [t*2 *, t*3 *]:* During this transition interval, switch *S* and diodes *D*2 and *D*3 are turned OFF, and diodes *D*1 and *D*4 are conducted. The current flow path is shown in Fig. 3(c). The energy stored in leakage inductance *Lk* 1 instantly flows through the diode *D*1 to charge capacitor *C*1. The energy is released to magnetizing inductor *Lm* through coupled inductor *T*1, which is serially connected to *C*1, *C*2, and *C*3, and secondary winding *N*2; *Lk*2 discharges the energy that is stored in charge output capacitor *Co* and loads *R*. This mode ends when decreasing *iLk*1 is equal to increasing *iLm* at *t* = *t*3

$$v_{Lm} = -V_{c1} \quad (6)$$

$$\Delta i_{Lm} = \frac{-V_{c1}}{L_m} \cdot (t_3 - t_2). \quad (7)$$

*Mode IV [t*3 *, t*4 *]:* During this interval, switch *S* and diode *D*4 are turned OFF, and diodes *D*1,*D*2 , and *D*3 are conducted. The current flow path is shown in Fig. 3(d). Leakage inductance *Lk* 1 continues to release energy to charge capacitor *C*1 through diode *D*1. Magnetizing inductor *Lm* through coupled inductor *T*1 transfers energy to capacitors *C*2 and *C*3. The energy that is stored in capacitor *CO* is constantly discharged to load *R*. This mode ends when decreasing *iLk*1 is zero at *t* = *t*4

$$v_{Lm} = -V_{c1} \tag{8}$$

$$\Delta i_{Lm} = \frac{-V_{c1}}{L_m} \cdot (t_4 - t_3). \tag{9}$$

*Mode V [t*4, *t*5*]:* During this interval, diodes *D*2 and *D*3 are conducted. The current flow path is shown in Fig. 3(e). Magnetizing inductor *Lm* constantly transfers energy to secondary winding *N*2 and charges capacitors *C*2 and *C*3. The energy that is stored in capacitor *CO* is constantly discharged to load *R*. This mode ends when switch S is turned ON at the beginning of the next switching period

$$v_{Lm} = \frac{-V_{c2}}{n} = \frac{-V_{c3}}{n} \tag{10}$$

$$\Delta i_{Lm} = \frac{-V_{c2}}{n \cdot L_m} \cdot (t_5 - t_4) = \frac{-V_{c3}}{n \cdot L_m} \cdot (t_5 - t_4). \tag{11}$$

B. DCM Operation

*Mode I [t*0, *t*1*]:* During this interval, switch *S* and *D*4 are conducted, and diodes *D*1*, D2*, and *D*3 are turned OFF. The current flowpath is shown in Fig. 4(a).Magnetizing inductor*Lm* with leakage inductance *Lk* 1 stores energy from source energy *V*in. Meanwhile, source energy *V*in is also serially connected to capacitors *C*1*, C*2, and *C*3, and secondary winding *N*2 to charge capacitor *Co* and load *R*. This mode ends when switch *S* is turned OFF at *t* = *t*1

$$v_{Lm} = V_{\text{in}} = \frac{V_o - V_{\text{in}} - V_{c1} - V_{c2} - V_{c3}}{n} \tag{12}$$

$$\Delta i_{Lm} = \frac{V_{\text{in}}}{L_m} \cdot (t_1 - t_0) = \frac{V_o - V_{\text{in}} - V_{c1} - V_{c2} - V_{c3}}{n \cdot L_m} \cdot (t_1 - t_0). \tag{13}$$

*Mode II [t*1 *, t*2 *]:* During this transition interval, switch *S* and diodes *D*2 and *D*3 are turned OFF, and diodes *D*1 and *D*4 are conducted. The current flow path is shown in Fig. 4(b). The energy stored in leakage inductance *Lk* 1 instantly flows through the diode*D*1 to charge capacitor *C*1 ; this energy is also released to magnetizing inductor *Lm* through the coupled inductor *T*1 series that is connected to *C*1*, C*2 , and *C*3 , secondary winding *N*2 , and *Lk*2 to

charge output capacitor *Co* and load *R*. This mode ends when decreasing *iD*4 is zero at *t* = *t*2

$$v_{Lm} = -V_{c1} \tag{14}$$

$$\Delta i_{Lm} = \frac{-V_{c1}}{n \cdot L_m} \cdot (t_2 - t_1). \tag{15}$$

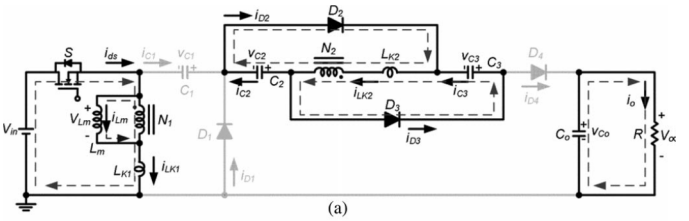

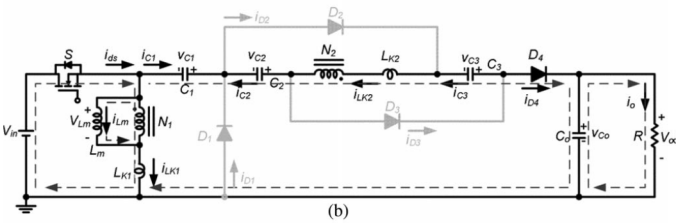

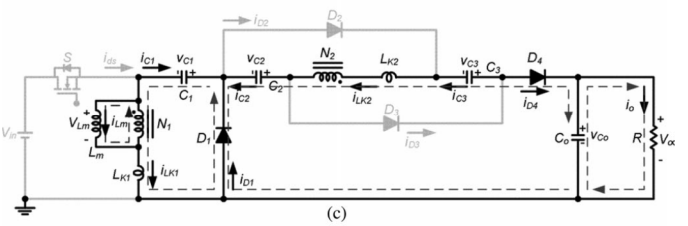

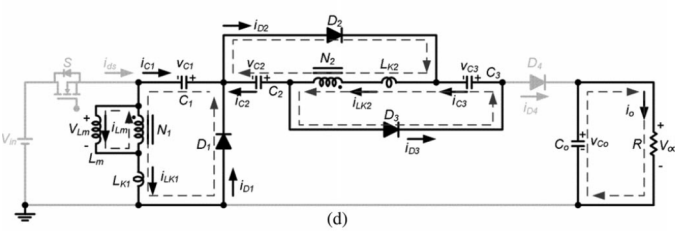

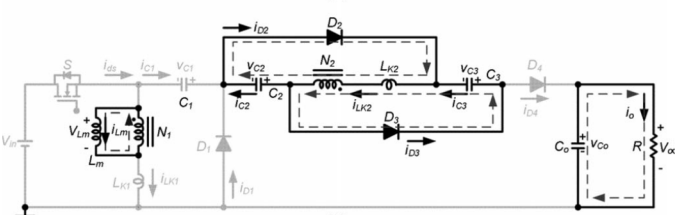

Fig. 3 Current flow path in five operating modes during one switching period in CCM operation: (a) Mode I, (b) Mode II, (c) Mode III, (d) Mode IV, and (e) Mode V

*Mode III [t*2, *t*3]*:* During this transition interval, switch *S* and diode *D*4 are turned OFF, and diodes *D*1*, D2*, and *D*3 are conducted. The current flow path is shown in Fig. 4(c). Leakage inductance *Lk* 1 continues to release energy to charge capacitor *C*1 through diode *D*1. Magnetizing inductor *Lm* transfers energy to capacitors *C*2 and *C*3 through coupled inductor *T*1. The energy stored in capacitor *Co* is constantly discharged to load *R*. This mode ends when decreasing *iLk*1 is zero at *t* = *t*3

$$v_{Lm} = -V_{c1} = \frac{-V_{c2}}{n} = \frac{-V_{c3}}{n} \tag{16}$$

$$\Delta i_{Lm} = \frac{-V_{c1}}{n \cdot L_m} \cdot (t_3 - t_2) = \frac{-V_{c2}}{n \cdot L_m} \cdot (t_3 - t_2) = \frac{-V_{c3}}{n \cdot L_m} \cdot (t_3 - t_2). \tag{17}$$

*Mode IV [t*3 *, t*4 *]:* During this interval, switch *S*, diodes *D*1 and *D*4 are turned OFF, and diodes *D*2 and *D*3 are conducted.

The current flow path is shown in Fig. 4(d).Magnetizing inductor *Lm* constantly transfers energy to secondary winding *N*2 and charges capacitors *C*2 and *C*3. The energy that is stored in capacitor *Co* is constantly discharged to load *R*. This mode ends when decreasing *iLm* is zero at *t* = *t*4

$$v_{Lm} = \frac{-V_{c2}}{n} = \frac{-V_{c3}}{n} \tag{18}$$

$$\Delta i_{Lm} = \frac{-V_{c2}}{n \cdot L_m} \cdot (t_5 - t_4) = \frac{-V_{c3}}{n \cdot L_m} \cdot (t_4 - t_3). \tag{19}$$

*Mode V [t*4 *, t*5 *]:* During this interval, the switch and all the diodes are turned OFF. The current flow path is shown in Fig. 4(e). The energy that is stored in capacitor *CO* is constantly discharged to load *R.* This mode ends when switch S is turned

ON at the beginning of the next switching period

$$v_{Lm} = 0 \tag{20}$$

$$\Delta i_{Lm} = 0. \tag{21}$$

III. STEADY-STATE ANALYSIS

A. CCM Operation

Only steady-state analysis is considered during CCM operation, and the leakage inductances at primary and secondary sides are disregarded. Applying a volt-second balance on the magnetizing inductance *Lm* yields

$$\int_0^{DT_S} V_{\text{in}}\,dt + \int_{DT_S}^{T_S} (-V_{C1})dt = 0 \tag{22}$$

$$\int_0^{DT_S} (nV_{\text{in}})dt + \int_{DT_S}^{T_S} (-V_{C2})dt = 0 \tag{23}$$

From which the voltage across capacitors*C*1 and*C*2 are obtained as follows:

$$V_{C1} = \frac{D}{1-D} \cdot V_{\text{in}} \tag{24}$$

$$V_{C2} = V_{C3} = n \cdot V_{C1} = \frac{n \cdot D}{1-D} \cdot V_{\text{in}}. \tag{25}$$

At Mode I, the output voltage is *Vo* = *V*in + *VC* 1 + *VN* 2 +*VC* 2+ *VC* 3. Voltage gain *VO* /*V*in can be obtained as follows:

$$\int_0^{DT_S} (V_o - V_{\text{in}} - V_{C1} - 2 \cdot V_{C2})dt + \int_{DT_S}^{T_S} (-V_{C2})dt = 0 \tag{26}$$

$$V_o = V_{\text{in}} + V_{C1} + \frac{1+D}{D} \cdot V_{C2} \tag{27}$$

$$\frac{V_o}{V_{\text{in}}} = \frac{n \cdot D + n + 1}{1-D} \tag{28}$$

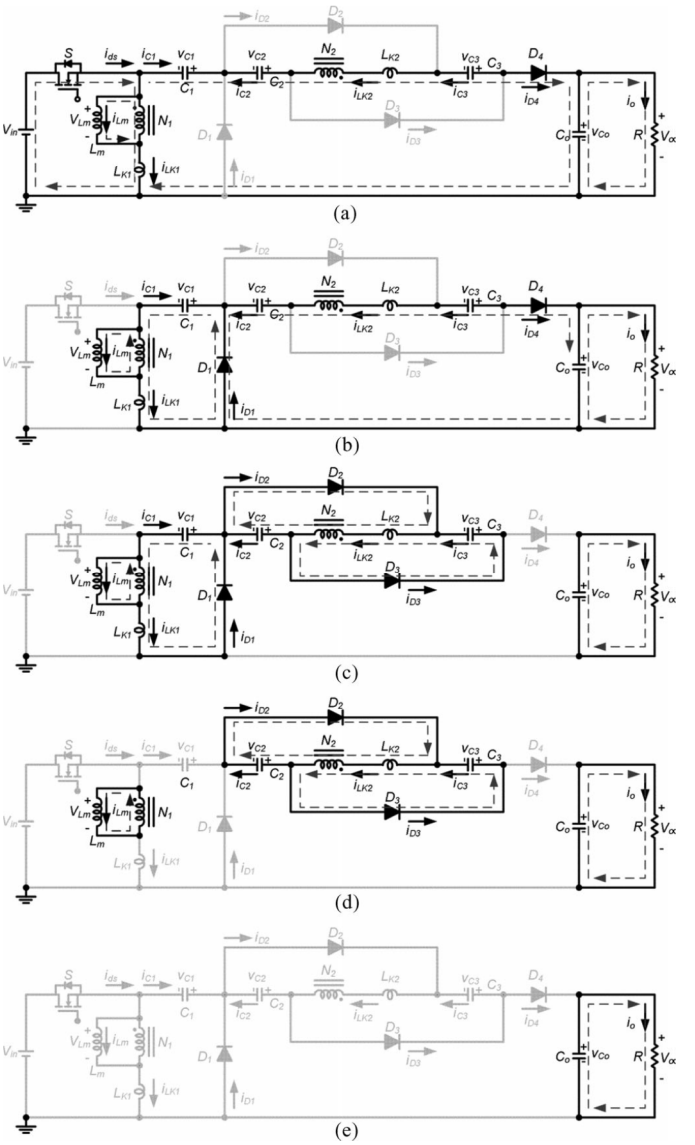

Fig. 4 Current flow path in five operating modes during one switching period in DCM operation: (a) Mode I, (b) Mode II, (c) Mode III, (d) Mode IV, and (e) Mode V

B. BCM Operating Conditions

The leakage inductances at primary and secondary sides are disregarded in this approach. We refer to (12) and (16) in applying volt-second balance on magnetizing inductance *Lm*, deriving

$$\int_0^{DT_S} V_{\text{in}} dt + \int_{DT_S}^{D_L T_S} (-V_{C1}) dt = 0 \qquad (29)$$

Where *DLTS* is the time duringwhich current *iLm* declines from peak current to zero

$$D_L \leq (1 - D). \qquad (30)$$

From (16), (29), and (30), the voltage across capacitors *C*2 and *C*3 are obtained

$$V_{C1} = \frac{D}{D_L} \cdot V_{\text{in}} \qquad (31)$$

$$V_{C2} = V_{C3} = n \cdot V_{c1} = \frac{n \cdot D}{D_L} \cdot V_{\text{in}}. \qquad (32)$$

On the basis of (12) and (18), the voltage across *Lm* can be determined using the volt-second balance principle

$$\int_0^{DT_S} (V_o - V_{\text{in}} - V_{C1} - 2 \cdot V_{C2}) dt + \int_{DT_S}^{(D_L + D)T_S} (-V_{C2}) dt = 0 \qquad (33)$$

$$V_o = V_{\text{in}} + V_{c1} + \frac{2 \cdot D + D_L}{D} \cdot V_{c2}. \qquad (34)$$

Substituting (31) and (32) into (34) yields the voltage gain in

DCM operation; *DL* is defined as follows:

$$\frac{V_o}{V_{\text{in}}} = \frac{(2 \cdot n + 1) \cdot D + (n + 1) \cdot D_L}{D_L} \qquad (35)$$

$$D_L = \frac{(2 \cdot n + 1) \cdot D}{\frac{V_o}{V_{\text{in}}} - (n + 1)}. \qquad (36)$$

In terms of *IN* 1 = *nIo,* input current peak *i*in, peak and magnetizing current peak *iLm,* peak are determined by

$$i_{\text{in,peak}} = i_{Lm,\text{peak}} + (n+1) \cdot i_{o,\text{peak}} \tag{37}$$

$$i_{Lm,\text{peak}} = \frac{V_{\text{in}}}{L_m} \cdot DT_S. \tag{38}$$

On the basis of (35), (37), and (38), the input current is determined as follows:

$$I_{\text{in}} = \frac{V_{\text{in}} \cdot D^2 \cdot T_S}{2 \cdot L_m} + \frac{(n+1) \cdot I_{\text{in}}}{V_o/V_{\text{in}}}. \tag{39}$$

Substituting (35) into (39) yields the DCM operation voltage gain and normalized magnetizing inductance time constant τLm

$$\frac{V_o}{V_{\text{in}}} \cdot \left(\frac{V_o}{V_{\text{in}}} - (n+1) \right) = \frac{V_o \cdot D^2 \cdot T_S}{2 \cdot L_m \cdot I_o} \tag{40}$$

$$\tau_{Lm} = \frac{L_m}{R \cdot T_S} = \frac{D^2}{2 \cdot \left((\frac{V_o}{V_{\text{in}}})^2 - \frac{V_o}{V_{\text{in}}} \cdot (n+1) \right)} \tag{41}$$

$$\frac{V_o}{V_{\text{in}}} = \frac{(n+1) \pm \sqrt{(n+1)^2 + \frac{2 \cdot D^2}{\tau_{Lm}}}}{2}. \tag{42}$$

When the proposed converter is operating in BCM, the CCM, and DCM operations have equal voltage gains. Boundary normalized magnetizing inductance time constant τLmB can be obtained by

$$\tau_{LmB} = \frac{D(D-1)^2}{2(2n+1)(nD+n+1)}. \tag{43}$$

C. Instantaneous MPPT Accuracy

To estimate the accuracy of MPPT, the instantaneous MPPT accuracy is defined as

$$\eta_{\text{MPPT}} = \frac{P_{\text{PV}}(t)}{P_{\text{MPPT}}(t)} \times 100\% \tag{44}$$

Where *P*pv (*t*) is the result of voltage *V*pv (*n*) multiplied by current *I*pv (*n*); *P*MPPT(*t*) denotes the real maximum PV output power that is obtained from a PV module or PV simulator.

IV. EXPERIMENTAL RESULTS

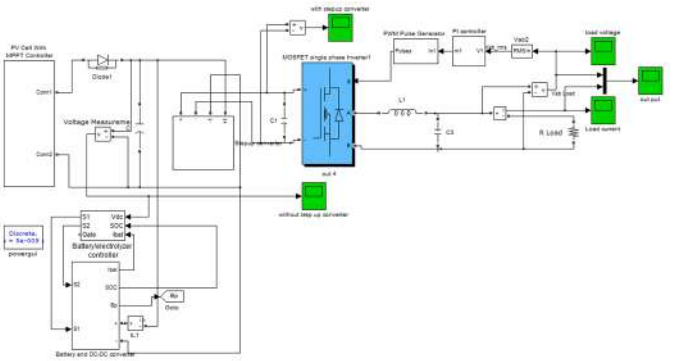

Fig 5 High Step up Solar Power Optimizer with DC Micro Grid System

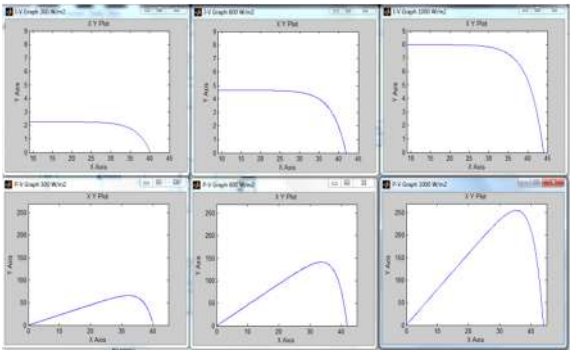

Fig. 6 PV panel charecteristics

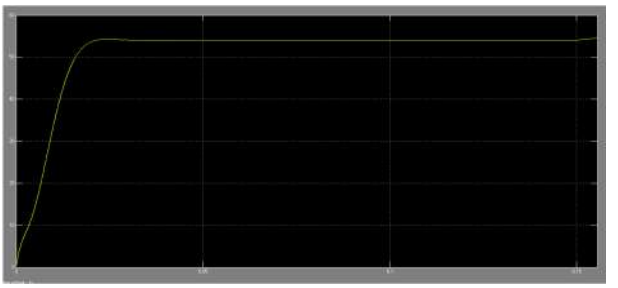

Fig. 7 voltage without boost converter

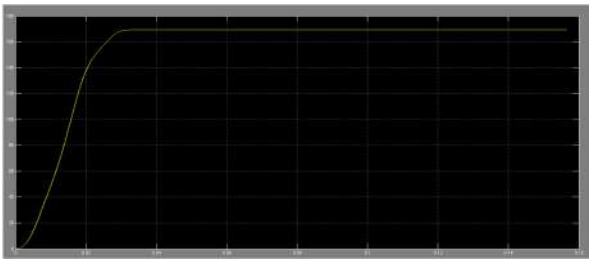

Fig. 8 DC output voltage with boost converter

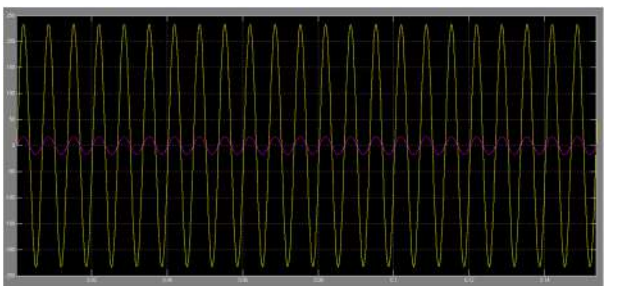

Fig. 9 load current & load voltage

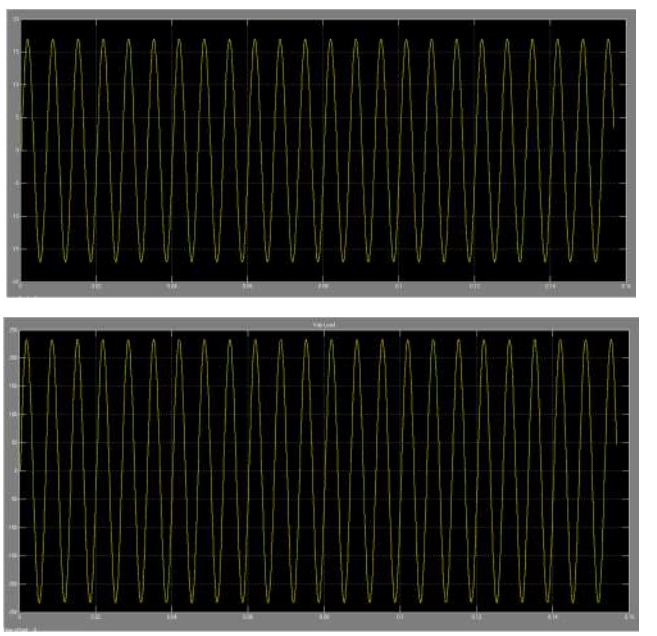

Fig.10 a) load current b) load voltage

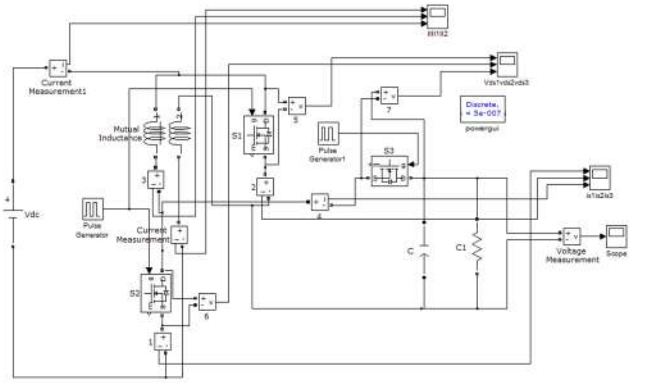

Fig 11 step up converter used in proposed system

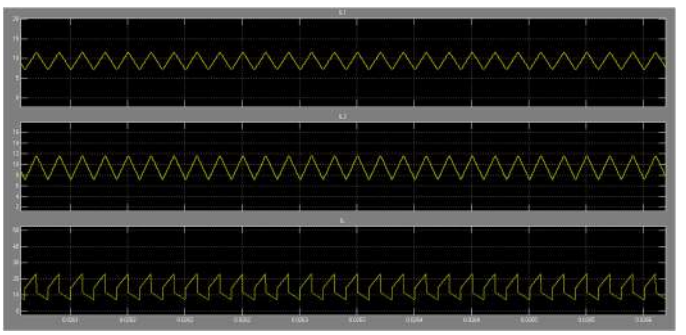

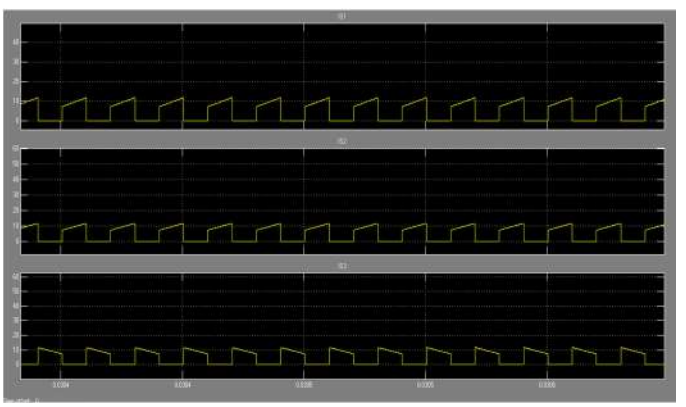

Fig 12 step up converter waveforms a) inductor currents b) switch currents c) switch voltages

V. CONCLUSION

The high step-up SPO uses the coupled inductor with an appropriate turn's ratio design and switched-capacitor technology to achieve a high-voltage gain that is 20 times higher than the input voltage. Because the leakage inductance energy of a coupled inductor is recycled and the voltage stress across the active switch S is constrained, the low *R*DS(ON) of active switch can be selected to improve maximum efficiency up to 96.7%. As a result, full load efficiency reaches 92.8%. The highest MPPT accuracy is 99.9% and the highest average accuracy is 97.9% at *P*PV = 150 W. A 300 W SPO with a high step-up voltage gain and MPPT functions are implemented and verified.

VI. Acknowledgment

This paper is based on M. Tech. project carried out by the student of pydah college of engineering & technology, Kakinada studying M.Tech (Power Electronics) The project had been completed by Mr. VRS KUMAR bearing H.T.no.:126T1D4312 under the guidance of Mr. P. VIJAYA RAMARAO.

REFERENCES

1. Y. Fang and X. Ma, "A novel PVmicroinverter with coupled inductors and double-boost topology," *IEEE Trans. Power Electron.*, vol. 25, no. 12, pp. 3139–3147, Dec. 2010.

2. A. Ch. Kyritsis, E. C. Tatakis, and N. P. Papanikolaou, "Optimum design of the current-source flyback inverter for decentralized grid-connected photovoltaic systems," *IEEE Trans. Energy Convers.*, vol. 23, no. 1, pp. 281–293, Mar. 08
3. P. Tsao, "Simulation of PV systems with power optimizers and distributed power electronics," in *Proc. IEEE Photovolt. Spec. Conf.*, Jun. 2010, pp. 389–393.
4. D. D.-C. Lu and V. G. Agelidis, "Photovoltaic-battery-powered DC bus system for common portable electronic devices," *IEEE Trans. Power Electron.*, vol. 24, no. 3, pp. 849–855, Feb. 2009.
5. L. Zhang, K. Sun,Y. Xing, L. Feng, andH.Ge, "A modular grid-connected photovoltaic generation system based on DC bus," *IEEE Trans. Power Electron.*, vol. 26, no. 2, pp. 523–531, Feb. 2011.
6. S. M. Chen, K. R. Hu, T. J. Liang, L. S. Yang, and Y. H. Hsieh, "Implementation of high step-up solar power optimizer for DC micro grid application," in *Proc. IEEE Appl. Power Electron Conf.*, Feb. 2012, pp. 28–32.
7. A. Pratt, P. Kumar, and T. V. Aldridge, "Evaluation of 400 V DC distribution in telco and data centers to improve energy efficiency," in *Proc. IEEE Int. Telecommun. Energy Conf.*, Sep./Oct. 2007, pp. 32–39.
8. L. Zhang, K. Sun,Y. Xing, L. Feng, andH.Ge, "A modular grid-connected photovoltaic generation system based on DC bus," *IEEE Trans. Power Electron.*, vol. 26, no. 2, pp. 523–531, Feb. 2011.
9. S.M. Chen, T. J. Liang, L. S. Yang, and J. F. Chen, "A boost converter with capacitor multiplier and coupled inductor for AC module applications," *IEEE Trans. Ind. Electron.,* Early Access Articles, vol. PP, no. 99, p. 1.
10. A. C. Nanakos, E. C. Tatakis, and N. P. Papanikolaou, "A weightedefficiency-oriented design methodology of flyback inverter for AC photovoltaic modules," *IEEE Trans. Power Electron.*, vol. 27, no. 7, pp. 3221– 3233, Jul. 2012.
11. S. Zengin, F. Deveci, and M. Boztepe, "Decoupling capacitor selection in DCMflyback PV micro-inverters considering harmonic distortion," *IEEE Trans. Power Electron.*, Early Access Articles, vol. pp., no. 99, p. 1.
12. B. Axelrod, Y. Berkovich, and A. Ioinovici, "Switched-capacitor/switched-inductor structures for getting transformerless hybrid DC-DC PWM converters," *IEEE Trans. Circuits Syst. I, Reg. Papers*, vol. 55, no. 2, pp. 687–696, Mar. 2008.
13. O. Abutbul, A. Gherlitz, Y. Berkovich, and A. Ioinovici, "Step-up switching-mode converter with high voltage gain using a switched- capacitor circuit," *IEEE Trans. Syst. I, Fundam. Theory Appl.*, vol. 50, no. 8, pp. 1098–1102, Aug. 2003.
14. S. C. Tan, S. Bronstein, M. Nur, Y. M. Lai, A. Ioinovici, and C. K. Tse, "Variable structure modeling and design of switched-capacitor converters," *IEEE Trans. Circuits Syst. I, Reg. Papers*, vol. 56, no. 9, pp. 2132– 2142, Sep. 2009.
15. G. Zhu and A. Ioinovici, "Switched-capacitor power supplies: DC voltage ratio, efficiency, ripple, regulation," in *Proc. IEEE Int. Symp. Circuits syst.*, May 1996, pp. 553–556.
16. F. L. Luo, "Switched-capacitorized DC/DC converters," in *Proc. IEEE Conf. Ind. Electron. Appl.*, May 2009, pp. 1074–1079.

17. L. S.Yang, T. J. Liang, and J. F.Chen, "TransformerlessDC-DC converters with high step-up voltage gain," *IEEE Trans. Ind. Electron.*, vol. 56, no. 8, pp. 3144–3152, Aug. 2009.
18. B. Axelrod, Y. Berkovich, and A. Ioinovici, "Transformerless DC-DC converters with a very high DC line-to-load voltage ratio," in *Proc. IEEE Int. Symp. Circuits syst.*, May 2003, vol. 3, pp. 435–438.
19. F. L. Luo and H. Ye, "Positive output multiple-lift push-pull switchedcapacitor Luo-converters," *IEEE Trans. Ind. Electron.*, vol. 51, no. 3, pp. 594–602, Jun. 2004.
20. M. Zhu and F. L. Luo, "Enhanced self-lift cˆuk converter for negative-topositive voltage conversion," *IEEE Trans. Power Electron.*, vol. 25, no. 9, pp. 2227–2233, Apr. 2010.
21. Y. Jiao, F. L. Luo, and M. Zhu, "Voltage-lift-type switched-inductor cells for enhancing DC-DC boost ability: Principles and integrations in Luo converter," *IET Trans. Power Electron.*, vol. 4, no. 1, pp. 131–142, Jan. 2011.
22. J. W. Baek, M. H. Ryoo, T. J. Kim, D. W. Yoo, and J. S. Kim, "High boost converter using voltage multiplier," in *Proc. Annu. IEEE Conf. Ind. Electron. Soc.*, 2005, pp. 567–572.
23. R. J.Wai and R. Y. Duan, "High step-up converter with coupled-inductor," *IEEE Trans. Power Electron.*, vol. 20, no. 5, pp. 1025–1035, Sep. 2005.
24. S. K. Changchien, T. J. Liang, J. F. Chen, and L. S. Yang, "Novel high step-up DC–DC converter for fuel cell energy conversion system," *IEEE Trans. Ind. Electron.*, vol. 57, no. 6, pp. 2007–2017, Jun. 2010.
25. S. M. Chen, T. J. Liang, L. S. Yang, and J. F. Chen, "A safety enhanced, high step-up DC-DC converter for AC photovoltaic module application," *IEEE Trans. Power Electron.*, vol. 27, no. 4, pp. 1809–1817, Apr. 2012.
26. Q. Zhao and F. C. Lee, "High-efficiency, high step-up DC-DC converters," *IEEE Trans. Power Electron.*, vol. 18, no. 1, pp. 65–73, Jan. 2003.
27. Y. Zhao, W. Li, Y. Deng, X. N. He, S. Lambert, and V. Pickert, "High step-up boost converter with coupled inductor and switched capacitor," in *Proc. IET Power Electron. Machines Drives Conf.*, Apr. 2010, pp. 1–6.
28. W. Yu, J. S. Lai, H. Qian, and C. Hutchens, "High-efficiency MOSFET inverter with H6-type configuration for photovoltaic nonisolatedAC-module applications," *IEEE Trans. Power Electron.*, vol. 26, no. 4, pp. 1253– 1260, Apr. 2011.
29. C. Restrepo, J. Calvente, A. Romero, E. Vidal-Idiarte, and R. Giral, "Current-mode control of a coupled-inductor buck–boost DC–DC switching converter," *IEEE Trans. Power Electron.*, vol. 27, no. 5, pp. 2536– 2549, May 2012.
30. K. H. Hussein, I. Muta, T. Hshino, and M. Osakada, "Maximum photovoltaic power tracking: An algorithm for rapidly changing atmospheric conditions," in *Proc. Inst. Elect. Eng.*, Jan. 1995, vol. 142, no. 1, pp. 59–64.
31. C. W. Tan, T. C. Green, and C. A. Hernandez-Aramburo, "An improved maximum power point tracking algorithm with current-mode control for photovoltaic applications," in *Proc. IEEE Int. Conf. Power Electron. Drive Sys.*, 2005, vol. 1, pp. 489–494.

INTERNATIONAL JOURNAL OF MULTIDISCIPLINARY EDUCATIONAL RESEARCH
ISSN : 2277-7881; IMPACT FACTOR - 2.972; IC VALUE:5.16
VOLUME 3, ISSUE 10(4), OCTOBER 2014

DUAL BUCK CONVETER FED FULL BRIDGE INVERTER FOR RENEWABLE ENERGY POWER GENERATION

Mr. S RAMBABU
sainam.rambabu@gmail.com
Under the guidance of
Ms.M.PAVANI
ASSISTANT PROFESSIOR
PYDAH COLLEGE OF ENGINEERING, KAKINADA

Abstract—In this paper, a Dual Buck Conveter Fed Full Bridge Inveter is developed and applied for injecting the real power of the renewable power into the grid to reduce the harmonic distortion, switching power loss and electromagnetic interference caused by the switching operation of power electronic devices. The dual-buck converter converts 2 dc capacitor voltage sources to a dc output voltage with three levels and balances these two dc capacitor voltages. The output voltage of the dual-buck converter supplies to the full-bridge inverter. Two dc capacitors, a dual-buck converter, a full-bridge inverter, and a filter configure the five-level inverter. The input of the dual-buck converter is 2 dc capacitor voltage sources. The power electronic switches of the full-bridge inverter are switched in low frequency synchronous with the utility voltage to convert the output voltage of the dual-buck converter to a five-level ac voltage. The output current of the five-level inverter is controlled to generate a sinusoidal current in phase with the utility voltage to inject into the grid. A hardware prototype is developed to verify the performance of the developed renewable power generation system. The experimental results are done by using MATLAB/SIMULINK software.

Key words: dual buck converter, inverter, renewable energy

I. INTRODUCTION

The conventional single-phase inverter topologies for gridconnection include half-bridge and full bridge [1]–[4]. The half-bridge inverter is configured by one capacitor arm and one power electronic arm. The dc bus voltage of the half-bridge inverter must be higher than double of the peak voltage of the output ac voltage. The output ac voltage of the half-bridge inverter is two levels. The voltage jump of each switching is the dc bus voltage of the inverter. The full-bridge inverter is configured by two power electronic arms. The voltage jump of each switching is double the dc bus voltage of the

inverter if the bipolar modulation is used, and it is the dc bus voltage of the inverter if the unipolar modulation is used. All power electronic switches operate in high switching frequency in both half-bridge and fullbridge inverters. The switching operationwill result in switching loss. The loss of power electronic switch includes the switching loss and the conduction loss. The conduction loss depends on the handling power of power electronic switch. The switching loss is proportional to the switching frequency, voltage jump of each switching, and the current of the power electronic switches.

The power efficiency can be advanced if the switching loss of the dc–ac inverter is reduced. Multilevel inverter can effectively reduce the voltage jump of each switching operation to reduce the switching loss and increase power efficiency. The number of power electronic switches used in the multilevel inverter is larger than that used in the conventional half-bridge and full-bridge inverters. Moreover, its control circuit is more complicated. Thus, both the performance and complexity should be considered in designing the multilevel inverter [8], [9]. However, interest in the multilevel inverter has been aroused due to its advantages of better power efficiency, lower switching harmonics, and a smaller filter inductor compared with the conventional half-bridge and full-bridge inverters.

The conventional single-phase multilevel inverter topologies include the diode-clamped, the flying capacitor, and the cascade H-bridge types [10]–[15], as shown in Fig. 1. Fig. 1(a) shows the basic configuration of a diode-clamped multilevel inverter. As can be seen, it is configured by two dc capacitors, two diodes, and four power electronic switches. Two diodes are used to conduct the current loop, and four power electronic switches are used to control the voltage levels. The output voltage of the basic diode-clamped multilevel inverter has three levels. The voltage difference of each level is *V*dc/2 (the voltage on a capacitor). Since the voltages of two dc capacitors are used to form the voltage level of the multilevel inverter, the voltages of these two dc capacitors must be controlled to be equal. The control for balancing these two dc capacitors is very important in controlling the diode-clamped multilevel inverter, and it is very hard under the light load [16]–[19].

If the five-level output voltage is expected, extra two diodes and four power electronic switches are required [11], [20]. Fig. 1(b) shows the circuit configuration of a basic flying capacitor multilevel inverter. As can be seen, it is configured by three dc capacitors and four power electronic switches. The

voltage on each dc capacitor is controlled to be *V*dc/2, and the output voltage of the basic flying capacitor multilevel inverter has three levels. The voltage difference of each level is also *V*dc/2 (the voltage on a dc capacitor). These three dc capacitors must be controlled for maintaining their voltages to be *V*dc/2 in the charge and discharge processes. Therefore, its control circuit is more complicated. If five-level output voltage is required, an extra dc capacitor and four power electronic switches are required [11], [13], [14]. Fig. 1(c) shows the circuit configuration of the basic cascade H-bridge multilevel inverter [8]–[11], [15], [21]. As can be seen, it is configured by two full-bridge inverters connected in cascade. The dc bus voltage of each full-bridge inverter is *V*dc/2, and the output voltage of each full-bridge inverter can be controlled to be *V*dc/2, 0, and −*V*dc/2. Thus, the voltage levels of the output voltage of the cascade full-bridge multilevel inverter are *V*dc, *V*dc/2, 0, −*V*dc/2, and −*V*dc. This topology has advantages of fewer components being required compared with other multilevel inverters under the output voltage with the same levels, and its hardware circuit can be modularized because the configuration of each full bridge is the same. However, this topology has the disadvantages that two independent dc voltage sources are required.

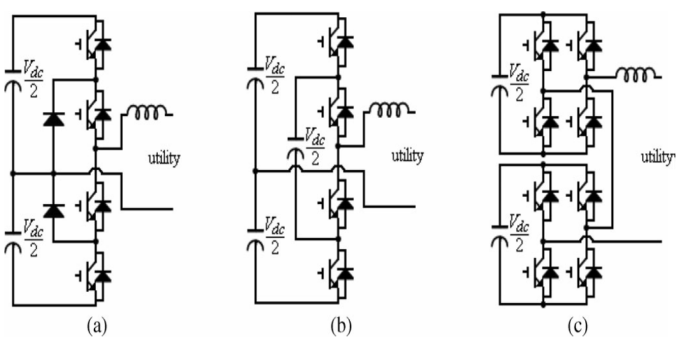

Fig. 1. Circuit configuration of conventional single-phase multilevel inverter (a) Diode clamped. (b) Flying capacitor. (c) Cascade H-bridge

In this paper, a five-level inverter is developed and applied for injecting the real power of the renewable power into the grid. This five-level inverter is configured by two dc capacitors, a dual-buck converter, a full-bridge inverter, and a filter [22]. The five-level inverter generates an output voltage with five levels and applies in the output stage of the renewable power generation system to generate a sinusoidal current in phase with the utility voltage to

inject into the grid. The power electronic switches of the dual-buck converter are switched in high frequency to generate a three-level voltage and balance the two input dc voltages. The power electronic switches of the full-bridge inverter are switched in low frequency synchronous with the utility to convert the output voltage of the dual-buck converter to a five-level ac voltage. Therefore, the switching power loss, harmonic distortion, and electromagnetic interference (EMI) caused by the switching operation of power electronic devices can be reduced, and the control circuit is simplified. Besides, the capacity of output filter can be reduced. A hardware prototype is developed to verify the performance of the developed renewable power generation system.

II. CIRCUIT CONFIGURATION

Fig. 2 shows the circuit configuration of the five-level inverter applied to a photovoltaic power generation system. As can be seen, it is configured by a solar cell array, a dc–dc converter, a five-level inverter, two switches, and a digital signal processor (DSP)-based controller. Switches *SW*1 and *SW*2 are placed between the five-level inverter and the utility, and they are used to disconnect the photovoltaic power generation system from the utility when islanding operation occurs. The load is placed between switches *SW*1 and *SW*2. The output of the solar cell array is connected to the input port of the dc–dc converter. The output port of the dc–dc converter is connected to the five-level inverter. The dc–dc converter is a boost converter, and it performs the functions of maximum power point tracking (MPPT) and boosting the output voltage of the solar cell array. This five-level inverter is configured by two dc capacitors, a dualbuck converter, a full-bridge inverter, and a filter. The dual-buck converter is configured by two buck converters. The two dc capacitors perform as energy buffers between the dc–dc converter and the five-level inverter. The output of the dual-buck converter is connected to the full-bridge inverter to convert the dc voltage to ac voltage. An inductor is placed at the output of the fullbridge inverter to form as a filter inductor for filtering out the high-frequency switching harmonic generated by the dual-buck converter.

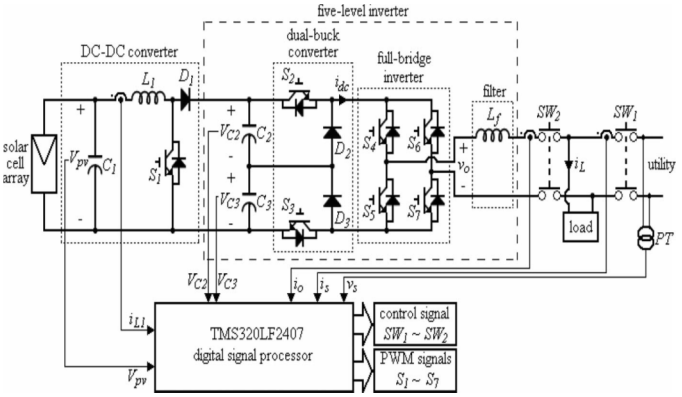

Fig. 2. Circuit configuration of the developed photovoltaic power generation system

III. OPERATION OF FIVE-LEVEL INVERTER

The operation of this five-level inverter can be divided into eight modes. Modes 1–4 are for the positive half-cycle, and modes 5–8 are for the negative half-cycle. Fig. 3 shows the operation modes of five-level inverter. As can be seen, the power electronic switches of the full-bridge inverter are switched in low frequency and synchronously with the utility voltage to convert the dc power into ac power for commutating. As seen in Fig. 3(a)–(d), the power electronic switches *S*4 and *S*7 are in the ON state, and the power electronic switches *S*5 and *S*6 are in the OFF state during the positive half-cycle. On the contrary, the power electronic switches *S*4 and *S*7 are in the OFF state, and the power electronic switches *S*5 and *S*6 are in the ON state during the negative half-cycle. Since the dc capacitor voltages *VC*2 and *VC*3 are balanced by controlling the five-level inverter, the dc capacitor voltages *VC*2 and *VC*3 can be represented as follows:

$$V_{C2} = V_{C3} = \frac{1}{2} V_{\mathrm{dc}}. \qquad (1)$$

The operation modes of this five-level inverter are stated as follows.

Mode 1: Fig. 3(a) shows the operation circuit of mode 1. The power electronic switch of the dual-buck converter *S*2 is turned ON and *S*3 is turned OFF. DC capacitor *C*2 is discharged through *S*2, *S*4, the filter inductor, the utility, *S*7,

and *D*3 to form a loop. Both output voltages of the dual-buck converter and five-level inverter are *V*dc/2.

Mode 2: Fig. 3(b) shows the operation circuit of mode 2. The power electronic switch of the dual-buck converter *S*2 is turned OFF and *S*3 is turned ON. DC capacitor *C*3 is discharged through *D*2, *S*4, the filter inductor, the utility, *S*7, and *S*3 to form a loop. Both output voltages of the dual-buck converter and fivelevel inverter are *V*dc/2.

Mode 3: Fig. 3(c) shows the operation circuit of mode 3. Both power electronic switches *S*2 and *S*3 of the dual-buck converter are turned OFF. The current of the filter inductor flows through the utility, *S*7, *D3, D2*, and *S*4. Both output voltages of the dualbuck converter and five-level inverter are 0.

Mode 4: Fig. 3(d) shows the operation circuit of mode 4. Both power electronic switches *S*2 and *S*3 of the dual-buck converter are turned ON.DCcapacitors*C*2 and*C*3 are discharged together through *S*2, *S*4, the filter inductor, the utility, *S*7, and *S*3 to form a loop. Both output voltages of the dual-buck converter and five-level inverter are *V*dc.

Modes 5–8 are the operation modes for the negative halfcycle. The operations of the dual-buck converter under modes 5–8 are similar to that under modes 1–4, and the dual-buck converter can also generate three voltage levels *V*dc/2, *V*dc/2, 0, and *V*dc, respectively. However, the operation of the full-bridge inverter is the opposite. The power electronic switches *S*4 and *S*7 are in the OFF state, and the power electronic switches *S*5 and *S*6 are in the ON state during the negative half-cycle. Therefore, the output voltage of the five-level inverter for modes 5–8 will be $-V$dc/2, $-V$dc/2, 0, and $-V$dc, respectively.

Considering operation modes 1–8, the full-bridge inverter converts the dc output voltage of the dual-buck converter with three levels to an ac output voltage with five levels which are *V*dc, *V*dc/2, 0, $-V$dc/2, and $-V$dc.

The operation of power electronic switches *S*2 and *S*3 should guarantee the output voltage of the dual-buck converter is higher than the absolute of the utility voltage. The waveforms of output voltage of five-level inverter and utility voltage are shown in Fig. 4.

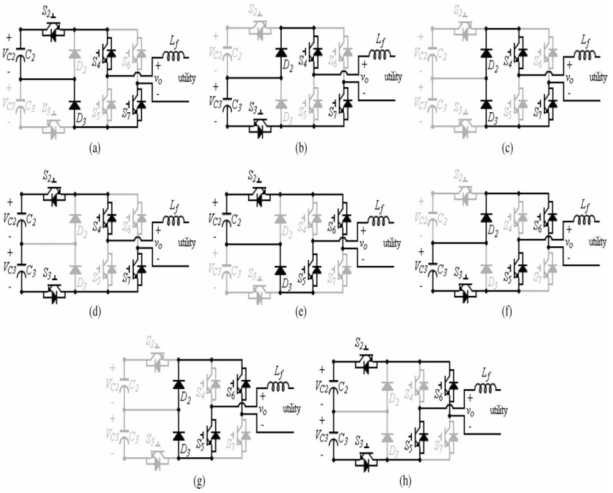

Fig. 3. Operation modes of the five-level inverter (a) Mode 1 (b) Mode 2 (c) Mode 3 (d) Mode 4 (e) Mode 5 (f) Mode 6 (g) Mode 7 (h) Mode 8

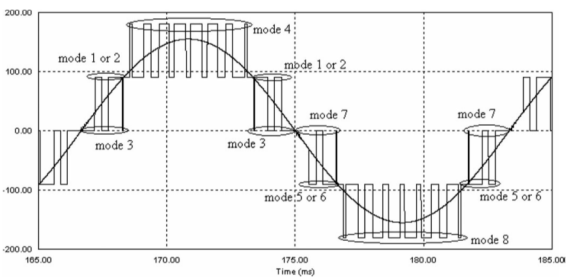

Fig. 4. Waveforms of output voltage and utility voltage

Due to the operation of full-bridge inverter, the voltage and current in the dc side of full-bridge inverter are their absolute values of the utility voltage and the output current of the fivelevel inverter. When the absolute of the utility voltage is smaller than *V*dc/2, the output voltage of the dual-buck converter should change between *V*dc/2 and 0. Accordingly, the power electronics of five-level inverter is switched between modes 1 or 2 and mode 3 during the positive half-cycle. On the contrary, the power electronics of five-level inverter is switched between modes 5 or 6 and mode 7 during the negative half-cycle. One of the power electronic switches *S*2 and *S*3 is in the OFF state and the other is switched in high frequency during one PWM period. Fig. 5(a) shows the equivalent circuit for the dc side of the five-level inverter under $|vs| < V\text{dc}/2$. As seen in Fig. 5(a), the equivalent circuit is a

conventional buck converter. DC voltage source *Vcx* may be dc capacitor voltage *VC*2 or *VC*3, and it depends on which power electronic switch *S*2 or *S*3 is switching in high frequency. As the power electronic switch is turned ON, the change rate of the output current can be represented as follows:

$$\frac{d|i_o|}{dt} = \frac{V_{Cx} - |v_s|}{L} \qquad (2)$$

Where *L* is the inductance of the filter inductor the change rate of the output current is positive. Thus, the output current |*io* | increases when the power electronic switch is turned ON. As the power electronic switch is turned OFF, the change rate of the output current can be represented as follows:

$$\frac{d|i_o|}{dt} = \frac{-|v_s|}{L}. \qquad (3)$$

The change rate of the output current is negative, meaning the output current |*io* | will decrease when the power electronic switch is turned OFF. As seen in (2) and (3), the output current |*io* | can be controlled by controlling the ON/OFF operation of the power electronic switch to track a reference current signal. When the absolute of the utility voltage is higher than *V*dc/2, the output voltage of the dual-buck converter should be changed between *V*dc and *V*dc/2. Accordingly, the five-level inverter is operated in mode 4, and 1 or 2 during the positive half-cycle, and it is switched in mode 8, and 5 or 6 during the negative half cycle.

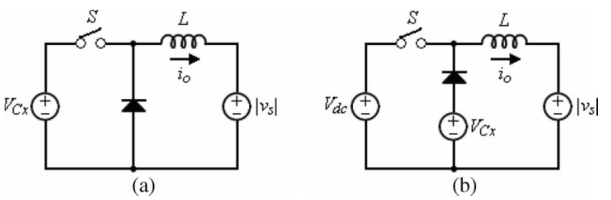

Fig. 5. Equivalent circuit. (a) |*vs* | < *V*dc /2. (b) |*vs* | > *V*dc /2

One of power electronic switches *S*2 and *S*3 is still turned ON and the other is switched in high frequency during one PWM period. Fig. 5(b) shows the equivalent circuit for the dc side of the five-level inverter under |*vs* | > *V*dc/2. The dc voltage source Vdc is the summation of dc capacitor voltages *VC*2 and *VC*3. As seen in Fig. 5(b), it differs from the conventional buck converter, where voltage source *VCx* is connected to the diode in series. Voltage source *Vcx* may be dc capacitor voltage *VC*2 or *VC*3, and it depends on

which power electronic switch *S*3 or *S*2 is switching in high frequency. As the power electronic switch is turned ON, the change rate of the output current can be represented as follows:

$$\frac{d|i_o|}{dt} = \frac{V_{\rm dc} - |v_s|}{L}. \qquad (4)$$

The change rate of the output current |*io* | is positive, meaning the output current |*io* | increases when the power electronic switch is turned ON. As the power electronic switch is turned OFF, the change rate of the output current can be represented as follows:

$$\frac{d|i_o|}{dt} = \frac{V_{Cx} - |v_s|}{L}. \qquad (5)$$

The change rate of the output current |*io* | is negative, and the output current |*io* | inductor current will be decreased when the power electronic switch is turned OFF. As seen in (4) and (5), the output current |*io* | can also be controlled to track a reference current signal by controlling the ON/OFF operation of the power electronic switches under |*vs* | > *V*dc/2.

Hence, the output current of the five-level inverter can be controlled to track a reference current signal, which is a sinusoidal current in phase with the utility voltage by controlling the ON/OFF operation of the power electronic switches *S*2 and *S*3. Meanwhile, the five-level inverter will generate a five-level output voltage varying with the change of the utility voltage. The switching loss, filter inductor, and EMI are reduced because the voltage difference of each voltage level is only *V*dc/2.

IV. VOLTAGE BALANCE OF FIVE-LEVEL INVERTER

Balancing the voltages of dc capacitors is very important in controlling the multilevel inverter. The voltage balance of dc capacitor voltages *VC*2 and *VC*3 can be controlled by the power electronic switches *S*2 and *S*3 easily. When the absolute of the utility voltage is smaller than *V*dc/2, one power electronic switch either *S*2 or *S*3 is switched in high frequency and the other is still in the OFF state. Which power electronic switch is switched in high frequency depends on the dc capacitor voltages *VC*2 and *VC*3. If dc capacitor voltage *VC*2 is higher than dc capacitor voltage *VC*3, power electronic switch *S*2 is switched in high frequency. In this situation, the voltage source *VCx* in Fig. 5(a) is *VC*2, and *C*2 will be discharged. Thus, the dc capacitor voltages *VC*2 decreases and

*VC*3 does not change. On the contrary, power electronic switch *S*3 is switched in high frequency when voltage *VC*3 is higher than voltage *VC*2. In this situation, the voltage source *VCx* in Fig. 5(a) is *VC*3. Thus, the dc capacitor voltages *VC*3 decreases and *VC*2 does not change. In this way, the voltage balance of *C*2 and *C*3 can be achieved. When the absolute of the utility voltage is higher than *V*dc/2, one power electronic switch either *S*2 or *S*3 is switched in high frequency and the other is still in the ON state. Which power electronic switch is switched in high frequency depends on the dc capacitor voltages *VC*2 and *VC*3. If dc capacitor voltage *VC*2 is higher than dc capacitor voltage *VC*3, the power electronic switch *S*3 is switched in high frequency. The voltage source VCx in Fig. 5(b) is dc capacitor voltage VC2. When the power electronic switch S3 is turned ON, both C2 and C3 are discharged.

However, only C2 supplies the power when the power electronic switch S3 is turned OFF. Thus, C2 will discharge more power than that of C3. On the contrary, the power electronic switch S2 is switched in high frequency when dc capacitor voltage VC3 is higher than dc capacitor voltage VC2. The voltage source VCx in Fig. 5(b) is dc capacitor voltage VC3. When the power electronic switch S2 is turned ON, both C2 and C3 are discharged.

However, only C3 supplies the power when the power electronic switch S2 is turned OFF. Thus, C3 will discharge more power than that of C2. In this way, the voltage balance of C2 and C3 can be achieved. As mentioned earlier, the operation of power electronic switches S2 and S3 can be summarized as Table I. The voltages of capacitors C2 and C3 can be easily balanced compared with the conventional multilevel inverter.

TABLE I

ON/OFF STATE OF *S*2 AND *S*3

		$\lvert v_s\rvert<V_{dc}/2$	$\lvert v_s\rvert>V_{dc}/2$
$V_{C2}>V_{C3}$	S_2	PWM	on
	S_3	off	PWM
$V_{C2}<V_{C3}$	S_2	off	PWM
	S_3	PWM	on

V. CONTROL BLOCK DIAGRAM

The developed photovoltaic power generation system consists of a dc–dc power converter and the five-level inverter. The five-level inverter performs the functions of converting the dc power into high-quality ac power and

injecting it into the utility, balancing two dc capacitor voltages *VC*2 and *VC*3 , and detecting the islanding operation. The dc–dc converter boosts the output voltage of the solar cell array and performs the MPPT to extract the maximum output power of the solar cell array. The controllers of both the dc–dc converter and the five-level inverter are explained as follows.

A. Five-Level Inverter

Fig. 6 shows the control block diagram of five-level inverter. In the operation of the five-level inverter, the dc bus voltage must be regulated to be larger than the peak voltage of the utility, and the dc capacitor voltages of *C*2 and *C*3 must be controlled to be equal. Besides, the five-level inverter must generate a sinusoidal current in phase with the utility voltage to be injected into the utility. As seen in Fig. 6, the voltages of dc capacitors *C*2 and *C*3 are detected and then added to obtain a dc bus voltage *V*dc. The added result is subtracted from a dc bus setting voltage *Vdcset*. The dc bus setting voltage *Vdcset* is larger than the peak voltage of the utility. The subtracted result is sent to a P-I controller. An islanding detection is also incorporated into the control of the five-level inverter. The concept of this islanding detection was proposed by authors [23]. However, it will not be addressed in this paper.

As seen in Fig. 6, the utility current is detected and sent to an RMS detection circuit. The output of the RMS detection circuit is sent to a hysteresis comparator that contains a low threshold value and a high threshold value. If the RMS value of the utility current is smaller than the low threshold value, the output of the hysteresis comparator is high, meaning the condition of islanding operation or power balance occurs. On the contrary, the output of the hysteresis comparator is low when the RMS value of the utility current is larger than the high threshold value, meaning the utility is normal. The output of the hysteresis comparator is sent to a signal generator. The output signal of the signal generator is an islanding control signal *Sa.* The islanding control signal is a dc signal with unity amplitude if the output of the hysteresis comparator is low. On the contrary, the islanding control signal is a square wave with a frequency of 20 Hz (disturbance signal for islanding detection) when the output of the hysteresis comparator is high. The outputs of the PI controller and signal generator are sent to a multiplier, and the product of the multiplier is the amplitude of the reference signal.

The utility voltage is detected and then sent to a phase-lock loop (PLL) circuit to generate an unity-amplitude sinusoidal signal whose phase is in

phase with the utility voltage. The outputs of the multiplier and the PLL circuit are sent to the other multiplier. The product of this multiplier is the reference signal of the output current for the five-level inverter. The output current of the five-level inverter is detected by a current sensor.

The reference signal and detected signal for the output current of the five-level inverter are sent to a subtractor. The subtracted result is sent to a current-mode controller. The output of the current-mode controller is sent to a PWM circuit to generate a PWM signal. The detected dc capacitor voltages *VC*2 and *VC*3 are also sent to a comparator to obtain signal *Sb* . When dc capacitor voltage *VC*2 is higher than dc capacitor voltage *VC*3, *Sb* is a high value. On the contrary, *Sb* is a low value when dc capacitor voltage *VC*2 is smaller than dc capacitor voltage *VC*3. DC voltage *V*dc is also sent to an amplifier with a gain of 0.5 to obtain voltage signal *V*dc/2. The detected utility voltage is sent to an absolute circuit to obtain voltage signal |*vs*|.

Voltage signals *V*dc/2 and |*vs* | are compared to obtain signal *Sc*. When *V*dc/2 > |*vs* |, *Sc* is a high value. On the contrary, *Sc* is a low value when *V*dc/2 < |*vs* |. The output signal of the PWM circuit and signals *Sb* and *Sc* are sent to the mode selection circuit. The output of the mode selection circuit will generate the control signals of power electronic switches *S*2 and *S*3 according to Table I. The detected utility voltage is also sent to a comparator to obtain complementary square signals that are synchronous with the detected utility voltage. The complementary square signals are the control signals of the power electronic switches of the full-bridge inverter. As mentioned earlier, only two power electronic switches *S*2 or *S*3 in the five-level inverter should be switched in high frequency, and only one of them is switched in high frequency at any time, and the voltage level of every switching is *V*dc/2. Therefore, the five-level inverter can reduce the switching loss effectively.

B. DC–DC Converter

Fig. 7 shows the control block of the dc–dc converter. The input of the dc–dc converter is the output of the solar cell array. A ripple voltage with a frequency double that of the utility will appear in the dc bus voltage *V*dc, while the five-level inverter injects real power into the utility. The function of MPPT will be degraded, while the output voltage of solar cell array contains a ripple voltage. Therefore, the ripple voltage superimposed on the dc bus voltage *V*dc must be blocked by the dc–dc converter for improving the function of MPPT. Accordingly, the dual control loops, an outer voltage control loop, and an inner

current control loop are applied to control the dc–dc converter. Since the output voltage of the dc–dc converter is the dc bus voltage that is controlled to be a constant voltage by the five-level inverter, the outer voltage control loop is used to regulate the output voltage of the solar cell array. The inner current control loop is applied to control the inductor current to approach a constant current to block the ripple voltage of dc bus voltage *V*dc. The perturbation and observation method is adopted to obtain the function of MPPT [24], and it is incorporated into the controller of the dc–dc converter. The output of the MPPT controller is the desired output voltage of the solar cell array, and it is the reference voltage of the outer voltage control loop. The output voltage of the solar cell array is perturbed first, and then the output power variation of the solar cell array is observed to determine the next perturbation for the output voltage of the solar cell array. The output power of the solar cell array is calculated from the product of the output voltage of the solar cell array and the inductor current. Therefore, the output voltage of the solar cell array and the inductor current are detected and sent to a MPPT controller to determine the desired output voltage of the solar cell array. The detected output voltage and desired output voltage of the solar cell array are sent to a subtractor, and the subtracted result is sent to a P-I controller. The output of the P-I controller is the reference signal of the inner current control loop. The reference signal and the detected inductor current are sent to a subtractor, and the subtracted result is sent to an amplifier to complete the inner current control loop. The output of the amplifier is sent to the PWM circuit. The output signal of the PWM circuit is the driving signal for the power electronic switch of the dc–dc converter. For protecting the renewable power generation system from the voltage rise, the MPPT function will be disabled and the power electronic switch *S*1 will be turned OFF when the inverter stage is interrupted after detecting the islanding operation.

Therefore, the output voltage of solar cell array is limited to the open-circuit voltage of solar cell array, and the dc bus voltage *V*dc is also limited.

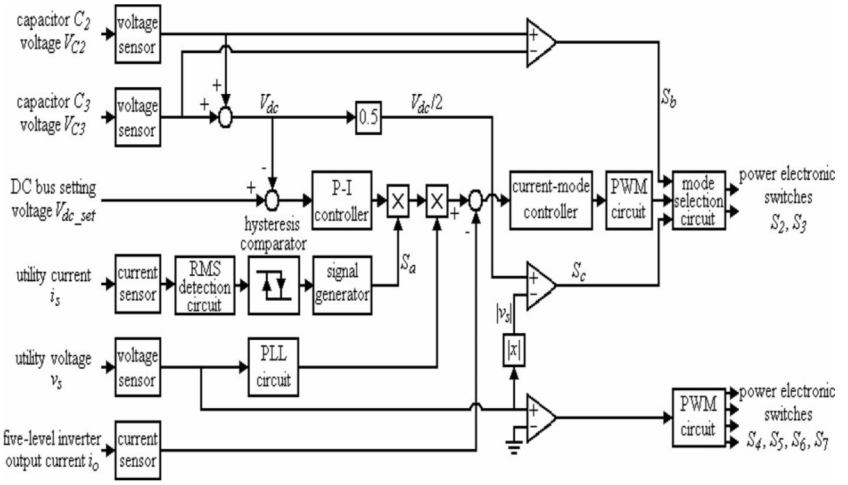

Fig. 6. Control block diagram of five-level inverter

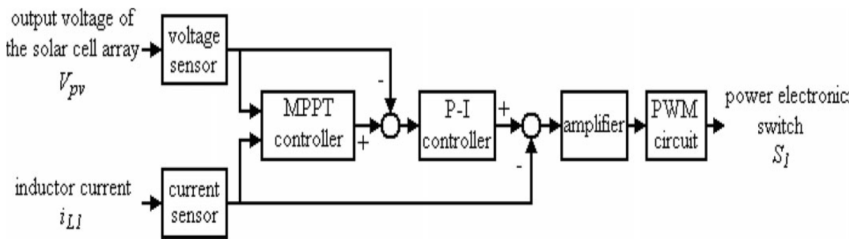

Fig. 7. Control block of the dc–dc converter

TABLE II

MAJOR PARAMETERS USED IN THE EXPERIMENTS

Solar module	
Rate of maximum power	75W
Open voltage	21.7V
Short current	5.0A
DC-DC converter	
Capacitor (C_1)	470μF
Inductor (L_1)	2mH
Switch frequency	20kHz
Five-level inverter	
DC bus capacitor (C_2 and C_3)	2,200μF
Filter inductor (L_f)	1.4mH
DC bus setting voltage	170V
Switch frequency (PWM)	20kHz
Utility voltage	110V
Utility frequency	60Hz

VI. EXPERIMENTAL RESULTS

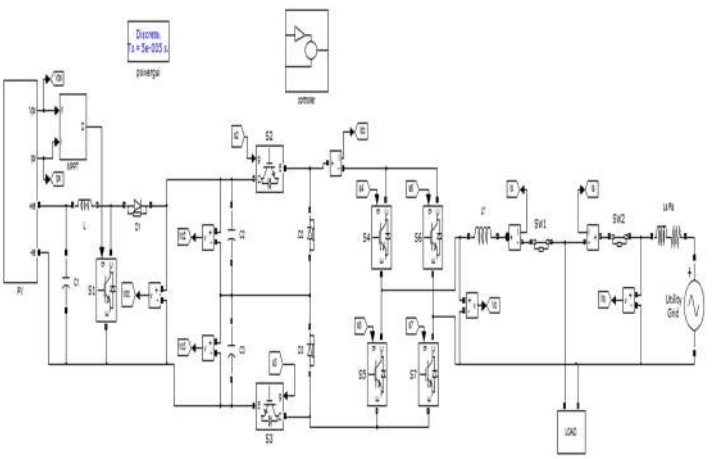

Fig 7 simulation diagram of Five-Level Inverter for Renewable Power

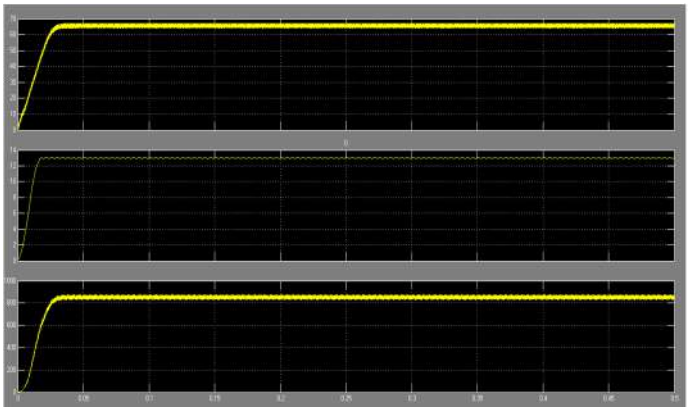

Fig 8 Experimental results of MPPT performance for the developed photovoltaic power generation system

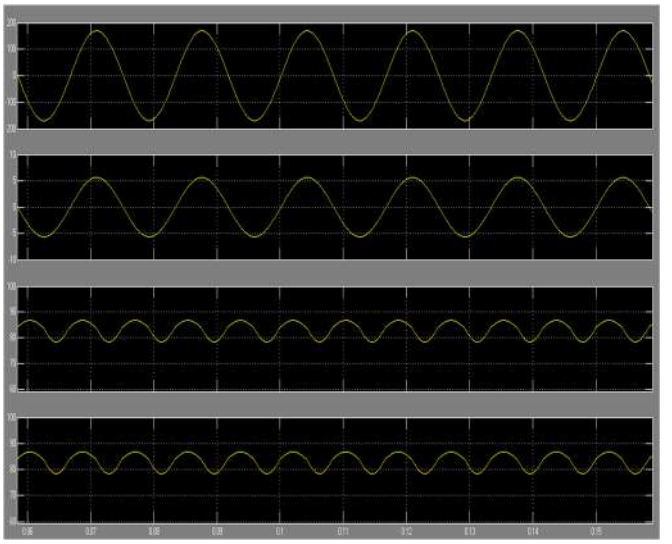

Fig 9 Experimental results of the five-level inverter. (a) Utility voltage. (b) Output current of the five-level inverter. (c) DC capacitor voltage *VC* 2 (d) DC capacitor voltage *VC* 3

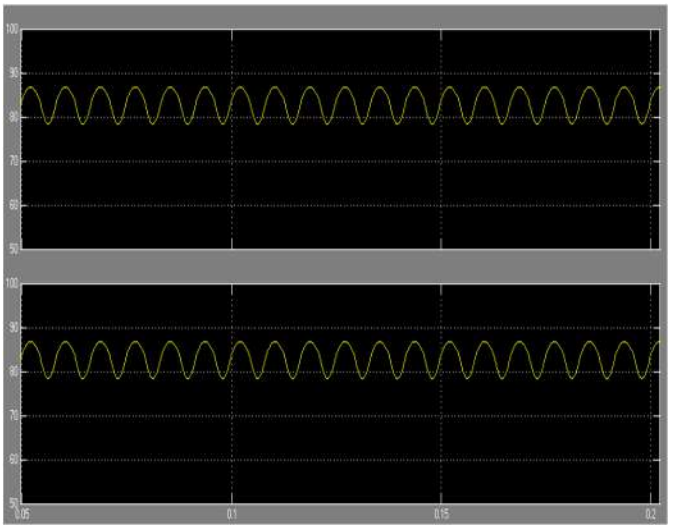

Fig 10 Experimental results for the dc–dc converter of the developed photovoltaic power generation system. (a) Voltage ripple of dc capacitor *C*2 (b) Voltage ripple of dc capacitor *C*3

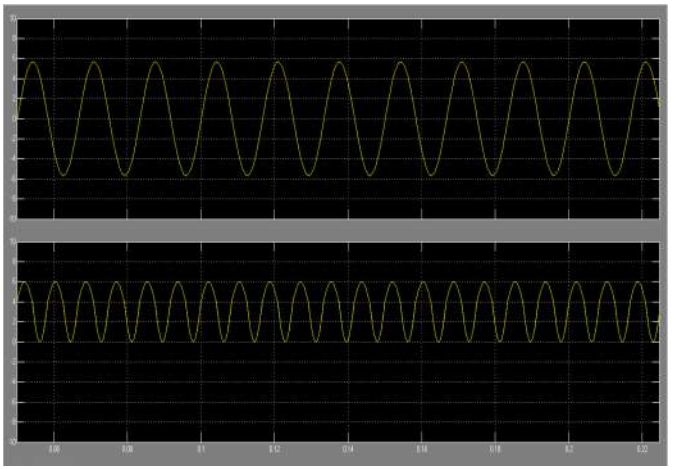

Fig 11 Experimental results for full-bridge inverter of the five-level inverter. (a) Output current of the full-bridge inverter *io* (b) Input current of the full bridge inverter *i*dc

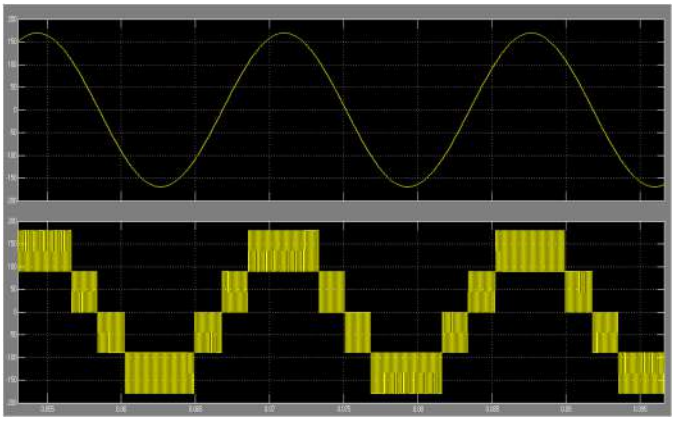

Fig 12 Experimental results of the five-level inverter. (a) Utility voltage. (b) Output voltage of the full-bridge inverter

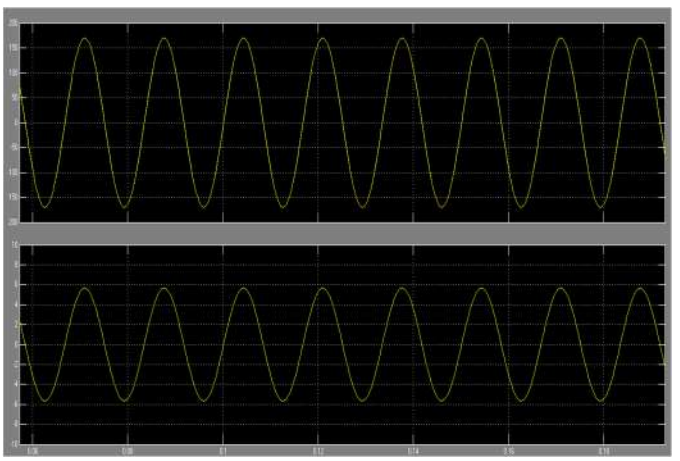

Fig 13 Experimental results for the developed photovoltaic power generation system under the distorted utility voltage. (a) Utility Voltage. (b) Output current of the five-level inverter

VII. CONCLUSION

A Dual Buck Converter Fed Full Bridge Inverter for Renewable Energy Power Generation was proposed in this paper. The five-level inverter can perform the functions of regulating the dc bus voltage, converting solar power to ac power with sinusoidal current and in phase with the utility

voltage, balancing the two dc capacitor voltages, and detecting islanding operation. The experimental results show the developed photovoltaic power generation system with dual buck converter, and the five-level inverter improves the performance.

VI. Acknowledgment

This paper is based on M. Tech. project carried out by the student of pydah college of engineering & technology, Kakinada studying M.Tech (Power Electronics) The project had been completed by Mr. S. RAMBABU bearing H.T.no.: 126T1D4313 under the guidance of Ms. M PAVANI.

REFERENCES

1. D. Puyal, L. A. Barragan, J. Acero, J. M. Burdio, and I. Millan, "An FPGA-based digital modulator for full- or half-bridge inverter control," *IEEE Trans. Power Electron.*, vol. 21, no. 5, pp. 1479–1483, Sep. 2006.
2. O. Lopez, F. D. Freijedo, A. G. Yepes, P. Fernandez-Comesaa, J. Malvar, R. Teodorescu, and J. Doval-Gandoy, "Eliminating ground current in a transformerless photovoltaic application," *IEEE Trans. Energy Convers.*, vol. 25, no. 1, pp. 140–147, Mar. 2010.
3. B. R. Lin and C. L. Huang, "Implementation of a Shunt-series compensator for nonlinear and voltage sensitive load," in *Proc. IEEE Power Electron. Motion Control Conf.*, 2006, pp. 1–5.
4. U. S. Selamogullari, D. A. Torrey, and S. Salon, "A systems approach for a stand-alone residential fuel cell power inverter design," *IEEE Trans. Energy Convers.*, vol. 25, no. 3, pp. 741–749, Sep. 2010.
5. J.Gafford,M.Mazzola, J. Robbins, and G. Molen, "Amulti-kilowatt highfrequency ac-link inverter for conversion of low-voltage dc to utility powervoltages," in *Proc. IEEE Power Electron. Spec. Conf.*, 2008, pp. 3707–3712.
6. T. H. Ai, J. F. Chen, and T. J. Liang, "A random switching method for HPWM full-bridge inverter," *IEEE Trans. Ind. Electron.*, vol. 49, no. 3, pp. 595–597, Jun. 2002.
7. C. Y. Chen, Y. H. Lin, J. F. Chen, and R. L. Lin, "Design and implementation of DSP-based voltage frequency conversion system," in *Proc. Int. Symp. Comput. Commun. Control Autom.*, May 2010, pp. 435–438.
8. M. Chithra and S. G. B. Dasan, "Analysis of cascaded H bridge multilevel inverters with photovoltaic arrays," in *Proc. Int. Conf. Emerging Trends Elect. Comput. Technol.*, Mar. 2011, pp. 442–447.
9. N. Yousefpoor, S. H. Fathi, N. Farokhnia, and S. H. Sadeghi, "Application of OHSW technique in cascaded multi-level inverter with adjustable dc sources," in *Proc. Int. Conf. Electric Power Energy Convers. Syst.*, 2009, pp. 1–6.
10. S. De, D. Banerjee, K. Siva Kumar, K. Gopakumar, R. Ramchand, and C. Patel, "Multilevel inverters for low-power application," *IET Power Electron.*, vol. 4, no. 4, pp. 384–392, Apr. 2011.
11. A. Nami, F. Zare, G. Ledwich, A. Ghosh, and F. Blaabjerg, "Comparison between symmetrical and asymmetrical single phase multilevel inverter with diode-clamped topology," in *Proc. IEEE Power Electron. Spec. Conf.*, Jun. 2008, pp. 2921–2926.

12. E. Ozdemir, S. Ozdemir, and L. M. Tolbert, "Fundamental-frequencymodulated six-level diode-clamped multilevel inverter for three-phase stand-alone photovoltaic system," *IEEE Trans. Ind. Electron.*, vol. 56, no. 11, pp. 4407–4415, Nov. 2009.
13. A. Nami, F. Zare, A. Ghosh, and F. Blaabjerg, "A hybrid cascade converter topology with series-connected symmetrical and asymmetrical diodeclamped H-Bridge cells," *IEEE Trans. Power Electron.*, vol. 26, no. 1, pp. 51–65, Jan. 2011.
14. A. A. Boora, A. Nami, F. Zare, A. Ghosh, and F. Blaabjerg, "Voltagesharing converter to supply single-phase asymmetrical four-level diodeclamped inverter with high power factor loads," *IEEE Trans. Power Electron.*, vol. 25, no. 10, pp. 2507–2520, Oct. 2010.
15. P. Samuel, R. Gupta, and D. Chandra, "Grid interface of wind power with large split-winding alternator using cascaded multilevel inverter," *IEEE Trans. Energy Convers.*, vol. 26, no. 1, pp. 299–309, Mar. 2011.
16. O. Bouhali, B. Francois, E. M. Berkouk, and C. Saudemont, "DC link capacitor voltage balancing in a three-phase diode clamped inverter controlled by a direct space vector of line-to-line voltages," *IEEE Trans. Power Electron.*, vol. 22, no. 5, pp. 1636–1648, Sep. 2007.
17. G. P. Adam, S. J. Finney, A. M. Massoud, and B. W.Williams, "Capacitor balance issues of the diode-clampedmultilevel inverter operated in a quasi two-state mode," *IEEE Trans. Ind. Electron.*, vol. 55, no. 8, pp. 3088–3099, Aug. 2008.
18. G. P. Adam, S. J. Finney, B. W. Williams, and M. T. Mohammed, "Twolevel operation of a diode-clamped multilevel inverter," in *Proc. IEEE Int. Symp. Ind. Electron.*, Jul. 2010, pp. 1137–1142.
19. C. Xia, X. Gu, T. Shi, and Y. Yan, "Neutral-point potential balancing of three-level inverters in direct-driven wind energy conversion system," *IEEE Trans. Energy Convers.*, vol. 26, no. 1, pp. 18–29, Mar. 2010.
20. X. Ruan, B. Li, Q. Chen, S. C. Tan, and C. K. Tse, "Fundamental considerations of three-level dc–dc converters: Topologies, analyses, and control," *IEEE Trans. Circuits Syst. I: Reg. Papers*, vol. 55, no. 11, pp. 3733–3743, Dec. 2008.
21. F. Khoucha, M. S. Lagoun, A. Kheloui, and M. El Hachemi Benbouzid, "A comparison of symmetrical and asymmetrical three-phase H-bridge multilevel inverter for DTC induction motor drives," *IEEE Trans. Energy Convers.*, vol. 26, no. 1, pp. 64–72, Mar. 2011.
22. H. D. Sun, M. Y. Park, J. H. Park, H. G. Kim, T. W. Chun, and E. C. Nho, "NovelH-bridge multi-level inverter with dc-link switches," in *Proc. IEEE*
Int. Conf. Power Electron. ECCE Asia, 2011, pp. 1734–1741.
23. J. M. Shen, H. L. Jou, and J. C. Wu, "Grid-Connected power converter with islanding detection and active power filter functions," in *Proc. IEEE Int. Symp. Power Electron. Distrib. Generation Syst.*, Jun. 2010, pp. 501– 506.
24. G. J. Yu, Y. S. Jung, J. Y. Choi, and G. S. Kim, "A novel two-mode MPPT control algorithm based on comparative study of existing algorithms," *Solar Energy*, vol. 76, no. 4, pp. 455–463, 2004.
25. *IEEE Recommended Practice for Utility Interface of Photovoltaic (PV) Systems*, IEEE Std 929-2000, 2000.
26. *Safety of Power Converters for Use in Photovoltaic Power Systems—Part 2: Particular Requirements for Inverters*, IEC 62109-2, Ed.1, 2011.

INTERNATIONAL JOURNAL OF MULTIDISCIPLINARY EDUCATIONAL RESEARCH
ISSN : 2277-7881; IMPACT FACTOR - 2.972; IC VALUE:5.16
VOLUME 3, ISSUE 10(4), OCTOBER 2014

DUAL ACTIVE BRIDGE (DAB) CONVERTER STAGE WITH HIGH FREQUENCY SST'S BETWEEN AC & DC DISTRIBUTION SYSTEMS

Mr. B. SATYA VARAPRASAD
satyaeee0205@gmail.com
Under the guidance of
Ms. B. LALITHA KUMARI
ASSISTANT PROFESSIOR
PYDAH COLLEGE OF ENGINEERING , KAKINADA

Abstract— This paper proposes a new voltage and power balance control for the cascaded H-Bridge converter-based SST. The solid-state transformer (SST) is an interface device between ac distribution grids and dc distribution systems. The SST consists of a cascaded multilevel ac/dc rectifier stage, a dual active bridge (DAB) converter stage with high-frequency transformers to provide a regulated 400-V dc distribution, and an optional dc/ac stage that can be connected to the 400-V dc bus to provide residential 120/240 Vac . However, due to dc-link voltage and power unbalance in the cascaded modules, the unbalanced dc-link voltages and power increase the stress of the semiconductor devices and cause overvoltage or overcurrent issues. Based on the single-phase *dq* model, a novel voltage and the power control strategy is proposed to balance the rectifier capacitor voltages and the real power through parallel DAB modules. Furthermore, the intrinsic power constraints of the cascaded H-Bridge voltage balance control are derived and analyzed. With the proposed control methods, the dc-link voltage and the real power through each module can be balanced. The SST switching model simulation is presented using MATLAB.

Key words: DAB, cascaded H-Bridge, SST

I. INTRODUCTION

The solid-state transformer (SST) is the interface device between the distribution system and the electricity consumer's in future smart grid systems. As the interface between power transmission grids and the consumers, the distribution power system currently requires 60 Hz transformers for voltage transformation. These conventional copper-and-iron based transformers possess many undesirable properties including bulky size, environmental concerns and especially power quality susceptibility. As the development of the dc distribution system and the increase of the penetration

of distributed generations, an intelligent transformer with the capability to actively manage the power and allowing for the easy connection of the distribution resources is becoming indispensable.

In the proposed electric configuration of the smart grid system shown in Fig. 1, low voltage (120 V), residential class distributed renewable energy resource (DRER), distributed energy storage device (DESD), and loads are connected to the 400-V dc distribution bus and then to distribution bus (12-kV three phase or 7.2-kV single phase) through a SST. The SST is used to enable active management of DRER, DESD, and loads, rather than a 60-Hz conventional transformer.

The SST has the features of instantaneous voltage regulation, voltage sag compensation, fault isolation, power factor correction, harmonic isolation, and dc output [1]–[4]. The SST has a 400-V dc port that will facilitate more efficient connection of certain classes of DRERs and DESDs. Acting very much like an energy router, each SST has bidirectional energy flow control capability allowing it to control active and reactive power flow and to manage the fault currents on both low- and high-voltage sides. Its large control bandwidth provides the plug-and-play feature for distributed resources to rapidly identify and respond to changes in the system.

This paper proposes a 20-kVA cascaded H-Bridge multilevel converter-based SST to directly interface with 7.2-kV singlephase distribution voltage level. As shown in Fig. 2, the SST consists of a cascaded multilevel ac/dc rectifier, dual active bridge (DAB) converterswith high-frequency transformers. The regulated 400-V dc bus is distributed for easier connection of battery and other distributed resources.

The rectifier stage is a seven-level cascaded H-Bridge converter, which controls the input power factor and regulates the 3.8-kV high-voltage dc link. The DAB converter regulates the 400-V-low-voltage dc bus and additional dc/ac inverters can be added to provide a 60 Hz 120/240-V ac residential voltage. One of the main disadvantages of the cascaded H-bridge rectifier is the voltage unbalance of the dc-link voltages at different H-Bridges [5]–[7], [12], [13], [18], [20]. Relevant research mainly focuses on the unbalance issues in static synchronous compensator (STATCOM) or drive applications and no powercontrol method has been mentioned. The proposed voltage and balance control in this paper have the following features: balanced dc-bus voltage,

balanced real power, equally distributed reactive power between H-bridges, and using simple phase-shift pulsewidth modulation (PWM).

In [5]–[7], low-frequency PWM techniques for STATCOM are presented. The dc-link voltage is balanced by using different switching patterns to charge and discharge each H-Bridge capacitor, but the reactive power is not controlled. Barrena *et al.* [8] present an individual voltage-balancing strategy to balance the dc-link voltage with PWM. The method maintains delivered reactive power equally distributed among all H-Bridges. However, the method is based on the STATCOM application and no power unbalance constraints are mentioned in this paper. Iman-Eini *et al.* [9] present a method that ensures the dc-link voltages converge to the reference value when load power is different. The method results in different switching frequencies for the H-Bridges and a complicated controller implementation. Leon *et al.* [10] and Barrena *et al.* [11] present different PWM methods to balance the dc-link voltages, however the balance range and power control are not included. In contrast to the STATCOM and drive application, the SST requires a highfrequency modulation and both real and reactive power control. Furthermore, due to the intrinsic constraint of the cascaded rectifier topology, the voltage balance control is limited and the power balance control is therefore required. In this paper, the modeling of the SST, including ac/dc rectifier, DAB converter are developed. A single-phased *dq* vector controller is designed for the rectifier stage; therefore the real power and reactive power can be controlled independently. Based on the single-phase *dq* control, a voltage balance control method is proposed to resolve the voltage unbalance that could appear on the dc links of different H-bridges.

The limitation and the power unbalance range of the cascaded H-Bridge rectifier are derived. Meanwhile, a power balance control method is proposed to regulate the real power transferring through the DAB parallel modules. The proposed voltage and power control are verified by the switching model simulation. Finally, a SST scale-down prototype is implemented by using 600-V insulatedgate bipolar transistor (IGBT) devices. The experiments are presented to verify the real and reactive power control, power factor correction, voltage sag compensation, and proposed voltage balance control.

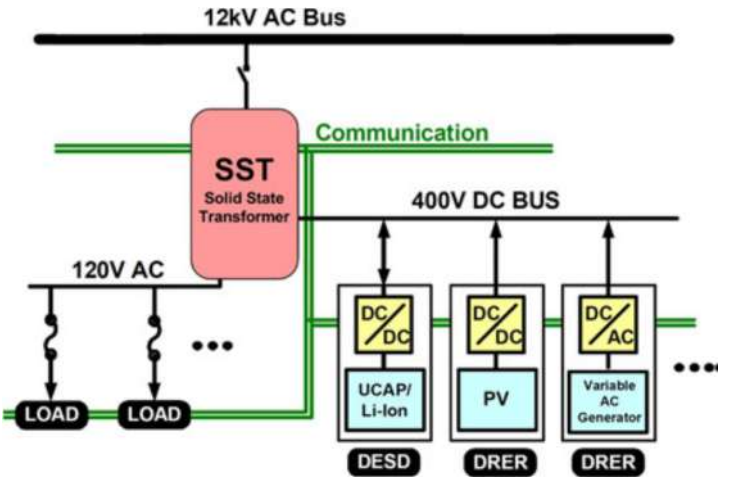

Fig. 1 SST at one residential home (SST: solid-state transformer, DRER: distributed renewable energy resource, DESD: distributed energy storage device).

II. SST MODELING AND CONTROL

The modeling and control of the SST, including the cascaded multilevel ac/dc rectifier, DAB converters with high-frequency transformers are developed in this section.

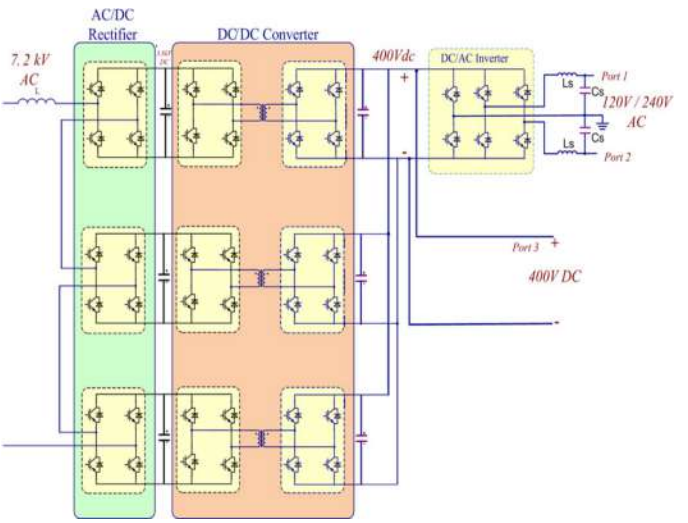

Fig. 2 Topology of the proposed SST

The basic configuration of the proposed 20-kVASST is shown in Fig. 2. The SST is rated as single-phase input voltage 60 Hz, 7.2 kV, output voltage 400-V dc. The first stage of the SST is a high-voltage cascaded H-Bridge ac/dc rectifier that converts 60 Hz, 7.2-kV ac to three cascaded 3.8-kV dc links. The second stage consists of three high-voltage high-frequency dc/dc converters that convert 3.8 kV to 400-V dc bus and then additional inverter can be connected to 400-V dc bus to invert 400-V dc to 60-Hz, 240/120 V. The switching devices in high-voltage H-bridges and low-voltage H-bridges are 6.5-kV IGBT and 600-V IGBT, respectively. The switching frequency of the 6.5-kV IGBT devices is 1 kHz, because the device current is very low resulting in low switching losses. The 20-kVA SST unit is envisioned as a building block for construction of a larger rated SST. The controller of each stage in the SST is independent from each other. The rectifier controller regulates the input power factor and 3.8-kV high-voltage dc link. The DAB controller regulates the 400-V low-voltage dc bus, and the inverter controller regulates the 240/120-V output ac voltage.

A. Rectifier Single-Phase dq Vector Control

The ac/dc rectifier stage converts the single-phase 7.2-kV ac voltage to three dc-link voltages while controlling the reactive power at the input side. The rectifier consists of three cascaded H-bridges with each reference dc-link voltage 3.8 kV. The average differential equations of the rectifier are

$$\frac{di_a}{dt} = \frac{3E}{L_s} d_a - \frac{V_{\text{pcca}}}{L_s} - \frac{R_s}{L_s} i_a \qquad (1)$$

$$\frac{dE}{dt} = -\frac{E}{R_L C} - \frac{d_a i_a}{C} \qquad (2)$$

Where, *ia* is the input current, *V*pcca is the input voltage, *Rs* is the input line resistance, *Ls* is the input inductor,*E* is the dc-link voltage, *RL* is the equivalent output impedance of the rectifier stage, *C* is the rectifier dc capacitor, and *da* is the rectifier PWM duty cycle.

The single-phase *dq* vector control is applied in the rectifier controller. An imaginary phase M, lagging the original phase A by 90◦, is hypothesized. The differential equations for the imaginary phase are

$$\frac{di_m}{dt} = \frac{3E}{L_s} d_m - \frac{V_{\text{pccm}}}{L_s} - \frac{R_s}{L_s} i_m \qquad (3)$$

$$\frac{dE_m}{dt} = -\frac{E_m}{R_L C} - \frac{d_m i_m}{C} \qquad (4)$$

Where, *im* is the input current of the imaginary phase, *V*pccm is the input voltage of the imaginary phase, *Em* is the dc-link voltage of the imaginary phase, *dm* is the rectifier PWM duty cycle of the imaginary phase. Based on the small ripple approximation, *Em*=*E*. Then, combine the equations for two phases, and rewrite the equations

$$\frac{d\vec{i}_{\mathrm{am}}}{dt} = \frac{3E}{L_s}\vec{d}_{\mathrm{am}} - \frac{\vec{V}_{\mathrm{pccam}}}{L_s} - \frac{R_s}{L_s}\vec{i}_{\mathrm{am}} \tag{5}$$

$$\frac{dE}{dt} = -\frac{E}{R_L C} - \frac{\vec{d}_{\mathrm{am}}^{T}\vec{i}_{\mathrm{am}}}{2C} \tag{6}$$

where

$$\vec{i}_{\mathrm{am}} = \begin{bmatrix} i_a \\ i_m \end{bmatrix}, \vec{d}_{\mathrm{am}} = \begin{bmatrix} d_a \\ d_m \end{bmatrix}, \vec{V}_{\mathrm{pccam}} = \begin{bmatrix} V_{\mathrm{pcca}} \\ V_{\mathrm{pccm}} \end{bmatrix}.$$

The single-phase *dq* transformation is applied to the (5) and (6) [14], and the differential equations in *dq* coordinates are divided

$$[x]_{\mathrm{dq}} = [T] \cdot [x]_{\mathrm{am}} \tag{7}$$

Where

$$T = \begin{bmatrix} \sin(\theta) & -\cos(\theta) \\ \cos(\theta) & \sin(\theta) \end{bmatrix}, \theta = \omega t, \omega = 2\pi f_L$$

fL is line frequency.

Then, the *dq*-axis equation of the single-phase H-bridge rectifier is given in (8) and (9)

$$\frac{d}{dt}\begin{bmatrix} i_d \\ i_q \end{bmatrix} = \frac{3E}{L_s}\begin{bmatrix} d_d \\ d_q \end{bmatrix} - \frac{1}{L_s}\begin{bmatrix} v_{\mathrm{pccd}} \\ v_{\mathrm{pccq}} \end{bmatrix} - \begin{bmatrix} \frac{R_s}{L_s} & -\omega \\ \omega & \frac{R_s}{L_s} \end{bmatrix}\begin{bmatrix} i_d \\ i_q \end{bmatrix} \tag{8}$$

$$\frac{dE}{dt} = -\frac{E}{R_L C} - \frac{1}{2C}\begin{bmatrix} d_d \\ d_q \end{bmatrix}^{T}\begin{bmatrix} i_d \\ i_q \end{bmatrix}. \tag{9}$$

The function of the rectifier controller is to control the reactive power (or power factor) and regulate the dc-link voltages. With the chosen phase-locked loop, the voltage vector is aligned with the direction of the *d*-axis during steady state. The grid-voltage component in the *d*-direction is equal to its peak value and the *q*-component of the grid voltage is equal to zero. Thus, the *d*-

component of the current vector (in steady state parallel to the grid-voltage vector) becomes the active current component (*d*-current) and the *q*-component of the current vector becomes the reactive current component (*q*-current) [15]. The decoupled *dq* vector controller for each H-bridge is shown in Fig. 3. The three sinusoidal pulse width modulation (SPWM) carriers for the cascaded H-bridge are phase shifted so that the rectifier has seven voltage levels to reduce the voltage stress and harmonics. Depending on the reactive power reference in the SST controller *i*qref, the SST can generate or absorb reactive power to the power grid.

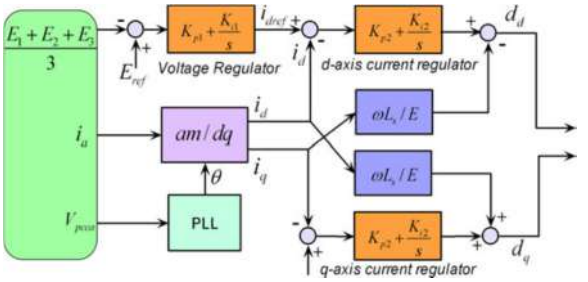

Fig. 3 Rectifier single-phase *dq* decoupled controller

B. Modeling and Control of DAB

The DAB consists of a high-voltage H-Bridge, a highfrequency transformer and a low-voltage H-bridge as shown in Fig. 4. The rectifier regulates the high-voltage dc-link voltage and controls the input current to be sinusoidal from the ac input. The low-voltage dc link is regulated by the DAB converter [16], [19].

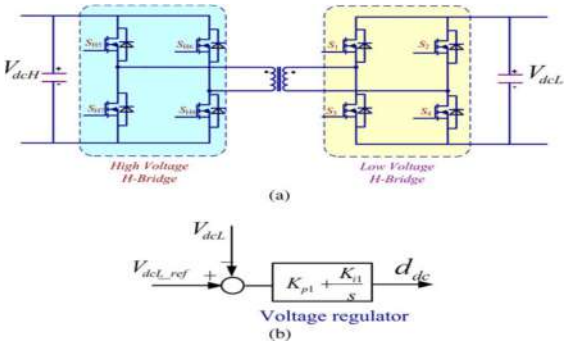

Fig. 4 (a) DAB circuit and (b) DAB voltage controller

The DAB topology offers zero voltage switching, relatively low-voltage stress for the switches, low passive component ratings and complete symmetry of configuration that allows seamless control for bidirectional power flow. Real power flows from the bridge with leading phase angle to the bridge with lagging phase angle, the amount of transferred power is controlled by the phase angle difference and the magnitudes of the dc voltages at the two ends as given by (10)

$$P_o = \frac{V_{\mathrm{dcH}} V'_{\mathrm{dcL}}}{2Lf_H} d_{\mathrm{dc}}(1 - d_{\mathrm{dc}}) \qquad (10)$$

Where, *V*dcH is input side high dc-link voltage, *fH* is switching frequency, *L* is leakage inductance, *V* _ dcL is output side low dc bus voltage referred to input side, and *d*dc is the ratio of time delay between the two bridges to one-half of switching period. For the DAB converter, the phase-shift control is applied to regulate the low-voltage dc voltage to the reference 400 V under different load conditions. First the difference between the low dc voltage *V*dc and the reference voltage is compared. Then, the phase-shift angle is adjusted by the proportional-integral (PI) controller to regulate *V*dcL according to this voltage error.

III. VOLTAGE AND POWER BALANCE CONTROL

Since the rectifier stage of the SST consists of three H-Bridges in series, the voltage unbalance could appear on the dc-link voltages (*E*1*, E2*, and *E*3, as shown in Fig. 5) due to the device loss mismatching and H-Bridge real power differences. The unbalance issue worsens when the SST operates at no load or light load condition, because a small power difference is a significant percentage of the real power and will result in a large voltage unbalance at no load or light load condition. The unbalanced voltage will cause the capacitor or IGBT device overvoltage in the H-Bridge and trigger the system overvoltage protection. The DAB stage consists of three DAB modules in parallel. The power unbalance (*P*1*, P*2, and *P*3, as shown in Fig. 5) can be caused by the transformer parameter mismatching (such as leakage inductance or turns ratio) and dc-link voltage differences. The power unbalance will cause a device overcurrent issue and result in unbalance heat distributions. Section III-A introduces the proposed voltage balance control for the cascaded H-Bridge rectifier and illustrates the three dc-link voltages can be balanced in a 20% power unbalance condition. Section III-B derives the maximum real power

unbalance range in which the voltage balance control can maintain the balanced dc links. If the power unbalance is out of the derived range, the voltage balance control will not be able to balance the dc-link voltages, therefore the DAB power balance control is needed to regulate the H-Bridge real power. Section III-C describes the proposed power balance control method, which guarantees the power unbalance of the DAB modules is within the required range so that the three dc-link voltages can always be balanced with the proposed voltage balance control.

A. Voltage Balance Control

The single-phase *dq* vector controller for the rectifier stage regulates the total dc-link voltage and controls the reactive power. Based on the single-phase *dq* control, a voltage balance control method is proposed to resolve the voltage unbalance on the dc links of different H-bridges. The voltage balance control basically adjusts the modulation signals *da*1*, da*2, and *da*3 individually to achieve different real power distributions of the H-Bridges. Fig. 6 illustrates the proposed voltage balance controller. In Fig. 6, the *dd* and *dq* are calculated according to the single-phase *dq* vector control. The individual dc-link voltages of the first two H-Bridges, *E*1 and *E*2 are compared with the dc-link voltage reference *E*ref to generate *d*-axis compensation $\Delta dd1$ and $\Delta dd2$ by a PI regulator. Then, $\Delta dd1$ and $\Delta dd2$ are added to the original *dd.* Therefore, *dd*1 for the first H-Bridge and *dd*2 for the second H-Bridge are adjusted so that the real power distribution can be changed. The real power of the H-Bridge with a lower dc-link voltage is increased, and the real power with a higher dc-link is decreased to eliminate the voltage unbalance. For the third H-Bridge, $\Delta dd3 = -\Delta dd1 - \Delta dd2$, so the total dc-link voltage regulation is not affected. Meanwhile, the *q*-axis current references are still independent form the *d*-axis, which means the reactive power, can be controlled independently.In order to verify the proposed voltage control, the switching model simulation of the 20-kVA SST is implemented in MATLAB/Simulink. The SST topology is shown in Fig. 5 and the simulation parameters are shown in Table I. The parameter selections are described in [17]. In the simulation, the real power *P*1*, P*2, and *P*3 of the three H-Bridges are controlled by connecting different resistors to the 3.8-kV dc links, *E*1*, E2*, and *E*3 as shown in Fig. 5. Before 0.83 s, the three H-Bridges transfer the same amount of real power, $P1 = P2 = P3 = 1.0$ p.u. (20 kW/3). Then, at 0.83 s, *P*2 and *P*3 are decreased to 0.8 p.u., $P1 = 1.0$ p.u., $P2 = P3 = 0.8$ p.u. (20% load unbalance).

Two different cases are simulated. The three H-Bridge dc-link voltages become unbalanced after the power change. The H-bridge that transfers more power has the highest dc-link voltage. With the voltage balance controller, the three dc-link voltages are equally regulated in the steady state. This simulation demonstrates that with voltage balance control, even if there is 20% power unbalance from the parallel dc/dc converters, the dc-link voltages can still be balanced. The different resistors simulate a 20% power difference, which is caused by no power balance control in the DAB modules. So when the power balancing control is implemented in DAB, the power difference is dominated by converter power losses, the power unbalance is much smaller than 20%. This guarantees the three dc-link voltage can always be balanced with the proposed voltage balance control.

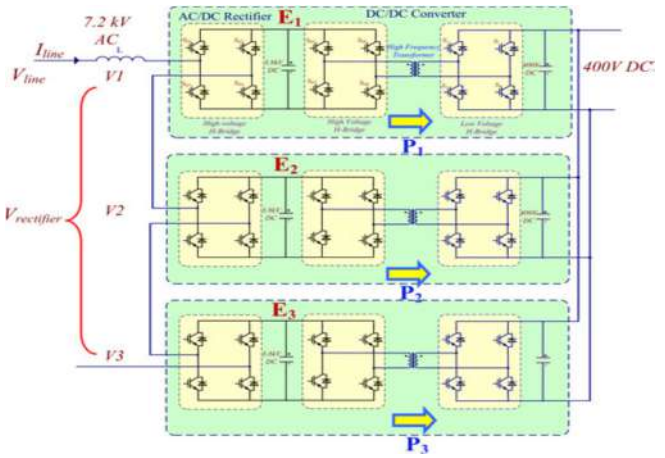

Fig. 5 Voltage and power unbalance in SST topology

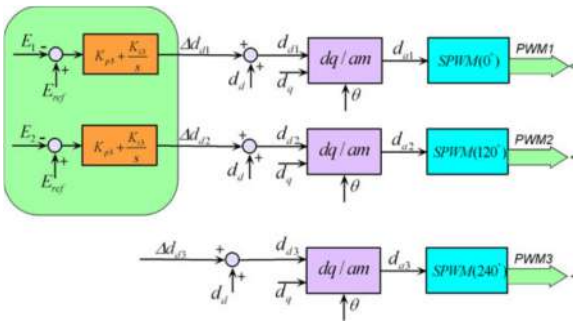

Fig. 6. Proposed voltage balance control based on the single-phase *dq* vector.

TABLE I

SIMULATION PARAMETERS

Input AC voltage (single phase)	7.2kV
Power rating	20kVA
Line inductance L_s	230mH
High voltage DC capacitor	30uF
High voltage DC reference	3.8kV
Low voltage DC capacitor	2mF
Low voltage DC reference	400V
Transformer leakage inductance	165mH
Switching frequency for rectifier	1kHz
Switching frequency for DAB	3kHz
Rectifier control parameters (P, I)	0.3, 12
DAB control parameters (P, I)	1.5e-3, 0.2

B. Voltage Balance Constraints

The proposed voltage controller can maintain the balanced dc-link voltage when the real power is different for each HBridge. However, due to the intrinsic constraints of the cascaded H-Bridge structure, in order to maintain the dc-link balanced, the real power unbalance range of the H-Bridges is limited. This limitation is determined by the input ac voltage, dc-link voltage reference, input inductance, and the number of H-bridges. As shown in Fig. 7, the constraints of the voltage vectors are given by (11)–(21). The derivations are based on the assumption of a unity power factor at the SST rectifier input

$$V_1 + V_2 + V_3 = V_{\text{line}} - j\omega L I_{\text{line}} \tag{11}$$

$$V_1 = (d_1 + jq_1)E,\ V_2 = (d_2 + jq_2)E$$

$$V_3 = (d_3 + jq_3)E \tag{12}$$

Where, *Vn* is the *N*th H-Bridge voltage vector, *V*line is the single phase input ac voltage, *I*line is the input ac current, *dn* and *qn* are the *d*-axis and *q*-axis duty cycle generated by the controller, and *E* is the dc-link reference voltage of each H-Bridge. Rearrange the (11) and (12)

$$V_{\text{line}} - j\omega L I_{\text{line}} = (d_1 + jq_1)E + (d_2 + jq_2)E + (d_3 + jq_3)E$$
$$= E(d_1 + d_2 + d_3) + jE(q_1 + q_2 + q_3). \quad (13)$$
$$\text{So, } d_1 + d_2 + d_3 = \frac{V_{\text{line}}}{E}, \quad q_1 + q_2 + q_3 = \frac{-j\omega L I_{\text{line}}}{E}. \quad (14)$$

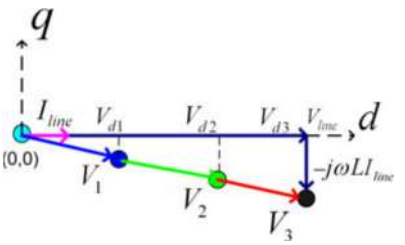

Fig. 7 Rectifier voltage vector constrains

The real power *PN* and reactive power *QN* of the *N*th Hbridge is calculated as

$$P_1 + jQ_1 = I_{\text{line}}V_1 = I_{\text{line}}(d_1 + jq_1)E \quad (15)$$
$$P_2 + jQ_2 = I_{\text{line}}V_2 = I_{\text{line}}(d_2 + jq_2)E \quad (16)$$
$$P_3 + jQ_3 = I_{\text{line}}V_3 = I_{\text{line}}(d_3 + jq_3)E. \quad (17)$$

So from (15)–(17)

$$P_1 = I_{\text{line}}d_1E,\ P_2 = I_{\text{line}}d_2E,\ P_3 = I_{\text{line}}d_3E. \quad (18)$$

The total input power $P_{\text{in}} = \sum_{1}^{N=3} P_n = I_{\text{line}}V_{\text{line}}$, so

$$I_{\text{line}} = \frac{P_{\text{in}}}{V_{\text{line}}}. \quad (19)$$

Substitute *I*line in (14) with (19), then *d*1, *d*2, and *d*3 are derived as

$$d_1 = \frac{P_1}{P_{\text{in}}}\frac{V_{\text{line}}}{E}, \quad d_2 = \frac{P_2}{P_{\text{in}}}\frac{V_{\text{line}}}{E}, \quad d_3 = \frac{P_3}{P_{\text{in}}}\frac{V_{\text{line}}}{E}. \quad (20)$$

Without loss of generality, assume *d*1 ≥ *d*2 ≥ *d*3, the reactive power is equally distributed and no overmodulation *d*21+ *q*21 ≤1.

According to (14) $q_1 + q_2 + q_3 = \frac{-j\omega L I_{\text{line}}}{E}$, so $d_1 \leq \sqrt{1 - (\frac{\omega L I_{\text{line}}}{3E})^2}$.

Substitute d_1 with (20), then the maximum power P_1 should meet the

$$\frac{P_1}{\sum_1^N P_n} \leq \frac{E}{V_{\text{line}}} \sqrt{1 - \left(\frac{\omega L I_{\text{line}}}{NE}\right)^2} \qquad (21)$$

where, N is the number of H-Bridges.

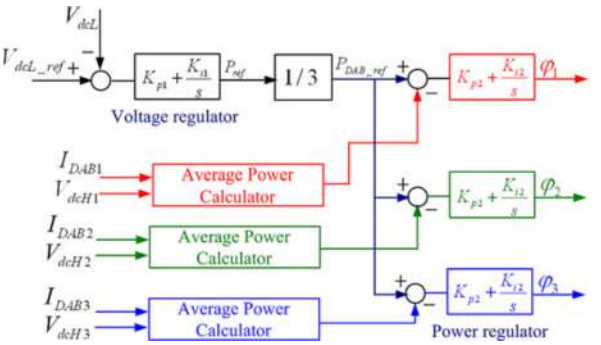

Fig. 8 Power balance controller

In order to balance the dc-link voltages, the real power of each H-Bridge has to be within the range presented in (21). In other words, if the power unbalance is too large, the H-Bridge will not be able to maintain the balanced dc-link voltage. For the designed SST system, according to (21), the maximum power unbalance occurs when the maximum power *P*1 = 37% Pin. When the SST is under light load condition, the power unbalance becomes much more severe because the device loss and transformer parameter mismatch account for a significant percentage of the total power, the power balance equation (21) cannot be assured. Therefore, a power balance control is needed to regulate the H-Bridge real power.

C. Power Balance Control

Due to the parameter variation of the high-frequency transformers, such as leakage inductance and turns ratio, the three DAB currents can be different, which results in a power unbalance of the threeDABmodules.Apower balance controlmethod is proposed to regulate the real power transferring through the DAB parallel modules. As shown in Fig. 8, the voltage regulator compares the low-voltage dc voltage *V*dcL with the reference *V*dcL ref and generates the power references *P*ref for the three DAB modules. Then, the

power regulator compares the calculated average power of each DAB module with *P*ref and generates the phase-shift angles □1, □2, and □3 for the three DAB modules. In the calculation, $P = _ \pi 0 V$dcH*ip dt*, the primary dc voltage *V*dcH can be considered constant in a switching cycle. So the power calculation involves only the summation of current, which is easily implemented in DSP.

The switching model simulation is implemented to verify the proposed power balance control. In the simulation, different leakage inductance values are simulated for the three transformers: 165, 165, and 115 mH (30% variation). The DAB module with smaller leakage inductance has large current and transfers more powerThe transformer current and the power transferring through each DAB module is balanced. So the power balance control guarantees the power unbalance of the parallel DAB modules meets the (21), so that the dc-link voltages can always be balanced with the proposed voltage balance control.

TABLE II

SST PROTOTYPE PARAMETERS

Input inductance	3.5mH
DC Capacitor	900uF
DC voltage reference	400V
Switching frequency of prototype	10kHz
Rectifier control parameters (P, I)	0.3, 12

IV. EXPERIMENTAL RESULTS

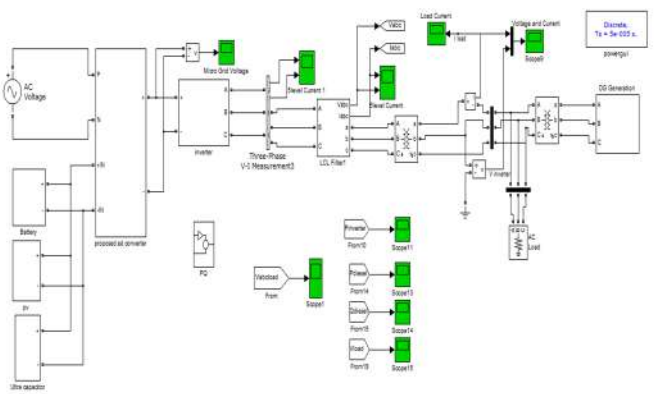

Fig 9 simulation diagram of proposed system

Fig 10 GRID ACTIVE POWER

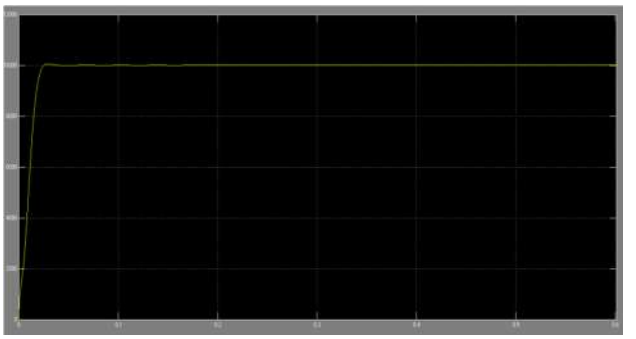

Fig 11 GRID REACTIVE POWER

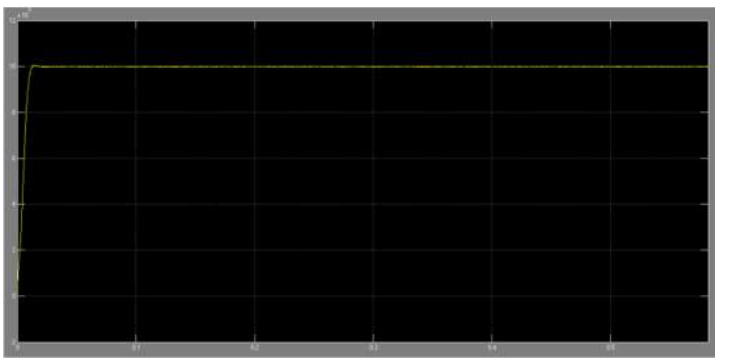

Fig 12 inverter active power

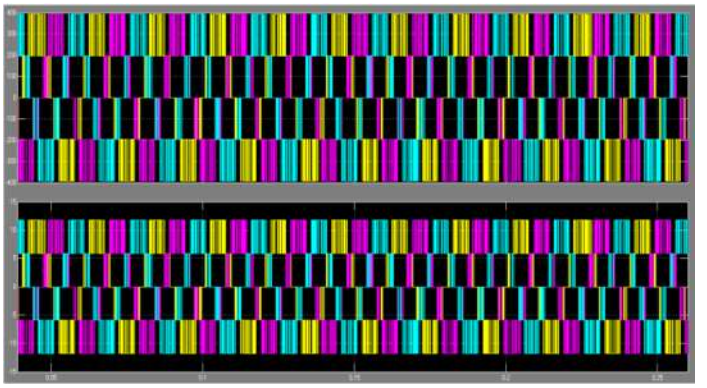

Fig 13 inverter voltage & currents

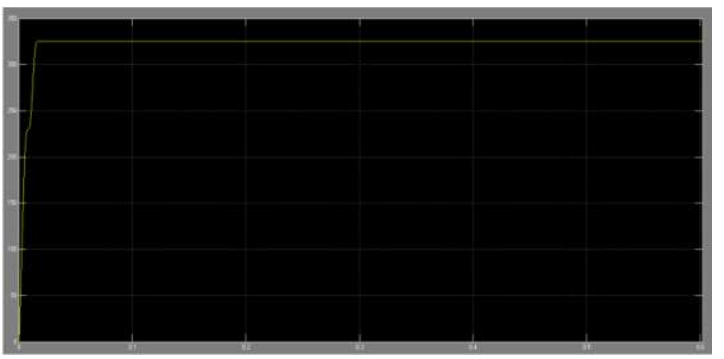

Fig 14 load RMS voltage

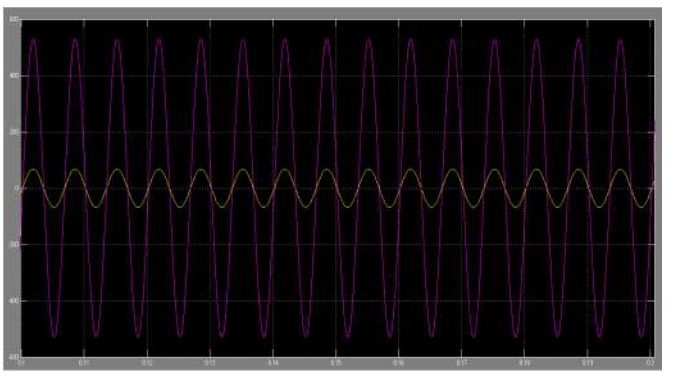

Fig 15 load voltage & current

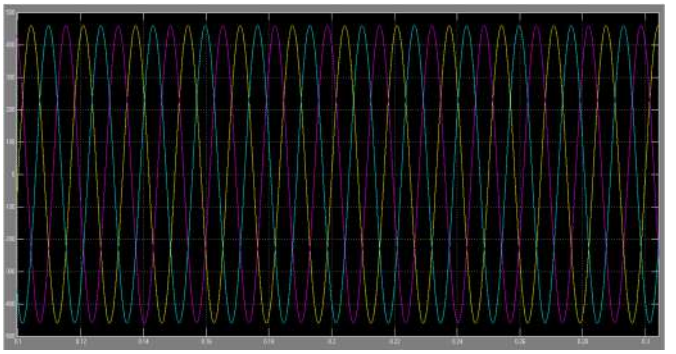

Fig 16 load voltages

V. CONCLUSION

The single-phase *dq* vector modeling and control of the SST, including ac/dc rectifier, DAB converter is developed. A new voltage balance control method is proposed to resolve the voltage unbalance of the dc links in different H-bridges. In this paper, a cascaded H-Bridge converter-based SST is proposed to interface between 7.2-kV ac grid and a 400-V dc distribution in smart grid systems. The power intrinsic unbalance constraints of the voltage balance control for the cascaded H-Bridge rectifier is derived and verified by simulations and experiments. Meanwhile, a power balance control method is proposed to regulate the real power transferring through the parallelmodules. Finally, the switching model simulation and SST scale-down prototype are implemented with the proposed controller.

VIII.Acknowledgment

This paper is based on M. Tech. project carried out by the student of pydah college of engineering & technology, Kakinada studying M.Tech (Power Electronics) The project had been completed by MR. B. SATYA VARAPRASAD bearing H.T.no.: 126T1D4314 under the guidance of B. LALITHA KUMARI.

REFERENCES

1. J. S. Lai and F. Peng, “Multilevel converters—A new breed of power converter,” *IEEE Trans. Ind. Electron.*, vol. 32, no. 3, pp. 509–517, May/Jun. 1996.
2. E. R. Ronan, S. D. Sudhoff, S. F. Glover, and D. L. Galloway, “A power electronic-based distribution transformer,” *IEEE Trans. Power Del.*, vol. 17, no. 2, pp. 537–543, Apr. 2002.

3. J. S. Lai, A. Maitra, A. Mansoor, and F. Goodman, "Multilevel intelligent universal transformer for medium voltage applications," in *Proc. Conf. Rec. Ind. Appl.Conf., 40th IAS Annu. Meeting.*,Oct. 2005, vol. 3, pp. 1893–1899.
4. T. Zhao, J. Zeng, S. Bhattacharya, M. E. Baran, and A. Q. Huang, "An average model of solid state transformer for dynamic system simulation," in *Proc. IEEE Power Energy Soc. Gen. Meeting*, Jul. 2009, pp. 1–8.
5. Y. Liu, A. Q. Huang, W. Song, S. Bhattacharya, and G. Tan, "Smallsignal model-based control strategy for balancing individual DC capacitor voltages in cascade multilevel inverter-based STATCOM," *IEEE Trans. Ind. Electron.*, vol. 56, no. 6, pp. 2259–2269, Jun. 2009.
6. Q. Song, W. Liu, Z. Yuan, W. Wei, and Y. Chen, "DC voltage balancing technique using multi-pulse optimal PWM for cascade H-bridge inverters based STATCOM," in *Proc. IEEE 35th Annu. Power Electron. Spec. Conf.*, 2004, pp. 4768–4772.
7. C. Cecati, A. Dell'Aquila, M. Liserre, and V. G. Monopoli, "Design of H-bridge multilevel active rectifier for traction systems," *IEEE Trans. Ind. Appl.*, vol. 39, no. 5, pp. 1541–1550, Sep./Oct. 2003.
8. J. A. Barrena, L.Marroyo, M. A. R.Vidal, and J. R. T.Apraiz, "Individual voltage balancing strategy for PWM cascaded h-bridge converter-based STATCOM," *IEEE Trans. Ind. Electron*, vol. 55, no. 1, pp. 21–29, Jan. 2008.
9. H. Iman-Eini, J.-L. Schanen, S. Farhangi, and J. Roudet, "A modular strategy for control and voltage balancing of cascaded H-bridge rectifiers," *IEEE Trans. Power Electron.*, vol. 23, no. 5, pp. 2428–2442, Sep. 2008.

INTERNATIONAL JOURNAL OF MULTIDISCIPLINARY EDUCATIONAL RESEARCH
ISSN : 2277-7881; IMPACT FACTOR - 2.972; IC VALUE:5.16
VOLUME 3, ISSUE 10(4), OCTOBER 2014

A CYCLO-CONVERTER BASED LFAC SYSTEM INTERFACED WITH THE MAIN POWER GRID FOR WIND POWER

Mr. S. RAJASEKHAR
s.raja226@gmail.com
Under the guidance of
Mr. P. VIJAYA RAMARAO
ASSISTANT PROFESSIOR
PYDAH COLLEGE OF ENGINEERING , KAKINADA

Abstract—This paper presents a low-frequency ac (LFAC) transmission system for offshore wind power. Off shore wind power plants are expected to represent a significant component of the future electric generation portfolio due to greater space availability and better wind energy potential in offshore locations The LFAC system is interfaced with the main power grid with a cyclo-converter. The wind power plant collection system is dc based, and connects to the LFAC transmission line with a 12-pulse thyristor converter. A method to design the system's components and controls is set forth. Simulation results are provided to illustrate the system's performance. Simulation results are presented by using MATLAB/SIMULINK.

Key words: wind power, cyclo-converter.

I. INTRODUCTION

In this paper, a novel LFAC transmission topology is analyzed. The proposed system differs from previous work [11]–[13] in that the wind turbines are assumed to be interconnected with a medium-voltage (MV) dc grid, in contrast with current practice, where the use of MV ac collection grids is standard [14]. The integration of offshore wind power plants with the main power grid is a subject of ongoing research [3]–[5]. Presently, high-voltage ac (HVAC) and high-voltage dc (HVDC) are well-established technologies for transmission [6]. HVAC transmission is advantageous because it is relatively straightforward to design the protection system and to change voltage levels using transformers. However, the high capacitance of submarine ac power cables leads to considerable charging current, which, in turn, reduces the active power transmission capacity and limits the transmission distance. HVAC is adopted for relatively short (up to 50–75 km) underwater transmission distances [7]. Two classes of HVDC systems exist, depending on the types of power-electronic devices used:

1) line-commutated converter HVDC (LCC-HVDC) using thyristors

2) voltage-source converter HVDC (VSC-HVDC) using self-commutated devices, for example, insulated-gate bipolar transistors (IGBTs) [8].

The main advantage of HVDC technology is that it imposes essentially no limit on transmission distance due to the absence of reactive current in the transmission line [9]. LCC-HVDC systems are capable of handling power up to 1 GW with high reliability [7]. LCCs consume reactive power from the ac grid and introduce low-order harmonics, which inevitably results in the requirement for auxiliary equipment, such as capacitor banks, ac filters, and static synchronous compensators [4]. On the other hand, VSC-HVDC systems are able to independently regulate active and reactive power exchanged with the onshore grid and the offshore ac collection grid. The reduced efficiency and cost of the converters can be identified as drawbacks of VSC-HVDC systems [6]. Power levels (typically on the order of 300–400MW) and reliability are lower than those of LCC-HVDC [7], [9]. HVDC is applied for distances greater than 100 km for offshore wind power transmission. Besides HVAC and HVDC, high-voltage low-frequency ac (LFAC) transmission has been recently proposed [10]–[13]. In LFAC systems, an intermediate-frequency level is used, which is created using a cyclo-converter that lowers the grid frequency to a smaller value, typically to one-third its value.

In general, the main advantage of the LFAC technology is the increase of power capacity and transmission distance for a given submarine cable compared to 50-Hz or 60-Hz HVAC. This leads to substantial cost savings due to the reduction in cabling requirements and the use of normal ac breakers for protection. DC collection is becoming a feasible alternative with the development of cost-effective and reliable dc circuit breakers [15], and studies have shown that it might be advantageous with respect to ac collection in terms of efficiency and improved production costs [16].

The required dc voltage level can be built by using high-power dc–dc converters [17], [18] and/or by the series connection of wind turbines [19]–[22]. For example, multi-MW permanent-magnet synchronous generators with fully rated power converters (Type-4 turbines) are commonly used in offshore wind plants. By eliminating grid-side inverters, a medium-voltage dc collection system can be formed by interconnecting the rectified output of the generators [23]. The main reason for using a dc collection system with LFAC transmission is that the wind turbines would not need to be redesigned to output low-

frequency ac power, which would lead to larger, heavier, and costlier magnetic components (e.g., step-up transformers and generators). The design of the dc collection system is outside the scope of this paper.

At the sending end of the proposed LFAC system, a dc/ac 12-pulse thyristor-based inverter is used to generate low-frequency (20- or 16 2/3-Hz) ac power, as shown in Fig. 1. At the onshore substation (the receiving end), a thyristor-based cycloconverter is used as an interface between the low-frequency side and the 60- or 50-Hz onshore power grid. Thyristor-based converters can transmit more power with increased reliability and lower cost compared to VSC-HVDC systems. However, large filters are necessary at both ends to suppress low-order harmonics and to supply reactive power. Furthermore, the system can be vulnerable to main power grid disturbances.

The proposed LFAC system could be built with commercially available power system components, such as the receiving-end transformers and submarine ac cables designed for regular power frequency. The phase-shift transformer used at the sending end could be a 60-Hz transformer derated by a factor of three, with the same rated current but only one-third of the original rated voltage. Another advantage of the proposed LFAC scheme is its feasibility for multiterminal transmission, since the design of multiterminal HVDC is complicated [24], [25], but the analysis of such an application is not undertaken herein. In summary, LFAC transmission could be an attractive technical solution for medium-distance transmission (i.e., in between HVAC and HVDC) [12].

The objective of this paper is to set forth as a design process for an LFAC system for point-to-point transmission. The system configuration and control strategies are outlined in Section II. The selection of the major system components is discussed in Section III-A, and filter design is discussed in Section III-B. A design example and time-domain simulation study of the proposed LFAC system are provided in Sections IV and V, respectively. Section VI concludes this paper.

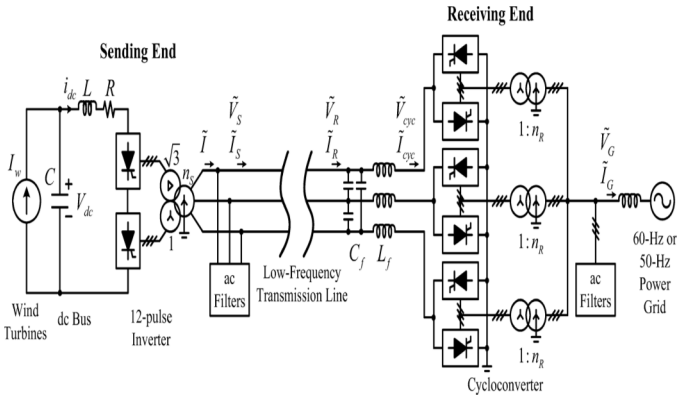

Fig. 1 Configuration of the proposed LFAC transmission system

II. SYSTEM CONFIGURATION AND CONTROL

The proposed LFAC transmission system is shown in Fig. 1, assuming a 60-Hz main grid. At the sending end, a medium-voltage dc collection bus is formed by rectifying the ac output power of series-connected wind turbines [16]. A dc current source represents the total power delivered from the wind turbines. A dc/ac 12-pulse thyristor-based inverter is used to convert dc power to low-frequency (20-Hz) ac power. It is connected to a three-winding transformer that raises the voltage to a higher level for transmission. AC filters are used to suppress the 11th, 13th, and higher-order (23rd) current harmonics, and to supply reactive power to the converter. A smoothing reactor is connected at the dc terminals of the inverter. At the receiving end, a three-phase bridge (6-pulse) cycloconverter is used to generate 20-Hz voltage. A filter is connected at the low-frequency side. At the grid side, ac filters are used to suppress odd current harmonics, and to supply reactive power to the cycloconverter.

Simply put, the operation of the LFAC transmission system can be understood to proceed as follows. First, the cycloconverter at the receiving end is activated, and the submarine power cables are energized by a 20-Hz voltage. In the meantime, the dc collection bus at the sending end is charged using power from the wind turbines. After the 20-Hz voltage and the dc bus voltage are established, the 12-pulse inverter at the sending end can synchronize with the 20-Hz voltage, and start the transmission of power. In reality, more sophisticated schemes for system startup would have to be devised, based nevertheless on this operating principle.

A. Sending-End Control

The control structure for the sending-end inverter is shown in Fig. 2. The controller regulates the dc bus voltage by adjusting the voltage at the inverter terminals. The cosine wave crossing method [26] is applied to determine the firing angle

$$\alpha_S = \arccos\left(\frac{V^*}{V_P}\right) \qquad (1)$$

Where is the peak value of the cosine wave.Note that and (using common notation), since the converter is in the inverter mode of operation [27]. And (line-to-neutral, rms) are related by [28]

$$V = \frac{6\sqrt{6}V_S}{\pi n_S}\cos(\alpha_S). \qquad (2)$$

A phase-locked loop (PLL) provides the angular position of the ac-side voltage, which is necessary for generating the firing pulses of the thyristors. It also outputs the rms value of the fundamental component of the voltage, which is used in the firing-angle calculation.

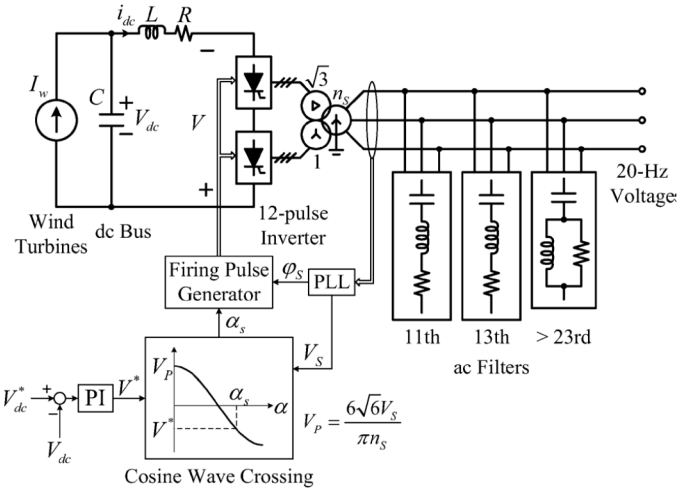

Fig. 2 Sending-end inverter control

B. Receiving-End Control

The structure of the cyclo-converter controller at the receiving end is illustrated in Fig. 3. The control objective is to provide a constant 20-Hz

voltage1 of a given rms value (line-to-neutral). The fundamental component of the cyclo-converter voltage is obtained with the signal conditioning logic depicted in Fig. 4. The firing angles are determined with the cosine wave crossing method, as shown in Fig. 5, which uses phase- as an example. The firing angles of the phase- positive and negative converters (denoted as "*aP*" and "*aN*" in Fig. 3) are and, respectively. For the positive converter, the average voltage at the 20-Hz terminals is given by [28]

$$V_{aP} = \frac{3\sqrt{6}V_G}{\pi n_R}\cos(\alpha_{aP}) \qquad (3)$$

Where the rms value of the line-to-neutral voltage at the grid side, and is the turn's ratio of the transformers. The condition ensures that average voltages with the same polarity are generated from the positive and negative converter at the 20-Hz terminals [30]. The firing pulses and are not simultaneously applied to both converters, in order to obtain a noncirculating current mode of operation. This functionality is embedded in the "Bank Selector" block of Fig. 3, which operates based on the filtered current. Note (for later use) that the maximum line-to-neutral rms value of the 20-Hz cycloconverter voltage is [26]

$$V_{\text{cyc}}^{\max} = \frac{3\sqrt{3}V_G}{\pi n_R} \qquad (4)$$

And that a voltage ratio is defined as

$$r = \frac{V_{\text{cyc}}}{V_{\text{cyc}}^{\max}}. \qquad (5)$$

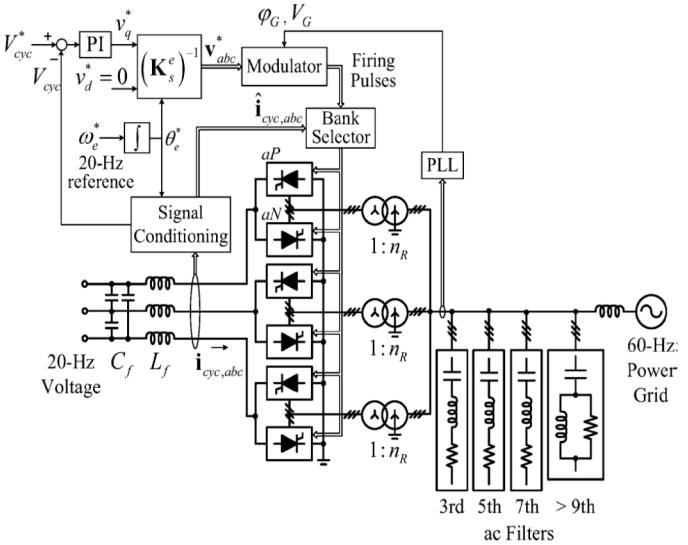

Fig. 3 Receiving-end cyclo-converter control

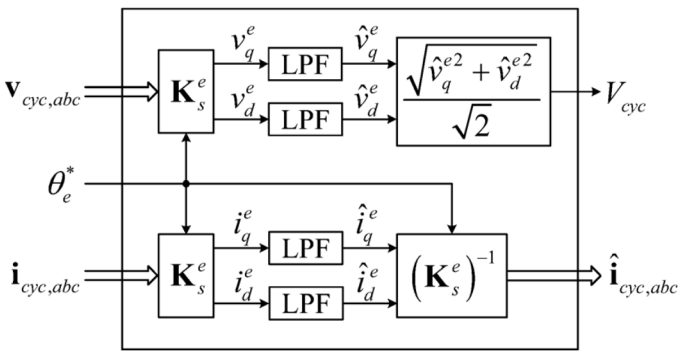

Fig. 4 Details of the signal conditioning block. (LPF first-order low-pass filters, with time constants equal to 0.05 s and 0.01 s for the voltage and current, respectively.)

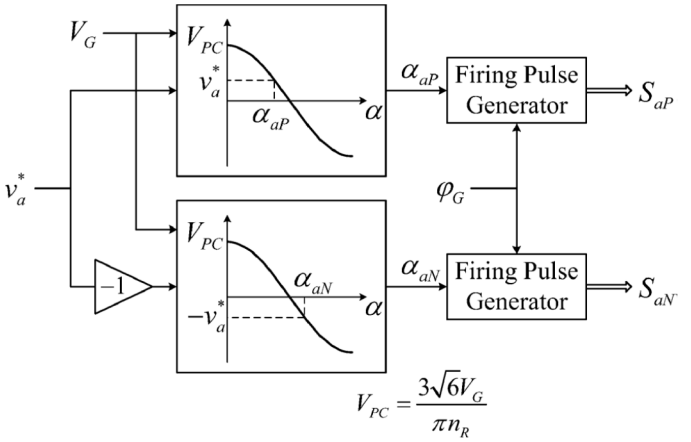

Fig. 5 Modulator for phase

In practice, the theoretical maximum value 1 cannot be achieved, due to the leakage inductance of the transformers, which was ignored in the analysis.

III. SYSTEM DESIGN

A. Main Power Components

The main power components are selected based on a steady state analysis of the LFAC transmission system shown in Fig. 1, under the following assumptions:

- Only fundamental components of voltages and currents are considered. The receiving end is modeled as a 20-Hz voltage source of nominal magnitude.
- The power losses of the reactor, thyristors, filters, and transformers are ignored.
- The resistances and leakage inductances of transformers are neglected.
- The ac filters are represented by an equivalent capacitance corresponding to the fundamental frequency.
- The design is based on rated operating conditions (i.e., maximum power output).

At the steady state, the average value of the dc current is equal to, so the power delivered from the wind turbines is

$$P_w = V_{\mathrm{dc}} I_w. \tag{6}$$

For the 12-pulse converter, the rms value of the current at the transmission side is [28]

$$I = \frac{2\sqrt{6}}{\pi} \frac{I_w}{n_S}. \tag{7}$$

Hence, (7) can be written as

$$I = M P_w \tag{8}$$

With

$$M = \frac{2\sqrt{6}}{\pi n_S V_{\mathrm{dc}}}. \tag{9}$$

Let $\tilde{V}_S = V_S \underline{/0^\circ}$ and $\tilde{I}$ denote the phasors of the line-to-neutral voltage and line current, respectively. Since $-\tilde{I}$ lags $\tilde{V}_S$ by α_S [28], it follows that $\tilde{I} = I \underline{/180^\circ - \alpha_S}$. The active power delivered by the 12-pulse inverter is given by

$$P_S = P_w = 3V_S I \cos(\alpha_S - 180^\circ) = -3V_S I \cos(\alpha_S) > 0. \tag{10}$$

Substitution of (8) into (10) yields

$$\cos(\alpha_S) = -\frac{1}{3MV_S} \tag{11}$$

and

$$\sin(\alpha_S) = \sqrt{1 - \frac{1}{9M^2 V_S^2}}. \tag{12}$$

The reactive power generated from the 12-pulse inverter is

$$Q_S = 3V_S I \sin(\alpha_S - 180^\circ) = -3V_S I \sin(\alpha_S). \tag{13}$$

From (10)–(13), it follows that:

$$Q_S = P_S \tan(\alpha_S) = -P_S\sqrt{9M^2V_S^2 - 1}. \qquad (14)$$

The negative sign in (13) and (14) indicates that the 12-pulse inverter always absorbs reactive power. Equation (14) shows that can be expressed as a function. Based on the aforementioned analysis, the steady-state single-phase equivalent circuit of the LFAC transmission system is shown in Fig. 6. The equivalent capacitance of the sending-end ac filters at the fundamental frequency. The transmission line is modeled by a -equivalent (positive-sequence) circuit using lumped parameters. The well-known hyperbolic trigonometric expressions for and are used [31]. Given a power rating of a wind power plant, the maximum reactive power that is absorbed by the 12-pulse inverter can be estimated according to (14), which yields

$$Q_{\text{rated}} = P_{\text{rated}}\sqrt{3M^2V_o^2 - 1} \qquad (15)$$

Where is the nominal transmission voltage level (line-to-line rms). Here, it is assumed that the sending-end ac filters supply the rated reactive power to the inverter. Therefore

$$C_{\text{eq}} = \frac{Q_{\text{rated}}}{\omega_e V_o^2} \qquad (16)$$

In addition, the apparent power rating of the transformer at the sending end should satisfy

$$S_{tS} > \sqrt{P_{\text{rated}}^2 + Q_{\text{rated}}^2} = \sqrt{3}P_{\text{rated}}MV_o. \qquad (17)$$

At the 60-Hz grid side, the reactive power capacity of the ac filters and the apparent power rating of the transformers depend on the cycloconverter's voltage ratio, which is a design parameter, and the 20-Hz side power factor [30], which can be estimated as follows. For a given transmission cable, the voltage ratings (nominal and maximum voltage), the current rating, and the distributed cable parameters (resistance, inductance, and capacitance per unit length) are known. Here, it is assumed that a power cable is chosen to transmit the rated wind power plant power without violating the cables voltage and current ratings. (The relationship between active power through the cable and maximum transmission distance given a certain cable will be discussed later.) For simplicity, it is further assumed that the rms value of

line-to-line voltage at both sending and receiving ends and the current is approximately equal to the current rating of the cable.

Since the ac filters are designed to supply all reactive power to the 12-pulse inverter at the sending end, the reactive power injected into the 20-Hz side of the cycloconverter can be estimated by using

$$Q_{\text{cyc}}^{20} \approx \text{Im}\{Y'\}V_o^2 + \omega_e 3C_f V_o^2 - 3I_{\text{rated}}^2 \text{Im}\{Z'\} - 3I_{\text{rated}}^2 \omega_e L_f \quad (18)$$

Where the first two terms represent the reactive power generated from the cable and the capacitor of the *LC* filter, and the last two terms represent the reactive power consumed by the cable and the *LC* filter's inductor. The active power injected into the cyclo-converter from the 20-Hz side can be estimated by using

$$P_{\text{cyc}}^{20} \approx P_{\text{rated}} - \text{Re}\{Y'\}V_o^2 - 3I_{\text{rated}}^2 \text{Re}\{Z'\} \quad (19)$$

Where the last two terms represent the power loss of the cable The 20-Hz side power factor can be estimated according to (18) and (19).

The 60-Hz side power factor at the transformers' grid side terminals can be obtained using the 20-Hz power factor and the voltage ratio based on the analysis and calculations of ([30, p. 358]). Then, the apparent power rating of each of the three receiving-end transformers should satisfy

$$S_{tR} > \frac{P_{\text{cyc}}^{20}}{(3)(\text{PF}^{60})}. \quad (20)$$

Also, it is assumed that the grid-side ac filters are designed to supply the rated amount of reactive power to the cyclo-converter.

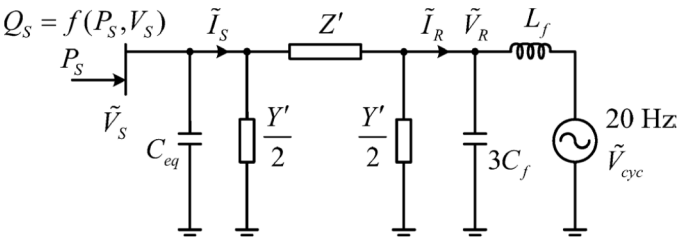

Fig. 6 Equivalent circuit of the LFAC transmission system at fundamental frequency

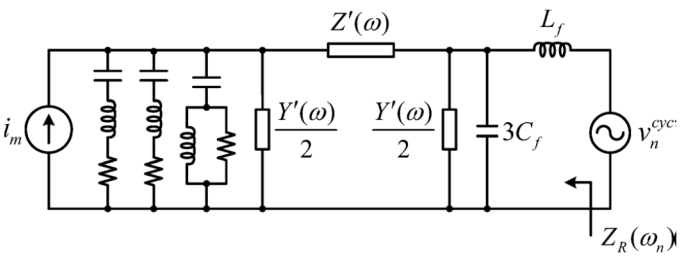

Fig. 7 Equivalent circuit of the LFAC transmission system for harmonic analysis

B. Filter Design

At the sending end, the 12-pulse inverter produces harmonics of order can be represented as a source of harmonic currents (Fig. 7). These current harmonics are filtered by two single-tuned filters for the 11th and 13th harmonic, and one damped filter for higher-order harmonics (23rd). Generally, the filter design is dependent on the reactive power supplied at fundamental frequency (also known as the filter size) and the required quality factor [32]. The total reactive power requirement of these filters can be estimated based on (15). Here, it is assumed that the total reactive power requirement is divided equally among the three filters. The quality factor for each filter can be determined using the method presented in ([32, Ch. 6]. A high quality factor 100) is used for the single-tuned filters, and a low quality factor is used for the high-pass damped filter. Finally, with the capacitance and quality factor known, the inductance and resistance of each filter can be determined. With such filter design, the 12-pulse-related current harmonics originating at the sending end are essentially absent from the transmission line.

At the receiving end, there are two groups of filters, namely, the ac filters at the 60-Hz side and the *LC* filter at the 20-Hz side. At the 60-Hz side, if the cyclo-converter generates exactly one-third of the grid frequency, and it can be shown [30, p. 360] that the line current has only odd harmonic components (3rd, 5th, 7th, etc). Sub-harmonic and inter-harmonic components are not generated. Here, three single-tuned filters and one damped filter are used to prevent these harmonic currents from being injected into the 60-Hz power grid. These filters are designed with a procedure similar to that for the ac filters at the sending end.

At the 20-Hz side, the line-to-neutral voltage has harmonics of order 3, 5, 7.... without sub-harmonic and inter-harmonic components [30, p. 306]. However, the harmonic components of order equal to integer multiples of three are absent in the line-to-line voltage. Therefore, as seen from the 20-Hz side, the cyclo-converter acts as a source of harmonic voltages of orders (Fig. 7). The design of the *LC* filter has two objectives:

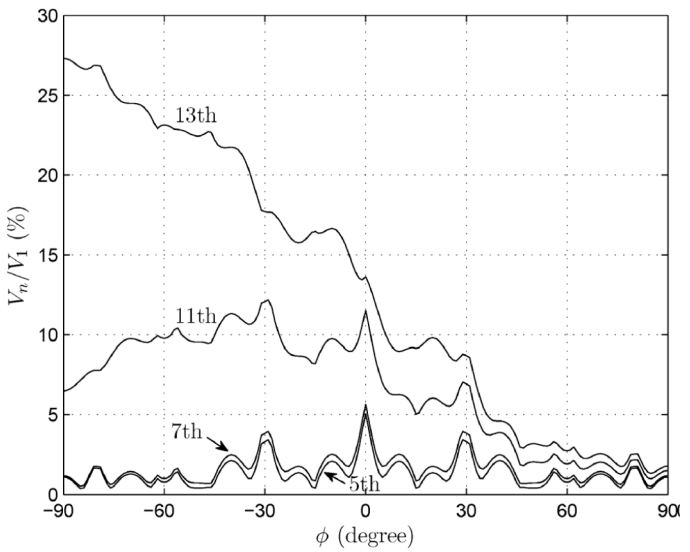

Fig. 8 Harmonic voltage amplitudes generated by the cyclo converter at the 20-Hz side.

IV. SIMULATION RESULTS

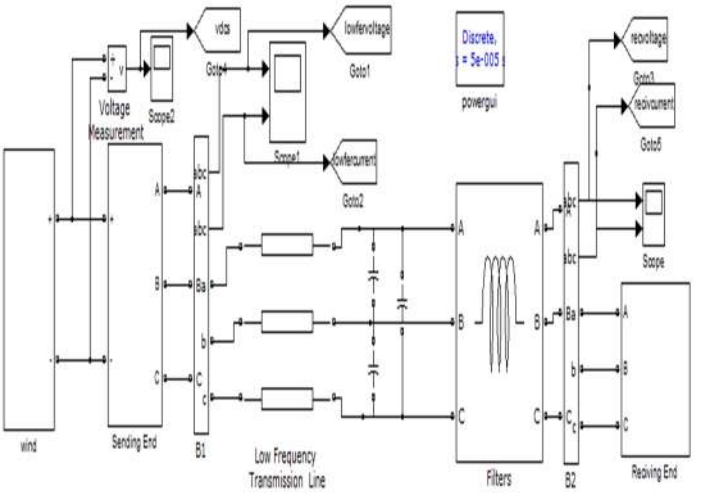

Fig 9 simulation diagram of propose system

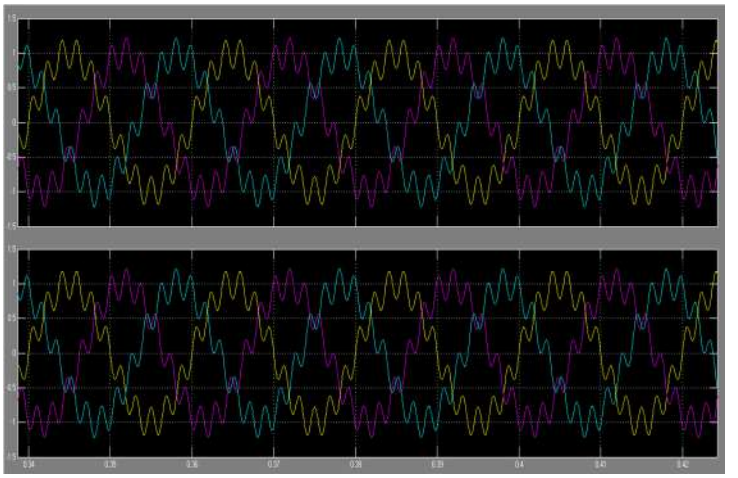

Fig 10 voltage & current

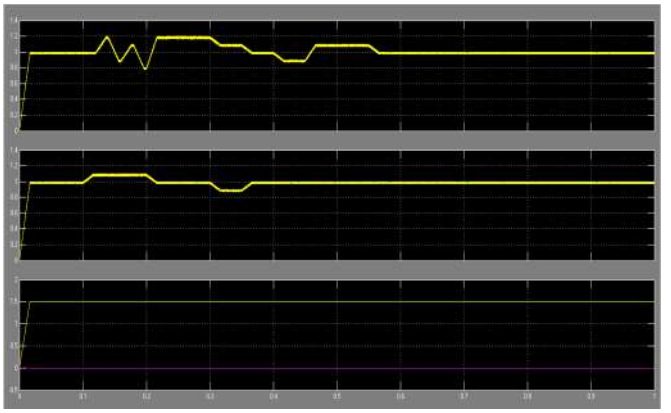

Fig 11 DC voltage, active & reactive power

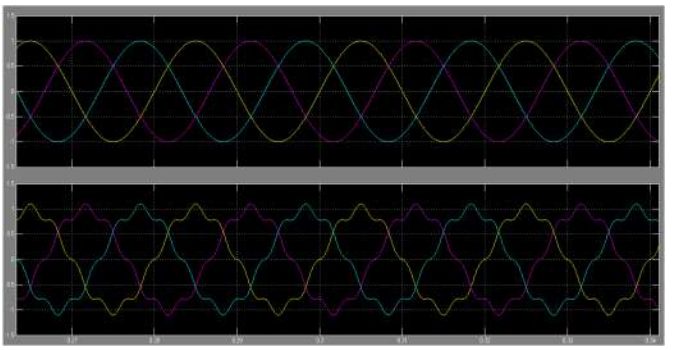

Fig 12 grid voltage & current

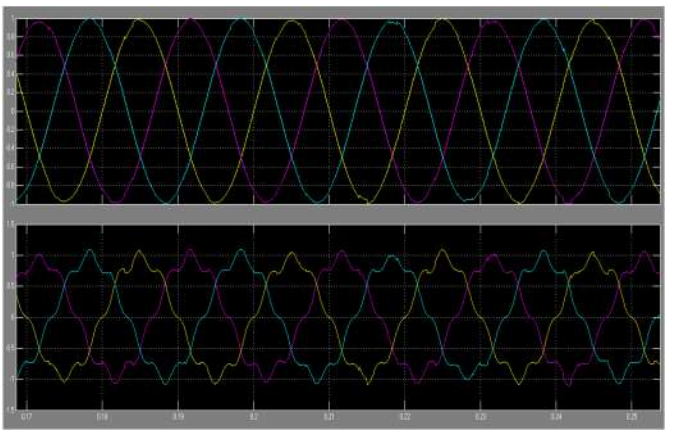

Fig 13 receiving end voltage & current

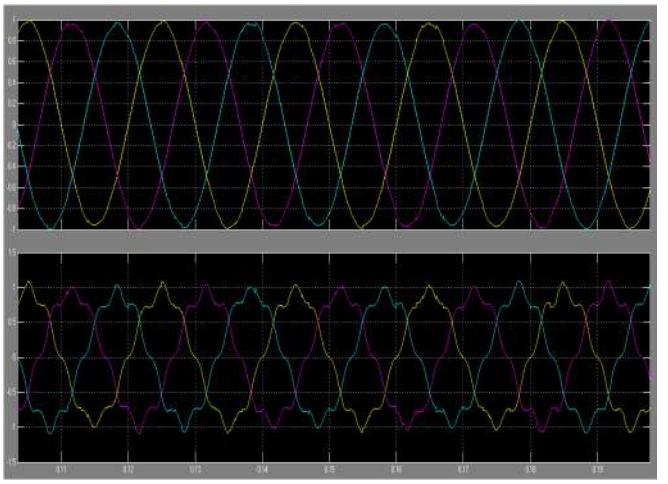

Fig 14 sending end voltage & current

V. CONCLUSION

The use of a low frequency can improve the transmission capability of submarine power cables due to lower cable charging current. The proposed LFAC system appears to be a feasible solution for the integration of offshore wind power plants over long distances, and it might be a suitable alternative over HVDC systems in certain cases. A low-frequency ac transmission system for offshore wind power has been proposed. A method to design the system's components and control strategies has been discussed. Furthermore, it might be easier to establish an interconnected low-frequency ac network to transmit bulk power from multiple plants. In order to make better-informed decisions, it is necessary to perform a complete technical and economic comparison among HVAC, HVDC, and LFAC, evaluating factors, such as the transmission efficiency, investment and operating costs, and the performance under system transients.

VI. Acknowledgment

This paper is based on M. Tech. project carried out by the student of pydah college of engineering & technology, Kakinada studying M.Tech (Power Electronics) The project had been completed by Mr. S. RAJASEKHAR bearing H.T.no.:126T1D4315 under the guidance of Mr. P. VIJAYA RAMARAO.

REFERENCES

1. National Grid Electricity Transmission, London, U.K., 2011 offshore development information statement, Tech. Rep., Sep. 2011. [Online]. ODIS/Cu rrentStatement
2. T. Mai, R. Wiser, D. Sandor, G. Brinkman, G. Heath, P. Denholm, D. J. Hostick, N. Darghouth, A. Schlosser, and K. Strzepek, "Exploration of high-penetration renewable electricity futures study," National Renewable Energy Laboratory, Golden, CO, Tech. Rep. NREL/TP-6A20- 52409-1, National Renewable Energy Laboratory.
3. N. B. Negra, J. Todorovic, and T. Ackermann, "Loss evaluation of HVAC and HVDC transmission solutions for large offshore wind farms," *Elect. Power Syst. Res.*, vol. 76, no. 11, pp. 916–927, Jul. 2006.
4. S. Bozhko,G.Asher, R. Li, J. Clare, and L.Yao, "Large offshore DFIGbased wind farm with line-commutated HVDC connection to the main grid: Engineering studies," *IEEE Trans. Energy Convers.*, vol. 23, no. 1, pp. 119–127, Mar.
5. O. Gomis-Bellmunt, J. Liang, J. Ekanayake, R. King, and N. Jenkins, "Topologies of multiterminal HVDC-VSC transmission for large offshore wind farms," *Elect. Power Syst. Res.*, vol. 81, no. 2, pp. 271–281, Feb. 2011.
6. P. Bresesti, W. L. Kling, R. L. Hendriks, and R. Vailati, "HVDC connection of offshore wind farms to the transmission system," *IEEE Trans. Energy Convers.*, vol. 22, no. 1, pp. 37–43, Mar. 2007.
7. S. V. Bozhko, R. Blasco-Giménez,R. Li, J. C. Clare, andG.M.Asher, "Control of offshoreDFIG-based wind farm grid with line-commutated HVDC connection," *IEEE Trans. Energy Convers.*, vol. 22, no. 1, pp. 71–78, Mar. 2007.
8. J. Arrillaga*, High Voltage Direct Current Transmission*, 2nd ed. London, U.K.: Institution of Electrical Engineers, 1998
9. N. Flourentzou, V. G. Agelidis, and G. D. Demetriades, "VSC-based HVDC power transmission systems: An overview," *IEEE Trans. Power Electron.*, vol. 24, no. 3, pp. 592–602, Mar. 2009.

INTERNATIONAL JOURNAL OF MULTIDISCIPLINARY EDUCATIONAL RESEARCH
ISSN : 2277-7881; IMPACT FACTOR - 2.972; IC VALUE:5.16
VOLUME 3, ISSUE 10(4), OCTOBER 2014

TWO STRING BUCK BOOST CONVERTERS IN PV PANELS WITH TWO MPPT'S FOR DISTRIBUTION SYSTEM

Mr. T SIVA KUMAR
siva.tanknda@gmail.com
Under the guidance of
Ms.M.PAVANI
ASSISTANT PROFESSIOR
PYDAH COLLEGE OF ENGINEERING, KAKINADA

Abstract— The proposed MPPT topology consists of buck and boost converters to deal with wide output voltage range of PV panels. This paper develops the operational control of two maximum power point trackers (MPPTs) for two-string photovoltaic (PV) panels in dc distribution systems. This dc distribution system is connected to ac grid via a bidirectional inverter. Two PV strings and two MPPTs are implemented in this system. To accurately determine the input current of MPPTs, the PV-string configuration check is accomplished online. The perturbation and observation method are applied for maximum power point tracking. Moreover, the current balancing of two MPPT modules in parallel is achieved. In this paper, the system configuration and the operational principle of the proposed MPPT are first introduced. Afterward, the perturbation and observation method and the mode transition are demonstrated. Flowcharts of the online PV-string configuration check and current balancing are explained.

Key words: MPPT, buck-boost converters

I. INTRODUCTION

In the utilization of solar power and fuel cell generations [1], [2] for residential buildings, dc distribution systems provide higher conversion efficiency than traditional ac distribution systems because most of the energy storage units and home appliances are also dc types. DC distribution systems [1]–[6] have been used in isolated power systems such as aircraft, spacecraft, and ship, which are not connected to the ac utility grid. The trend of employing renewable energy sources is drawing more and more attention in recent years for reducing fossil fuel exhaustion and carbon emission. For a typical dc distribution system shown in Fig. 1, the power conversion losses can be reduced by adopting the dc bus to minimize the power conversion stages. Therefore, this paper develops the maximum power point trackers (MPPTs)

for two-string photovoltaic (PV) panels in a conventional 5-kW dc distribution system to obtain high utilization rate of the solar power. Maximum power point tracking [7]–[12] is an essential issue in solar energy sources because the installation cost of PV panels is high and the conversion efficiency from solar power to electrical power is low.

The conventional maximum power point tracking techniques include hill climbing [7], perturb and observe (P&O) [7]–[9], incremental conductance [10], fractional open-circuit voltage [11], fractional short-circuit current [12], fuzzy logic and neural network [13], and others [7]. The P&O and fractional open-circuit voltage methods are easy in implementation.

The convergence speed of fuzzy logic and neural network schemes is fast. Detailed comparisons of different maximum power point tracking techniques are discussed in [7]. The conventional converter topologies of MPPTs can be classified into buck type [14], boost type [15], and buck–boost type [16]. If the PV panels are connected in series to gain higher output voltage than the dc-bus voltage, the buck converter is used. On the contrary, the boost converter is employed in low PV output voltage situations. However, both buck and boost converters are not suitable for dealing with high voltage variation in the PV output end. Consequently, a buck–boost combination converter is used in this paper to solve problems of high voltage variation. PV panels are generally connected in series or in parallel to form PV arrays [17]–[21] so that the power level can be increased. Recent research works [18]–[22] indicate that total maximum power of multiple PV panels can be obtained effectively via multi-string MPPTs. The developed two MPPTs are implemented in a 5-kW dc distribution system as shown in Fig. 2. This dc distribution system is connected to ac grid through a 5-kW bidirectional inverter. For wide application, the two-string MPPTs are proposed to satisfy different power requirements. Each MPPT has 2.5-kW rating and can be operated independently or in parallel.

When the MPPT supplies power to dc appliances, such as water heaters of which power is less than 2.5 kW, it will be operated under standalone. Moreover, it can also supply to a 5-kW home system with parallel configuration. Besides, the peak efficiency of a device is generally at the half-load condition. A single-string MPPT will have lower efficiency under the 5 kW (higher load) or 200 W (lower load) conditions. The two-string MPPTs can improve the efficiency under light or heavy load conditions. The operational

principles of the MPPTs will be introduced. Both buck and boost operational modes can be achieved by the proposed topology.

The P&O method is adopted for tracking maximum power and the mode transition is obtained via the employed scheme. Configuration check will be proceeded online to confirm the correct operation of the MPPTs when the PV panels are plugged or unplugged. Current balancing of the MPPTs is also accomplished to meet the desired criterion. The maximum power tracking accuracy is verified by the programmable power supply. The shadow effect of the PV panels is also identified by the experimental results. The measured waveforms demonstrate configuration check and current balancing of the MPPTs. Power conversion efficiencies are compared at both buck and boost modes.

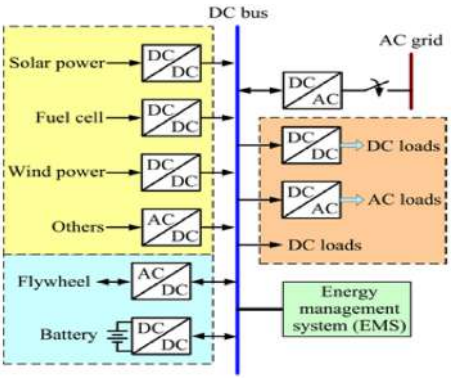

Fig. 1 Typical dc distribution system

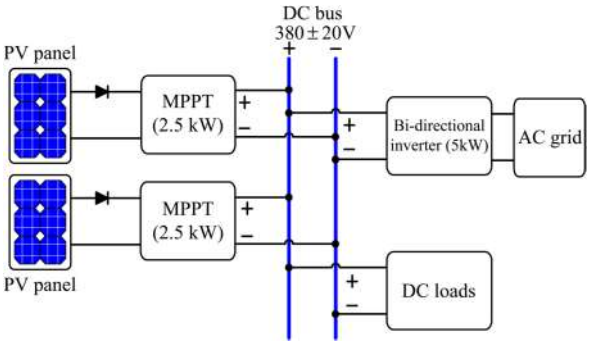

Fig. 2 Configuration of the 5-kW dc distribution system

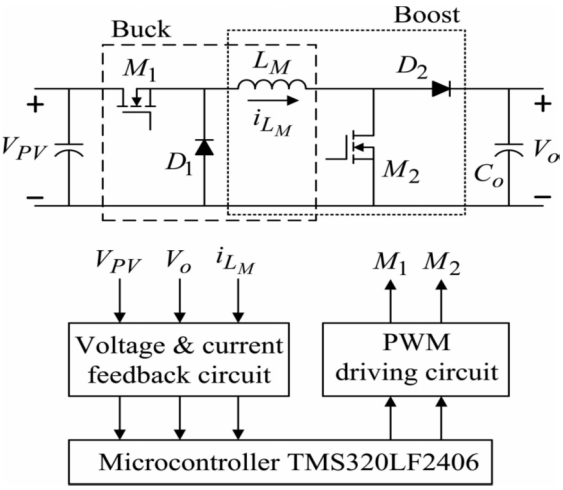

Fig. 3 Circuit configuration of the proposed MPPT module

II. SYSTEM CONFIGURATION AND OPERATIONAL PRINCIPLE

Fig. 3 shows the circuit configuration of the proposed MPPT module. The circuit topology consists of two power switches, two power diodes, and one inductor. If the PV panel voltage is higher than the output voltage, the converter will be operated in buck mode. On the other hand, it will be operated in boost mode. The MPPT module is controlled by the microcontroller TMS320LF2406 manufactured by Texas Instruments Inc. The PV voltage *V*PV, output voltage *Vo,* and inductor current *iLM* are sensed by the feedback circuit to determine the operational modes and the duty ratio of the power switches. The operational modes, maximum power tracking method, online PV-string configuration check, and current balancing control scheme are introduced in the following section.

A. Operational Modes and Mode Transition

The proposed MPPT module can be operated in both buck and boost modes. In the dc distribution system, the input voltage of the MPPT module is the PV-panel voltage, and the output voltage is the dc-bus voltage. In the case of PV-panel voltage higher than dc-bus voltage, the converter will be operated in buck mode and the power switch *M*2 is kept turned OFF. The equivalent circuits of the modes 1 and 2 are drawn in Fig. 4(a). Detailed analyses of the buck operation are described in the following.

1) Mode 1: The power switch *M*1 is turned ON. The inductance *LM* is magnetized by the voltage *V*PV – *Vo* through the power diode *D*2. The variation of the inductance current ΔiLM can be expressed as

$$\Delta i_{L_M} = \frac{(V_{\mathrm{PV}} - V_o)}{L_M} t_{\mathrm{on},M_1} \qquad (1)$$

Where *V*PV is the PV-panel voltage, *Vo* is the output voltage, *t*on*, M1* is the turn-on time of the power switch *M*1, and *T* is the switching period.

2) Mode 2: The power switch *M*1 is turned OFF. The inductance *LM* is demagnetized by the output voltage *Vo* through the power diodes *D*1 and *D*2. The variation of the inductance current ΔiLM can be expressed as

$$\Delta i_{L_M} = \frac{(-V_o)}{L_M} t_{\mathrm{off},M_1} \qquad (2)$$

Where *t*off, M1 is the turn-on time of the power switch *M*1 The duty ratio of *M*1 can be derived by using (1) and (2)

$$D_{M_1} = \frac{t_{\mathrm{on},M_1}}{T} = \frac{V_o}{V_{\mathrm{PV}}} \qquad (3)$$

If the PV-panel voltage is always lower than dc-bus voltage, the converter is operated in boost mode and its equivalent circuits are shown in Fig. 4(b). In the boost operation, the power switch *M*1 is kept turned ON. The two operation modes are the following:

1) Mode 3: The power switch *M*2 is turned ON. The inductance *LM* is magnetized by the PV-panel voltage *V*PV through the power switches *M*1 and *M*2;

2) Mode 4: The power switch *M*2 is turned OFF. The inductance *LM* is demagnetized by the voltage *Vo* – *V*PV through the power switch *M*1 and the power diode *D*2. The duty ratio of *M*2 can be derived via similar procedure in the buck mode

$$D_{M_2} = \frac{V_o - V_{\mathrm{PV}}}{V_o}. \qquad (4)$$

The critical control issue of the proposed circuit topology is the transition between buck and boost modes. If the PV-panel voltage and the dc-bus voltage are very close to each other, voltage and current fluctuations may

occur due to incorrect operations of the power switches. To prevent the fluctuation problem, the mode transition scheme is implemented as shown in Fig. 5.

If the converter is operated in buck mode and *V*PV is approaching *Vo,* the duty ratio of *M*1 will be increased to 100%. Then, the operation mode is changed to boost mode and the duty ratio of *M*2 will be initially set as 0.5%. On the other hand, when the converter is operated in boost mode and *V*PV is approaching *Vo*, the duty ratio of *M*2 will be decreased to 0%. During the mode transition, the input and output voltages of the MPPT will be very close. To avoid the over current fault and decrease the switching loss, the switch*M*1 is kept turned ON and the switch *M*2 is kept turned OFF in one perturbation period. This period is referred as the bypass mode. Then, the operation mode is changed to buck mode and the duty ratio of*M*1 will be initially set as 0.5%.

B. Maximum Power Point Tracking

The P&O method is adopted in this paper to obtain maximum power. The voltage and current parameters are necessary in the P&O method to calculate PV-panel power. In the calculation of PV-panel power, the operation mode of the developed MPPT should be determined first. When the MPPT is operated in buck mode, the output current is continuous and is equal to the inductor current *iLM.* Therefore, the output voltage *Vo* and the inductor current *iLM* can be employed to determine the power. If the MPPT is operated in boost mode, the input current will be continuous and equals inductor current *iLM.* Hence, the power is calculated via the PV-panel voltage *V*PV and the inductor current *iLM.* Due to the wide input voltage range, a large perturbation with a low input voltage will result in a high current spike under heavy load condition, while a low perturbation with a high input voltage might weaken the power response and the MPPT will determine a wrong maximum power. For applying to the wide input voltage range, the MPPT will be perturbed with step size 10–15 V and 1.3% duty ratio during a P&O period (8.32 ms). Moreover, this step size with inductance 1 mH will have current spikes under 1 A.

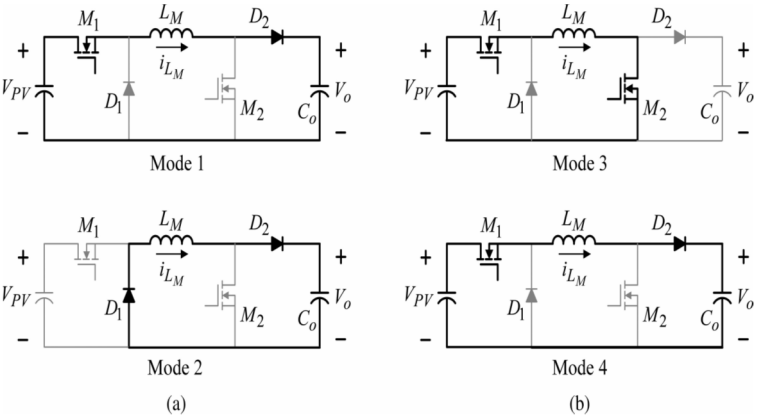

Fig. 4 Operational modes of the developed circuit topology: (a) mode 1 and mode 2 in buck operation; (b) mode 3 and mode 4 in boost operation.

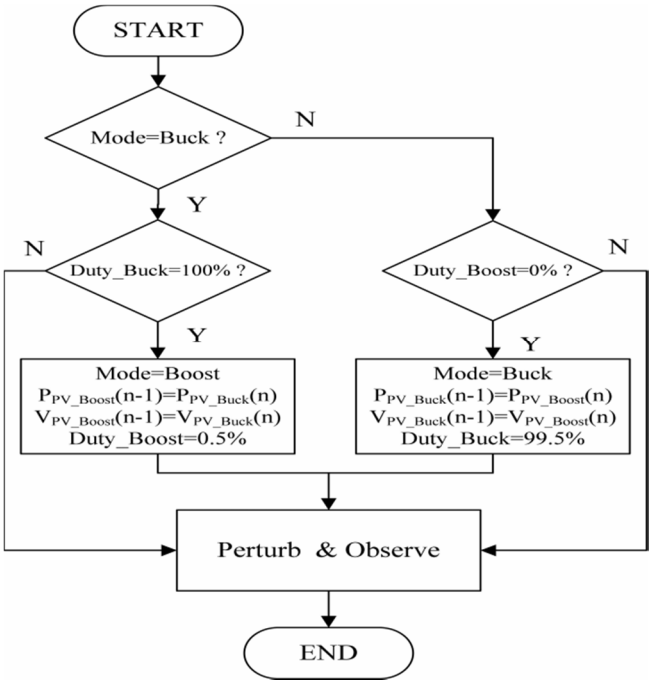

Fig. 5 Flowchart of the mode transition scheme

C. Online PV-String Configuration Check

The possible connected configurations of the MPPTs are shown in Fig. 6. In the standalone configuration, the MPPTs may be operated in different modes due to different solar illumination. Therefore, the microcontroller should calculate the power and determine the duty ratio of each MPPT individually.

In the parallel configuration, the input voltages of the MPPTs will be very close. The determination of online PV-string configurations is based on this phenomenon. However, the input voltages of the MPPTs may be close in standalone mode due to their similarity of the solar illumination. In this case, the microcontroller will continuously check the voltage differences of the MPPTs for 91.6 ms to ensure the correct configuration. The developed two-string MPPTs are implemented in a 5-kW dc distribution system with a bidirectional inverter. The switching frequencies of the MPPT and the inverter are different, of which the MPPT is 25 kHz and the inverter is 20 kHz. Their switching noises might affect the accuracy of the signal sampling, especially under a high-load condition. In this paper, the timer counter of the MPPT will be synchronized with the inverter to improve the performance of the dc distribution system.

The MPPT will perturb and observe the power variation at the zero crossing of the inductor current of the inverter with less noise interference. Due to the slow power variation of the PV panels, the MPPT will perturb the input voltage once every ten cycles (83.2 ms) of the zero crossing, as shown in Fig. 7(a). For determining the correct configuration, the MPPT will check the voltage variations of the PV1 and the PV2 twice. Therefore, the period of the configuration check is 91.6 ms.

The proposed online PV-string configuration check strategy is drawn in Fig. 7(b). First, the controller will check the input voltages of the MPPTs. If the input voltage of the MPPT is higher than the threshold voltage 150 V, this MPPT will be labelled as online, and vice versa. Then, the configuration check will be executed if both input voltages are higher than the threshold voltage. For example, if the MPPT module 1 is online and the MPPT module 2 is plugged, the controller will continuously examine the voltage difference for 91.6 ms. If two input voltages of both MPPTs are very close (within 10 V), the connecting configuration will be diagnosed to be the parallel mode. On the contrary, the connecting configuration is labelled as standalone mode. In the

proposed configuration check scheme, the parallel disturbance test is proceeded to verify the configuration check. The controller will disturb the duty ratio of one MPPT to ensure the connecting modes. After the configuration check was completed, the operation mode (buck/boost) is determined by the controller.

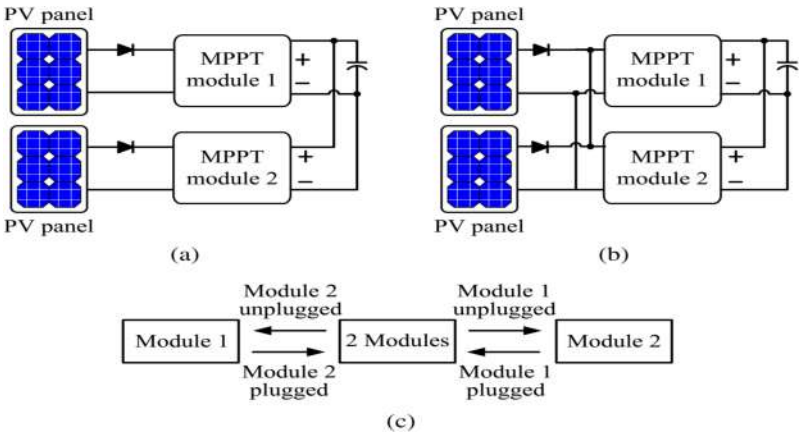

Fig. 6 Connected configurations of the two MPPTs: (a) standalone; (b) parallel; (c) possible configuration changing conditions

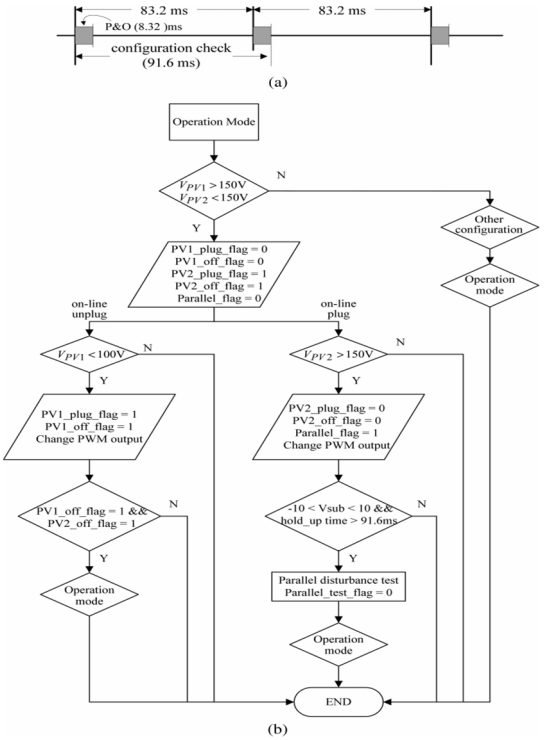

Fig. 7. (a) Timing diagram of the proposed MPPT. (b) Flowchart of the online PV-string configuration check scheme.

D. Current Balancing Control Scheme

Because the feedback circuits, PWM driving circuits, and circuit parameters of the two MPPTs are not identical, imbalance of the two inductor currents may occur when they are connected in parallel. The MPPT being operated with higher current will have shorter life time due to the higher operational temperature and the higher electrical stress. To prevent the thermal problem and to enhance the component reliability, the current balancing control algorithm is proposed in Fig. 8.

In the parallel connection mode, the microcontroller will check the difference of the inductor currents, which is defined as

$$I_{\text{diff}} = I_{\text{PV1}} - I_{\text{PV2}} \qquad (5)$$

Where *I*PV1 is the inductor current of MPPT module 1 and *I*PV2 is the inductor current of MPPT module 2.

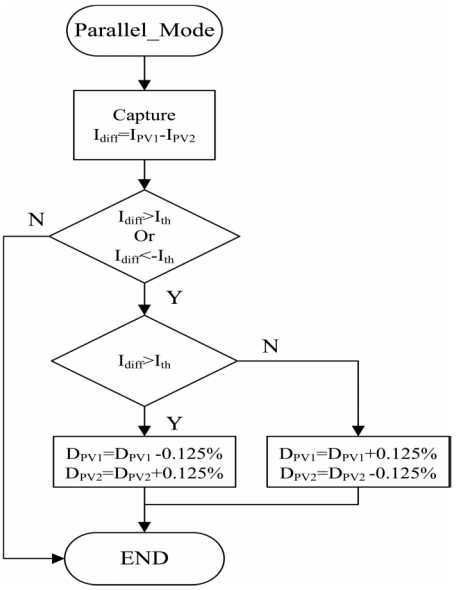

Fig. 8 Flowchart of the current balancing control algorithm

III. EXPERIMENTAL RESULTS

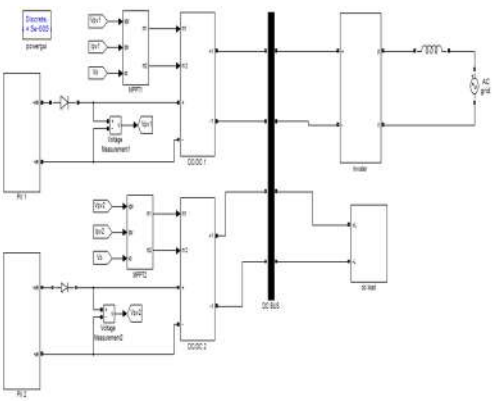

Fig 9 simulation diagram of proposed system

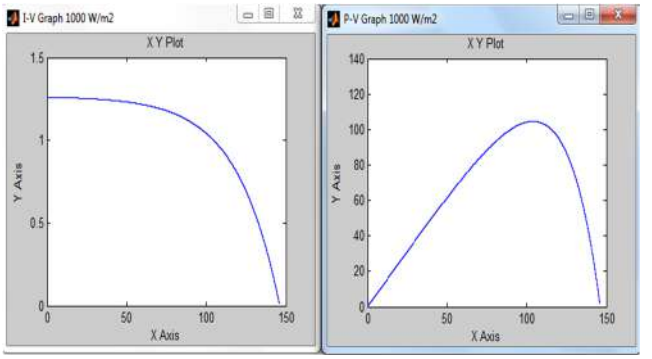

Fig 10 PV panel characteristics

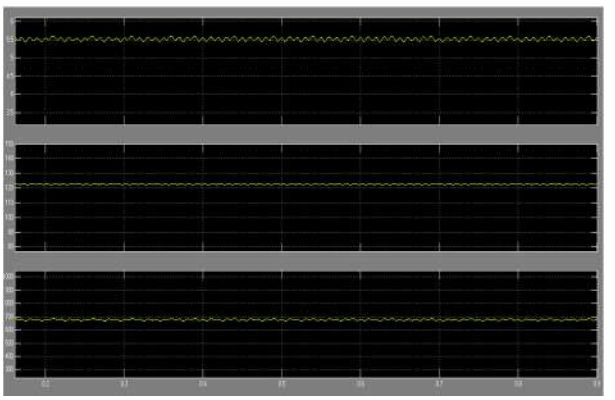

Fig 11 Buck boost load current voltage power

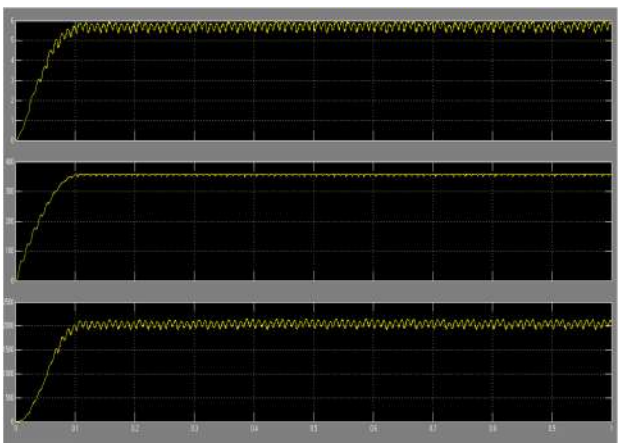

Fig 12 Buck boost output current voltage power

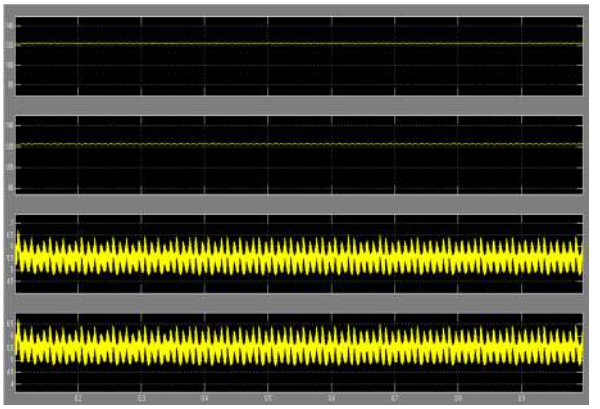

Fig 13 both PV voltages & currents

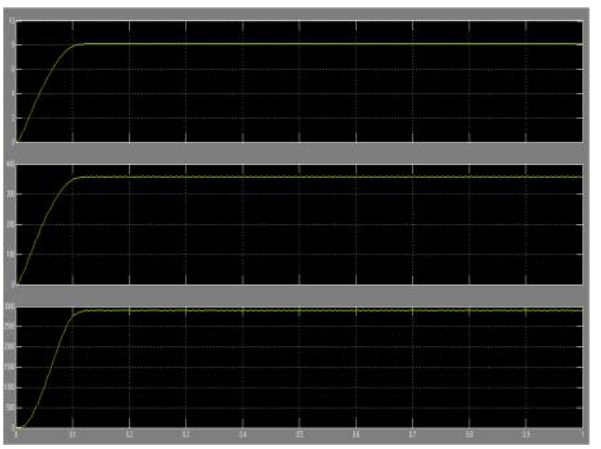

Fig 14 DC load current, voltage & power

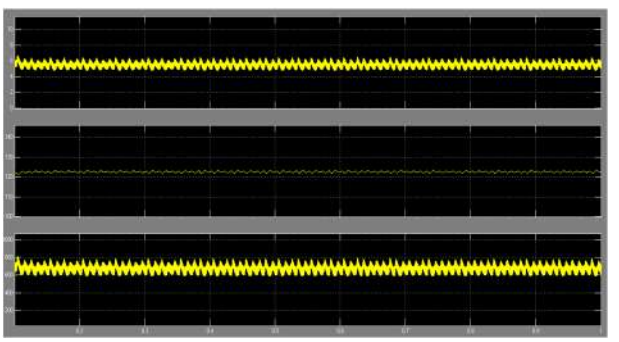

Fig 15 PV 2 current voltage & power

IV. CONCLUSION

This paper developed the operational control of two maximum power point trackers (MPPTs) for two-string photovoltaic (PV) panels in dc distribution systems. This dc distribution system is connected to ac grid via a bidirectional inverter. To accurately determine the input current of MPPTs, the PV-string configuration check is accomplished online. The two-string MPPTs in dc distribution system are developed in this paper. This circuit topology is suitable for wide input voltage applications. The mode transition is smoothly achieved by the employed strategy. To ensure the correct operations of two MPPTs, the proposed online PV-string configuration check verifies the connecting configuration. The online plugged and unplugged are successfully obtained in both standalone and parallel modes.

VI. Acknowledgment

This paper is based on M. Tech. project carried out by the student of pydah college of engineering & technology, Kakinada studying M.Tech (Power Electronics) The project had been completed by MR. T SIVA KUMAR bearing H.T.no.: 126T1D4316 under the guidance of Ms. M PAVANI.

REFERENCES

1. D. J. Hammerstrom, "AC versus DC distribution systems—did we get it right?" in *Proc. IEEE Power Eng. Soc. Gen. Meet.*, Jun. 2007, pp. 1–5.
2. G.-S. Seo, J. Baek, K. Choi, H. Bae, and B. Cho, "Modeling and analysis of DC distribution systems," in *Proc. IEEE 8th Int. Conf. Power Electron. ECCE Asia*, May–Jun. 2011, pp. 223–227.
3. M. E. Baran and N. R. Mahajan, "DC distribution for industrial systems: Opportunities and challenges," *IEEE Trans. Ind. Appl.*, vol. 39, no. 6, pp. 1596–1601, Nov./Dec. 2003.
4. A. Stupar, T. Friedli, J. Minibock, and J. W. Kolar, "Towards a 99% efficient three-phase buck-type PFC rectifier for 400-V DC distribution systems," *IEEE Trans. Power Electron.*, vol. 27, no. 4, pp. 1732–1744, Apr. 2012.
5. Y. C. Chang and C. M. Liaw, "Establishment of a switched-reluctance generator-based common DC microgrid system," *IEEE Trans. Power Electron.*, vol. 26, no. 9, pp. 2512–2527, Sep. 2011.
6. A. Kwasinski and C. N. Onwuchekwa, "Dynamic behavior and stabilization of DC microgrids with instantaneous constant-power loads," *IEEE Trans. Power Electron.*, vol. 26, no. 3, pp. 822–834, Mar. 2011.

7. T. Esram and P. L.Chapman, "Comparison of photovoltaic arraymaximum power point tracking techniques," *IEEE Trans. Energy Convers.*, vol. 22, no. 2, pp. 439–449, Jun. 2007.
8. N. Femia, G. Petrone, G. Spagnuolo, and M. Vitelli, "Optimization of perturb and observe maximum power point tracking method," *IEEE Trans. Power Electron.*, vol. 20, no. 4, pp. 963–973, Jul. 2005.
9. A. K. Abdelsalam, A. M. Massoud, S. Ahmed, and P. N. Enjeti, "High-performance adaptive perturb and observe MPPT technique for photovoltaic-based microgrids," *IEEE Trans. Power Electron.*, vol. 26, no. 4, pp. 1010–1021, Apr. 2011.
10. A. Safari and S. Mekhilef, "Simulation and hardware implementation of incremental conductance MPPT with direct control method using Cuk converter," *IEEE Trans. Ind. Electron.*, vol. 58, no. 4, pp. 1154–1161, 2011.
11. M. Adly,H. El-Sherif, and M. Ibrahim, "Maximum power point tracker fora PV cell using a fuzzy agent adapted by the fractional open circuit voltagetechnique," in *Proc. IEEEInt. Conf.Fuzzy Syst.*, Jun. 2011, pp. 1918–1922.
12. M. A. S. Masoum, H. Dehbonei, and E. F. Fuchs, "Theoretical and experimental analyses of photovoltaic systems with voltage- and current-based maximum power-point tracking," *IEEE Trans. Energy Convers.*, vol. 17, no. 4, pp. 514–522, Dec. 2002.
13. M. Veerachary, T. Senjyu, and K. Uezato, "Neural-network-based maximum-power- point tracking of coupled-inductor interleaved-boostconverter- supplied PV system using fuzzy controller," *IEEE Trans. Ind. Electron.*, vol. 50, no. 4, pp. 749–758, Aug. 2003.
14. B. N. Alajmi, K. H. Ahmed, S. J. Finney, and B. W. Williams, "Fuzzylogic- control approach of a modified hill-climbing method for maximum power point in microgrid standalone photovoltaic system," *IEEE Trans. Power Electron.*, vol. 26, no. 4, pp. 1022–1030, Apr. 2011.
15. R. F. Coelho, F. Concer, and D. C. Martins, "A study of the basic DC–DC converters applied in maximum power point tracking," in *Proc. IEEE Brazilian Power Electron. Conf.*, Sep./Oct. 2009, pp. 673–678.
16. E. Koutroulis, K. Kalaitzakis, and N. C. Voulgaris, "Development of a microcontroller-based, photovoltaic maximum power point tracking control system," *IEEE Trans. Power Electron.*, vol. 16, no. 1, pp. 46–54, Jan. 2001.
17. S. Chun and A. Kwasinski, "Analysis of classical root-finding methods applied to digital maximum power point tracking for sustainable photovoltaic energy generation," *IEEE Trans. Power Electron.*, vol. 26, no. 12, pp. 3730–3743, Dec. 2011.

18. G. R. Walker and P. C. Sernia, "Cascaded DC–DC converter connection of photovoltaic modules," *IEEE Trans. Power Electron.*, vol. 19, no. 4, pp. 1130–1139, Jul. 2004.
19. L.-J. Gao, R. A. Dougal, S.-Y. Liu, and R. A. Iotova, "Parallel-connected solar PV system to address partial and rapidly fluctuating shadow conditions," *IEEE Trans. Ind. Electron.*, vol. 56, no. 5, pp. 1548–1556, May 2009.
20. W. Chen, X. -B. Ruan, H. Yan, and C. K. Tse, "DC/DC conversion systems consisting of multiple converter modules: Stability, control, and experimental verifications," *IEEE Trans. Power Electron.*, vol. 24, no. 6, pp. 1463–1474, Jul. 2009.
21. T. Noguchi, S. Togashi, and R. Nakamoto, "Short-current pulse-based maximum-power-point tracking method for multiple photovoltaic-andconverter module system," *IEEE Trans. Ind. Electron.*, vol. 49, no. 1, pp. 217–223, Feb. 2002.
22. M. Miyatake, M. Veerachary, F. Toriumi, N. Fujii, and H. Ko, "Maximum power point tracking of multiple photovoltaic arrays: A PSO approach," *IEEE Trans. Aerosp. Electron. Syst.*, vol. 47, no. 1, pp. 367–380, Jan. 2011.

INTERNATIONAL JOURNAL OF MULTIDISCIPLINARY EDUCATIONAL RESEARCH
ISSN : 2277-7881; IMPACT FACTOR - 2.972; IC VALUE:5.16
VOLUME 3, ISSUE 10(4), OCTOBER 2014

SINUSOIDAL PULSE WIDTH MODULATION BASED MULTIPLE-LOOP DIGITAL CONTROL METHOD INVERTER SYSTEM

Ms. V.N.D SAILAJA
Under the guidance of
Ms. B. LALITHA KUMARI
ASSISTANT PROFESSIOR
PYDAH COLLEGE OF ENGINEERING , KAKINADA

Abstract—To keep phase balance and improve output voltage quality, a novel multiple-loop control system in 400-Hz inverter power supply based on unipolar sinusoidal pulse width modulation (SPWM) is proposed. The causes of phase imbalance in a three phase combined inverter power system are analyzed, and a new multiple-loop control strategy based on phase control is presented to eliminate it. For reducing the total harmonic distortion (THD) of high-power inverter output, unipolar SPWM is added with this new control strategy. The designs of drive circuit and snubber circuit are discussed to eliminate dead time effects and voltage oscillation. The stability of the control system is analyzed and the power system and the control strategies are realized with digital signal processing. Contrastive simulation results indicate the advantages and the correctness of this novel controller for inverter.

I. INTRODUCTION

A novel multiple-loop control strategy for the 400-Hz inverter based on unipolar SPWM is proposed in this paper, which is the added phase feedback loop based on traditional three-loop control, and inverter output voltage phase can follow the given signal automatically; at the same time, the value of total harmonic distortion (THD) of output voltage could be reduced with unipolar SPWM, and the quality of output can be improved. A medium frequency inverter power system is widely used in many engineering fields. For obtaining high power output, a combined three-phase inverter power system which constituted with three single-phase inverters is used to supply stable and reliable high power. The combined three phase inverter power system is constructed by three single-phase inverters; compared with other three-phase inverters, this system has better performance on unbalanced loads and adaptability of the work condition. A good combined inverter system has two criteria: phase balance and low harmonics. To keep phase balance, a phase control method is widely used in the control system.

In 1988, Harada *et al*. studied the use of phase control in a dc–ac converter and indicated that this method is especially suitable for small uninterruptible power supply (UPS) systems [2]. In 1996, Abdel-Rahim designed a multiple feedback loop control scheme for single-phase voltage-source UPS inverters with an *L–C* filter, and the experimental verification of a laboratory model of the UPS system under the proposed closed-loop operation was provided for both linear and nonlinear loads [3]. Phase control is also used in new energy generation resources widely [4]–[6]; Ciobotaru *et al*. proposed an accurate and less-disturbing active anti-islanding method suitable for grid-connected converters using phase-locked loop (PLL)-based grid synchronization [7]; a novel digital phase-locked loop algorithm for single-phase photovoltaic systems which uses two virtual phases is proposed by Choi *et al*. [8], and Zhang *et al*. from Xi'an University of Technology proposes a new digital PLL method for single-phase grid-connected power conversion systems, which consisted of an even harmonics elimination network, a grid voltage feed-forward network, and a fictions instantaneous power feedback phase correction network [9], but these strategies are not suitable for the medium frequency 400-Hz inverter system. Meanwhile, for obtaining the high-quality output voltage of the inverter system, increasing switching frequency and changing circuit parameters are the most used methods to reduce harmonics.

But there are some problems encountered when the aforementioned methods are applied: high switching frequency cannot be used in a high power situation, because high current shock would be generated when power switches turn ON/OFF with high speed, and in this situation, switches will be damaged. Changing circuit parameters is the other method to improve the quality of output voltage, such as increasing values of inductance and capacitance, but the phase-frequency characteristic of output will also be changed in such situations, so it cannot eliminate the phase imbalance radically. The principle and implementation methods of phase feedback control are analyzed, filter parameters based on unipolar SPWM are derived, and the stability of the control system is analyzed. Digital control parameters and main circuit parameters are derived by simulation experiments. To eliminate the dead time effects in the inverter system, a drive board which includes a drive circuit and snubber circuit is designed, and the inverter system based on the multiple-loop control strategy is constructed, experimental results show that the inverter system can make phase difference between each phase is less than 2◦, and the THD of output voltage can be limited within 2%.

This paper is organized as follows. In Section II, the theory of three-loop control is analyzed, and the influence of control parameters to the system is studied. In Section III, the theory and design of phase feedback control in inverter system are presented, and the stability of the system is proved. Filter, drive circuit, and snubber circuit of the inverter system based on unipolar SPWM are designed in Section IV. In Section V, the realization of the multiple-loop digital control system based on digital signal processing (DSP) is presented. In Sections VI and VII, simulation and a practical experiment are performed, the results show that the inverter system can make a phase difference of less than 2◦ between each phase, and the THD of output voltage can be controlled within 2%. Finally, the conclusions are presented.

II. ANALYSIS OF THREE-LOOP CONTROL SYSTEM

The three-phase combined inverter system is constituted by the same three single inverters, which are *Y*-connected with each other, so it is reasonable that the single phase is taken as an example to study characteristics of the inverter system. In single phase, a full bridge structure is adopted as the main circuit of the inverter [14], while the insulated gate bipolar transistor (IGBT) is chosen as a switch component to perform energy transfer and power conversion, as Fig. 1 shows. Before the load, the *LC* filter is constructed by capacitance and inductance, which is used for filtering high-order harmonics. Drive signals of IGBTs matched by a triangular wave and sinusoidal wave are provided by the drive board, and this process is realized by DSP.

A traditional three-loop control structure is shown as part I of Fig. 2; from inner to exterior there are instantaneous capacitor current feedback control, instantaneous voltage feedback, and effective voltage feedback. The main function of instantaneous capacitor-current feedback is adjusting waveform of output voltage; instantaneous voltage feedback keeps phase balance and increases dynamic response of the inverter system; and keeping the output voltage effective value at a standard value is the main function of effective voltage feedback.

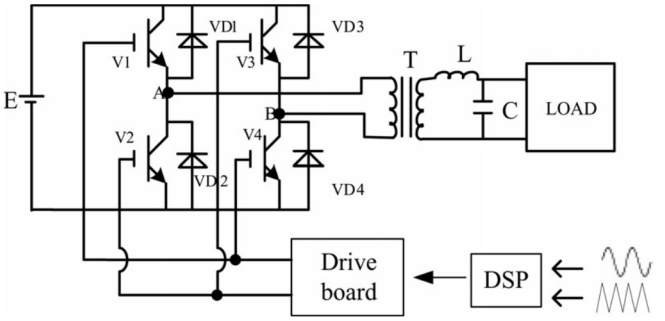

Fig. 1. Main circuit of the single phase inverter

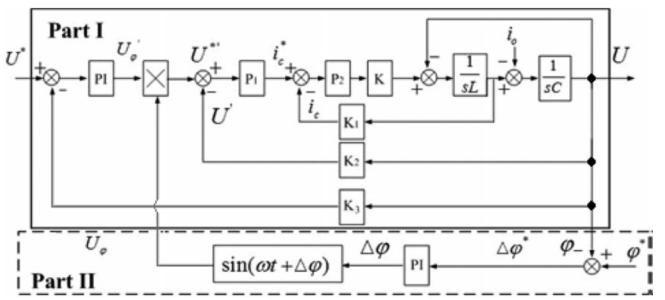

Fig. 2. Block of multiple-loop control

The phase of output voltage is mainly controlled by an instantaneous voltage feedback loop, which usually used a proportional controller in digital control strategy. Theoretically, when parameters of the main circuit are constants, and with a higher instantaneous voltage control coefficient being preferred, the phase difference between output voltage and sine references would be lower. Actually in a digital control system, the proportional coefficient *P*2 (see Fig. 2) must be appropriately valued, because the inverter system would be oscillated if *P*2 was too high, and then system would break down. There are three reasons which caused this phenomenon: 1) *Sampled error*: interferences would be included in sampled signals which came from the main circuit, so the sampled signals must be regulated by a modulated circuit before coming into DSP, such as amplitude limited circuit, absolute value calculated circuit, and analog filtered circuit. While the signal is regulated, interferences are also generated, so, sampled signals would be also added other interferences when they though modulated circuit.

2) *Calculating error:* Signals are calculated in DSP, sometimes mantissa of digital signals would be rounded off, and after many calculating steps, errors would be accumulated, so they would have a serious effect with inverter system. 3) *Neutral point excursion*: neutral point is used for calculating sampled voltage once in every seven periods. But errors would be generated in these calculating processes, and these errors would make neutral point excursion; when the next computational process begins, the wrong neutral point would lead to wrong calculation, and then a wrong sinusoidal signal would be obtained. As stated previously, phase imbalance could not be eliminated radically only by instantaneous voltage feedback.

Moreover, phase of the inverter system would also be affected by parameters of the main circuit. The THD of output voltage is an important parameter index for the inverter power system, because the waveform quality of output voltage can be embodied by THD. Furthermore, *LC* filter parameters have great influences on THD; values of inductance and capacitance are in inverse ratio to THD. The higher the *LC* parameters, the lower the THD, and the better the output waveform will be. But high filter parameters will delay output voltage phase, because when changing the parameters of the filter, phase-frequency characteristics of the filter will also be changed so *LC* parameters cannot be infinite, and the contradiction between phase equilibrium and output voltage waveform quality is reflected in this way.

In the combined three-phase inverter system, every single phase is not exactly the same as other phases; it means that individual differences exist in every single phase, such as different main circuit parameters, element characters, and control conditions. When three single-phase inverters are combined with a whole inverter system, these differences will be magnified, and when three single-phase inverters are Y-connected with each other, the phase difference between any two phases cannot be 120◦.

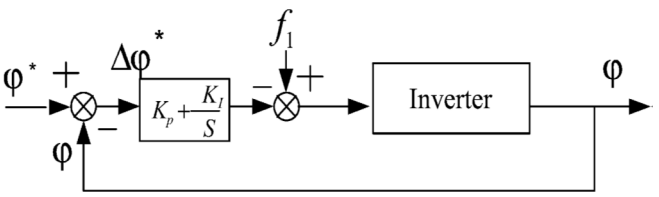

Fig. 3. Block of phase feedback control

III. PHASE FEEDBACK CONTROL

A. Principle of Phase Feedback Control

The multiple-loop control method is proposed in this paper, which is based on phase feedback control; the structure is shown in Fig. 2. The principle of this control method is that the phase difference $\Delta\square\square$ is obtained by the phase subtraction of output voltage and reference phase, and then $\Delta\square\square$ is adjusted by the PI regulator, and $U_\square$ is the adjusted signal. This adjusted signal is multiplied with the sine signal, which is the output of effective voltage feedback; the superposed signal which is of corrected phase and amplitude can be considered as the input of inner loops, and after being adjusted by instantaneous capacitor current feedback and instantaneous voltage feedback, the signal is put into inverter for modulation.

The block of phase feedback control is shown in Fig. 3, where $KP + KI$ S is the expression of the PI regulator, the input signal $\square\square$ is the phase of sine references, $\square$ is the phase of output voltage, $\Delta\square\square$ is the phase difference of the output signal and standard signal, $f1$ is the frequency of the standard signal, and $f1$ = 400 Hz [15], [16].

B. Design of the Phase Feedback Controller

When output voltage is sampled, phase and amplitude are contained in the sampled signal. In order to realize phase control, the phase information should be extracted from the sampled signal [17]. After phase detection, rectification, and filtration, the ultimate sampled signal includes phase information only, and this adjusted signal can be considered as the dc signal, so the PI regulator can be used for regulating it. When the system is in a steady state, steady errors of the phase difference between the output signal and sine references can be eliminated by introducing the integral role of the PI regulator. An integral separation PI controller is used for increasing efficiency and accuracy of the regulator. The calculation principle of PI control is that, set a threshold $\alpha = 5^\circ$, when phase difference $|\Delta\square| > \alpha$, using P regulator for fast approximating the reference value, and when $|\Delta\square| \leq \alpha$, using the PI regulator. In the latter case, the phase difference is too small to use the P regulator; if the P regulator is used in this situation, this will result in overregulation, and the whole system would be oscillated seriously.

C. Stability of the Multiple-Loop Inverter System

The three-phase combined inverter is constructed by three independent phase inverters, so we can take one phase as an example to model and analyze. The open-loop transfer function of the single-phase inverter system is shown as follows:

$$G(s) = \frac{U(s)}{U_c(s)} = \frac{R}{LCRs^2 + (L + RC)s + R} \quad (1)$$

$$G(s) = \frac{U_0(s)}{U_i(s)} = \frac{R_C RCs + R + P_1 P_2}{LC(R + R_C)s^2 + [L + (R_L + R_C)RC + R_L R_C C]s + (R + R_L + P_1 P_2)} \quad (2)$$

where *RC* and *RL* are the equivalent resistances of the capacitance and inductor, respectively, and *R* is the load.

As the phase feedback control loop is added, the stability of the system could be reduced, but this effect could be weakened by choosing suitable digital control parameters. To ensure the rapidity and stability of the inverter system, P controllers are used in instantaneous voltage/current feedback control, and PI controllers are used in effective voltage feedback and phase feedback control. The proportional coefficient of instantaneous capacitor-current feedback is 1.5; the proportional coefficient of instantaneous voltage feedback is 1.2, the proportional controller coefficient of effective voltage feedback is 1.2, the integral controller coefficient of effective voltage feedback is 0.4, the proportional controller coefficient of phase feedback is 1.8, and the integral controller coefficient of phase feedback is 0.1.

In that case, when the output of the inverter system has a large difference with the reference signal, the multiple-loop control system adjusts the output to meet the phase and amplitudes of the reference signal in few cycles, and the high-quality output of the inverter system is obtained.

IV. UNIPOLAR SPWM

A. Principle of Unipolar SPWM

Generally, output THD can be reduced by increasing *LC* filtering parameters, but higher filter parameters would lag output voltage phase [18], for keeping phase balance and getting satisfied output voltage waveform; bipolar SPWM is replaced by unipolar SPWM [19]. In this modulation method, without changing parameters of the *LC* filter, satisfied output quality could be obtained with small digital controller parameters. Because the output

frequency of the inverter bridge is twice the switch frequency, the THD of the output can be reduced in the low switch frequency; in the mean time, the phase of output voltage can meet the requirements without changing the parameters of the *LC* filter.

B. Filter Design Based on Unipolar SPWM

In unipolar SPWM, the value of filter inductor depends on maximum ripple of inductor current, which is 15% of peak output current with loads [20]. In this paper, the single phase output power is 10 kVA, output voltage is 115 V, and output frequency is 400 Hz; based on the above, the parameters are calculated as follows:

$$\Delta I_L = 15\% \times \sqrt{2}\frac{P_O}{U_O} = 15\% \times \sqrt{2} \times \frac{10 \times 10^3}{115} = 18.44\,\text{A}. \tag{3}$$

Assumption that, *U*AB is the output pulse voltage of inverterbridge, *Ud* is the voltage of the dc bus, duty ratio *d* = *U*AB/*Ud*, as formula $\Delta i = U/L\,\Delta t$, expression of inductor current is

$$\Delta I_L = \frac{U_d - U_{\text{AB}}}{L} \times \frac{d}{2f} = \frac{(U_d - U_{\text{AB}})U_{\text{AB}}}{2L \times U_d \times f}. \tag{4}$$

According to (4), the inductor current is maximum when *U*AB = *Ud*/2 , so

$$\Delta I_L = \frac{U_d}{8Lf} \Rightarrow L = \frac{U_d}{8f \times \Delta I_L} = \frac{380}{8 \times 26400 \times 18.44} \approx 100\,\mu\text{H} = 0.1\,\text{mH} \tag{5}$$

After inductance is confirmed, capacitance can be determined by the cut-off frequency of the *LC* filter. In unipolar SPWM, the harmonic wave of output voltage is two or more times of switch frequency, so the cut-off frequency of the filter can be calculated as 10% of the lowest output voltage harmonic

$$\frac{1}{2\pi\sqrt{LC}} = \frac{2f}{10} \Rightarrow C \geq \frac{100}{4 \times f^2 \times 4\pi^2 \times L}. \tag{6}$$

Inserting the inductance in the above formula, the capacitance can be calculated as follows:

$$C \geq \frac{100}{4 \times f^2 \times 4\pi^2 \times L} = \frac{100}{4 \times 26400 \times 4\pi^2 \times 1 \times 10^{-4}} \approx 10\,\mu\text{F}. \tag{7}$$

Actually, the components in the inverter system are not ideal elements and output voltage will be affected by dead-time effects, so that output signals could include low-order harmonics. For reducing output harmonics, *LC* filter parameters in practical experiments should be higher than simulation.

C. Design of a Drive Board and Snubber Circuit

The main function of a drive circuit is drive signal amplification, ensuring steep transitions and the correct operation of the IGBTs [21]. Moreover, the drive circuit can provide electrical isolation between the control circuit and main circuit. Based on the M57962 drive chip produced by Mitsubishi Electric, a new drive circuit is designed. To avoid short through the inverter bridge, a capacitance *Cb* is set between pins 12 and 13. The larger the capacitance, the longer the dead time will be; a resistance *Rn* is set between pins 8 and 12 to provide overload protection of the system; the threshold value will be decreased with increasing resistance. The connection diagrams are shown in Fig. 4. Over voltages can occur when an IGBT is turned ON or OFF.

Thus, snubber circuits are added between the collector and emitter of each IGBT [22], as shown in Fig. 5. When the IGBT is turned ON, energy of leakage inductance will be absorbed by snubber resistance and load; the energy which is originally consumed by the IGBT would be reduced, so that the IGBT can be protected. In the snubber circuit, the snubber resistance is 1 kΩ and the capacitance is 4.4 nF.

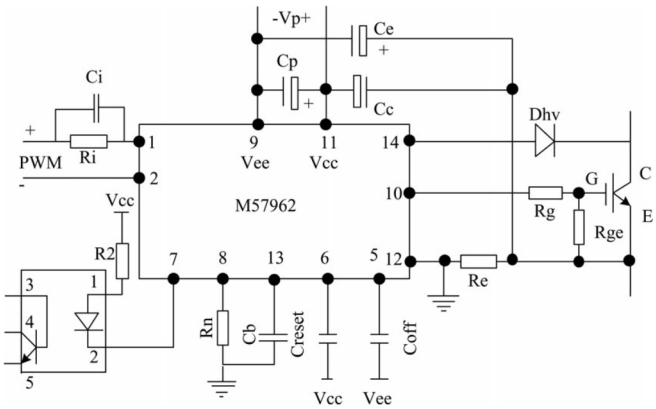

Fig. 4. Connection diagrams of drive circuit

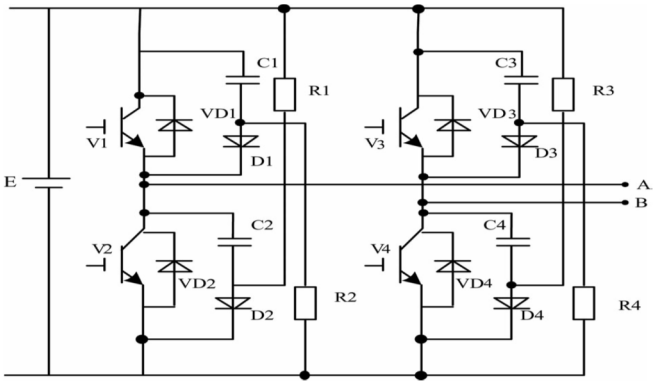

Fig. 5. Snubber circuit of IGBT

V. DIGITAL MULTIPLE-LOOP CONTROL

A. Phase Feedback Control System

Working mode of the IGBT can be controlled by SPWM signals, which are generated by matching between period register (TxPR) and compare register (TxCMPR) [23]. Counting type of TxPR is set as increase and decrease mode, and the compared value is set in TxCMPR as a threshold value. Counter starts at zero. When the counted number is up to the compared value, compared matching is triggered; when the counted number is up to the peak of TxPR, periodic matching is triggered, counting type turns to decrease at the same moment, and matching also happens in the same way. In the inverter system, carrier wave frequency can be changed by entering different TxPR values. During these processes, levels of pulsating signals are skipped, which are of different pulse widths.

In the inverter power system, a carrier to noise ratio (CTNR) $N = fc/f$ is constant; with the change in the value of TxPR (carrier frequency fc), the output voltage frequency of the inverter also changes. The inverter output voltage amplitude is U, frequency is f, amplitude of sine references is U□, frequency of sine reference is f□, and phase difference is Δ□ [24], [25]

$$U^* \sin 2\pi f^* t = U \sin(2\pi f t + \Delta\varphi). \qquad (8)$$

If the output signal and reference signal were identical, that is to say

$$2\pi f^* t = 2\pi f t + \Delta\varphi \quad (9)$$

$$f - f^* = \frac{\Delta\varphi}{2\pi t}. \quad (10)$$

From (8), if Δ□ > 0, the output voltage leads to sine references, the value of TxPR increases, and the frequency of output voltage reduces; if Δ□ < 0, the output voltage lags behind the sine references, the value of TxPR reduces, frequency of output voltage increases. The phase difference Δ□ would be eliminated after adjusting, and phases of input and output signals maintain the balance working status. When the phase difference exists in the inverter system, output voltage is sampled by the Hall voltage sensor; the sampled signal is filtered, amplitude is limited by the regulated circuit, and then the corrected signal is put into DSP for calculation. At the same time, the event manager of DSP starts counting from zero; when the sinusoid signal goes down to zero point, the counting number is loaded into the register, and making subtraction with the standard number which is the same point of sine references. Δ□ looks like a controlled variable, and phase feedback control is used for eliminating Δ□ [26], [27]. When the output voltage is out of sync with the reference signal, Δ□ could be obtained by DSP counter. After PI is regulated, the corrected signal which involved the right phase information is compensated into sine references, and the combined signal is multiplied with the output of effective voltage feedback; the multiplied signal regulated by instantaneous capacitor-current feedback and instantaneous voltage feedback would then be modulated in the inverter system. This process is a dynamic loop and the modulation occurs as long as phase differences between the output and input signal exist. After a few periods of regulation, output and input signals get synchronized. When phase differences become 0, there is no output signal of phase feedback, and the inverter system will work in this balance state.

B. Realization in DSP

Implementation of the bipolar SPWM signal in DSP is that, defined in a sine data table, the value of each point in this table can be calculated by carrier frequency (frequency of a triangular wave), and the number of points in one period is CTNR. The value of TxPR is set as same as the pulse number of each program period; and the value of TxCMPR is set as the pulse number when the level is triggered. Counter type is set as increase and decrease mode, and level changed until counting to the value of TxCMPR, output of this

process is a group of pulse signals with same amplitude and different width. Unipolar SPWM could be considered as the intersection between a triangular wave and a group of opposite poles sinusoid signals, so a pair of polarity-reversed sinusoidal tables should be defined [28], and the value of TxCMPR is also set as before. In bipolar SPWM, IGBTs have the same drive signals, and one DSP output signal is enough to drive IGBTs, but in unipolar SPWM, diagonal IGBTs have the same drive signals, and IGBTs on the same side have complementary signals, so two types of drive signals should be output from DSP.

In inverter system digital implementation with DSP, the stability of the inverter system should also be considered. For increasing the stability of the system, the sampled singles must be eliminated, and some digital filter methods are used. In instantaneous capacitor-current feedback, instantaneous voltage feedback, and phase feedback control loops, the filter method based on single value decomposition is used for eliminating the interferences which could affect the stabilization of the inverter system, and in an effective voltage feedback control loop, because sampled signals are calculated every seven cycles and real time is not necessary, the moving average filter method is used. Some assistance functions of DSP for the inverter system are shown in Fig. 6. For reducing system damage caused by a sudden increase and decrease in voltage, digital soft starting is used in the inverter system, that is to say, modulation degree of sinusoid signal increases slowly until the value needed is achieved, and hence this starting method could reduce system damage effectively. Except that, analog-to-digital conversion, digital filter for sampling current, voltage, and phase signals can be realized in DSP. Module functions can be realized by programming for DSP, and the signals are collected and sent to the SPWM wave to IGBT for calculating.

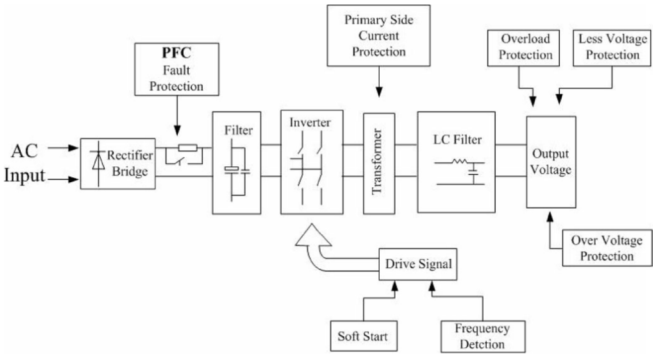

Fig. 6. Function of DSP for inverter system

VI. SYSTEM SIMULATION RESULTS

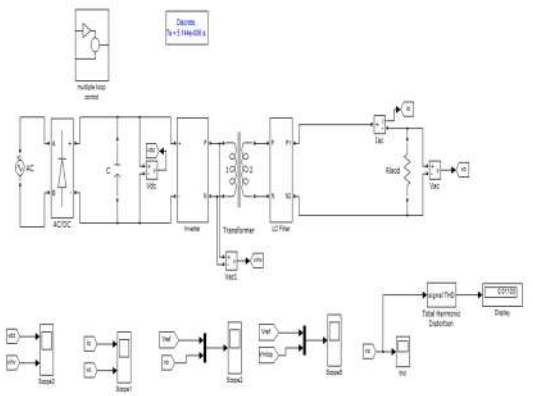

Fig 7 multiple 400 Hz closed loop inverter 1 ohm

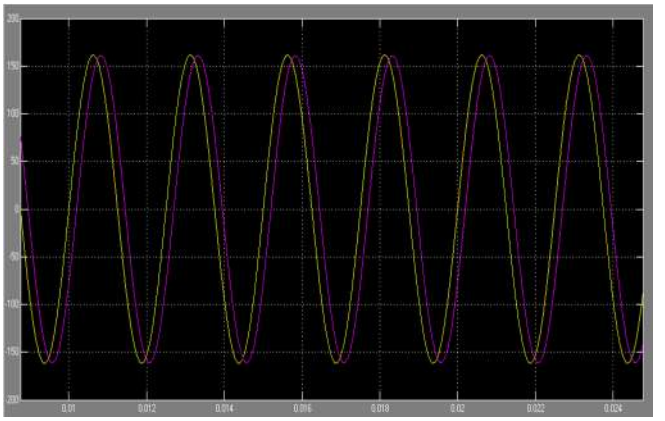

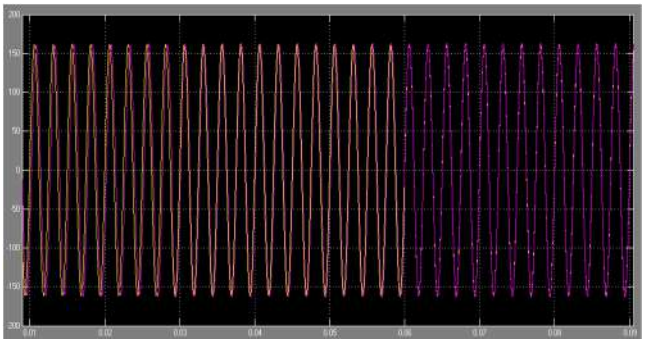

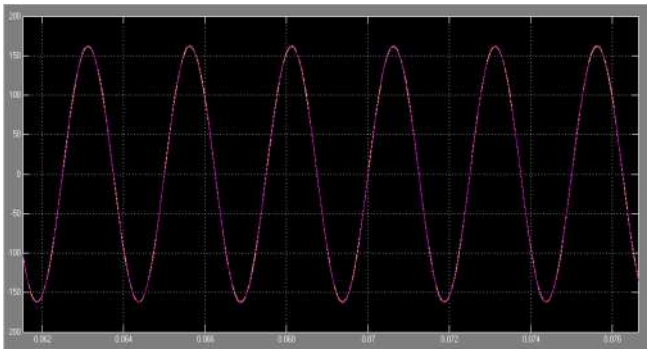

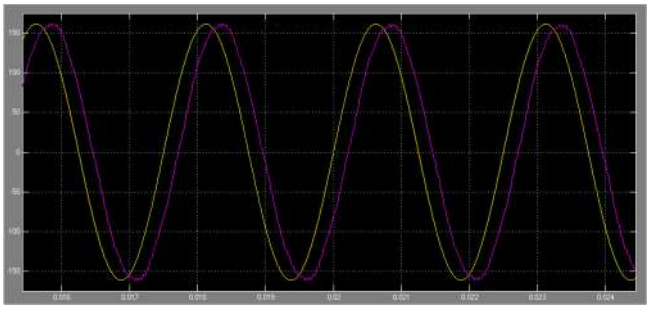

Fig 8 Simulation result with 1-Ω resistance load (a) Result with three-loop control. (b) Result with phase feedback control. (c) Detailed drawings of start and finish time in (b)

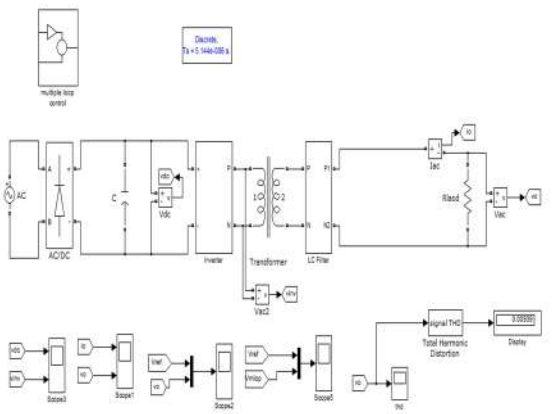

Fig 9 multiple 400 Hz closed loop inverter 6 ohm

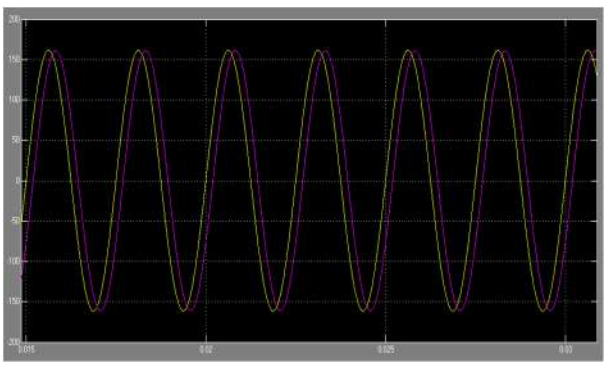

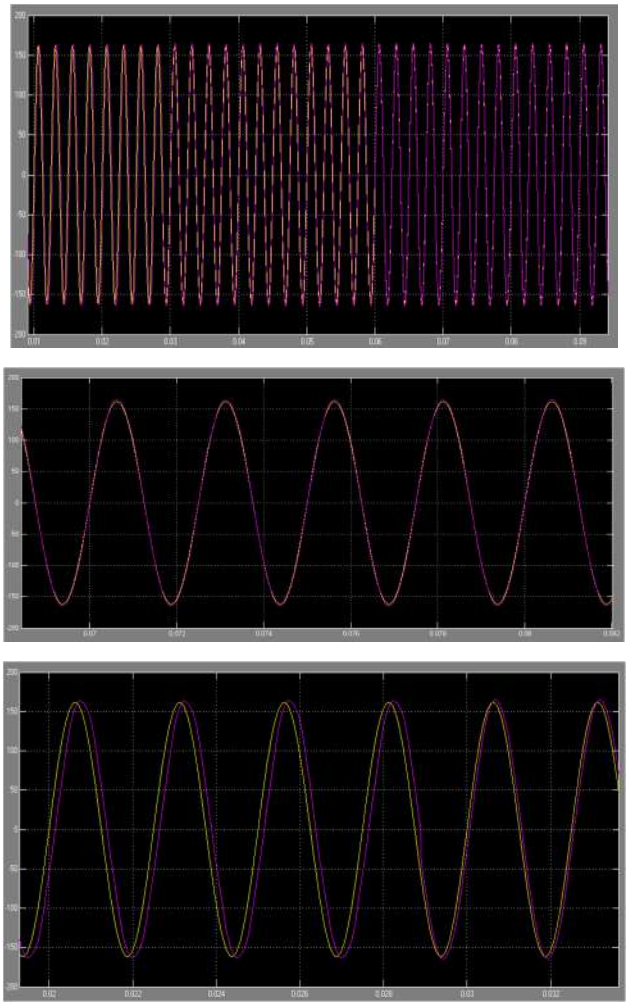

Fig 10 Simulation result with 6-Ω resistance load (a) Results with three loop control. (b) Results with phase feedback control. (c) Detailed drawings of start and finish time in (b).

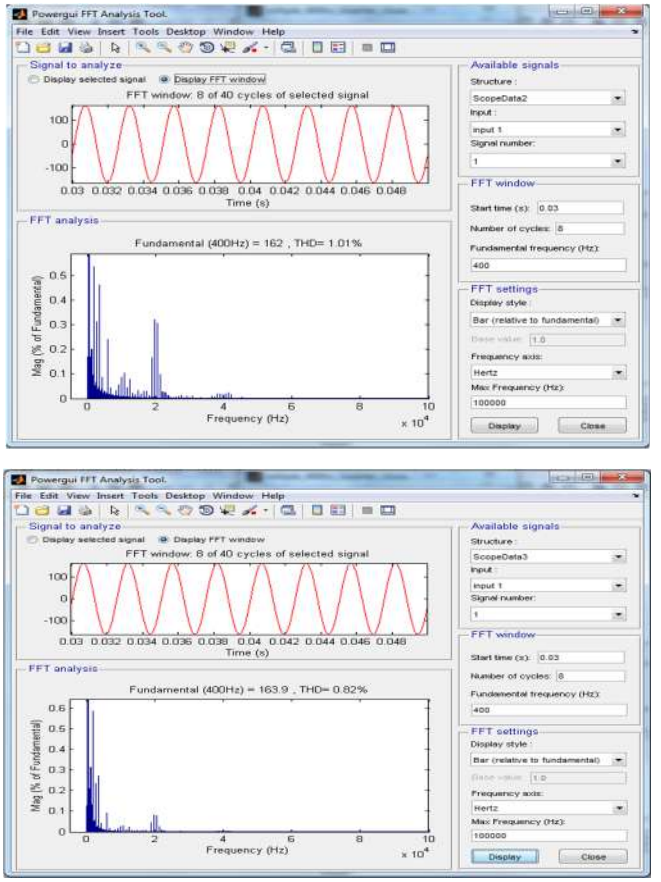

Fig Simulation waveform and THD analysis (a) Result with three-loop control. (b) Result with phase feedback control

VIII. CONCLUSION

The phase imbalance and output quality of the three-phase combined inverter power system can be improved. The guidelines for the design of the phase controller have been discussed; the stability of the multiple-loop control system has been analyzed; and LC filter parameters, drive board, and snubber circuit structure design have been presented. This paper has presented a new novel multiple-loop control system for a 400-Hz inverter power system based on unipolar SPWM, which is added phase control feedback based on traditional three-loop control. By these hardware designs, dead time effects and voltage oscillation across the IGBT can be eliminated effectively. Simulation experimental results with different loads show that the phase of output voltage

can be adjusted in a short time, and the THD of the inverter system can be improved greatly compared to traditional control strategy. The three-phase combined inverter system based on multiple-loop control strategy is constructed, and experimental results show that the THD of output voltage can be controlled to 2%, and the phase difference of the three-phase inverter system can be controlled to 2◦, and kept the instable working state. The future work will focus on the new control method of a three-phase inverter which is based on the DQ reference frame, and a high frequency link can be used in the inverter for increasing power transmission efficiency.

VIII. Acknowledgment

This paper is based on M. Tech. project carried out by the student of pydah college of engineering & technology, Kakinada studying M.Tech (Power Electronics) The project had been completed by Ms. V.N.D SAILAJA bearing H.T.no.: 126T1D4317 under the guidance of B. LALITHA KUMARI.

REFERENCES

1. A. M. Hava and N. O. C¸ etin, "A generalized scalar PWM approach with easy implementation features for three-phase. Three-wire voltage-source inverters," *IEEE Trans. Power Electron.*, vol. 26, no. 5, pp. 1385–1395, May 2011.
2. K. Harada, H. Sakamoto, and M. Shoyama, "Phase-controlled DC-AC converter with high-frequency switching," *IEEE Trans. Power Electron.*, vol. 3, no. 4, pp. 406–411, Oct. 1988.
3. N. M. Abdel-Rahim and J. E. Quaicoe, "Analysis and design of a multiple feedback loop control strategy for single-phase voltage-source UPS inverters," *IEEE Trans. Power Electron.*, vol. 11, no. 4, pp. 532–541, Jul. 1996.
4. M. Ciobotaru, V. Agelidis, and R. Teodorescu, "Accurate and lessdisturbing active anti-islanding method based on PLL for grid-connected PV Inverters," in *Proc. Rec. IEEE Annu. Power Electron. Spec. Conf.*, Jun. 2008, pp. 4569–4576.
5. N. Anani, O. A. Al-Ali, P. Ponnapalli, S. R. Al-Araji, and M. A. Al-Qutayri, "Synchronization of a single-phase photovoltaic generator with the grid," in *Proc. IEEE Int. Conf. Computer Tool (EUROCON)*, Apr. 2011, pp. 1–4.
6. D. Velasco, C. Trujillo, G. Garcer´a, and E. Figueres, "An active antiislanding method based on phase-PLL perturbation," *IEEE Trans. Power Electron.*, vol. 26, no. 4, pp. 1056–1066, Apr. 2011.
7. M. Ciobotaru, V. G. Agelidis, R. Teodorescu, and F. Blaabjerg, "Accurate and less-disturbing active antiislanding method based on

PLL for gridconnected converters," *IEEE Trans. Power Electron.*, vol. 25, no. 6, pp. 1576–1584, Jun. 2010.

8. J. W. Choi, Y. K. Kim, and H. G. Kim, "Digital PLL control for singlephase photovoltaic system," *IEEE Proc. Electron. Power Appl.*, vol. 153, no. 1, pp. 40–46, Jan. 2006.
9. Q. Zhang, X. D. Sun, Y. R. Zhong, M. Matsui, and B. Y. Ren, "Analysis and design of a digital phase-locked-loop for single-phase grid-connected power conversion systems," *IEEE Trans. Ind. Electron.*, vol. 58, no. 8, pp. 3581–3592, Aug. 2011.
10. Y. X. Xie, L. Zhou, and H. Peng, "Homopoty algorithm research of the inverter harmonic elimination PWMmodel," *Proc. CSEE*, vol. 20, no. 10, pp. 23–26, 2000.
11. Y. W. Li, M. Pande, N. R. Zargari, and B. Wu, "An input power factor control strategy for high-power current-source induction motor drive with active front-end," *IEEE Trans. Power Electron.*, vol. 25, no. 2, pp. 352– 359, Feb. 2010.
12. X. H. Wang, X. B. Ruan, S. W. Liu, and C. K. Tse, "Full feedforward of grid voltage for grid-connected inverter with LCL filter to suppress current distortion due to grid voltage harmonics," *IEEE Trans. Power Electron.*, vol. 25, no. 12, pp. 3119–3127, Dec. 2010.
13. F. D. Freijedo, J. Doval-Gandoy, O. Lopez, and E. Acha, "A generic openloop algorithm for three-phase grid voltage/current synchronization with particular reference to phase, frequency, and amplitude estimation," *IEEE Trans. Power Electron.*, vol. 24, no. 1, pp. 94–107, Jan. 2009.
14. S. Dasgupta, S. K. Sahoo, S. K. Panda, and G. A. J. Amaratunga, "Singlephase inverter-control techniques for interfacing renewable energy sources with microgrid—Part II: Series-connected inverter topology to mitigate voltage-related problems along with active power flow control," *IEEE Trans. Power Electron.*, vol. 26, no. 3, pp. 732–746, Mar. 2011.
15. S. K. Chung, H. B. Shin, and H.W. Lee, "Precision control of single-phase PWM inverter using PLL compensation," *IEEE Proc. Electron. Power Appl.*, vol. 152, no. 2, pp. 429–436, Mar. 2005.
16. Y. X. Wu, M. A. Shafi, A. M. Knight, and R. A. McMahon, "Comparison of the effects of continuous and discontinuous PWM schemes on power losses of voltage-sourced inverters for induction motor drives," *IEEE Trans. Power Electron.*, vol. 26, no. 1, pp. 182–191, 2011.
17. H. Pham,H. Fujita, K. Ozaki, andN.Uchida, "Phase angle control of highfrequency resonant currents in a multiple inverter system for zone-control induction heating," *Power Electron.*, vol. 26, no. 11, pp. 3357–3366, Nov. 2011.

18. X. Q. Yi, X. J. Pei, and T. Hou, "Study of single pole double frequency SPWM of combinatorial three phase inverter on DSP," *Power Electron.*, vol. 41, no. 6, pp. 77–79, Jun. 2007.
19. A. B. Afarulrazi, M. Zarafi,W. M. Utomo, and A. Zar, "FPGA implementation of Unipolar SPWM for single phase inverter," in *Proc. Int. Conf. Comput. Appl. Ind. Electron.*, Dec. 2010, pp. 671–676.
20. H. X. Yu, Y. C. Ji, andM. Lin, "An advanced harmonic elimination PWM technique implemented in ac choppers," *Proc. CSEE*, vol. 25, no. 5, pp. 68–73, Mar. 2005.
21. D. L. Chen and G. L. Wang, "Differential buck DC–DC chopper mode inverterswith high-frequency link," *IEEE Trans. Power Electron.*, vol. 26, no. 5, pp. 1444–1451, May 2011.
22. H. G. Zhang, Q. Wang, E. H. Chu, X. C. Liu, and L. M. Hou, "Analysis and implementation of a passive lossless soft-switching snubber for PWM inverters," *IEEE Trans. Power Electron.*, vol. 26, no. 2, pp. 411–426, Feb. 2011.
23. Z. L. Yao, L. Xiao, and Y. G. Yan, "Control strategy for series and parallel output dual-buck half bridge inverters based on DSP control," *IEEE Trans. Power Electron.*, vol. 24, no. 2, pp. 434–444, Feb. 2009.
24. H. Liao, S. S.Qiu, and J. Zhang, "The technology of software phase-locked for UPS based on F2812," *Electron. Appl.*, vol. 27, no. 5, pp. 68–71, Mar. 2008.
25. X. Q. Zhu, "Research on digital control of UPS based on TMS320F240," *Power Electron.*, vol. 39, no. 6, pp. 116–119, Nov. 2005.
26. S. K. Chung, "A phase tracking system for three phase utility interface inverters," *IEEE Trans. Power Electron.*, vol. 15, no. 3, pp. 431–438, May 2000.
27. Y. R. Shayan and T. Le-Ngoc, "All digital phase-locked loop: Concepts design and applications," in *IEE Proc. F Radar Signal*, vol. 36, no.1, pp. 53–56, Feb. 1989.
28. H. M. Kojabadi, Y. Bin, I. A. Gadoura, L. C. Chang, and M. Ghribi, "A novel DSP-based current-controlled PWM strategy for single phase grid connected inverters," *IEEE Trans. Power Electron.*, vol. 21, no. 4, pp. 985–993, Jul. 2006.

INTERNATIONAL JOURNAL OF MULTIDISCIPLINARY EDUCATIONAL RESEARCH
ISSN : 2277-7881; IMPACT FACTOR - 2.972; IC VALUE:5.16
VOLUME 3, ISSUE 10(4), OCTOBER 2014

VOLTAGE BALANCING TECHNIQUE FOR REACTIVE POWER COMPENSATION IN 3-LEVEL NPC INVERTERS USING TPWM TECHNIQUE

MS. CH. RAMYA
ramyachodi@gmail.com
Under the guidance of
Mr. P. VIJAYA RAMARAO
ASSISTANT PROFESSIOR
PYDAH COLLEGE OF ENGINEERING , KAKINADA

Abstract— This paper presents a comparison with two already known strategies in which a sinusoidal waveform at two and six times the output frequency are injected. This technique, suitable for reactive power compensation and for inverters operating with a relatively low switching frequency, consists in adding a square wave at six times the output frequency. A novel technique to balance the voltage of the two split dc capacitors of a 3-Level neutral-point-clamped inverter using triangular carrier pulse width modulation is presented. Subsequently, the current contribution to the midpoint of the dc bus is then analyzed for different modulation indexes and operating conditions. Based on this analysis, a small-signal averaged model, suitable for control design purposes is presented.

***Index Terms*— FACTS, SSSC, STATCOM, VSC**

I. INTRODUCTION

One of the main control challenges in 3-L NPC inverters is to keep the voltage across the two dc-split capacitors balanced. The development of FACTS devices, which aim for the transmission network to operate close to its thermal limit by providing a fast dynamic control, has been boosted in recent times by the emergence of new semiconductor devices such as high-voltage insulated-gate bipolar transistors (IGBTs). The well-known neutral point clamped (NPC) 3-level (3-L) inverter has been widely used in this type of applications. These inverters are often based on well proven solutions, also used in other high-integrity demanding applications such as steel mill processes, ship propulsion, and ship dredger pumps. These are 3-L NPC IGBT-based inverters, where each has a power in the range of 3.5 MVA.

The use of space vector pulse width modulation (SVPWM) techniques, widespread these days, presents limitations to control the midpoint voltage at

very low power factor operation and high modulation indexes, as is often the case of FACTS devices. Moreover, there are applications where the use of traditional triangle carrier modulation is preferred. For instance when the output waveforms are non-sinusoidal, as is the case of active filters, or when the topology requires additional balancing loops, for instance anti-saturation control of magnetic devices connected at the inverter output, i.e., coupling transformers.

II. VOLTAGE BALANCING TECHNIQUE

This section begins by describing the compensation techniques based on sinusoidal second and sixth harmonic injection, followed by the newly proposed compensation method. The explanation of the voltage balancing technique is based on the 3-L NPC inverter seen in Fig. 1. The explanation assumes that the inverter is supplied by a three phase set of pure sinusoidal currents (1). However, the simulation results show later on in this paper that the analysis and proposed techniques are also valid for an unbalanced supply system.

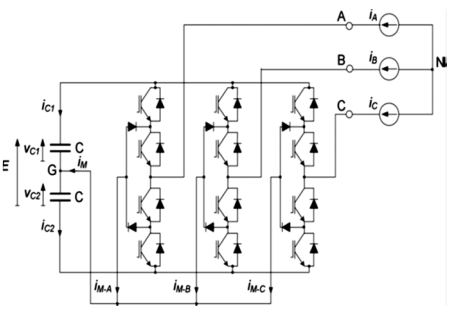

Fig. 1 Three-level NPC inverter configuration with ideal sinusoidal current sources

Also, the output voltage of the inverter is produced by comparing the reference waveform showed in (2), with two level shifted triangular carrier waveforms to obtain a 3-L output. In addition, the injection of a third harmonic waveform, as seen in (3), is a well recurred method to increase the magnitude of the output voltage, about 15% higher where K_3 takes a value of 1/6

$$
\begin{aligned}
i_A &= \hat{I}\sin(\omega t + \phi) \\
i_B &= \hat{I}\sin\left(\omega t - {}^{2\pi}/_{3} + \phi\right) \\
i_C &= \hat{I}\sin\left(\omega t + {}^{2\pi}/_{3} + \phi\right) \qquad (1) \\
v_A &= {}^{E}/_{2}\, m_1 \sin(\omega t) \\
v_B &= {}^{E}/_{2}\, m_{11} \sin\left(\omega t - {}^{2\pi}/_{3}\right) \\
v_C &= {}^{E}/_{2}\, m_1 \sin\left(\omega t + {}^{2\pi}/_{3}\right) \qquad (2) \\
v_3 &= {}^{E}/_{2}\, m_1 K_3 \sin(3\omega t) \qquad (3)
\end{aligned}
$$

Where $m1$ is the modulation index and K_3 is the amount of third harmonic injection.

A. Sinusoidal Second Harmonic Injection

This method consists in injecting a negative sequence second harmonic voltage waveform, superimposed to the fundamental output waveform defined in (4). Since the second harmonic components are negative sequence, a negative sequence of those will be in phase with the positive fundamental sequence

$$
\begin{aligned}
v_{A-2\sin} &= v_A + {}^{E}/_{2}\, m_2 \sin(2\omega t + \phi_2) \\
v_{B-2\sin} &= v_B + {}^{E}/_{2}\, m_2 \sin\left[2\left(\omega t + {}^{2\pi}/_{3}\right) + \phi_2\right] \\
v_{C-2\sin} &= v_C + {}^{E}/_{2}\, m_2 \sin\left[2\left(\omega t - {}^{2\pi}/_{3}\right) + \phi_2\right] \qquad (4)
\end{aligned}
$$

Where $m2$ is the modulation index for the compensation waveform

The effect of this technique in the modulation reference waveforms is seen in Fig.2 (a), where the modulation index for the reference and injected waveform is 0.6 and 0.1, respectively. The magnitude of the injected waveform in these figures has been exaggerated for clarity purposes. One of the disadvantages of this method is that second harmonic voltage components are heavily penalized in most power quality legislations. To overcome this problem, the injection of a sinusoidal waveform at six times the supply frequency can be used instead.

B. Sinusoidal Sixth Harmonic Injection

It is well known that harmonics multiple of three times the output frequency are zero sequence, that is, they are in phase across all three phases and are, therefore, inherently cancelled out at the output of a three-phase system. Moreover, even harmonics contribute with a nonzero average value of current to the midpoint in the same way as explained in the previous section. This method consists in injecting a sinusoidal waveform at six times the supply frequency as seen in (5). The effect of this method on the output waveform is showed in Fig. 2(b) for a $m1$ index of 0.6 and a modulation index of the injected waveform $m6$ of 0.1

$$\begin{aligned} v_{A-6\sin} &= v_A + {}^{E}/_{2} m_{6-\sin} \sin(6\omega t + \phi_{6-\sin}) \\ v_{B-6\sin} &= v_B + {}^{E}/_{2} m_{6-\sin} \sin(6\omega t + \phi_{6-\sin}) \\ v_{C-6\sin} &= v_C + {}^{E}/_{2} m_{6-\sin} \sin(6\omega t + \phi_{6-\sin}) \end{aligned} \qquad (5)$$

where $m6$ is the modulation index for the compensation waveform.

One of the potential disadvantages of using this method in large power inverter systems is the relatively high switching frequency that is required to materialize the sixth harmonic component. This has a frequency of 300 and 360 Hz, respectively for supply frequencies of 50 or 60 Hz. Large power inverters normally operate at relatively low switching frequencies, below 1 kHz. The next section proposes a voltage balancing method that aims to overcome this problem.

C. Squared Sixth Harmonic Injection

This technique can be seen as an evolution of that presented in the previous section and consists in injecting a squared wave at six times the supply frequency. Since the injection of a squared wave can be regarded as the addition of a dc offset of a given magnitude to the reference waveform that changes sign every 30 electrical degrees, its practical implementation is likely to be simpler, especially in inverters operating with a low switching frequency. This injected waveform can be expressed as

$$v_{A-6sq} = v_A + v_{6-sq}$$
$$v_{B-6sq} = v_B + v_{6-sq}$$
$$v_{C-6sq} = v_A + v_{6-sq}$$
$$v_{6-sq} = {}^{E}/_{2} m_{6-sq} \operatorname{sign}\left[\sin\left(6\omega t + \phi_{6-sq}\right)\right]. \qquad (6)$$

The effect of this technique on the inverter output waveform is illustrated in Fig. 2(c) for a *m*1 index of 0.6 and a modulation index of the injected waveform*m*6 of 0.1. The next section evaluates the ability of the three compensation approaches described so far to control de midpoint voltage.

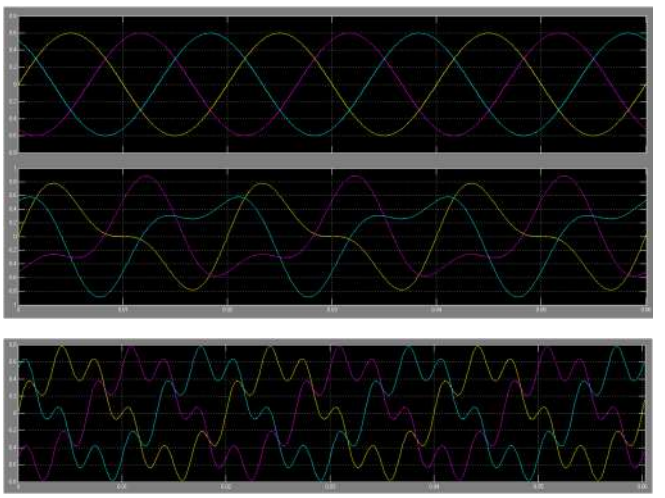

Fig. 2. Line-to-midpoint output voltage for: (a) sinusoidal second harmonic injection; (b) sinusoidal sixth harmonic injection; (c) squared sixth harmonic injection. Continuous line: *vA* ; dashed line: *vB* ; dotted line: *vC* , normalized with respect to E/2.

III. ANALYSIS OF THE AVERAGE CURRENT CONTRIBUTION TO THE MIDPOINT AND AN AVERAGE MODE

This section begins by analyzing the current contribution to the midpoint for the three voltage balancing techniques explained in the previous section. Subsequently, a sensitivity analysis for different modulation indexes and phase-shift angles is performed. Next, a small signal averaged model of the midpoint balance control loop, suitable for control design purposes, is proposed.

A. Analysis of the Current Contribution to the Midpoint

As already explained in the instantaneous duty ratio *d* of the portion of the phase input current that flows to the midpoint is defined as

$$d_K = \begin{cases} 1 + 2v_K/E & \left(-E/2 \le v_K < 0\right) \\ 1 - 2v_K/E & \left(0 \le v_K \le -E/2\right) \end{cases} \qquad (7)$$

where *k = A, B, or C*

Consequently, the instantaneous contribution of any phase to the midpoint current is obtained by multiplying the duty ratio *dK* by the phase current (1)

$$i_{M-K} = d_K i_K . \qquad (8)$$

Since the voltage drift of the midpoint is a comparatively slower varying process than the instantaneous voltage ripple present in the dc bus, the effectiveness of the midpoint voltage control can be evaluated by considering the mean dc midpoint current over an entire line period *T*. This is calculated in a straight forward manner as

$$\bar{i}_{M-K} = \frac{1}{T}\int_0^T i_{M-K}\, dt \qquad (9)$$

where the total average current contribution to the midpoint is

$$\begin{aligned} \bar{i}_M &= \bar{i}_{M-A} + \bar{i}_{M-B} + \bar{i}_{M-C} \\ &= \frac{1}{T}\int_0^T (i_{M-A} + i_{M-B} + i_{M-C})\, dt. \end{aligned} \qquad (10)$$

The effect that the injection of a negative sequence second harmonic, sinusoidal sixth harmonic and squared sixth harmonic, have on the midpoint current can be visually seen by looking at the waveforms in Figs. 4–5 respectively, corresponding to phase A.

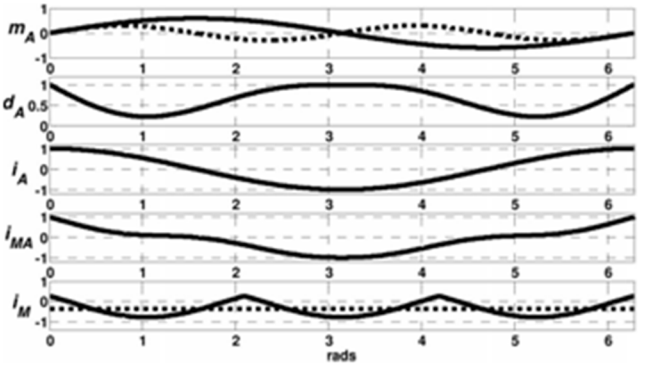

Fig. 3. Second harmonic compensation for $m1 = 0.6$ and $m2 = 0.3$.

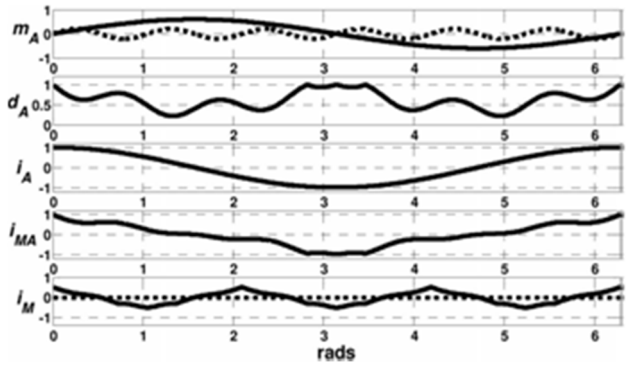

Fig. 4. Sixth harmonic sinusoidal compensation for $m1 = 0.6$ and $m6 - \sin = 0.2$.

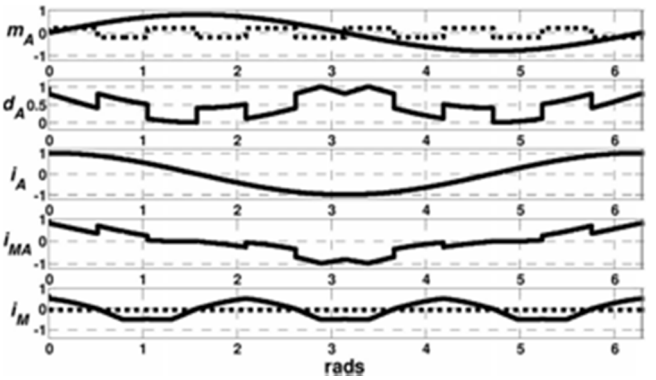

Fig. 5. Sixth harmonic squared injection at six times the supply frequency for $m1 = 0.6$ and $m6-sq = 0.2$.

These waveforms have been computed using the MATLAB software using (1)–(10) for a modulation index of the fundamental waveform of $m1$ = 0.6. The modulation index for the compensation waveforms where $m2$ = 0.3, $m6-\sin$ = 0.2, and $m6-\mathrm{sq}$ = 0.2 and the phase angle of the injection waveforms was set to zero, that is, $\Phi_2 = 0$, $\Phi_6-\sin = 0$, and $\Phi_6-\mathrm{sq} = 0$. The first two waveforms on top of every figure show the fundamental and the compensating waveforms in continuous and dotted lines. The second waveform depicts the instantaneous duty ratio d of the current to the midpoint. The third waveform shows the current i_A flowing into phase A, 90^0 out of phase with respect to the output voltage. The fourth waveform shows the current contribution of phase A to the midpoint, calculated by direct multiplication of the second and third waveforms, as seen in (8). Finally, the last set of waveforms show the instantaneous overall current contribution to the midpoint made by all three phases, using a continuous trace and its average value over the entire period, using a dotted trace. The voltages and currents are normalized with respect to E/2 and the phase peak current, respectively. It can be seen by visual inspection how the average current has a negative value, more significant in the case of the second harmonic injection Fig. 3(a). The usual third harmonic current ripple, which creates a third harmonic voltage ripple in the midpoint, is also present.

B. Limit of the Injection Waveforms

The sum of the reference and compensating waveform should not exceed the dc-bus voltage E/2. Consequently the compensating waveform must comply with the following expression at all times

$$v_{\mathrm{COMP}} \leq E/2 - v_{A,B,C} \qquad (20)$$

$$v_{\mathrm{COMP}} \leq E/2 - v_{A,B,C} \qquad (11)$$

where v_{COMP} can be either $v_{A,B,C}-2\sin$, $v_{A,B,C}-6\sin$, or $v_{A,B,C}-6\mathrm{sq}$ as defined in (4)–(6), respectively. Also, $v_{A,B,C}$ is expressed in (2) and (3) if third harmonic injection is used.

The maximum modulation index for the injection waveforms has been calculated by solving (11) for the angle $(\omega t)_{\mathrm{MAX}}$ that achieves the peak value in expressions (4)–(6). This angle has been calculated by solving the equation that

equates the angle derivative expression to zero, following basic mathematic principles.

Using those, the maximum modulation index for the compensating waveform has been calculated for several values of the modulation index *m*1 of the reference waveform, close to the maximum $2/\sqrt{3}$, where third harmonic injection has been used and the results are shown. The second harmonic, sinusoidal sixth harmonic, squared sixth harmonic and SPWM are represented using continuous, dashed, dashed–dotted and dotted traces, respectively. Also, in that figure, the resultant average current that flows to the midpoint *IM*, normalized with respect to the peak value of the line current is also shown. These results are compared with the current that is obtained using the well-known SPWM technique for a 3-L-NPC inverter.

In that figure, it can be seen how the maximum compensating waveform that can be injected is gradually reduced as the modulation index for the reference waveform is increased, until it reaches its maximum value of $m_1 = 2/\sqrt{3}$, where no compensating waveform can be introduced. On the contrary, SPWM can produce a mid-point balancing current even at the maximum modulation index. How second harmonic injection has a higher balancing effect, whereas sinusoidal and squared harmonic injection can produce compensating currents with similar values. This is explained, despite squared sixth harmonic injection having a higher balancing action than sinusoidal sixth harmonic injection, because the latter allows having an injection waveform of a magnitude higher than that of the former.

It is important to mention that the contribution of the proposed techniques to the midpoint balancing current can be easily increased at certain times at the expenses of sacrificing the magnitude of the reference waveform. That is, the value of *m*2, *m*6−sin, or *m*6−sq, depending on whichever technique is used, can be temporarily increased by subsequently reducing the value of *m*1, to bring the midpoint back into balance, as it will be seen in the simulation results seen in Section IV.

C. Small Signal Averaged Model of the Split Capacitors

Midpoint Balance

The averaged model of the split capacitors midpoint balance loop is obtained by averaging the output capacitor currents and voltages over a supply cycle, that is, by neglecting the instantaneous ripple. The analysis also

assumes that the dc bus voltage v_0 is stable and has a constant average value of E. This assumption is justified, even at the low switching frequencies typical of large converter systems, by the criteria chosen to design the dc-link capacitors. This, with the purpose of avoiding any overvoltage across the power devices, aims to reduce the voltage switching ripple to a very low value by including enough capacitance. For that reason, the voltage unbalance within one switching cycle for the different modulation methods has not been considered.

TABLE I

Im /*m*2 And *Im* /*m*6 Gains in the First Linear Operating Region

	K_M
Second harmonic	1.27
Sinusoidal 6th harmonic	0.323
Squared 6th harmonic	0.454

By looking at the diagram of Fig. 1, it can be easily deducted that voltage balance of the midpoint capacitors is

$$\bar{v}_{C2} - \bar{v}_{C1} = \frac{1}{C}\int_0^T (\bar{i}_{C2} - \bar{i}_{C1})\,dt = \frac{1}{C}\int_0^T \bar{i}_M\,dt \quad (21)$$

$$\bar{v}_{C2} - \bar{v}_{C1} = \frac{1}{C}\int_0^T (\bar{i}_{C2} - \bar{i}_{C1})\,dt = \frac{1}{C}\int_0^T \bar{i}_M\,dt \quad (12)$$

Expressing this equation in the S domain, and relating the average midpoint current *IM* to the peak phase current and the modulation index of the compensating waveform by means of the K_M ratio (14) seen in Table I, the following transfer function is obtained:

$$\frac{V_{C2} - V_{C1}}{m_2(or\ m_6)} = \frac{\hat{I}\sin(\phi)\,K_M}{CS} \quad (13)$$

$$\frac{V_{C2} - V_{C1}}{m_2(or\ m_6)} = \frac{\hat{I}\sin(\phi)\,K_M}{CS} \quad (22)$$

$$K_M = \frac{I_M}{\hat{I}m_2} \text{ or } K_M = \frac{I_M}{\hat{I}m_{6-\sin}} \text{ or } K_M = \frac{I_M}{\hat{I}m_{6-sq}}. \quad (14)$$

$$K_M = \frac{I_M}{\hat{I}m_2} \text{ or } K_M = \frac{I_M}{\hat{I}m_{6-\sin}} \text{ or } K_M = \frac{I_M}{\hat{I}m_{6-sq}}. \quad (11)$$

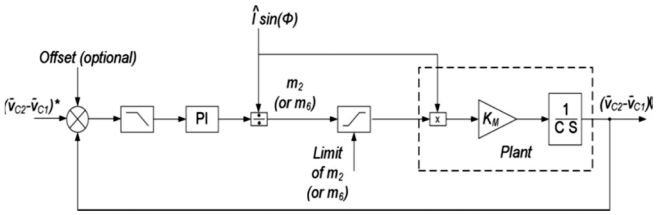

Based on this transfer function, a control loop structure valid for reactive power compensation is proposed where a usual PI controller is employed in combination with a low-pass, first order filter, to suppress the voltage ripple components (15).

The control output is normalized by dividing it by the peak reactive component of the phase current, a straightforward operation in usual digital control systems. An optional offset has been added to the set point to allow introducing step changes to evaluate the performance of the control loop. The cross-over frequency of the first order filter is selected to mitigate the third harmonic ripple components present across the capacitors (150 Hz for a 50 Hz system), for example at 15 Hz or 94.25 rad/s. Subsequently, the PI loop can be tuned using conventional techniques, for instance, aiming to achieve a reasonable Phase Margin. Although, as explained in the next Section IV, the dynamic response achieved using this control strategy is sufficient for most large power electronics applications, other suitable strategies compatible with the proposed compensating techniques could also be devised

$$\text{Controller } TF = \frac{1}{\left(S/\omega_P + 1\right)} K_P \frac{(S + iT_n)}{S} \qquad (15)$$

$$\text{Controller } TF = \frac{1}{\left(S/\omega_P + 1\right)} K_P \frac{(S + iT_n)}{S} \qquad (23)$$

IV. SIMULATION EVALUATION

The operation of the control strategy proposed in Fig. 12 has been validated, first in simulation and then experimentally, on a 690 Vac, 100 A, 120 kVA, 3-L NPC inverter, based on IGBT devices switching at 600 Hz. Each of the split capacitors had a capacitance value of 6.6 mF and the positive and negative dc link terminals of the inverter were supplied by a 950 V external rectifier unit, with the midpoint left floating. The phase-shift angle of the injection waveforms with respect to the reference waveform has been chose to be Φ_2 = 0, Φ_6−sin = 0, Φ_6−sq = 0 for a greater compensation effect. The

simulation results for a step response when second harmonic compensation is selected are shown in Fig. 13. The inverter was supplied by a set of ideal current sources of 90-A RMS and the RMS phase-to-neutral output voltage was 310 V.

To validate the averaged model described in the previous section, the control loop as shown in Fig. 12 has been made run in parallel with the complete inverter simulation. In that figure, the left and right-hand plots show the response to a 0 to 50 V and 0 to 50 to 0 V offset step respectively. The continuous thin and thick lines represent the instantaneous and averaged v_{C2} - v_{C1} waveforms, which show close correspondence. The step set point is depicted in the figure using a dotted thin trace. The control parameters where chosen as ω_P = 94.24 rads/s; K_P = 0.0863 and i_{TN} = 2.93. The same results were obtained for sixth harmonic squared and sinusoidal compensation, but are not shown in this paper for the shake of briefness. The control loop achieves an open-loop bandwidth of 2.64 Hz, a settling time of 0.784 s (for a 1% error criteria) and an overshoot of 12%. Therefore, with the proposed adjustment, it will take about 40 line cycles to complete a step response. Although this may seem a long time, in practice, due to the amount of capacitance present in the dc link, the dc-link midpoint voltage balance changes relatively slowly. This is confirmed in the experimental section and in several industrial applications where this strategy has been implemented.

In the experimental validation, the inverter output terminals were connected to an 18 mH inductive load and it was operated in current control mode. To verify the ability to control the midpoint, an offset step of 50 V was introduced when the output current was controlled to be 70A RMS and the results are shown, for second harmonic, sinusoidal sixth harmonic, and squared sixth harmonic compensation, respectively.

The first two waveforms show the capacitor voltages v_{C1} and v_{C2}, the third waveform the inverter output voltage with respect to the midpoint of the dc-link capacitors v_{AG} and the bottom waveform shows the output current i_A. The proportional gain K_P for second and sixth harmonic was chosen to be 0.3 and 0.85, respectively, whereas the integral term iTn and the filter crossover frequency were 2.93 and 94.24 rad/s, respectively, in all three cases (15). These waveforms show how the midpoint voltage balance can be successfully controlled for all the proposed strategies. A similar response was obtained for a falling 50Vto 0Vstep response. By looking at the results, it is very hard to

appreciate substantial differences between response obtained using sinusoidal and squared sixth harmonic injection. Therefore, the main difference between these two techniques lies in the easier implementation offered by the squared harmonic injection at low switching frequencies. In the waveforms of Fig. 14, a dip in the output current during the midpoint transient can be observed, which highlights a limitation of the proposed compensation techniques. This is due to the output voltage required to control the output current, already operating close to its limit in this experiment, diminishing to accommodate the midpoint compensating waveforms. This effect is significantly greater in the case of the sixth harmonic injection strategies as their compensation power is about three or four times smaller than that of the second harmonic strategy.

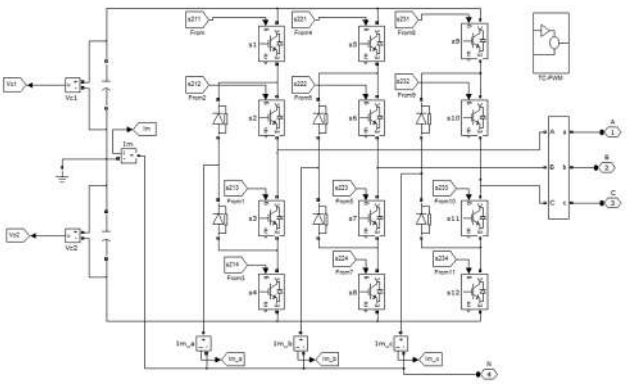

Fig 6 simulation diagram of proposed system

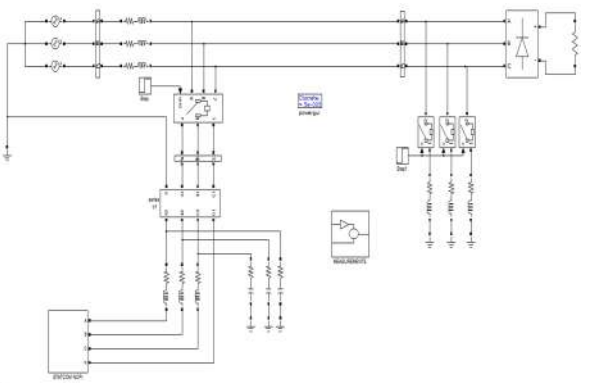

Fig 7 simulation diagram of STATCOM Neutral Clamped Point Inverter

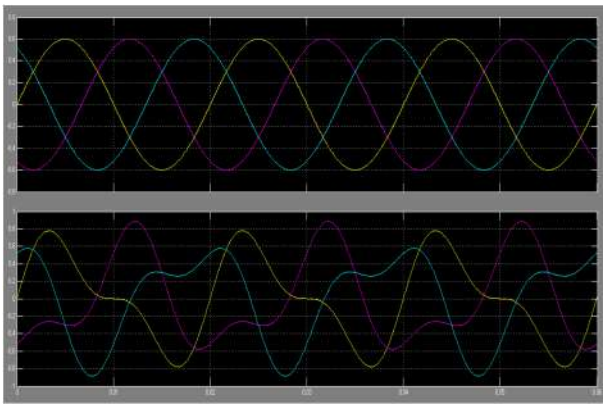

Fig 8 sinusoidal second harmonic injection

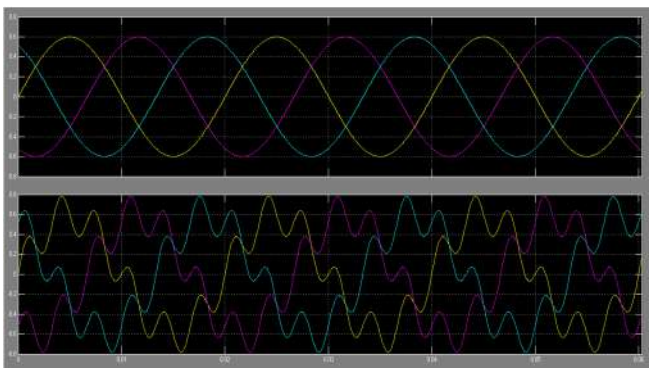

Fig.9 sinusoidal sixth harmonic injection

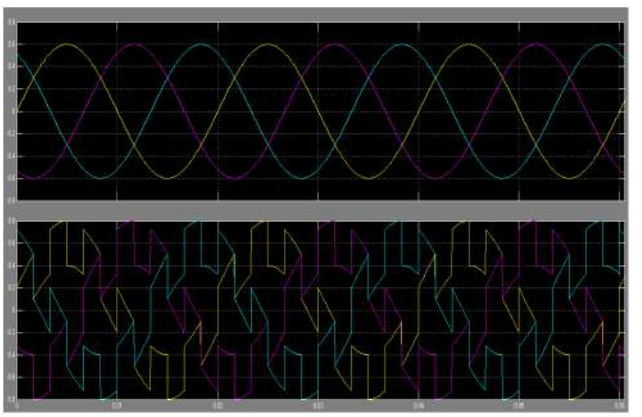

Fig 10 squared sixth harmonic injection

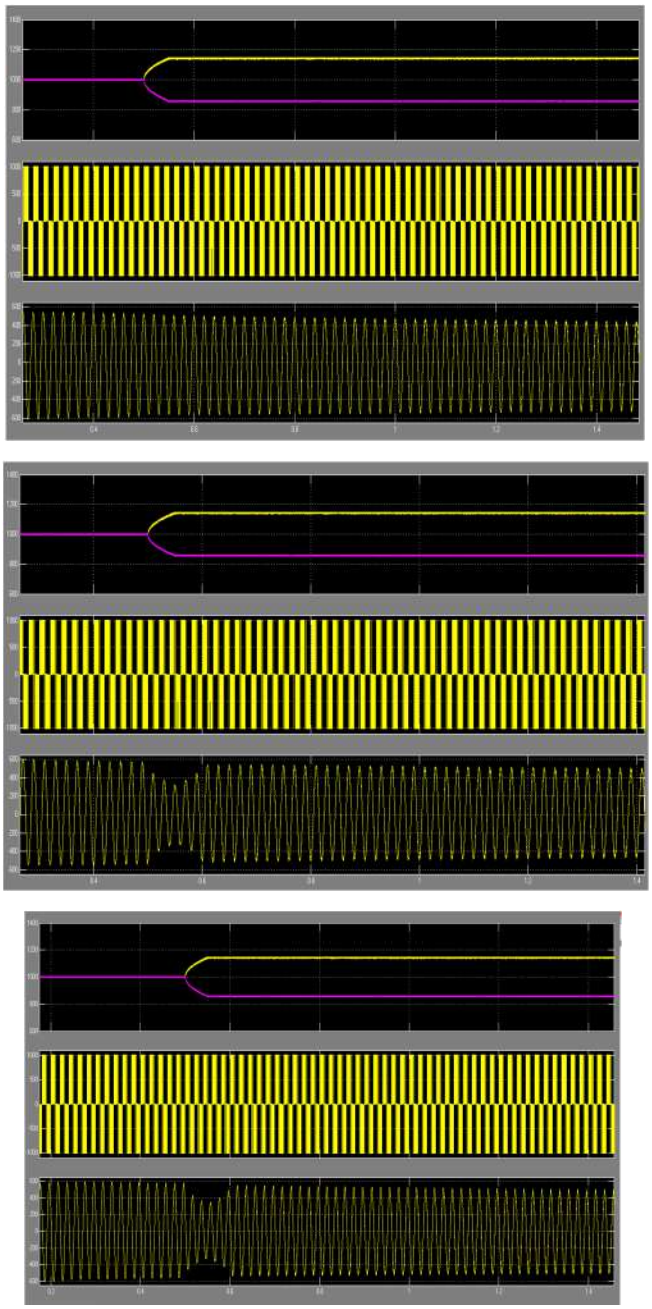

Fig 11 Instantaneous response for a mid-point imbalance step of 0 to 50 V, 70 A RMS. (a) sinusoidal second harmonic injection; (b) sinusoidal sixth harmonic

injection; (c) squared sixth harmonic injection. First waveform: *vc* 1, second waveform: *vc* 2, third waveform *v*AG, fourth waveform: *iA*.

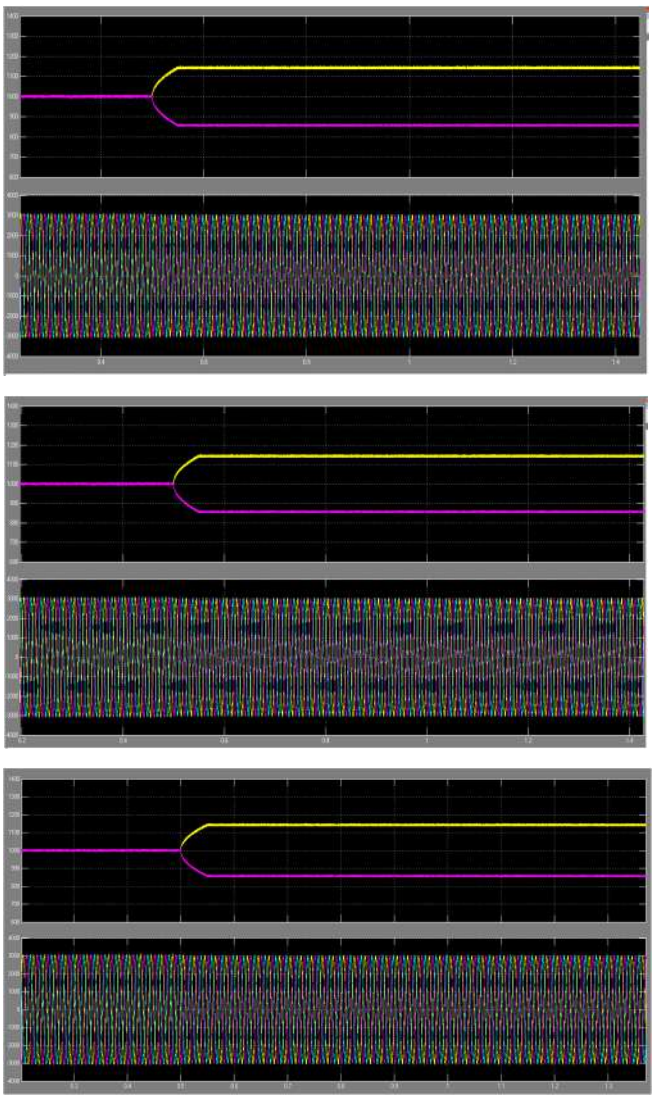

Fig Instantaneous response for a mid-point imbalance step of 0– 50 V, 35 A RMS, unbalanced load: (a) sinusoidal second harmonic injection; (b) sinusoidal sixth harmonic injection; (c) squared sixth harmonic injection. First waveform: *vc* 1, second waveform: *vc* 2, third waveform *iA*, fourth waveform: *iB*.

V. CONCLUSION

The results conclude that, although the three techniques are valid, second harmonic injection has a major effect in balancing the inverter midpoint and the even harmonics that it introduces are negligible and only present during transients. This paper has presented a novel technique to balance the voltage of the two split dc capacitors of a 3-L neutral-point clamped inverter, suitable for reactive power compensation, when triangular carrier PWM modulation is employed. It consists in injecting a squared waveform at six times the supply frequency. Subsequently, it has been compared with two already known strategies based on the injection of a negative-sequence second harmonic and a sinusoidal sixth harmonic waveform.

The contribution of current to the inverter midpoint of these techniques has been analyzed as a performance measure. Subsequently a small signal averaged model, suitable for control design purposes has been presented and a control strategy has been proposed. However, out of the two sixth harmonic injection methods that do not produce even harmonics at the inverter output, the proposed squared waveform technique is preferred, as it has a slightly greater compensation effect on the dc midpoint and is easier to implement, particularly, in systems employing a low modulation index.

VI. Acknowledgment

This paper is based on M. Tech. project carried out by the student of pydah college of engineering & technology, Kakinada studying M.Tech (Power Electronics) The project had been completed by MS. CH. RAMYA bearing H.T.no.:126T1D4318 under the guidance of Mr. P. VIJAYA RAMARAO.

REFERENCES

1. N. G. Hingorani and L. Gyugyi, *Understanding FACTS. Concepts and Technology of Flexible AC Transmission Systems*. Piscataway, NJ: IEEE Press, Dec. 1999.
2. *Convertible Static Compensator (CSC) for New York Power Authority: Final Report*, EPRI, Palo Alto, CA, and New York Power Authority, White Plains, NY, 2003, 1001809.
3. D. Alvira, M. Torre, J. Bola, U. Burdalo, M. Marquez, M. A. Rodriguez, J. Chivite, A. Hernandez, and S. A´ Ivarez, "The use of a static synchronous series compensator (SSSC) for power flow control in the 220 kV Spanish transmission network," *Water energy Int.*, vol. 68, no. 1, pp. 68–69, 2011.

4. H. Akagi, "Large static inverters for industry and utility applications," *Proc. IEEE*, vol. 89, no. 6, pp. 976–983, Jun. 2001.
5. B. Wu, *High-Power Inverters and AC Drives*. New York: Wiley, 2006.
6. (2013). [Online]. Available: http\\.www.ingeteam.com
7. S. Fukuda and Y. Matsumoto, "Optimal regulator based control of NPC boost rectifiers for unity power factor and reduced neutral point potential variations," in *Proc. 32nd IEEE IAS Annu. Meeting Ind. Appl. Conf.*, Oct. 5–9, 1997, vol. 2, pp. 1455–1462.
8. N. Celanovic and D. Borojevic, "A comprehensive study of neutral-point voltage balancing problem in three-level neutral-point-clamped voltage source PWM inverters," in *Proc. 14th Annu. Appl. Power Electron. Conf. Expo.*, Mar 14–18, 1999, vol. 1, pp. 535–541.
9. O. Alonso, L. Marroyo, P. Sanchis, E. Gubia, and A. Guerrero, "Analysis of neutral-point voltage balancing problem in three-level neutral-pointclamped inverters with SVPWM modulation," in *Proc. 28th Annu. IEEE Ind. Electron. Soc.Conf.]* Nov. 5–8, 2002, vol. 2, pp. 920–925.
10. O. Alonso, "An´alisis, dise˜no y control de convertidores multinivel del tipo NPC," Ph.D. dissertation, Dept. Electr. Electron. Eng., Universidad P´ublica de Navarra (UPNA), Pamplona, Spain, 2006.

INTERNATIONAL JOURNAL OF MULTIDISCIPLINARY EDUCATIONAL RESEARCH
ISSN : 2277-7881; IMPACT FACTOR - 2.972; IC VALUE:5.16
VOLUME 3, ISSUE 10(4), OCTOBER 2014

SINGLE STAGE DC/DC CONVERTER & DC/AC CONVERTER FOR PV-BATTERY APPLICATIONS

Mr. V. RAMA LAKSHMI
ramalakshmi.vaddi@gmail.com
Under the guidance of
Ms.M.PAVANI
ASSISTANT PROFESSIOR
PYDAH COLLEGE OF ENGINEERING , KAKINADA

Abstract— This paper addresses a dc/dc converter & dc/ac converter suitable for an energy storage system with an additional function of galvanic isolation. An energy storage device such as an electric double layer capacitor is directly linked to one of the dc buses of the dc/dc converter without any chopper circuit. Nevertheless, the dc/dc converter dc/ac converter can continue operating when the voltage across the energy storage device droops along with its discharge. Theoretical calculation and experimental measurement reveal that power loss and peak current impose limitations on a permissible dc-voltage range. In this project verifies that the dc/dc converter can charge and discharge the capacitor bank properly. Moreover, the dc/dc converter & dc/ac converter can charge the capacitor bank from zero to the rated voltage without any external pre charging circuit. In this project, a new converter called reconfigurable solar converter (RSC) for photovoltaic (PV)-battery application, mainly utility-scale PV battery application is presented. The major notion of the new converter is to use a single-stage three phase grid-tie solar PV converter to perform dc/ac and dc/dc operations. This converter solution is urging for PV-battery application, since it reduces the number of conversion stages, thereby developing efficiency and reducing cost, weight, and volume. In this project, a combination of analysis and simulation tests is used to show the attractive performance features of the suggested RSC.

Key words: RSC, PV-battery, power electronics

I. INTRODUCTION

Nowadays, photovoltaic (PV) plants are receiving a very great attention due to their intrinsic ability to directly transform solar energy in electrical energy. Nevertheless, electricity generated from photovoltaic plants can rarely offer immediate response to load demand, as these sources do not

deliver a regular supply immediately compatible with consumption needs. In stand-alone PV plants, energy storage (typically based on electrochemical batteries), together with the help of additional generation systems (such as those powered by fuel engines), is on the basis of regularization of PV generation and of full satisfaction of load consumptions.

In grid-linked PV plants – theoretically - energy storage is not essential or useful, due to the availability of the distribution grid that should work as an ideal container of the electrical energy (theoretically, it can work both as an ideal generator and, also, as an ideal load). But, in this last years, an important attention has been devoted to the use of energy storage also in grid-linked PV plants, with the main aim of overcoming some important power quality problems of real distribution grids and for making PV plants more and more useful and attractive.

This project presents a new single-stage solar converter called reconfigurable solar converter (RSC). The key notion of the RSC is to use a single power conversion system to achieve different operation methods for example PV to grid (dc to ac), PV to battery (dc to dc), batter to grid (dc to ac), and battery/PV to grid (dc to ac) for solar PV systems with energy storage. The RSC notion evolved from the fact that energy storage combination for utility-scale solar PV systems makes sense if there is an enough gap or a minimal overlap between the PV energy storage and release time.

II. Reconfigurable Solar Converter

A. Preface

The diagram of the suggested RSC is shown in Fig.1. The RSC consists of some changes to the usual three-phase PV inverter system. These changes let the RSC to involve the charging task in the usual three-phase PV inverter system. Letting that the usual utility-scale PV inverter system contains a three-phase voltage source converter and its related parts, the RSC needs extra cables and mechanical switches, as shown in Fig. 1. Optional inductors are integrated if the ac filter inductance is not sufficient for the charging function.

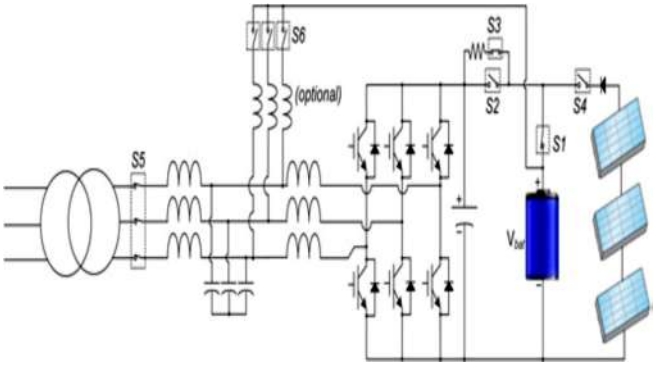

Fig. 1 Schematic of the proposed RSC circuit

B. Operation Methods of the RSC

All feasible operation methods for the RSC are shown in Fig. 2. In Method 1, the PV is directly linked to the grid over a dc/ac operation of the converter with prospect of maximum power point tracking (MPPT) monitor and the S1 and S6 switches stay open. In Method 2, the battery is charged with the PV panels over the dc/dc operation of the converter by closing the S6 switch and opening the S5 switch. In this method, the MPPT function is achieved; thus, maximum power is produced from PV.

There is an alternative method that both the PV and battery offer the power to the grid by closing the S1 switch. This operation is shown as Method 3. In this method, the dc-link voltage that is the similar to the PV voltage is imposed by the battery voltage; thus, MPPT monitor is not possible. Method 4 represents an operation method that the energy stored in the battery is offered to the grid. There is another method, Method 5 that the battery is charged from the grid. This method is not shown in Fig. 2.

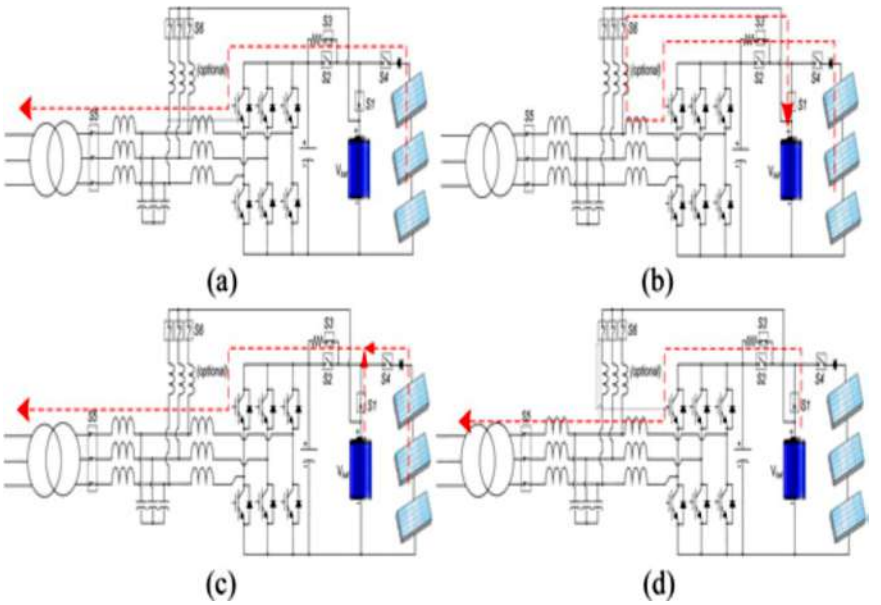

Fig. 2. All operation methods of the RSC. (a) Method 1—PV to grid. (b) Method 2—PV to battery.

(c) Method 3—PV/battery to grid. (d) Method 4—battery to grid.

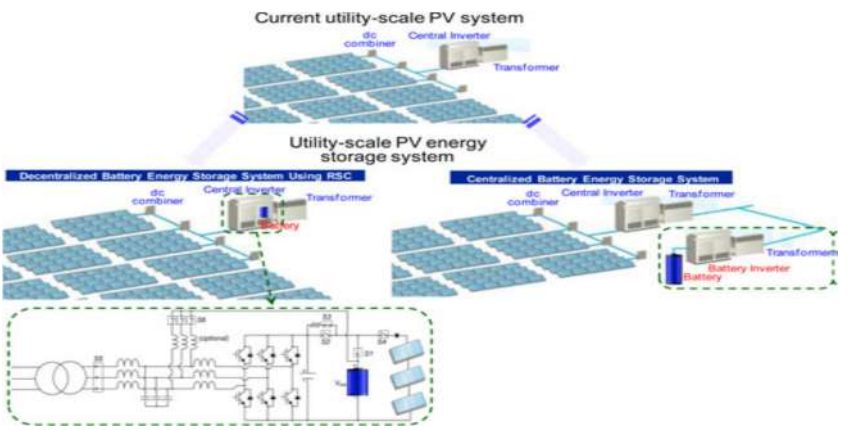

Fig.3. Utility-scale PV-energy storage systems with the RSC and the current state-of-the-art solution

C. System Gains of Solar PV Power Plant with the RSC Method I

The RSC method I offers major gains to system planning of utility-scale solar PV power plants. The current state-of-the-art technology is to combine the energy storage into the ac side of the solar PV system. An example of viable energy storage solutions is the ABB issued energy storage (DES) solution that is a complete package up to 4MW, which is linked to the grids directly and, with its communication means, can be used as a mean for peak shifting in solar PV power plants. The RSC method I permits not only the system owners to have an flexible ability that assists them to arrange and run the power plant correspondingly although manufacturers to present a cost-aggressive dispersed PV energy storage solution with the RSC. Fig. 3 shows examples of the PV energy storage solutions with the RSC and the current state-of-the-art tools. The technical and financial gains that the RSC solution is able to offer are more apparent in larger solar PV power plants. Specially, a large solar PV power plant using the RSCs can be monitored more efficiently and its power can be dispatched more economically since of the flexibility of operation. Developing a full operation characteristic of a solar PV power plant with the RSC is further than the scope of this project. But, different system monitors as shown in Fig. 4 can be suggested based on the requested power from the grid operator *P*req and available generated power form the plant *P*gen. These two values being results of an optimization problem (such as unit commitment methods) serve as variables to monitor the solar PV power plant accordingly. In other words, in response to the request of the

grid operator, different system monitor plans can be realized with the RSC-based solar PV power plant as follows:

1) System monitor 1 for *P*gen > *P*req;

2) System monitor 2 for *P*gen < *P*req;

3) System monitor 3 for *P*gen = *P*req;

4) System monitor 4 for charging from the grid

(Operation Method 5)

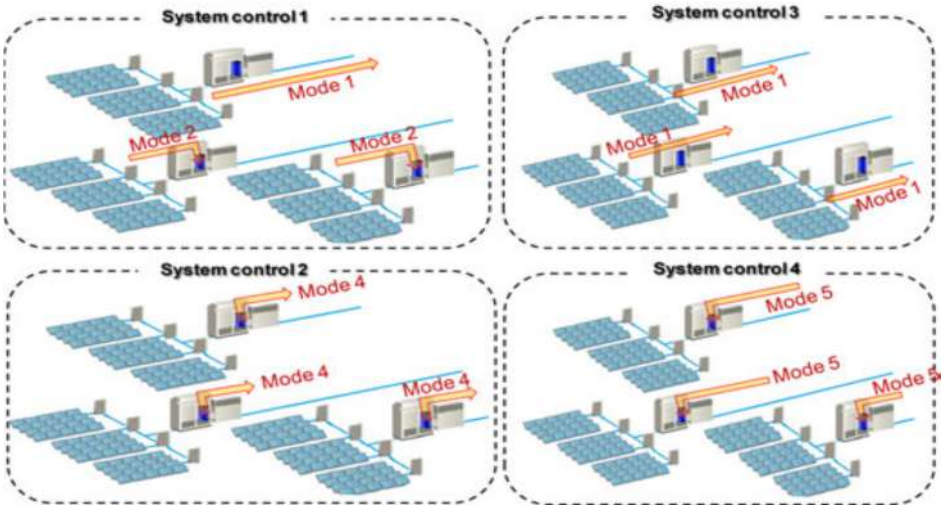

Fig.4. Example of different system operation methods of a RSC-based solar PV power plant

III. RSC MONITOR

A. Monitor of the RSC in the DC/AC Operation Methods (Methods 1, 3, 4, and 5)

The dc/ac operation of the RSC is used for delivering power from PV to grid, battery to grid, PV and battery to grid, and grid to battery. The RSC performs the MPPT algorithm to deliver maximum power from the PV to the grid. Like the usual PV inverter control, the RSC control is implemented in the synchronous reference frame. The synchronous reference frame proportional integral current monitor is employed. In a reference frame rotating synchronously with the fundamental excitation, the fundamental excitation signals are transformed into dc signals. As a result, the current regulator forming the innermost loop of the monitor system is able to regulate ac currents over a wide frequency range with high bandwidth and zero steady-state error. For the pulse width modulation (PWM) scheme, the usual space vector PWM scheme is used.

Fig. 5 presents the overall monitor block diagram of the RSC in the dc/ac operation. For the dc/ac operation with the battery, the RSC monitor should be matched with the battery management system (BMS), which is not shown in Fig. 5.

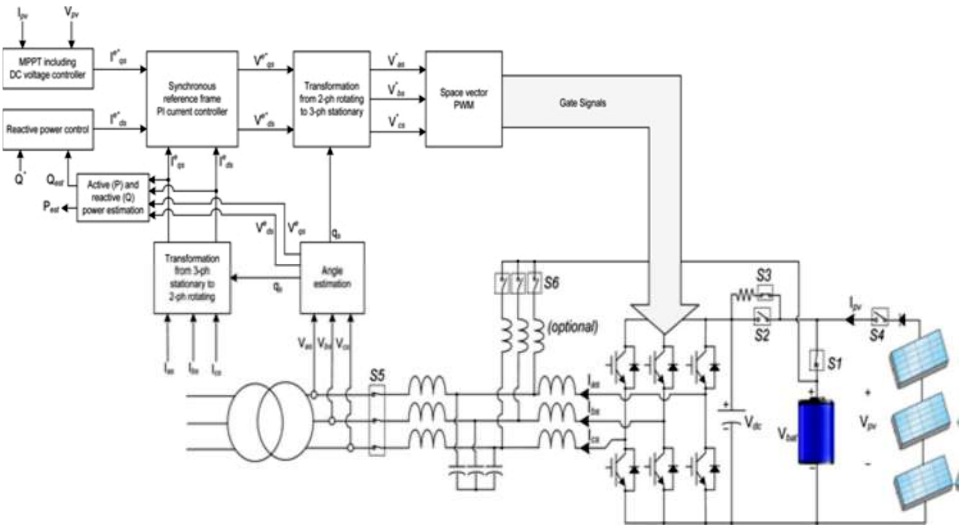

Fig.5. Overall control block diagram of the RSC in the dc/ac operation

B. Monitor of the RSC in the DC/DC Operation Method (Method 2)

The dc/dc operation of the RSC is also used for delivering the maximum power from the PV to the battery. The RSC in the dc/dc operation is a boost converter that monitors the current flowing into the battery. In this research, Li-ion battery has been selected for the PV-battery systems. Li-ion batteries need a stable current, stable voltage type of charging algorithm. In other words, a Li-ion battery should be charged at a set current level until it achieves its final voltage. At the last voltage, the charging process should switch over to the stable voltage method, and offer the current essential to possess the battery at this final voltage. Thus, the dc/dc converter performing charging process must be able of offering stable monitor for maintaining either current or voltage at a stable value, depending on the state of the battery. Typically, a few percent capacity losses happen by not performing stable voltage charging. But, it is not uncommon only to use stable current charging to simplify the charging monitor and process. The latter has been used to charge the battery. Thus, from the monitor point of view, it is just sufficient to monitor only the inductor current. Like the dc/ac operation, the RSC performs the MPPT algorithm to convey maximum power from the PV to the battery in the dc/dc operation. Fig.6 shows the overall monitor block diagram of the RSC in the dc/dc operation. In this method, the RSC monitor should be managed with the BMS, which is not shown.

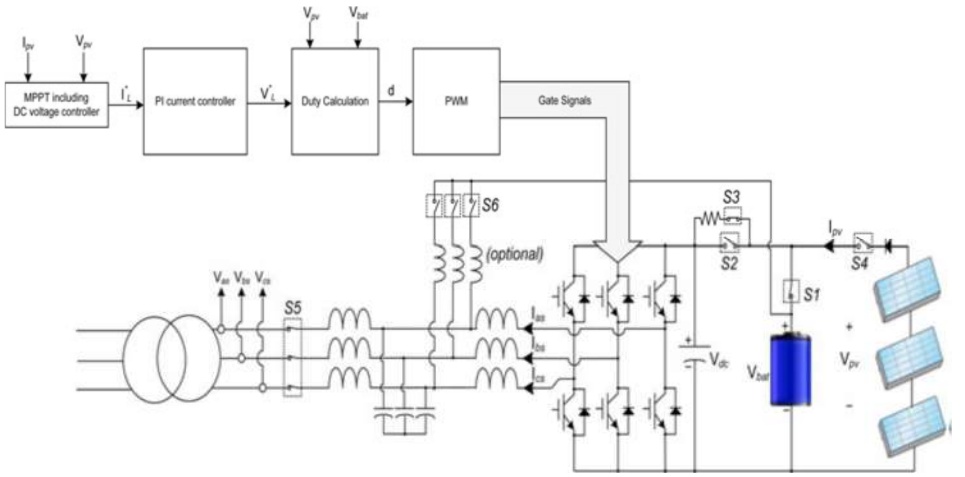

Fig.6. Overall monitor block diagram of the RSC in the dc/dc operation

C. Strategy Issues and Changes to the Usual Three-Phase PV Converter

One of the most vital conditions of the project is that a new power conversion solution for PV battery systems must consist least difficulty and changes to the usual three-phase solar PV converter system. Thus, it is essential to explore how a three-phase dc/ac converter works as a dc/dc converter and what changes should be made. It is widespread to use a *LCL* filter for a high-power three-phase PV converter and the RSC in the dc/dc operation is probable to use the inductors already existing in the *LCL* filter. There are chiefly two types of inductors, coupled three-phase inductor and three single-phase inductors that can be used in the RSC circuit. Using all three phases of the coupled three-phase inductor in the dc/dc operation affects a major drop in the inductance value due to inductor core saturation. The reduction in inductance value needs inserting additional inductors for the dc/dc operation which has been marked as “optional” in Fig. 1. To shun extra inductors, only one phase can do the–dc/dc operation. But, when only one phase, for example phase B, is used for the dc/dc operation with only either upper or lower three insulated-gate bipolar transistors (IGBTs) are turned OFF as balancing switching, the flowing current occurs in phases A and C through filter capacitors, the coupled inductor, and switches, ensuing in radically high current ripple in phase B current.

To stop the flowing current in the dc/dc operation, the following two solutions are suggested; 1) all unemployed upper and lower IGBTs must be turned OFF; 2) the coupled inductor is exchanged by three single-phase inductors.

Whereas the primary solution with a coupled inductor is straightforward, using three single phase inductors makes it possible to use all three phase legs for the dc/dc operation. There are two methods to use all three phase legs for the dc/dc operation:

1) Synchronous operation,

2) Interleaving operation.

In the primary solution, all three phase legs can work synchronously with their own current control. In this task, the battery can be charged with a higher current compared to the case with one-phase dc/dc operation. This leads to a faster charging time due to higher charging current capability. But, each phase operates with higher current ripples. Higher ripple current flowing into the battery and capacitor can have negative results on the lifetime of the battery and capacitors.

To beat the aforementioned problem associated with the synchronous operation, phases B and C can be moved by applying a phase offset. For the interleaving operation using three phase legs, phases B and C are moved by 120◦ and 240◦, respectively. The inductor current control in interleaving operation needs a different inductor current sampling scheme, as shown in Fig. 9. Generally, for digital control of a dc/dc converter, the inductor current is tested at either the beginning or center point of PWM to confine the average current that is unbound from switching noises. For two phase interleaving that two phases are 180◦ apart, there is no need to change the sampling scheme, since the average inductor currents for both phases can be attained with the usual sampling scheme.

But, for three-phase interleaving, a changed sampling scheme is needed to compute the average currents for all three phases. Thus, the sampling points for phases B and C must be moved by 120◦ and 240◦, respectively, which may entail that computation needed inductor current control for each phase should be done asynchronously. Using the interleaving operation reduces the ripples on the charging current flowing into the battery. Thus, the filter capacitance value can be decreased considerably.

IV. Results

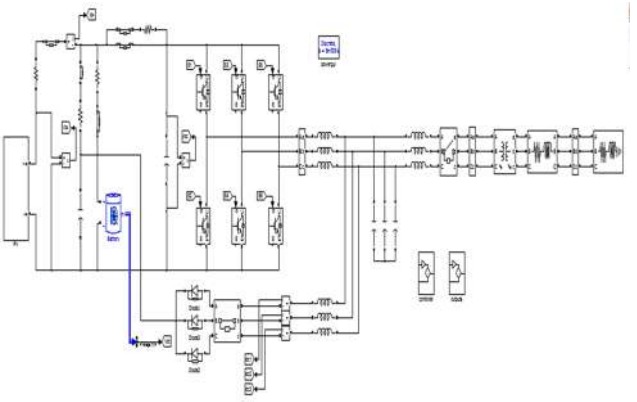

Fig 7 simulation diagram of DC to DC converter

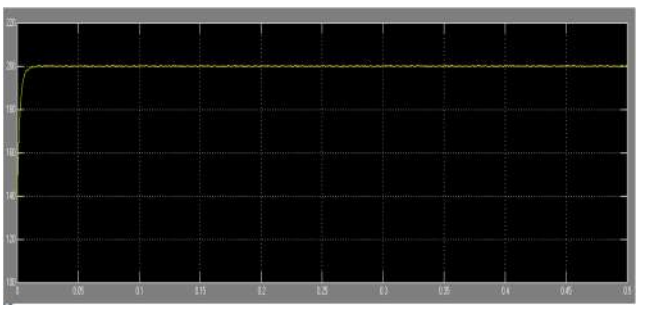

Fig 8 PV voltage

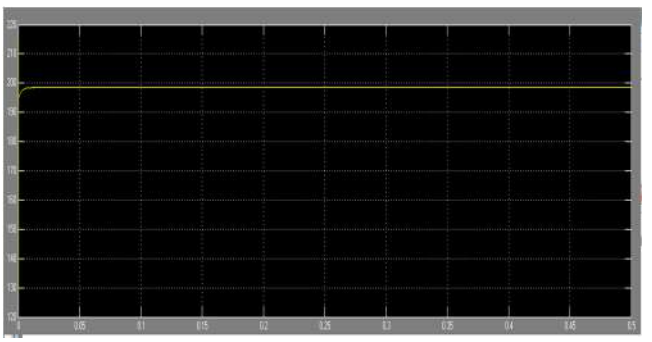

Fig 9 Battery Voltage

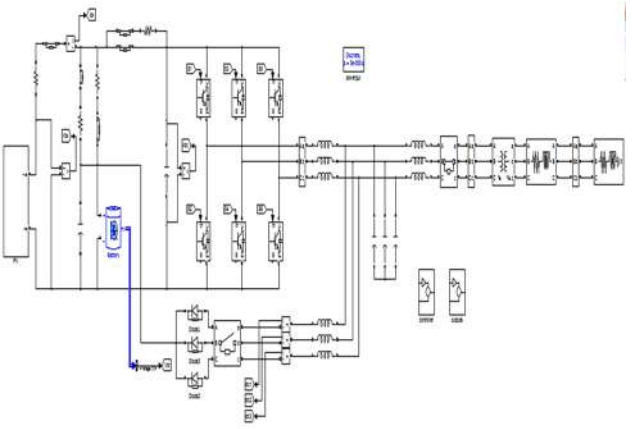

Fig 10 simulation diagram of DC TO AC converter

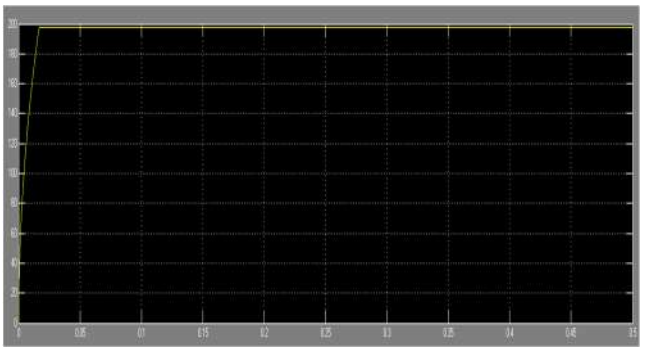

Fig 10 PV Voltage

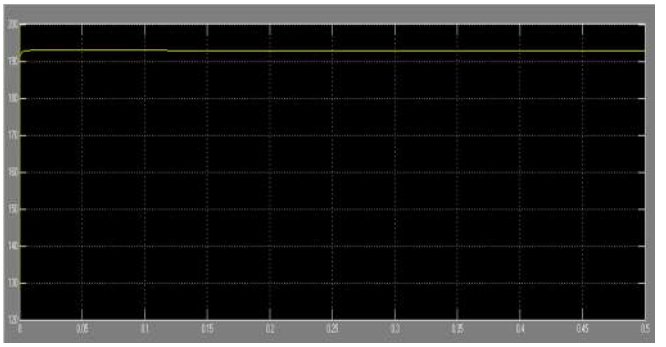

Fig 11 Battery Voltage

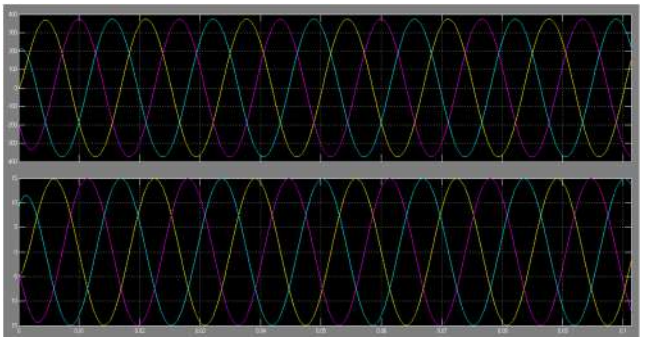

Fig 12 Grid Voltage & Current

V. Conclusion

A passive MPPT technique, to be utilized mostly in large grid-connected PV plants, has been introduced and discussed; it is essentially based on the energy storage capabilities of batteries that are proposed to be put in parallel to a proper number of PV sub-fields, so as to be used in a distributed manner. If well designed in their location, in their nominal voltage value and in their capacity, batteries can naturally catch the MPP of each PV subfield, also compensating for critical unbalanced solar irradiation conditions. Furthermore, the presence of an energy storage system can make more and more attractive grid-connected PV plants, due to some important additional capabilities not commons of currently conceived grid connected PV plants, as: a more great availability in favor of the AC power grid; a significant reduction of unfavorable requests of occasional peaks of load power demand; the possibility to substitute other expensive (and often not renouncing) apparatus for utility grid power quality improvements, as UPS and active filters; the possibility to be integral with other different renewable resources, with minor expenses and with great economical advantages. Finally, a conspicuous number of batteries distributed on board to a single PV module could be on the basis of the development of AC PV modules, to be directly connected to LV distribution grids and characterized by high quality of AC voltage, high efficiency and high availability.

Simulation results have been presented to verify the concept of the RSC and to demonstrate the attractive performance characteristics of the RSC. These results confirm that the RSC is an optimal solution for PV-battery power conversion systems.

VI. Acknowledgment

This paper is based on M. Tech. project carried out by the student of pydah college of engineering & technology, Kakinada studying M.Tech (Power Electronics) The project had been completed by Ms. V. RAMA LAKSHMI bearing H.T.no.: 126T1D4301 under the guidance of Ms. M PAVANI.

VII. References

1. U.S. Department of Energy, "Solar energy grid integration systems-energy storage (SEGIS-ES)," May 2008.
2. D. Bundestag, "Gesetz zur Neuregelung des Rechts der erneuerbaren Energien im Strombereich und zur A¨ nderung damit zusammenha ¨ngender Vorschriften," Bundesgesetz-blatt, 2008.
3. H. Konishi, T. Iwato, and M. Kudou, "Development of large-scale power conditioning system in Hokuto mega-solar project," in *Proc. Int. Power Electron. Conf.*, 2010, pp. 1975–1979.
4. J. H. Enslin and D. B. Snyman, "Combined low-cost, high efficient inverter, peak power tracker and regulator for PV applications," *IEEE Trans. Power Electron.*, vol.6, no. 1, pp. 73–82, Jan. 1991.
5. H. Ertl, J. W. Kolar, and F. Zach, "A novel multicell dc-ac converter for applications in renewable energy systems," *IEEE Trans. Ind. Electron.*, vol. 49, no. 5, pp. 1048–1057, Oct. 2002.
6. C. Zhao, S. D. Round, and J. W. Kolar, "An isolated three-port bidirectional dc/dc converter with decoupled power flow management," *IEEE Trans. Power Electron.*, vol. 23, no. 5, pp. 2443–2453, Sep. 2008.
7. M. Bragard, N. Soltau, R. W. De Doncker, and A.Schiemgel, "Design and implementation of a 5 Kw photovoltaic system with Li-ion battery and additional dc/dc converter," in *Proc. IEEE Energy Convers. Congr. Expo.*, 2010, pp. 2944–2949.
8. W. Li, J. Xiao, Y. Zhao, and X. He, "PWM plus phase angle shift control scheme for combined multiport dc/dc converters," *IEEE Trans. Power Electron.*, vol. 27, no. 3, pp. 1479–1489, Mar. 2012.
9. N.Benavidas and P.Chapman, "Power budgeting of a multiple-input buck-boost converter," *IEEE Trans. Power Electron.*, vol. 20, no. 6, pp. 1303–1309, Nov. 2005.
10. P. Barrade, S.Delalay, and A. Rufer, "Direct connection of super capacitors to photovoltaic panels with on-off maximum power point

tracking," *IEEE Trans. Sustainable Energy*, vol. 3, no. 2, pp. 283–294, Apr. 2012.

11. S. J. Chiang, K. T. Chang, and C. Y.Yen, "Residential photovoltaic energy storage system," *IEEE Trans. Ind. Electron.*, vol. 45, no. 3, pp. 385–394, Jun. 1998.
12. Z. Zhao, M. Xu, Q. Chen, J. Lai, and Y. Cho, "Derivation, analysis, and implementation of a boostbuck converter-based high-efficiency PV inverter," *IEEE Trans. Power Electron.*, vol. 27, no. 3, pp. 1304–1313, Mar. 2012.
13. C. Ho, H. Breuninger, S. Pettersson, G. Escobar, L. Serpa, and A. Coccia, "Practical design and implementation procedure of an interleaved boost converter using SiC diodes for PV applications," *IEEE Trans. Power Electron.*, vol. 27, no. 6, pp. 2835–2845, Jun.2012.
14. M. Bragard, N. Soltau, R. W. De Doncker, and A.Schmiegel, "Design and implementation of a 5 kW PV system with Li-ion battery and additional dc/dc converter," in *Proc. IEEE Energy Convers. Congr. Expo.*, 2010, pp. 2944–2949.
15. H. Konishi, T. Iwato, and M. Kudou, "Development of large-scale power conditioning system in Hokuto mega-solar project," in *Proc. Int. Power Electron. Conf.*, 2010, pp. 1975–1979.
16. J. H. Enslin and D. B. Snyman, "Combined low-cost, high efficient inverter, peak power tracker and regulator for PV applications," *IEEE Trans. Power Electron.*, vol. 6, no. 1, pp. 73–82, Jan. 1991.

INTERNATIONAL JOURNAL OF MULTIDISCIPLINARY EDUCATIONAL RESEARCH
ISSN : 2277-7881; IMPACT FACTOR - 2.972; IC VALUE:5.16
VOLUME 3, ISSUE 10(4), OCTOBER 2014

PV BASED SINGLE & THREE PHASE INTEGRATED ENERGY SYSTEMS FOR MICRO GRIDS

Ms. K ANITHA
rithisha.eee205@gmail.com
Under the guidance of
Ms. B. LALITHA KUMARI
ASSISTANT PROFESSIOR
PYDAH COLLEGE OF ENGINEERING, KAKINADA

Abstract— This paper presents PV based Single & Three Phase Integrated Energy Systems for Micro Grids. Almost always, these entities have their own power converters for grid interfacing and energy processing. Having individual converters has advantages like more flexible individual control and simpler design but does not encourage functionality merging. The proposed Distributed generation systems usually include local energy sources, storages, and loads. Reduction of semiconductors to arrive at a more compact integrated design is thus not possible. Addressing this concern, a number of integrated energy generation systems that use 25% lesser semiconductors are proposed. The systems can be single or three phase depending on the types of sources, storages, and loads assembled. They can operate in the grid-tied or stand-alone mode with no compromise in performances expected, when compared with other solutions using more switches. For verifying the practicalities of the proposed integrated systems, experimental testing has already been performed on two example systems assembled in the laboratory.

Index Terms— Distributed generation (DG), energy systems, micro grids, pulse width-modulated converters.

I. INTRODUCTION

For greater controllability, energy storages appear to be unavoidable even though their capacities can be reduced if there are more source types in the systems. The installed energy storages also need not be of the same type. Distributed Generation (DG) by local green energy sources has gained worldwide attention because of the ever-growing energy demand, gradual depletion of fossil fuels, and environmental concerns linked to the burning of fossil fuels. Accompanying this interest is an equally intensive effort devoted to energy storages like batteries, ultra capacitors, and flywheels. Energy stored in these mediums can appropriately be used for smoothing variations linked to

most green (usually renewable) sources, which at present are major shortcomings. Another way of smoothing the variations is to design the DG systems with different types of sources, whose generation characteristics must complement each other. There is however no guarantee that a continuous stream of energy will always be produced if the sources are mostly uncontrollable like renewable sources.

They should instead be designed with a variety, for example, a combination of ultra-capacitors and batteries for fulfilling the power and energy density requirements of the considered system. In short, that means a typical comprehensive energy system would unlikely be a single-source system. Rather, it would include many entities needed for meeting the local generation, storage, utilization, and grid-tied requirements. Almost always, these entities would have their own power converters for processing energy to a form suitable for storage or consumption. This is no doubt the most flexible arrangement, which certainly is an advantage. Other advantages can also be thought of, but for certain, including too many individual converters to a system might at times introduce too much costly redundancy.

This might be the case for renewable systems, whose energy generations are usually intermittent. Power converters connected to them might therefore operate below their rated capacities for a sizable period of time. It might hence be of interest to perform some integration rather than use multiple individual converters as per existing practice. For that, a number of integrated energy systems using 25% lesser semiconductors are proposed here for DG. Operating principles and advantages of the systems proposed are first clarified before considering their likely performance tradeoffs. These tradeoffs cannot be avoided by most (if not all) reduced semiconductor topologies but can surely be minimized for the systems proposed. Relevant explanation can be found in a later section, together with experimental results for proving the practicalities of the systems proposed.

II. ENERGY GENERATION SYSTEMS WITH NONINTEGRATED POWER CONVERTERS

Fig. 1(a) shows the typical block representation of a common solar energy generation system drawn here for example. Each source or storage included is accompanied by its own dc–dc boost or charging converter tied to a common dc link. The harnessed energy is then forwarded to a dc–ac inverter

for conditioning before channeling it to the grid. The inverter can either be single or three phase, even though the latter is explicitly drawn in the diagram. It is also not necessary for the dc–ac inverter to tie to the grid if the energy generated is meant for immediate load consumption in an islanded local microgrid. The dc–ac inverter in an islanded microgrid can also be replaced by a dc–dc converter if the loads are dc by nature. DC network is certainly a possibility, but based on present advancement, ac output would probably continue to dominate for many more years.

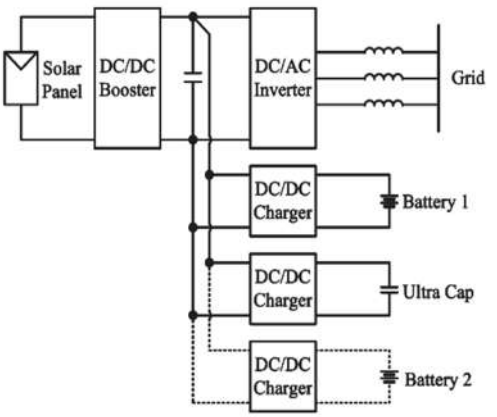

(a)

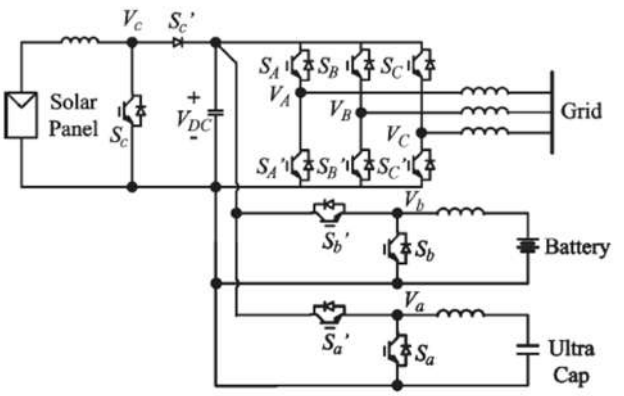

(b)

Fig. 1. Example (a) block diagram and (b) circuit layout of nonintegrated energy system.

To reveal more details of Fig. 1(a), its individual blocks are filled with some simple representative circuits. The resulting circuit shown in Fig. 1(b) uses 12 semiconductor devices in total. Eleven of the devices are controllable switches with the remaining one being an uncontrollable diode. The diode *Sc* can be replaced by a controllable switch if the indicated solar panel in Fig. 1(b) is replaced by another type of source that can absorb backward flow of energy. Regardless of that, the system shown in Fig. 1(b) clearly lacks integration. Its formation is simply by connecting individual well-known converters to a common dc link. The system is thus fully decoupled with each converter having virtually no influence on the others. Surely, this is an advantage, but because of the intermittent nature of the solar source (in fact, most renewable sources) and battery charging process, most of the converters would likely not operate continuously at their rated capacities. The resulting system built with multiple individual converters is hence neither cost effective nor compact single- and three-phase energy systems are now described as follows.

III. INTEGRATED ENERGY GENERATION SYSTEMS

A. Method of Integration

The integration principles are better explained by referring first to the nonintegrated energy system shown in Fig. 1(b). For easier viewing, two of its phase legs with switches *{SA, S'A, S'a, Sa}* are drawn separately, as shown in Fig. 2(a). For each of the illustrated phase legs, its two switches must be switched in complement, meaning that, when one switch is on, the other must be off. Terminal voltage of the considered phase leg can then produce two discrete values identified as *V*dc and 0 V. The same applies to the other phase leg shown in Fig. 2(a). Terminal voltages of the two phase legs can then be any of the four sets of values indicated in Table I.

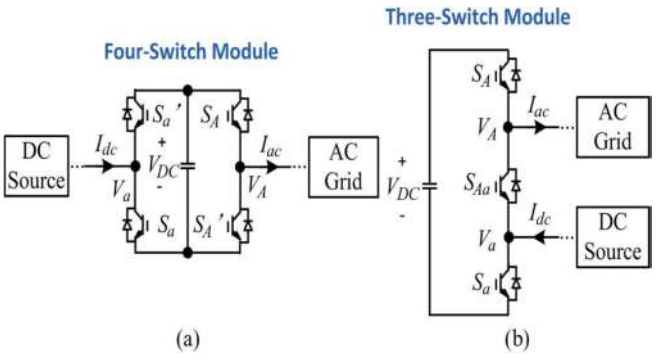

Fig.2. Illustration of (a) nonintegrated four-switch and (b) integrated three switch topologies.

TABLE I

SWITCHING STATES AND OUTPUT VOLTAGES OF FIG. 2(a)

S_A	S_A'	S_a'	S_a	V_A	V_a
ON	OFF	ON	OFF	V_{DC}	V_{DC}
ON	OFF	OFF	ON	V_{DC}	0
OFF	ON	OFF	ON	0	0
OFF	ON	ON	OFF	0	V_{DC}

TABLE II

SWITCHING STATES AND OUTPUT VOLTAGES OF FIG. 2(b)

S_A	S_{Aa}	S_a	V_A	V_a
ON	ON	OFF	V_{DC}	V_{DC}
ON	OFF	ON	V_{DC}	0
OFF	ON	ON	0	0

Instead of two independent phase legs, the switches can be rearranged as shown in Fig. 2(b) while still providing two terminal voltages. Instead of four switches, only three switches labeled as *{SA, SAa, Sa}* are used. That represents a saving of 25%, which can be sizable if more switches are considered. Among the three switches, two of them will be turned on to tie the terminal voltages to either the same or different dc rails at any instant. The three possibilities are summarized in Table II, which, when compared with Table I, tells a constraint faced by the three-switch topology. To be more precise, the terminal voltages of the three-switch topology cannot produce the fourth combination of *VA* = 0 V and *Va* = *V*dc, which certainly is a tradeoff incurred by saving one switch. The overall system design should therefore be planned such that influences from this tradeoff on the terminal voltages are kept to a minimum. Discussion on this issue can be found in the next section.

Applying the same integration to the remaining two pairs of phase legs with switches *{SB, S'B , S'b, Sb}* and *{SC, S'C , S'c , Sc}* then results in the integrated energy system shown in Fig. 3. The system in Fig. 3 uses nine switches as compared to 12 for the nonintegrated system shown in Fig. 1(b). The same six terminal voltages are retained with the upper three produced by the dc–ac inverter formed by the upper three switches *{SA, SAa, Sa}* and middle three switches *{SB, SBb, Sb}*. On the other hand, the lower three voltages are produced by three dc–dc converters formed by the middle three

switches *{SB, SBb, Sb}* and lower three switches *{SC, SCc, Sc}*. The middle three switches are obviously shared by the inverter and converters, which will surely introduce some constraints as already identified (fourth combination of $VA = 0$ V and $Va = V$dc cannot be produced).

Before progressing forward, it is appropriate to share here that the same nine-switch topology has earlier been used as an ac–ac converter for dual motor drives, rectifier-inverter systems, and uninterruptible power supplies. In those attempts, the six converter terminals are organized as either two sets of three-phase ac outputs or one set of three-phase ac input and one set of three-phase ac output. They have so far been proven fine, but with serious limitations imposed. The limitations can be summarized as either a very limited phase shift between the two sets of ac terminals or a doubling of dc-link voltage caused by strict amplitude sharing. These constraints would make the 25% saving in semiconductors not so attractive. Methods for minimizing them are therefore of interest and are discussed here in the context of energy systems. Concentrating on energy systems also has the merit of merging ac and dc circuits using the nine-switch topology, which so far has not been tried by other researchers.

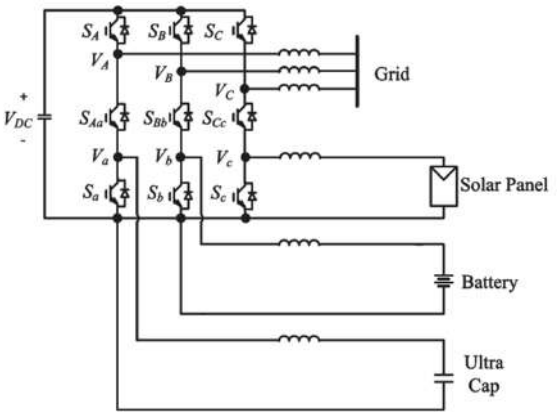

Fig. 3. Integrated three-phase energy system with multiple sources and storages

B. Modulation Principles

Referring again to those two simplified illustrations shown in Fig. 2, making them produce the same terminal voltages would demand that they share the same modulation theories. Some constraints would however be

accompanying the three switch topology shown in Fig. 2(b) since it uses lesser switches. A convenient way of explaining the three-switch modulation is hence to focus on the more established independent phase legs shown in Fig. 2(a) first, before shifting the knowledge with constraints added to Fig. 2(b).

With the circuit shown in Fig. 2(a), the phase leg tied to the dc source is, in theory, controlled by a dc reference and a triangular or saw-tooth carrier. The second phase leg tied to a phase of the three-phase ac grid is similarly controlled by a sinusoidal reference and a triangular carrier (saw-tooth carrier not considered here since it has no spectral benefit). Strictly, carriers of the two phase legs need not be the same, but in practice, using one carrier has the benefit of involving only one timer. It is hence advisable to use a common carrier and two independent references for the circuit shown in Fig. 2(a). The same independence cannot be introduced to the integrated topology shown in Fig. 2(b), whose sinusoidal reference for the upper terminal must always be placed above its linear reference for the lower terminal. Such placement helps to avoid the fourth restricted state of $VA = 0$ V and $Va = V$dc.

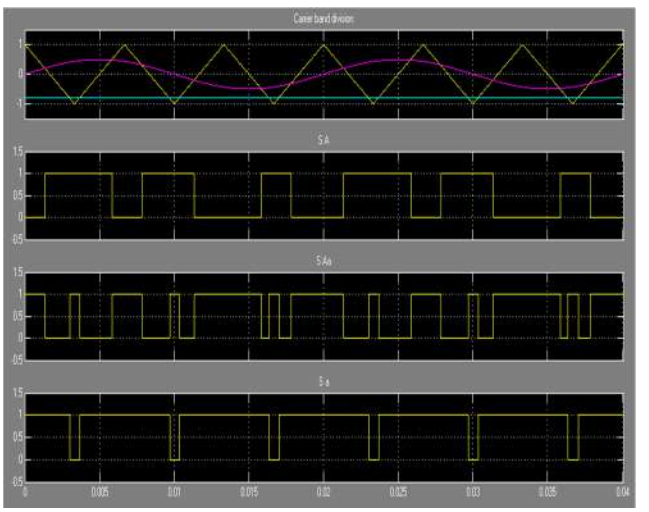

Fig. 4. Carrier band division and gating signal generation per phase leg

An example illustrating the three-switch modulation is shown in Fig. 4, where a single carrier band is clearly divided into $h1$ and $h2$. The upper subband $h1$ is assigned to the upper terminal and hence confines the sinusoidal reference. Similarly, the lower subband $h2$ is assigned to the lower terminal and hence encompasses the linear reference. Comparing the

references with the single common carrier based on the following rules then leads to those gating signals for *SA* and *Sa* shown at the bottom of Fig. 4

$$S_A = \begin{cases} 1, & \text{reference} \geq \text{carrier} \\ 0, & \text{reference} < \text{carrier} \end{cases}$$
$$S_a = \begin{cases} 0, & \text{reference} \geq \text{carrier} \\ 1, & \text{reference} < \text{carrier.} \end{cases} \quad (1)$$

To ensure that only two switches are on and hence produce any of the three combinations shown in Table II, the gating signal for the middle switch *SAa* must be derived from the earlier two based on the following:

$$S_{Aa} = S_A \oplus S_a - (!S_A) \oplus (!S_a) \quad (2)$$

where is the logical XOR operator and !*SA* and !*Sa* are the complements of *SA* and *Sa* with deadtime added. Operating on !*SA* and !*Sa* is recommended since it automatically creates the deadtime needed by *SAa* to avoid shorting the three switches simultaneously. The full set of gating signals obtained (e.g., bottom of Fig. 4) is thus always in agreement with the allowed states summarized in Table II. Another concern noted with the modulation process is the dc offset added to the sinusoidal reference for centering it within *h*1. Like triplen [15]–[17], this offset is added to all phases of a three phase system and will therefore be cancelled in the line-to-line voltages.

C. Parameters and Constraints

As mentioned earlier, the lower subband *h*2 in Fig. 4 is assigned to the lower terminal of the three-switch topology shown in Fig. 2(b). Given that it is tied to a dc source, the usual parameter of interest would be the duty ratio *d* or fractional on time of the lower switch *Sa*. The range of variation of *d* and its accompanied gain *G*dc(= 1/(1 − *d*)) can accordingly be determined as

$$(1 - 0.5h_2) \leq d \leq 1 \qquad 2/h_2 \leq G_{\text{dc}} < \infty. \quad (3)$$

For interfacing the dc source to the ac grid, *G*dc must usually be high so as to minimize the number of dc sources or storages connected in series. With fewer entities in series, problems like shading and unbalanced charging are less prominent, inferring that mechanisms for preventing them might not be necessary. The overall system is hence simplified, which certainly is a strong reason for keeping *h*2 small and *G*dc high.

Referring now to the upper terminal of the three-switch topology shown in Fig. 2(b), since it is tied to an ac source, its parameter of interest would be the modulation index *M*. Referring to Fig. 4, *M* represents the amplitude of the sinusoidal reference, which, in theory, is also equal to the resulting buck gain *G*ac. Its value can vary within the range spelled in (4), where the factor of 1.15 is added for representing triplen insertion

$$0 \leq M \leq 1.15 \times h1/2. \qquad (4)$$

The value of *M* is also known to vary inversely with the dc-link voltage *V*dc(*M* $\propto 1/V$dc) in the case of a fixed ac grid voltage. Lowering *V*dc therefore requires *M* and, hence, *h*1 to be high. That means *h*2 = 2− *h*1 in Fig. 4 must be low, which, for the proposed energy system, is fine since a high dc gain *G*dc is needed, as explained earlier. The proposed energy system is therefore a more suitable system for applying the three-switch topology shown in Fig. 2(b) rather than those ac–ac converters suggested. In those references, *V*dc is doubled because *M* is set to a maximum of only 0.5.

D. Other Integrated Configurations

Instead of the system shown in Fig. 3, the three-switch topology shown in Fig. 2(b) can be used to form other energy systems. Two proposed examples are shown in Fig. 5(a) and (b), where, again, three three-switch phase legs are shown. In general, the number of three-switch phase legs connected in parallel can be any positive integer number. It depends on the number of sources, storages, and loads connected together. Where needed, traditional two-switch phase legs can also be added in parallel to the three-switch phase legs. This extension is relatively straightforward.

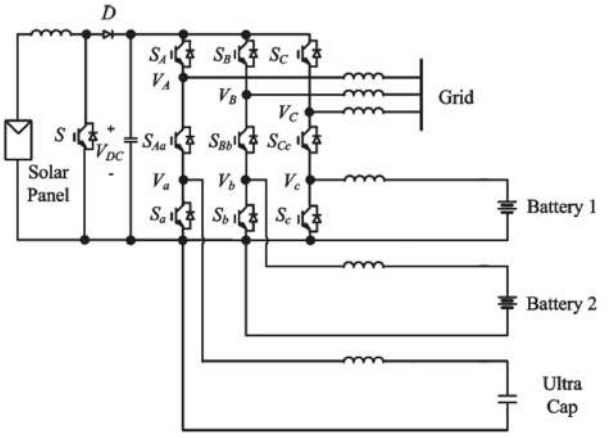

(a)

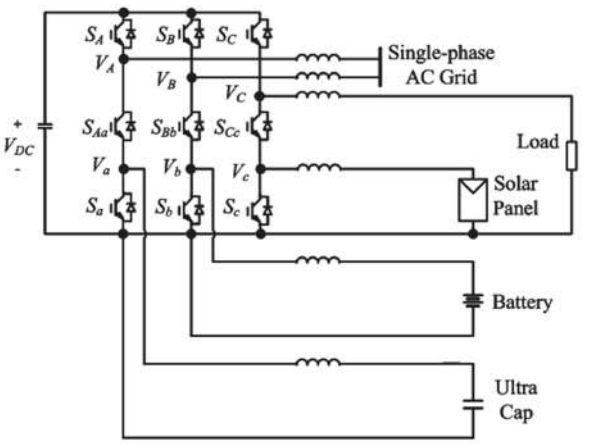

(b)

Fig. 5. Other integrated configurations for (a) three- and (b) single-phase grid-tied energy conversions.

Rather, the intention for including Fig. 5(a) is to show the additional possibility of connecting a solar panel (indicated only as an example) to the dc link through its dc–dc converter. Unlike Fig. 3, no source is now connected to the lower three dc terminals, which are instead tied to three storages (two batteries and an ultra-capacitor). The system however retains its three-phase ac grid interfacing like in Fig. 3. For illustrating single-phase grid interfacing, Fig. 5(b) is referred to instead, where two of its upper terminals are used for

single-phase grid interfacing. The same dc offset as in Fig. 4 must still be added to the two 180◦ phase-shifted sinusoidal references for the two upper terminals, which, when subtracted, will not appear in the ac voltage ($VA - VB$). Since the third upper terminal is now not used for grid interfacing, it can either be removed together with switch *SC* or tied to a dc load, as shown in Fig. 5(b). Other connections to the lower three dc terminals in Fig. 5(b) remain unchanged as in Fig. 3.

IV. THREE-SWITCH VERSUS FOUR-SWITCH TOPOLOGY

A. DC-Link Voltage

As described earlier, the four-switch topology shown in Fig. 2(a) is divided into two independent phase legs with no restriction on their modulation parameters. Choosing the ac terminal voltage *VA* as the base (= 1 p.u.), the minimum dclink voltage *V*dc is then given by 1.74 p.u. if *VA* is assumed to be a phase of a three-phase ac grid. This value is obtained by substituting the maximum modulation index of *M* = 1.15 to the standard definition of *M* = *VA*/(*V*dc/2). On the other hand, if a single-phase ac system is considered, the minimum *V*dc would change to 2 p.u. since the maximum *M* is now one. Converting from three- to single-phase system is thus a simple multiplication by 1.15, which is also applicable to the three switch topology shown in Fig. 2(b).

Unlike the four-switch topology, the maximum modulation index of the three-switch topology in a three-phase system is not *M* = 1.15 but is rather given by the expression in (4). The minimum dc-link voltage *V*dc of the three-switch topology is thus computed as (3.48/*h*1) p.u. for the three-phase systems shown in Figs. 3 and 5(a). [As mentioned earlier, a multiplication factor of 1.15 needs to be included for the single-phase system shown in Fig. 5(b).] In percentage term, it represents an increase given by

$$\Delta V_{\mathrm{dc}} = \frac{\left(\frac{3.48}{h_1}\right) - 1.74}{1.74} \times 100\% = \left(\frac{2}{h_1} - 1\right) \times 100\%, \qquad 1 \le h_1 \le 2. \qquad (5)$$

Variation of (5) is shown in Fig. 6, from which it is read that the increase is 100% or doubled when *h*1 = 1 or *M* = 0.5. This doubling of dc-link voltage is experienced by those ac–ac converters proposed in [12] and [13], which conceptually can be reduced here by increasing *h*1. For example, if *h*1 is

raised to 1.6 and 1.8, the increase ΔVdc would be 25% and 11%, respectively. It is hence important to keep one subband much wider than the other ($h1 >> h2$ shown in Fig.4), which, fortunately, is a requirement enforced by the proposed energy systems. This identification has so far not been discussed in the open literature.

When dividing the carrier band, it is also of concern to mention here that the upper subband $h1$ must include all upper references and the lower subband $h2$ must include all lower references. That indirectly means that the highest modulating references in both subbands will decide on the appropriate level to divide in the full carrier band. These references correspond to the highest upper and lower terminal voltages that the inverter can manage.

B. Switch Currents and Overall System Losses

Instantaneous current stresses experienced by the switches can be found by considering the individual terminal currents and converter states summarized in Tables-I and II for the four-switch and three-switch topologies. For clarity, positive reference currents for the terminals are defined here as those of *I*ac and *I*dc shown in Fig. 2(a) and (b). Positive current through a switch is also defined as current flowing through its transistor, which then means that negative current flows through its anti parallel diode.

TABLE III

Currents through switches at different output voltages for four-switch topology

S_A	S_A'	S_a'	S_a	V_A	V_a
I_{ac}	0	$-I_{dc}$	0	V_{DC}	V_{DC}
I_{ac}	0	0	I_{dc}	V_{DC}	0
0	$-I_{ac}$	0	I_{dc}	0	0
0	$-I_{ac}$	$-I_{dc}$	0	0	V_{DC}

With these definitions, the four-switch topology shown in Fig. 2(a) can easily be analyzed by considering which switches from its two phase legs are turned on. The turned-on switches will carry the respective terminal currents, which then lead to those entries shown in Table III for each pair of corresponding terminal voltages. The table shows that each switch of the nonintegrated four-switch topology carries a terminal current, which is not true for the integrated three-switch topology. For example, to produce *VA* = *Va* = *V*dc, the first row of Table II indicates that the upper two switches *SA* and *SAa* of the threeswitch topology must be turned on, which then lead to

currents $-(I\text{dc} - I\text{ac})$ and $-I\text{dc}$ flowing through them. The current flowing through *SA* is obviously decided by two terminal currents and not one. The same determination can be applied to the other two states listed in Table II with their resulting current expressions summarized in Table IV. Table IV is, in principle, applicable to the three systems shown in Fig. 3 and Fig. 5(a) and (b) since they use the same three-switch topology and the same three operating states.

TABLE IV

Currents through switches at different output voltages for three-switch topology

S_A	S_{Aa}	S_a	V_A	V_a
$-(I_{dc}-I_{ac})$	$-I_{dc}$	0	V_{dc}	V_{dc}
I_{ac}	0	I_{dc}	V_{dc}	0
0	$-I_{ac}$	$I_{dc}-I_{ac}$	0	0

The currents obtained in Tables III (first three rows only) and IV can then be compared for each pair of terminal voltages produced. The conclusions drawn are summarized hereinafter.

1. By eliminating one switch, the middle switch *SAa* of the three-switch topology carries the same current as either *S'A* or *S'a* of the four-switch topology, depending on the state presently being assumed.
2. The current through *SA* of the three-switch topology has an interval over which its current is $-(I\text{dc} - I\text{ac})$. Otherwise, it is closely similar to the current flowing through *SA* of the four-switch topology.
3. The current through *Sa* of the three-switch topology is similar to that flowing through the same switch of the four-switch topology, except for an interval over which the current is $(I\text{dc} - I\text{ac})$.

It should be noted here that the absolute amplitude of the current $(I\text{dc} - I\text{ac})$ depends on the amount of boosting introduced and the individual current polarities (e.g., charging or discharging, terminals connected to sources, storages, or loads). Instantaneous current stresses might therefore be raised, but that does not imply the same for the overall system losses. On average, if a good mix of different entities is tied to the integrated system, its losses should be either comparable or slightly raised as compared to its nonintegrated counterpart. The slightly higher losses are mainly caused by the slightly higher dc-link voltage needed by the integrated system, as understood from Fig. 4.

To demonstrate, the overall losses of the nonintegrated and integrated energy systems shown in Figs.1(b) and 3 have been computed based on the simulation approach proposed. Switches used for the simulation are 600-V/50-A insulated gate bipolar transistors (IGBTs), whose parameters. For both systems, energy flow has been tuned to flow from the solar source to the ac grid and storages. For small $h2 \leq 0.4$, this is in accordance to the earlier suggested band sizing requirement. The results show that, for smaller $h2$, losses of the nonintegrated energy system increase because of the lower dc terminal voltages and hence higher dc terminal currents if the system power is kept constant. The integrated system, on the other hand, has its losses reduced because of the lower dc-link voltage associated with a smaller $h2$. This trend is applicable to both three-phase systems shown in Figs. 3 and 5(a), except for higher loss values anticipated with Fig. 5(a) because of its additional switch *S*, diode *D*, and other passive components.

The evaluation is next performed with the three-phase grid in Fig. 1(b) replaced by a single-phase grid and a resistive load like those shown in Fig. 5(b) for the single-phase integrated system. Results obtained for both systems can be found in Table VI, which, upon compared, show lower losses for the integrated system. The reason might probably be linked to the third upper terminal supplying a positive current to the dc load. The earlier notated upper current *I*ac is thus always positive, which, when subtracted from *I*dc, will always lead to a smaller (*I*dc − *I*ac) for the third three-switch phase leg. Since its currents are reduced, its losses will reduce accordingly too.

V. CONTROL PRINCIPLES

The control schemes for the integrated energy system shown in Fig. 3 are explained in detail. This does not compromise generality since the other two discussed systems in Fig. 5(a) and (b) and the nonintegrated system shown in Fig. 1(b) share the same control principles. The same control schemes were, in fact, used for single- and threephase experimental testings, whose results are shown in a later section. It is hence appropriate to consider only Fig. 3 with its upper dc–ac inverter control discussed now with reference to the upper half of Fig. 7. In that representation, the dclink voltage *V*dc is first measured, before being regulated by a classical proportional (P)-integral (I) (PI) controller to follow a defined command V^*dc. Where the inner current loop, being much faster, is replaced by a time lap and a low-pass-filter block for representing computational delay and capacitor charging dynamics. The P and

I gains are then chosen as $Kp1 = 0.1$ and $Ki1 = 10$ to give enough phase margin for maintaining the overall system stability.

The PI output, being the active current amplitude needed for keeping Vdc constant, is then multiplied with a unit sine synchronized with the ac grid voltage Vgrid by a standard phaselocked loop. The resulting ac signal I^*ac represents the in-phase active current reference fed to the inner current loop. The inner current controller can no longer be a PI controller, whose steady-state error is not zero because of its finite gain at the ac frequency of interest. A P–Resonant (PR) controller is used instead, whose transfer expression is written as

$$G_{\mathrm{PR}}(s) = K_{p2} + \frac{2K_{i2}\omega_c s}{s^2 + 2\omega_c s + \omega_0^2} \qquad (6)$$

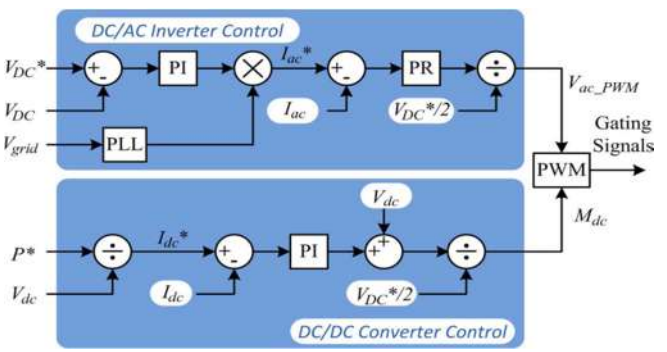

Fig. 7. Per-phase illustration of the overall control schemes

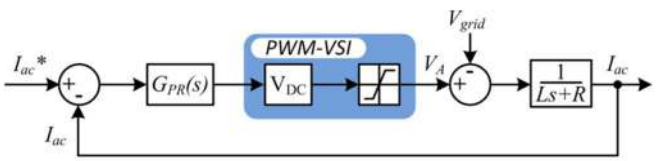

Fig. 8. Per-phase ac inner current loop

Where K_{p2} and K_{i2} are the controller gains and ωc and ωo are the angular cutoff and fundamental frequencies, respectively. Bode diagrams of (6) will, in theory, have a high resonant peak at the 50-Hz frequency of interest. This peak will gradually tend toward infinity as $\omega c \rightarrow 0$.

The final tracking performance of the inner current loop can be verified by referring to its control block diagram drawn separately in Fig. 8. Filter impedance ($R + sL$) and grid voltage Vgrid have now been included in

the figure for arriving at its closed-loop transfer function written in (7). The derived transfer function clearly has two terms for informing that, if the controller gains are chosen high enough, *I*ac will follow its reference *I**ac exactly with little influence from *V*grid

$$I_{\mathrm{ac}}=\frac{G_{\mathrm{PR}}(s)V_{\mathrm{dc}}}{G_{\mathrm{PR}}(s)V_{\mathrm{dc}}+sL+R}I_{\mathrm{ac}}^{\star}-\frac{1}{G_{\mathrm{PR}}(s)V_{\mathrm{dc}}+sL+R}V_{\mathrm{grid}} \quad (7)$$

The controller gains, on the other hand, cannot be too high if the system is to be kept stable. To balance the tradeoff, Bode diagrams of the open-loop transfer function of Fig. 8 are plotted in Fig. 9. In addition to those obtained with the PR controller, relevant plots obtained with a P controller are also included in Fig. 9 for the design. The design procedure read from then suggests choosing a P gain K_{p2} for the P controller so that the system is stable with good transient response. For that, K_{p2} = 0.1 is chosen, which gives more than 90^{O} of phase margin at the system crossover frequency (instant at which magnitude response drops to 0 dB). The system is thus stable.

The second step is to design the resonant gain so that acceptably small steady-state errors are produced, together with a satisfactory phase margin. The chosen resonant gain here is K_{i2} = 10, which will alter only the magnitude response around 50 Hz and not at the crossover frequency. The final phase margin is thus still more than 60^{O}, which, needless to say, represents a stable system. Cutoff frequency ωc can next be chosen, whose purpose is mainly to lessen selectiveness by widening the bandwidth around the resonant peak. This can be helpful if the 50-Hz resonance frequency varies slightly but should not be excessive since the resonant peak amplitude drops significantly as ωc increases.The resulting signal from the properly designed PR controller then forms the required ac modulating reference (upper sinusoidal reference in Fig. 4) needed for switching pulse generation. For that, a timer counting from zero to one and then back is used for realizing a positively displaced triangular carrier, unlike that shown in Fig. 4. The ac modulating reference should therefore be changed according to (8), whose effect is still to place the reference centrally within the upper subband *h*1

$$V'_{\mathrm{ac_PWM}}=0.5V_{\mathrm{ac_PWM}}h_1+1-0.5h_1. \quad (8)$$

Attention should next be focused on the control scheme shown at the bottom of Fig. 7 for the dc–dc converters. In that scheme, a power reference (or voltage reference in some cases) is first created by an algorithm linked to the

source or storage. For the case of a solar module, the power reference is usually decided by an appropriate maximum-power-point-tracking algorithm. The determined power reference can then be divided by the measured input voltage to create a current reference I^{*}_{dc} for tracking by the dc boost current I_{dc}. Tracking is enforced here by a simple PI controller, whose high dc gain helps to force zero dc steady-state error. Tuning of this PI controller is presently well established and can, in fact, be done in Matlab after setting the desired closed-loop bandwidth to be a fifth of the switching frequency or lower.

VI. RESULTS

Single-phase grid-tied system with two of its upper terminals connected to one phase of a 155-V 50-Hz three-phase ac grid and a local single-phase ac load of 30 Ω. The third upper terminal was tied to a local dc load of 13 Ω, while the lower three terminals were connected to three separate dc sources of 30 V each. Two 180° phase-shifted sinusoidal and four linear references were thus needed. In the figure, two upper sinusoidal references and a single linear load reference at M_{dc} = 0.33 were shown occupying the upper subband with a width of $h1/2$ = 0.8. Also shown in the figure were three lower linear references clustering around M_{dc} = 0.15 for the dc sources. They occupy the lower narrower subband with a width of $h2/2$ = 0.2.

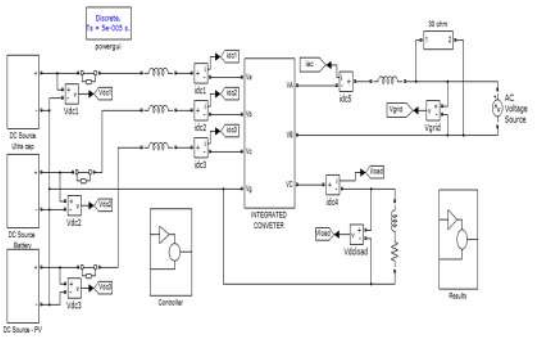

Fig. 9 Integrated single-phase energy system with multiple sources and storages transient 1

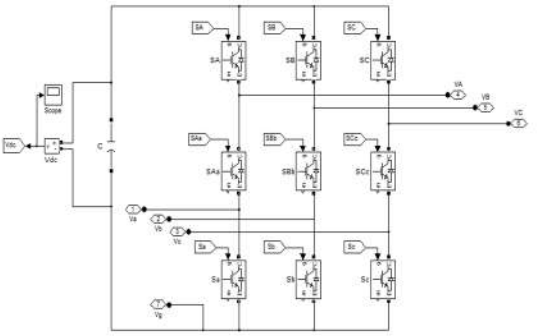

Fig 10 Integrated converter

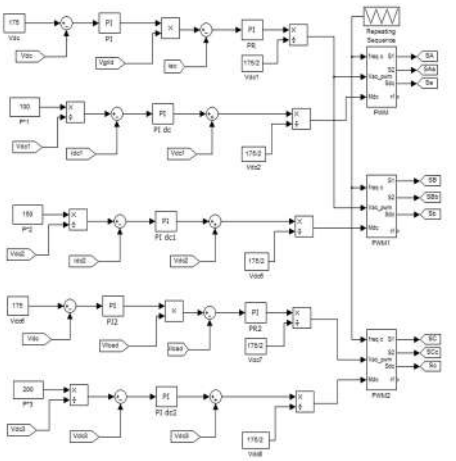

Fig 11 Integrated single phase controller

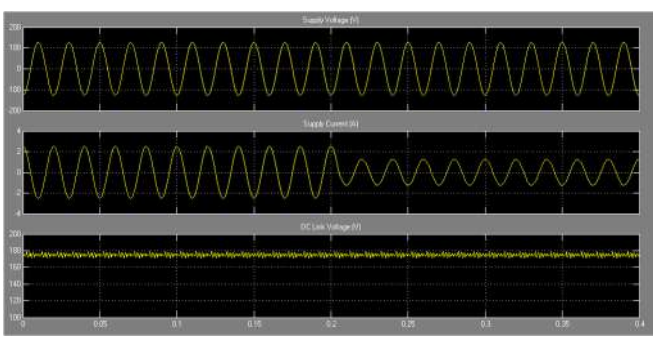

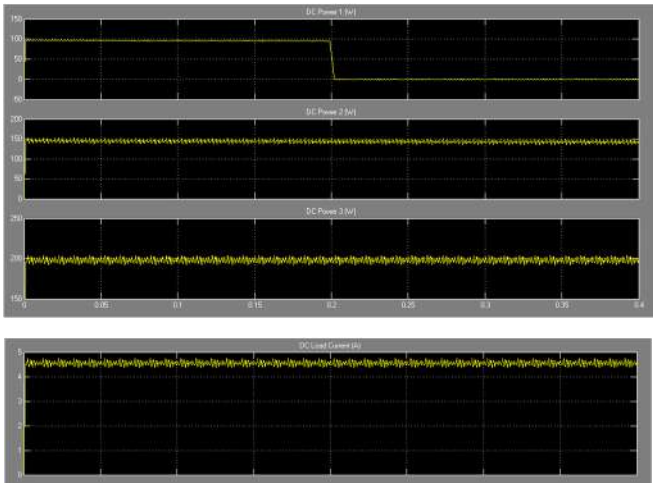

Fig. 12 Experimental waveforms of single-phase system in Transient 1

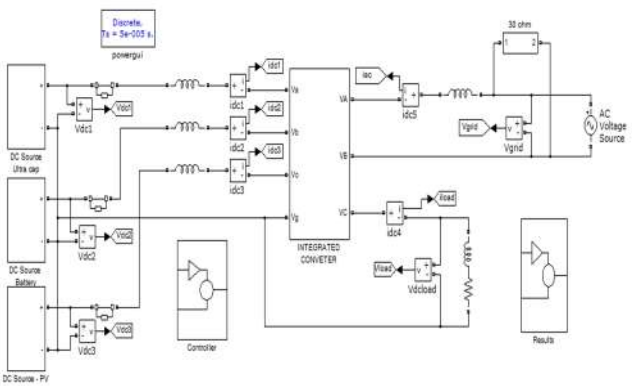

Fig. 13 Integrated single-phase energy system with multiple sources and storages transient 2

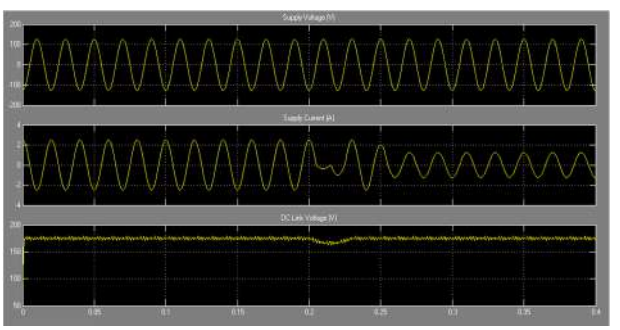

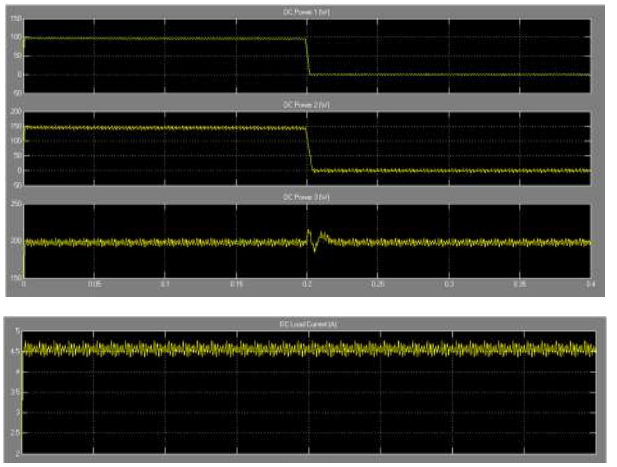

Fig. 14 Experimental waveforms of single-phase system in Transient 2

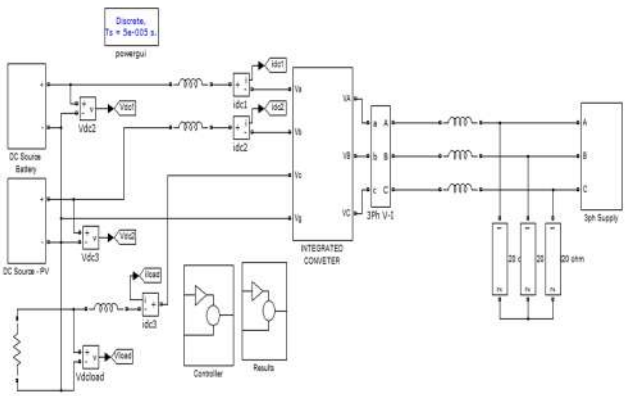

Fig 15 Integrated three-phase energy system with multiple sources and storages

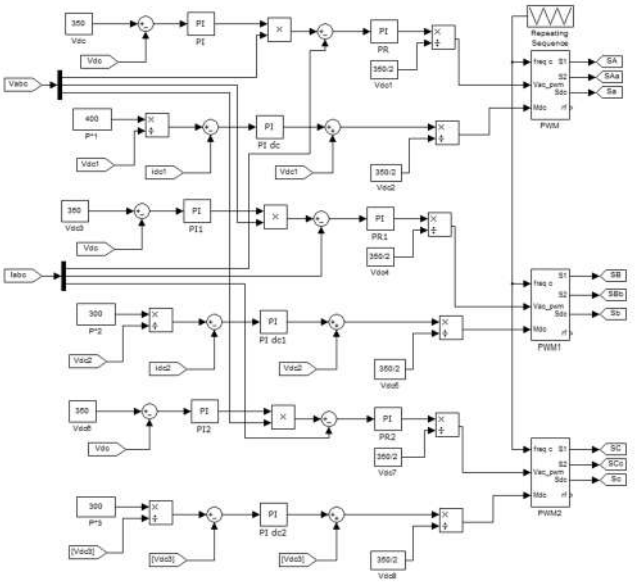

Fig 16 Integrated three phase controller transient-1

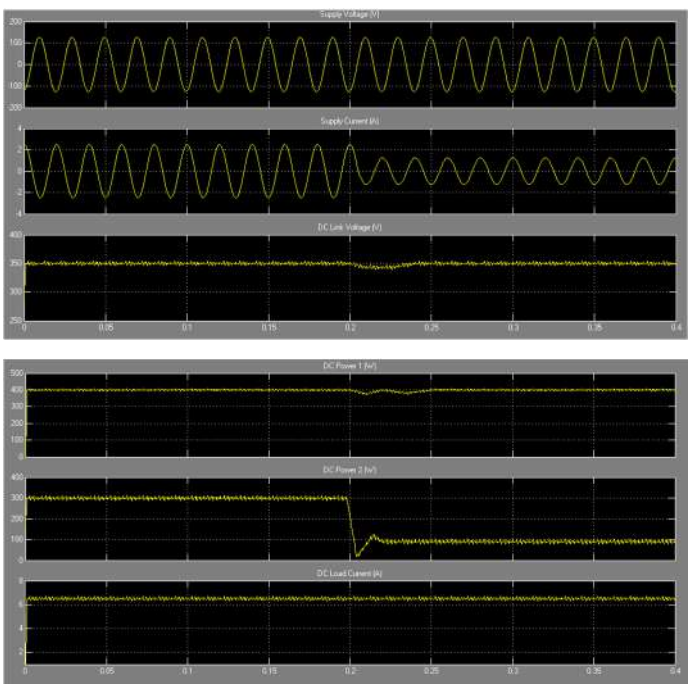

Fig 17 Experimental waveforms of three-phase system Transient 1

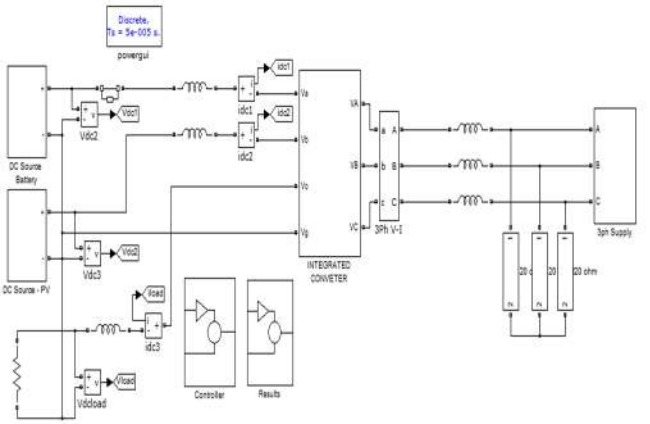

Fig 18 Integrated three phase controller transient-2

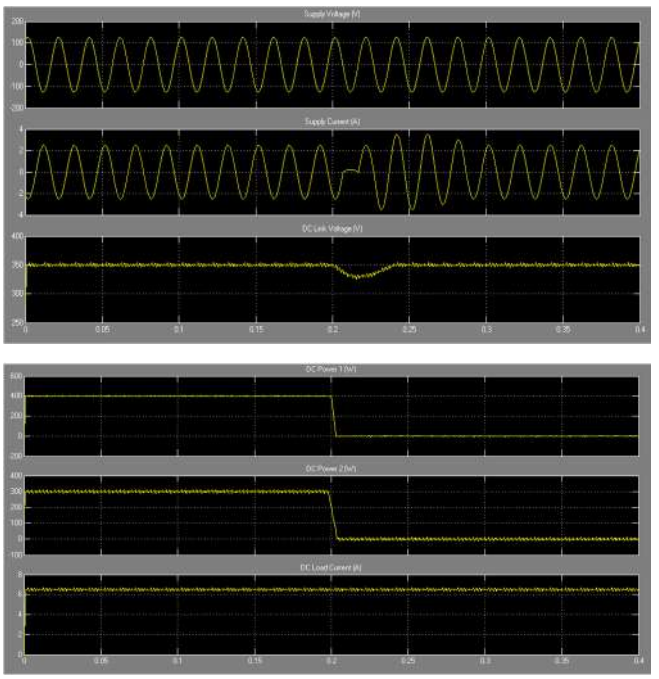

Fig 19 Experimental waveforms of three-phase system Transient 2

VII. CONCLUSION

This paper presents PV based Single & Three Phase Integrated Energy Systems for Micro Grids. This paper has proposed a number of integrated

energy systems based on a compact converter topology. Through proper design, the proposed systems are shown to output equally good terminal waveform quality while yet gaining advantages like reduced switch count and compactness. Surely, some tradeoffs cannot be avoided but can be minimized through proper modulation planning and, hence, do not constitute a major problem.

VIII.Acknowledgment

This paper is based on M. Tech. project carried out by the student of pydah college of engineering & technology, Kakinada studying M.Tech (Power Electronics) The project had been completed by Ms. K ANITHA bearing H.T.no.: 126T1D4302 under the guidance of B. LALITHA KUMARI.

IX.REFERENCES

1. W. Li, G. Joos, and J. Belanger, "Real-time simulation of a wind turbine generator coupled with a battery supercapacitor energy storage system," *IEEE Trans. Ind. Electron.*, vol. 57, no. 4, pp. 1137–1145, Apr. 2010.
2. "Control and performance evaluation of a flywheel energy-storage system associated to a variable-speed wind generator," *IEEE Trans. Ind. Electron.*, vol. 53, no. 4, pp. 1074–1085, Jun. 2006.
3. S. J. Chiang, K. T. Chang, and C. Y. Yen, "Residential photovoltaic energy storage system," *IEEE Trans. Ind. Electron.*, vol. 45, no. 3, pp. 385–394, Jun. 1998.
4. S. Vazquez, S. M. Lukic, E. Galvan, L. G. Franquelo, and J. M. Carrasco, "Energy storage systems for transport and grid applications," *IEEE Trans. Ind. Electron.*, vol. 57, no. 12, pp. 3881–3895, Dec. 2010.
5. C. Liu, K. T. Chau, and X. Zhang, "An efficient wind–photovoltaic hybrid generation system using doubly excited permanent-magnet brushless machine," *IEEE Trans. Ind. Electron.*, vol. 57, no. 3, pp. 831–839, Mar. 2010.
6. J. P. Barton and D. G. Infield, "Energy storage and its use with intermittent renewable energy," *IEEE Trans. Energy Convers.*, vol. 19, no. 2, pp. 441– 448, Jun. 2004.
7. S. Lemofouet and A. Rufer, "A hybrid energy storage system based on compressed air and supercapacitors with maximum efficiency point tracking (MEPT)," *IEEE Trans. Ind. Electron.*, vol. 53, no. 4, pp. 1105–1115, Jun. 2006.
8. J. M. Carrasco, L. G. Franquelo, J. T. Bialasiewicz, E. Galvan, R. C. P. Guisado, M. A. M. Prats, J. I. Leon, and N. Moreno-Alfonso,

"Powerelectronic systems for the grid integration of renewable energy sources: A survey," *IEEE Trans. Ind. Electron.*, vol. 53, no. 4, pp. 1002–1016, Jun. 06

9. C. B. Jacobina, I. S. de Freitas, C. R. da Silva, M. B. de Rossiter Correa, and E. R. C. da Silva, "Reduced switch-count six-phase AC motor drive systems without input reactor," *IEEE Trans. Ind. Electron.*, vol. 55, no. 5, pp. 2024–2032, May 2008.
10. C. B. Jacobina, I. S. de Freitas, and E. R. C. da Silva, "Reduced-switchcount six-leg converters for three-phase-to-three-phase/four-wire applications," *IEEE Trans. Ind. Electron.*, vol. 54, no. 2, pp. 963–973, Apr. 2007.
11. G. Mondal, K. Gopakumar, P. N. Tekwani, and E. Levi, "A reducedswitch- count five-level inverter with common-mode voltage elimination for an open-end winding induction motor drive," *IEEE Trans. Ind. Electron.*, vol. 54, no. 4, pp. 2344–2351, Aug. 2007.
12. T. Kominami and Y. Fujimoto, "Inverter with reduced switching-device count for independent AC motor control," in *Proc. IEEE IECON*, Nov. 2007, pp. 1559–1564.
13. C. Liu, B. Wu, N. R. Zargari, D. Xu, and J. R. Wang, "A novel threephase three-leg AC/AC converter using nine IGBTs," *IEEE Trans. Power Electron.*, vol. 24, no. 5, pp. 1151–1160, May 2009.
14. C. Liu, B. Wu, N. R. Zargari, and D. Xu, "A novel nine-switch PWM rectifier–inverter topology for three-phase UPS applications," in *Proc. IEEE EPE*, Sep. 2007, pp. 1–10.

INTERNATIONAL JOURNAL OF MULTIDISCIPLINARY EDUCATIONAL RESEARCH
ISSN : 2277-7881; IMPACT FACTOR - 2.972; IC VALUE:5.16
VOLUME 3, ISSUE 10(4), OCTOBER 2014

TRANSIENT STABILITY & VOLTAGE UNBALANCES IMPROVEMENT USING TCSC & SFCL

Mr. B. SAI KRISHNA
bavireddysaikrishna@gmail.com
Under the guidance of
Mr. P. VIJAYA RAMARAO
ASSISTANT PROFESSIOR
PYDAH COLLEGE OF ENGINEERING , KAKINADA

Abstract— Voltage unbalance in the source cause control error in the systems, influences the power equipment by causing a reduction in the power generation capacity of the generator and a decrease in the output of the other facilities in the transmission line. Railway system uses a single-phase source that is supplied through a Scott transformer from a three-phase transmission system. The electric railway system has rapidly changing load characteristics; unbalance is generated to the rapidly changing loads. Subsequently, the unbalanced load causes an unbalanced transmission line. Many flexible ac transmission systems are applied to transmission lines to compensate for and control electric power. This proposal brings the application of a superconducting fault current limiter to improve the voltage unbalance in a transmission system linked to a Scott transformer with transient simulations.

Key words: SFCL, Facts, Railway system, TCSC

I. INTRODUCTION

Railway system uses a single-phase source supplied through a Scott transformer from a 3-phase transmission system and has rapidly changing load characteristics in time. These characteristics can cause voltage unbalances. From the utility viewpoint, single-phase loads that cause voltage unbalances in the transmission line are constantly being increased. In response to the unbalances, flexible AC transmission systems (FACTs) are applied to control transmission system power flow and to improve system stability. A thyristor-controlled series capacitor (TCSC) is one of the practical devices that can improve the implementation of FACTs. Actual line voltage and current information is quite important TCSC control scheme. However, voltage and current unbalance produced by an electric railway load causes serious TCSC control errors. This problem can influence system stability. In particular, a voltage and current unbalances after fault will cause further

problems. The remainder of this paper is organized as follows. Section II details a transmission line with a TCSC system and unbalanced loads in an electric railway system. In Section III, faults in the transmission line with a TCSC system and electric railway are analyzed using SFCL modeling. In Section IV, a method is proposed for improving the transmission line using SFCL. Simulations and analysis in this paper are performed using the PSCAD/EMTDC software package.

TABLE I

PARAMETERS OF MODELED SFCL

Parameter	Z_n [Ω]	T_F [s]	a_1	a_2	b_1	b_2
Value	10-20	0.01	-40	-120	10-20	3

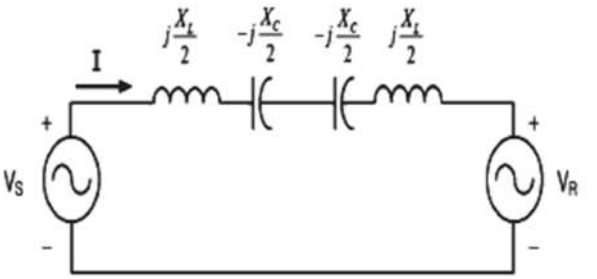

Fig. 1. Series compensation concept for a power system

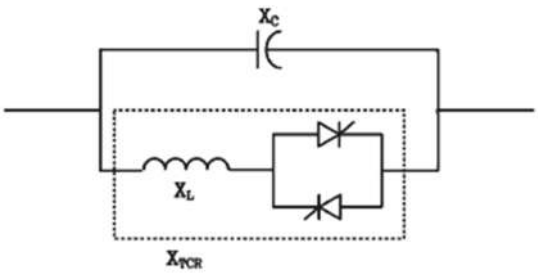

Fig. 2. Configuration of a typical TCSC

II. TRANSMISSION LINE WITH TCSC AND ELECTRIC RAILWAY

A. TCSC-Compensated Transmission:

Power transmitted between a sending-end bus and a receiving-end bus in an AC transmission system is dependent on the series impedance. Further, impedance of a transmission line consists mainly of inductive reactance, with resistance accounting for only 5–10% of impedance. If a series capacitor is inserted into transmission line, the inductive reactance of transmission line could be compensated by a capacitive supply. This concept of series compensation is illustrated in Fig. 1. Typical configuration of a TCSC from a steady state perspective involves a fixed capacitor (FC) with a thyristor controlled reactor (TCR). TCSC structure is shown in Fig. 2. TCR consists of bi-directional thyristor valves and a fixed reactor with inductance *L*.

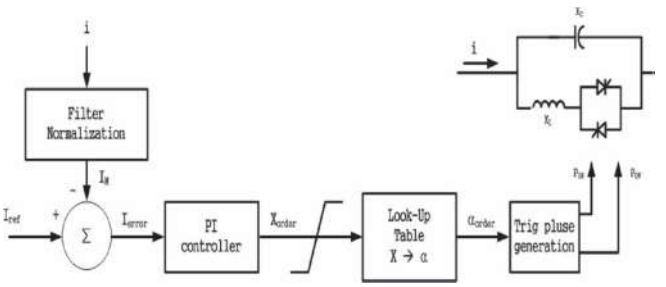

Fig. 3 TCSC closed-loop constant current control methodology

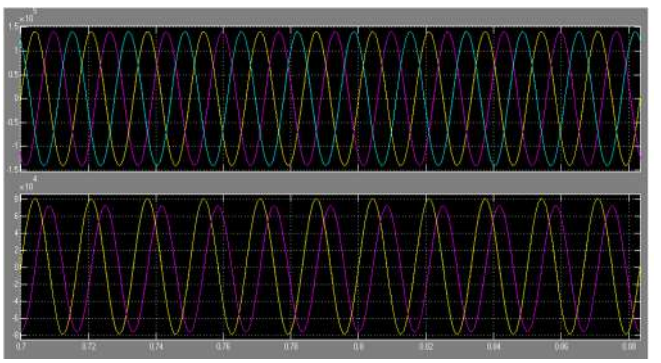

Fig. 4 Typical primary and secondary voltages of a Scott transformer under a T-phase load

B. Operation and Control of a TCSC System:

In Fig. 2, the equivalent impedance *X*TCSC of TCSC is as follows:

$$X_{TCSC} = \frac{X_C X_{TCR}}{X_C - X_{TCR}} = \frac{X_C X_L}{X_C / (\pi\,(2(\pi-\alpha)+\sin 2\alpha)) - X_L}. \quad (1)$$

Where *XL* is the reactance of the fixed reactor, α is firing angle of the thyristor measured from the zero crossing, and *XC* is reactance of the fixed capacitor. Control of α typically applies open-loop control or closed loop control. Fig. 3 details a schematic of a constant current closed-loop control. In Fig. 3, *Iref* is desired transmission line current, *IM* is actual current, and *Ierror* is difference between *Iref* and *IM*. In particular, *Ierror* is an important quantity in this control loop. A current unbalance can cause serious issues for TCSC control.

C. Unbalanced Load in an Electric Railway System:

An electric railway characteristic that most utilities are concerned with is current unbalance produced by large single-phase loads. These unbalanced currents cause 3-phase voltage unbalance. To minimize voltage unbalances in 3-phase power feed networks, Scott transformers are widely used. Nevertheless, an unbalance can be generated owing to large rapidly changing single-phase loads. Fig. 4 shows an unbalance in a 3-phase transmission line voltage produced by a single-phase load in T-phase of the railway.

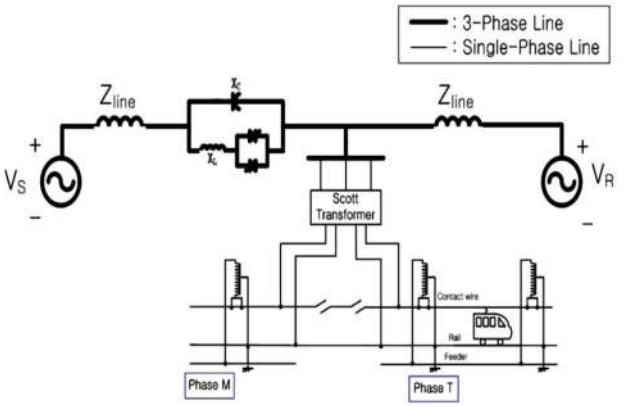

Fig. 5. Transmission system connected with a railway

III. MODELING THE SFCL AND FAULT OF THE TRANSMISSION LINE IN AN ELECTRIC RAILWAY

A. Resistor-Type SFCL Modeling:

In order to limit a fault current, many models for the SFCL have been developed: resistor-type, reactor-type, transformer type, etc. In this study, we modeled a resistor-type SFCL that is mostly basic and used widely which represents the experimental studies for superconducting elements of SFCL. Quench characteristics and recovery characteristics of a resistor-type SFCL are modeled. An impedance of the SFCL according to time *t* is given as follows:

$$Z(t) = \begin{cases} 0 & (t < t_0) \\ Z_{\mathrm{n}}\left[1 - \exp\left(-\frac{t-t_0}{T_{\mathrm{F}}}\right)\right]^{\frac{1}{2}} & (t_0 \le t < t_1) \\ a_1(t-t_1) + b_1 & (t_1 \le t < t_2) \\ a_2(t-t_2) + b_2 & (t \ge t_2) \end{cases} \quad (2)$$

where *Zn* and *TF* are the impedance saturated normal temperature and time constant. In addition, *t*0, *t*1, and *t*2 are the quench-starting time, first recovery-starting time, and secondary recovery-starting time, respectively. *a*1, *a*2, *b*1, and *b*2 are coefficients of the first-order linear function to denote the experimental results of the recovery characteristics of the SFCL. The values used for the parameters are listed in Table I. The recovery time of the SFCL is set to the value until fault clearing to protect the TCSC and transmission line.

B. Fault Modeling of the Transmission Line in the Electric Railway:

An electric railway is connected to a 154 kV transmission line through a Scott transformer in Korea. Fig. 5 shows a transmission system connected with railway equivalent model. A TCSC facility is installed to control power flow in transmission line, and an electric railway includes a single phase load that causes a voltage unbalance. Table II shows the transmission and electric railway system parameters of simulation. In addition, the self- and mutual impedance of transmission and rail of the Korean electric railway system were considered [1]. Here, in order to analyze the influence of an electric railway connection on the transmission line fault, we simulated a fault situation. Fig. 6 shows fault location on the transmission line with TCSC. Fault starting time is 0.4 s and fault duration time is 0.1 s. Fig. 7(a) and (b) show simulation results for a 3-phase fault for an electric railway connection, respectively. In case of fault on the transmission line without electric railway, 3-phase voltage decreased owing to fault and after fault removal, there is a transient

phenomenon that has a small offset voltage but returned to a steady state. In addition, this simulation showed a small magnitude difference between offset voltages. Current is generated a large transient current during fault and reach to steady state, load current, after fault removal. In contrast, large offset voltages are represented in simulation result about fault on transmission line with electric railway such as Fig. 7(b). Especially, voltage of phase B is increased up to 350 kV in a moment. In addition, voltage unbalances of transmission line became more serious compared with above case. Line currents are also increased and caused unbalance owing to transient voltage. We think that closing phase angle control of TCSC system is influenced by generated transient voltage and current as the cause of these results. This phenomenon will cause problem about voltage stability and malfunction of protection scheme in the transmission grid. These results show that an electric railway connection aggravates voltage unbalance in the transmission line.

TABLE II

PARAMETERS OF TRANSMISSION LINE FAULT SIMULATION

Component	Parameter		Value
3-phase source	Zero sequence impedance [%]		0.257+j1.336
	Positive, negative impedance [%]		0.072+j0.757
Transmission line	Zero sequence impedance [%/km]		0.056+j0.196
	Positive, negative impedance [%/km]		0.01+j0.1
Scott transformer	M-phase (Main transformer)	Capacity [MVA]	15
		Ratio [kV]	154/55
		Impedance [%]	10
	T-phase (Teaser transformer)	Capacity [MVA]	15
		Ratio [kV]	133/55
		Impedance [%]	10
Autotransformer		Capacity [MVA]	10
		Ratio [kV]	55/27.5
		Capacity [%]	0.45

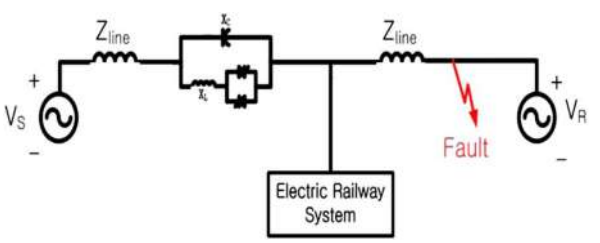

Fig. 6. Transmission line three-phase fault simulation equivalent circuit and fault location

IV. METHOD FOR IMPROVING THE VOLTAGE UNBALANCE USING THE SFCL FROM THE LINE FAULT

We propose a method to improve voltage unbalance using an SFCL. If a transmission line fault occurs, fault current is decreased by the SFCL. After fault is cleared, voltage unbalance produced by railway's single-phase loads can quickly be reduced. As a result, a transmission and electric railway system return to the steady state. In particular, SFCL has advantage of fast operation within 1/4 cycle. The operation characteristics of conventional relay and breaker are greater than 5–15 cycles.

A. Case Study:

As mentioned in the fault modeling, a single-phase load in an electric railway is one of the causes of voltage unbalance in the transmission system. However, the proposed method using SFCL can alleviate this problem. SFCL was installed in the transmission line between TCSC and electric railway in the case study simulation using the PSCAD/EMTDC software package. SFCL decreased the voltage unbalance.

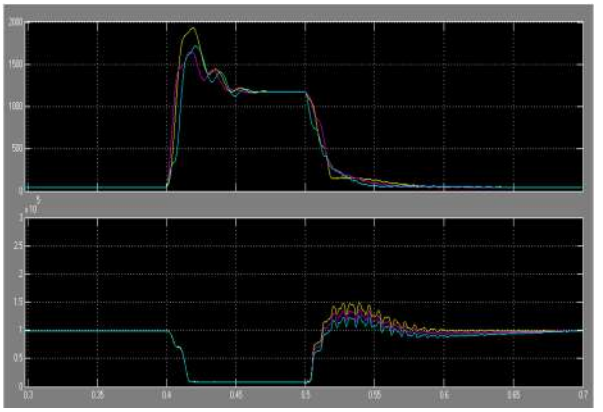

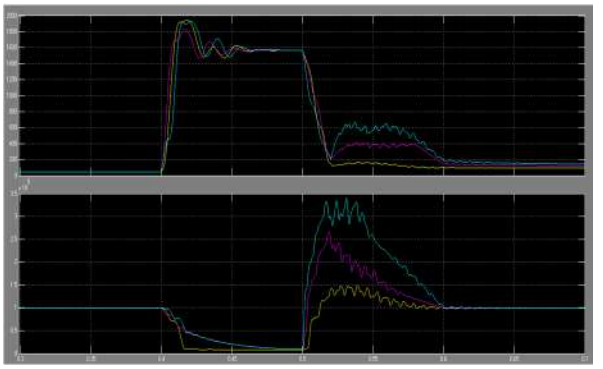

Fig. 7. Voltage and current results from the simulation: (a) without railway and (b) with railway

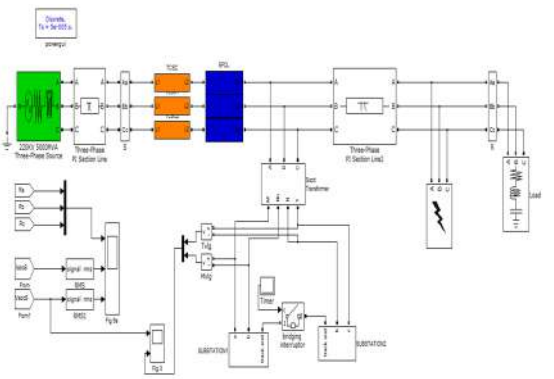

Fig. 8. Transmission system with an electric railway system and SFCL

Fig. 8 shows the transmission system including an electric railway and SFCL. Fig. 9(a) and (b) show the results when SFCL has an impedance of 10 and 20 Ω, respectively. The results showed fault current limiting characteristics and improvement in voltage unbalance. In addition, we discovered following features: 1) the larger resistance of a resistor type SFCL, the more voltage unbalance was improved. 2) In SFCL operating process, there are differences of recovery time between superconducting elements owing to unbalance fault current shown in Fig. 7(b). If a fault occurs, the proposed method clears voltage unbalance and protects TCSC. Thus, transmission system can quickly return to operating in a conventional state. As a result, we will expect improvement effect for the problems about voltage stability and protection scheme malfunction.

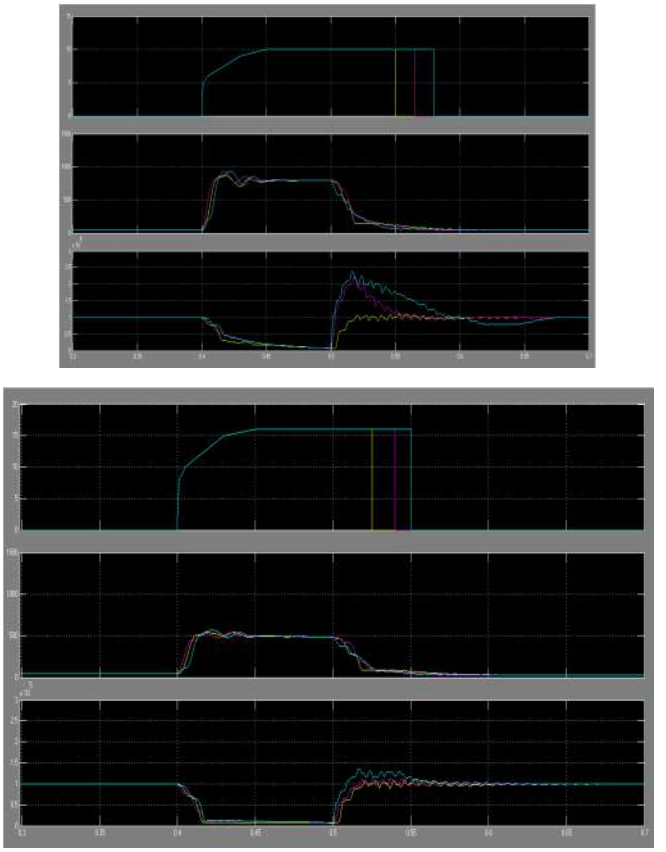

Fig. 9.Fault current limiting, improvement in voltage unbalance, and SFCL quenching characteristics of the proposed method: SFCL impedances of (a)10Ω and (b)20 Ω.

V. CONCLUSION

This paper proposed a method to reduce voltage unbalance for a TCSC-compensated transmission line using an SFCL. First, the configuration and operation of a compensated transmission line and connected electric railway system were modeled and detailed. Next, voltage unbalance in transmission line was studied when line fault occurs. Finally, the method for alleviating this problem with SFCL was considered. The proposed method showed the following improvements for transmission line faults: 1) the fault current was decreased as compared to the existing system fault current and 2) voltage unbalance in the transmission system was quickly improved after the fault was

removed. In future, we will study a protection scheme using an SFCL for a compensated transmission system to improve system stability.

VI. Acknowledgment

This paper is based on M. Tech. project carried out by the student of pydah college of engineering & technology, Kakinada studying M.Tech (Power Electronics) The project had been completed by Mr. B. SAI KRISHNA bearing H.T.no.:126T1D4303 under the guidance of Mr. P. VIJAYA RAMARAO.

REFERENCES

1. H.-S. Shin, S.-M. Cho, J.-S. Huh, J.-C. Kim, and D.-J. Kweon, "Application on of SFCL in automatic power changeover switch system of electric railway," *IEEE Trans. Appl. Supercond.*, vol. 22, no. 3, p. 5600704, Jun. 2012.
2. S. T. Senini and P. J.Wolfs, "Novel topology for correction of unbalanced load in single phase electric traction systems," in *Proc. IEEE Power Electron. Spec. Conf.*, 2002, vol. 3, pp. 1208–1212.
3. T. Uzuka, S. Ikedo, and K. Ueda, "A static voltage fluctuation compensator for AC electric railway," in *Proc. IEEE Power Electron. Spec. Conf.*, 2004, vol. 3, pp. 1869–1873.
4. A. D. Del Rosso, C. A. Canizares, and V. M. Dona, "A study of TCSC controller design for power system stability improvement," *IEEE Trans. Power Syst.*, vol. 18, no. 4, pp. 1487–1496, Nov. 2012.
5. S. S. N. Singh and A. K. David, "Optimal location of FACTs devices for congestion management," *Elect. Power Syst. Res.*, vol. 58, no. 2, pp. 71– 79, Jun. 2001.
6. J.-U. Lim, J.-C. Seo, and S.-I. Moon, "Selection of optimal TCSC location to keep the steady-state voltage profile within limits," presented at the KIEE Conf., 1998.
7. A. Kazemi and B. Badrzadeh, "Modeling and simulation of SVC and TCSC to study their limits on maximum loadability point," *Int. J. Elect. Power Energy Syst.*, vol. 26, no. 8, pp. 619–626, Oct. 2004.
8. Y. Tang, R. Yu, and M. Yan, "Research on the synchronous voltage reversal control model of TCSC," in *Proc. Int. Conf. Power Syst. Technol.*, Oct. 24–28, 2010, pp. 1–6.
9. T.-H. Chen, "Criteria to estimate the voltage unbalances due to high-speed railway demands," *IEEE Trans. Power Syst.*, vol. 9, no. 3, pp. 1672–1678, Aug. 1994.

10. S.-H. Chang, K.-H. Oh, and J.-H. Kim, "Analysis of voltage unbalance in the electric railway system using two-port network model," *KIEE Trans.*, vol. 50A, pp. 248–254, May 2001.
11. J.-S. Kim, S.-H. Lim, J.-F. Moon, J.-C. Kim, and O.-B. Hyun, "Analysis on the protective coordination on neutral line of main transformer in power distribution substation with superconducting fault current limiter," *KIEE Trans.*, vol. 58, no. 11, pp. 2089–2094, Nov. 2009.
12. H. R. Kim, S.-W. Yim, O.-B. Hyun, J. Sim, and S.-Y. Oh, "Analysis on recovery characteristics of superconducting fault current limiters," presented at the Proc. Conf. Magn. Technol., Philadelphia, PA, USA, Aug. 27–31, 2007, MT-20.
13. S.-H. Lim, S.-R. Lee, H.-S. Choi, and B.-S. Han, "Analysis of operational characteristics of flux-lock type SFCL combined with Power compensator," *IEEE Trans. Appl. Supercond.*, vol. 15, no. 2, pp. 2043–2046, Jun. 2005.

INTERNATIONAL JOURNAL OF MULTIDISCIPLINARY EDUCATIONAL RESEARCH
ISSN : 2277-7881; IMPACT FACTOR - 2.972; IC VALUE:5.16
VOLUME 3, ISSUE 10(4), OCTOBER 2014

BIDIRECTIONAL POWER FLOW CONTROLLER FOR THE ELECTRIC VEHICLE AND DC OR AC GRID

Ms. J. RAMESH
rameshjanga004@gmail.com
Under the guidance of
Ms. M. PAVANI
ASSISTANT PROFESSIOR
PYDAH COLLEGE OF ENGINEERING , KAKINADA

Abstract— The inductances of the traction motor windings are used for bidirectional converter operation to transfer power eliminating the need for extra inductors for the charging and vehicle-to-grid converter operations. These operations are in addition to the vehicle traction mode operation. This paper presents converter topology that has bidirectional power flow capability between an electric vehicle and the dc or ac supply or grid. The electric power train system size and weight can be minimized with this approach. The concept has been analyzed MATLAB software. Experimental results are also provided with electric machines. The interleaving technique has been used with the inductors to share the current and reduce the converter switching stresses.

Key words: electric vehicle, Bidirectional power flow, Matlab

I. INTRODUCTION

Several research activities for integrating the batter charging system with the traction drive have been reported. In one approach, the traction motor windings have been used as the inductors for the converter to develop the charging system without any additional component. The three-phase supply is connected with each phase of the machine and the battery is always connected to the dc bus. The research showed the use of a poly-phase machine for the charger. Other topologies have been used for battery charging systems with traction motor windings used as filter components. The multipurpose use of the power electronic converter in the drive train of an electric vehicle has become an interesting topic for minimizing the system size, weight, and cost. This paper presents the analysis, design, an experiments of the integrated traction drive and power converter for electric/hybrid vehicle applications. The electric machine has been analyzed using coupled simulation of finite-element and dynamic analysis software.

The weight and size of the converter are challenging issues in the case of on-board chargers which otherwise provides the flexibility of charging the vehicle anywhere. The vehicle is not driven during the period of charging, and hence, the traction motor and inverter of the power train can be used as an integral part of the converter. The windings of the traction motor can serve as the inductors of the power converter along with power devices of the traction inverter to transfer power. The power converter of the electric vehicle can draw power from the grid when it requires, and also can deliver power to the grid in the peak time when the grid needs power. During a significant part of the day, most vehicles remain idle in the parking lot when the integrated power converter can use the traction motor and its drive to transfer power to the grid.

An on-board integrated charger has been proposed with reconfiguration of the stator windings of a special electric machine. A battery charger is developed for the electric scooter, where interior permanent magnet traction motor is used for charging with power factor correction. The interleaving technique is another interesting approach used in designing dc–dc converters for reduced switching stresses and increased efficiency. The approach reduces the size and power rating of the converter passive components. Low EMI and low stress in the switches can be expected from the interleaved converter phase legs.

In this paper, an integrated motor converter is proposed that can be used as the traction motor drive, a battery charger, and a power converter to transfer energy from vehicle-to-grid (V2G) through reconfiguration of the inverter topology using relays or contactors. The traction inverter with the proposed reconfiguration method can also transfer power from the vehicle to a dc grid and from a dc grid to the vehicle using the traction motor windings with the appropriate relay settings. The three phase machine windings and the three inverter phase legs can be utilized with an interleaved configuration to distribute the current and reduce the converter switching stresses. The battery voltage is increased in the boost mode to an output reference voltage level within the limits of the machine ratings. A soft starter method using PWM control has been used to reduce the starting current overshot when connecting to a dc grid. In a dc grid connected mode, the voltage drop across the inductor will be the difference between the inverter output voltage and the dc grid voltage. The dc grid voltage provides more stable voltage to counteract the rate

of change of inductor current and the current ripple is controlled in a better fashion in a dc grid connected mode.

The proposed converter system can also be used for transferring power between a single-phase ac grid and the vehicle in either direction without any extra component. The rated conditions of the motor and utility interface are quite similar. The inverter is able to regulate the motor phase current in the entire speed range. When changing from the motor control mode to ac grid connected mode of operation, the back EMF voltage is replaced with the grid voltage. Considering the operating conditions with the grid, motor inductance would be enough to handle the grid connected modes of operation. Also, in the blocked rotor condition, motor magnetizing inductance dominates and contributes to the phase inductance significantly. For high enough inductance required in case of ac grid, the rotor can be locked which will give high inductance in the blocked rotor condition. In the charging mode, the machine is thermally stable with no electromechanical power flow through the air gap of the machine. The machine ratings are within limits in all the operating modes as there is only electric loading, and no magnetic loading except during traction operation. The current limit is higher in converter modes compared to the traction mode current limit.

The power converter and controller have been modeled using MATLAB/Simulink. The proposed converter reconfiguration method is advantageous for reducing the size and component of the electric power train while providing bidirectional power flow capability with connections to either dc or ac supplies.

II. PROPOSED TOPOLOGY

Different types of topologies have been developed for electric vehicles for battery charging and bidirectional power flow between the battery and the power supply. However, the traction inverter uses the standard six-switch configuration that has elements of the various power converter topologies. The proposed converter topology utilizing the traction inverter along with the switches used for reconfiguration is shown in Fig. 1(a) and (b) shows the detailed switch or relay arrangements required for different modes of operations. Several different configurations can be obtained by appropriate positioning of the switches, which results in a novel methodology for bidirectional power transfer between a vehicle battery and dc or ac grid. Including the use of the topology as the traction inverter during vehicle

operation this power converter can be operated in five different modes: 1) power flow from the battery to the dc grid, 2) power flow from the dc grid to the battery, 3) traction mode, 4) power flow from the battery to single-phase ac grid and 5) power flow from a single-phase ac grid to the battery.

The reconfiguration switches can be realized with relays or contactors depending on the ratings of the currents. Those relays and contactors are controlled in a coordinated way to accommodate the different modes of use. The contactors with optimum current capacity should be used to minimize the size of the contactor. The size of the contactor has to be accommodated based on the current rating chosen. To minimize the space and size of the contactors, all the switches can be integrated into a single package.

The switches will be controlled for the different modes of operation using State 1 and State 2 conditions given in Table I. Fig. 1(b) shows the details of the configuration in the routing box with the switches which relates to the operations of the switches according to Table I. The terminal numbers are shown in Fig. 1(b) inside the switches which are changed to different positions for the different configurations. When the converter is to connect to a dc grid, Switch 4 will be in State 1 to isolate from the ac grid. When the converter is to connect to an ac grid Switch 5 will be in State 1 to isolate from the dc grid. Thus, the traction converter can be connected to either a dc or an ac grid. Fig. 2 shows the OFF condition where all the switches are in State 1; in this situation, there will be no power transfer. If there is any fault in one or multiple phases in the motor the converter configuration will be switched to State 1 as shown in Fig. 2, and there will be no power transfer between the grid and the battery. The usual protection schemes for a traction inverter will take over. The system has inherent fault protection capability, and extra protection is not needed.

TABLE I

SWITCH POSITIONS AND CONVERTER STATES

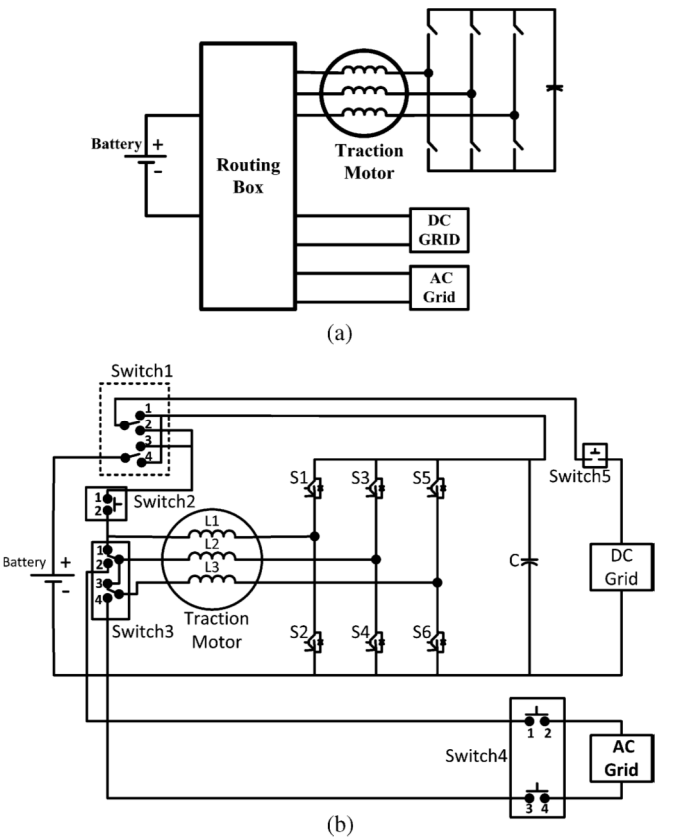

Fig. 1. Converter with switches capable of interfacing with both ac and dc grid (a) combined and (b) details

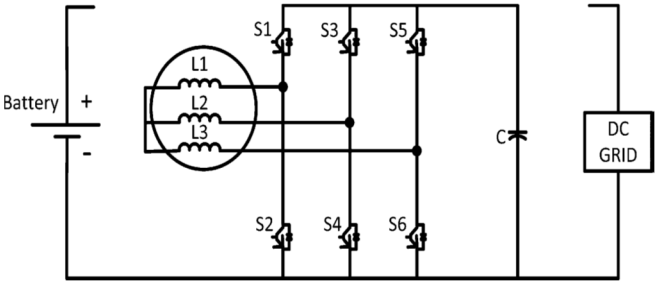

Fig. 2. Circuit with all switches in State 1

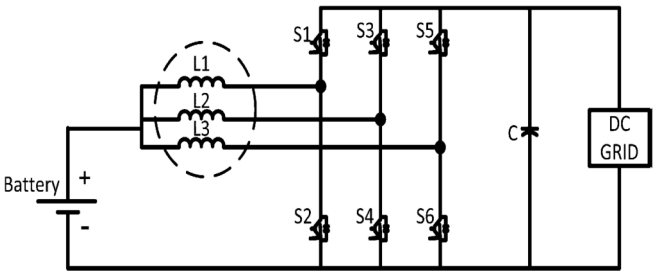

Fig. 3. Circuit with Switch 2 and Switch5 in State 2 for V2G boost or G2V buck operation with vehicle side inductors interleaved.

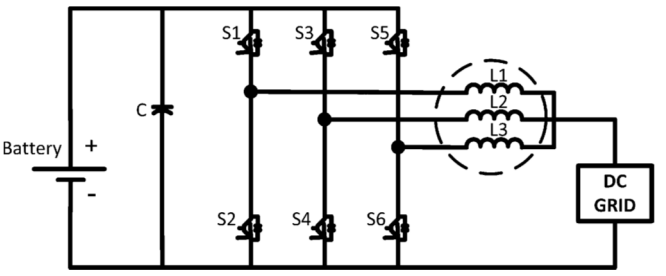

Fig. 4. Circuit with Switch 3 and Switch 4 are in State 1 for V2G buck or G2V boost operation with dc grid side inductors interleaved.

Power is transferred from the vehicle battery to the dc grid using the boost mode of operation for the converter with Switch 2 and Switch 5 in State 2, and the other switches in State 1; power from the vehicle battery to the dc grid can also be transferred in buck mode with Switch 3 and Switch 4 in State 1 and the other switches in State 2. When power transfer is needed from dc

grid to the vehicle, Switch 2 and Switch 5 are in State 2 for buck operation and Switch 3 and Switch 4 are in State 1 for boost operation. From Fig. 3, it can be observed that for V2G boost operation, the interleaved technique can be applied on the battery side with the three inductances and three legs of the converter; for G2V boost operation, the interleaved technique can be applied on the dc grid side to reduce the switching stresses. The proposed converter can be used for traction mode with Switch1 in State 2 and other switches in State 1 as shown in Fig. 5.

This converter can be used for bidirectional power transfer between a single-phase ac grid and the vehicle battery. For this configuration, Switch 1 and Switch 5 are kept in State 1, while all switches are to be in State 2. The two phases of traction motor windings are connected with the single-phase ac grid side and another switch connects with the battery as shown in Fig. 6. Power can flow in either direction with buck or boost modes of operation.

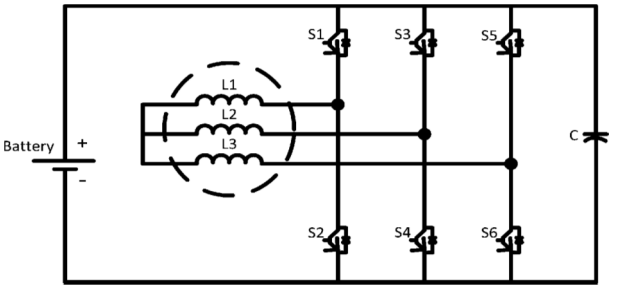

Fig. 5. Circuit with Switch 1 is in State 2 for traction mode operation

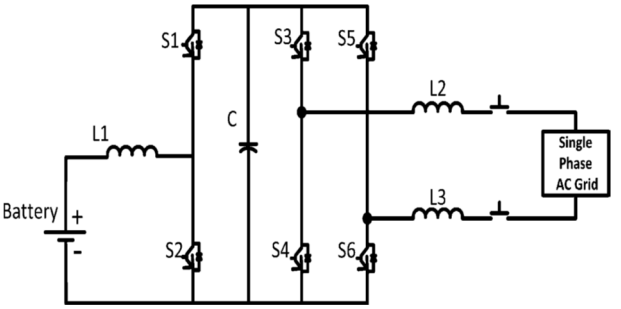

Fig. 6. Circuit configuration for bidirectional interface with a single-phase ac grid

Operating mode 1 in Fig. 3 and operating mode 2 in Fig. 4 have been verified in simulation. Operating mode 1 is experimentally verified using two

types of machines. Although, operating mode 2 in Fig. 4 is different from operating mode 1, the converter is symmetrical for these two modes and for experiments they are similar. Therefore, verifying operating mode 1 experimentally is sufficient for both modes. The operation mode in Fig. 5 is the typical traction machine operation which is used in the motor drives of electric and hybrid vehicles.

The typical traction inverter and its controller are designed to have enough bandwidth to regulate the motor phase currents with reasonable ripple on them. The voltage that appears across the motor inductances is dependent on the inverter dc bus voltage, amount of motor inductance, motor back EMF voltage, and the switching frequency of the controller. When the inverter switches to the grid connection mode, the effect of back EMF voltage is replaced by the grid voltage and the rest of the elements would stay close to the motor operation. In fact, current regulation during traction at low speed is much more challenging than the grid connected operation since the back EMF voltage is quite small at low speeds. Therefore, the machine inductance would be suitable for all the operating modes, since it is just the configuration of the winding of the machine, and the machine inductances are typically large values. The performance depends on the machine specifications. The maximum current limit is within the thermal limit of the machine, and the ripple in current is dictated by the fixed inductance of the machine as the machine windings cannot be changed. The bus capacitor is selected to handle the voltage ripple and the appropriate switching frequency is selected beyond the acoustic range of frequencies. If there is an option to design the machine with the intention of applying the proposed reconfigurable converters, then the machine can be designed with higher current capability for faster charging and higher winding inductance for minimizing current ripple without degradation of traction operation.

TABLE II

PARAMETER SPECIFICATION FOR ANALYSIS

Input voltage range	100V – 250V
Maximum output voltage	650V
Machine Phase Inductance	4.98mH
Output Capacitance	3300μF
Load Resistance	20Ω
Maximum Input current	30A

Traction machines can be of induction, permanent magnet, or switched reluctance machine types. Inductance variations for permanent magnet synchronous and induction machines with respect to the position change are minimal. However, there are variations of the inductance value at different rotor positions for interior permanent magnet and switched reluctance machines. With a dc grid, the rotor is not required to be locked as it will be aligned with the maximum inductance path. Consequently, the ripple will be lower. With an ac grid, the flux produced from ac voltage can move the rotor or vibrate the rotor. In this case, the rotor needs to be locked. The mutual inductances have not been modeled in this analysis. There can be phase imbalance due to the mutual inductance. Phase current controls with individual phase current measurements are already in place in a typical traction drive. The current controller would act to compensate for the variations in the inductance and balance the phase currents. The difference in the current ripple between the phases could still be an issue, but is not expected to be a significant one.

Three-phase machines have been considered in this research as this is the practical scenario with all the traction machines. However, if the phase number is larger than three, three phases will be used and other phases can be distributed and connected to those three branches or the extra phases could be left disconnected depending on the mode of operation. All modes of operation as described in Fig. 3 –Fig. 6 are similarly applicable.

III. SYSTEM ANALYSIS

The converter configuration shown in Fig. 3 can be operated as a simple boost converter if the frequency and duty cycle of the bottom three IGBTs and the top three IGBTs are the same. The system matrix of the converter is

$$A = \begin{bmatrix} \frac{-r_L}{L} & \frac{-D'}{L} \\ \frac{D'}{C} & \frac{-1}{R_L C} \end{bmatrix}$$

where *rL* is the internal resistance of the inductor, *D* is duty cycle, D^{l} is (1 – *D*), *L* is the combination of the motor windings, and *RL* is the combined resistance on the grid side. The system stability can be analyzed using the system matrix.

The converter specifications for stability analysis are given in Table II. For the input voltage range of 100–250 V with the desired output voltage of 650 V, the real part of the system poles are observed to be negative (see Fig. 7). The system is stable within these input–output voltage ranges.

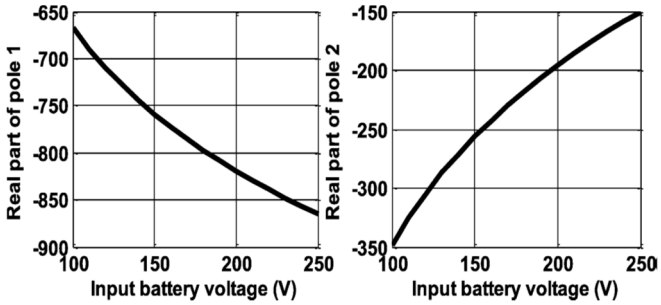

Fig. 7. Effect of input voltage change on the system pole 1 and pole 2

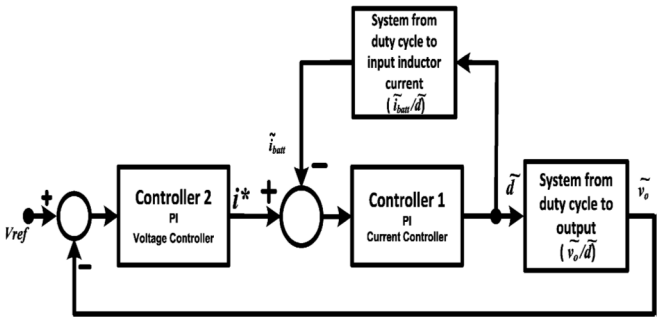

Fig. 8. System block diagram with closed-loop feedback control

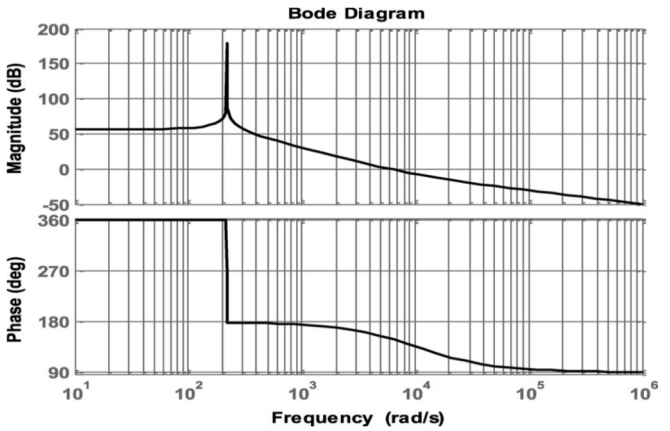

Fig. 9. Frequency response from duty cycle to output voltage

The transfer functions of duty cycle to output voltage and of duty cycle to battery current can be derived as follows from the small signal analysis of the converter with a PI controller

$$\frac{\tilde{v}_o}{\tilde{d}} = \frac{\frac{-I_{\text{batt}}}{C}\left(s - \frac{D'V_o}{I_{\text{batt}}L}\right)}{s^2 + \left(\frac{1}{R_L C}\right)s + \frac{D'^2}{LC}}$$

$$\frac{\tilde{i}_{\text{batt}}}{\tilde{d}} = \frac{\frac{V_o}{L}\left(s + \frac{1}{R_L C} + \frac{D'I_{\text{batt}}}{V_o C}\right)}{s^2 + \left(\frac{1}{R_L C}\right)s + \frac{D'^2}{LC}}.$$

The converter characteristics in terms of parameter sensitivity and bandwidth analysis can be analyzed with the closed-loop transfer functions. The corner frequency of the closed-loop system is

$$f = \frac{D'}{\sqrt{LC}}.$$

The frequency response of the system for 60% duty cycle with the bandwidth of 6 kHz is shown in Fig. 9. The response would change with change in duty cycle which suggests the parameter dependency of the system transfer function. The converter system with feedback control as shown in Fig. 8 depends on the duty cycle nonlinearly, which makes it challenging to design this converter within the stability and bandwidth limits. The bode diagram is from the analytical model, which has been used to select the converter parameters.

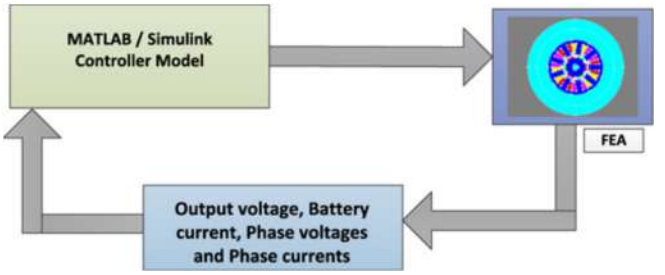

Fig. 10. Coupled simulation of Flux 2-D and MATLAB/Simulink

IV. SIMULATION RESULTS

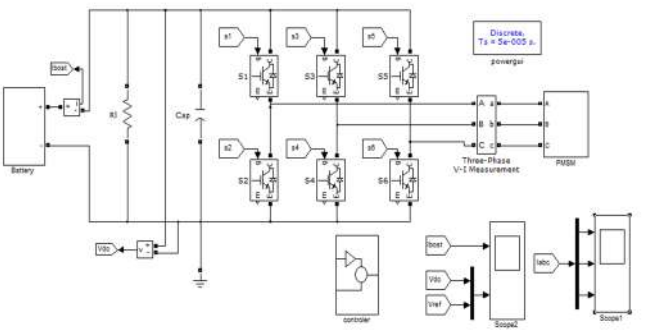

Fig 11 Integrated Electric Motor Drive and Power Electronics pmsm

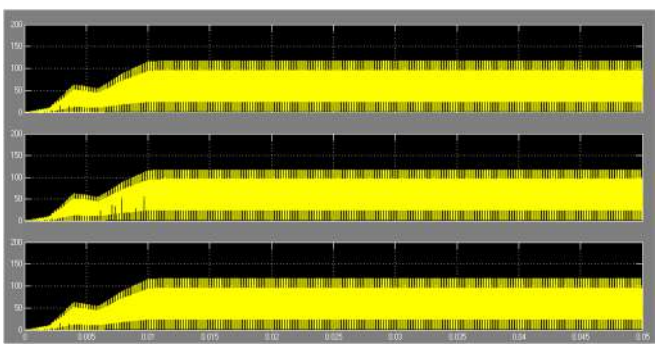

Fig 12 Integrated Electric Motor Drive and Power Electronics pmsm current

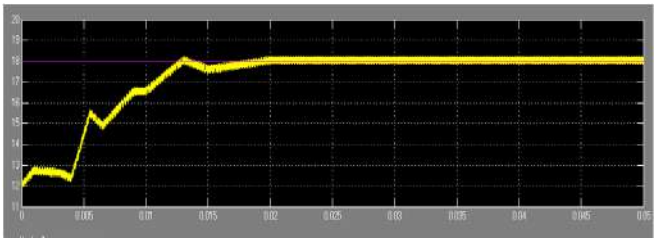

Fig 13 Integrated Electric Motor Drive and Power Electronics pmsm voltage

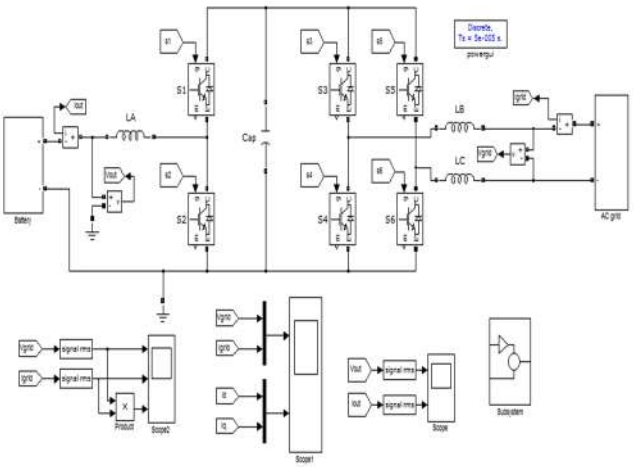

Fig 14 electric motor IM ac grid

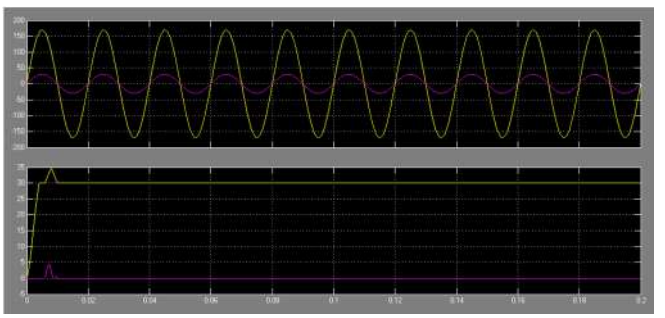

Fig 15 voltage & current of AC grid

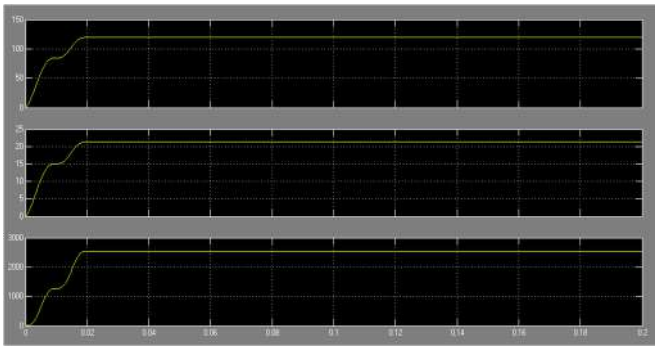

Fig 16 r.m.s value of voltage & current

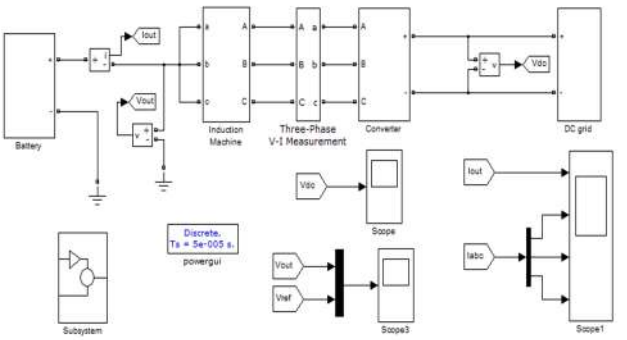

Fig 17 electric motor IM dc grid

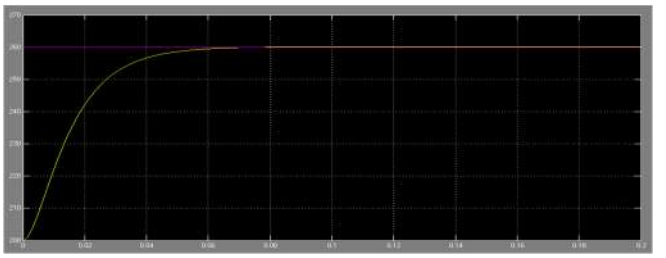

Fig output voltage & reference voltage

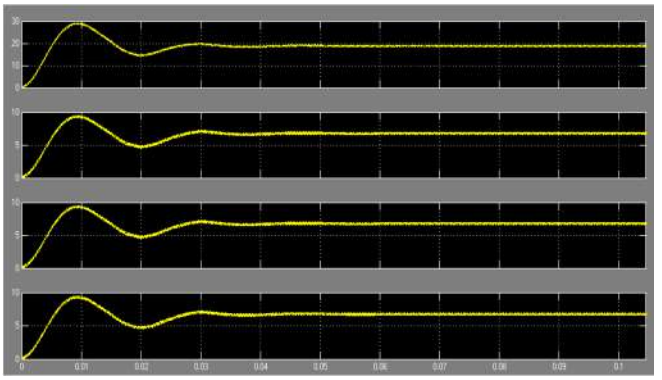

Fig output & three phase current

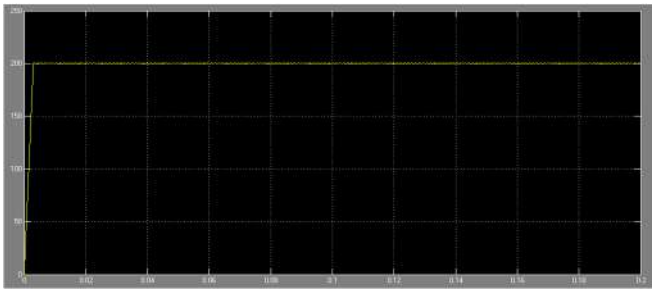

Fig DC output voltage

VI. CONCLUSION

Bidirectional Power Flow Controller for the Electric Vehicle and DC or AC Grid method have been proposed in this paper, where traction machine windings can be used as the inductors of the converter to transfer power between a vehicle battery and either a dc or an ac grid. The converter reconfiguration concept is useful in minimizing the size and parts in the power train of an electric vehicle. The machine-converter coupled simulation results showed that the integrated converter can be used for the power transfer with versatility without significantly extra power elements. The experimental results verified that the proposed integrated converter can work in both directions for V2G and G2V; additionally, it has the advantages of utilizing the interleaving technique in both V2G and G2V modes of operations.

VII. Acknowledgment

This paper is based on M. Tech. project carried out by the student of pydah college of engineering & technology, Kakinada studying M.Tech (Power Electronics) The project had been completed by Ms. J. RAMESH bearing H.T.no.: 126T1D4304 under the guidance of Ms. M PAVANI.

REFERENCES

1. S. Lacroix, E. Laboure, andM.Hilairet, "An integrated fast battery charger for electric vehicle," in *Proc. IEEE Veh. Power and Propulsion Conf.*, Oct. 2010, pp. 1–6.
2. M. Milanovic, A. Roskaric, and M. Auda, "Battery charger based on double-buck and boost converter," in *Proc. IEEE Int. Symp. Ind. Electron.*, Jul. 1999, vol. 2, pp. 747–752.
3. A. G. Cocconi, "Combined motor drive and battery recharge system," U.S. Patent 5 341 075, 23 Aug. 1994.
4. S. K. Sul and S. J. Lee, "An integral battery charger for four-wheel drive electric vehicle," *IEEE Trans. Ind. Appl.*, vol. 31, no. 5, pp. 1096–1099, Sep./Oct. 1995.
5. D. Thimmesch, "An SCR inverter with an integral battery charger for electric vehicles," *IEEE Trans. Ind. Appl.*, vol. IA-21, no. 4, pp. 1023–1029, Jul./Aug. 1985.
6. L. Solero, "Nonconventional on-board charger for electric vehicle propulsion batteries," *IEEE Trans. Veh. Technol.*, vol. 50, no. 1, pp. 144–149, Jan. 2001.
7. S. Haghbin, S. Lundmark, M. Alak¨ula, and O. Carlson, "An isolated high power integrated charger in electrified vehicle applications," *IEEE Trans. Veh. Technol.*, vol. 60, no. 9, pp. 4115–4126, Nov. 2011.
8. G. Pellegrino, E. Armando, and P. Guglielmi, "An integral battery charger with Power Factor Correction for electric scooter," in *Proc. IEEE Electric Mach. Drives Conf.*, May 2009, pp. 661–668.
9. N. M. L. Tan, T. Abe, and H. Akagi, "A 6-kW, 2-kWh Lithium-Ion battery energy storage system using a bidirectional isolated DC-DC converter," in *Proc. Power Electron. Conf.*, Jun. 2010, pp. 46–52.
10. S. Dwari and L. Parsa, "An efficient high-step-up interleaved DC–DC converter with a common active clamp," *IEEE Trans. Power Electron.*, vol. 26, no. 1, pp. 66–78, Jan. 2011.

11. O. Hegazy, J. Van Mierlo, and P. Lataire, "Analysis, modeling, and implementation of a multidevice interleaved DC/DC converter for fuel cell hybrid electric vehicles," *J. Power Electron.*, vol. 27, pp. 4445–4458, Jul. 2011.
12. O. Hegazy, J. Van Mierlo, and P. Lataire, "Control and analysis of an integrated bidirectional DC/AC and DC/DC converters for plug-in hybrid electric vehicle applications," *J. Power Electron.*, vol. 11, no. 4, pp. 408– 417, Jul. 2011.
13. O. Ellabban, O. Hegazy, J. Van Mierlo, and P. Lataire, "Dual loop digital control design and implementation of a dsp based high power boost converter in fuel cell electric vehicle," in *Proc. IEEE Int. Conf. Optim. . Electr. Electro. Equipment*, May 2010, pp. 610–617.
14. M. N. Arafat, S. Palle, Y. Sozer, and I. Husain, "Transition control strategy between standalone and grid-connected operations of voltage-source inverters," *IEEE Trans. Ind. Appl.*, vol. 48, no. 5, pp. 1516–1525, Sep./Oct. 2012.

INTERNATIONAL JOURNAL OF MULTIDISCIPLINARY EDUCATIONAL RESEARCH
ISSN : 2277-7881; IMPACT FACTOR - 2.972; IC VALUE:5.16
VOLUME 3, ISSUE 10(4), OCTOBER 2014

ENHANCEMENT OF THREE-PHASE SHUNT ACTIVE POWER FILTERS WITH CURRENT CONTROL STRATEGY WITH FSTPI

Ms. K. SRINIVASULU
kokkanti.srinu@gmail.com
Under the guidance of
Ms. B. LALITHA KUMARI
ASSISTANT PROFESSIOR
PYDAH COLLEGE OF ENGINEERING , KAKINADA

Abstract—This paper proposes Three-Phase Shunt Active Power Filters with Current Control Strategy with FSTPI. The total cost to implement the proposed APF becomes lower, owing to the minimized current sensors and the use of a four-switch three-phase inverter (FSTPI). The proposed scheme requires only two current sensors at the supply side. In order to make the supply currents sinusoidal, an effective harmonic compensation method is developed with the aid of a conventional proportional-integral (PI) and vector PI controllers. The absence of the harmonic detector not only simplifies the control scheme but also significantly improves the accuracy of the APF, since the control performance is no longer affected by the performance of the harmonic tracking process. Despite the simplified hardware, the performance of the APF is improved significantly compared to the traditional control scheme, thanks to the effectiveness of the proposed compensation scheme.

Key words: APF's, 3 phase 4 wire inverter

I. INTRODUCTION

In order to improve the power quality of distribution networks as well as to meet these restriction standards, two main solutions have been introduced: *LC* passive filters and active power filters (APFs). *LC* passive filters are traditionally utilized to compensate the harmonic currents since they are simple and low-cost solution. The increasing use of nonlinear loads such as adjustable speed drives, electric arc welders, and switching power supplies causes large amounts of harmonic currents inject into distribution systems. These harmonic currents are responsible for voltage distortion, increasing power losses and heat on networks and transformers, and causing operational failure of electronic equipment. Due to these problems, harmonic restriction standards such as IEEE-519 or IEC 61000-3-2 have been published

to demand those harmonic currents injected into utility networks to be below the specified values.

However, they are often large and heavy. Furthermore, the compensation capability of a passive filter is typically fixed and relies heavily on a network's impedance, thus potentially causing undesired resonance problems. In contrast, shunt APFs are recognized as a flexible solution for harmonic current compensation since they are capable of compensating harmonic currents generated by many types of nonlinear loads as well as providing fast responses to load variations. A typical control scheme of a shunt APF is illustrated in Fig. 1. The purpose of an APF is to generate harmonic currents (*iF,abc*) having the same magnitude and opposite phase with the harmonics produced by the nonlinear load, and to ensure that the supply currents (*iS,abc*) contain only the fundamental component. In order to realize the desired goals, as shown in Fig. 1, the traditional control scheme requires several steps such as load current measurement, harmonic current detection, and reference filter current generation, and filter current control. Since the APF must generate non-sinusoidal currents, the design of the current controller for the APF is a challenging task. Various control methods have been developed in the literature such as proportional-integral (PI) control, dead-beat control, and hysteresis control. Due to the limitation of the control bandwidth, the PI controller is not a suitable solution for the APF applications since the current controller must deal with harmonic currents, which are high-frequency signals. In contrast, the dead-beat control method is able to provide fast control response, but the control performance relies significantly on knowledge of the APF parameters. Despite the simple and robust feature of the hysteresis controller, this approach also has an inherent drawback: switching frequency variation, which causes a difficulty in design of an output filter for the APF and results in unwanted resonance problems with the networks. In addition, in order to achieve good current performance, the hysteresis band must be set as small as possible. It results in a significant increasing of the switching frequency and consequently introduces higher switching loss on the APF.

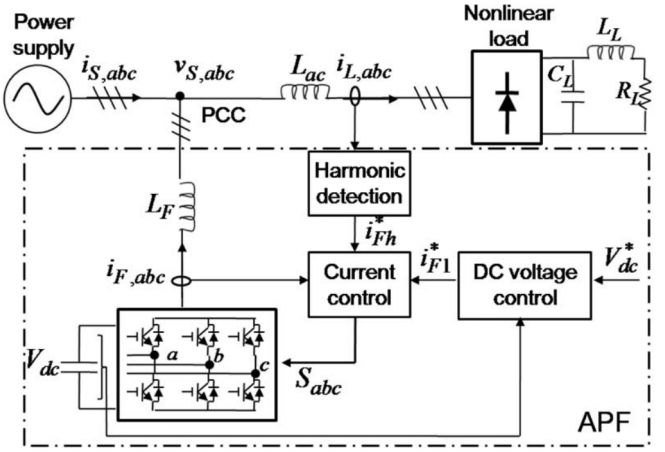

Fig. 1 Typical control scheme of a shunt APF

In recent years, several high-performance current controllers have been developed for APFs to achieve good control performance. In these control schemes, the current controllers are employed in the fundamental reference frame, consisting of a proportional controller plus multiple sinusoidal signal integrators, a PI controller plus a series of resonant controllers, or vector PI (VPI) controllers. In fact, the VPI controller is an alternative version of resonant controller that has superior and robust characteristics when compensating high-order harmonic currents. These control schemes are capable of providing good control performances thanks to high-performance current controllers. However, as illustrated in Fig. 1, the performance of the APF relies on not only the current controller but also the harmonic currents detector. The harmonic detector aims to extract the harmonic components presented in the load currents whose output becomes the reference filter current for the APF. Thus, the performance of this process critically impacts on the accuracy of the APF. The harmonic detector is typically employed by using filters such as high-pass, low-pass, adaptive filters, or through complex mathematical functions. However, by using these filters, it is difficult to achieve both fast response and good steady-state harmonic tracking performance because of a compromise: if the filters are designed to achieve good steady-state performance, their response becomes slow and vice-versa. As a result, the use of a harmonic detector in the control scheme may have an adverse effect on both the accuracy and response of an APF.

In order to avoid the use of harmonic detectors, indirect current control schemes have been introduced in where the supply currents (*iS,abc*) are directly measured and regulated to be sinusoidal. Hysteresis controller was used in the current control loop to force the supply current to be sinusoidal. However, as mentioned earlier, this method has a drawback, i.e., the variation of the switching frequency, so that the supply current regularly contains many switching noises. Meanwhile, the PI controller and the proportional controller are utilized, respectively. They obviously have a limitation on the control bandwidth and are unable to accurately regulate high-frequency signals such as harmonic currents. Consequently, it is hard to achieve a good performance of the supply currents. Authors demonstrated that indirect control method is able to provide better performances compared to direct one since it can prevent inaccurate tracking performances of the harmonic detector. Nevertheless, in this control scheme, two sets of current sensors are required. In addition, the reference supply current is given based on the supply voltage which is assumed to be a pure sinusoidal waveform. Thus, the performance of the supply current is degraded when the supply voltage is distorted.

Adopting the advantage of indirect current control schemes, i.e., the absence of a harmonic detector, this paper proposes an advanced control strategy to enhance the APF performance. In the proposed control scheme, the supply currents are directly measured and regulated to be sinusoidal by an effective harmonic compensator, which is developed based on a PI plus VPI controllers and implemented in the fundamental reference frame. Owing to the effectiveness of the proposed PI-VPI controller, the harmonic currents produced by the nonlinear load can be accurately compensated without the demand of a load current measurement and harmonic detector. The absence of the harmonic detector not only simplifies the control scheme but also significantly improves the accuracy of the APF since the control performance is no longer affected by the performance of the harmonic tracking process. Moreover, the total cost to implement the proposed APF is lower, owing to the minimized current sensors and the use of a four-switch three-phase inverter (FSTPI). Despite the simplified hardware, the performance of the APF is significantly improved compared to the traditional control scheme thanks to the superiority of the proposed compensation scheme. And also, the proposed control algorithm is capable of mitigating harmonic currents as well as reactive power to achieve unity power factor condition at the supply side. The

proposed control scheme is theoretically analyzed, and a 1.5-kVA APF is built in the laboratory to validate the feasibility of the proposed control strategy.

II. CONTROL STRATEGY

A. Structure of a Shunt APF:

Three-phase diode rectifiers are widely used as the front-ends of industrial ac drives. These types of loads introduce harmonic currents into the networks, which have odd orders: $6n \pm 1$(n = 1, 2, 3....) of the fundamental frequency. Since these harmonic currents cause serious problems and deteriorate the power quality of the distribution networks, the shunt APF was developed to compensate those harmonic currents and consequently to improve the power quality. As illustrated in Fig. 1, a shunt APF is basically a three phase voltage source inverter (VSI) connected in parallel with a nonlinear load at the point of common coupling through an inductor *LF*. The energy storage of the APF is a large capacitor located at the dc-link side of the inverter. The nonlinear load can be presented as a RL or RLC load connected to the power supply through a three-phase diode rectifier as shown in Fig. 1. As stated earlier, the APF must generate the harmonic currents to compensate harmonics produced by the nonlinear load and to make the supply currents sinusoidal. To fulfill these demands, the traditional control scheme requires a harmonic detector and current controller where both loops must be designed properly to achieve good control performance. However, it may cause excessive complexity in the design process.

B. Proposed Control Strategy:

In order to simplify the control scheme and to enhance the accuracy of the APF, an advanced control strategy is proposed, as shown in Fig. 2. In Fig. 2, the proposed control scheme is implemented by using only the supply current (*iSa* and *iSb*) without detecting the load current (*iL,abc*) and filter current (*iF,abc*). Thereby, the load current sensors and filter current sensors in the typical shunt APF shown in Fig. 1 can be eliminated. And also, the harmonic current detection is omitted.

Due to the absence of harmonic detection, the proposed control scheme can be implemented with only two loops: the outer voltage control and the inner current control. The outer loop aims to keep dc-link voltage of the APF constant through a PI controller, which helps the APF deal with load variations. The output of this control loop is the reference active current in the

fundamental reference frame (*i□ Sd*). Meanwhile, the reference reactive current (*i□ Sq*) is simply set to be zero, which ensures the reactive power provided by the power supply to be zero. And, the reactive power caused by loads is supplied by the shunt APF. The inner loop is then used to regulate the supply current in the fundamental reference frame (*iS,dq*) by using the proposed PI-VPI current controller. The output of this loop becomes the control signal (*v□ F,ab*) applied to the four-switch APF which is implemented by the FSTPI. Since the current control is executed without the harmonic detector, the control performance of the APF only relies on the current controller. In the next section, the analysis and design of the proposed current controller will be presented.

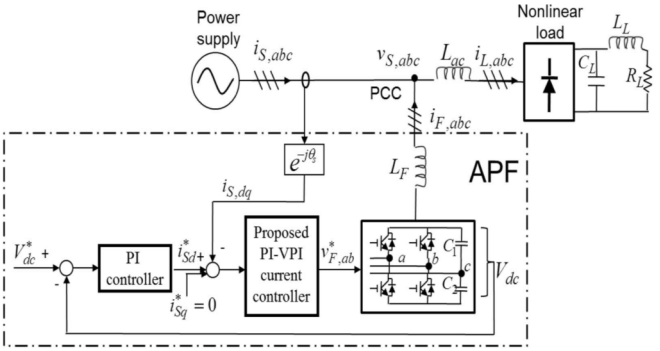

Fig. 2 Proposed control scheme for three-phase shunt APF

III. CURRENT CONTROL SCHEME USING PI PLUS VPI CONTROLLERS IN FUNDAMENTAL REFERENCE FRAME

A. Proposed Current Controller

As illustrated in Fig. 1, harmonic components are detected from the load current by means of the harmonic detector whose output is the reference filter current for the APF. Since the reference filter current is a non-sinusoidal signal, design of current controller for an APF is a challenging task. A series of resonant controllers tuned at harmonic frequencies is typically required for achieving good current performance. In contrast, in the proposed control scheme shown in Fig. 2, the supply current is directly sensed, and the current controller is executed to regulate the supply current to be sinusoidal. Normally, a conventional PI controller employed in the fundamental reference frame is sufficient for regulating the sinusoidal signals since these signals behave as dc signals in this frame. However, in the APF system, it is

impossible to force the supply currents to be sinusoidal by using only a PI controller because the supply currents are not directly but indirectly controlled by regulating the filter currents which are the non-sinusoidal signals. In fact, due to the limitation of the control bandwidth, the PI controller is unable to adequately regulate the high frequency signals, e.g., harmonic currents. As a result, the desired control target of the APF cannot be achieved by using only PI current controller.

In order to effectively regulate the supply currents to be sinusoidal, the current controller must have high gains at harmonic frequencies, which can be achieved by means of multiple resonant controllers tuned at harmonic frequencies. The transfer function of multiple proportional resonant controllers in the s-domain is given as

$$G_{\mathrm{PR}} = \sum_{h=1,5,7,11,13\ldots} K_{ph} + \frac{2K_{rh}s}{s^2 + (h\omega_s)^2} \qquad (1)$$

where *Kph* and *Krh* are the proportional and resonant gains of the resonant controller, respectively, *h* is the order of harmonic currents, and ωs is the fundamental frequency of the supply voltage.

However, as shown in (1), each resonant controller has a responsibility to regulate only one harmonic component. Thus, the controller complexity and computational burden are significantly increased if large numbers of harmonic currents are required to be compensated.

In fact, each pair of $h = 6n \pm 1$ harmonic currents behave as $h = 6n$ harmonic currents in the fundamental reference frame. Thus, it is possible to perform a resonant controller tuned at $h = 6n$ multiples of ωs in this reference frame to regulate a pair of $h = 6n \pm 1$ harmonic currents. The transfer function of the PI controller plus resonant controllers in the s-domain is given as

$$G_{\mathrm{PI\text{-}R}} = K_{p1} + \frac{K_{i1}}{s} + \sum_{h=6,12,18\ldots} K_{ph} + \frac{2K_{rh}s}{s^2 + (h\omega_s)^2} \quad (2)$$

Where *Kp*1 and *Ki*1 are the proportional and integrator gains of the PI controller, respectively, $h = 6n$ is the order of harmonics in the fundamental reference frame with $n = 1, 2, 3 \ldots$. In (2), the aim of the PI controller is to regulate the fundamental current whereas resonant controllers are used to control the harmonic currents. However, the delay time caused by the effect of

the APF and digital implementation must be taken into account if the high-order harmonics are compensated. A compensation term is added to (2) to compensate the delay time, the transfer function of the PI-R controller becomes

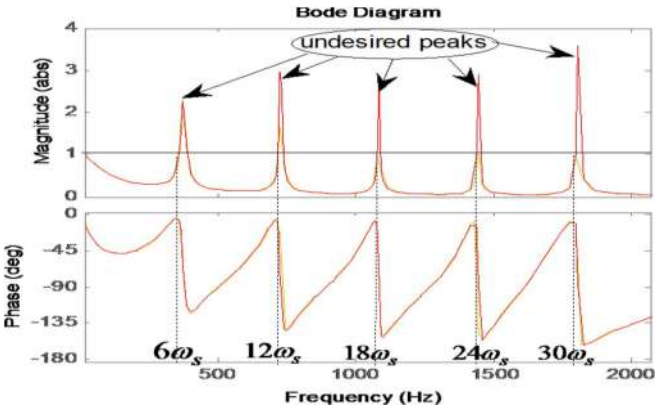

Fig. 3. Closed-loop Bode diagram of PI-R controller with compensation method given in (3) with $N = 2$, $h = 6n$, and $n = 1...5$.

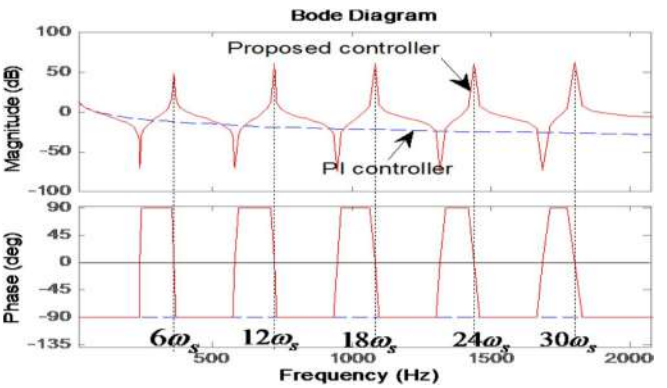

Fig. 4. Open-loop Bode diagrams of the conventional PI and proposed controller.

$$G_{\text{PI-R}} = K_{p1} + \frac{K_{i1}}{s} + \sum_{h=6,12,18\ldots} K_{ph} + 2K_{rh}\frac{s\cos(h\omega_s NT_s) - h\omega_s \sin(h\omega_s NT_s)}{s^2 + (h\omega_s)^2} \quad (3)$$

where N is the number of samples and TS is the sampling period. The best result is obtained when $N = 2$.

The compensation method given in (3) only considers the delay time caused by digital implementation and neglect the effect of the APF: the stability margins are reduced, and undesired peaks appear in the closed-loop frequency response when the order of the compensated harmonic increases as shown in Fig. 3. In order to overcome these problems, an alternative solution of the resonant controller, the VPI controller, has been introduced. The transfer function of the VPI controllers in the s-domain is

$$G_{\text{VPI}} = \sum_{h=6,12,18\ldots} 2\frac{K_{ph}s^2 + K_{rh}s}{s^2 + (h\omega_s)^2}. \qquad (4)$$

The VPI controller is able to cancel the coupling term with the form1/($sLF + RF$) by selecting the resonant gain as $Krh = KphRF/LF$, where LF and RF are the inductance and the equivalent resistance of the LF inductor, respectively. Owing to this advantage, the VPI controller is able to remove anomalous peaks appearing in the closed-loop response without demand of delay compensation. Adopting the superiority of the VPI controllers over resonant controllers, VPI controllers given in (4) are used to replace resonant controllers in (2), the transfer function of the proposed PI-VPI current controller in the s-domain is given as follows:

$$G_{\text{PI-VPI}} = K_{p1} + \frac{K_{i1}}{s} + \sum_{h=6\ldots30} 2\frac{K_{ph}s^2 + K_{rh}s}{s^2 + (h\omega_s)^2}. \qquad (5)$$

In order to investigate the superior characteristics of the proposed PI-VPI controller over the traditional PI controller, Fig. 4 describes open-loop Bode diagram for the traditional PI and the proposed controllers given in (5) for the case of $h = 6n$, $n = 1. . . 5$, $\omega s = 2\pi 60$ rad/s, $Kph = 1$, and $Krh = KphRF/LF$. As illustrated in Fig. 4, at low frequency (less than 20 Hz), the gains of both the PI and proposed controllers are high and comparable, but at high frequencies, i.e., selected resonant frequencies ($6\omega s$, $12\omega s$, $18\omega s$, $24\omega s$, and $30\omega s$), the gain of the PI controller is significantly reduced while the proposed controller produces very high gains for ensuring zero steady-state errors in compensating the harmonic currents.

As mentioned earlier, the PI-R controller given in (3) is also able to produce high gains at selected resonant frequencies and overcome the limitation of the PI controller. However, as presented in Fig. 3, undesired peaks appear in the closed-loop frequency response of the PI-R controller when it compensates high-order harmonic components. In contrast, the proposed PI-VPI controller is capable of preventing this problem owing to its pole-zero cancellation capability with the *LF* inductor.

Taking into account the *LF* inductor model defined by (6), the closed-loop transfer function of the proposed current control is defined in (7), shown at the bottom of the next page

$$G_{L_F} = \frac{1}{sL_F + R_F}. \qquad (6)$$

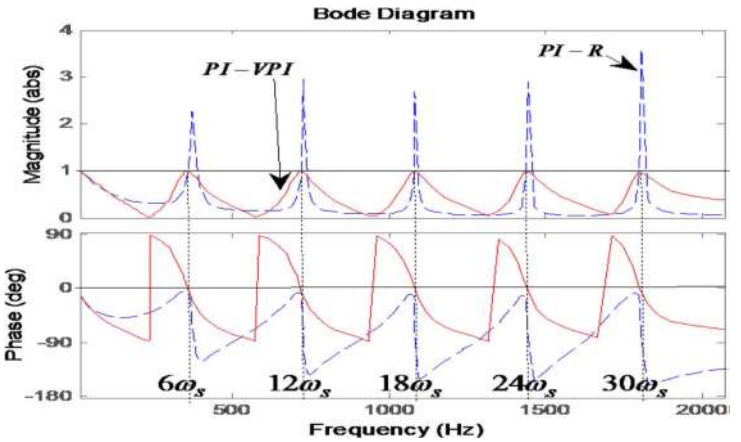

Fig. 5. Closed-loop Bode diagrams of the PI-VPI and PI-R controller

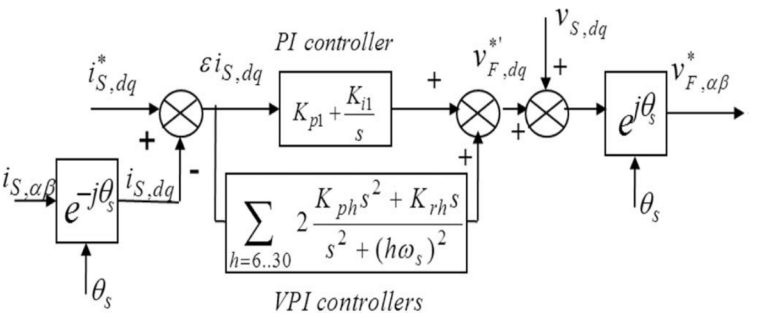

Fig. 6. Block diagram of the proposed current control scheme

Fig. 5 presents the Bode diagram of the closed-loop transfer function for the proposed controller and the PI-R controller with $h = 6n$, $n = 1 \ldots 5$, $Kph = 1$, and $Krh = KphRF/LF$. As shown in Fig. 5, the proposed controller provides unity gain and zero phase-shift for all selected resonant frequencies while there are undesired peaks in the closed loop of the PI-R controller. Thus, the use of VPI controllers significantly improves the stability margin and accuracy of the proposed current controller.

The complete proposed current control scheme using the PI-VPI controller is shown in Fig. 6. Since the proposed current controller is designed in the fundamental reference frame, the measured supply current $iS,\alpha\beta$ first must be transformed from the stationary to the fundamental reference frame iS,dq. The proposed current controller is then executed to regulate this current follow its reference $i\square S,dq$. The outputs of the current controllers $v\square'F,dq$ and the feedforward supply voltage term vS,dq are added together and then transformed in the stationary reference frame through an inverse rotational transformation to obtain the command voltage $v\square F,\alpha\beta$, which is the control signal for the APF.

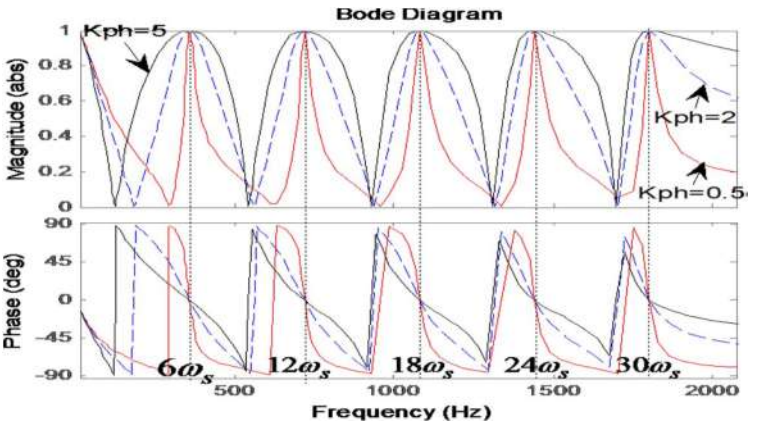

Fig. 7. Closed-loop Bode diagrams of the VPI controllers with *Kph* = 0.5, *Kph* = 2, and *Kph* = 5.

B. Current Controller Design:

In order to design the gains for the PI-VPI controller and to investigate the effect of these gains on the control performance, the closed-loop transfer function of the PI-VPI current controller defined in (7) is analyzed. By selecting the resonant gain as $Krh = KphRF/LF$ and $Ki1 = Kp1RF/LF$, the closedloop transfer function of the PI-VPI controller becomes (8), shown at the bottom of the page.

In (8), *Kph* and *Kp*1 are the only gains that need to be tuned. In fact, *Kp*1 is the integrator gain of the PI controller that does not affect the harmonic compensation performance of the VPI controller. Thus, for the sake of simplification, *Kp*1 is kept constant, and *Kph* is changed to determine the control performance of the VPI controller. The Bode diagram is illustrated in Fig. 7 with *Kph* = 0.5, *Kph* = 2, and *Kph* = 5. As shown in Fig. 7, at selected resonant frequencies, the VPI controller provides a unity gain and zero phase-shift, regardless of the value of *Kph*. Moreover, the narrowest bandwidth is achieved with*Kph* = 0.5, which indicates that the VPI controller is more selective and obtain better steady-state performance if *Kph* is a smaller value. In harmonic compensation application, the steady-state performance is regarded as the most critical index; thus it prefers to choose *Kph* to be a small value (*Kph* < 1).

$$G_C = \frac{G_{\text{PI-VPI}} G_{L_F}}{1 + G_{\text{PI-VPI}} G_{L_F}} = \sum_{h=6...30} \frac{(K_{p1} + 2K_{ph})s^3 + (K_{i1} + 2K_{rh})s^2 + K_{p1}(h\omega_s)^2 s + K_{i1}(h\omega_s)^2}{L_F s^4 + (K_{p1} + 2K_{ph} + R_F)s^3 + (K_{i1} + 2K_{rh} + L_F(h\omega_s)^2)s^2 + (R_F + K_{p1})(h\omega_s)^2 s + +K_{i1}(h\omega_s)^2} \quad (7)$$

$$G_C = \sum_{h=6...30} \frac{(K_{p1}L_F + 2K_{ph})s^2 + 2K_{ph}K_{p1}s + K_{p1}L_F(h\omega_s)^2}{L_F s^3 + (K_{p1}L_F + 4K_{ph})s^2 + (2K_{ph}K_{p1} + L_F(h\omega_s)^2)s + K_{p1}L_F(h\omega_s)^2} \quad (8)$$

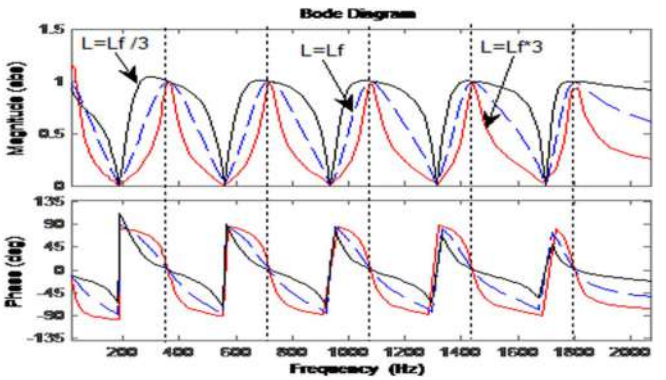

Fig. 8. Closed-loop Bode diagrams of the VPI controllers with variation of the inductor parameters

However, we should not select a too small *Kph* since it may degrade the dynamic responses of the APF. The controller gains obtained by using aforementioned design process are kept constant during whole operating time. However, the inductor parameters are changed during operation, so that the relationship, *Krh = KphRF /LF* , is no longer satisfied. Fig. 8 shows the Bode diagram of (7) in order to investigate the robustness of the VPI controller against the inductor parameter variation. As can be seen in Fig. 8, the VPI controller still maintains a unity gain and zero phase-shift at a selected resonant frequency regardless of the different inductor parameter, which means that the inductor parameter variation has no effect on the stability and steady-state performance of the APF.

C. Discrete-Time Implementation of the VPI Controllers:

An important step to realize any digital controller is discretization, which transfers the controller from the continuous time to the discrete-time type to be implemented with digital processors such as microcontrollers or digital signal processors (DSPs). Because of the narrow band and infinite gain

characteristics of the resonant and VPI controllers, a slight displacement of the resonant poles causes a significant loss of performance. Therefore, the selection of a discretization technique is critical and significantly impacts on the accuracy and control performance of the VPI controllers. To achieve accurate resonant pole placement, the transfer function of the VPI controller in the z-domain must be determined as follows:

$$G_{\mathrm{VPI}}(z)=\frac{K_{ph}+(K_{rh}T_s-2K_{ph})z^{-1}-(K_{rh}T_s-K_{ph})z^{-2}}{1-2\cos(h\omega_s T_s)z^{-1}+z^{-2}} \tag{9}$$

Where *z* is the shift operator

The transfer function given in (9) provides an accurate resonant pole placement, but the trigonometric portion of the formula, i.e., the cosine function, must be online calculated and consumes a large amount of execution time as part of the control scheme, particularly when the control algorithm is implemented in low-performance microprocessors or DSPs. So as to avoid this large calculation time, the cosine function is approximated by means of a Taylor series as given by

$$\cos(h\omega_s T_s)=1-\frac{(h\omega_s T_s)^2}{2}+\frac{(h\omega_s T_s)^4}{24}-\frac{(h\omega_s T_s)^6}{720}+\ldots. \tag{10}$$

A higher order approximation results in a more precise result, but an approximation of fourth order also can provide sufficient accuracy and high performance with significantly reduced computation time for the VPI controllers. Therefore, a fourth order approximation is used to replace the cosine function in (9). The transfer function of the VPI controller in the z-domain can now be rewritten as

$$G_{\mathrm{VPI}}(z) = \frac{K_{ph}+(K_{rh}T_s-2K_{ph})z^{-1}-(K_{rh}T_s-K_{ph})z^{-2}}{1-2\left(1-\frac{(h\omega_s T_s)^2}{2}+\frac{(h\omega_s T_s)^4}{24}\right)z^{-1}+z^{-2}}. \tag{11}$$

IV. DESCRIPTION OF THE WHOLE CONTROL STRATEGY

Fig. 9 illustrates the block diagram of whole proposed control strategy. As aforementioned, the proposed control scheme contains two main loops: the dc-link voltage control and the supply current control. In addition, since the

proposed current controller is employed in the fundamental reference frame, a phase-locked loop (PLL) is required to track the phase of the supply voltage which is needed for coordinate transformation and synchronization.

A. DC-Link Voltage Control Loop:

As stated earlier, this control loop aims to keep dc-link voltage of the shunt APF constant through a simple PI regulator, whose output is the reference active current in the fundamental reference frame as follows:

$$i_{Sd}^{*} = \left(K_{\mathrm{pdc}} + \frac{K_{\mathrm{idc}}}{s}\right)(V_{\mathrm{dc}}^{*} - V_{\mathrm{dc}}) \qquad (12)$$

where *Kp*dc and *Ki*dc are the proportional and integrator gains of the PI controller, respectively, and *V* □ dc and *V*dc are reference and measured dc-link voltages of the APF, respectively.

In fact, since the four-switch APF has only two switching legs, the four-switch APF needs a higher dc-link voltage reference (*V* □ dc) compared to the traditional six-switch APF as mentioned in Table I. In addition, since the dc-link voltage of the APF contains small ripples at harmonic frequencies due to harmonic currents, a low-pass filter (LPF) is designed to eliminate all ripples in the feedback measurement of the dc-link voltage, which helps in smoothing the reference current *i*□ *Sd*.

In the proposed control scheme, the role of the dc-link voltage controller is not only to ensure a proper operation of the APF but also to help the APF deal with load variations. In this paper, even though the load current measurement is not used, the load changes can be detected indirectly through dc link voltage variations. Hence, by detecting and regulating the dc-link voltage, the shunt APF can recognize and respond against load variations without the load current measurement.

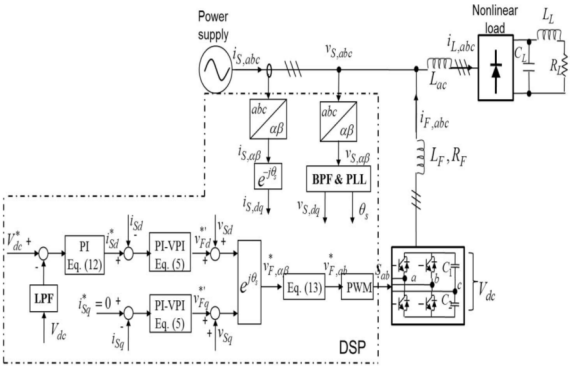

Fig. 9 Block diagram of the proposed control scheme

TABLE I

SYSTEM PARAMETERS

Supply voltage RMS line-line	127 V
Supply frequency	60 Hz
5th harmonic supply voltage	10% of the fundamental component
7th harmonic supply voltage	5% of the fundamental component
DC-link reference voltage for the six-switch APF V_{dc}^{*}	260 V
DC-link reference voltage for the four-switch APF V_{dc}^{*}	420 V
DC-link capacitor for four-switch APF C_1=C_2	1000 μF
DC-link capacitor for six-switch APF C=C_1+C_2	2000 μF
Filter resistance R_F	0.05 Ω
Filter inductance L_F	2 mH
Nonlinear RLC load	$R_{L(\min)}$=12.5 Ω, $R_{L(\max)}$=20 Ω, L_L=1 mH, C_L=2200 μF

B. Supply Current Control Loop:

This loop regulates the supply current by means of the proposed current control scheme shown in Fig. 6. The reference active current $i* Sd$ is the output of the dc-link voltage control loop given in (13), while the reference reactive current $i* Sq$ is simply set to be zero. Consequently, the reactive power caused by loads can be fully compensated by the APF, and also unity power factor condition is achieved at the supply side.

C. Control Signal Computation for the Four-Switch APF:

The traditional three-phase VSI is commonly used to implement an APF. In this paper, in order to accomplish a low cost APF topology, the four-switch APF is introduced by replacing the traditional three-phase VSI with the FSTPI without degrading the performance of the proposed control strategy. The FSTPI, which is composed of four power switching devices and two split capacitors, has been applied for low-cost ac motor drives. In Fig. 9, the control signal in the stationary reference frame ($v^*_{F,\alpha\beta}$) obtained after executing the current controller is changed into control signals of the four-switch APF as the following equations:

$$v^*_{Fa} = \sqrt{\frac{3}{2}} v^*_{F\alpha} + \sqrt{\frac{1}{2}} v^*_{F\beta}$$
$$v^*_{Fb} = \sqrt{2} v^*_{F\beta} \qquad (13)$$

Where v^*_{Fa} and v^*_{Fb} are the control signals for leg a and b of the four-switch APF, respectively.

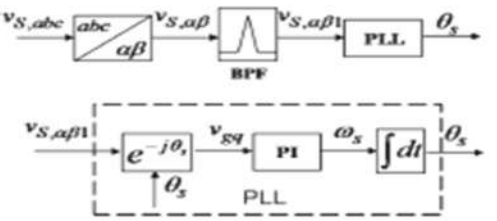

Fig.10 control diagram

D. Supply Voltage PLL:

The aim of this loop is to track the phase of the supply voltage, which is a necessary component for any converter interfacing with grid. In practical distribution network, supply voltage is regularly not pure sinusoidal but contains harmonic components, which may affect to the accuracy of the PLL. To overcome this problem, a band pass filter (BPF) tuned at the fundamental frequency of the supply voltage is implemented to reject all of the harmonic components contained in supply voltage, and its output contains only the fundamental component which is used as the input of the PLL block. The block diagram of the improved PLL is illustrated in Fig. 10. Even though the BPF used in the PLL can cause a small time delay in tracking the phase angle

of the supply voltage, it is negligible because the PLL usually operates at steady-state condition before the

APF is active.

TABLE II

CURRENT CONTROLLER GAINS

$K_{p1} = 4$	$K_{i1} = 100$	$K_{p18} = 0.3$	$K_{r18} = 7.5$
$K_{p6} = 0.8$	$K_{r6} = 20$	$K_{p24} = 0.1$	$K_{r24} = 2.5$
$K_{p12} = 0.6$	$K_{r12} = 15$	$K_{p30} = 0.1$	$K_{r30} = 2.5$

V. SIMULATION RESULTS

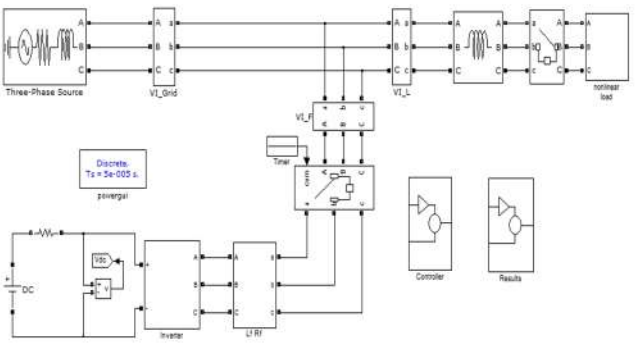

Fig 11. Simulation diagram of proposed system

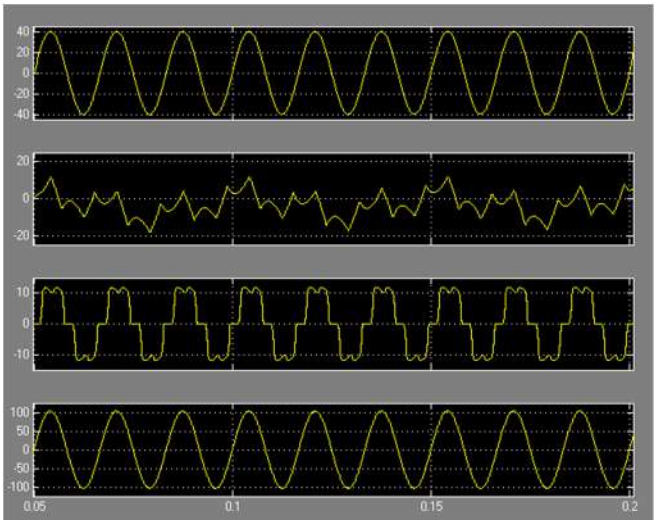

Fig. 12 Steady-state performance with PI current controller under RL load

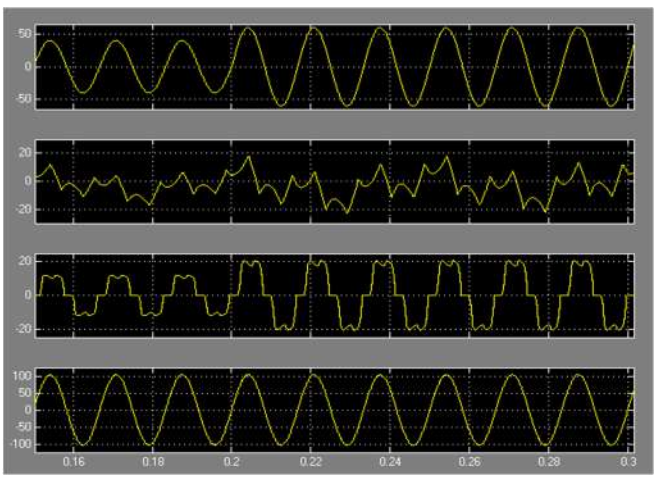

Fig. 13 Steady-state performance with proposed control scheme under RL load

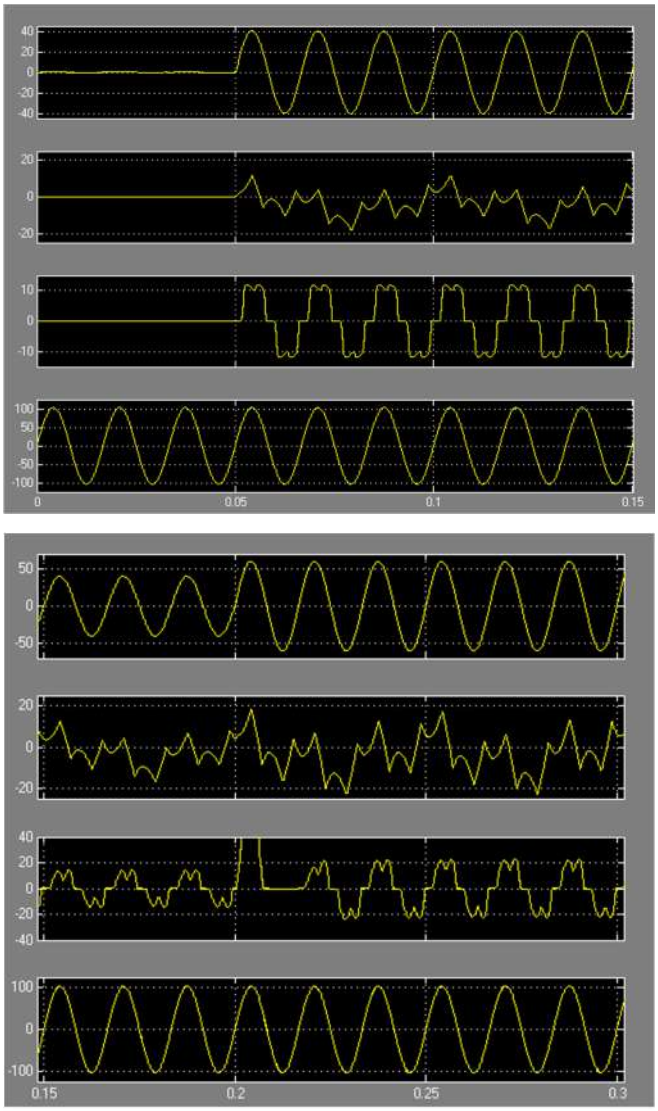

Fig. 14. Dynamic responses of proposed control scheme under RL load variations: (a) load applied (b) load changed

VI. CONCLUSION

The outputs of the proposed control strategy was verified through various simulation results, where the proposed control strategy presented good steady-state performance with nonlinear RL and RLC loads as well as good dynamic response against load variations: the supply current is almost perfect sinusoidal and in-phase with the supply voltage even under the distorted voltage condition. The simulation results verified that the absence of a harmonic detector results in faster transient responses as well as assures notches free in steady-state performances of the supply current. Moreover, we also confirmed that the FSTPI can be used to implement the APF without any degradation in the APF performance.

VIII.Acknowledgment

This paper is based on M. Tech. project carried out by the student of pydah college of engineering & technology, Kakinada studying M.Tech (Power Electronics) The project had been completed by Ms. K. SRINIVASULU bearing H.T.no.: 126T1D4305 under the guidance of B. LALITHA KUMARI.

REFERENCES

1. *Recommended Practice for Harmonic Control in Electric Power Systems*, IEEE Std. 519-1992, 1992.
2. *Limits for Harmonic Current Emission*, IEC 61000-3-2, 2001.
3. H. Akagi, "New trends in active filters for power conditioning," *IEEE Trans. Ind. Appl.*, vol. 32, no. 2, pp. 1312–1332, Nov./Dec. 1996.
4. F. Z. Peng, "Application issues of active power filters," *IEEE Ind. Appl. Mag.*, vol. 4, no. 5, pp. 21–30, Sep./Oct. 1998.
5. H. Akagi, E. H. Watanabe, and M. Aredes, *Instantaneous Power Theory and Applications to Power Conditioning*, M. E. El-Hawari, Ed New York: Wiley, 2007.
6. S. Buso, L. Malesani, and P. Mattavelli, "Comparison of current control techniques for active filters applications," *IEEE Trans. Ind. Electron.*, vol. 45, no. 5, pp. 722–729, Oct.
7. L.Malesani, P. Mattavelli, and S. Buso, "Robust dead-beat current control for PWM rectifiers and active filters," *IEEE Trans. Ind. Appl.*, vol. 35, no. 3, pp. 613–620, May/Jun. 1999.
8. S. Rahmani, N. Mendalek, and K. Al-Haddad, "Experimental design of a nonlinear control technique for three-phase shunt active power filter," *IEEE Trans. Ind. Electron.*, vol. 57, no. 10, pp. 3364–3375, Oct. 2010.

9. H. Hu, W. Shi, Y. Lu, and Y. Xing, "Design considerations for DSP controlled 400 Hz shunt active power filter in an aircraft power system," *IEEE Trans. Ind. Electron.*, vol. 59, no. 9, pp. 3624–3634, Sep. 2012.
10. Z. Chen, Y. Luo, and M. Chen, "Control and performance of a cascaded shunt active power filter for aircraft electric power system," *IEEE Trans. Ind. Electron.*, vol. 59, no. 9, pp. 3614–3623, Sep. 2012.
11. L. Asiminoaei, F. Blaabjerg, and S. Hansen, "Detection is key—Harmonic detection methods for active power filter applications," *IEEE Ind. Appl. Mag.*, vol. 13, no. 4, pp. 22–33, Jul.Aug. 2007.
12. R. R. Pereira, C. H. da Silva, L. E. B. da Silva, G. Lambert-Torres, and J. O. P. Pinto, "New strategies for application of adaptive filters in active power filters," *IEEE Trans. Ind. Appl.*, vol. 47, no. 3, pp. 1136–1141, May/Jun. 2011.
13. Bhattacharya and C. Chakraborty, "A shunt active power filter with enhanced performance using ANN-based predictive and adaptive controllers," *IEEE Trans. Ind. Electron.*, vol. 58, no. 2, pp. 421–428, Feb. 2011.
14. F. A. S. Neves, H. E. P. de Souza, M. C. Cavalcanti, F. Bradaschia, and E. J. Bueno, "Digital filters for fast harmonic sequence component separation of unbalanced and distorted three-phase signals," *IEEE Trans. Ind. Electron.*, vol. 59, no. 10, pp. 3847–3859, Oct. 2012.
15. R. I. Bojoi, G. Griva, V. Bostan, M. Guerriero, F. Farina, and F. Profumo, "Current control strategy for power conditioners using sinusoidal signal integrators in synchronous reference frame," *IEEE Trans. Power Electron.*, vol. 20, no. 6, pp. 1402–1412, Nov. 2005.
16. C. Lascu, L. Asiminoaei, I. Boldea, and F. Blaabjerg, "Frequency response analysis of current controllers for selective harmonic compensation in active power filters," *IEEE Trans. Ind. Electron.*, vol. 56, no. 2, pp. 337– 347, Feb. 2009.
17. L. Limongi, R. Bojoi, G. Griva, and A. Tenconi, "Digital current-control schemes," *IEEE Ind. Electron. Mag.*, vol. 3, no. 1, pp. 20–31, Mar. 2009.
18. C. Lascu, L. Asiminoaei, I. Boldea, and F. Blaabjerg, "High performance current controller for selective harmonic compensation in active power filters," *IEEE Trans. Power Electron.*, vol. 22, no. 5, pp. 1826–1835, Sep. 2007.
19. B. N. Singh, A. Chandra, and K. Al-Haddad, "Performance comparison of two current control techniques applied to an active filter," in *Proc. 8thICHQP*, Athens, Greece, Oct. 14–16, 1998, vol. 1, pp. 133–138.
20. J. W. Dixon, J. M. Contardo, and L. A. Moran, "A fuzzy-controlled active front-end rectifier with current harmonic filtering characteristics and minimum sensing variables," *IEEE Trans. Power Electron.*, vol. 14, no. 4, pp. 724–729, Jul. 1999.

INTERNATIONAL JOURNAL OF MULTIDISCIPLINARY EDUCATIONAL RESEARCH
ISSN : 2277-7881; IMPACT FACTOR - 2.972; IC VALUE:5.16
VOLUME 3, ISSUE 10(4), OCTOBER 2014

A MULTI OBJECTIVE CURRENT & POWER CONTROLLER FOR DISTRIBUTED GENERATION (DG) RESOURCES

MS. K. SRAVANI SANDHYA
katta.sravanasandhya@gmail.com
Under the guidance of
Mr. P. VIJAYA RAMARAO
ASSISTANT PROFESSIOR
PYDAH COLLEGE OF ENGINEERING , KAKINADA

Abstract— The proposed strategy provides compensation for active, reactive, and harmonic load current components during connection of DG link to the grid. The proposed control method of this paper does not need a phase-locked loop in control circuit and has fast dynamic response in providing active and reactive power components of the grid-connected loads. The dynamic model of the proposed system is first elaborated in the stationary reference frame and then transformed into the synchronous orthogonal reference frame. The transformed variables are used in control of the voltage source converter as the heart of the interfacing system between DG resources and utility grid. By setting an appropriate compensation current references from the sensed load currents in control circuit loop of DG, the active, reactive, and harmonic load current components will be compensated with fast dynamic response, thereby achieving sinusoidal grid currents in phase with load voltages, while required power of the load is more than the maximum injected power of the DG to the grid. The effectiveness of the proposed control technique in DG application is demonstrated with injection of maximum available power from the DG to the grid, increased power factor of the utility grid, and reduced total harmonic distortion of grid current.

Key Terms— distributed generation (DG), renewable energy sources, voltage source converter (VSC).

I. INTRODUCTION

Over the past two decades, declines in the costs of small scale electricity generation, increases in the reliability needs of many customers, and the partial deregulation of electricity markets have made DG technology more attractive to businesses and households as a supplement to utility-supplied power. Distributed Generation (DG) technology also known as dispersed generation technology is electricity generating plant connected to a

distribution grid rather than the transmission network. There are many types and sizes of DG facilities. These include wind farms, solar photovoltaic (PV) systems, hydroelectric power, or one of the new smaller generation technologies.

The DG concept emerged as a way to integrate different power plants, increasing the DG owner's reliability and security, providing additional power quality benefits of the power grid and improving the air quality as a result of lower greenhouse gas emissions of air pollutants. In addition, the cost of the distribution power generation system using the renewable energies is on a falling trend and is expected to fall further as demand and production increase. DG technology can come from conventional technologies such as motors powered by natural gas or diesel fuel or from renewable energy technologies, such as solar PV cells and wind farms. However, the increasing number of DG units in electrical networks requires new techniques for the operation and management of the power networks in order to maintain or even to improve the power supply reliability and quality in the future. As a consequence, the control of DG unit should be improved to meet the requirements for the electrical network. Therefore, design of a control technique, which considers different situations of the electrical networks, becomes of high interest for interconnection of DG units to the power grid. Numerous control techniques and strategies have been proposed and reported for the control and connection of DG units to the electrical grid. An overview of different control and synchronization techniques for DG systems has been presented. Different hardware structures for the DG system, control strategies for the grid-side converter, and control strategies under fault conditions were addressed. Different implementation techniques like *dq*, stationary, and natural frame control structures were presented, and their major characteristics were pointed out. A discussion about different controllers in DG system and their ability to compensate low-order harmonic components presented in the utility grid was given. Finally, an overview of grid synchronization strategies, their influences, and roles in the control of DG system on normal and faulty grid conditions were discussed.

A control concept was proposed that provides sharing of harmonic load currents between parallel connected converters without mutual communication. In this paper, a converter operates as an active inductor at a certain frequency to absorb the harmonic current components. However, the exact calculation of grid inductance in real-time systems is not simple, and it

can deteriorate the performance of the proposed control strategy. The fact that power grids are faced with unexpected and unavoidable disturbances and uncertainties complicates the design of a practical plug-and play converter-based DG interface. A robust interfacing scheme for DG converters featuring robust mitigation of converter grid resonance at parameter variation, grid-induced distortion, and current-control parametric instabilities is presented. To ensure high disturbance rejection of grid distortion, converter resonance at parameter variation, and parametric instabilities, an adaptive internal model for the capacitor voltage and grid side current dynamics is included within the current-feedback structure. A control algorithm of three-phase voltage source converter (VSC) has been proposed for integration of renewable energy resources to the main grid through an output *L*-type or *LCL*-type filter. The proposed controller provides active damping of the *LCL* resonance mode, robustness with respect to grid frequency, and impedance uncertainty. A control technique is proposed to determine which power lines should be inserted into the power network to optimize voltage profile during the presence of DG. An algorithm is suggested in order to design feasible line drop compensation parameters. This algorithm guarantees the satisfaction of voltage constraints for all possible variations in DG output. DG unit was modelled as a PV node, and its control was coordinated with existing volt/var controls to minimize distribution losses. a centralized control algorithm is proposed to operate the control devices using a communication. The proposed control technique aims that active control of DG output and volt/var regulators be in desirable level in order to allow for higher levels of distributed resource integrations. A loss reduction and approximate power flow formula were suggested in the search for optimal feeder configuration for loss minimization. The impact of DG technology on distribution feeder reconfiguration was described.

Several other control strategies of interfacing system between DG resources and electrical grid proposed and presented for different objectives. In all the proposed methods, a solution has been proposed for an important problem in electrical networks. In this paper, the authors propose a design of a multipurpose control strategy for VSC used in DG system. The idea is to integrate the DG resources to the power grid. With the proposed approach, the proposed VSC controls the injected active power flow from the DG source to the grid and also performs the compensation of reactive power and the

nonlinear load current harmonics, keeping the grid current almost sinusoidal during connection of extra loads to the grid.

The exact feedback linearization theory is applied in the design of the proposed controller. This control technique allows the decoupling of the currents and enhances their tracking of the fast change in the active and reactive power. This paper shows the complete simulation and experimental validation of the proposed method for all its features, i.e., active and reactive power generation along with current harmonic compensation. This paper is organized as follows. The proposed system's model is introduced and discussed in detail in Section II, with a particular focus on the reference current generator. Sections III and IV are related to the modelling of the proposed DG system, with focus on the dynamic and state-space model analysis for control and the current control implementation.

Simulation results of the proposed system are presented in Section V for different conditions. Section VI is related to the experimental results and contains a description of the testing setup followed by a complete experimental validation of the proposed control technique. The experimental results are presented for the grid-connected VSC that generates maximum active power of DG source and compensates for unwanted reactive and harmonic load current component nonlinear loads, thus achieving complete power quality features.

II. PROPOSED DG MODEL

Fig. 1 shows the schematic diagram of the proposed system. Conventional signs of voltages and currents components are also indicated in this schema, where *Rc* and *Lc* represent the equivalent resistance and inductance of the ac filter, coupling transformer, and connection cables; *Rs* and *Ls* represent the grid resistance and inductance up to the point of common coupling (PCC), respectively; *vk* (*k* = 1, 2, 3) is the supply voltage components at the PCC; *vsk* is the grid voltage components; *v*dc is the dc-link voltage; and *isk*, *ilk*, and *ick* are grid, load, and DG current components, respectively. In addition, the DG resources and additional components are represented as a dc current source which is connected to the dc side of the converter.

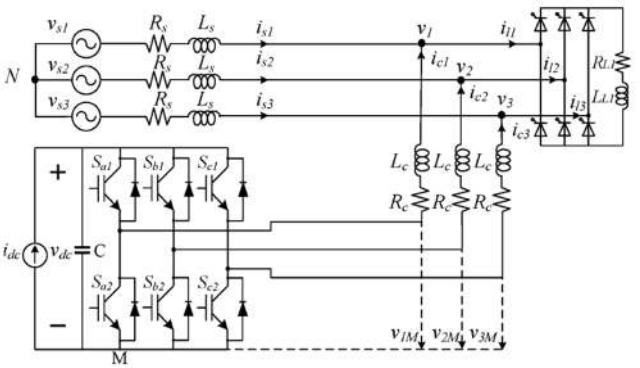

Fig. 1. Schematic diagram of the proposed DG system

III. VOLTAGE AND CURRENT COMPONENTS IN THE SPECIAL REFERENCE FRAMES

The proposed control technique in this paper is based on the analysis of voltage and current vector components in the special reference frames, e.g., 123(abc) to $\alpha\beta$ and $\alpha\beta$ to *dq* transformation. The Clarke transformation maps the three phase instantaneous voltages and currents in the 123 phases into the instantaneous voltages and currents on the $\alpha\beta$-axes. In the next step, the $\alpha\beta$ reference frame is transformed to the rotating synchronous reference frame, i.e., in *dq*-components. The synchronous reference frame uses a reference frame transformation module, to transform the grid current and voltage waveforms into a reference frame that rotates synchronously with the grid voltage. By means of this, the control variables become dc values; thus, filtering and controlling can be achieved easily.

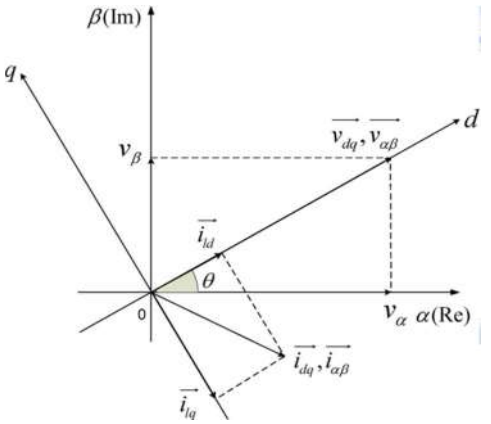

Fig. 2. Voltage and current components in special reference frames

Fig. 2 shows the voltage and current components in $\alpha\beta$ and *dq* reference frames. Considering *d*-axis vector in the direction of voltage vector in this transformation, the *q*-component of voltage in rotating synchronous reference frame is always zero (*vq* = 0). Therefore, the instantaneous angle of grid voltage can be calculated as

$$\theta = \tan^{-1} \frac{v_\beta}{v_\alpha}. \qquad (1)$$

In other words, if we consider the instantaneous angle of load voltage by (1), the reference voltage vector will be in the direction of *d*-axis vector of load voltage, and *q*-axis vector of load voltage will be zero.

According to Fig. 2, the magnitude of the voltage at the PCC can be calculated as

$$v_{\mathrm{ref}} = |\overrightarrow{v_d}| = |\overrightarrow{v_{dq}}| = |\overrightarrow{v_{\alpha\beta}}| = \sqrt{v_\alpha^2 + v_\beta^2}. \qquad (2)$$

In the next stage, reference currents of the DG control loop must be calculated according to the objectives of the proposed DG model.

A. Calculation of Reference Current to Supply Load Active Power

In fundamental frequency, the active power injected from DG link to the grid is

$$P = \frac{3}{2}(v_d I_{cd} + v_q I_{cq}) \qquad (3)$$

where capital letters are related to fundamental frequency of the currents. Therefore, by considering the first assumption (*vq* = 0), *d*-component of reference current to provide active current in fundamental frequency can be calculated by

$$I_{cd}^{*} = \frac{2}{3}\frac{P_{\text{ref}}}{v_d} \qquad (4)$$

where *P*ref is maximum power of the VSC in fundamental frequency and I^{*}_{cd} is the *d*-component of DG link reference current in fundamental frequency. Due to limited output power of proposed VSC, reference current must be restricted. Calculation of *d*-component of reference current with this method makes it possible to control the maximum active power injection into the grid by changing *P*ref. *P*ref depends on DG system capacity, capacity of power electronic interfacing devices and transformers.

B. Calculation of Harmonic Components of d-Axis Reference Current

In the *dq* reference frame, the fundamental current component can be seen as a dc component, and as a consequence, the harmonic load currents can be extracted with high-pass filters (HPFs). The main problem with this method is the delay that occurs when the control system is digitally implemented. To minimize the influence of the HPF phase responses, by means of a low-pass filter (LPF), a minimal phase HPF (MPHPF) can be obtained, and the transfer function of this LPF has order and cutoff frequency as the same as HPF. Thus, the MPHPF can be obtained simply by the difference between the input signal and the filtered one, which is equivalent to performing $H_{\text{MPHPF}}(s) = 1 - H_{\text{LPF}}(s)$. A double-precision filter using the Chebyshev type-II fifth-order LPF is used for this purpose. The filter considered has a cutoff frequency *fc* = (*f*/2)(*f* = 50 Hz) which promises the extraction of dc components in the nonlinear load currents. Therefore, i_{ld} can be expressed as

$$i_{ld} = \tilde{i}_{ld} + I_{ld} \qquad (5)$$

Where $\hat{i}_{ld}$ is alternative *d*-component of load current which is related to harmonic components of load current and I_{ld} is the dc term of load current which is related to fundamental frequency of load current. To use DG link as an active power filter, harmonic components of the nonlinear load current must be supplied. For this purpose, *d*-component of nonlinear link reference

current is achieved by doing the sum of currents in (4) and alternative terms of load current in (5)

$$i^*_{cd} = \tilde{i}_{ld} + \bar{I}\,cd. \qquad (6)$$

C. Calculation of Reference Current to Supply Load Reactive Power

In *dq* frame, quadrature component of load current is perpendicular to direct component of voltage ($v_d \perp i_{lq}$). As a result, *q*-component of load current indicates required reactive power of the load. To compensate load reactive power, DG must provide a current with *q*-component equal to i_{lq}. For this purpose, it is sufficient to set *q*-component of DG's reference current equal to *q*-component of the load current as

$$i^*_{cq} = i_{lq}. \qquad (7)$$

The term of i^*_{cq} is the *q*-component of DG link reference current. By this consideration, total load reactive current and harmonic components of *q*-axis are compensated.

IV. MODELING OF THE DG SYSTEM

For the purposes of this paper, the electric power grid is composed of the generation system, the transmission, or the distribution system, and the loads. The DG source and additional components are represented as a dc current source connected to the dc side of the proposed converter. To draw an appropriate plan to control the integration of DG resources to the power grid, a dynamic analytical model of the proposed power system should be developed.

A. Proposed Model Analysis

Kirchhoff's laws of voltage and current applied to the proposed model shown in Fig. 1 provide a general equation in the stationary reference frame in a three-phase system as

$$\sum_{i=1}^{3} v_{iM} = \sum_{i=1}^{3} \left(L_c \frac{di_{ci}}{dt} + R_c i_{ci} + v_i + v_{NM} \right). \qquad (8)$$

A null value for the zero voltage component is assumed. Since the absence of neutral wire is considered, the zero current component is also null, with the assumption that the grid voltages are balanced. By taking into account these assumptions, the ac neutral point voltage term can be obtained as

$$v_{NM} = \frac{(v_{1M} + v_{2M} + v_{3M})}{3} = \frac{1}{3}\sum_{i=1}^{3} v_{iM}. \qquad (9)$$

The switching function s_k of the k_{th} leg of the VSC can be expressed as

$$S_k = \begin{cases} 1, & \text{if } T_k \text{ is on and } T_k' \text{ is off} \\ 0, & \text{if } T_k \text{ is off and } T_k' \text{ is on.} \end{cases} \qquad (10)$$

Thus, with $vkM = S_k V_{dc}$ and substituting in (8) and (9), a set of dynamic equations describing the switched model of the proposed DG model is developed. This model is general, complete, and makes no assumptions other than the use of ideal switches. Therefore, (11) can be expressed as

$$\frac{di_{ck}}{dt} = -\frac{R_c}{L_c} i_{ck} + \frac{1}{L_c}\left(S_k - \frac{1}{3}\sum_{j=1}^{3} S_j\right) v_{dc} - \frac{v_k}{L_c} \qquad k = 1, 2, 3. \quad (11)$$

Equation (11) represents phase *k* dynamic equation of the proposed VSC. By (11), the switching state function can be defined as

$$D_{nk} = \left(S_k - \frac{1}{3}\sum_{j=1}^{3} S_j\right). \qquad (12)$$

Equation (12) shows that the value of *Dnk* depends on the switching state *n* and on the phase *k*. In other words, *Dnk* depends simultaneously on the switching functions of the three legs of the interfaced VSC. This shows the interaction between the three phases.

By substituting (12) into (11), dynamic equation of the proposed model can be expressed as

$$\frac{d}{dt}\begin{bmatrix} i_{c1} \\ i_{c2} \\ i_{c3} \end{bmatrix} = -\frac{R_c}{L_c}\begin{bmatrix} 1 & 0 & 0 \\ 0 & 1 & 0 \\ 0 & 0 & 1 \end{bmatrix}\begin{bmatrix} i_{c1} \\ i_{c2} \\ i_{c3} \end{bmatrix} + \frac{1}{L_c}\begin{bmatrix} D_{n1} \\ D_{n2} \\ D_{n3} \end{bmatrix} v_{dc} - \frac{1}{L_c}\begin{bmatrix} v_1 \\ v_2 \\ v_3 \end{bmatrix}. \quad (13)$$

V. STATE-SPACE MODEL

By use of Park transformation matrix, the dynamic equation of proposed model can be transformed to the *dq* frame as

$$\frac{d}{dt}\begin{bmatrix} i_{cd} \\ i_{cq} \end{bmatrix} = \begin{bmatrix} -\frac{R_c}{L_c} & \omega \\ -\omega & -\frac{R_c}{L_c} \end{bmatrix} \begin{bmatrix} i_{cd} \\ i_{cq} \end{bmatrix} + \frac{1}{L_c}\begin{bmatrix} D_{nd} \\ D_{nq} \end{bmatrix} v_{\mathrm{dc}} - \frac{1}{L_c}\begin{bmatrix} v_d \\ v_q \end{bmatrix}. \quad (14)$$

As the sum of the three-phase currents is zero, there is no homopolar component ($ic0 = 0$); therefore, the ac neutral point voltage does not affect any transformed current. This voltage can be deduced as

$$v_{NM} = \frac{v_0 - v_{0M}}{\sqrt{3}}. \quad (15)$$

It can be seen that the v_{NM} only depends on homopolar voltage components of the converter (v_{0M}) and the grid (v_0). In addition, when the voltage of power grid is balanced, the averaged value of v_0 is zero; therefore, voltage v_{NM} depends only on the homopolar component of the ac voltages of the interfaced converter. Considering the original position of the load voltage vector in *d*-axis, voltage vector of *q*-axis will be zero ($v_q = 0$), and the other vector's value will be equal to *EL* ($v_d = E_L$), which is the value of the line-to-line rms voltage of grid voltage. Therefore, (14) can be written as

$$\frac{d}{dt}\begin{bmatrix} i_{cd} \\ i_{cq} \end{bmatrix} = \begin{bmatrix} -\frac{R_c}{L_c} & \omega \\ -\omega & -\frac{R_c}{L_c} \end{bmatrix} \begin{bmatrix} i_{cd} \\ i_{cq} \end{bmatrix} + \frac{1}{L_c}\begin{bmatrix} D_{nd} \\ D_{nq} \end{bmatrix} v_{\mathrm{dc}} - \frac{1}{L_c}\begin{bmatrix} E_L \\ 0 \end{bmatrix} \quad (16)$$

where the homopolar component has been omitted.

A. Current Control Technique for Proposed DG Model

In order to obtain a low overshoot, high accuracy, and fast dynamic response to provide load active and reactive power and also harmonic current components of the grid-connected loads, two equations in the equivalent model of the proposed system (14) must be controlled in two different and independent loops. As we mentioned before, all the Park-transformed variables of the DG system will become a constant value in steady-state condition. By referring to (14) and considering $\lambda = L_c(di_c/dt) + R_c i_c$, switching state functions can be calculated as

$$D_{nd} = \frac{\lambda_d - L_c\omega i_{cq} + v_d}{v_{dc}} \qquad (17)$$

$$D_{nq} = \frac{\lambda_q + L_c\omega i_{cd}}{v_{dc}}. \qquad (18)$$

As shown in (17) and (18), the cross coupling terms $L_c\omega i_{cq}$ and $L_c\omega i_{cd}$ exist in circuit of current control loop, and the blocks that contain $L_c\omega$ have the objective of decoupling influenced between both current control loops in the *d*- and *q*-axes. Note that the original control inputs D_nd and D_nq consist of combination of a nonlinearity cancelation part and a linear decoupling compensation part. To achieve a fast dynamic response and zero steady-state errors, particularly during connection of nonlinear loads to the grid, which main grid is polluted by these types of loads, a proportional–integral (PI)-type regulator is needed. The parameter of the proposed regulator can be obtained as

$$(\lambda_{dq}) = k_p(\Delta i_{cdq}) + k_i \int (\Delta i_{cdq})\, dt \qquad (19)$$

where terms *kp* and *ki* are proportional and integral gains, respectively, and (Δ*icdq*) = (*i*□*cdq*) − (*icdq*) denotes a comparison of the calculated reference currents and the actual DG injection currents generated by the VSC which create error signals and control the switches of the inverter according to objectives of the interconnection of DG system to the grid. The transfer function of the PI regulator for current control loops of proposed strategy is given as

$$G_i(s) = \frac{\lambda_d(s)}{\Delta I_d(s)} = \frac{\lambda_q(s)}{\Delta I_q(s)} = k_p + \frac{k_i}{s}. \qquad (20)$$

To design PI regulator in circuit of current controller, it is necessary to decouple the model of the system by adding the measured voltage of *d*-axis and cross coupling terms as shown in Fig. 3, where *L*□ and *v*□ are estimated values of coupling inductance and grid voltages. Thus, the inner control loops of the current *icd* can be simplified as shown in Fig. 4. As shown in Fig. 3, the current loops of *icd* and *icq* are the same. Thus, in *dq* reference frame, decoupled control for the reactive and active power can be conveniently achieved by independently controlling the *d*- and *q*-axis currents.

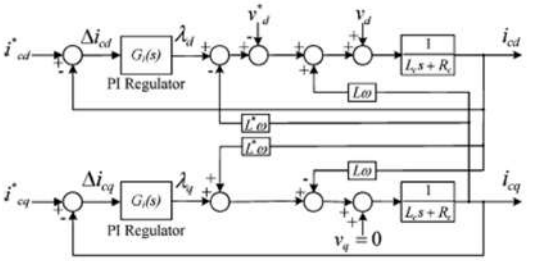

Fig. 3. Inner control loop of the *icd* and *icq*.

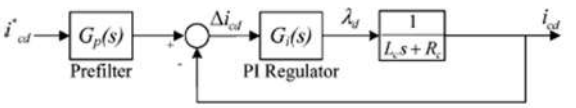

Fig. 4. Equivalent diagram of *d*-axis current control loop

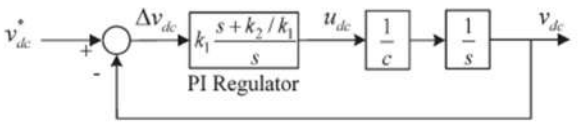

Fig. 5. Control loop of the dc voltage.

The closed-loop transfer function of the current loop can be calculated as

$$\frac{I_{cq}(s)}{I_{cq}^{*}(s)} = \frac{I_{cd}(s)}{I_{cd}^{*}(s)} = \frac{k_p}{L_c}\frac{s + \frac{k_i}{k_p}}{s^2 + \frac{(R_c + k_p)}{L_c}s + \frac{k_i}{L_c}}. \qquad (21)$$

The transient response of the currents will be affected by the presence of the zero in (21). In particular, the actual percent overshoot will be much higher than expected. For the optimal value of the damping factor $\zeta = \sqrt{1/2}$, the theoretical overshoot is 20.79%. To eliminate the effect of zero on transient response in (21), a prefilter is added as shown in Fig. 4. The response of the current loops becomes that of a second-order transfer function with no zero. Comparison between general model of a second-order transfer function $\omega^2 n/(s^2 + 2\xi\omega n s + \omega^2 n)$ and (21) leads to the following design relations:

$$k_p = 2L_c\zeta\omega_n - R_c \qquad k_i = L_c \cdot \omega_n^2 \qquad (22)$$

where ω_n is natural undamped angular frequency and depends on the specific time response.

VI. SIMULATION ANALYSIS AND RESULTS

In order to demonstrate the high performance of the proposed control technique, the complete system model was simulated using the "Power System Blockset" simulator operating under the Matlab/Simulink environment. The schematic diagram and principle of the proposed model and the control technique in an ac grid are shown in Fig. 6. The test model contains a power converter with power rating of 20 kVA. The maximum available value of DG source active power is 8 kW, which is also the active power reference included in the simulations. At first, capabilities of DG resources and flexibility of proposed control strategy to control the proposed VSC in providing active, reactive, and harmonic current components of different loads are shown, and the capabilities of proposed control method on reactive power tracking with constant output active power are considered. In addition, the simulated results have been used to analyze the total harmonic distortion (THD) of the utility grid current amid severe varying load conditions. During the simulation process, constant dc voltage sources have been considered as a DG source.

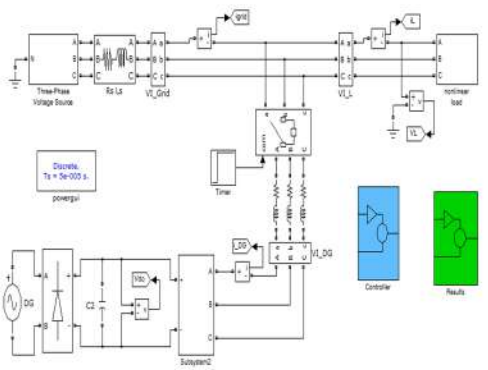

Fig 6 simulation diagram of proposed system

In addition, the active power which is delivered from the DG link to the ac grid is considered to be constant. This assumption makes it possible to evaluate the capability of the proposed control strategy to track the fast change in the active and reactive power, independent of each other. For this purpose, when one of them is changed, another one must be constant.

Fig. 7. Load voltage, load, grid, and DG currents before and after connection of DG and before and after connection and disconnection of additional load into the grid.

A. Connection of DG Link to the Grid to Supply Harmonic Current Components and Nonlinear Load Increment

A full-wave thyristor converter supplies a load with resistance of 20 Ω and 10-mH inductors in each phase. This nonlinear load draws harmonic currents from the grid continuously. The DG link is connected to the ac grid at t = 0.1 s. This process is continued until t = 0.2; at this moment, another full-wave thyristor converter similar to the prior load is connected to the grid, and it is disconnected from the grid at t = 0.35 s. Fig. 7 shows the load voltage (vl), load current (il), grid current ($i$grid), and DG current (iDG) in phase (a). As shown in this figure, after the connection of DG link to the grid at t = 0.1 s, the grid current becomes zero, and all the active and reactive current components including fundamental and harmonic frequencies are provided by DG link ($i$grid = $i$load − iDG). In this case, load current is completely equal to reference current of converter; therefore, VSC injects the maximum available power of DG source to the power grid. As a result, the injected current from the grid will be zero. The load current is fed from nonlinear link continuously until the connection of additional load to the grid.

Fig. 8(a) shows that, after connection of additional load to the power grid at t = 0.2 s, converter injects the maximum active and reactive power by connection of DG source to the grid. However, in this case, the maximum power of proposed converter is less than the power which is needed to supply the grid-connected loads. Therefore, the remaining power is injected by the

utility grid. As shown in this figure, the utility grid injects high-power quality current waveforms even under the connection of nonlinear loads to the grid, and load harmonic currents are provided by DG. There are some sharp edges on current waveforms which are related to high-order harmonic frequencies and created during switching of thyristor converters.

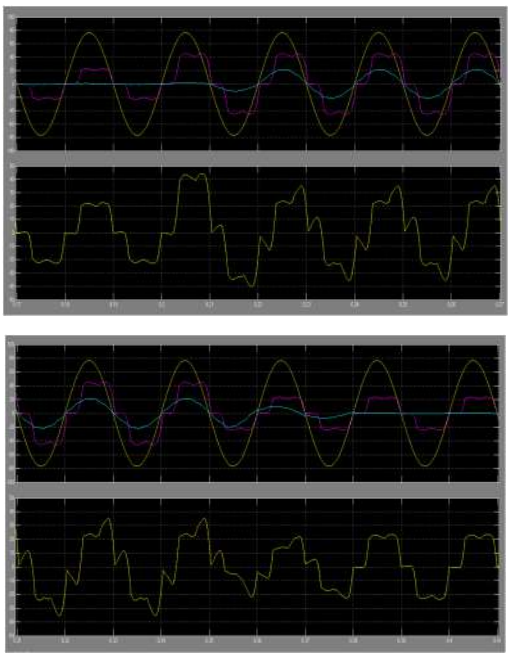

Fig. 8. Grid, load, DG currents, and load voltage (a) before and after connection of additional load and (b) before and after disconnection of additional load.

In addition, the production in control circuit of DG system is delayed for around one cycle. This is due to the settling time of proposed MPHPF filter, in DG's control loop. Fig. 8(b) shows that, with the same delay as before, additional load is removed at t = 0.35 s. As shown in this figure, after the pass of the transient times, the injected current from grid to the load becomes zero, and DG link supplies all the required power to supply the proposed nonlinear load.

Fig. 9 shows that, after the transient times during connection of additional load to the main grid, the load voltage and grid current are in phase,

and the grid does not need to provide reactive and harmonic currents for the load which is shown for three phases.

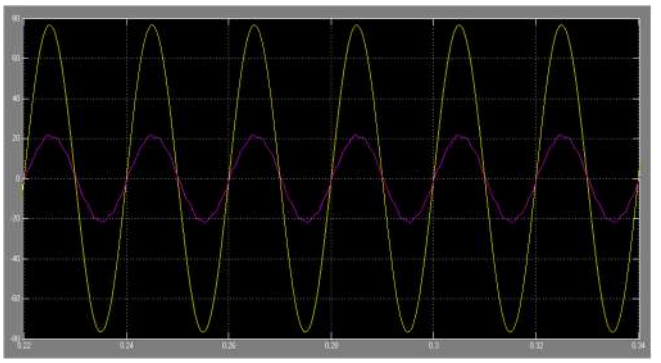

Fig. 9. Phase-to-neutral voltage and grid current for phase-A

The ability of control loop to track the reference current trajectories of *d*- and *q*-axes, during connection of DG link to the grid and, also, connection of additional load to the grid, is shown in Fig. 10. Fig. 10(a) shows that, before connection of additional load to the grid, the actual *d*- and *q*-axis current components of DG's control loop track their reference trajectory precisely. However, according to Fig. 10(b), after connection of additional load to the grid, the actual *d*-axis current component of DG tracks half of its reference trajectory which is equal to its maximum active power (reference active power), and all the reference trajectories of reactive current change.

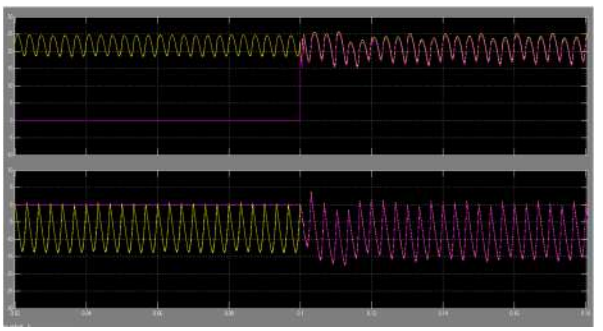

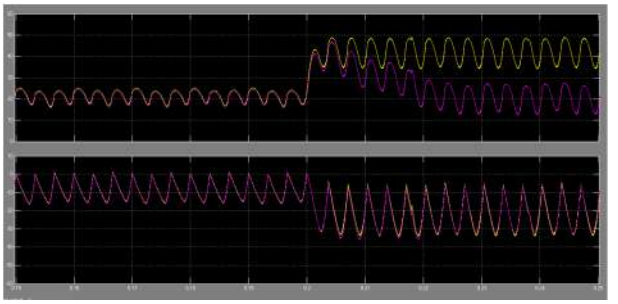

Fig. 10. Reference currents track the load current (a) after interconnection of DG resources and (b) after additional load increment.

B. Connection of DG Link to an Unbalanced Grid

The ability of proposed DG link to track load current components for unbalanced grid voltage is evaluated. At first, a nonlinear load similar to the prior load is added to the PCC at t = 0.45 s. At t = 0.55 s, the grid voltage is unbalanced. Fig. 11 shows three-phase grid voltages, load current, grid current, and DG link current. As shown in Fig. 11, load harmonic current components are provided by DG link, and grid currents are maintained sinusoidal during balanced and unbalanced grid voltages. In addition, load voltage and grid current are kept in phase (the grid does not provide reactive current). The proposed control scheme provides balanced current injection from the DG link. Therefore, since the grid voltage unbalance forces unbalanced current in the load, the grid current is unbalanced. Depending on the power converter current ratings and voltage unbalance severity, it could be possible to compensate the grid currents unbalance by injecting unbalance currents from the DG link, but this is not the purpose of the present control scheme.

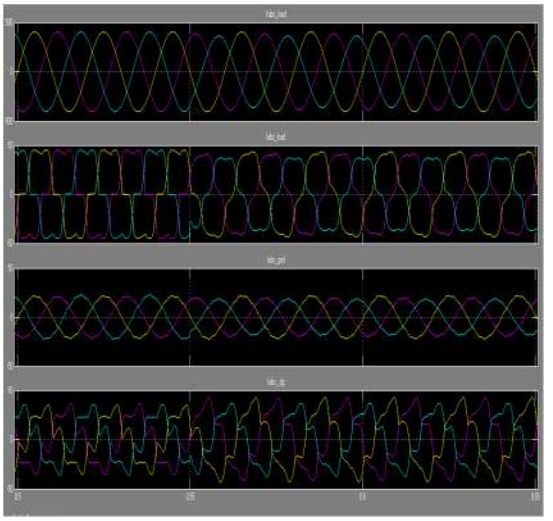

Fig. 11 Load voltage, load, grid, and DG currents during connection of DG link to the unbalanced grid voltage.

VII. CONCLUSION

A multi objective control algorithm for the grid-connected converter has been proposed and presented in this paper. Due to sensitivity of phase-locked loop to noises and distortion, its elimination can bring benefits for robust control against distortions in DG applications. Flexibility of the proposed DG in both steady-state and transient operations has been verified through simulation and experimental results. Also, the problems due to synchronization between DG and grid do not exist, and DG link can be connected to the power grid without any current overshoot. One other advantage of proposed control method is its fast dynamic response in tracking reactive power variations; the control loops of active and reactive power are considered independent. By the use of the proposed control method, DG system is introduced as a new alternative for distributed static compensator in distribution network. The results illustrate that, in all conditions, the load voltage and source current are in phase and so, by improvement of power factor at PCC, DG systems can act as power factor corrector devices.

The results indicate that proposed DG system can provide required harmonic load currents in all situations. The proposed control technique can be used for different types of DG resources as power quality improvement devices in a customer power distribution network.

Table-I

System parameters

Parameter	Value
Grid voltage	230 V
Interfacing inductance	4.6 mH
DC-link capacitance	1020 μF
DC-link voltage setpoint	610 V
Switching/Sampling frequency	10 kHz
Fundamental frequency	50 Hz
Linear load resistance	40 Ω
Linear load inductance	100 mH
Nonlinear load resistance	180 Ω

VIII. Acknowledgment

This paper is based on M. Tech. project carried out by the student of pydah college of engineering & technology, Kakinada studying M.Tech (Power Electronics) The project had been completed by MS. K. SRAVANI SANDHYA bearing H.T.no.:126T1D4306 under the guidance of Mr. P. VIJAYA RAMARAO.

REFERENCES

1. E. Pouresmaeil, D. Montesinos-Miracle, O. Gomis-Bellmunt, and J. Bergas-Jané, "A multi-objective control strategy for grid connection of DG (distributed generation) resources," *Energy*, vol. 35, no. 12, pp. 5022–5030, Dec. 2010.
2. F. Blaabjerg, R. Teodorescu, M. Liserre, and A. V. Timbus, "Overview of control and grid synchronization for distributed power generation systems," *IEEE Trans. Power Electron.*, vol. 53, no. 5, pp. 1398–1409, Oct. 2006.
3. F. Blaabjerg, Z. Chen, and S. Kjaer, "Power electronics as efficient interface in dispersed power generation systems," *IEEE Trans. Power Electron.*, vol. 19, no. 5, pp. 1184–1194, Sep. 2004.
4. G. Saccomando and J. Svensson, "Transient operation of grid-connected voltage source converter under unbalanced voltage conditions," in *Proc. IAS*, Chicago, IL, Oct. 2001, vol. 4, pp. 2419–2424.
5. R. Teodorescu and F. Blaabjerg, "Flexible control of small wind turbines with grid failure detection operating in stand-alone or grid-connected mode," *IEEE Trans. Power Electron.*, vol. 19, no. 5, pp. 1323–1332, Sep. 2004.

6. M. Kazmierkowski, R. Krishnan, and F. Blaabjerg, *Control in Power Electronics—Selected Problems*. New York: Academic, 2002.
7. E. Twining and D. G. Holmes, "Grid current regulation of a three-phase voltage source inverter with an *LCL* input filter," *IEEE Trans. Power Electron.*, vol. 18, no. 3, pp. 888–895, May 2003.
8. T. Zhou and B. François, "Energy management and power control of a hybrid active wind generator for distributed power generation and grid integration," *IEEE Trans. Ind. Electron.*, vol. 58, no. 1, pp. 95–104, Jan. 2011.
9. M. Singh, V. Khadkikar, A. Chandra, and R. K. Varma, "Grid interconnection of renewable energy sources at the distribution level with power quality improvement features," *IEEE Trans. Power Del.*, vol. 26, no. 1, pp. 307–315, Jan. 2011.
10. M. F. Akorede, H. Hizam, and E. Pouresmaeil, "Distributed energy resources and benefits to the environment," *Renewable Sustainable Energy Rev.*, vol. 14, no. 2, pp. 724–734, Feb. 2010.
11. C. Mozina, "Impact of green power distributed generation," *IEEE Ind. Appl. Mag.*, vol. 16, no. 4, pp. 55–62, Jun. 2010.
12. B. Ramachandran, S. K. Srivastava, C. S. Edrington, and D. A. Cartes, "An intelligent auction scheme for smart grid market using a hybrid immune algorithm," *IEEE Trans. Ind. Electron.*, vol. 58, no. 10, pp. 4603–4611, Oct. 2011.
13. E. Twining and D. G. Holmes, "Grid current regulation of a three-phase voltage source inverter with an *LCL* input filter," *IEEE Trans. Power Electron.*, vol. 18, no. 3, pp. 888–895, May 2003.
14. M. K. Ghartemani and M. Iravani, "A method for synchronization of power electronic converters in polluted and variable-frequency environments," *IEEE Trans. Power Syst.*, vol. 19, no. 3, pp. 1263–1270, Aug. 2004.
15. U. Borup, F. Blaabjerg, and P. N. Enjeti, "Sharing of nonlinear load in parallel-connected three-phase converters," *IEEE Trans. Ind. Appl.*, vol. 37, no. 6, pp. 1817–1823, Nov./Dec. 2001.
16. Y. A.-R. I. Mohamed, "Mitigation of grid-converter resonance, gridinduced distortion and parametric instabilities in converter-based distributed generation," *IEEE Trans. Power Electron.*, vol. 26, no. 3, pp. 983–996, Mar. 2011.
17. H. Karimi, A. Yazdani, and R. Iravani, "Robust control of an autonomous four-wire electronically-coupled distributed generation unit," *IEEE Trans. Power Del.*, vol. 26, no. 1, pp. 455–466, Jan. 2011.
18. V. Calderaro, V. Galdi, and A. Picolo, "Distribution planning by genetic algorithm with renewable energy units," in *Proc. Bulk Power Syst. Dyn. Control*, Cortina d'Ampezzo, Italy, 2004, vol. 1, pp. 375–380.

19. M. Kim, R. Hara, and H. Kita, "Design of the optimal ULTC parameters in distribution system with distributed generations," *IEEE Trans. Power Syst.*, vol. 24, no. 1, pp. 297–305, Feb. 2009.
20. J.-H. Teng, C.-Y. Chen, C.-F. Chen, and Y.-H. Liu, "Optimal capacitor control for unbalanced distribution systems with distributed generations," in *Proc. IEEE ICSET*, Singapore, 2008, pp. 755–760.
21. H. Hatta, S. Uemura, and H. Kobayashi, "Demonstrative study of control system for distribution system with distributed generation," in *Proc. IEEE/PES Power Syst. Conf. Expo.*, Seattle, WA, 2009, pp. 1–6.
22. M. E. Baran and F. F. Wu, "Network reconfiguration in distribution systems for loss reduction and load balancing," *IEEE Trans. Power Del.*, vol. 4, no. 2, pp. 1401–1407, Apr. 1989.
23. C. C. Liu, S. J. Lee, and K. Vu, "Loss minimization for distribution feeders: Optimality and algorithms," *IEEE Trans. Power Del.*, vol. 4, no. 2, pp. 1281–1289, Apr. 1989.
24. J. Olamaei, T. Niknam, and G. Gharehpetian, "Impact of distributed generators on distribution feeder reconfiguration," in *Proc. IEEE Lausanne Power Tech*, Lausanne, Switzerland, 2007, pp. 1747–1751.
25. S. Yang, Q. Lei, F. Z. Peng, and Z. Qian, "A robust control scheme for grid-connected voltage-source inverter," *IEEE Trans. Ind. Electron.*, vol. 58, no. 1, pp. 202–212, Jan. 2011.
26. J. He, Y. W. Li, and M. S. Munir, "A flexible harmonic control approach through voltage-controlled DG-grid interfacing converters," *IEEE Trans. Ind. Electron.*, vol. 59, no. 1, pp. 444–455, Jan. 2012.
27. I.-Y. Chung, W. Liu, D. A. Cartes, E. G. Collins, and S. Moon, "Control methods of inverter-interfaced distributed generators in a microgrid system," *IEEE Trans. Ind. Electron.*, vol. 46, no. 3, pp. 1078–1088, May/Jun. 2010.

INTERNATIONAL JOURNAL OF MULTIDISCIPLINARY EDUCATIONAL RESEARCH
ISSN : 2277-7881; IMPACT FACTOR - 2.972; IC VALUE:5.16
VOLUME 3, ISSUE 10(4), OCTOBER 2014

A PULSE WIDTH MODULATION DC–DC NON-ISOLATED BUCK CONVERTER USING THE THREE-STATE SWITCHING CELL

Ms. K. BHANU DEEPIKA
bhanudpk@gmail.com
Under the guidance of
Ms.M.PAVANI
ASSISTANT PROFESSIOR
PYDAH COLLEGE OF ENGINEERING , KAKINADA

Abstract—This paper presents a pulse width modulation dc–dc non-isolated buck converter using the 3SS cell, constituted by two active switches, two diodes, and two coupled inductors. Only part of the load power is processed by the active switches, reducing the peak current through the switches to half of the load current, as higher power levels can then be achieved by the proposed topology. The volume of reactive elements, i.e., inductors and capacitors, is also decreased since the ripple frequency of the output voltage is twice the switching frequency. Due to the intrinsic characteristics of the topology, total losses are distributed among all semiconductors. Another advantage of this converter is the reduced region for discontinuous conduction mode when compared to the conventional buck converter. The theoretical approach is detailed through qualitative and quantitative analyses by the application of the three-state switching cell to the buck converter operating in non-overlapping mode ($D < 0.5$).

Key words: DC-DC converter, conventional buck converter

I. INTRODUCTION

Conventional hard switching converters with a single active switch such as buck, boost, buck–boost, Cuk, single-ended primary-inductance converter (SEPIC), and Zeta typically present low power density, while attempts to further minimize the size of filter elements lead to increased switching losses, compromising the efficiency of the converters. Pulse width modulation (PWM) dc–dc converters are widely employed in numerous applications, e.g., audio amplifiers [1], uninterruptible power supplies [2], fuel cell powered systems [3], and fork lift vehicles [4], although many other ones can be easily found.

In order to overcome such limitation, several soft switching approaches have been introduced in the literature. Soft switching is supposed to reduce

the overlap between voltage and current during the commutation, and can be classified in either active or passive methods, as one must choose between the aforementioned snubbers for a given application. Active methods can reduce the switching losses by using auxiliary switches. Unfortunately, an auxiliary switch increases the complexity of both power and control circuits. Synchronization problems between control signals of the switches during transient also complicate the control strategy. Circuit cost is increased and reliability is affected by using active snubbers [5].

A passive lossless snubber can effectively restrict switching losses and electromagnetic interference (EMI) noise using no active components and no power dissipative components. No additional control is needed and no circulating energy is generated. Circuit structure is as simple as *RCD* (resistor–capacitor–diode) snubbers while circuit efficiency is as high as active snubbers and resonant converters [6], [7]. Low cost, high performance and high reliability are the distinct advantages of a passive lossless snubber [8]. However, soft switching may not be achieved for the entire load range, and besides the accurate design of the resonant tank is not a trivial task, even what is also valid when active snubbers are considered [9].

Significant effort has then been made to improve the characteristics of the traditional non-isolated dc–dc converters in the last few years. For instance, the study of a dc–dc buck converter with three-level buck clamping, zero voltage switching (ZVS), active clamping, and constant-frequency PWM is proposed in [10]. A family of converters is also derived, which combines the advantages of reduced voltage across the switches using a three-level commutation cell, and decreased switching losses obtained from a soft switching technique.

In the last few years, many converters based on the three state switching cells (3SSC) have been proposed. The cell can be obtained by the association of two two-state PWM cells (2SSC) interconnected to a center tap autotransformer, from which novel converters can be derived. General advantages over conventional topologies can be achieved, e.g., the inductor is designed for twice the switching frequency, with consequent reduction of size and weight; the current through the switches is half of the input current; part of the input power is delivered to the load by the transformer instead of the main switches, consequently reducing conduction and commutation losses; lower cost switches can be used. Many dc–dc converters based on the 3SSC

have been introduced in the last few years [13]–[18]. However, the aforementioned works are basically concerned with high voltage gain boost-based topologies dedicated to dc voltage step-up applications. Literature does not present further detailed studies regarding the remaining dc–dc non-isolated topologies using the 3SSC.

Within this context, this paper proposes the complete study of the dc–dc converter based on the 3SSC. Initially, some theoretical background on the 2SSC and the 3SSC is presented, leading to the conception of the improved buck converter using the so-called cell type *B*. Then, the converter operation in non-overlapping mode (NOM) is described, where the main characteristics of the topology are discussed. An experimental prototype is then implemented, while the detailed discussion of experimental results is supposed to validate the theoretical assumptions and also demonstrate the merit of the proposal.

II. 3SSC AND PROPOSED BUCK CONVERTER

The canonical switching cell is an approach that allows us to obtain and classify the classical dc–dc converters, from which some families of converters can be derived [19]. Buck, boost, and buck–boost converters, which are second-order systems, as well as Cuk, SEPIC, and Zeta, which are fourth-other systems, have a single switching cell that is part of their respective power stages. Literature has also shown appreciable effort to improve the characteristics of the original structures, even though the novel resulting topologies are more complex approaches with higher component count.

The aforementioned switching cell is composed of three terminals, which are active, passive, and common. Its behaviour is based on the complementary operation of two switches connected by the common terminal. In other words, one switch is turned ON while the remaining one remains turned OFF, and vice versa. Therefore, this arrangement can be called 2SSC. With the aim of achieving higher power density, switching frequency is usually increased, with consequent reduction of size and volume of reactive elements. Consequently, it leads to the increase of both switching losses and the volume of heat sinks. This practice, therefore, compromises the very reduction of physical dimensions in static power converters.

The aforementioned losses must then be reduced, and soft switching circuits using the resonance phenomenon have been widely proposed as a possible solution. By using well-known techniques such as ZVS and zero

current switching, the performance of converters can be improved. However, even though switching losses are mitigated or eliminated, conduction losses are still of major concern and may even increase depending on the adopted snubber. With the aim to further reduce voltage and/or current stress, the association of semiconductors or even converters in series or in parallel has been thoroughly investigated. Other topologies can also be obtained, such as multilevel converters [20]. It is also possible to increase the efficiency by the use of the 3SSC, which has been employed in recent publications [21] and is originally derived from the dc–dc push–pull converter. In order to obtain the cell type *B*, let us consider the classical push– pull topology shown in Fig. 1, which is formed by switches S1 and S2 , two rectifier diodes *D*1 and *D*2 in the secondary side, and a high-frequency transformer. The circuit corresponds to a dc–ac–dc conversion system. If the central tap transformer is considered ideal with unity turns ratio, the primary and secondary windings can be replaced by the respective magnetizing inductances, which are coupled and constitute an autotransformer.

The negative terminal of the output stage represented by *Vo,* which was formerly connected to the central tap of the transformer, is then connected to the negative pole of the input voltage source to generate a boost topology, as seen in Fig. 1(c). Otherwise, if connected to the positive pole, a buck–boost converter is derived. The cell type *B* can then be applied to the dc–dc buck converter substituting the 2SSC, while the resulting topology is presented in Fig. 2.

It can be seen that the 3SSC is formed by two controlled switches S1 and S2, two diodes *D*1 and *D*2, one autotransformer *T*1*, T*2, and one inductor *L*. Even though the resulting cell seems more complex with higher component count than the conventional 2SSC, the advantages over its counterpart will be clearly demonstrated in this study. For instance, the use of the 3SSC may lead to the need of switches with reduced current rating, which is desirable in step-down high-current applications. Considering that the operation of the switch and the diode of a same leg is complementary, two modes regarding the main switches can be obtained for the proposed topology. If the duty cycle *D* is higher than 0.5, overlapping mode (OM) occurs, where two switches remain turned ON at the same time. Otherwise, if $D < 0.5$, the converter operates in NOM, while only one switch remains turned ON in a given operating stage.

The proposed approach can be seen as the integration of the interleaving technique and the 3SSC. The following advantageous characteristics can be then addressed to the introduced topology:

1) Reduced size, weight, and volume of magnetic, which are designed for twice the switching frequency analogously to the interleaved buck converter.

2) The current stress through each main switch is equal to half of the total output current, allowing the use of semiconductors with lower current ratings.

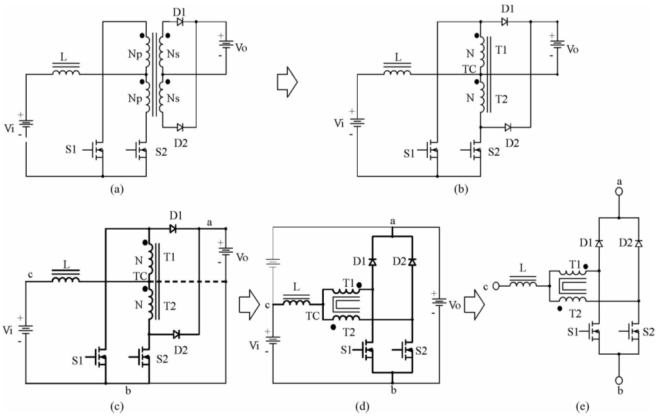

Fig. 1 3SSC type B

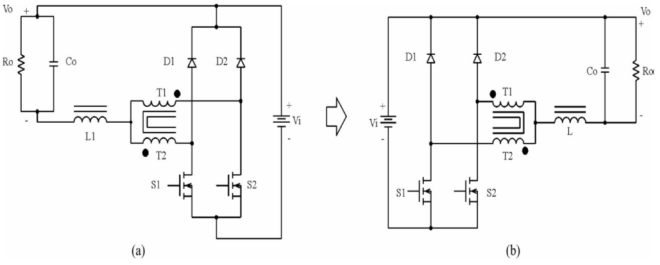

Fig. 2 Buck converter based on the 3SSC

3) Losses are distributed among the semiconductors, leading to better heat distribution and consequently more efficient use of the heat sinks.

4) Part of the input power, i.e., 50%, is directly transferred to the load through the diodes and the coupled inductors (autotransformers), and not through the main switches. As a consequence, conduction and switching losses are reduced. This is the main difference between the functionality of this approach and that of the interleaved buck topology.

5) The use of the 3SSC allows the parallel connection of switches and, therefore, inexpensive power devices and drives can be used.

6) Energy is transferred from the source to the load during most part of the switching period, which is a distinct characteristic of the proposed converter, since in other buck type converters, it only occurs during half of the switching period. As a consequence, reduction of current peaks and also conduction losses are expected.

7) The drive circuit of the main switches becomes less complex because they are connected to the same reference node, what does not occur in the interleaved buck converter.

For the detailed description of the dc–dc buck converter using the 3SSC in NOM, the following assumptions are made:

1) The converter operates in steady state; 2) switching frequency is constant and PWM is employed to drive the switches; 3) The gating signals of the switches are 180◦ displaced; 4) The turn's ratio of the autotransformer is unity; 5) The magnetizing current is much lower than the load current; 6) All semiconductor and passive elements are ideal.

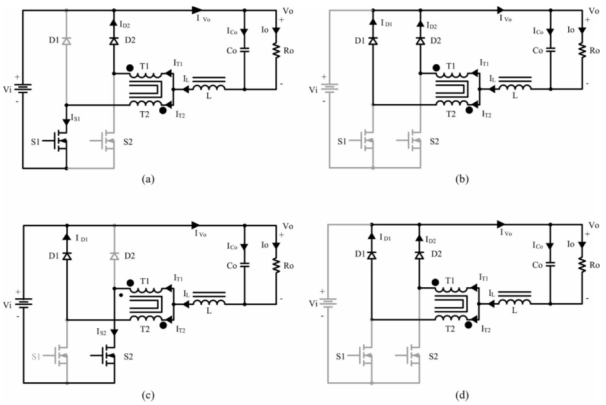

Fig. 3. Operating stages of the proposed converter in NOM-CCM. (a) First stage. (b) Second stage. (c) Third stage. (d) Fourth stage

A. Operation in NOM and Continuous Conduction Mode

(CCM) (D < 0.5)

The converter operation can be defined according to four operating stages as shown in Fig. 3. The respective main theoretical waveforms are presented in Fig. 4, where each one of the variables is defined as follows:

1) *Vg* (S1) , *Vg* (S2)—gating signals applied to switches S1 and S2 , respectively;

2) *IL* —current through inductor *L*, while the maximum and minimum values assumed by this quantity are *IM* and *Im*, respectively;

3) *I*S1—current through switch S1;

4) *ID* 1—current through diode *D*1;

5) *IV o*—current through the output stage, which is the sum of the currents through the output capacitor *ICo* and the load *Io;*

6) *V*S1—voltage across switch S1;

7) *VD* 1—voltage across diode *D*1;

8) *VL*—voltage across inductor *L*.

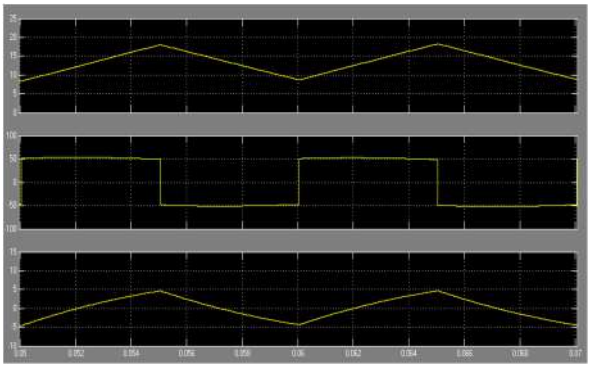

Fig. 4 Main theoretical waveforms for NOM-CCM

*First stage [t*0*, t*1*] [see Fig. 3(a)]:* Initially, switch S1 is turned ON, while switch S2 is turned OFF. The current through the inductor is divided in two parts. The first one flows through *T*1 and *D*2 with energy being delivered to the load. The second one flows through *T*2 and S1. Current sharing is maintained since the number of turns for *T*1 and *T*2 is the same. The current through *L* increases linearly. Windings *T*1 and *T*2 have the same impedance, and the voltages across them are equal to half of the input voltage *Vi* . This stage finishes when *S*1 is turned OFF.

Second stage [t1, t2] [see Fig. 3(b)]: Switch S1 is turned OFF, while switch S2 remains OFF. The voltage across inductor *L* is inverted. Diode *D*1 is forward biased while *D*2 remains conducting. The energy stored in *L* during the previous stage is then transferred to the load. The current flows through *T*1_*T*2 , according to the given polarity, what causes the magnetic flow in the core to be null. The current returns to the source analogously to the previous stage. This stage finishes when S2 is turned ON.

Third stage [t2, t3] [see Fig. 3(c)]: Due to symmetry of the circuit, this stage is similar to the first one, although switch S2 is turned ON instead and S1 remains turned OFF. Diode *D*1 keeps conducting and *D*2 is reverse biased.

Fourth stage [t3, t4] [see Fig. 3(d)]: This stage is similar to the second one, as the same equivalent circuit and operating conditions are valid in this case.

1) Output Characteristic of the Converter: The static gain expressions for the converter operating in CCM, discontinuous conduction mode (DCM), and critical conduction mode (CRM) are given by (1), (2), and (3), respectively. The procedure used to obtain such expressions is the same as that employed in [21] and will not be described here in detail. Expression (1) clearly shows that the static gain for the proposed converter in CCM is the same as that of the conventional buck converter

$$G_{\mathrm{CCM_NOM}} = \frac{V_0}{V_i} = D \tag{1}$$

$$G_{\mathrm{DCM_NOM}} = \frac{1}{2} \cdot \frac{D^2}{\gamma + D^2} \tag{2}$$

$$G_{\mathrm{CRM_NOM}} = \frac{1}{4} \pm \frac{1}{4} \cdot \left(\sqrt{1 - 16\gamma}\right) \tag{3}$$

where

$$\gamma = \frac{2LI_o}{V_i T_s} \tag{4}$$

and

Io—output current [A];

Ts—switching period [s];

D—duty cycle

From expressions (1)–(3), it is possible to determine the static gain of the proposed converter operating at $D < 0.5$, as obtained curves are presented in Fig. 5.

Analogously to the conventional buck converter, the output voltage is a function of the load current in DCM, and this operating region must be avoided. It is worth to mention that the maximum static gain in CRM occurs at $\gamma = 0.0625$ and $D = 0.25$ for the proposed converter. Considering the classic buck converter, the maximum gain in CRM is verified when $\gamma = 0.25$ and $D = 0.5$. In practical terms, it means that the CCM region is wider for the proposed converter. That is, for a given operating point, the necessary inductance becomes one fourth of that required for the classical buck converter.

2) Filter Elements: The ripple current through the inductor (ΔIL) is given as

$$\Delta I_L = \frac{T_s (1-2D) D}{2L} V_i. \qquad (5)$$

Expression (5) can be normalized so that the ripple current is obtained as

$$\beta = \frac{L \cdot \Delta I_L}{T_s V_i} = \frac{(1-2D) D}{2}. \qquad (6)$$

Expression (6) is plotted in Fig. 6, where one can see that the maximum ripple current occurs at $D = 0.25$ and $\beta = 0.0625$.

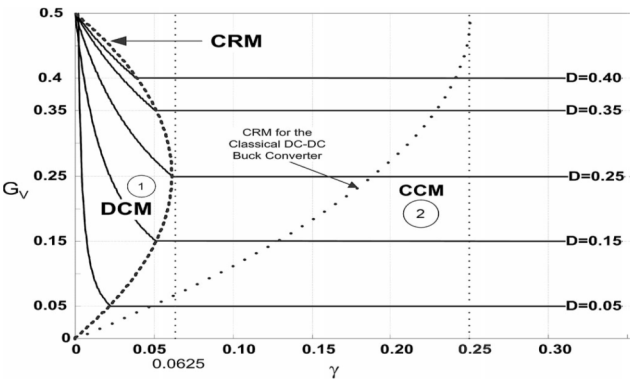

Fig. 5. Comparison between static gain curves of the conventional and proposed buck converters.

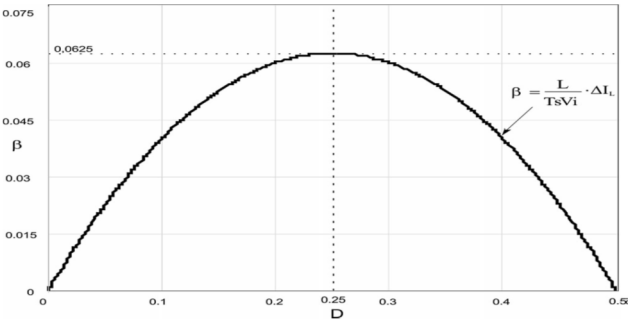

Fig. 6. Ripple current through the inductor in NOM

By choosing arbitrarily the ripple current, the inductance can be determined as

$$L = \frac{(1-2D)\,DT_sV_i}{2\Delta I_L} = \beta\frac{T_sV_i}{2\Delta I_L}. \qquad (7)$$

Considering the maximum ripple current which represents the worst case, the inductance can be obtained by

$$L = \frac{T_sV_i}{16\Delta I_L}. \qquad (8)$$

The critical inductance, whose value assures operation in

CCM, is given by

$$L_{\text{crit}} = \gamma\frac{V_iT_s}{4I_o}. \qquad (9)$$

The output capacitor can be determined as

$$C_o = \frac{\Delta I_L}{4\pi f_s\Delta V_o} \qquad (10)$$

where

ΔVo is the output voltage ripple [V] and

fs is the switching frequency [Hz].

III. DESIGN PROCEDURE

A design example of the proposed 3SSC buck converter, which is supposed to operate in NOM, is presented as follows.

The specifications are listed in Table I and were used in the implementation of an experimental prototype. Some important calculations are performed in order to show the loss mechanism. It is also worth to mention that both conduction and commutation losses are estimated under rated load condition.

A. Preliminary Calculation

Considering the operation in CCM, the static gain is

$$G = D = \frac{60}{200} = 0.3. \tag{11}$$

The output current is

$$I_o = \frac{P_o}{V_o} = \frac{1000}{60} = 16.667\text{A}. \tag{12}$$

B. Inductor

The inductance is given by (7) as

$$L = \frac{(1 - 2 \times 0.3) \times 0.3 \times 200 \times 33.33 \times 10^{-6}}{2 \times 3.33} = 120\ \mu\text{H}. \tag{13}$$

The rms and peak currents through the inductor are given by

(14) and (15), respectively

$$I_{L(\text{rms})} = \sqrt{I_o^2 + \left[\frac{V_i^2 T_s^2 D^2 (2D-1)^2}{48L^2}\right]} = 16.69\,\text{A} \tag{14}$$

$$I_{L(\text{pk})} = I_0 + \frac{V_i T_s (1-2D) D}{4L} = 18.33\,\text{A} \tag{15}$$

The core loss in the inductor can be obtained from

$$P_{Lb(\text{core})} = \Delta B^{2.4} \left(K_H f_L + K_E f_L^2\right) V_e = 0.098\,\text{W} \tag{16}$$

Where ΔB = 0.04 is the magnetic flux variation, KH = 4 ×

10−5 is the hysteresis loss coefficient, *fL* = 2 × *fs* = 60 kHz is the operating frequency of the inductor, *KE* = 4 × 10−10 is the eddy-current loss coefficient, and *Ve* = 42.5 cm3 is the core volume.

The copper loss in the inductor is given by

$$P_{L(\text{copper})} = \frac{\rho \cdot l_{Lt} \cdot N_L \cdot I_{L(\text{rms})}^2}{n_L \cdot S_f} = 0.976\,\text{W} \qquad (17)$$

where ρ = 2.078 ×10−6 Ω · m is the copper resistivity at 70 ◦C, *lLt* = 11.6 cm is the average length of one turn, *NL* = 25 is the number of turns of the inductor, *nL* = 15 is the number of wires in parallel, and *Sf* = 0.003221 cm is the cross-sectional area of copper wire AWG23.

C. Autotransformer

The maximum voltage across the windings is

$$V_{T1} = \frac{V_i}{2} = 100\,\text{V} \qquad (18)$$

The rms and peak currents through transformer *T*1 are given

by (19) and (20), respectively

$$I_{T(\text{rms})} = \frac{1}{2}\sqrt{I_o^2 + \left[\frac{V_i^2 T_s^2 D^2 (2D-1)^2}{48L^2}\right]} = 8.35\,\text{A} \quad (19)$$

$$I_{T(\text{pk})} = \frac{I_o}{2} + \frac{V_i T_s (1-2D) D}{8L} = 9.17\,\text{A}. \qquad (20)$$

The core loss in the autotransformer can be obtained from

$$P_{T(\text{core})} = \Delta B^{2.4} \left(K_H f_T + K_E f_T^2\right) V_e = 0.94\,\text{W} \qquad (21)$$

Where Δ*B* = 0.15 is the magnetic flux variation, *KH* = 4 ×10−5 is the hysteresis loss coefficient, *fT* = 2 × *fs* = 60 kHz is the operating frequency of the transformer, *KE* = 4 × 10−10 is the eddy-current loss coefficient, and *Ve* = 42.5 cm3 is the core volume.

The copper loss in the windings of the transformer is given by

$$P_{T(\text{copper})} = \frac{2\rho l_{Tt} N_T I_{T(\text{rms})}^2}{n_T S_f} = 0.94\,\text{W} \qquad (22)$$

Where ρ = 2.078 ×10−6 Ωm is the copper resistivity at 70 ◦C, *IT t* = 11.6 cm is the average length of one turn, *NT* = 14 is the number of turns of the 1:1 autotransformer, *nT* =5 is the number of wires in parallel, *Sf* =0.005176 cm is the cross-sectional area of copper wire AWG20.

D. Main Switches

The threshold voltage across one main switch is

*V*S1 = *Vi* = 200V. (23)

The average current *I*S1(avg) and the rms current *I*S1(rms) through the switch are given by (24) and (25), respectively

$$I_{S1(avg)} = \frac{1}{2} \times I_O \times D = 2.5\,\text{A} \tag{24}$$

$$I_{S1(rms)} = \sqrt{\frac{D}{4} \cdot \left[I_o^2 + \frac{V_i^2 T_s^2 D^2 (2D-1)^2}{48 L^2} \right]} = 4.57\,\text{A}. \tag{25}$$

MOSFET 5015VBR manufactured by APT was then chosen as the main switch, whose characteristics are drain to source voltage *V*DS = 500 V, diode forward voltage *VS* (*F*) = 1.3 V, drain current *ID* = 32 A, on resistance *R*DS (on) = 0.15, rise time *tr* = 14 ns, and fall time *tf* = 11 ns. The conduction loss regarding each main switch is

$$P_{S1(cond.)} = V_{S1(F)} \cdot I_{S1(avg)} + R_{DS(on)} \cdot I_{S1(rms)}^2 = 6.383\,\text{W} \tag{26}$$

The switching loss during turn ON and turn OFF for a single switch is

$$P_{S1(sw)} = \frac{f_s}{2}(t_r + t_f) I_{S1(avg)} V_{S1} = 0.188\,\text{W}. \tag{27}$$

IV. RESULTS

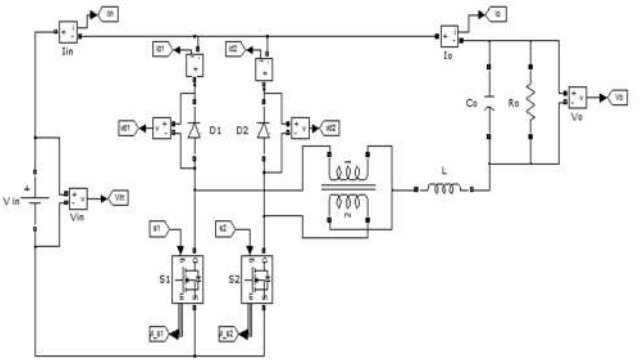

Fig.7 simulation diagram of three state switching cell 3ssc

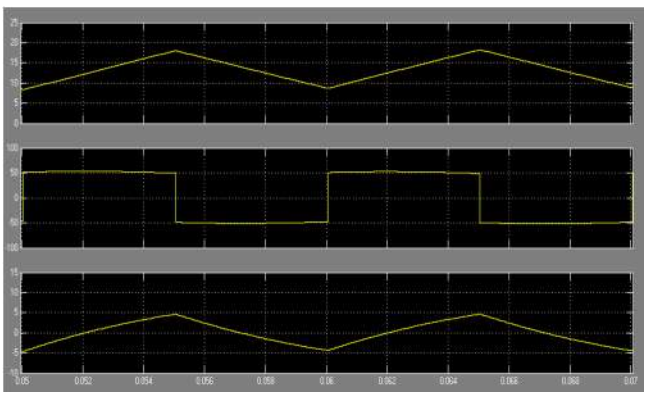

Fig. 8 Main theoretical waveforms for NOM-CCM Il Vl ico

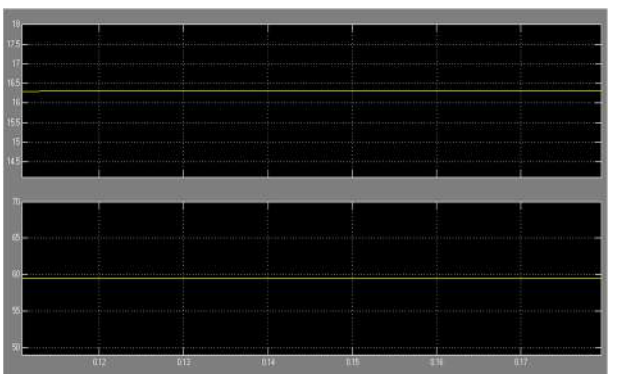

Fig. 4 Main theoretical waveforms for NOM-CCM Io Vo

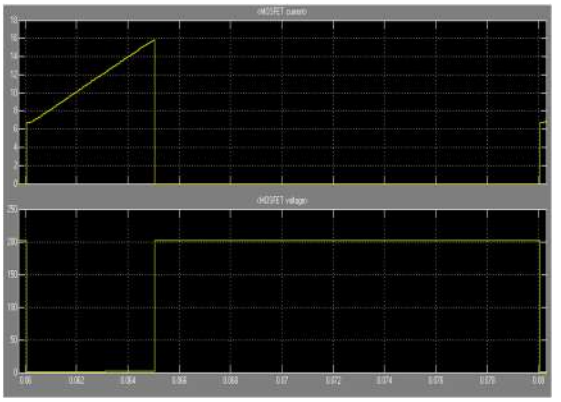

Fig. 4 Main theoretical waveforms for NOM-CCM Is1 Vs1

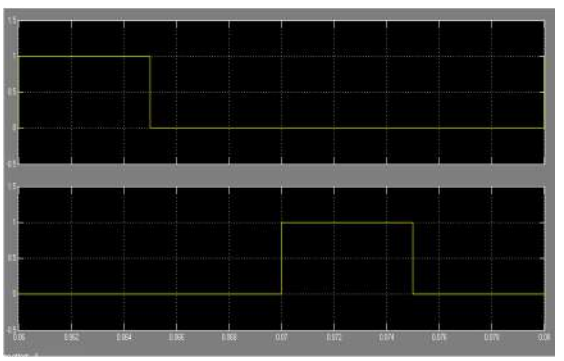

Fig. 4 Main theoretical waveforms for NOM-CCM Vgsi Vgs2

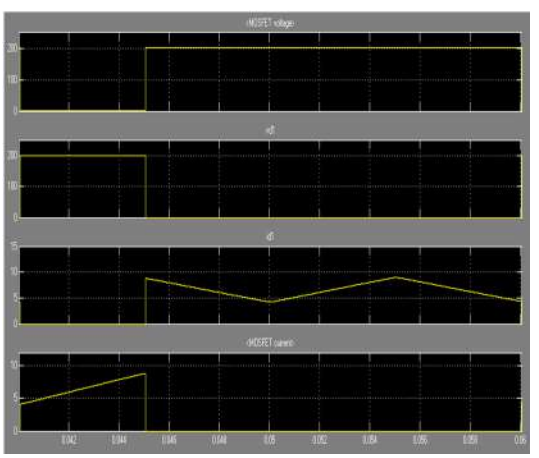

Fig. 4 Main theoretical waveforms for NOM-CCM Vs1 Vd1 Id1 Is1

V. CONCLUSION

In this paper dc–dc buck converter based on the 3SSC has been presented. When the 3SSC is employed, the current is distributed among the semiconductors. Despite the increase in the number of semiconductors, the current levels on these devices are reduced, enabling the use of inexpensive switches and simplified command circuits because the isolated drive is not required like in the interleaved buck converter. In front of these characteristics, its use is recommended for high-power high-current applications where the traditional approach may be inadequate, while good current sharing is achieved.

Furthermore, only part of the energy from the input source flows through the active switches, while the remaining part is directly transferred to the load without being processed by these switches, i.e., this energy is delivered to the load through passive components, such as the diodes and the transformer windings.

In addition, the overall losses are distributed among all semiconductors, reducing the heat sink efforts. The reactive components operate with twice the switching frequency, with significant reduction in weight and volume of such components. Considering the operation in NOM ($D < 0.5$) and the same ratings, the following characteristics can be addressed with the 3SSC-based converter if compared with the conventional buck topology:

1) increased number of semiconductor elements;

2) The operating area in CCM is wider;

3) The ripple current through the inductor is reduced, as well as the currents through the switches;

4) Reactive elements are designed for twice the switching frequency, causing the required critical inductance to be smaller, for instance;

5) Only 50% of the power is delivered to the load through the main switches due to the magnetic coupling between the transformer windings. Besides, an important advantage of the proposed converter operating in OM ($D > 0.5$) is the continuous nature of the input current, which is inherently discontinuous in the conventional buck converter, what may lead to the use of an input filter for some applications.

VI. Acknowledgment

This paper is based on M. Tech. project carried out by the student of pydah college of engineering & technology, Kakinada studying M.Tech (Power Electronics) The project had been completed by Ms. K. BHANU DEEPIKA bearing H.T.no.: 126T1D4307 under the guidance of Ms. M PAVANI.

REFERENCES

1. M. Berkhout and L. Dooper, "Class-D audio amplifiers in mobile applications," *IEEE Trans. Circuits Syst. I, Reg. Papers*, vol. 57, no. 5, pp. 992–1002, May 2010.
2. E. K. Sato,M. Kinoshita, Y. Yamamoto, and T. Amboh, "Redundant highdensity high-efficiency double-conversion uninterruptible power system," *IEEE Trans. Ind. Appl.*, vol. 46, no. 4, pp. 1525–1533, Jul./Aug. 2010.
3. S. V. Araujo, R. P. Torrico-Bascop´e, and G. V. Torrico-Bascop´e, "Highly efficient high step-up converter for fuel-cell power processing based on three-state commutation cell," *IEEE Trans. Ind. Electron.*, vol. 57, no. 6, pp. 1987–1997, Jun. 2010.
4. Z. Amjadi and S. S. Williamson, "Power-electronics-based solutions for plug-in hybrid electric vehicle energy storage and management systems," *IEEE Trans. Ind. Electron.*, vol. 57, no. 2, pp. 608–616, Feb. 2010.
5. G. Yao, Y. Shen,W. Li, and X. He, "A new soft switching snubber for the interleaved boost converters," in *Proc. 35th Annu. IEEE Power Electron. Spec. Conf.*, Jun. 2004, pp. 3765–3769.
6. I.Matsuura, K. M. Smith, Jr., and K. M. Smedley, "A comparison of active and passive switching methods for PWM converters," in *Proc. 29th Annu. IEEE Power Electron. Spec. Conf.*, May 1998, vol. 1, pp. 94–100.
7. G. Hua and F. C. Lee, "Soft-switching techniques in PWM converters," *IEEE Trans. Ind. Electron.*, vol. 42, no. 6, pp. 595–603, Dec. 1995.
8. K. Fujiwara and H. Nomura, "A novel lossless passive snubber for softswitching boost-type converters," *IEEE Trans. Power Electron.*, vol. 14, no. 6, pp. 1065–1069, Nov. 1999.
9. D. S. Oliveira, Jr., C. E. A. Silva, R. P. Torrico-Bascop´e, F. L. Tofoli, C. A. Bissochi, Jr., J. B. Vieira, Jr., V. J. Farias, and L. C. de Freitas, "Analysis, design, and experimentation of a double forward converter

with soft switching characteristics for all switches," *IEEE Trans. Power Electron.*, vol. 26, no. 8, pp. 2137–2148, Aug. 2011.

10. J. P. Rodrigues, S. A. Mussa,M. L.Heldwein, and A. J. Perin, "Three-level ZVS active clamping PWM for the dc–dc buck converter," *IEEE Trans. Power Electron.*, vol. 24, no. 10, pp. 2249–2258, Aug. 2009.
11. Y. Jang and M. M. Jovanovic, "Interleaved boost converter with intrinsic voltage-doubler characteristic for universal-line PFC front end," *IEEE Trans. Power Electron.*, vol. 22, no. 4, pp. 1394–1401, Jul. 2007.
12. D. J. Perreault and J. G. Kassakian, "Distributed interleaving of paralleled power converters," *IEEE Trans. Circuits Syst. I, Fundam. Theory Appl.*, vol. 44, no. 8, pp. 728–734, Aug. 1997.
13. S. V. Araujo, R. P. Torrico- Bascop´e, and G. V. Torrico-Bascop´e, "Highly efficient high step-up converter for fuel-cell power processing based on three-state commutation cell," *IEEE Trans. Ind. Electron.*, vol. 57, no. 6, pp. 1987–1997, Jun. 2010.
14. S. V. Araujo, R. P. Torrico-Bascop´e, G. V. Torrico-Bascop´e, and L. Menezes, "Step-up converter with high voltage gain employing threestate switching cell and voltagemultiplier," in *Proc. Power Electron. Spec. Conf.*, 2008, pp. 2271–2277.
15. R. A. da Camara, C.M. T. Cruz, and R. P. Torrico-Bascop´e, "Boost based on three-state switching cell for UPS applications," in *Proc. Brazilian Power Electron. Conf.*, 2009, pp. 313–318.
16. G. V. Torrico-Bascope, R. P. Torrico-Bascop´e, D. S. Oliveira, Jr., S. V. Ara´ujo, F. L. M. Antunes, and C. G. C. Branco, "A generalized high voltage gain boost converter based on three-state switching cell," in *Proc. IEEE Int. Symp. Ind. Electron.*, 2006, pp. 1927–1932.
17. G. V. Torrico- Bascop´e, R. P. Torrico-Bascop´e, D. S. Oliveira, Jr., S. V. Ara´ujo, F. L. M. Antunes, and C. G. C. Branco, "A high step-up converter based on three-state switching cell," in *Proc. IEEE Int. Symp. Ind. Electron.*, 2006, pp. 998–1003.
18. R. P. Torrico-Bascop´e, C. G. C. Branco, G. V. Torrico-Bascop´e, C. M. T. Cruz, F. A. A. de Souza, and L. H. S. C. Barreto, "A new isolated DC–DC boost converter using three-state switching cell," in *Proc. Appl. Power Electron. Conf. Expo.*, 2008, pp. 607–613.
19. E. E. Landsman, "A unifying derivation of switching regulator topologies," in *Proc. IEEE Power Electron. Spec. Conf.*, 1979, pp. 239–243.

20. S. Busquets-Monge, S. Alepuz, and J. Bordonau, "A bidirectional multilevel boost–buck dc–dc converter," *IEEE Trans. Power Electron.*, vol. 26, no. 8, pp. 2172–2183, Aug. 2011.
21. J. P. R. Balestero, F. L. Tofoli, R. C. Fernandes, G. V. Torrico-Bascop´e, and F. J. M. Seixas, "Power factor correction boost converter based on the three-state switching cell," *IEEE Trans. Ind. Electron.*, vol. 59, no. 3, pp. 1565–1577, Mar. 2012.
22. M. Roslan, K. H. Ahmed, S. J. Finney, and B.W.Williams, "Improved instantaneous average current-sharing control scheme for parallel-connected inverter considering line impedance impact in microgrid networks," *IEEE Trans. Power Electron.*, vol. 26, no. 3, pp. 702–716, Mar. 2011.
23. N. Genc and I. Iskender, "DSP-based current sharing of average current controlled two-cell interleaved boost power factor correction converter," *IET Power Electron.*, vol. 4, no. 9, pp. 1015–1022, 2011.
24. Y.-M. Chen, S.-Y. Tseng, C.-T. Tsai, and T.-F. Wu, "Interleaved buck converters with a single-capacitor turn-off snubber," *IEEE Trans. Aerosp. Electron. Syst.*, vol. 40, no. 3, pp. 954–967, Jul. 2004.
25. K. M. Smith, Jr. and K.M. Smedley, "Properties and synthesis of lossless, passive soft switching converters," in *Proc. 1st Int. Congr. Israel Energy Power Motion Control*, May 1997, pp. 112–119.
26. L. X. Chao, Z. Bo, Y. J. Sheng, J. Gallagher, and F. J. Gen, "A nonisolated voltage regulator module with integrating coupled-inductor," in *Proc. Power Electron. Spec. Conf.*, 2005, pp. 438–442.

INTERNATIONAL JOURNAL OF MULTIDISCIPLINARY EDUCATIONAL RESEARCH
ISSN : 2277-7881; IMPACT FACTOR - 2.972; IC VALUE:5.16
VOLUME 3, ISSUE 10(4), OCTOBER 2014

ELECTROLYTIC CAPACITOR-LESS DC ANTI-ISLANDING TECHNIQUE IN DC DISTRIBUTION SYSTEMS

Ms. K SURYA TEJASWI
suryatejaswi.225@gmail.com
Under the guidance of
Ms. B. LALITHA KUMARI
ASSISTANT PROFESSIOR
PYDAH COLLEGE OF ENGINEERING, KAKINADA

Abstract— In this paper, issues on PV interface for dc distribution systems are discussed for energy-efficient and reliable system implementation. In addition, this paper proposes a new anti-islanding technique for dc distribution as a system protection scheme. AC and dc PV interfaces are mathematically analyzed. This paper proposes a photovoltaic (PV) generation system interfaced with a dc distribution system. DC interface allows for the improvement of system efficiency by fully utilizing dc-based renewable sources and storage devices. In dc distribution, eliminating electrolytic capacitors in PV interfaces improves system reliability, increases system efficiency, and reduces cost. The operating principle is presented in detail and analysis shows that the proposed injected current perturbation technique is an effective solution for anti-islanding operation. A prototype converter features a simple structure with no electrolytic capacitor, which ensures a longer lifetime of the PV power circuit. Experimental results of the prototype circuit done by using simulink. The proposed anti-islanding technique shows fast response to the islanding condition in less than 0.2 s.

Key words: PV system, islanding technique

I. INTRODUCTION

In this trend, the research on optimization of the traditional power system by utilizing state-of-the-art power electronics is widely expanding [2]. Among the efforts, dc application approaches, such as dc distribution systems, are especially promising for the use of renewable power sources and dc loads. This paper proposes a new anti-islanding technique for dc-interfaced PV generation systems. The solution detects the island and disconnects the PV system from dc distribution in 0.2 s. Depending on the system configuration and operation principle, the technique can be utilized not only for system protection but also as a system control signal for operation mode change. DC

interface can be much more energy efficient than ac because power generated from dc sources, such as photovoltaics (PVs), can be directly supplied to the loads, which allows for a reduction of conversion loss by eliminating dc-ac and ac-dc conversion stages [3]. The penetration rate of distributed generation (DG) has rapidly increased as their feasibility and reliability improve through technology advances, and as environmental issues and sustainable developments have become a major concern [1]. DC interface systems have been applied in data centers, such that ac-dc and dc-ac conversions required for traditional uninterruptible power supplies can be completely eliminated [4]–[6].

This paper focuses on a PV generation system interfaced with dc distribution. The penetration rate has dramatically increased due to its attractive features, e.g., ease of installation, and static operation [16]. In conventional applications, PV generation system is interfaced with the ac utility. Generated energy must be converted to ac, which causes inefficacy of energy generation and usage. When PV generation is interfaced with dc distribution, the energy efficiency can be improved because redundant conversion is eliminated [17]–[20]. In addition, system lifetime issues can be improved by utilizing the advantages of dc distribution. An analytical evaluation of a variety of data center system architectures is presented in [4], where the feasibility of a 400-VDC distribution system is discussed. In view of system realization, design and control issues, such as operation modes and transition conditions, are discussed for data center applications in [6].

System performance of dc systems is maximized when the system components, such as dispersed generation sources, storage devices, and loads, are efficiently configured and managed, as shown in numerous studies related to system configuration and control schemes [7]–[11]. Low-voltage bipolar-type dc microgrid for a residential complex is proposed in [7]. Each house can share its generated power with others within the dc system.

Minimization of the energy exchanged with the ac utility, using a super capacitor as a storage device, enables the system energy efficiency to be optimized. Issues related to current-controlled bidirectional inverters are discussed in [8], where cost effective approaches are presented for system realization. In addition, several control methods are presented in [9]–[11] for dc system operation.

Research on dc system feasibility evaluation has also been widely conducted [12]–[15]. Loss comparison of dc distribution with conventional ac is made based on the system component models in [12] and [13], where an ac and dc hybrid system is also considered. In [14], availability evaluation of dc micro-grids is presented considering the system configurations and power converter topologies. Economic feasibility considering replacement and installation cost is discussed in [15]. Based on previous research, it is clear that a dc distribution system is an effective solution considering the increasing use of renewable sources and storage devices with dc preferred loads.

Module-integrated solutions, which address mismatch issues, typically utilize an electrolytic capacitor. The electrolytic capacitor is employed to block the alternate current fluctuation on the PV side from the ac system; however, it is also the main cause of power circuit failure [21]. In a dc distribution system, the decoupling capacitor is not necessary because there are no ac fluctuations. Thus, the short lifetime electrolytic capacitors can be eliminated, extending the PV generation system lifetime toward PV panel lifetime of 25 years. For system protection, there are many implementation challenges [22], [23]. In PV applications, anti-islanding technology is a key requirement for human safety and equipment protection.

In Section II, PV generation system structures are reviewed for system cost, efficiency, and reliability. In Section III, the analysis of PV voltage variation in an ac- and dc-interfaced PV generation system is presented and the feasibility of electrolytic capacitor-less converter implementation in dc distribution is verified. In Section IV, islanding operation is discussed and a new dc anti-islanding technique is proposed. In Section V, a dc PV interface is designed for building integrated photovoltaic (BIPV) modules and the prototype PV converter is implemented. Experimental results of the prototype PV converter are shown to verify the feasibility of this study. In Section VI, the conclusion is presented.

II. PV SYSTEM

Although PV panel cost has been continuously declining as a result of PV technology advances, it is still relatively expensive compared to conventional energy sources. In many countries, the installation of PV generation systems is driven by government grant and it is still an efficiency driven market due to the high cost. Therefore, efficiency and cost are the most important driving factors in the PV market [24], [25].

The centralized inverter architecture has been widely employed due to its high efficiency and low cost. Because one integrated inverter controls a group of PV modules in the centralized structure, as shown in Fig. 1(a), the efficiency of the PV power circuit is relatively high and the cost per watt is reduced due to its high power capacity. However, mismatch between panels caused by partial shading and panel characteristic differences make it difficult to achieve individual maximum power point tracking (MPPT) for each PV module [26].

String and multi-string structures have been used for improved harvest efficiency. In the string structure, energy lost due to mismatch is reduced by conditioning a single string of PV modules as shown in Fig. 1(b). However, the structure is not suitable for applications such as residential rooftop or BIPV generation system due to the partial shading problem and safety issues of high voltage wiring [27].

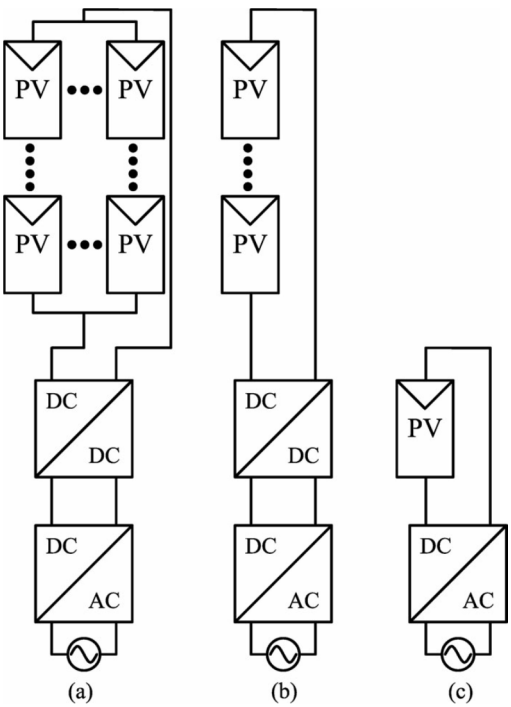

Fig. 1 PV generation system configurations in ac distribution: (a) centralized, (b) string, (c) ac module

Another solution is to have individual modules controlled by their own conditioners, as shown in Fig. 1(c). Harvest energy can be maximized and safety issues can be eliminated by attaching the conditioner at the back of the module such that users are not exposed to high dc voltage and installation becomes easier [28]. By applying the ac module concept, harvest efficiency can be kept high even in mismatch conditions. However, its relatively high cost and low efficiency compared to the centralized structure have been obstacles for its wide application.

In addition, the lifetime issue caused by the use of electrolytic capacitors for ac decoupling is also a drawback for this approach [25]. Because the module-integrated inverter is installed on the back of the PV module frame, the power circuit must sustain harsh conditions and high temperature. The lifetime of electrolytic capacitors, which is much shorter than that of other components and heavily depends on operating temperature, becomes the main obstacle to extending the lifetime of PV module generation systems [29], [30].

In this paper, a dc PV generation interface based on dc distribution is proposed as a compensatory solution to ac module concept. Retaining the advantages of the ac module concept, dc interfaced PV generation systems have lower cost and higher power conversion efficiency due to lower part count and less conversion stages from source to load. In addition, reliability issues are addressed by eliminating the short lifetime electrolytic capacitors in the PV power circuit.

III. ELECTROLYTIC CAPACITOR-LESS PV INTERFACE

Figs. 2 and 3 show the schematic of ac and dc distribution systems, respectively. Renewable sources, storage devices, and loads that are connected through their own ac-dc interfaces in the ac distribution system are directly connected to the dc link in the dc distribution system. An integrated ac-dc converter, shown in Fig. 3, controls the dc-link voltage and balances the power flow with the ac utility.

In the ac module concept, a PV converter enacts MPPT and output commutation current control. Because the output current must be injected to the ac utility in a sinusoidal manner, as shown in Fig. 4, large decoupling capacitors are required to keep

PV operation near its maximum power point (MPP) regardless of the sinusoidal alternate current. Electrolytic capacitors have been widely used for

decoupling due to their high energy density and relatively low cost. Due to the short lifetime of electrolytic capacitors, research focusing on increasing system lifetime is being widely investigated [28].

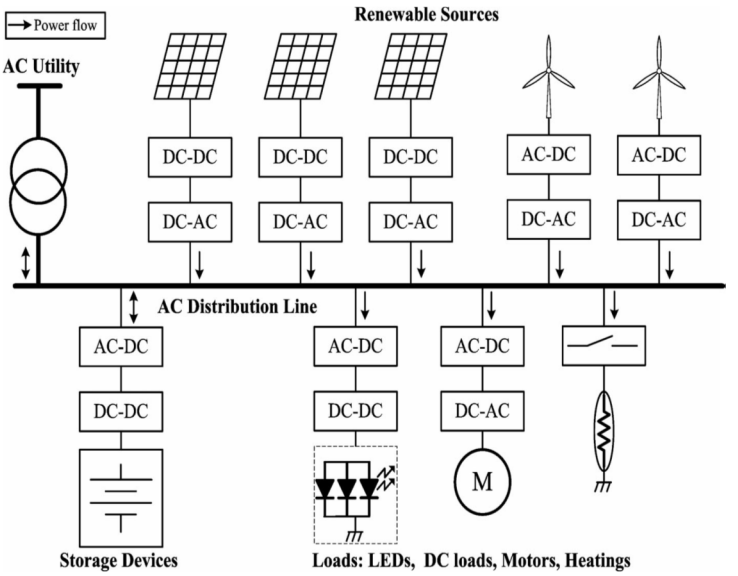

Fig. 2. Schematic of ac distribution with renewable generations and storage devices

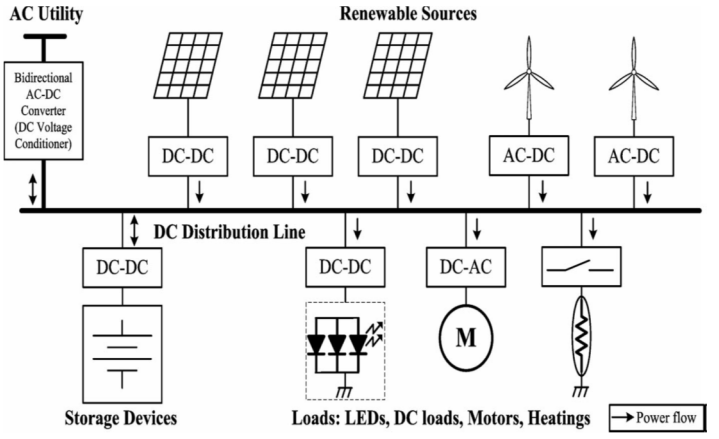

Fig. 3. Schematic of dc distribution with renewable generations and storage devices

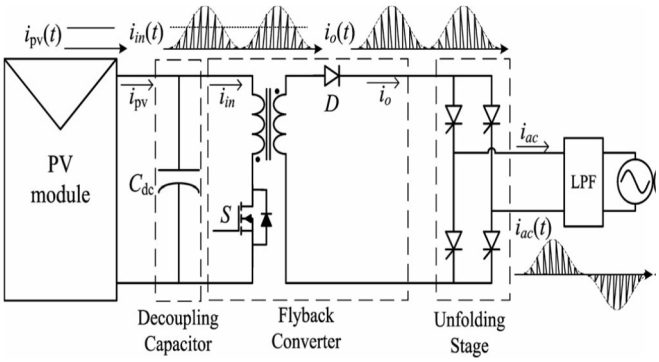

Fig. 4 Fly-back-type PV inverter with a thyristor unfolding stage

A. AC Utility Interactive PV System

Fig. 4 shows a conventional ac line interactive PV inverter, fly-back type converter followed by a thyristor unfolding stage, which is widely used for its low component count and ease of operation. Electrolytic capacitors are located between the PV module and converter to decouple ac fluctuations. Average PV module output power and instantaneous output power transferred to the ac utility are expressed as

$$P\text{pv} = V\text{pv} \cdot I\text{pv} \qquad (1)$$

$$P\text{ac}(t) = P\text{pv}(1 - \cos(2\omega\text{grid}t)) \qquad (2)$$

where Ppv , Vpv , Ipv , and ωgrid are the average power, voltage, and current of PV module, and grid angular frequency, respectively. Based on (1) and (2), voltage ripple at the PV side is

$$\Delta v_{\text{pv}} = \frac{I_{\text{pv}}}{2\omega_{\text{grid}} C_{\text{dc}}} \qquad (3)$$

Where Δvpv and Cdc are the operating voltage variation of PV module and PV dc-link capacitance, respectively.

If the PV voltage variation tolerance is chosen as 2% to ensure high harvest efficiency, a minimum capacitance of 10 mF is required for a 60-Hz ac

utility, 35-V MPP voltage, 200-W PV module application. The electrolytic capacitors relatively short lifetime, usually several thousand hours, is a limiting factor for product lifetime guarantees. Capacitor size reduction or elimination techniques using additional circuitries have been explored to tackle the issue [31].

B. DC Distribution Interactive PV Generation System

In dc distribution systems, an electrolytic capacitor-less PV interface can be implemented to improve lifetime of PV power circuits. The dc-link voltage is tightly regulated such that there are no ac fluctuations in the dc distribution system. Thus, electrolytic capacitors can be replaced with film capacitors, extending product lifetime for electric devices, such as PV interface or LED driver circuits. The lifetime of film capacitors is about ten thousands hours, which is an order of magnitude longer than electrolytic capacitor lifetimes [32].

Fig. 5(a) shows an equivalent circuit model of a PV module connected to a boost converter with a parallel capacitance. The PV is modelled as a constant current source and the boost converter is shown as a current load which is shown in Fig. 5(b). It is assumed that the boost converter employs boundary conduction mode (BCM) for this analysis. Considering the current through the capacitor *C*dc, the voltage variation at the PV module in dc distribution is

$$\Delta v_{\mathrm{pv}} = \frac{I_{Lp}}{8 \cdot C_{\mathrm{dc}} \cdot f_s} \qquad (4)$$

Where *ILp* and *fs* are the peak inductor current and switching frequency of boost converter, respectively. Voltage variation is proportional to current and reversely proportional to capacitance *C*dc and switching frequency *fs.* The relationship is similar to that of the ac module in (3), but a much smaller current and voltage variation occurs in a dc interface with the same capacitance because the dc PV converter switching frequency is in the range of tens of kilohertz, while the ac grid frequency ranges from 50 to 60Hz. A small capacitance of about 10 μF— one thousandth of ac case—is enough to meet the required 2% voltage ripple on the same 35-V MPP voltage, 200-W PV module application. In short, utilizing the lack of ac fluctuations in dc distribution, an electrolytic capacitor-less PV interface can be realized. DC distribution not

only enables efficiency improvement and cost reduction, but also helps improve system reliability.

IV. NEW ANTI-ISLANDING TECHNIQUE

Anti-islanding is a key requirement for PV conditioners interfaced with the ac utility to guarantee human safety and equipment damage protection. A variety of anti-islanding technologies have been developed that utilize the amplitude of voltage, frequency, phase, and harmonic characteristics [33]. DC distribution systems also require anti-islanding technology. In this section, a new anti-islanding technique is proposed for dc PV generation system.

A. Need for Anti-Islanding Method in DC Distribution

The ac utility can be considered as an infinite source, which means that it is not affected by other system components. Therefore, subsystems can be independently designed and implemented in ac distribution systems. However, it is more difficult to design reliable systems in dc distribution because all system components are directly connected to the dc link, which is easily affected by their operation. In a conventional system, bidirectional ac-dc converters are employed to tightly regulate the dc distribution voltage. The ac-dc converter balances energy exchange with the ac utility and the system goes into island condition when the converter is disconnected from the utility [3].With the ac-dc converter disabled, the dc distribution voltage must be regulated by another component or the system should be shut down for safety. In this case, charging/discharging of storage device can be enabled for dc-link voltage regulation. Using the storage interface, system efficiency can be improved by reducing the energy exchange with the ac utility. For effective dc system operation, several schemes have been proposed [7], [11], [17].

The anti-islanding method may seem to not be required, given the utilization of the ac-dc converter and energy buffer interface. However, it is still required for system protection. The ac-dc converter and energy buffer interface cannot perform properly in some conditions, such as when the devices are disconnected from a dc distribution system or renewable sources are islanded by an accident. Therefore, anti-islanding is essential in dc distribution systems for safety and protection.

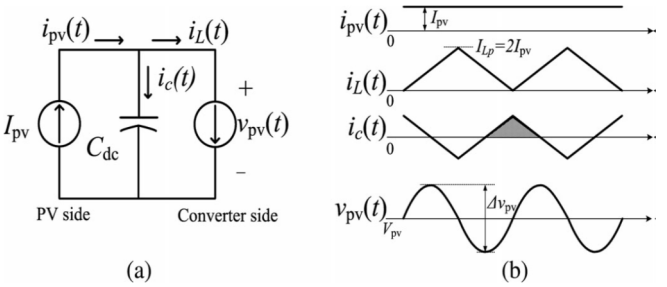

Fig. 5 PV voltage variation in dc distribution (a) Equivalent circuit model (b) Voltage and current waveforms

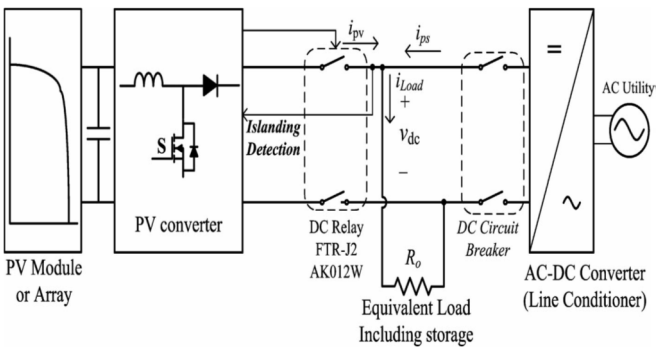

Fig. 6. DC system diagram with PV generation and line conditioner including protection devices

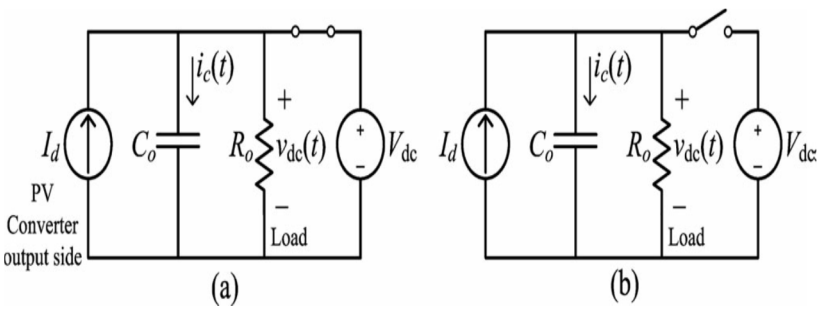

Fig. 7 Equivalent circuits of normal and island conditions (a) Normal condition. (b) Island condition

B. New DC Anti-Islanding Technique for DC Distribution System

Because voltage is the only measurable parameter in dc distribution system, while the frequency and phase can be measured for ac systems, a new dc anti-islanding algorithm is required to smoothly interconnect renewable sources to the dc distribution system. The system diagram including protection devices is shown in Fig. 6, where a PV converter, ac-dc converter, and equivalent resistance for the loads are connected to the dc link. DC circuit breakers and dc relays are utilized for safety and protection. When the difference between generated and consumed power is large enough to make the dc-link voltage reach the under or upper limit of operating voltage, the islanding condition can be easily detected. This is considered a passive method, like the over under voltage method in ac systems. However, based on the IEEE Standard 929–2000, the hardest islanding condition to detect is when the difference is near to zero because the dc-link voltage does not change quickly. Thus, an effective anti-islanding method should be able to detect the island in this worst case.

In this paper, the proposed anti-islanding algorithm is equipped with passive and active detection methods implemented in software. With the proposed injected current perturbation technique, the algorithm can detect the island condition within 0.2 s while maintaining high PV MPPT efficiency. For the analysis of islanding condition in dc distribution systems, equivalent circuits of normal and island conditions are shown in Fig. 7(a) and (b), respectively. The PV converter is modelled as a current source with an output capacitor *Co,* loads are modelled as an equivalent resistor, and the dc link is shown as a constant voltage source. The proposed anti-islanding algorithm is based on injected current perturbation. By causing a current imbalance for a short time at a scheduled frequency *fp,* as shown in Fig. 8, island conditions can be detected. In normal operation, ac-dc power converter is operating and the dc-link voltage is not affected by the current injection. However, without the dc-link regulation, the voltage is affected by the perturbation. If the fluctuation caused by injected current perturbation exceeds a set threshold value, algorithm increases the amount of perturbation as shown in Fig. 8, which creates positive feedback. The voltage change caused by the current imbalance is accelerated and the island is quickly detected by under voltage protection. The performance of the algorithm is determined by the perturbation factor *k*, perturbation frequency *fp,* and perturbation duration *Tp.* In addition, the effect of the algorithm on MPPT efficiency in normal operation should be considered.

Based on the equivalent circuit in Fig. 7, mathematical analysis is carried out. In the analysis, it is assumed that the resistor is exactly matched to the injected current before the perturbation, and injected current *id* is considered a constant current source, which means that switching ripple in PV converter output current is ignored. After islanding, the dc-link voltage is expressed as

$$\frac{dv_{\mathrm{dc}}(t)}{dt} = \frac{1}{C_o}\left(k \cdot I_d - \frac{1}{R_o} v_{\mathrm{dc}}(t)\right) \qquad (5)$$

where *v*dc(*t*), *Co* , *Id* , and *Ro* , are dc-link voltage, PV converter output capacitance, average current from PV converter to output capacitor, and equivalent resistance of the load, respectively. The solution of (5) can be expressed as

$$v_{\mathrm{dc}}(t) = k \cdot I_d \cdot R_o + [(V_{\mathrm{dc}} - k \cdot I_d \cdot R_o)e^{-1/(R_o C_o)t}] \quad (6)$$

where *V*dc is the initial voltage right before islanding occurs.

Nominal distribution voltage is assumed to be 380V.

Based on (6), the voltage drop curves as a function of time with different perturbation factor *k* values are shown in Fig and the circuit parameters are shown in Table I. As the factor *k* decreases, the detection time decreases. However, a smaller *k* creates larger perturbations on the PV input side, which is closely related to MPPT efficiency and the required PV output capacitance. Because large perturbations can affect the PV operating point and reduce MPPT efficiency, proper perturbation factor must be determined. The perturbation frequency *fp* exhibits a trade-off between detection time and MPPT efficiency. Thus, perturbation duration *Tp* should be determined considering dc-link voltage condition such as dc-link voltage ripple and voltage dynamics in normal operation.

TABLE I

SPECIFICATIONS OF A PROTOTYPE PV CONVERTER

Input Voltage (PV volt.)	0-145 V
Output Voltage (DC Line)	380 V
Maximum Power	120 W
C_{dc}	Film, 10 μF
Inductance, L	Core: RM14LP, 710 μH,
MOSFET, S	28NM50N, 500 V, 21A
Diode, D	SDT08S60, 600 V, 8A

V. RESULTS

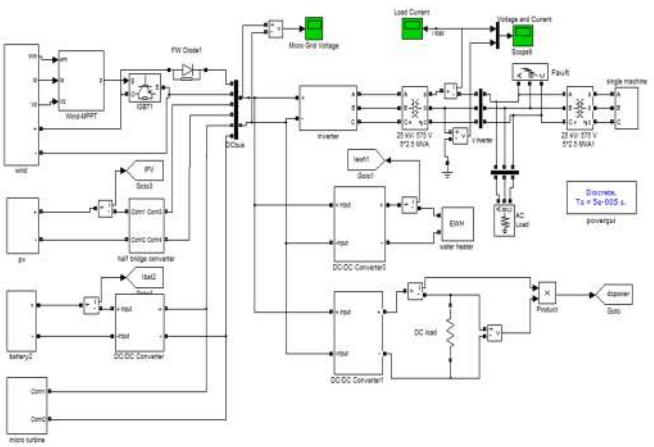

Fig. 8 Diagram of the proposed BCM boost power converter for dc PV interface with a digital signal processor

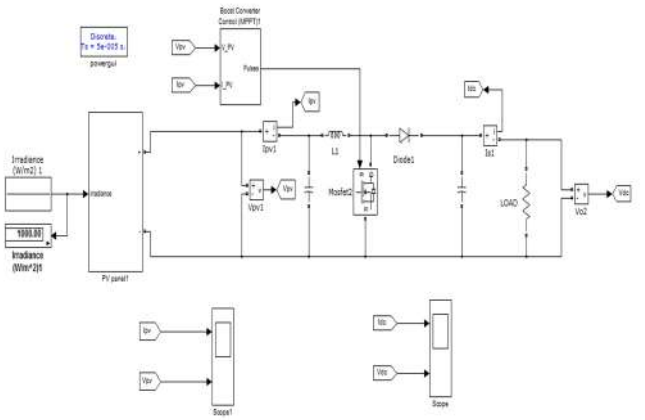

Fig 9 simulation diagram of PV with MPPT

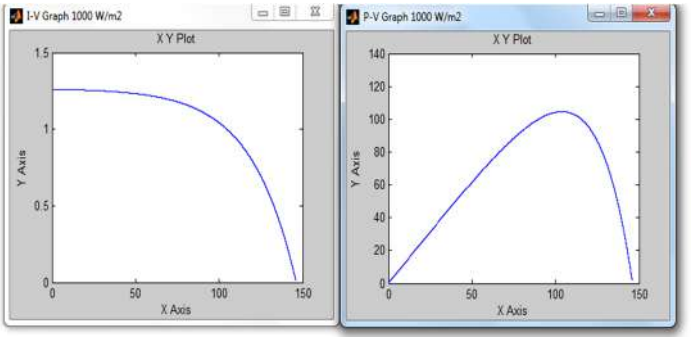

Fig 10 V-I and P-V characteristics

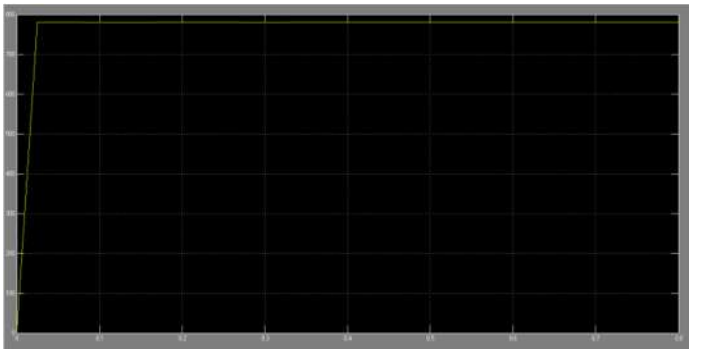

Fig 11 DC bus voltage

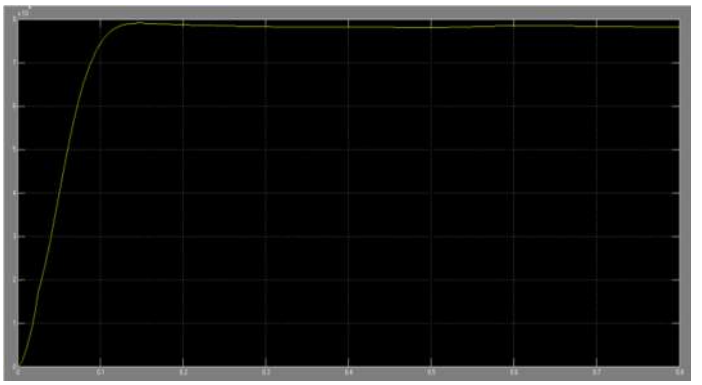

Fig 12 DC load power

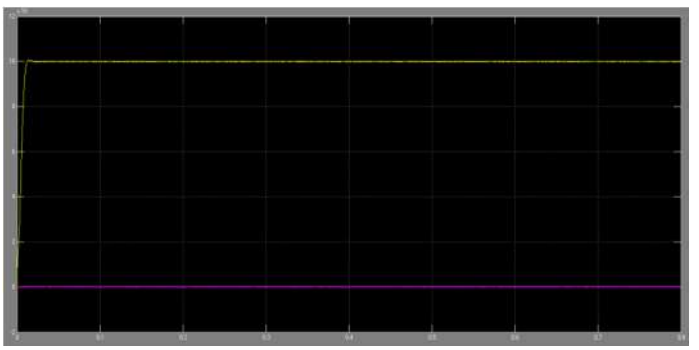

Fig 13 grid active & reactive powers

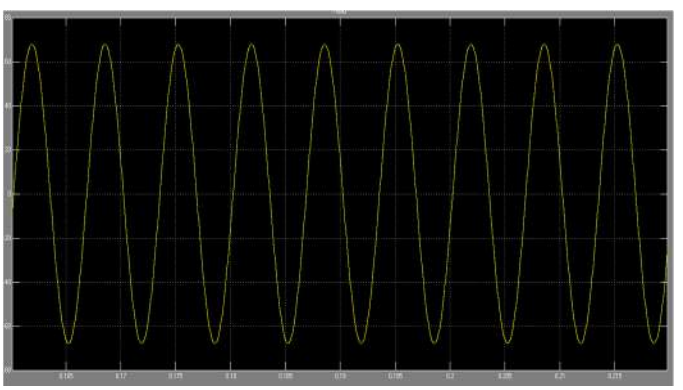

Fig 14 load current

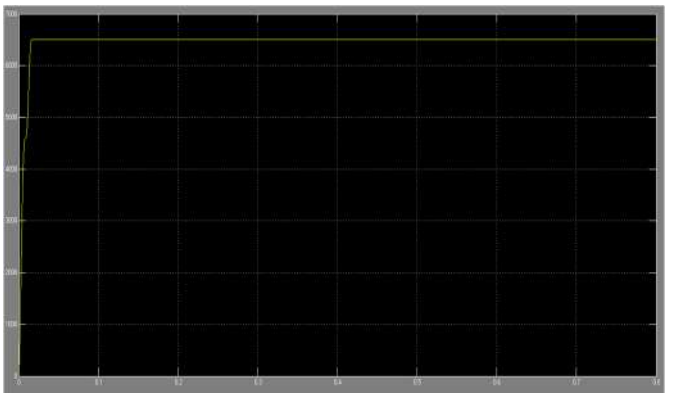

Fig 15 grid side RMS voltage

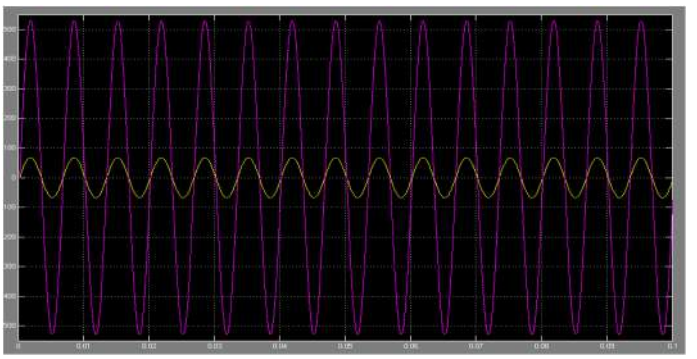

Fig 16 load voltage & current

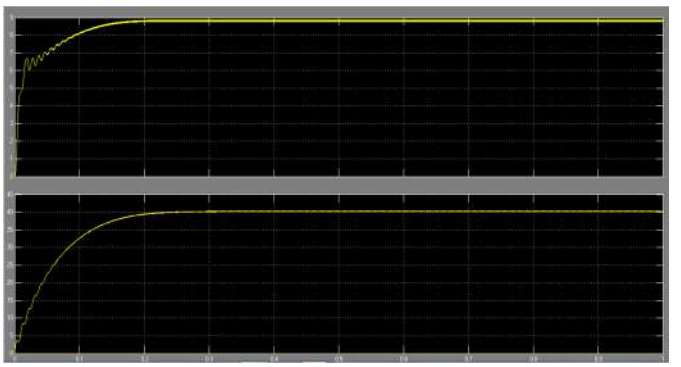

Fig 17 MPPT input voltage & current

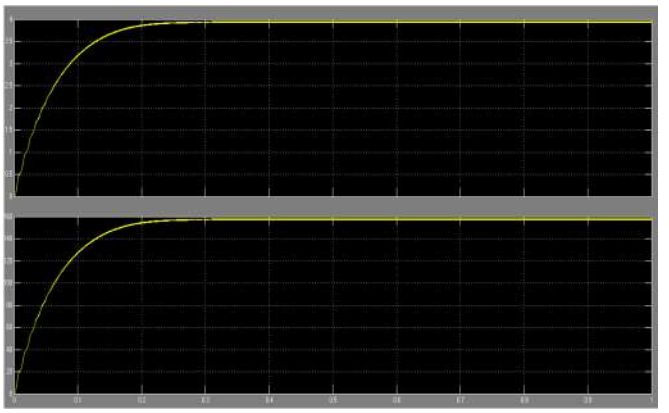

Fig 18 MPPT output voltage and current

VI. CONCLUSION

A new PV interface concept for dc distribution has been proposed. Utilizing the dc distribution system, electrolytic capacitors can be replaced with film capacitors at the PV dc link, which extends PV product lifetime. Islanding detection is a key requirement for dc distribution systems to ensure safety and protection. A new anti-islanding algorithm has been proposed for dc systems. Also, dc distribution systems achieve high efficiency with simple dc power converters by eliminating the ac-dc interface. This study should be helpful to implement high efficiency and long lifetime guaranteed PV interface converters without electrolytic capacitors. In addition, the experimental results have showed that the proposed dc anti-islanding algorithm detects the island condition within 0.2 s, as estimated from the analysis. The algorithm minimally affects the MPPT efficiency.

VIII. Acknowledgment

This paper is based on M. Tech. project carried out by the student of pydah college of engineering & technology, Kakinada studying M.Tech (Power Electronics) The project had been completed by Ms. K. SURYA TEJASWI bearing H.T.no.: 126T1D4308 under the guidance of B. LALITHA KUMARI.

REFERENCES

1. J.M. Guerrero, F. Blaabjerg, T. Zhelev, K. Hemmes, E. Monmasson, S. Jemei, M. P. Comech, R. Granadino, and J. I. Frau, “Distributed

generation: Toward a new energy paradigm," *IEEE Ind. Electron. Mag.*, vol. 4, no. 1, pp. 52–64, Mar. 2010.

2. F. Blaabjerg, Z. Chen, and S. B. Kjaer, "Power electronics as efficient interface in dispersed power generation systems," *IEEE Trans. Power Electron.*, vol. 19, no. 5, pp. 1184–1194, Sep. 2004.
3. D. Boroyevich, I. Cvetkovic, D. Dong, R. Burgos, F. Wang, and F. Lee, "Future electronic power distribution systems a contemplative view," in *Proc. IEEE Int. Conf. Optim. Electr. Electron. Equip.*, May 2010, pp. 1369–1380.
4. A. Pratt, P. Kumar, and T. V. Aldridge, "Evaluation of 400V DC distribution in telco and data centers to improve energy efficiency," in *Proc. IEEE Int. Telecommun. Energy Conf.*, Sep./Oct. 2007, pp. 32–39.
5. K. Hirose, "DC power demonstrations in Japan," in *Proc. IEEE Int. Conf. Power Electron.-ECCC Asia*, May/Jun. 2011, pp. 242–247.
6. D. Salomonsson, L. Soder, and A. Sannino, "An adaptive control system for a DC microgrid for data centers," *IEEE Trans. Ind. Appl.*, vol. 44, no. 6, pp. 1910–1917, Nov./Dec. 2008.
7. H. Kakigano, Y. Miura, and T. Ise, "Low-voltage bipolar-type DC microgrid for super high quality distribution," *IEEE Trans. Power Electron.*, vol. 25, no. 12, pp. 3066–3075, Dec. 2010.
8. T.-F. Wu, K.-H. Sun, C.-L. Kuo, and C.-H. Chang, "Predictive current controlled 5-kW single-phase bidirectional inverter with wide inductance variation for DC-microgrid applications," *IEEE Trans. Power Electron.*, vol. 25, no. 12, pp. 3076–3084, Dec. 2010.
9. Y.-C. Chang and C.-M. Liaw, "Establishment of a switched-reluctance generator-based common DC microgrid system," *IEEE Trans. Power Electron.*, vol. 26, no. 9, pp. 2512–2527, Sep. 2011.
10. P. C. Loh, D. Li, and F. Blaabjerg, "Autonomous control of interlinking converters in hybrid AC-DC microgrids with energy storages," in *Proc. IEEE Energy Convers. Congr. Expo.*, Sep. 2011, pp. 652–658.
11. L. Xu and D. Chen, "Control and operation of a DC microgrid with variable generation and energy storage," *IEEE Trans. Power Del.*, vol. 26, no. 4, pp. 2513–2522, Oct.
12. M. R. Starke, L. M. Tolbert, and B. Ozpineci, "AC vs. DC distribution: A loss comparison," in *Proc. IEEE/PES Transmiss. Distrib. Conf. Expo.*, Apr. 2008, pp. 1–7.

13. D. J. Hammerstrom, "AC versus DC distribution systems: Did we get it right?," in *Proc. IEEE Power Eng. Soc. Gen. Meet.*, Jun. 2007, pp. 1–5.
14. A. Kwasinski, "Quantitative evaluation of DC microgrids availability: Effects of system architecture and converter topology design choices," *IEEE Trans. Power Electron.*, vol. 26, no. 3, pp. 835–851, Mar. 2011.
15. B. A. Thomas, "Edison revisited: Impact of DC distribution on the cost of LED lighting and distributed generation," in *Proc. IEEE Appl. Power Electron. Conf. Expo.*, Feb. 2010, pp. 588–593.
16. R. Teodorescu, M. Liserre, and P. Rodriguez, *Grid Converters for Photovoltaic and Wind Power Systems*. Chichester, U.K.:Wiley, 2011, pp. 3–29.
17. K. Sun, L. Zhang, Y. Xing, and J. M. Guerrero, "A distributed control strategy based on DC bus signaling for modular photovoltaic generation systems with battery energy storage," *IEEE Trans. Power Electron.*, vol. 26, no. 10, pp. 3032–3045, Oct. 2011.
18. C.-M. Lai, C.-T. Pan, and M.-C. Cheng, "High-efficiency modular high step-up interleaved boost converter for DC-microgrid applications," *IEEE Trans. Ind. Appl.*, vol. 48, no. 1, pp. 161–171, Jan./Feb. 2012.

INTERNATIONAL JOURNAL OF MULTIDISCIPLINARY EDUCATIONAL RESEARCH
ISSN : 2277-7881; IMPACT FACTOR - 2.972; IC VALUE:5.16
VOLUME 3, ISSUE 10(4), OCTOBER 2014

SPACE VECTOR PULSE WIDTH AMPLITUDE MODULATION FOR VOLTAGE SOURCE INVERTER

Mr. T. M. RAYUDU
rayuduthumati@gmail.com
Under the guidance of
Mr. P. VIJAYA RAMARAO
ASSISTANT PROFESSIOR
PYDAH COLLEGE OF ENGINEERING, KAKINADA

Abstract—This paper proposes a space vector pulse width amplitude modulation (SVPWAM) method voltage source inverter. In addition, it is also verified that the output harmonic distortions of SVPWAM is lower than SPWM, by only using one-third switching frequency of the latter one. For a voltage source inverter, the switching loss is reduced by 87%, compared to a conventional sinusoidal pulse width modulation (SPWM) method. For a current source inverter, the switching loss is reduced by 60%. In both cases, the power density is increased by a factor of 2 to 3. The numbers are remarkable at this power rating. As a result, it is feasible to use SVPWAM to make the buck–boost inverter suitable for applications that require high efficiency, high power density, high temperature, and low cost. Such applications include electric vehicle motor drive or engine starter/alternator.

Key words: SVPWAM, VSI, BUCK-BOOST

I. INTRODUCTION

Currently two existing inverter topologies are used for hybrid electric vehicles (HEVs) and electric vehicles (EVs): the conventional three-phase inverter with a high voltage battery and a three-phase pulse width modulation (PWM) inverter with a dc/dc boost front end. The conventional PWM inverter imposes high stress on switching devices and motor thus limits the motor's constant power speed range (CPSR), which can be alleviated through the dc–dc boosted PWM inverter. Fig. 1 shows a typical configuration of the series plug-in electric vehicle (PHEV). The inverter is required to inject low harmonic current to the motor, in order to reduce the winding loss and core loss. For this purpose, the switching frequency of the inverter is designed within a high range from 15 to 20 kHz, resulting in the switching loss increase in switching device and also the core loss increase in the motor stator. To solve this problem, various soft-switching methods have been proposed [1]–[3]. Active

switching rectifier or a diode rectifier with small DC link capacitor has been proposed in [4], [5], [8]–[12]. Varies types of modulation method have been proposed previously such as optimized pulse-width-modulation [13], improved Space-Vector-PWM control for different optimization targets and applications [14]–[16], and discontinuous PWM (DPWM) [17]. Different switching sequence arrangement can also affect the harmonics, power loss and voltage/current ripples [18]. DPWM has been widely used to reduce the switching frequency, by selecting only one zero vector in one sector. It results in 50% switching frequency reduction. However, if an equal output THD is required; DPWM cannot reduce switching loss than SPWM. Moreover, it will worsen the device heat transfer because the temperature variation. A double 120 flattop modulation method has been proposed in [6] and [7] to reduce the period of PWM switching to only 1/3 of the whole fundamental period. However, these papers didn't compare the spectrum of this method with others, which is not fair. In addition, the method is only specified to a fixed topology, which cannot be applied widely.

This paper proposes a novel generalized space vector Pulse width amplitude modulation (SVPWAM) method for the buck/boost voltage source inverter (VSI) and current source inverter (CSI). By eliminating the conventional zero vector in the space vector modulation, two-third and one-third switching frequency reduction can be achieved in VSI and CSI, respectively. If a unity power factor is assumed, an 87% switching loss reduction can be implemented in VSI, and a 74% reduction can be implemented in CSI. A 1-kW boost-converter inverter system has been developed and tested based on the SVPWAM method. A 90% power loss reduction compared to SPWM has been observed. The two stage efficiency reaches 96.7% at the full power rating. The power volume density of the prototype is 2.3kW/L. The total weight of the system is 1.51 lb. Therefore, a high-efficiency, high-power density, high-temperature, and low cost 1-kW inverter is achieved by using an SVPWAM method.

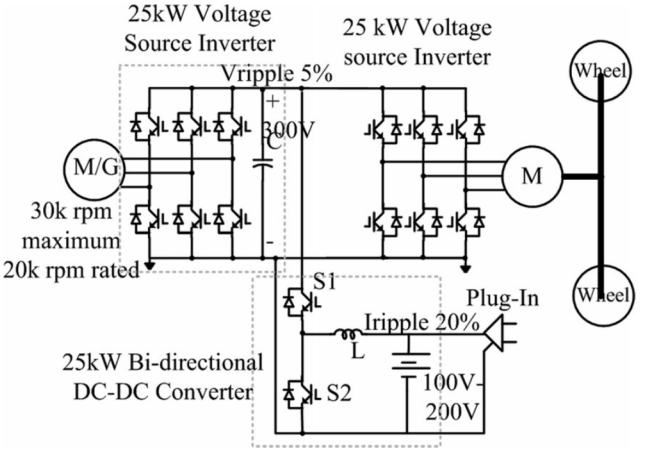

Fig. 1 Typical configuration of a series PHEV

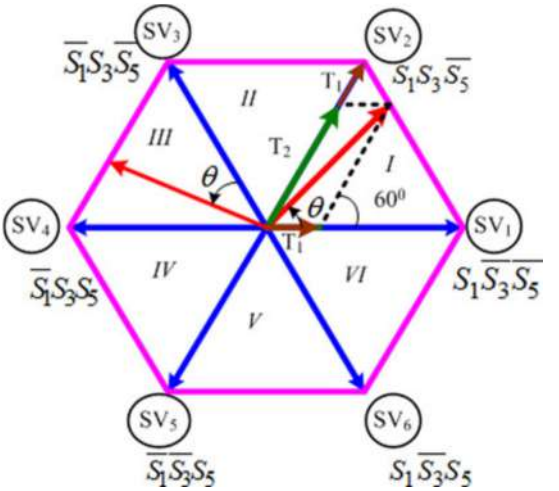

Fig. 2 SVPWAM for VSI

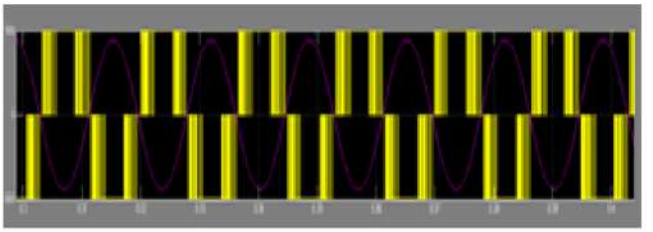

Fig. 3 DC-link voltage of SVPWAM in VSI

II. SVPWAM FOR VSI

A. Principle of SVPWAM Control in VSI

The principle of an SVPWAM control is to eliminate the zero vector in each sector. The modulation principle of SVPWAM is shown in Fig. 2. In each sector, only one phase leg is doing PWM switching; thus, the switching frequency is reduced by two-third. This imposes zero switching for one phase leg in the adjacent two sectors. For example, in sector VI and I, phase leg A has no switching at all. The dc-link voltage thus is directly generated from the output line-to-line voltage. In sector I, no zero vector is selected. Therefore, *S*1 and *S*2 keep constant ON, and *S*3 and *S*6 are doing PWM switching. As a result, if the output voltage is kept at the normal three-phase sinusoidal voltage, the dc-link voltage should be equal to line-to-line voltage *V*ac at this time. Consequently, the dc-link voltage should present a 6ω varied feature to maintain a desired output voltage. The corresponding waveform is shown in solid line in Fig. 3. A dc–dc conversion is needed in the front stage to generate this 6ω voltage. The topologies to implement this method will be discussed later.

The original equations for time period *T*1 and *T*2 are

$$T_1 = \frac{\sqrt{3}}{2} m \sin\left(\frac{\pi}{3} - \theta\right); \quad T_2 = \frac{\sqrt{3}}{2} m \sin(\theta) \qquad (1)$$

Where $\theta \in [0, \pi/3]$ is relative angle from the output voltage vector to the first adjacent basic voltage vector like in Fig. 2. If the time period for each vector maintains the same, the switching frequency will vary with angle, which results in a variable inductor current ripple and multi-frequency output harmonics.

Therefore, in order to keep the switching period constant but still keep the same pulse width as the original one, the new time periods can be calculated as

$$T_1'/T_s = T_1/(T_1 + T_2) \qquad (2)$$

The vector placement within one switching cycle in each sector is shown in Fig. 4. Fig. 5 shows the output line-to-line voltage and the switching signals of *S*1.

B. Inverter Switching Loss Reduction for VSI

For unity power factor case, the inverter switching loss is reduced by 86% because the voltage phase for PWM switching is within [−60◦, 60◦], at which the current is in the zero-crossing region. In VSI, the device voltage stress is equal to dc-link voltage *V*DC, and the current stress is equal to output current *ia*. Thus the switching loss for each switch is

$$\begin{aligned} P_{\mathrm{SW_I}} &= \frac{1}{2\pi}\left[\int_{-\pi/6}^{\pi/6} E_{\mathrm{SR}} \frac{|I_m \sin(\omega t)| \cdot V_{\mathrm{DC}}}{V_{\mathrm{ref}} I_{\mathrm{ref}}} \cdot f_{\mathrm{sw}}\, d\omega t \right. \\ &\quad \left. + \int_{5\pi/6}^{7\pi/6} E_{\mathrm{SR}} \frac{|I_m \sin(\omega t)| \cdot V_{\mathrm{DC}}}{V_{\mathrm{ref}} I_{\mathrm{ref}}} \cdot f_{\mathrm{sw}}\, d\omega t \right] \\ &= \frac{2-\sqrt{3}}{\pi} \cdot \frac{I_m V_{\mathrm{DC}}}{V_{\mathrm{ref}} I_{\mathrm{ref}}} E_{\mathrm{SR}} \cdot f_{\mathrm{sw}}, \end{aligned} \qquad (3)$$

Where *E*SR, *V*ref , *I*ref are the references.

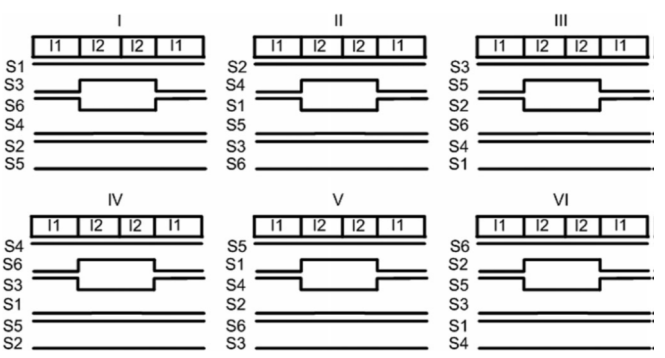

Fig. 4 Vector placement in each sector for VSI

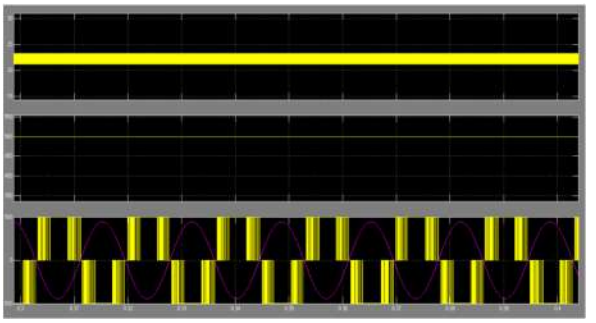

Fig. 5 Theoretic waveforms of dc-link voltage, output line-to-line voltage and switching signals

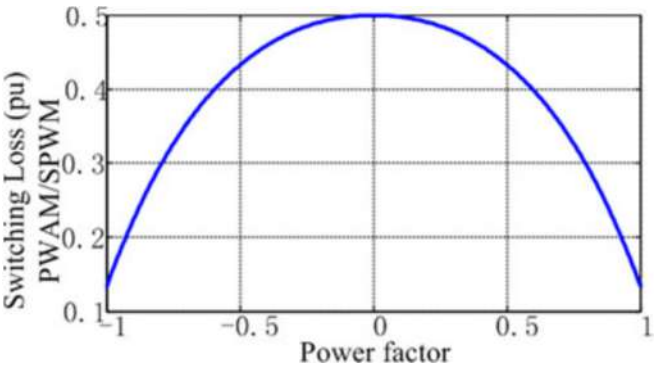

Fig. 6 (SVPWAM power loss/SPWM power loss) versus power factor in VSI

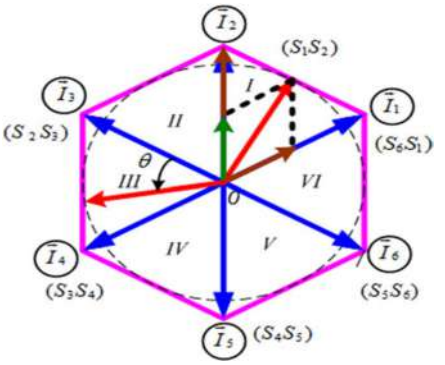

Fig. 7 Conventional CSI and its corresponding SVPWAM diagram

Since the SVPWAM only has PWM switching in two 60 sections, the integration over 2π can be narrowed down into integration within two 60◦

$$P_{\mathrm{SW_I}} = (2\sqrt{3})/\pi \cdot (I_m V_{\mathrm{DC}}/(V_{\mathrm{ref}} I_{\mathrm{ref}})) \cdot E_{\mathrm{SR}} \cdot f_{\mathrm{sw}}. \quad (4)$$

The switching loss for a conventional SPWM method is

$$P_{\mathrm{SW_I'}} = (2/\pi) \cdot (I_m V_{\mathrm{DC}}/(V_{\mathrm{ref}} I_{\mathrm{ref}})) \cdot E_{\mathrm{SR}} \cdot f_{\mathrm{sw}}. \quad (5)$$

In result, the switching loss of SVPWAM over SPWM is

f = 13.4%.

However, when the power factor decreases, the switching loss reduction amount decreases because the switching current increase as Fig. 6 shows. As indicated, the worst case happens when power factor is equal to zero, where the switching loss reduction still reaches 50%. In conclusion, SVPWAM can bring the switching loss down by 50–87%.

III. SVPWAM FOR CSI

A. Principle of SVPWAM in CSI

The principle of SVPWAM in CSI is also to eliminate the zero vectors. As shown in Fig. 7, for each sector, only two switches are doing PWM switching, since only one switch in upper phase legs and one switch in lower phase legs are conducting together at any moment. Thus, for each switch, it only needs to do PWM switching in two sectors, which is one-third of the switching period. Compared to SVPWM with single zero vector selected in each sector, this method brings down the switching frequency by one-third.

Similarly, the dc-link current in this case is a 6ω varied current. It is the maximum envelope of six output currents: $Ia, Ib, Ic, -Ia, -Ib, -Ic$, as shown in Fig. 8. For example, in sector I, *S*1 always keeps ON, so the dc-link current is equal to *Ia.* The difference between dc-link current in CSI and dc-link voltage in VSI is dc-link current in CSI is overlapped with the phase current, but dc-link voltage in VSI is overlapped with the line voltage, not the phase voltage.

The time intervals for two adjacent vectors can be calculated in the same way as (1) and (2). According to diagram in Fig. 7, the vector placement in each switching cycle for six switches can be plotted in Fig. The SVPWAM is implemented on conventional CSI through simulation. Fig. 10 shows the ideal waveforms of the dc current *I*dc, the output phase ac current and the

switching signals of *S*1. The switching signal has two sections of PWM in positive cycle, but no PWM in negative cycle at all.

B. Inverter Switching Loss Reduction for CSI

In CSI, the current stress on the switch is equal to the dc link current, and the voltage stress is equal to output line-to-line voltage, as shown the shadow area in Fig. Thus, the switching loss for a single switch is determined by

$$P_{\mathrm{SW_CSI}} = \frac{2-\sqrt{3}}{\pi} \frac{\overline{i_{\mathrm{dc}}} \cdot V_{\mathrm{l-lpeak}}}{V_{\mathrm{ref}} I_{\mathrm{ref}}} E_{\mathrm{SR}} f_{\mathrm{sw}}. \qquad (6)$$

When compared to discontinuous SVPWM, if the half switching frequency is utilized, then the switching loss of it becomes half of the result in (6). The corresponding switching loss ratio between SVPWAM and discontinuous SVPWM is shown

IV. Experiment Results

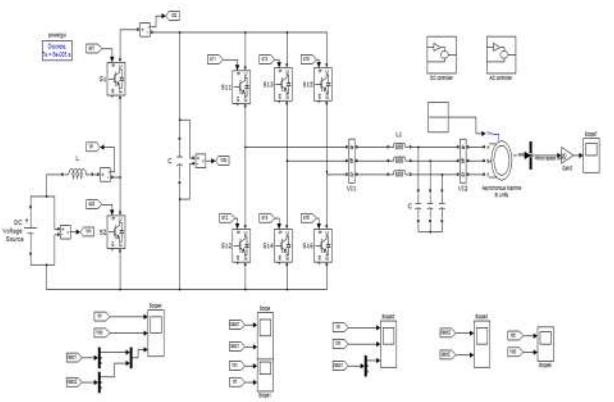

Fig 12 simulink diagram of system with DC source

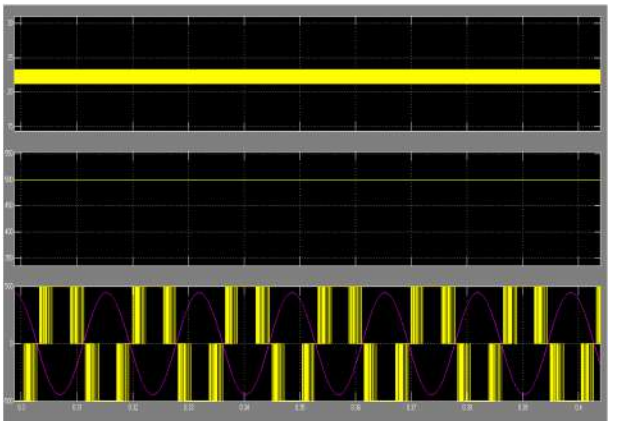

Fig Svpwm boost-buck Output voltage and input current voltage

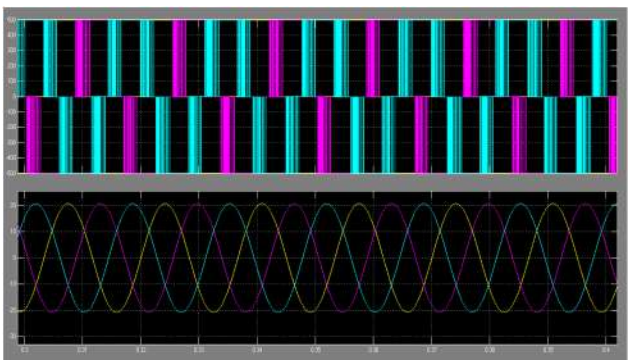

Fig svpwm boost-buck Output voltage and current

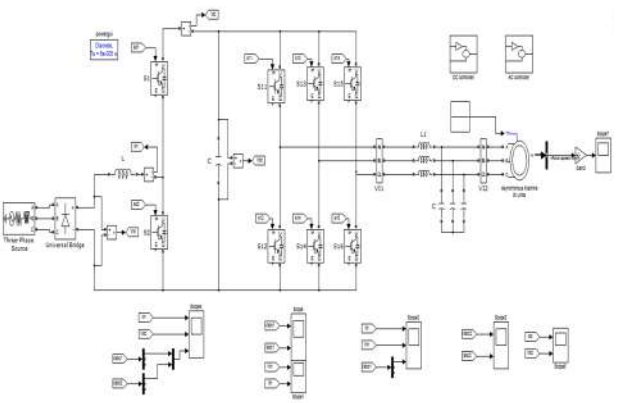

Fig simulation diagram of proposed system with AC-DC conversion

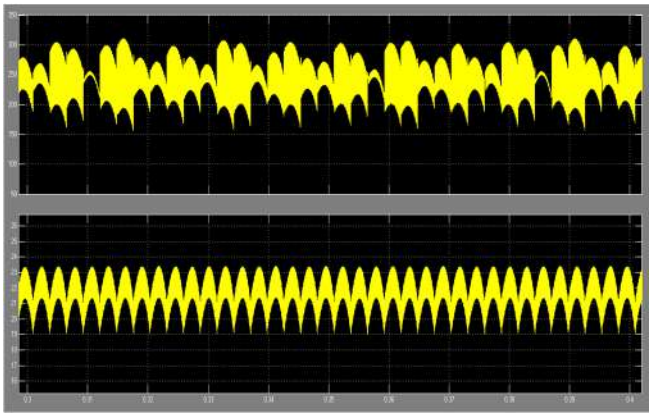

Fig input voltage, input current

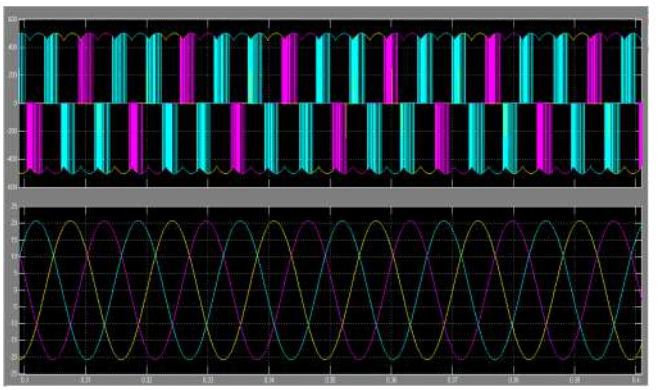

Fig output line-to-line voltage before LC filter, output current

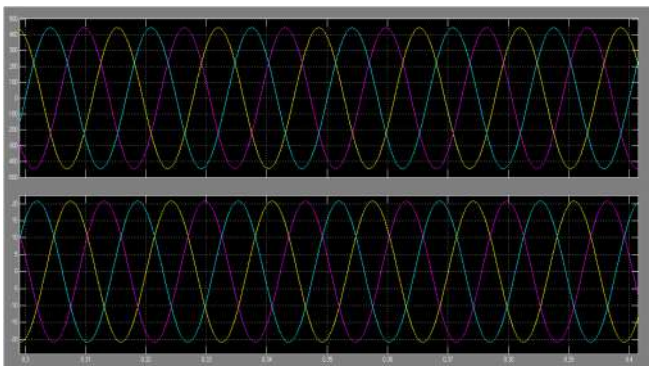

Fig output line-to-line voltage after, before LC filter, output current

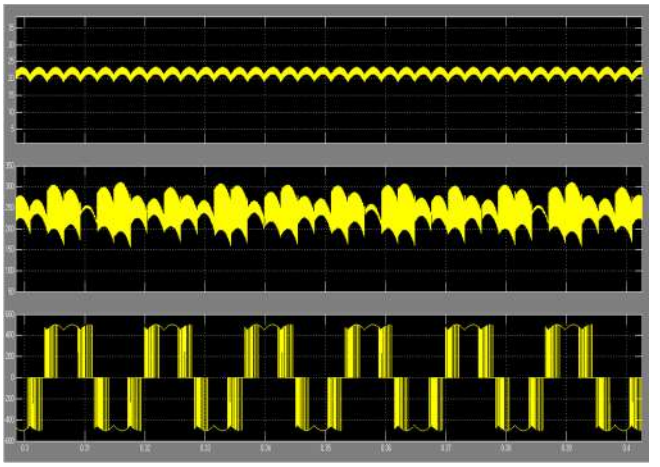

Fig Output voltage, input current & voltage

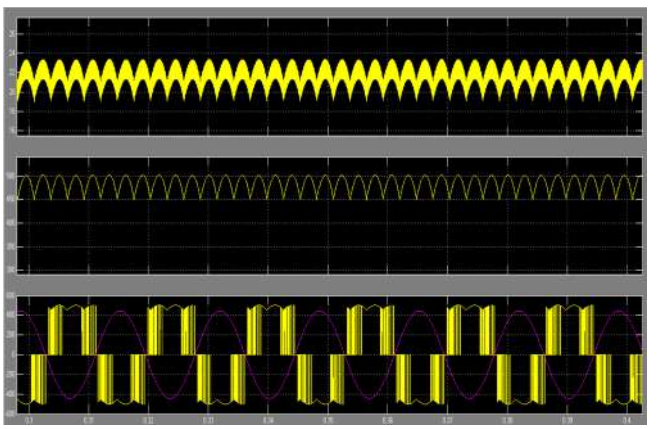

Fig Output voltage and input current

VIII. CONCLUSION

In this paper Space Vector Pulse width Amplitude Modulation for Voltage Source Inverter has been proposed. The SVPWAM control method preserves the following advantages compared to traditional SPWM and SVPWM method.

1. The cost is reduced by 30% because of reduced passives, heat sink, and semiconductor stress.
2. The power density is increased by a factor of 2 because of reduced dc capacitor and small heat sink is needed.

3. The switching power loss is reduced compared with the conventional SPWM inverter system.

A high-efficiency, high-power density, high-temperature, and low-cost inverter engine drive system has been simulated using MATLAB. The effectiveness of the proposed method in reduction of power losses has been validated by the experimental results that were obtained.

VI. Acknowledgment

This paper is based on M. Tech. project carried out by the student of pydah college of engineering & technology, Kakinada studying M.Tech (Power Electronics) The project had been completed by Mr. T. M. RAYUDU bearing H.T.no.:126T1D4309 under the guidance of Mr. P. VIJAYA RAMARAO.

REFERENCES

1. D. M. Divan and G. Skibinski, "Zero-switching-loss inverters for highpower applications," *IEEE Trans. Ind. Appl.*, vol. 25, no. 4, pp. 634–643, Jul./Aug. 1989.
2. W.McMurray, "Resonant snubbers with auxiliary switches," *IEEE Trans. Ind. Appl.*, vol. 29, no. 2, pp. 355–362, Mar./Apr. 1993.
3. J.-S. Lai, R. W. Young, Sr., G. W. Ott, Jr., J. W. McKeever, and F. Z. Peng, "A delta-configured auxiliary resonant snubber inverter," *IEEE Trans. Ind. Appl.*, vol. 32, no. 3, pp. 518–525, May/Jun. 1996.
4. J. S. Kim and S. K. Sul, "New control scheme for ac-dc-ac converter without dc link electrolytic capacitor," in *Proc. 24th Annu. IEEE Power Electron. Spec. Conf.*, Jun. 1993, pp. 300–306.
5. K. Rigbers, S. Thomas, U. Boke, and R. W. De Doncker, "Behavior and loss modeling of a three-phase resonant pole inverter operating with 120°A double flattop modulation," in *Proc. 41st IAS Annu. Meeting IEEE Ind. Appl. Conf.*, Oct. 8–12, 2006, vol. 4, pp. 1694–1701.
6. J. Shen, K Rigbers, C. P. Dick, and R. W. De Doncker, "A dynamic boost converter input stage for a double 120◦ flattop modulation based threephaseinverter," in *Proc. IEEE Ind. Appl. Soc. Annu. Meeting*, Oct. 5–9, 2008, pp. 1–7.
7. H. Fujita, "A three-phase voltage-source solar power conditioner using a single-phase PWM control method," in *Proc. IEEE Energy Convers. Congr. Expo.*, 2009, pp. 3748–3754.
8. H. Haga, K. Nishiya, S. Kondo, and K. Ohishi, "High power factor control of electrolytic capacitor less current-fed single-phase to three-phase power converter," in *Proc. Int. Power Electron. Conf.*, Jun. 21–24, 2010, pp. 443– 448.
9. X.Chen and M. Kazerani, "Space vectormodulation control of an ac-dc-ac converter with a front-end diode rectifier and reduced dc-link capacitor," *IEEE Trans. Power Electron.*, vol. 21, no. 5, pp. 1470–1478, Sep. 2006.

10. M. Hinkkanen and J. Luomi, "Induction motor drives equipped with diode rectifier and small dc-link capacitance," *IEEE Trans. Ind. Electron.*, vol. 55, no. 1, pp. 312–320, Jan. 2008.
11. J. Jung, S. Lim, and K. Nam, "A feedback linearizing control scheme for a PWM converter-inverter having a very small dc-link capacitor," *IEEE Trans. Ind. Appl.*, vol. 35, no. 5, pp. 1124–1131, Sep./Oct. 1999.
12. L. Malesani, L. Rossetto, P. Tenti, and P. Tomasin, "AC/DC/AC PWM converter with reduced energy storage in the dc link," *IEEE Trans. Ind. Appl.*, vol. 31, no. 2, pp. 287–292, Mar./Apr. 1995.
13. T. Bruckner and D. G. Holmes, "Optimal pulse-width modulation for three-level inverters," *IEEE Trans. Power Electron.*, vol. 20, no. 1, pp. 82–89, Jan. 2005.
14. F. Blaabjerg, S. Freysson, H.-H. Hansen, and S. Hansen, "A new optimized space-vector modulation strategy for a component-minimized voltage source inverter," *IEEE Trans. Power Electron.*, vol. 12, no. 4, pp. 704–714, Jul. 1997.
15. M. M. Bech, F. Blaabjerg, and J. K. Pedersen, "Random modulation techniques with fixed switching frequency for three-phase power converters," *IEEE Trans. Power Electron.*, vol. 15, no. 4, pp. 753–761, Jul. 2000.
16. F. Blaabjerg, D. O. Neacsu, and J. K. Pedersen, "Adaptive SVM to compensate dc-link voltage ripple for four-switch three-phase voltage-source inverters," *IEEE Trans. Power Electron.*, vol. 14, no. 4, pp. 743–752, Jul.1999.
17. L. Asiminoaei, P. Rodriguez, and F. Blaabjerg, "Application of discontinuous PWM modulation in active power filters," *IEEE Trans. Power Electron.*, vol. 23, no. 4, pp. 1692–1706, Jul. 2008.
18. B. P. McGrath, D. G. Holmes, and T. Lipo, "Optimized space vector switching sequences for multilevel inverters," *IEEE Trans. Power Electron.*, vol. 18, no. 6, pp. 1293–1301, Nov. 2003.
19. R. Zhang, V. H. Prasad, D. Boroyevich, and F. C. Lee, "Three-dimensional space vector modulation for four-leg voltage-source converters," *IEEE Trans. Power Electron.*, vol. 17, no. 3, pp. 314–326, May 2002.
20. R. Burgos, R. Lai, Y. Pei, F. Wang, D. Boroyevich, and J. Pou, "Space vector modulator for vienna-type rectifiersbased on the equivalence betweentwo- and three-level converters: A carrier-based implementation," *IEEE Trans. Power Electron.*, vol. 23, no. 4, pp. 1888–1898, Jul. 2008.
21. P. C. Loh, D. M. Vilathgamuwa, Y. S. Lai, G. T. Chua, and Y. Li, "Pulsewidth modulation of Z-source inverters," *IEEE Trans. Power Electron.*, vol. 20, no. 6, pp. 1346–1355, Nov. 2005.
22. F. Z. Peng, "Z-source inverter," *IEEE Trans. Ind. Appl.*, vol. 39, no. 2, pp. 504–510, Mar./Apr. 2003.

INTERNATIONAL JOURNAL OF MULTIDISCIPLINARY EDUCATIONAL RESEARCH
ISSN : 2277-7881; IMPACT FACTOR - 2.972; IC VALUE:5.16
VOLUME 3, ISSUE 10(4), OCTOBER 2014

PERFORMANCE OF A DG SYSTEM CONNECTED TO THREE-PHASE POWER CONVERTER & BOOST CONVERTER

Mr. K. MADHAVARAO
Under the guidance of
Ms. B. LALITHA KUMARI
ASSISTANT PROFESSIOR
PYDAH COLLEGE OF ENGINEERING, KAKINADA

Abstract:- This paper presents Performance of a DG System Connected to Three-Phase Power Converter & Boost Converter and the operation of a distributed generation (DG) system driven by a dc-dc step-up converter and a dc-ac voltage source inverter (VSI) interfaced with the power grid. To create a stable mode when different kinds of loads are connected locally or when working under contingency, the step-up converter must regulate the dc link voltage, allowing the VSI to stabilize its terminal voltage. The power flow between the grid and the DG is controlled by applying a power/voltage method that regulates the amplitude and the displacement of the grid voltage synthesized by the distributed generation, while a phase-locked loop algorithm is used to synchronize the grid and distributed generation. Additionally, a set of simulations are performed independent of the load type or its work regime.

Key words: DG system, VSI, boost converter

I. INTRODUCTION

A DG system operating at high performance requires a detailed evaluation of the feeder where the DG will be installed, plus an assessment of the load type the DG must supply locally and its working regime. Without these requirements, the effects of DG may be more harmful than beneficial: the insertion of new generation sources in the distribution system may cause transient effects due to switching operations, changing short-circuit levels, lower margin of stability, and inversion of the power flow through the distribution system, causing erroneous operations of the protection devices and islanding in part of the system.

THE use of distributed generation (DG) sources is currently being considered as a solution to the growing problems of energy demand. Apart from the consequent reduction in the size of the generating plants and the possibility of modular implementation, DG systems based on renewable energy sources are of great interest due to their low environmental impact and

technical advantages such as improvements in voltage levels and reduced power losses when a DG system is installed in radial lines. DG systems also promote cogeneration and improve overall system efficiency. In addition, the DG operation should not exceed the limits established by international standards for the following parameters: harmonic distortion, voltage imbalance, voltage fluctuations, and fast transients, whether the local load is unbalanced, nonlinear, or a dynamic load, such as a motor.

Recently, the use of power or current in the dq synchronous reference frame as control variables to command the voltage source inverter (VSI) connected to the grid has generated considerable interest from the scientific community. With either method, before or after the contingency takes place, the control variable remains the same, making the DG operate with limited capability to supply the load. On the other hand, two control algorithms were proposed to improve the grid-connected and intentional-islanding operations methods in which the DG system must detect the situation and switch from power or current to voltage as a control variable to provide constant rms voltage to the local loads.

The power flow is determined by controlling the amplitude and angle of displacement between the voltage produced by the DG and the grid voltage, i.e., the control variable is the same before and after the islanding mode occurs. The voltage control provides the capability to supply different kinds of loads to the DG system, such as linear, nonlinear, motor, balanced, or unbalanced, even if the DG operates in the islanding mode. These kinds of controls are suitable for DGs operating in parallel as each of the DGs are connected to the grid through a distribution transformer (DT). Conversely, the other approaches are more effective. Section II details the method used to drive both converters. Section III discusses the technique to control he power flow through the grid. Sections IV and V show the simulations and experimental setup to confirm the previous analysis, while the main points presented in this paper appear in the conclusion.

I. CHARACTERISTICS OF THE DG SYSTEM

Fig. 1 shows a diagram of the system used to analyze a typical connection of a DG system to a specific feeder, although studies to determine the best site for DG insertion should be performed before the operation analysis. A power plant represents a secondary source (DG systems), while in this study the standard grid is a basic configuration system found in 1547 standard (simulated system)

or a California Instruments LX 4500 source (experimental setup). Furthermore, the primary energy used in the proposed DG system is the same as the previously mentioned renewable energy sources.

A dc-dc converter is employed to equalize the dc link voltage and deliver energy for fast transients when required by the local load, while a dc-ac converter is used to guarantee the power quality delivered to customers (local load) and the specific feeder. To avoid disturbances between the dc-ac converter and the feeder, a phase-locked loop (PLL) algorithm associated with the zero voltage crossing detectors was used. Appendix I shows the design procedure for key passive components.

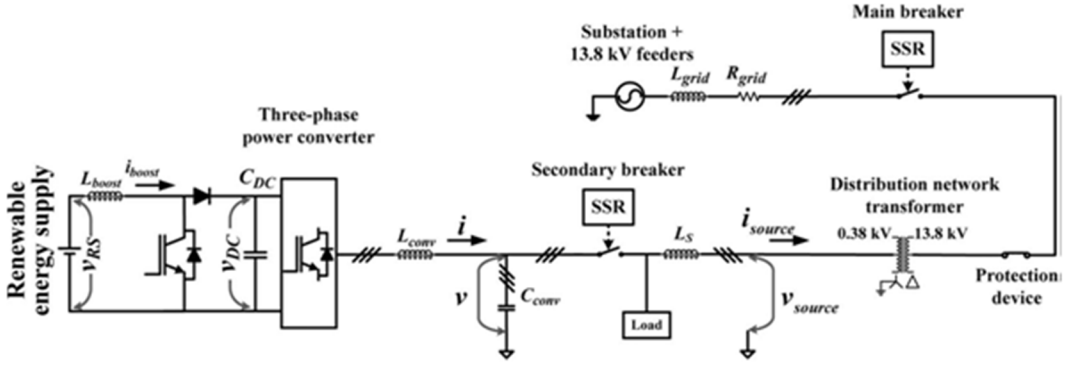

Fig. 1 General diagram of the distributed generation system

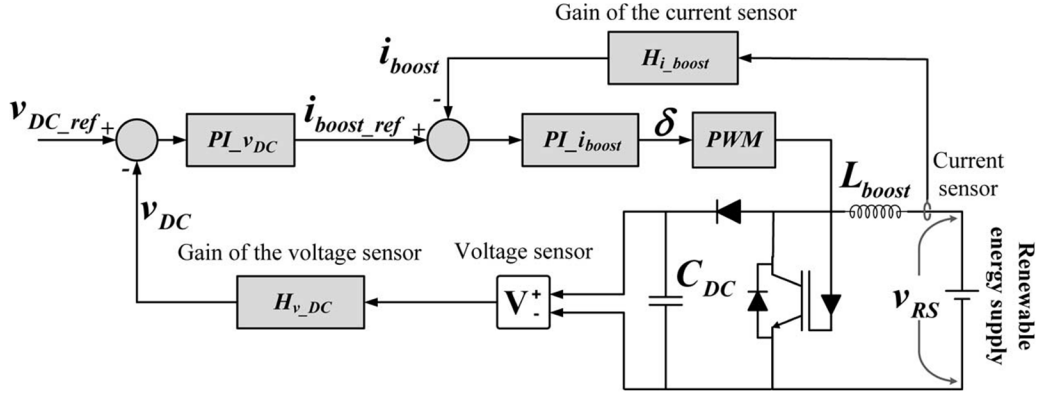

Fig. 2 Block diagram of the dc voltage/current control

A. DC-DC Converter:

A dc-dc step-up converter was used as an interface between the dc source and dc link of the three-phase dc-ac converter, as shown in Fig. 2. The step-up converter boosts the dc voltage and supplies the fast transients of energy required for the local load, thereby minimizing disturbances in the feeder current. The behaviour of the step-up converter is similar to a voltage source, and the power it delivers to the grid depends on the point of maximum power (PMP) defined by the dc source. The PMP is obtained using a tracking algorithm, based on the primary energy source. To keep the converters operating in a stable mode, proportional-integral (PI) controllers were used as a control technique to stabilize the L_{boost} current and dc voltage (v_{DC}). A method based on phase-margin (mf) and cutoff frequency (F_{CL}) was used to obtain the PIs constants (1) and (2) where the open loop gain (G_{OL}), angular frequency (ωF_{CL}), and mf define the PIs constants (k_{prop} and k_{int})

$$k_{prop}\frac{G_{OL}}{\omega_{F_{CL}}} = 1 \qquad (1)$$

$$k_{int} = k_{prop}\frac{\omega_{F_{CL}}}{tan(mf)}. \qquad (2)$$

TABLE I
PI CURRENT PARAMETERS OF THE DC-DC CONVERTER

F_{CL} (Hz)	mf (°)	V_{DC} (V)	L_{boost} (mH)	H_{i_boost}
400	80	1,000	5	1/250

TABLE II
PI VOLTAGE PARAMETERS OF THE DC-DC CONVERTER

F_{CL} (Hz)	mf (°)	V_{DC} (V)	C_{DC} (mF)	H_{v_DC}
50	60	1,000	12	1/1,500

Tables I and II display the main design parameters to determine the PIs constants of the boost converter namely, ***Hi boost*** and ***Hv DC*** gains for the dc current and voltage sensors, respectively.

B. *DC-AC Converter:*

Closed-loop controls of the output current and voltage were implemented to guarantee inverter voltage quality. PIs controllers were also used as the

control technique, while the design method of these PIs is the same as that used in the dc-dc step-up converter.

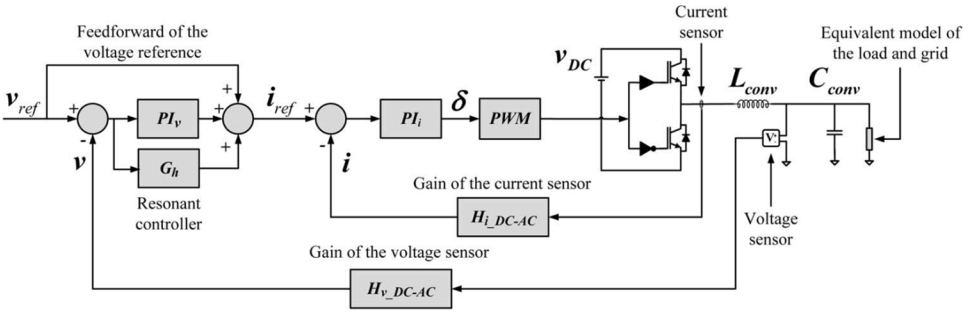

Fig. 3. Block diagram of the ac voltage/current control.

TABLE III
CURRENT PI PARAMETERS OF THE DC-AC CONVERTER

F_{CL} (Hz)	mf (°)	V_{DC} (V)	L_{conv} (mH)	$H_{i_DC\text{-}AC}$
1,200	70	1,000	2	$1/250$

TABLE IV
VOLTAGE PI PARAMETERS OF THE DC-AC CONVERTER

F_{CL} (Hz)	mf (°)	V_{DC} (V)	C_{conv} (μF)	$H_{v_DC\text{-}AC}$
120	70	1,000	15	$1/360$

TABLE V
MODIFIED PARAMETERS OF THE CONVERTERS

V_{DC} (V)	C_{DC} (μF)	H_{i_boost}	H_{v_DC}	$H_{i_DC\text{-}AC}$
330	2,800	$1/12$	$1/360$	$1/12$

Since the closed-loop cut-off frequency of the PI current controller was chosen one decade below the switching frequency, the PI of the current retains a good compensation capability in the frequency range of interest. To improve this capability, a feed forward of the reference voltage could be used to compensate the residual error in the closed-loop gain at low frequencies. Due to its high power and the need for a reduced switching frequency, the voltage controller exhibits a low regulation bandwidth (a few hundred Hertz).

To improve the control response of the output voltage regulator for fundamental and harmonic components, a resonant controller (3) is placed in parallel along with the conventional voltage PI, thereby reducing the converter impedance. In (3),(*h*) is the harmonic order, (ω_{ch}) is the bandpass round the resonance angular frequency, (ω_0) is the resonance angular frequency, and (k_{ih}) is the resonant controller gain.

A general block diagram demonstrating the control *v* is shown in Fig. 3. Tables III and IV present the main design parameters of the ac PIs, where in $\boldsymbol{H}i_DC-AC$ and $\boldsymbol{H}v_DC-AC$ are the ac current and voltage sensors gains, respectively

$$G_h = k_{ih}\frac{2\omega_{ch}s}{s^2 + 2\omega_{ch}s + (h\omega_0)^2}. \qquad (3)$$

C. *Grid Characteristics:*

In the simulations, the complete distribution system found in 1547 standard is composed of 13.8-kV feeders connected to a 69-kV radial line through 69/13.8-kV substation transformers, as shown in Fig. 1. To insert the DG at the distribution system, a 13.8/0.38 kV distribution network transformer is required to equalize the voltage levels. The line model employed in the simulations took into account the Bergeron's travelling wave method used by the Electromagnetic Transients Program, which utilized wave propagation phenomena and lineend reflections. Additionally, a set of switches was inserted between the DGs and distribution system, isolating them from each other to avoid the DG system supplies loads (loads placed in neighbouring feeders where the DG was installed) connected to the high voltage side of the distribution transform. Due to the high level of power and voltage, 12 kHz was used as the PWM switching frequency for both converters.

An experimental setup was built to substantiate the DG operation. The grid was represented by a California Instruments LX 4500 source and an isolated 220/220-V transformer; the power converter was commanded by an Analog Devices 21992 DSP, while the parameters to design the controllers are those in Tables I–IV, except for the parameters in Table V, which were calculated for a 3-kVA low scale prototype. To maintain their similarity with the simulations, the switching and sampling frequencies were also kept at 12 kHz.

The grid parameters (4) and (5) used in the experimental setup were calculated to have the same dynamic response as the simulated system. The main grid parameters of the equivalent model used in the experimental setup are represented by L_{grid}, R_{grid}, P_{SC}, f, and $V^2_{ABsource}$ (inductance and resistance (losses), short-circuit power, rated frequency, and rms voltage (phases A and B), respectively)

$$L_{grid} = \frac{V^2_{AB_{source}}}{2\pi P_{SC} f} \quad (4)$$

$$R_{grid} = \frac{(2\pi f) L_{grid}}{X}, \quad 1 < X < 100. \quad (5)$$

D. *Synchronization Algorithm:*

To connect the DG to the grid, it is essential to synchronize both systems, which is done by means of a PLL algorithm that computes the average of the internal product between v_{source} and the synchronous voltage ($v'_{\perp}$). If this equals zero in steady-state regime, $v'_{\perp}$ and v_{source} are perpendicular and synchronized. The integration of the angular frequency (ω) then defines the θ angle ($\theta = wt$) used as the argument to produce $v'_{\perp}$. Due to the high sampling and switching frequency $Ts \approx 0$, the delay block can be dismissed in the PLL closed loop transfer function

$$H_{CL} = \frac{PI_{PLL}}{s} = \frac{k_p s + k_i}{s^2 + k_p s + k_i}. \quad (6)$$

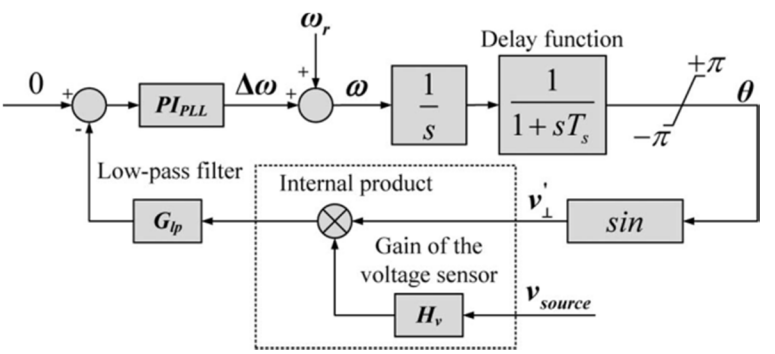

Fig. 4. PLL algorithm

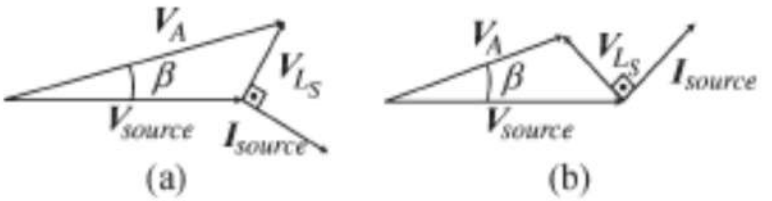

Fig. 5. Phasor diagrams. (a) Delivering active and reactive power. (b) Delivering active and absorbing reactive power.

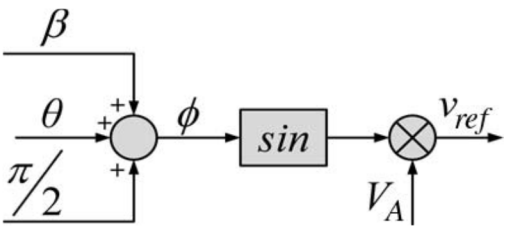

Fig. 6. Determination of the voltage reference

To compare the characteristic equation of the prototype transfer function with the PLL losed-loop transfer function (7), PI constants (8) and (9) can be adjusted by choosing the most suitable values for the natural undamped frequency (ωn) and damping ratio (ξ). To avoid stability problems, ωn should ideally be greater than one or two periods of the fundamental frequency, and the maximum overshoot lower than 30%.

A general description of the PLL algorithm is found in Fig. 4, where ωr, $\Delta\omega$, and $\boldsymbol{Hv}$ are the rated angular frequency (= $2\pi 60$), adjusted angular frequency, and voltage sensor gain (1/360) (voltage measured at the grid), respectively

$$\underbrace{s^2 + k_p s + k_i}_{\text{Characteristic equation of the PLL transfer function}} = \underbrace{s^2 + 2\xi\omega_n s + \omega_n^2}_{\text{Characteristic equation of the Prototype transfer function}} \quad (7)$$

$$k_p = 2\xi\omega_n \quad (8)$$

$$k_i = \omega_n^2. \quad (9)$$

III. POWER CONTROL THROUGH THE FEEDER

Energy produced by the renewable energy sources can be transferred to the grid by controlling the amplitude of the voltage produced by the DG, and the angle between the grid voltage and the DG voltage (β angle) through a coupling inductor (*LS*). This serves as an additional inductance placed to connect the DG to the grid, or the leakage inductance of the DT. If *LS* is a DT parameter, *vsource* must be measured on the high voltage side of the distribution network transformer. To achieve a controlled power flow from the DG to the grid, the DG voltage angle (*V A*) must be ahead of the grid voltage angle (*V Asource*). When this occurs, the DG delivers active power to the grid, as shown in Fig. 5. The same analysis can be applied to the ac voltage amplitude produced by the DG: if the amplitude of *V A* is greater than *V Asource* the DG delivers reactive power to the grid; however, if the amplitude of *V A* is less than *V Asource* the DG absorbs reactive power from the grid. The β angle is determined by the average power flowing to the grid (*Psource*), the connection reactance (*XLS*), the rms phase voltage (*VAsource*) synthesized by the grid, and the rms voltage produced (*VA*) by the DG according to (10). After defining the β angle, the DG voltage amplitude of ***V*** *A* must be adjusted according to (11), where *VAsource* and *XLS* are the same parameters described in (10). If *Qsource* = 0 the unity power factor (PF) to the feeder is obtained [34]. Additionally, *LS* is designed for a small voltage variation on the ac local voltage produced by the dc-ac inverter [16]. In Fig. 6, the voltage reference (*vref*) of the dc-ac power converter is determined by displacing θ by $\pi/2$ and adding the β angle to the result. The φ angle is then used as the argument of a sinusoidal function and multiplied by *VA* to obtain the voltage reference that must be synthesized at the VSI terminals

$$\beta = sin^{-1}\left(\frac{P_{source}\,|X_{L_S}|}{V_{A_{source}} V_A}\right) \qquad (10)$$

$$V_A = \sqrt{2}\left(\frac{V_{A_{source}}^2 - Q_{source}\,|X_{L_S}|}{V_{A_{source}}\cos\beta}\right). \qquad (11)$$

IV. SIMULATION ANALYSIS

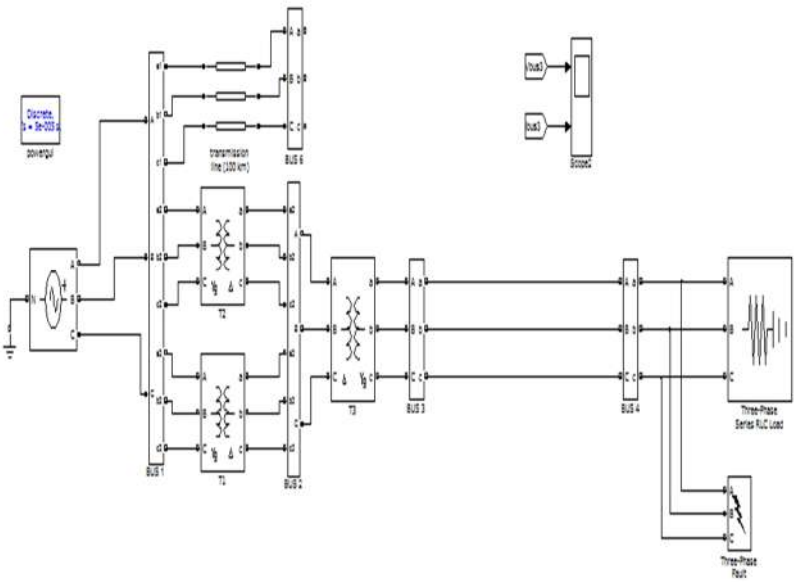

Fig 7 simulink diagram of proposed system without DVR

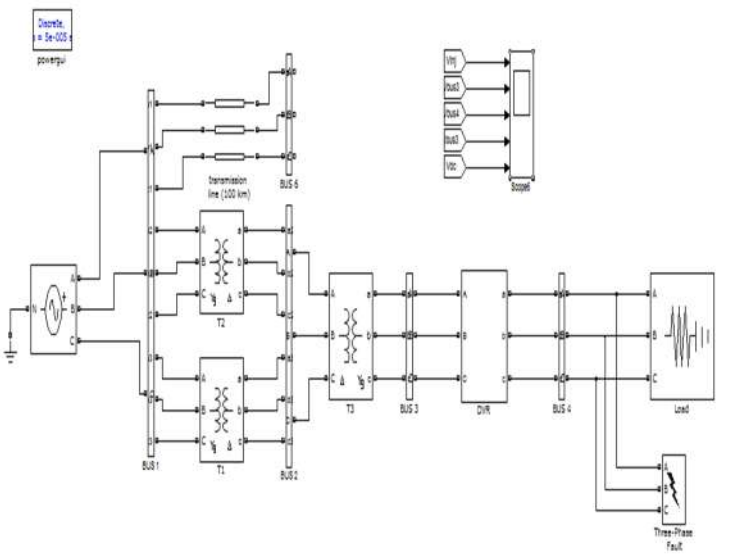

Fig 8 simulink diagram of proposed system with DVR

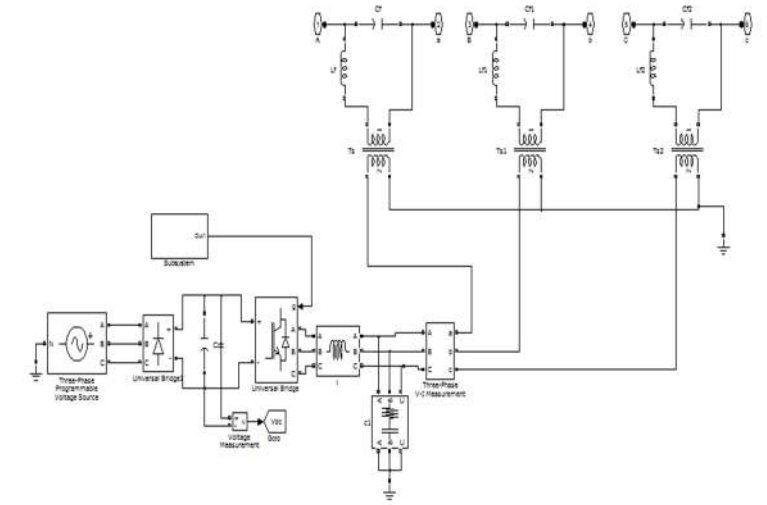

Fig 9 simulink diagram of proposed system

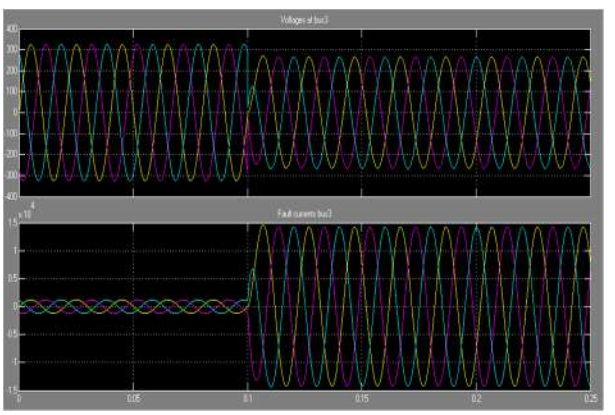

Fig. 10. (a) Voltages at bus3. (b) Fault currents, during downstream three-phase fault when the without DVR

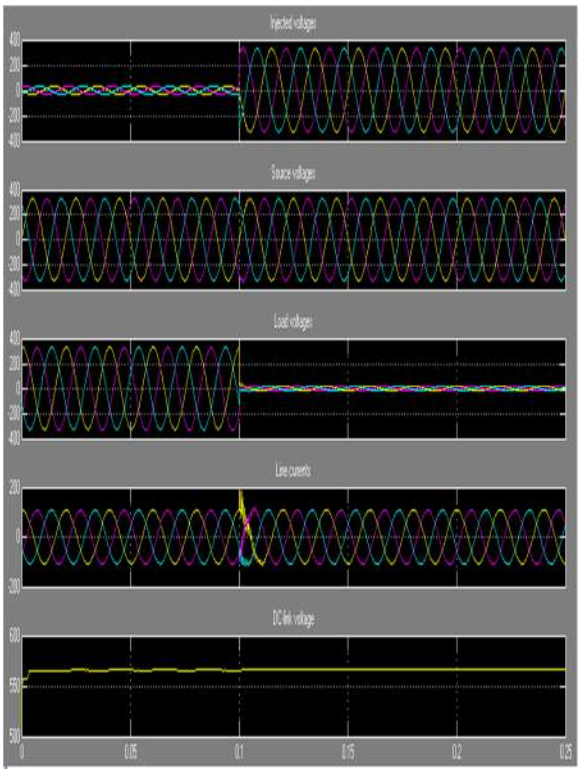

Fig. 11. (a) Injected voltages. (b) Source voltages. (c) Load voltages. (d) Line currents. (e) DC-link voltage, during the three-phase fault.

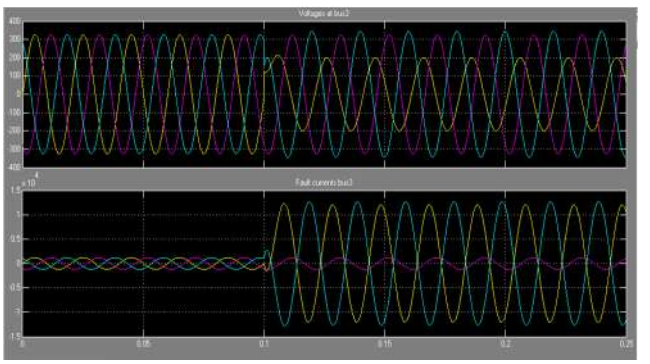

Fig. 12. (a) Voltages at bus3. (b) Fault currents, during downstream phase-to-phase fault when the without DVR

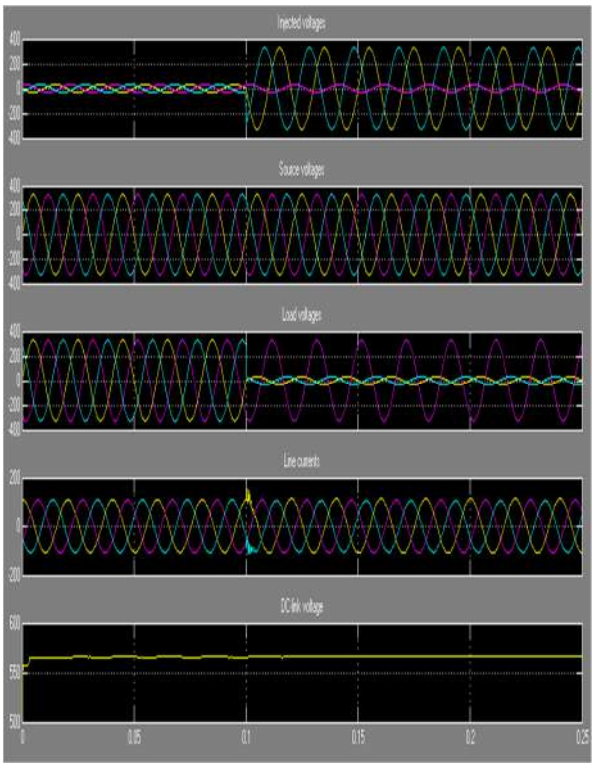

Fig. 13 (a) Injected voltages (b) Source voltages (c) Load voltages. (d) Line currents. (e) DC-link voltage, during the phase-to-phase fault.

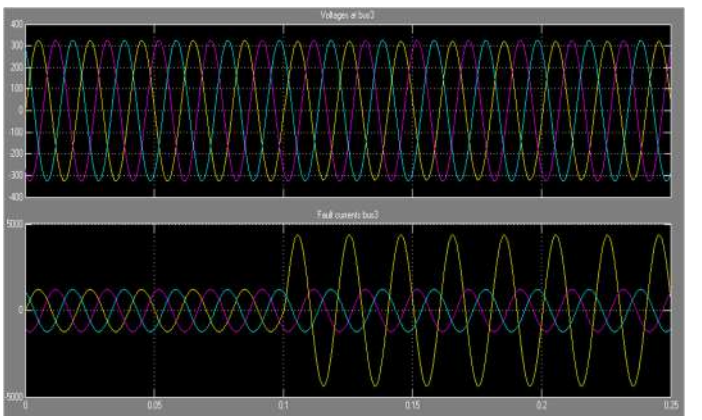

Fig. 14. (a) Voltages at bus3. (b) Fault currents, during the downstream single phase- to-ground fault when the without DVR

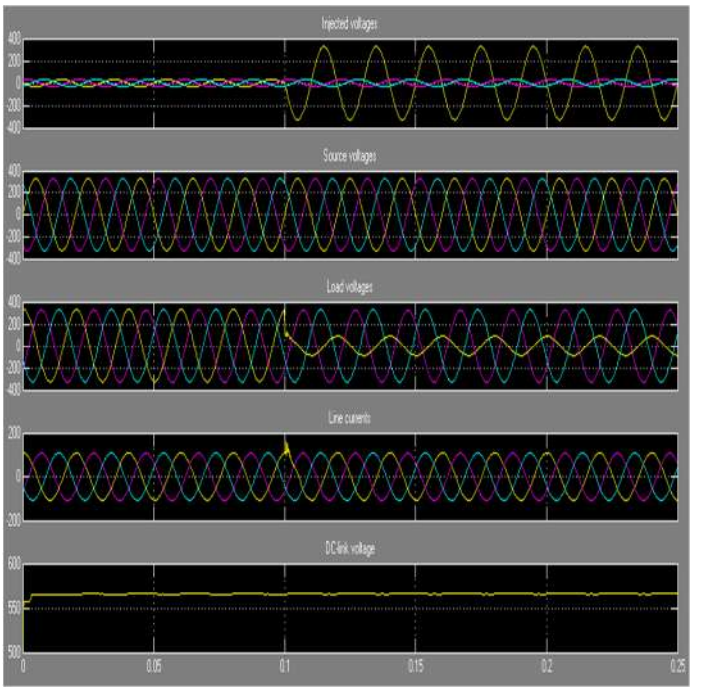

Fig. 15. (a) Injected voltages. (b) Source voltages. (c) Load voltages. (d) Line currents. (e) DC-link voltage, during the single phase- to-ground fault.

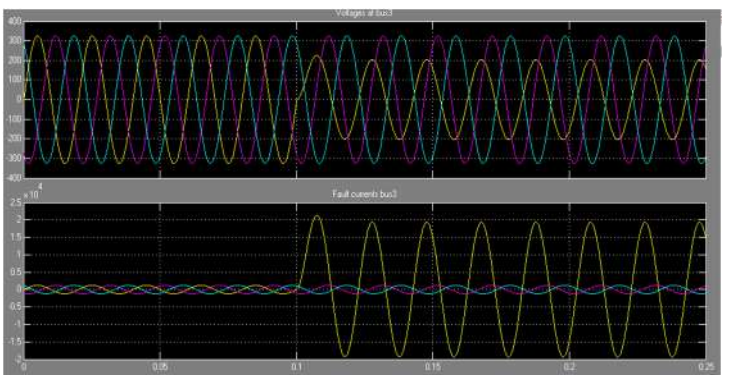

Fig. 16. (a) Voltages at bus3. (b) Fault currents, during the downstream single phase- to-ground arcing fault when the without DVR

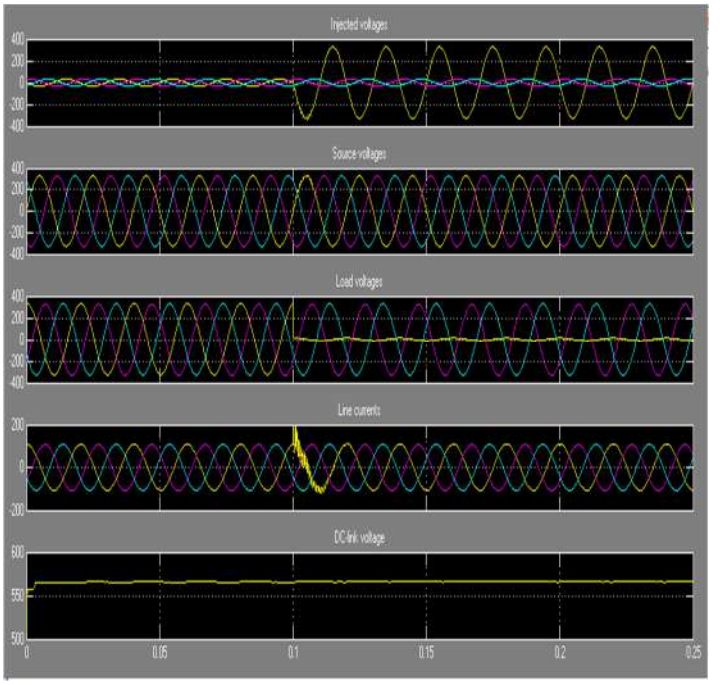

Fig. 8. (a) Injected voltages. (b) Source voltages. (c) Load voltages. (d) Line currents. (e) DC-link voltage, during the single phase- to- ground arcing fault

TABLE VI

INDUCTION MACHINE PARAMETERS USED IN THE SIMULATIONS AND EXPERIMENTAL SETUP

	Simulations	Experimental set-up
Stator resistance (r_s)	0.2761 Ω	5.43 Ω
Rotor resistance (r_r)	0.1645 Ω	6.09 Ω
Stator inductance (L_s)	2.191 mH	17.56 mH
Rotor inductance (L_r)	2.191 mH	17.56 mH
Mutual inductance (M)	76.14 mH	197 mH
Rated voltage	380/440 V	220/380 V
Rated power	20 HP	0.5 HP
Pole pairs (P)	2	2
Inertia (J)	0.1 kgm^2	0.0006 kgm^2
Rated frequency	60 Hz	60 Hz

VI. CONCLUSION

To improve the DG operation, the dc link voltage must be controlled, in this case by a dc-dc step-up converter. PI controllers associated with resonant regulators were used as a solution to produce distortion-free DG voltage, even when the local load is nonlinear or when distortion occurs in the grid voltage. This paper presents an alternative solution to connecting a DG system to the grid, whereby the amplitude and displacement of the voltage synthesized by the DG is regulated with respect to the grid voltage and the control variable before and after the contingency is always the same.

Additionally, a dc-dc step-up converter and a dc-ac VSI are used in a DG system as an interface with the power grid. The simulation and experimental results demonstrate that the connection of DG sources can have adverse effects, depending on the connection procedures. Although the PLL algorithm tracks as rapidly as possible, the frequency oscillations are slowly damped due to the limits of amplitude.

VII. Acknowledgment

This paper is based on M. Tech. project carried out by the student of pydah college of engineering & technology, Kakinada studying M.Tech (Power Electronics) The project had been completed by Mr. K. MADHAVARAO bearing H.T.no.: 126T1D4302 under the guidance of B. LALITHA KUMARI.

REFERENCES

1. M. G. Simões and F. A. Farret, *Integration of Alternative Sources of Energy*. Hoboken, NJ: Wiley, 2006.
2. A. Keyhani,M. N.Marwali, andM. Dai, *Integration of Green and Renewable Energy in Electric Power Systems*. Hoboken, NJ: Wiley, 2010.
3. S. Chowdhury, S. P. Chowdhury, G. A. Taylor, and Y. H. Song, "Mathematical modelling and performance evaluation of a stand-alone polycrystalline PV plant with MPPT facility," in *Proc. Power Energy Soc. Gen. Meeting—Conversion Delivery Electrical Energy 21st Century*, 2008, pp. 1–7.
4. Y. Wen-Chih and H. Wei-Tzer, "A load transfer scheme of radial distribution feeders considering distributed generation," *Proc CIS*, pp. 243–248, 2010.
5. D. D. Marquezini, D. B. Ramos, R. Q. Machado, and F. A. Farret, "Interaction between proton exchange membrane fuel cells and power converters for AC integration," *IET Renewable Power Gener.*, vol. 2, no. 3, pp. 151–161, Sep. 2008.
6. W. El-Khattam and M. M. A. Salama, "Distributed generation technologies, definitions and benefits," *Elect. Power Syst. Res.*, vol. 71, no. 2, pp. 119–128, Oct. 2004.

7. A. Barin, L. F. Pozzatti, L. N. Canha, R. Q. Machado, A. R. Abaide, and G. Arend, "Electrical power and energy systems multi-objective analysis of impacts of distributed generation placement on the operational characteristics of networks for distribution system planning," *Int. J. Elect. Power Energy Syst.*, vol. 32, no. 10, pp. 1157–1164, Dec.
8. S. Chaitusaney and A. Yokoyama, "Impact of protection coordination on sizes of several distributed generation sources," in *Proc. IPEC*, 2005, pp. 669–674.
9. IEEE Recommended Practices and Requirements for Harmonic Control in Electrical Power Systems, IEEE Std. 519, 1993.
10. Agância Nacional de Energia Elétrica—ANEEL, Procedimento de Distribuição de Energia Elétrica no Sistema Elétrico Nacional— PRODIST—Módulo 32010.
11. F. Blaabjerg, R. Teodorescu, M. Liserre, and A. V. Timbus, "Overview of control and grid synchronization for distributed power generation systems," *IEEE Trans. Ind. Electron.*, vol. 53, no. 4, pp. 1398–1409, Oct. 2006.
12. J. M. E. Huerta, J. Castello-Moreno, J. R. Fischer, and R. Garcia-Gil, "A synchronous reference frame robust predictive current control for threephase grid-connected inverters," *IEEE Trans. Ind. Electron.*, vol. 57, no. 3, pp. 954–962, Mar. 2010.
13. P. Rodriguez, A. V. Timbus, R. Teodorescu, M. Liserre, and F. Blaabjerg, "Flexible active power control of distributed power generation systems during grid faults," *IEEE Trans. Ind. Electron.*, vol. 54, no. 5, pp. 2583– 2592, Oct. 2007.
14. T. Hornik and Z. Qing-Chang, "A current-control strategy for voltagesource inverters in microgrids based on$H\infty$ and repetitive control," *IEEE Trans. Power Electron.*, vol. 26, no. 3, pp. 943–952, Mar. 2011.
15. I. J. Balaguer, L. Qin, Y. Shuitao, U. Supatti, and P. F. Zheng, "Control for grid-connected and intentional islanding operations of distributed power generation," *IEEE Trans. Ind. Electron.*, vol. 58, no. 1, pp. 147–157, Jan. 2011.
16. R. Q. Machado, S. Buso, and J. A. Pomilio, "A line-interactive singlephase to three-phase converter system," *IEEE Trans. Power Electron.*, vol. 21, no. 6, pp. 1628–1636, Nov. 2006.
17. F. Gao, S. Member, and M. R. Iravani, "A control strategy for a distributed generation unit in grid-connected and autonomous modes of operation," *IEEE Trans. Power Del.*, vol. 23, no. 2, pp. 850–859, Apr. 2008.
18. H. Kim, T. Yu, and S. Choi, "Indirect current control algorithm for utility interactive inverters in distributed generation systems," *IEEE Trans. Power Electron.*, vol. 23, no. 3, pp. 1342–1347, May 2008.
19. Agência Nacional de Energia Elétrica—ANEEL, Procedimento de Distribuição de Energia Elétrica no Sistema Elétrico Nacional— PRODIST—Módulo 82010.
20. J. M. Guerrero, J. C. Vasquez, J. Matas, L. G. de Vicuna, and M. Castilla, "Hierarchical control of droop-controlled AC and DC microgrids—A general approach toward standardization," *IEEE Trans. Ind. Electron.*, vol. 58, no. 1, pp. 158–172, Jan. 2011.
21. J. M. Guerrero, J. Matas, L. G. de Vicuna, M. Castilla, and J. Miret, "Wireless-control strategy for parallel operation of distributed-generation inverters," *IEEE Trans. Ind. Electron.*, vol. 53, no. 5, pp. 1461–1470, Oct. 2006.
22. J. M. Guerrero, J. Matas, V. L. Garcia de, M. Castilla, and J. Miret, "Decentralized control for parallel operation of distributed generation

inverters using resistive output impedance," *IEEE Trans. Ind. Electron.*, vol. 54, no. 2, pp. 994–1004, Apr. 2007.
23. Standard for Interconnecting Distributed Resources With Electric Power Systems, IEEE Std. 1547, 2003.
24. F. P. Marafão, S. M. Deckmann, J. A. Pomilio, and R. Q. Machado, "Metodologia de projeto e análise de algoritmos de sincronismo PLL," *SOBRAEP Revista da Associação Brasileira de Eletrônica de Potência*, vol. 10, no. 1, pp. 7–14, 2005.
25. V. Kaura and V. Blasko, "Operation of a phase locked loop system under distorted utility conditions," *IEEE Trans. Ind. Appl.*, vol. 33, no. 1, pp. 58– 63, Jan./Feb. 1997.
26. T. Esram and P. L. Chapman, "Comparison of photovoltaic array maximum power point tracking techniques," *IEEE Trans. Energy Convers.*, vol. 22, no. 2, pp. 439–449, Jun. 2007.
27. S. Buso, S. Fasolo, and P. Mattavelli, "Uninterruptible power supply multiloop control employing digital predictive voltage and current regulators," *IEEE Trans. Ind. Appl.*, vol. 37, no. 6, pp. 1846–1854, Nov./Dec. 2001.
28. P. Mattavelli, "A closed-loop selective harmonic compensation for active filters," *IEEE Trans. Ind. Appl.*, vol. 37, no. 1, pp. 81–89, Jan./Feb. 2001.
29. C. J. Gajanayake, D. M. Vilathgamuwa, P. C. Loh, R. Teodorescu, and F. Blaabjerg, "Z-source-inverter-based flexible distributed generation system solution for grid power quality improvement," *IEEE Trans. Energy Convers.*, vol. 24, no. 3, pp. 695–704, Sep. 2009.
30. R. Q. Machado, A. F. Q. Gonçalves, S. Buso, and J. A. Pomilio, "An electronic solution for the direct connection of a three-phase induction generator to a single-phase feeder," *SBA: Controle & Automação Sociedade Brasileira de Automatica*, vol. 20, no. 3, pp. 417–426, Jul./Sep. 2009.
31. IEEE Recommended Practice for Industrial and Commercial Power Systems Analysis, IEEE Std. 399, 1998.
32. IEEE Application Guide for AC High-Voltage Circuit Breakers Rated on a Symmetrical Current Basis, IEEE Std. C37.010, 2005.
33. J. Rocabert, G. M. S. Azevedo, A. Luna, J.M. Guerrero, J. I. Candela, and P. Rodríguez, "Intelligent connection agent for three-phase grid-connected microgrids," *IEEE Trans. Power Electron.*, vol. 26, no. 10, pp. 2993–3005, Oct. 2011.
34. E. Acha, C. R. Fuerte-Esquivel, H. Ambriz-Pérez, and C. Angeles- Camacho, *Facts Modelling and Simulation in Power Electronics*. Hoboken, NJ: Wiley, 2004.
35. E. J. Estébanez, V. M. Moreno, A. Pigazo,M. Liserre, and A. Dell'Aquila, "Performance evaluation of active islanding-detection algorithms in distributed-generation photovoltaic systems: Two inverters case," *IEEE Trans. Ind. Electron.*, vol. 58, no. 4, pp. 1185–1193, Apr. 2011.
36. K. Jae-Hyung, K. Jun-Gu, J. Young-Hyok, J. Yong-Chae, and W. Chung-Yuen, "An islanding detection method for a grid-connected system based on the goertzel algorithm," *IEEE Trans. Power Electron.*, vol. 26, no. 4, pp. 1049–1055, Apr. 2011.

37. A. M. McLandrich, "Sensorless control of a bidirectional boost converter for a fuel cell energy management system," M.S. thesis, Faculty Virginia Polytechnic Inst. State Univ., Blacksburg, VA, 2003.
38. R. Gopinath, K. Sangsun, H. Jae-Hong, P. N. Enjeti, M. B. Yeary, and J. W. Howze, "Development of a low cost fuel cell inverter system with DSP control," *IEEE Trans. Power Electron.*, vol. 19, no. 5, pp. 1256–1262, Sep. 2004.

INTERNATIONAL JOURNAL OF MULTIDISCIPLINARY EDUCATIONAL RESEARCH
ISSN : 2277-7881; IMPACT FACTOR - 2.972; IC VALUE:5.16
VOLUME 3, ISSUE 10(4), OCTOBER 2014

IFBTL DC/DC CONVERTER FOR WIND TURBINES IN A DC GRID

Ms. M. KAVYA
kmernedi6@gmail.com
Under the guidance of
Ms.M.PAVANI
ASSISTANT PROFESSIOR
PYDAH COLLEGE OF ENGINEERING , KAKINADA

Abstract—This paper presents an improved full-bridge three level (IFBTL) dc/dc converter for a wind turbine in a dc grid by inserting a passive filter into the dc/dc converter to improve the performance of the converter. The passive filter can effectively reduce the voltage stress of the medium frequency transformer in the IFBTL dc/dc converter. A modulation strategy, including two operation modes, is proposed for the IFBTL dc/dc converter. Then, a voltage balancing control strategy is proposed for the IFBTL dc/dc converter. Furthermore, the control of the wind turbine based on the IFBTL dc/dc converter in a dc-grid system is presented. Simulation results have been obtained by MATLAB/SIMULINK.

Key words: IFBTL, wind turbine, DC grid

I. INTRODUCTION

A number of converters are presented in [3]–[23]. The two level and three-level configurations are mainly considered here, since both of the two configurations have been widely used in the wind energy system [24]. The dc grid, with the advantages such as reactive power, harmonics, and so on [1], seems to be a promising solution of power collection system for the growing demand in the offshore wind power development. The offshore wind turbines may be directly connected into a dc grid to deliver dc power to a medium- or high-dc voltage network [2]. To realize the dc connection and power delivery, a high-efficient dc/dc converter is required. Normally, the voltage level of the dc network would be dozens of kilovolts which is much higher than the input voltage of the dc/dc converter [2].

Hence, a medium frequency transformer (MFT) operated at hundreds of hertz to several kilohertz would be installed in the dc/dc converter, which not only ensures that the input voltage can be boosted to a desired high output voltage, but also achieves the galvanic isolation between source and grid.

Besides, owing to the high-voltage level in the dc network, the usage of the diode bridges in the dc/dc converters could be advantageous. Fig. 1 shows several possible dc/dc converters for the dc-grid wind turbine, including the basic full-bridge (FB) two-level converter, the basic half-bridge (HF) three-level converter, the basic FB three-level converter, and the FB three-level converter based on sub-modules (SMs). The four converter configurations for an example of a 2.5-MW wind turbine system are considered in Table I. The system parameters are listed in the Appendix. The rated input voltage of the converters is 5.4 kV, and the 1700 V/600.

A insulated gate bipolar transistor (IGBT) (FZ600R17KE3) with the nominal device voltage *V*com at 100 FIT as 900 V is applied for the different converter configurations [25]. Although the required switch number for the FB two-level converter are not so many among the four configurations, the switches in the two-level configurations have to take the full dc-bus voltage. The voltage change rate d*v*/d*t* is high; therefore, it may cause large electromagnetic interference (EMI) [3]–[6].

As the three-level converters with the advantages in the aspects of power quality, semiconductor electrical and thermal stresses, and EMI for high-power applications [7]–[17], the switches in the basic HB three-level converter, FB three-level converter, and the SMs-based FB three-level converter only take half of the dc bus voltage, which effectively reduces d*v*/d*t* in comparison with the FB two-level converter. For the *N*-level configuration, a total number of 8($N-1$) switches are needed for the SMs-based FB converter, which is much more than 2($N-1$) and 4($N-1$) switches required in the basic HB and FB converters, respectively [7], [18]. Besides, the corresponding numbers of voltage sensors are normally required for the SMs, and the voltage balancing control would be complicated for the SMs-based FB converter [19].

The basic full-bridge three-level (FBTL) converter, with the advantage of the reduced voltage stress of the switches, reduced filter size, and improved dynamic response, is becoming highly suitable for medium-voltage and high-power conversion [7]. Although both the basic FBTL and the SMs-based FBTL configurations can create five-level output voltage to minimize voltage steps and reduce d*v*/d*t* in comparison with the basic HBTL configuration, particularly in the medium-voltage and high-power applications [18], [26], [27], the basic FBTL converter has a simpler circuit structure and less number

of switch devices than the SMs-based FBTL configuration, which leads to a small footprint and high reliability for the basic FBTL converter.

The FB converter has been evaluated to be a suitable choice for wind farm application from an energy efficiency point of view [28]. Hence, the isolated FBTL dc/dc converter is to be studied for high-power wind turbine systems in this paper. Some work about the isolated FBTL converter control has been reported, such as the chopping phase-shift (CPS) control and double phase-shift (DPS) control presented in [8] and [9], respectively, but they have a high-voltage change rate d*v*/d*t*, and thus may not be applicable for the medium-voltage and high power systems. So far, the application of the isolated FBTL dc/dc converter for offshore wind turbines within a dc grid has not been addressed in detail in the literature. In this paper, an improved FBTL (IFBTL) dc/dc converter is presented for an offshore wind turbine based on permanent magnet synchronous generators (PMSGs) in a dc grid as shown in Fig. 2, where the IFBTL dc/dc converter is applied to boost the dc voltage from a diode rectifier to a high voltage for the dc grid integration.

This paper is organized as follows. In Section II, the IFBTL dc/dc converter and the corresponding modulation strategy are proposed. In Section III, the voltage balancing control for the IFBTL dc/dc converter is proposed. Section IV presents the control of the wind turbine system based on the IFBTL dc/dc converter. A 1-kW prototype is built and tested in the laboratory, and the results verify the feasibility of the proposed converter topology, modulation strategy, and voltage balancing control strategy, which is reported in Section V. Finally, the main conclusions are drawn in Section VI.

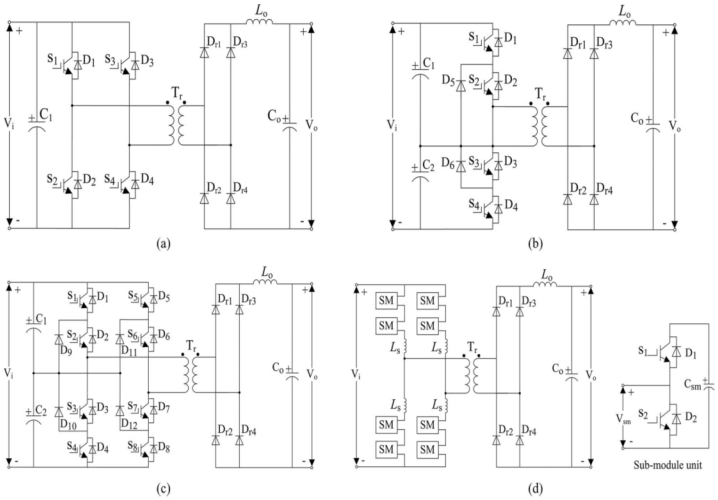

Fig. 1(a) Basic FB two-level converter (b) Basic HB three-level converter. (c) Basic FB three-level converter. (d) SMs based-FB three-level converter

TABLE I

POSSIBLE DC/DC CONVERTER OPTIONS

Converter topology		Valve number	Switch number in each valve	Valve voltage	Produced voltage level	Voltage balance control complexity	Voltage sensor
2-level	Basic FB converter	4	6×1.7 kV IGBTs	DC bus voltage	2	No	1
3-level	Basic HB converter	4	3×1.7 kV IGBTs	Half DC bus voltage	3	Easy	2
3-level	Basic FB converter	8	3×1.7 kV IGBTs	Half DC bus voltage	5	Easy	2
3-level	FB converter based on SMs	16	3 ×1.7 kV IGBTs	Half DC bus voltage	5	Calculation is proportional to the SMs number	8

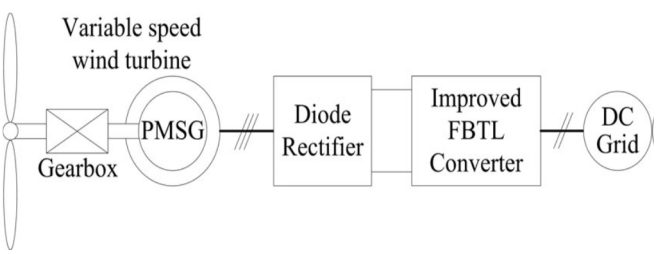

Fig. 2 Block diagram of the wind turbine connected to a dc grid

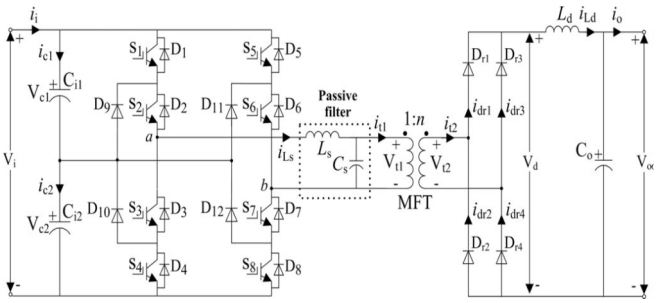

Fig. 3 Block diagram of the IFBTL dc/dc converter

II. IFBTL DC/DC CONVERTER

A. Converter Description

Fig. 3 shows the configuration of the IFBTL dc/dc converter, which is composed of eight switches (S1–S8), eight freewheeling diodes (D1–D8), four clamping diodes (D9–D12), an MFT, four rectifier diodes (D*r* 1–D*r* 4), a passive filter (*Ls* and *Cs*), an output filter inductor *Ld* , an output capacitor *Co* , and two voltage divided capacitors (*Ci* 1 and *Ci* 2), which are used to split the dc bus voltage *Vi* into two equal voltages *Vc* 1 and *Vc* 2 .

Different from the FBTL dc/dc converter, a passive filter is inserted into the IFBTL dc/dc converter as shown in Fig. 3 to improve the performance of the dc/dc converter [29], which can effectively overcome the problem that the nonlinear characteristics of semiconductor devices result in distorted waveforms associated with harmonics and reduce the voltage stress of the MFT, which is very significant for the power converter in the high-power application.

B. Proposed Modulation Strategy

The switches S1–S8 are switched complementarily in pairs with a pulse width modulation (PWM), i.e., pairs S1–S3, S4–S2, S5–S7, and S8–S6, respectively. The duty cycle for S1 is *D*. The way of phase shifting the PWM for other switch pairs results in the different operation modes as follows.

1) *Operation Mode I*: The PWM waveform for the pairs S8– S6, S5–S7, and S4–S2 lags behind that for pair S1–S3 by $(D - Dc)Ts/2$, $Ts/2$, and $(D - Dc + 1)Ts/2$ respectively as shown in Fig. 4(a). *Ts* is the switching cycle. The overlap time between S1–S3 and S8–S6 is $DcTs/2$, which is also for S4–S2 and S5–S7. *Dc* is defined as the overlap duty ratio.

2) *Operation Mode II*: The PWM waveform for pair S8– S6 leads before that for pair S1–S3 by $(D - Dc)Ts/2$, and the PWM waveform for pairs S4–S2 and S5-S7 lags behind that for the pair S1–S3 by $(1 - D + Dc)Ts/2$ and $Ts/2$, respectively, as shown in Fig. 4(b). The overlap time between S1–S3 and S8–S6, and between S4–S2 and S5–S7 is also both $DcTs/2$.

The main difference between the two operation modes is the capacitor charge and discharge situations in each half cycle as shown in Fig. 4. In operation mode I, capacitor *Ci* 2 discharges more energy than capacitor *Ci* 1 in each half cycle as shown in Fig. 4(a), while capacitors *Ci* 1 and the *Ci* 2 exchange their situations in operation mode II as shown in Fig. 4(b). In operation mode II, capacitor *Ci* 1 discharges more energy than capacitor *Ci* 2 in each half cycle. The two operation modes can be alternatively used for the adaptive voltage balancing control, which will be described in Section III. The steady-state operations of the converter under the proposed modulation strategy are explained with the assumption that $Ci\,1 = Ci\,2$. Fig. 4 shows the simulation waveforms of the IFBTL dc/dc converter in one cycle *Ts* under operation modes I and II, respectively. The system parameters are given in the Appendix.

In Fig. 4, voltages *V*ab, $Vt\,1$, $Vt\,2$ and currents *i*Ls, $it\,1$, $it\,2$ are all periodic waveforms with period *Ts*. Currents $ic\,1$, $ic\,2$, and *i*Ld are with the period $Ts/2$. Owing to the passive filter in the IFBTL dc/dc converter, the performance of voltages $Vt\,1$, $Vt\,2$ and currents $it\,1$, $it\,2$ associated with the MFT is effectively improved, which is significant for the IFBTL dc/dc converter in the applications of the medium-voltage and high-power system. From Fig. 4, it is easy to see that the charge and discharge situations (*ic* 1 and *ic* 2) of capacitors *Ci* 1 and *Ci* 2 are the main difference between the operation modes I and II, which would affect the capacitor voltages *Vc* 1 and *Vc* 2. The other performances of the converter are nearly the same.

III. VOLTAGE BALANCING CONTROL STRATEGY

A voltage balancing control strategy is proposed for the IFBTL dc/dc converter in this section, which can be realized by alternating the operation modes I and II.

A. In Operation Mode I

In Fig. 4(a), both the capacitor currents *ic* 1 and *ic* 2 are with the period of $Ts/2$. In the first half cycle, the charge or discharge situations for

capacitors *Ci* 1 and *Ci* 2 in stages A, C, and E are the same. In stage B, current *ic* 2 is more than *ic* 1 , while *ic* 2 is far less than *ic* 1 in stage D as shown in Fig. 4(a). Owing to that, the periods of stages B and D are $(D - Dc)Ts/2$. Suppose *Vc* 1 = *Vc* 2 =*Vi* /2; *Ci* 2 would provide more energy to the load than *Ci* 1 in the first half cycle under the operation mode I. The situation in the second half cycle is similar to that in the first half cycle.

Consequently, voltage *Vc* 1 would be increased and voltage *Vc* 2 would be reduced in operation mode I as shown in Fig. 4(a), which would result in the trend that voltage *Vc* 1 would be more than *Vc* 2 in operation mode I.

B. In Operation Mode II

The same to operation mode I, the charge and discharge situations for capacitors *Ci* 1 and *Ci* 2 in stages A, C, and E are the same as in the first half cycle. The only difference is that current *ic* 2 is less than *ic* 1 in stage D, while *ic* 2 is far more than *ic* 1 in stage B in operation mode II as shown in Fig. 4(b), which is contrary to that in operation mode I. The periods for stages B and D are both $(D - Dc)\,Ts/2$. Suppose *Vc* 1 = *Vc* 2 = *Vi* /2; *Ci*1 would provide more energy to the load than *Ci* 2 in the first half cycle under the operation mode II. The situation in the second half cycle is similar to the first half cycle. Therefore, voltage *Vc* 1 would be reduced and voltage *Vc* 2 would be increased in operation mode II as shown in Fig. 4(b), which would result in the trend that voltage *Vc* 1 would be less than *Vc* 2 in operation mode II.

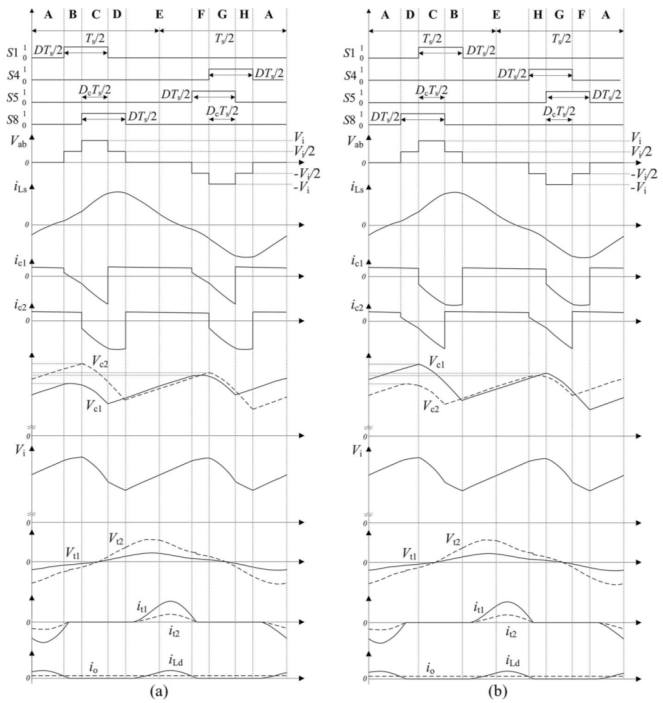

Fig. 4. Key waveforms of the IFBTL dc/dc converter (a) In operation mode I. (b) In operation mode II

C. Proposed Voltage Balancing Control Strategy

Based on the aforesaid analysis, *Vc* 1 would be more than *Vc* 2 in operation mode I, and *Vc* 1 would be less than *Vc* 2 in operation mode II. Consequently, a control strategy is proposed for the capacitor voltage balancing as shown in Fig. 5 where a comparator is used here with two input voltages *Vc* 1 and *Vc* 2. If *Vc* 1 is more than *Vc* 2, the operation mode in the next half cycle is selected as II. On the contrary, the operation mode I is selected in the next half cycle when *Vc* 1 is less than *Vc* 2.

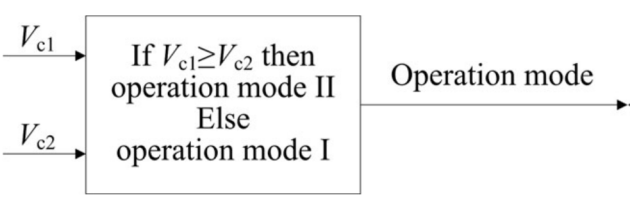

Fig. 5 Block diagram of the proposed voltage balancing control for IFBTL converter

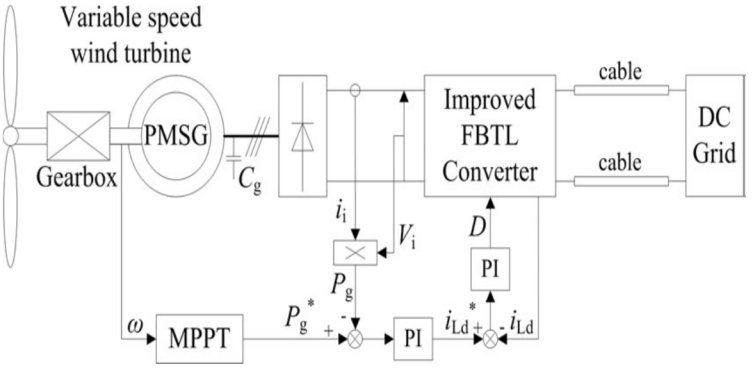

Fig. 6 Block diagram of the control for the VSWT based on a PMSG and an IFBTL dc/dc converter

IV. CONTROL OF AN IFBTL CONVERTER-BASED WIND TURBINE

Fig. 6 shows the control structure of the variable-speed wind turbine (VSWT) based on a PMSG and an IFBTL dc/dc converter, where the wind turbine is connected into the dc grid. The optimal power $P*g$ can be obtained with the measured wind turbine speed ω based on the maximum power point tracking method [30]. Neglecting the power electronics losses, the power relationship can be presented as

$$Pg = Vi\ Ii = Vo\ iLd \qquad (1)$$

Where Pg is the generator power and ii is the input current of the IFBTL converter. A PI regulator is used as the power controller and produces the current reference $i*Ld$. The other PI regulator is used as the current controller and produces the duty cycle D for the IFBTL converter so as to follow the optimal power of the VSWT.

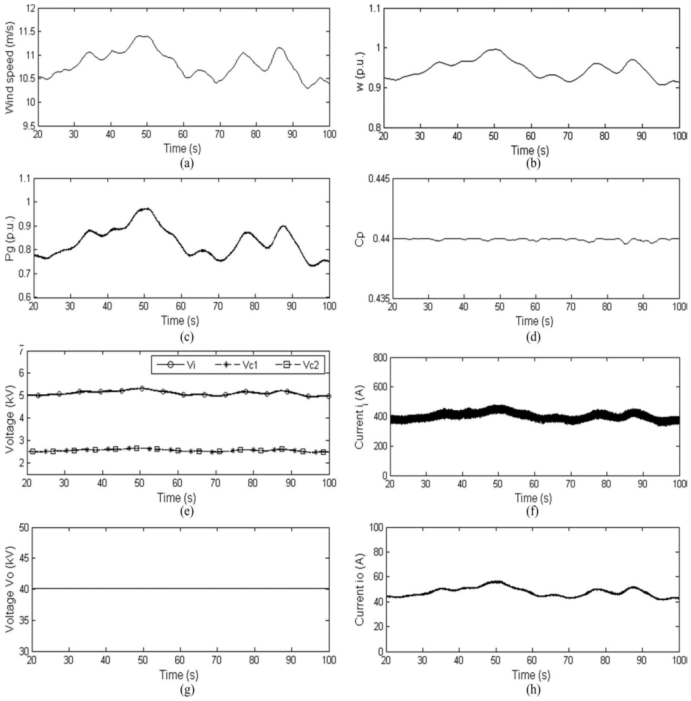

Fig. 7 (a) Wind speed (b) Wind turbine speed ω. (c) Power *Pg.* (d) Power coefficient *Cp.* (e) Voltages *Vi, Vc* 1, and *Vc* 2. (f) Current I*i.* (g) Voltage *Vo. (*h) Current *io.*

V. EXPERIMENTAL RESULTS

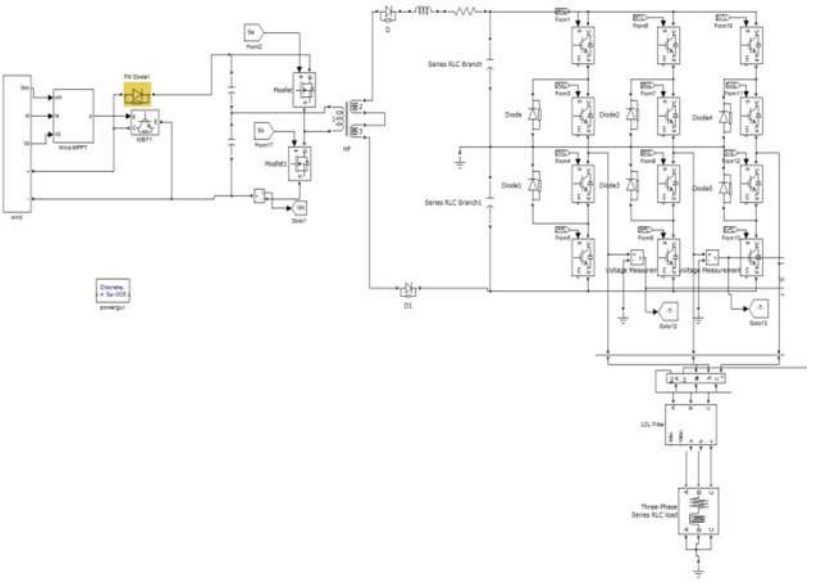

Fig 8 simulation diagram of proposed system

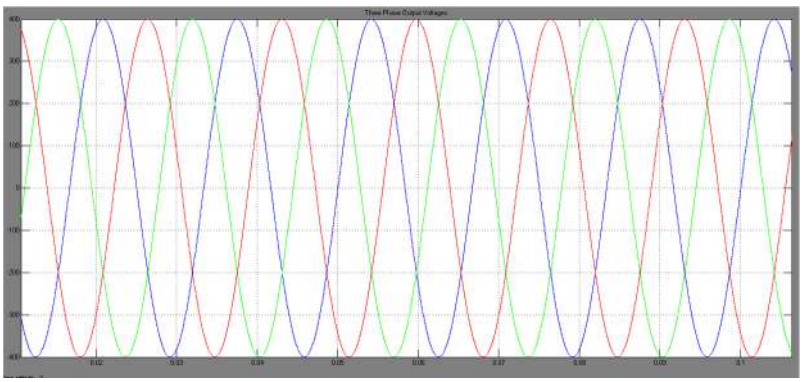

Fig 9 three phase load voltage

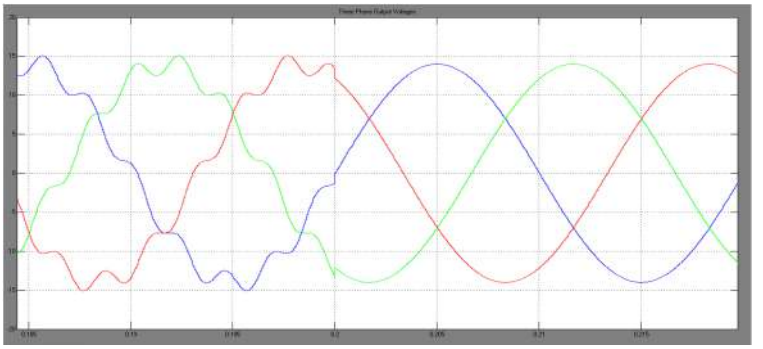

Fig 10 three phase load current

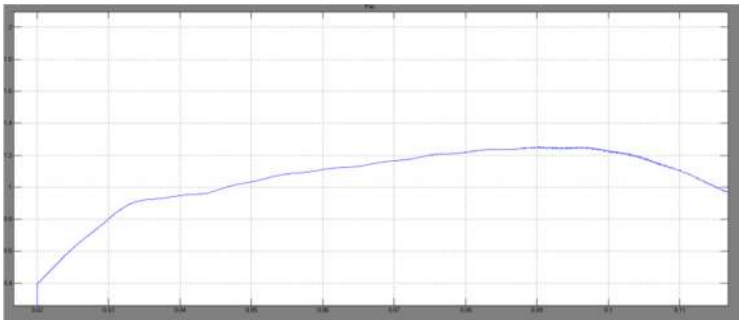

Fig 11 wind speed

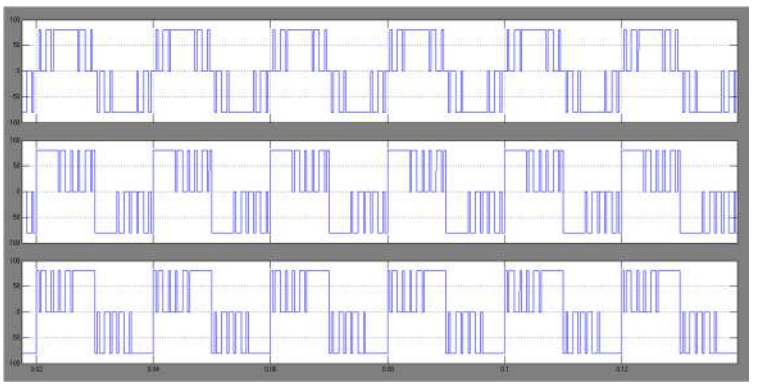

Fig 12 Three phase voltages

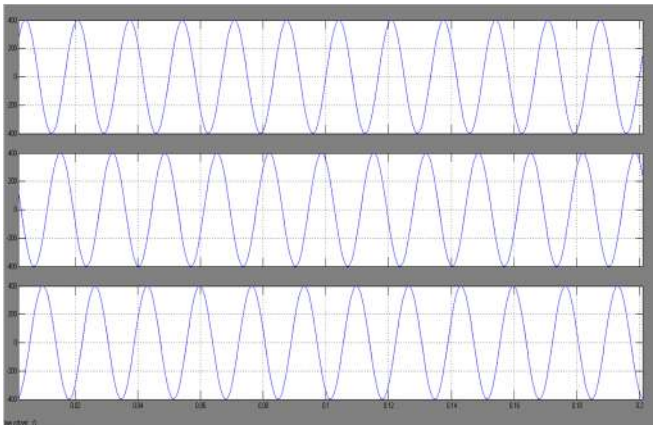

Fig 13 three phase load voltages

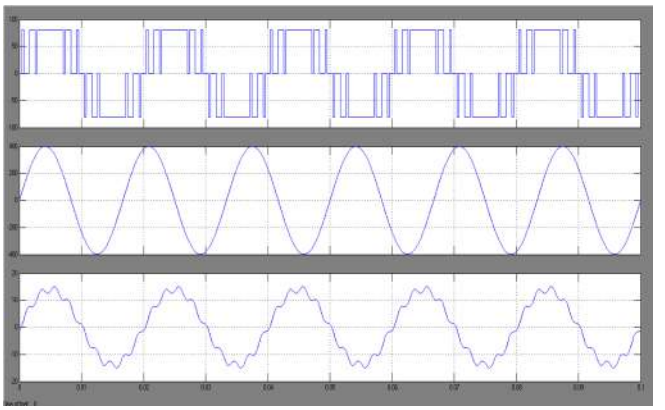

Fig 14 three level inverter line voltage load and load current

VI. CONCLUSION

This paper has presented IFBTL DC/DC Converter for Wind Turbines in a DC Grid. A voltage balancing control strategy is proposed for the IFBTL dc/dc converter, where the alternation of the proposed two operation modes can keep the capacitor voltage balanced. The corresponding modulation strategy, including operation modes I and II, is proposed for the IFBTL dc/dc converter. The proposed two operation modes are discussed in detail. With the passive filter and the modulation strategy, the voltage stress of the transformer in the IFBTL dc/dc converter can be effectively reduced, which is very significant in the medium-voltage and high-power application. The

control of the wind turbine system based on the IFBTL dc/dc converter is presented as well.

VI. Acknowledgment

This paper is based on M. Tech. project carried out by the student of pydah college of engineering & technology, Kakinada studying M.Tech (Power Electronics) The project had been completed by Ms. M. KAVYA bearing H.T.no.: 126T1D4310 under the guidance of Ms. M PAVANI.

REFERENCES

1. C. Meyer, M. Hoing, A. Peterson, and R. W. De Doncker, "Control and design of dc grids for offshore wind farms," *IEEE Trans. Ind. Appl.*, vol. 43, no. 6, pp. 1475–1482, Nov./Dec. 2007.
2. J. Robinson, D. Jovcic, and G. Jo´os, "Analysis and design of an offshore wind farm using a MV DC grid," *IEEE Trans. Power Delivery*, vol. 25, no. 4, pp. 2164–2173, Oct. 2010.
3. F. Blaabjerg, Z. Chen, and B. S. Kjaer, "Power electronics as efficient interface in dispersed power generation systems," *IEEE Trans. Power Electron.*, vol. 19, no. 5, pp. 1184–1194, Sep. 2004.
4. F. Blaabjerg, F. Iov, Z. Chen, and K. Ma, "Power electronics and controls for wind turbine systems," in *Proc. IEEE Int. Energy Conf. Exhib.*, Dec. 2010, pp. 333–344.
5. N. Mohan, T. M. Undeland, and W. P. Robbins, *Power Electronics: Converters, Applications, and Design*, 3rd ed. New York: Wiley, 2003.
6. N. Y. Dai, M. C.Wong, and Y. D. Han, "Application of a three-level NPC inverter as a three-phase four-wire power quality compensator by generalized 3DSVM," *IEEE Trans. Power Electron.*, vol. 21, no. 2, pp. 440–449, Mar. 2006.
7. X. Ruan, B. Li, Q. Chen, S. C. Tan, and C. K. Tse, "Fundamental considerations of three-level dc-dc converters: Topologies, analyses, and control," *IEEE Trans. Circuits Syst. I, Reg. Papers*, vol. 55, no. 11, pp. 3733–3743, Dec. 2008.
8. Z. Zhang and X. Ruan, "ZVS PWM full-bridge three-level converter," in *Proc. 4th Int. Power Electron. Motion Control Conf.*, 2004, pp. 1085–1090.
9. Z. Zhang and X. Ruan, "A novel double phase-shift control scheme for full-bridge three-level converter," in *Proc. 20th Annu. IEEE Appl. Power Electron. Conf. Expos.*, Mar. 2005, pp. 1240–1245.

10. P. J. Grbovic, "High-voltage auxiliary power supply using seriesconnected MOSFETs and floating self-driving technique," *IEEE Trans. Ind. Electron.*, vol. 56, no. 5, pp. 1446–1455, May 2009.
11. P. J. Grbovi´c, P. Delarue, P. Le Moigne, and P. Bartholomeus, "A bidirectional three-level dc-dc converter for the ultra capacitor applications," *IEEE Trans. Ind. Electron.*, vol. 57, no. 10, pp. 3415–3430, Oct. 2010.
12. P. M. Barbosa, F. Canales, J. M. Burd´ıo, and F. C. Lee, "A three-level converter and its application to power factor correction," *IEEE Trans. Power Electron.*, vol. 20, no. 6, pp. 1319–1327, Nov. 2005.
13. J. R. Pinheiro and I. Barbi, "The three-level ZVS-PWM dc-to-dc converter," *IEEE Trans. Power Electron.*, vol. 8, no. 4, pp. 486–492, Oct. 1993.
14. S. Inoue and H. Akagi, "A bidirectional isolated dc-dc converter as a core circuit of the next-generation medium-voltage power conversion system," *IEEE Trans. Power Electron.*, vol. 22, no. 2, pp. 535–542, Mar. 2007.
15. M. Malinowski, K. Gopakumar, J. Rodriguez, andM. A. P´erez, "A survey on cascaded multilevel inverters," *IEEE Trans. Ind. Electron.*, vol. 57, no. 7, pp. 2197–2206, Jul. 2010.
16. S. Kouro, M. Malinowski, K. Gopakumar, J. Pou, L. G. Franquelo, B.Wu, J. Rodriguez, M. A. P´ere, and J. I. Leon, "Recent advances and industrial applications of multilevel converters," *IEEE Trans. Ind. Electron.*, vol. 57, no. 8, pp. 2553–2580, Aug. 2010.
17. J. Rodriguez, S. Bernet, B. Wu, J. O. Pontt, and S. Kouro, "Multilevel voltage-source-converter topologies for industrial medium-voltage drives," *IEEE Trans. Ind. Electron.*, vol. 54, no. 6, pp. 2930–2945, Dec. 2007.
18. S. Kenzelmann, A. Rufer, M. Vasiladiotis, D. Dujic, F. Canales, and Y. R. de Novaes, "A versatile dc–dc converter for energy collection and distribution using the modular multilevel converter," in *Proc. 14th Eur. Conf. Power Electron. Appl.*, Aug./Sep. 2011, pp. 1–10.
19. M. Saeedifard and R. Iravani, "Dynamic performance of a modular multilevel back-to-back HVDC system," *IEEE Trans. Power Delivery*, vol. 25, no. 4, pp. 2903–2912, Oct. 2010.

20. M. A. Parker, N. Chong, and R. Li, "Fault-Tolerant control for a modular generator-converter scheme for direct-drive wind turbines," *IEEE Trans. Ind. Electron.*, vol. 58, no. 1, pp. 305–315, Jan. 2011.
21. R. Mel´ıcio, V. M. F. Mendes, and J. P. S. Catal˜ao, "Comparative study of power converter topologies and control strategies for the harmonic performance of variable-speed wind turbine generator systems," *Energy*, vol. 36, no. 1, pp. 520–529, Jan. 2011.
22. P. Samuel, R. Gupta, and D. Chandra, "Grid interface of wind power with large split-winding alternator using cascaded multilevel inverter," *IEEE Trans. Energy Convers.*, vol. 26, no. 1, pp. 299–309, Mar. 2011.
23. M. N. Slepchenkov, K. M. Smedley, and J. Wen, "Hexagram-converter based STATCOM for voltage support in fixed-speed wind turbine generation systems," *IEEE Trans. Ind. Electron.*, vol. 58, no. 4, pp. 1120–1131, Apr. 2011.
24. B.Wu, Y. Lang, N. Zargari, and S. Kouro, *Power Conversion and Control of Wind Energy Systems*. Hoboken, NJ: Wiley, 2011.
25. S. S. Fazel, S. Bernet, D. Krug, and K. Jalili, "Design and comparison of 4-kV neutral-point-clamped, flying-capacitor, and series-connected H bridge multilevel converters," *IEEE Trans. Ind. Appl.*, vol. 43, no. 4, pp. 1032–1040, Jul./Aug. 2007.
26. C. M.Wu,W. H. Lau, and H. Chung, "A five-level neutral-point-clamped H-bridge PWM inverter with superior harmonic suppression: Atheoretical analysis," in *Proc. IEEE Int. Symp. Circuits Syst.*, Orlando, FL, May 30– Jun. 2, 1999, vol. 5, pp. 198–201.
27. Z. Cheng and B. Wu, "A novel switching sequence design for five-level NPC/H-bridge inverters with improved output voltage spectrum and minimized device switching frequency," *IEEE Trans. Power Electron.*, vol. 22, no. 6, pp. 2138–2145, Nov. 2007.
28. L. Max and S. Lundberg, "System efficiency of a DC/DC converter-based wind farm," *Wind Energy*, vol. 11, no. 1, pp. 109–120, 2008.
29. K. Hyosung, K. Jang-Hwan, and S. Seung-Ki, "A design consideration of output filters for dynamic voltage restorers," in *Proc. 35th IEEE Power Electron. Spec. Conf.*, 2004, pp. 4268–4272.
30. Z. Chen, J. M. Guerrero, and F. Blaabjerg, "A review of the state of the art of power electronics for wind turbines," *IEEE Trans. Power Electron.*, vol. 24, no. 8, pp. 1859–1875, Aug. 2009.

INTERNATIONAL JOURNAL OF MULTIDISCIPLINARY EDUCATIONAL RESEARCH
ISSN : 2277-7881; IMPACT FACTOR - 2.972; IC VALUE:5.16
VOLUME 3, ISSUE 10(4), OCTOBER 2014

DISASTER MANAGEMENT IN ANDHRA PRADESH – A STUDY OF HUDHUD CYCLONE

Dr. B. Sunitha Padmavathi
HOD, Department of Public Administration
Govt. City College, Hyderabad

Abstract

The present study discusses on preliminary survey on the awareness levels of different classes of people on disaster alarm and management systems. This provided a fundamental initiative for developing a plan for a green and smart city. 57% of the survey included the participants from age group 15- 35 age and 43% from age group above 35 years age. 49% are from the educational sector, 21% are from the government and private sector, and 30% from others. 31% are part of cyclones, 9% are part of floods, 59% are part of landslides. The survey revealed that 70% increase in the awareness levels of disaster alarm systems. 50% of people were aware of disaster management system before tsunami while it increased by 44% after the tsunami. The technological development has catered a better scope in facing disasters of this sort. The public-private participatory approach would bring better results in developing a better disaster alarming, management, and green city.

Keywords: Disaster alarming system, Disaster management system, smart city etc.

Introduction

India is vulnerable to natural hazards, particularly floods, drought, cyclones, earthquakes, landslides, etc. About 5700 kilometers of India's coastline is exposed to cyclones of severe intensity and magnitude. The most severe cyclone to hit India over the last few decades was the Odisha Super Cyclone in 1999 wherein more than10, 000 people died. The enactment of the Disaster Management Act, of 2005 and the National Policy on Disaster Management, of 2009 facilitated the adoption of a proactive approach to dealing with disasters, which is being practiced in the Coastal States as well.Andhra Pradesh (A.P.) is highly prone to natural disasters. Floods and cyclones are a recurrent phenomenon in Andhra Pradesh.

Susceptibility to disasters is compounded by frequent occurrences of manmade disasters such as fire, industrial accidents, etc. While accurate data is in the process of being collated and analyzed; the floods in Kurnool and other coastal districts in October-November 2009 have reversed the development growth experienced by Andhra Pradesh in the last decade. Frequent disasters like the Hud Hud Cyclone lead to the erosion of development gains and restricted options for disaster victims. Physical safety, especially for vulnerable groups, is routinely threatened by natural hazards. Recent floods and the cyclones in A.P. have very clearly illustrated the need for multi-hazard prevention, response, and recovery plans for natural hazards so that threat to human life and property is minimized. Disaster management is a development problem; preparedness and mitigation planning will have to be taken up in perpetuity and in tandem with environmental and developmental concerns in the State.

The State Disaster Management Plan establishes the policies and structure for State government management of disasters; Prevention, Mitigation, Preparedness, Response, Relief, and Recovery. The State Disaster Management Plan (SDMP) is for Floods, Cyclones, Earthquakes, Industrial accidents (chemical spills), Oil spills, Dam breaches, and Mine disasters. This plan assigns responsibilities for actions and tasks that the State will take to provide for the safety and welfare of its citizens against the threat of natural, technological, and human-caused disasters.

The state plan is prepared with an emphasis on close coordination with the National Disaster Management Plan (NDMP) of the National Disaster Management Authority (NDMA). It establishes a base on which further plans, procedures, guidelines, logistical arrangement plans, district-level DM plans, and mandal-level DM plans can be prepared.

Facing Hudhud Cyclone: The two cyclone-prone States are hoping to lower the disaster-related death toll even further this year. Odisha's 1999 'super cyclone' killed 10,000 people. The October 2013 'Phailin', that battered Odisha and Andhra Pradesh, claimed less than 50 lives. The States are aiming to further lower the human loss caused by the latest 'Hudhud' cyclone, which hit the east coast exactly a year after

Phailin, by bringing it below last year's toll. What has made this feat possible? It's a combination of advancements in weather monitoring technology, preparedness by respective State administrations and coordination with disaster mitigation and defense personnel to tackle natural calamities.

Tropical Cyclone Hudhud formed in the Northern Indian Ocean on October 8, 2014 and began to track westward across the Bay of Bengal. As a very severe tropical cyclone, it gained more strength before landfall on October 12, 2014 between Visakhapatnam (Vizag) and Srikakulam in Andhra Pradesh.

With each passing hour, the intensity of Hudhud has increased and with every increase, the threat to Andhra Pradesh coastal areas also increased. From the past Category 1 strength, cyclone Hudhud intensified to Category 2 strength by Saturday morning, by afternoon it had intensified into Category 3 cyclone. The maximum sustained

wind speed as per US Joint Typhoon Warning Centre (JTWC) update was 105 knots (close to 194 km/hr), gusting at 130 knots (close to 240 kmph).

Evacuation of 450,000 people on in coastal Andhra

The Andhra Pradesh government has started evacuating people from the coastal villages in anticipation of severe cyclone Hudhud. The cyclone is on its course to hit the Visakhapatnam coast Sunday forenoon. According to Katta Hymavati, special commissioner, state disaster management, arrangements for evacuation of 456,000 people from 500 villages have been made. Storm surge of about 1 to 2 meters (3.2 to 6.4 feet) above astronomical tide would inundate low lying areas of east Godavari, Visakhapatnam, Vijayanagaram and Srikakulam districts of north coastal Andhra Pradesh at the time of landfall. Hudhud is capable to cause widespread damage to infrastructure and disrupt power and communications in low-lying coastal areas.

The Indian state of Andhra Pradesh is very vulnerable to natural disasters, especially cyclones and floods, as it is a coastal region. It has the longest coastline on the Eastern coast and an overall second-largest coastline of India which is more vulnerable to cyclones as compared to the Western coast. The Indian Red Cross Society in collaboration with the Canadian Red Cross has been implementing the community-based Disaster Risk Reduction (CBDRR) program since 2010 in Andhra Pradesh covering 32 communities spread across 12 districts. The CBDRR program was initiated to build disaster-resilient communities in the program villages. The communities have shown vast improvements in dealing with disasters since the program was initiated. Recently, a severe cyclonic storm, 'Hudhud' caused severe impact in 4 out of the 12 program districts.

Satellite, web technology help Andhra Pradesh, Odisha minimize Hudhud cyclone damage

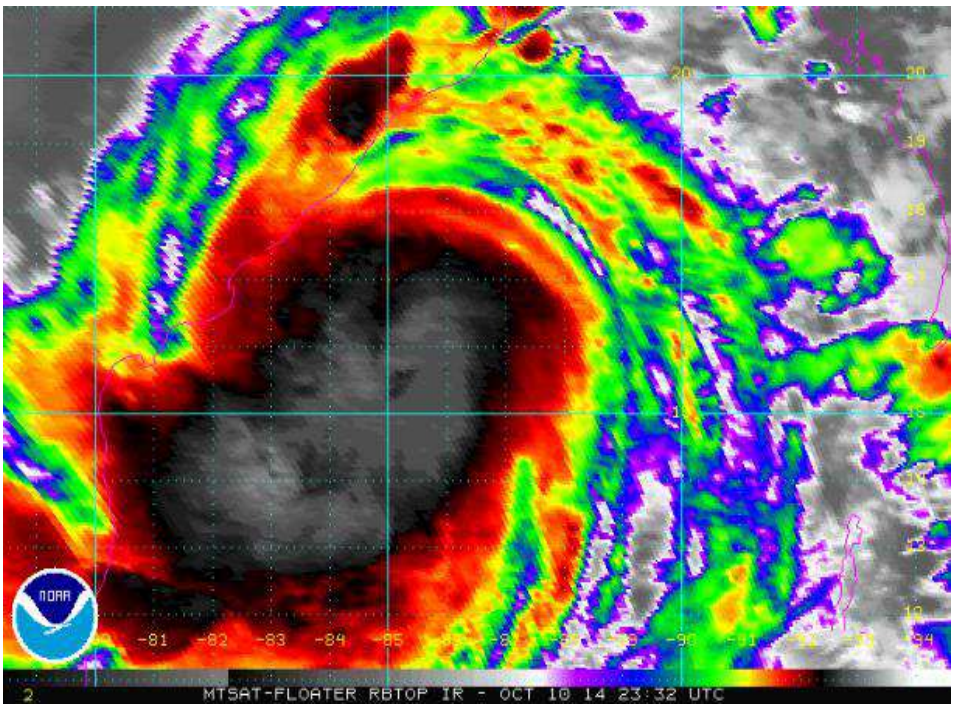

It's a combination of advancements in weather monitoring technology, preparedness by respective State administrations, and coordination with disaster mitigation and defense personnel to tackle natural calamities. For nearly a week, meteorology experts from the India Meteorological Department (IMD) have been putting out bulletins on the formation, movement and alerts on the potential intensity of the Hudhud cyclone. The Hyderabad-based, INCOIS and later NASA of US also stepped in as the cyclone gathered momentum to pitch in with their technology inputs, which included satellite imagery, wave, wind speed and potential rainfall data.

The continuous bulletins giving alerts and warnings helped the State Government of Andhra Pradesh and Odisha gear up preparations to minimize loss, especially humans while taking steps to reduce

economic destruction as well. Learning from the havoc of the super cyclone, the IMD and other meteorology agencies, built-up infrastructure like a network of satellite, ocean, and ground-based technological tools to improve the accuracy of forecasts, as they tracked Phailin.

Interestingly, the IMD's forecasts, which differed from those of some global agencies and raised a controversy, finally proved right in the case of Phailin. The preparedness of both the Odisha and AP Governments in co-ordination with the National Disaster Response Force efforts proved fruitful in keeping damages to the minimum. If the IMD has been continuously feeding satellite information, the Hyderabad-based Indian National Coastal, Ocean Information Systems (INCOIS) has been putting out real time data on the cyclone giving the progress of various parameters like wave height, and wind speeds, which have proved to be accurate with a 15 per cent margin of error, scientists told.

Better infrastructure

Both AP and Odisha, which perennially face the threat of natural disasters like cyclones and floods, have been improving their forecast and relief-cum-rehabilitation infrastructure. A series of Doppler Radars, weather stations, ocean-based buoys, and tracking systems are being set up, though at a slow pace. The NDRF, under the National Disaster Management Authority, is also proposing to set up some units and training facilities in the coastal States.

The AP Government's initiative to use crowdsourcing, by seeking pictures of the cyclone's impact, contributions for a specially designed Website on the National Remote Sensing Centre through an Android app, and a Facebook page and optimally utilizing the imagery from the Centre, has also brought in encouraging response to improve administrative steps in handling natural disasters.It is said that 146 cyclone relief shelters have been opened in the coastal districts. National Disaster Response Force has deployed 19 teams (each comprising 45 to 50 members) to undertake rescue and relief missions.

In addition, a large number of Army personnel have also been kept ready in Visakhapatnam. In Srikakulam, sea conditions were

rough this morning. Met department has warned that extensive damage to 'kutcha' houses, uprooting of big trees and partial disruption of power and communication lines and minor disruption of rail and road traffic are expected.

Under the influence of the system, rainfall, at most places heavy (6.5 - 12.4 cm) to very heavy (12.5 - 24.4 cm) at a few places and isolated extremely heavy (24.5 cm) would occur over west & east Godavari, Visakhapatnam, Vizianagaram and Srikakulam districts of north Andhra Pradesh and Ganjam, Gajapati, Koraput, Rayagada, Nabarangpur, Malkangiri, Kalahandi and Phulbani districts of south Odisha during the next 48 hours, met department said Rainfall would also occur at most places, with heavy to very heavy rainfall at isolated places, over Krishna, Guntur and Prakasham districts of Andhra Pradesh and north coastal Odisha during the same period. Squally winds, with speed reaching 50-60 kmph and gusting to 70 kmph at some places would prevail along and off north Andhra Pradesh and south Odisha coasts during the next 12 hours.

The wind speed would gradually increase to 140-150 kmph gusting to 165 kmph around the time of landfall along & off north Andhra Pradesh (East Godavari, Visakhapatnam, Vizianagaram and Srikakulam districts) and 80-90 kmph along and off adjoining districts of south Andhra Pradesh (West Godavari, Krishna districts) and south Odisha(Ganjam, Gajapati, Koraput and Malkangiri districts). The Andhra Pradesh government has asked all government employees to remain on duty over the weekend. In Visakhapatnam, the administration has opened 175 shelters and moved close to 40,000 people from the coastal villages. In Srikakulam, people of 250 villages in 11 mandals which may be affected have been evacuated. In Vizianagaram, at least 15,000 people have been evacuated, according to Collector M Naik.

Precautionary steps are taken to minimize Cyclone Hudhud impact

Joint Secretary Arvind Kumar, Officer on Special Duty for Relief, said people were reluctant to leave behind their belongings as they claimed there was no security. "But the district administration and police will ensure that there is no theft or any untoward incident in the villages while they are at the shelters," he said. "The cyclone may move north, so we are evacuating all those living in the coastal village as a precautionary measure," said Collector Gaurav Uppal. While human casualties are not expected due to the massive evacuation, power and telecommunication lines will be uprooted, leading to widespread disruption. A warning has been issued that flooding and uprooted trees will cut off escape routes, national and state highways and traffic is being regulated to ensure that nobody is caught in the flash floods caused by heavy rainfall.

Guidelines for design and construction of cyclone/tsunami shelters: National Disaster Management Division, India

The construction of shelters along vulnerable coastal areas is one of the important cyclone mitigation measures. These guidelines address conditions in the north Bay of Bengal, where storm surge conditions are among the most extreme worldwide in case of a cyclone. The work contains recommendations for the planning and design of shelters, covering such topics as: sustainable year-round uses, construction methods and selection of materials, accommodation capacity, location, the height of the cyclone shelter, inner design, structural specifications, water supply and toilets, and sewerage. Detailed design drawings are provided. This 26-page guide was published by the GoI-UNDP Disaster Risk Management Programme and four valuable reports from the associated workshop are included in the annex. Also included is a final chapter on the preparation of Killas or earth mounds, which have become an essential part of cyclone hazard minimization to protect livestock from the cyclone surge.

AP to adopt Odisha model of disaster management

The Andhra Pradesh government is planning to adopt a disaster management system like the one prevailing in Odisha, which frequently faces floods and cyclones. According to sources, impressed by the efficient cyclone relief work being put in by around 559 personnel from the Odisha Fire Services Department and Odisha Disaster Rapid Action Force (ODRAF) since October 13, Chief Minister N Chandrababu Naidu is learned to have asked State DGP and State fire services DG to adopt the Odisha model. States Andhra Pradesh & Odisha have relentlessly and successfully handled the pre & post-Hudhud cyclone conditions in minimizing human loss and in providing shelter and rehabilitation during the havoc. The deft handling of the delicate situation has been appreciated by International, National, and Local Organisations, Institutions, and authorities. This may be emulated by the other States and Rehabilitation and Disaster Management Institutions and Authorities.

The last few decades have seen an exponential increase in disasters striking different parts of the globe. The Indian Sub-Continent has a

multi–hazard profile on account of its unique geo-climatic conditions. The complex nature of disasters, urbanization and expansion of slums, increased vulnerability of rural populace to deteriorating ecosystems, and related issues like climate change have fuelled the intensity of disaster impacts. While hazards are largely unavoidable, especially with the growing threat of climate change and alterations in habitat, they only become disasters when communities' coping mechanisms are unable to manage their impacts. The recent experiences during the Uttarakhand, Phailin, HudHud, and Kashmir flood response constantly remind us of the need to invest in improved contingency planning, emergency communication & coordination, and capacity development of relevant stakeholders in risk mitigation and management. To combat such situations as far as cyclones are concerned: Putting in place an integrated web-based early warning dissemination system to connect to the last mile, is a pre-requisite to save human lives. The infrastructure of public and private buildings, roads, bridges, powerhouses and stations, water supply, food distribution, and other essential commodities needs to be made disaster resilient in phased manner but in shortest possible time. There is need to have IT/GIS based models for prevention, preparedness, mitigation and early response to disasters. These could be in the form of developing a Risk Atlas based on hazard risk vulnerability assessment of coastal areas of the country, which could help in locating vulnerable hotspots and making these resilient to disasters. This Risk Atlas can also be utilised for relief management purposes.

References

1. "Tropical Cyclone Formation Alert – Issued at 1330 UTC, 7 October 2014.". Joint Typhoon Warning Center.
2. "Tropical Weather Outlook for North Indian Ocean Issued at 0600 UTC of October 7, 2014.". India Meteorological Department.
3. "Cyclonic Storm Hudhud over north Andaman Sea & adjoining southeast Bay of Bengal.". India Meteorological Department.

4. "Very Severe Cyclonic Storm, HUDHUD over the Bay of Bengal (7-14 October 2014): A Report". India Meteorological Department.
5. "Hudhud intensifies Andhra Pradesh, Odisha on high alert". India Today. India Today.
6. "Cyclone Hudhud Effect: 38 Trains Cancelled on October 12". 11 October 2014.
7. "Cyclone Hudhud Heads for Odisha, After Battering Andaman and Nicobar Islands". NDTV. 8 October 2014.
8. "Cyclone Hudhud: 1.11 lakh people in Andhra Pradesh evacuated".
9. "Cyclone warning centre at Vizag also hit by Hudhud". news. biharprabha.com. IANS. 12 October 2014.
10. "Relief operations begin in cyclone-hit Andhra". 13 October 2014.
11. "Hudhud rips through Visakhapatnam airport". Times of India (Hyderabad). 14 October 2014.
12. "Cyclone Hudhud triggers Heavy rainfall in Southern Odisha". news. biharprabha.com. IANS. 12 October 2014.